National Research Council Canada
Conseil national de recherches Canada

ASSOCIATE COMMITTEE ON GEOTECHNICAL RESEARCH

SNOW PROPERTY MEASUREMENT WORKSHOP

APRIL 1 - 3, 1985
CHATEAU LAKE LOUISE
ALBERTA, CANADA

SPONSORED BY

SNOW AND ICE SUBCOMMITTEE
ASSOCIATE COMMITTEE ON GEOTECHNICAL RESEARCH

COMPILED BY

P.R. KRY

TECHNICAL MEMORANDUM 140

APRIL 1987

NRCC 27594

PRICE $25.00

Canada

88-04444/

The Associate Committee on Geotechnical Research is one of about thirty special committees which assist the National Research Council in its work. Formed in 1945 to deal with an urgent wartime problem involving soil and snow, the Commiteee is now performing its intended task of coordinating Canadian research studies concerned with the physical and mechanical properties of Snow and Ice, Peatlands, Permafrost, Urban Engineering Terrain Problems, Soil and Rock Engineering, and Marine Geotechnical Engineering. The Committee consists of about twenty Canadians appointed as individuals and not as representatives, each for a three-year term. Enquiries will be welcomed and should be addressed to: The Secretary, Associate Committee on Geotechnical Research, c/o Institute for Research in Construction, National Research Council of Canada, Ottawa, Ontario, K1A 0R6.

This publication is one of a series being produced by the Associate Committee on Geotechnical Research of the National Research Council of Canada. It may therefore be reproduced without amendment, provided that the Institute is told in advance and that full and due acknowledgement of this publication is always made. No abridgment of this report may be published without the written authority of the Secretary of the ACGR. Extracts may be published for purposes of review only.

****

Le Comité associé de recherches géotechniques est l'un des quelque trente comités spécieux qui assistent le Conseil national de recherches dans ses fonctions. Créé en 1945 pour s'occuper de problèmes ayant trait aux sols et à la neige et urgents par suite de la guerre, le Comité remplit maintenant le rôle qui lui était destiné, celui de coordonner au Canada les recherches portant sur les propriétes physiques et mécaniques du sol canadien. Il s'acquitte de ses fonctions par l'intermédiaire des sous-comités de la neige et de la glace, des marécages, du pergélisol, des problèmes l'ingénierie urbaine relatifs au terrain et de génie du sol et des roches, et de génie géotechnique marin. Le Comité se compose d'environ vingt canadiens nommés à titre individuel, et répondrons avec plaisir à vos demandes de renseignement. Veuillez les adresser à:

Le Secrétaire
Comité associé de recherches géotechniques
a/s Institut de recherche en construction
Conseil national de recherches
Ottawa, Ontario K1A 0R6

La présente publication fait partie d'une série réalisée par le Comité associé de recherches géotechniques du Conseil national de recherches. Elle peut donc être reproduite telle quelle à condition que l'institut en soit prévenue au préalable et que l'on mentionne toujours la présente publication. Il est interdit de publier tout résume du présent rapport sans le consentement écrit du secrétaire du CARG, seuls sont authorisée les extraits cités dans un comptes rendus.

NATIONAL RESEARCH COUNCIL CANADA
CONSIEL NATIONAL DE RECHERCHES CANADA

Associate Committee on Geotechnical Research

SNOW PROPERTY MEASUREMENT WORKSHOP

April 1-3, 1985
Chateau Lake Louise
Alberta, Canada

Sponsored by

Snow and Ice Subcommittee
Associate Committee on Geotechnical Research

Compiled by

P.R. Kry

TECHNICAL MEMORANDUM 140

April 1987

NRCC 27594

Acknowledgement

The organizing committee of this Workshop,

Dr. G. Irwin
Dr. P. R. Kry
Dr. D. Male
Dr. D. McClung
Dr. R. Perla
Mr. P. Schearer
Dr. R. Yong,

wish to express their gratitude to the Associate Committe on Geotechnical Research for its support in encouraging research and communication between researchers bound together by a focus on the material snow. Thanks are also due the NRC staff who assisted with the organization beyond the responsibilities of their normal work: Mr. Paul Anhorn, technical officer at Revelstoke, Mr. Michael Demuth, temporary assistant at Revelstoke, and Mrs. Beverly Richardson, secretary at Vancouver. Gratitude is especially extended to the workshop participants, through whose efforts this memorandum on measurement techniques was created. It is hoped their efforts will succeed in improving communication and understanding amongst researchers whose efforts enlarge our understanding of that common Canadian material: snow.

TABLE OF CONTENTS

Page

Preface 1

Workshop Program 3

Workshop Participants 7

Papers

"Mechanical and Physical Properties of Snow" by M. Fukue and R. Yong 11

"Avalanche Occurrence as Revealed by Time Lapse Photography, Kananskis Country, Alberta" by F. A. deScally, J. S. Gardner and H. J. Mcpherson 33

"Snow Microstructure Measurements Using Stereology" by J. Dozier, R.E. Davis and R. Perla 59

"Dilution Method for Measuring Liquid Water in Snow: Field Tests in a Subalpine Snowpack" by R. Perla, R. E. Davis, J. Dozier and E. R. Lachapelle 71

"Abnormally Enriched Elemental Concentrations in Urban and Rural Snow" by J.J. Drake, S. Vermette, S. Landsberger and A. Simsons 79

"Field Studies on Stress Waves in Natural Snowcover" by R.L. Brown, and A. Hansen 89

"Snow Properties in Actual Field Conditions and Stability Analysis" by M. Fukue 111

"Use of Index Measurements in Studies of Snow Under Vertical Loading" by G.J. Irwin 137

"Energy Analysis of Confined Compression and Shear Behavior of Snow" by R.N. Yong 165

"Experience Gained Operating Snow Pillows on a Near Real Time Basis in the Mountainous Areas of Alberta" by G.A. Coles, D.R. Graham, and R.D. Allison 193

"Remote Monitoring of Depth of Snow on Ground With a Micrologger" by S.N. Edey, D.J. Buckley, M.J.L. Lalonde and C.F. Nicholls 207

"Extrapolating Snow Measurement on the Marmot Creek Experimental Basin" by P.Y. Bernier 215

"Trends in Snow Surveying in Canada" by B.E. Goodison, J.E. Glynn, D. Harvey, and J.E. Slater 231

"Snowpack Measurements in a Forested Environment" by D.A. Daugharty and R.B.B. Dickison 255

"Snowmelt and Runoff During Rain-On-Snow in Forest and Adjacent Clearcut" by P.G. Beaudry and D.L. Golding 285

"Observations on Floating Snowpacks: Lakes, Rivers and the Sea" by P. Adams, T. Prowse and H. Granberg 313

"Measurement of Blowing Snow Properties Using Optical Attenuation Devices" by J.W. Pomeroy, T. Brown and D.H. Male 347

"Measurements of the Concentration of Falling Snow" by J.R. Stallabrass 389

"Snow-Drifting: A review of the Process and of Modelling Methods" by R.J. Kind 411

"Winter Precipitation, Snowpack, and Atmospheric Conditions in the Southern Canadian Rockies" by N.H. Thyer, F.D. Barlow and F.E. Robitaille 435

"A Comparison of Various Snow Gauges on the Canadian Prairies Over Five Winters" by K.H. Jones 455

"Impact of Automation on Winter Precipitation Measurement" by B.E. Goodison 471

"Snow Retention in a Large Cutblock", by A.M.K. Nip and R.H. Swanson 491

"Soil Heat Flux, Wetting Front Advance and Ice Layer Growth in Cold Dry Snow Covers" by P. Marsh and M. Woo 497

PREFACE

The objective of this workshop was to discuss problems associated with measurement of snow properties. This objective was formulated by a group of people who became the organizing committee for this workshop through their volunteer activities on a Working Group of the Snow and Ice Subcommittee of the Associate Committee on Geotechnical Research. At its twenty-sixth meeting, the Snow and Ice Subcommittee established a Working Group to identify snow research in Canada, review it and its application, identify deficiencies and recommend ways to overcome those deficiencies. To achieve this mandate, the Working Group compiled a bibliography of researchers whose publications indicated their research involved the material snow. A letter survey was formulated and sent to these researchers. From the results of that survey the objective of this workshop was clearly defined. No other concern was so clearly enunciated, except for the lack of funds and manpower, as the need for better and new techniques to quantify the properties of the material snow. Not only are there deficiencies in our abilities to measure known properties, but sometimes there are difficulties in clearly defining the physical quantities that give rise to the macroscopic behavior that we strive to understand and predict.

The Snow and Ice Subcommittee of the National Research Council Associate Committee on Geotechnical Research fulfills the role of identifying research needs for Snow and Ice problems in Canada and promoting research to address perceived deficiencies. During the period of active hydrocarbon exploration in the Arctic offshore, the Snow and Ice Subcommittee focused much of its attention on ice related problems and identified and promoted needed research through a number of workshops similar in format to this one. In recognition of the fact that snow research had not been as actively supported, the Subcommittee formed the Snow Advisory Working Group to provide needed advice on the state of research related to snow within Canada.

The Snow Advisory Working Group compiled a bibliography of more recent research which involved snow and identified over 200 researchers with an interest in snow. The Group noted that the snow research effort in Canada was fragmented. This was reflected by the fact that there were a large number of people who devoted a small fraction of their time to snow problems. There was a need for improved communication. By bringing people together in a workshop format it was felt that beneficial exchanges of manpower, funds, equipment or knowledge could be facilitated. To identify the topic which provided the major impediment to research in snow, the Group distributed a letter survey to 240 researchers. Ninety replies were received; an overwhelming 40% response rate.

The responses to the letter survey indicated that most of the research projects within Canada were directed either at snow cover distribution or prediction of snow melt and runoff. The research projects were grouped as follows:

Studies of snow cover distribution in arctic alpine, prairies and forest environments	27 projects
Prediction of snow melt and runoff	26 projects
Interaction of forests and vegetation with snow	13 projects
Collection of snowfall data and development of instrumentation for data collection	13 projects
Properties of snow: mechanical, thermal, electro-magnetic, metamorphism	11 projects
Avalanches	10 projects
Chemistry and impurities of snow	7 projects
Snow drifting	6 projects
Influence of snow on traffic, mobility	6 projects
Influence of snow on soil freezing and soil moisture	6 projects
Snow and buildings	3 projects.

Suitable instrumentation and problems with instruments were cited most frequently as an impediment to research. Nearly as frequently, the lack of data or reliable data was cited as an impediment. These results lead the Snow Advisory Working Group to become the organizing committee for a workshop on Snow Property Measurement. An auxiliary objective was to promote the interaction of groups of researchers who would not normally come together. With those as goals, the sessions for this workshop were advertised and have resulted in the submission of the papers collected in this volume.

The workshop agenda has been included in this publication to indicate the groupings of papers. The list of attendees has been included to facilitate communication amongst the researchers whose projects involve snow.

WORKSHOP PROGRAM

April 1, 1985

8:30-6:30 MEASUREMENT OF SNOW STRUCTURE AND ITS MECHANICAL AND PHYSICAL PROPERTIES
CHAIRMAN: Dr. R. Yong

8:30 M. Fukue and R. Yong: Mechanical and physical properties of snow.

F.A. de Scally, J.S. Gardner and H.J. McPherson: Avalanche occurrence as revealed by time lapse photography, Kananaskis, Alberta.

J. Dozier and R. Perla: Structure of snow.

10:00 COFFEE

10:30 R. Perla, R.E. Davis, J. Dozier and E.R. LaChapelle: Dilution method for measuring liquid water in snow: field tests in a subalpine snowpack.

J. Drake, S. Vermette, S. Landsberger and A. Simsons: Abnormally enriched elemental concentrations in urban and rural snow.

11:30 DISCUSSION

12:30 LUNCH

2:00 R.L. Brown and A. Hansen: Field studies on stress waves in natural snowcover.

H.B. Granberg: A Swedish snow density sampler.

M. Fukue: Snow properties in actual field conditions and stability analysis.

3:00 COFFEE

3:45 G.J. Irwin: Use of index measurements in studies of snow under vertical loading.

D.M. McClung: Creep constitutive properties of snow from field measurements.

R. Yong: Confined compression and shear of snow: energy concept.

5:00 DISCUSSION

April 2, 1985

8:30-5:30 MEASUREMENT OF SNOWCOVER DISTRIBUTION/WATER EQUIVALENT
CHAIRMAN: Dr. P. Adams

8:30 G.A. Coles, D.R. Graham and R.D. Allison: Experience gained operating snow pillows on a near real time basis in the mountainous areas of Alberta.

S.N. Edey, D.J. Buckley, M.J.L. Lalond and C.F. Nicholls: Remote monitoring of depth of snow on ground with a micrologger.

P.Y. Bernier: Extrapolating snow measurement on the Marmot Creek Experimental Basin.

10:00 COFFEE

10:30 B.E. Goodison, J.E. Glynn, D. Harvey and J.E. Slater: Trends in snow surveying in Canada.

11:00 DISCUSSION

12:00 LUNCH

2:00 D.A. Daugharty and R.B.B. Dickison: Snowpack measurements in a forested environment.

3:00 COFFEE

3:30 P.G. Beaudry and D.L. Golding: Snowmelt and runoff during rain-on-snow in forest and adjacent clearcut.

P. Adams, T. Prowse and H. Granberg: Observations on floating snowpacks.

4:30 DISCUSSION

April 3, 1985

8:30-1:00 MEASUREMENT OF PRECIPITATION AND BLOWING SNOW
CHAIRMAN: Dr. B. Goodison

8:30 J.W. Pomeroy, T. Brown and D.H. Male: Measurement of blowing snow properties using optical attenuation devices.

J.R. Stallabrass: Measurements of the concentration of falling snow.

R.J. Kind: Snow drifting: A review of the processes and of modelling methods.

10:00 DISCUSSION

10:30 COFFEE

April 3 - continued

11:00 N.H. Thyer, F.D. Barlow and F.E. Robitaille: Winter precipitation, snowpack, and atmospheric conditions in the Southern Canadian Rockies.

K.H. Jones: A comparison of various snow gauges on the Canadian Prairies over five winters.

B.E. Goodison: Impact of automation on winter precipitation.

12:30 DISCUSSION

1:00 LUNCH

WORKSHOP PARTICIPANTS

PETER ADAMS
Watershed Ecosystems
Trent University
Peterborough, Ontario, K9J 7B8

PAUL ANHORN
Division of Building Research
National Research Council
Box 2759
Revelstoke, British Columbia
V0E 2S0

RICK BARLOW
Atmospheric Sciences Department
Alberta Research Council
2411 - 11135 83 Avenue
Edmonton, Alberta T6G 2C6

PIERRE Y. BERNIER
Northern Forest Research Centre
Canadian Forestry Service
5320 - 122 Street
Edmonton, Alberta T6H 3S5

JEFF BOYD
CMH Heliskiing
Box 1660
Banff, Alberta TOL 0C0

BERNI CLAUS
Consultant
854 Keith Road
West Vancouver, B.C. V7T 1M3

DAVID DAUGHARTY
Department of Forest Resources
University of New Brunswick
Fredericton, N.B. E3B 5A3

FES A. deSCALLY
Department of Geography
University of Waterloo
Waterloo, Ontario N2L 3G1

EIZI AKITAYA
Institute of Low Temperature Science
Hokkaido University
Sapphoro, Japan

DICK ALLISON
Water Survey Section
Alberta Environment
200 5 Ave. South
Lethbridge, Alberta

PIERRE BEAUDRY
Research Section
British Columbia Ministry of Forests
Bag 5000
Smithers, B.C. V0J 2N0

GEORGE L. BLAISDELL
Department of Civil Engineering and
Engineering Mechanics
Montana State University
Bozeman, Montana 59717

ROBERT L. BROWN
Department of Civil Engineering and
Engineering Mechanics
Montana State University
Bozeman, Montana 59717

GERALD A. COLES
Water Survey Section
Alberta Environment
11th Floor - 9820 - 106 Street
Edmonton, Alberta T5K 2J6

MICHAEL DEMUTH
Division of Building Research
National Research Council
Box 2759
Revelstoke, B.C. V0E 2S0

R.B.B. DICKISON
Department of Forest Resources
University of New Brunswick
Bag Service 44555
Fredericton, N.B. E3B 6C2

JEFF DOZIER
Department of Geography
University of California
Santa Barbara, California 93106

JOHN J. DRAKE
Department of Geography
McMaster University
Hamilton, Ontario L8S 4M1

STUART EDEY
Agrometeorology Section
Land Resource Research Institute
Agriculture Canada
Central Experimental Farm, Bldg. 74
Ottawa, Ontario K1A 0C6

M. FUKUE
Tokai University
Shimizu, Japan

DAVID R. GLUNS
British Columbia Ministry of Forests
518 Lake Street
Nelson, B.C. V1L 4C6

DOUGLAS L. GOLDING
Faculty of Forestry
University of British Columbia
Vancouver, B.C. V6T 1W5

BARRY GOODISON
Canadian Climate Centre
Atmospheric Environment Service
4905 Dufferin Street
Downsview, Ontario M3H 5T4

DAVID R. GRAHAM
River Forecast Centre
Alberta Environment
10th Floor Oxbridge Place
9820 - 106th Street
Edmonton, Alberta T5K 2J6

ANDREW HANSEN
Department of Civil Engineering
and Engineering Mechanics
Montana State University
Bozeman, Montana 59717

G. JERRY IRWIN
Vehicle Mobility Section
Defence Research Establishment Suffield
Ralston, Alberta T0J 2N0

GEORGE HOLECEK
Alberta Environment
10th Floor Oxbridge Place
9820 - 106 Street
Edmonton, Alberta T5K 2J6

JANICE B. JOHNSON
Show Avalanche Section
B.C. Ministry of Transportation and
Highways
940 Blanshard Street
Victoria, B.C. V8W 3E6

KEN H. JONES
Scientific Services
Atmospheric Environment Service
P.O. Box 4080
Regina, Saskatchewan S4P 3W5

PETER JORDAN
Consultant
3046 West 7th Avenue
Vancouver, B.C. V6K 1Z8

R.J. KIND
Department of Mechanical and
Aeronautical Engineering
Carlton University
Ottawa, Ontario K1S 5B6

RICK KRY
Research Department
Esso Resources Canada Limited
339 - 50th Avenue S.E.
Calgary, Alberta T2G 2B3

WAYNE LAUGHREN
Aanderaa Instruments Ltd.
560 Alpha Street
Victoria, B.C. V8Z 1B2

DAVID M. McCLUNG
Division of Building Research
National Research Council
3904 West 4th Avenue
Vancouver, B.C. V6R 1P5

DAVID H. MALE
Division of Hydrology
University of Saskatchewan
Saskatoon, SASK. S7N OWO

JIM. W. MASON
Atmospheric Sciences Department
Alberta Research Council
720 - 4445 Calgary Trail South
Edmonton, Alberta T6H 5R7

ALLEN NIP
Research Branch
Alberta Forest Service
Postal Bag 6343
Spruce Grove, Alberta TOE 2CO

DAVID NORCROSS
Wardens Service
Parks Canada
Lake Louise TOL 1EO

BARRY NORTHEY
Forest Land Use Branch
Alberta Forest Service
9945 - 108 Street
Edmonton, Alberta T5K 2G6

RON PERLA
National Hydrology Research Institute
Environment Canada
Box 313
Canmore, Alberta TOL OMO

JOHN W. POMEROY
Division of Hydrology
University of Saskatchewan
Saskatoon, Saskatchewan S7N OWO

TERRY D. PROWSE
National Hydrology Research Institute
Environment Canada
Ottawa, Ontario K1A OE7

DAVID RENFROE
Aanderaa Instruments Ltd.
560 Alpha Street
Victoria, B.C. V8Z 1B2

FRANK ROBITAILLE
Atmospheric Sciences Department
Alberta Research Council
2411 - 11135 - 83 Avenue
Edmonton, Alberta T6G 2C6

PETER SCHAERER
Division of Building Research
National Research Council
3904 West 4th Avenue
Vancouver, B.C. V6R 1P5

ROBERT S. SCHEMENAUER
Cloud Physics Research Division
Atmospheric Environment Service
4905 Dufferin Street
Downsview, Ontario M3H 5T4

V.G. (FRED) SCHLEISS
Snow Research and Avalanche
Warning Section
Parks Canada
Box 350
Revelstoke, B.C. VOE 2SO

DAVID SKJONSBERG
Snow Research and Avalanche
Warning Section
Parks Canada
Box 350
Revelstoke, B.C. VOE 2SO

RICHARD SOMMERFELD
Rocky Mountain Forest and Range
Experiment Station
U.S. Forest Service
240 Prospect Street
Fort Collins, Colorado, 80526

JIM R. STALLABRASS
Division of Mechanical Engineering
National Research Council
Ottawa, Ontario K1A OR6

LYLE A. SUTHERLAND
University of Alberta
10427B - 145 Street
Edmonton, Alberta T5N 2X9

DAVID TOEWS
British Columbia Ministry of Forests
518 Lake Street
Nelson, B.C. V1L 4C6

DAVID WILFORD
British Columbia Ministry of Forests
R.R. #2
Smithers, B.C. V0J 2N0

H.R. WHITELEY
School of Engineering
University of Guelph
Guelph, Ontario N1G 2W1

RAYMOND N. YONG
Geotechnical Research Centre
McGill University
817 Sherbrooke Street West
Montreal, Quebec H3A 2K6

MECHANICAL AND PHYSICAL PROPERTIES OF SNOW

by

M. Fukue

Tokai University
Shimizu, Japan

R.N. Yong

Geotechnical Research Centre
McGill University, Montreal
Canada

presented at

SNOW PROPERTY MEASUREMENTS WORKSHOP

Lake Louise, Alberta

1-3 April, 1985

TECHNICAL MEMORANDUM 140

Compiled By

P.R. Kry

NRCC 27594

MECHANICAL AND PHYSICAL PROPERTIES OF SNOW

by

Masaharu Fukue[1] and Raymond N. Yong[2]

ABSTRACT

For the better understanding of the mechanical properties of snow, a comprehensive study on the deformation mechanism and failure criterion was made.

In this study, the most basic properties in dead load confined compression, strain controlled confined compression and direct shear performance were described on the basis of the adhesion theory.

INTRODUCTION

From the mechanical point of view, snow is loose material composed of viscous solid particles which exist near the melting point. Therefore, the mechanical properties of snow can be expressed by three key terms, i.e., loose, viscous particles and melting point.

The term "loose" directly means the compressibility of snow. However, the compression behaviour is very complicated in terms of strain hardening resulting from the viscous deformation of particles. Because snow materials are present near the melting point, the viscous deformation of snow causes the contact area between particles to increase, especially in poorly bonded and granular snows (Fukue, 1979).

---

[1] Tokai University, Shimizu, Japan.

[2] Geotechnical Research Centre, McGill University, Montreal, Canada.

This process is defined as the strain hardening of snow.

Therefore, under loading the change in snow properties such as viscosity, strength and density, should be taken into account in the deformation mechanism.

Fukue (1979) obtained an approximate relationship between the increase in contact area of spherical particles and viscous axial strain, based on geometrical consideration. This relationship has been examined experimentally by a statistical method and is significantly used in the study for the theoretical development of failure criterion and stress-strain relationships. The study deals with strain hardening as one of the most basic and important properties which may control the mechanical behaviour, and examines the deformation mechanism and failure criterion.

COMPRESSION SHEAR AND DIRECT SHEAR

Considering a loose grain structure as illustrated in Fig. 1, the problem to be solved becomes more clear. Under macroscopic principal stresses, σ_1 and σ_3, the microscopic forces, p and q, will be developed, where it is obvious that the stress ratio σ_1/σ_3 differs from p/q. Therefore,the conventional shear stress theory can hardly apply to this loose material.

Furthermore, under uniaxial compression, the failure plane which will be exerted by an external force often appears as a horizontal plane for which the macroscopic shear stress is nearly zero.

Under this situation, the mechanical performance of snow can be divided into compression shear and direct shear, as can be seen in the plate penetration performance shown in Fig. 2.

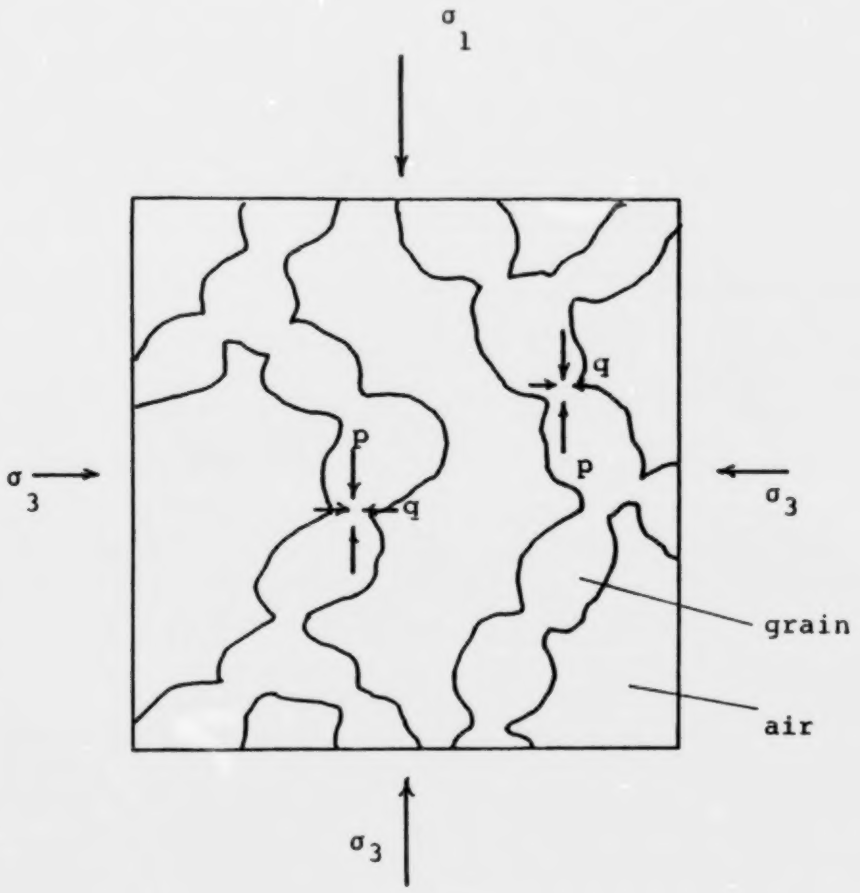

σ_1
σ_3
σ_3
σ_3
p
q
p
q
grain
air

Fig.1 Macroscopic stresses and microscopic internal forces in loose grain structure.

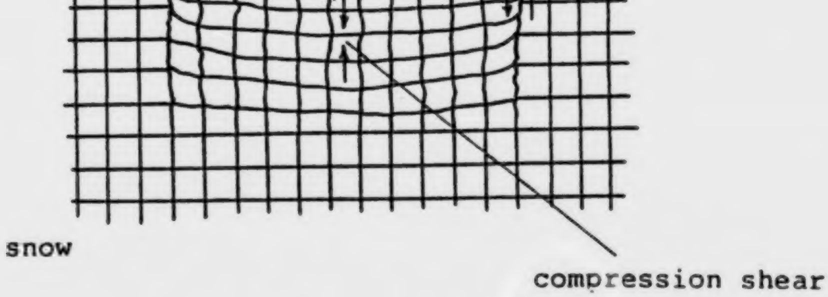

force
shear
snow
compression shear

Fig.2 Compression shear and direct shear under plate penetration.

ADHESION THEORY

Beyond the yield point of snow structural strength, snow particles deform viscously. If snow is poorly sintered, i.e., for poorly age-hardened or granular snows, the increase in the contact area between particles takes place with the volume change. In this case, an increase in structural strength can be expected due to an increase in the adhesion associated with the contact area.

The contact area between particles during compressive deformation was given by the following expression, based on a geometrical consideration, and assuming spherical particles to be in a loose state:

$$S = a\ \varepsilon_v(1 - b\ \varepsilon_v) \tag{1}$$

where

S = the increase in contact area caused by axial viscous strain, ε_v,

a and b = the parameters associated with snow type.

Therefore, the structural strength resulting from an increase in the contact area is defined as strain hardening, expressed by:

$$\alpha(\varepsilon_v) = A_d\ S \tag{2}$$

where A_d is the adhesion per unit area at contact.

On the other hand, the compressive viscosity associated with strain hardening can be assumed as:

$$\mu_c = \alpha\ S \tag{3}$$

where α is the parameter which may depend upon snow type. Taking the first approximation of Eq. (1) the compressive viscosity can be expressed by:

$$\mu_c = \alpha\ a\ \varepsilon_v \tag{4}$$

where ε_v is the compressive viscous strain.

STRAIN HARDENING UNDER LOADING

Under uniaxial compression, the stress-strain relationship of pure viscous materials can be expressed by:

$$\alpha = \mu_c \dot{\varepsilon}_v \qquad (5)$$

where $\dot{\varepsilon}_v$ is the compressive strain rate.

Therefore, for viscous materials with high compressibility, the stress-strain relationship can be expressed from Eqs. (3) and (5) as follows:

$$\sigma = \alpha S \dot{\varepsilon}_v$$

$$= \alpha \; a \; \varepsilon_v \; (1 - b \; \varepsilon_v) \; \dot{\varepsilon}_v \qquad (6)$$

Taking the first approximation of Eq. (6), the relationship can be expressed by:

$$\sigma = \alpha a \; \varepsilon_v \; \dot{\varepsilon}_v \qquad (6)'$$

(1) Dead load compression

Under a constant load, i.e., $\sigma = \sigma'$, Eq. (6)' is rewritten as

$$2\sigma t = \alpha \; a \; \varepsilon_v^{\,2} \qquad (7)$$

Then

$$\varepsilon_v = \sqrt{\frac{2 \; \sigma' \; t}{\alpha \; a}} \qquad (8)$$

where t is time.

Figure 3 shows the relationship between volumetric strain and time in confined compression under a dead load of 341 and 227 g/cm^2, at a temperature of -13°C. It is apparent that from the figure, the total volumetric strain (ε) is given by:

$$\varepsilon = \varepsilon_f + \varepsilon_0 + \varepsilon_v \qquad (9)$$

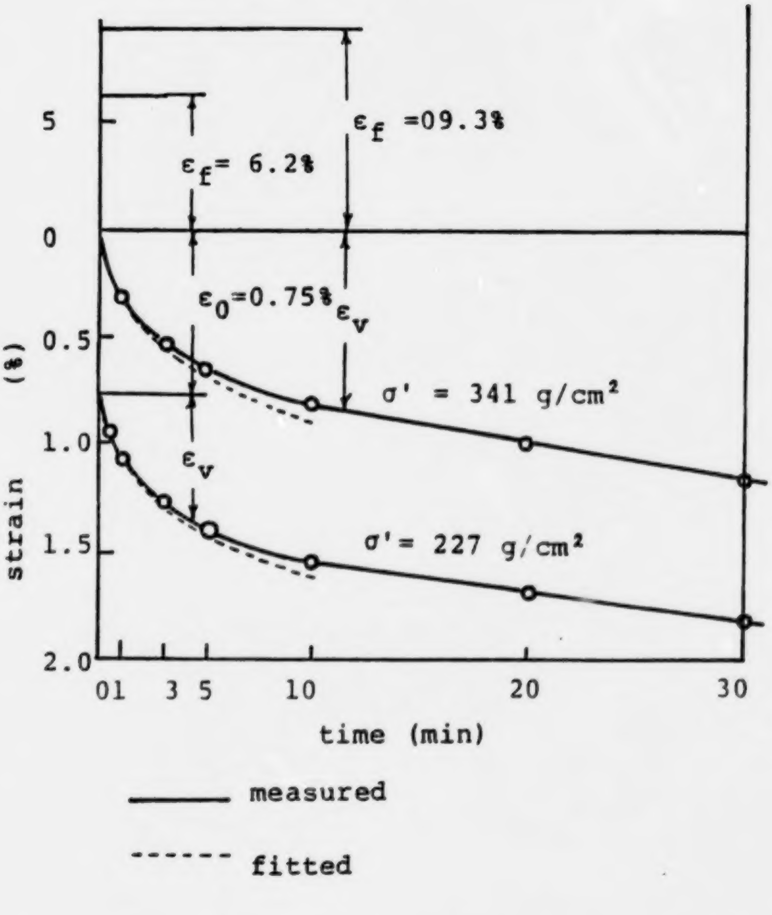

Fig.3 Volumetric strains of snow under single dead load.

where ε_f is defined as the failure strain due to compression shear failure (micro-fracture), ε_0 is defined as the foregoing viscous strain resulting from the continuous particle's rearrangement without micro-fracture and ε_v is defined as the viscous strain (creep strain) which will contribute to strain hardening.

Using Eq. (8), the total strain under a dead load can be expressed by:

$$\varepsilon = \varepsilon_f + \varepsilon_0 + \sqrt{\frac{2\sigma' t}{\alpha a}} \qquad (10)$$

It is noted that ε_f and ε_0 are also a function of normal load. The ε_f increases with dead load until critical density is reached (Fukue, 1979), as shown in Fig. 4.

As can be seen in Fig. 3, the relation between ε_v and time is almost the same for both curves obtained for the different normal load. This may be dependent on which different intensity of dead load provides the different ε_f and ε_0. Therefore, it may be possible that the value of αa is independent of dead load if the same type of granular snow is initially concerned. However, this does not mean that strain hardening is the same under different dead loads, because the different values in ε_f and ε_0 provide different densities when the viscous strain ε_v starts. Therefore, a different contact number should be taken into account for the initial condition.

Assuming that the strain hardening is proportional to the contact area, strain hardening is expressed by Eq. (2). Similarly, under dead load, strain hardening can be expressed by:

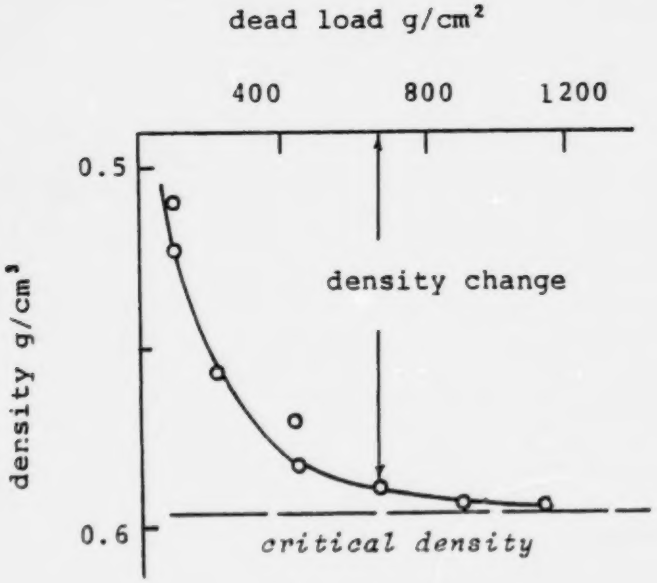

Fig.4 Density change under single dead load to obtain the critical density. Each density change results from failure strain.

$$\alpha(\varepsilon_v) = A_d\ a^* \sqrt{\frac{2\sigma' t}{\alpha\ a}} \qquad (11)$$

where

A_d = the adhesion per unit area at contact, and

a^* = the parameter concerned with initial density at which the viscous strain ε_v begins.

The approximate fitting using Eq. (8) gives slightly higher than actual compressibility, as shown in Fig. 3. This may result from the age hardening effect, and the increase in contact number related to the volume change. However, if the density concerned is relatively low, the effect of the change in contact number during volume change becomes less. Note that the increase in contact number has been observed on the thin sections of compressed snow samples, (Fukue, 1979).

(2) Direct shear

Recognizing that direct shear performance takes place during the strain hardening, as expressed by Eq. (11), if snow is initially granular, it is possible to express;

$$\tau_f(\varepsilon_v) = k\ \sigma(\varepsilon_v) \qquad (12)$$

where

τ_f = the shear strength, and

$k\ \sigma(\varepsilon_v)$ = the strain hardening due to normal load.

From Eqs. (11) and (12), shear strength is expressed by:

$$\tau_f = k\ A_d\ a^*\ \varepsilon_{vf} \qquad (13)$$

where

$$\varepsilon_{vf} = \sqrt{\frac{2\sigma'\ t_f}{\alpha\ a}}$$

The ε_{vf} is compressive viscous strain until shear failure.

Figure 5 shows saw-toothed type stress-deformation curves for initially granular snow in direct shear performance. Each development of stress which appears in the saw-toothed type curves is considered to be due to strain hardening. Therefore, shear failure and strain hardening repeatedly take place alternatively.

As mentioned above, a^* is dependent upon density after the foregoing strain. However, the relation between $kA_d a^*$ and σ can be examined using an arbitrary σ' and αa .

If we choose $\sigma' = 341$ g/cm^2, $\alpha a = 4.546 \times 10^9$ g/cm^2 sec, the relation between $k A_d a^*$ and σ , (which can be obtained using the experimental values of τ_f and t_f), and Eq. (13), becomes linear as shown in Fig. 6. The shear strength of granular snow can be given by the following expression:

$$\tau_f = \epsilon_{vf} C(\sigma + D) \tag{14}$$

If σ is relatively large, Eq. (14) is expressed by:

$$\tau_f = \epsilon_{vf} C \sigma \tag{15}$$

where $kA_d a^* = C \sigma$

then

$$\tau_f = \sigma C \sqrt{\frac{2\sigma'}{\alpha a} \frac{\gamma}{\dot{\gamma}}} \tag{16}$$

where

$t_f = \gamma/\dot{\gamma}$,

γ = the shear strain at failure, and

$\dot{\gamma}$ = the shear strain rate.

On the other hand, the shear strength of granular snow is

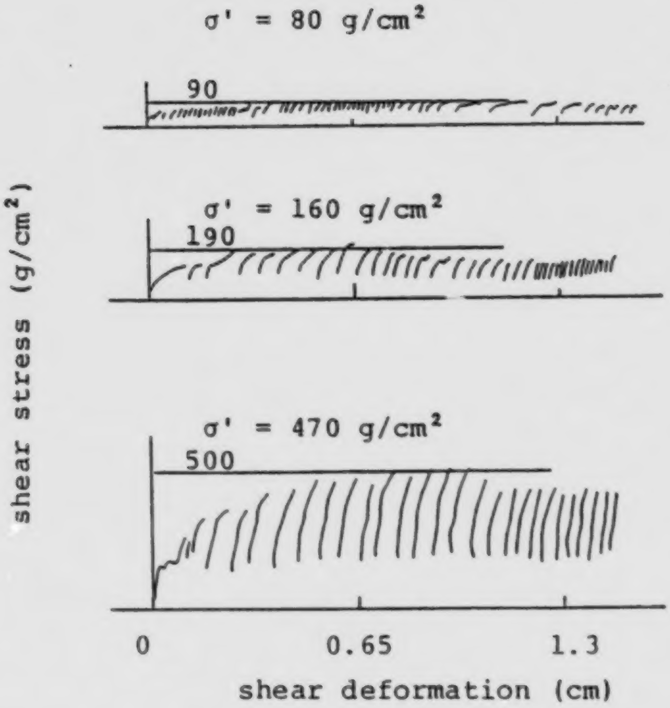

Fig.5 Typical stress-strain curve of snow in direct shear test at a strain rate of 0.8 %/sec.

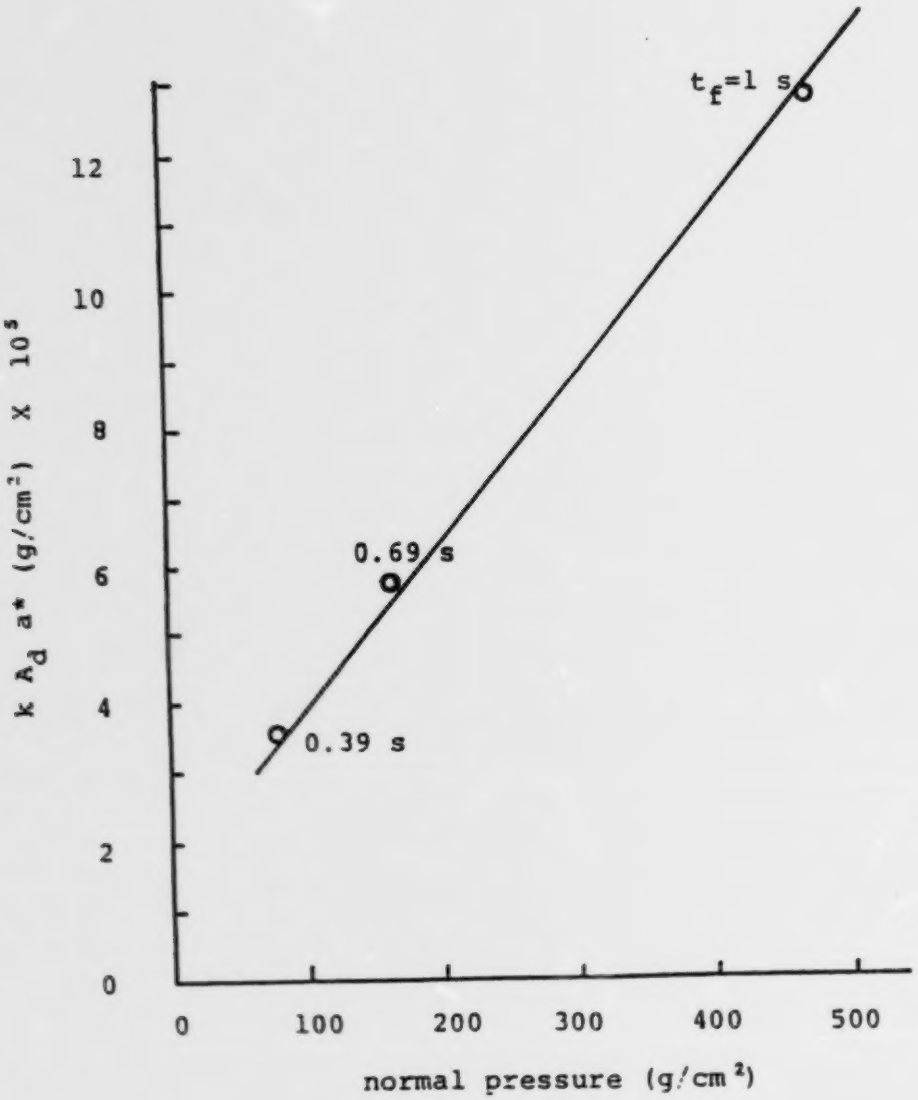

Fig.6 Relationship between K A_d a* and σ' based on the experimental data.

empirically expressed by a form:

$$\tau_f = \sigma \tan \phi' \qquad (17)$$

where

σ = the normal stress, and

ϕ' = the angle of internal friction.

Then from Eqs. (16) and (17), the following relation can be obtained:

$$\tan \phi' = C^* \sqrt{\frac{\gamma}{\dot{\gamma}}} \qquad (18)$$

Thus the angle of internal friction is dependent upon the shear strain rate unless $\gamma/\dot{\gamma}$ is constant.

From the experimental result, the values of $C^*\sqrt{\gamma}$ are 3.2 and 11 sec for strain rates of 0.04 and 0.0085/sec, respectively, at a temperature of -13°C.

The trend described above is very common. Note that the linear relationship between shear strength and normal pressure has been empirically accepted by many researchers but the rate effect on shear strength has not been well understood.

(3) Strain controlled confined compression

In confined compression with a constant strain rate, the stress-strain relationship of granular snows can be expressed by Eq. (6) to some extent. On the other hand, the stress cannot exceed the strength which is equal to the strain hardening for granular snow. Thus, from Eqs. (2) and (6), we obtain:

$$\dot{\varepsilon}_v \geqq \frac{A_d}{\alpha} \qquad (19)$$

where the maximum strain rate which satisfies the condition (19) is defined as the critical strain rate of granular snow, $\dot{\varepsilon}_c$. The critical strain rate of granular snow in confined compression is approximately 0.002/sec, i.e., 0.2%/sec, which is comparable to that of poorly-bonded snow under unconfined compression, at a temperature of -13°C, though the initial density may have some affect on it.

Therefore, at a temperature of -13°C, the following condition can be obtained:

$$A_d \geqq 0.002\ \alpha \qquad (20)$$

or

$$A_d a \geqq 0.002\ \alpha\ a \qquad (20)'$$

It is noted that $\alpha\ a$ is 4.546×10^9 g/cm^2 sec in dead load compression, and $A_d a$ is 9×10^6g/cm^2 in strain controlled confined compression at nearly the critical strain rate. The $A_d a$ value is obtained from the actual stress-strain relationship using Eq. (6)'.

If the strain rate concerned is lower than the critical value, the stress-strain relationship presented by Eq. (6) or (6)' is real. If not, the relationship becomes imaginary, as illustrated in Fig. 7. The trend shown in Fig. 7 is very common in actual compression performance of snows.

A continuous confined compression provides compression shear failure one after another until density reaches threshold value (Yong and Fukue, 1977). Under a confined condition, lateral stresses will be developed gradually by the volume change, and then the strain-hardening and compression shear failure will occur at the same time but in different parts, as a result of the lateral constraint.

This provides a saw-toothed type stress-strain relationship as shown in Fig. 8. Therefore, the total strain exerted consists mainly of the failure strain and viscous strain, ϵ_f and ϵ_v, res-

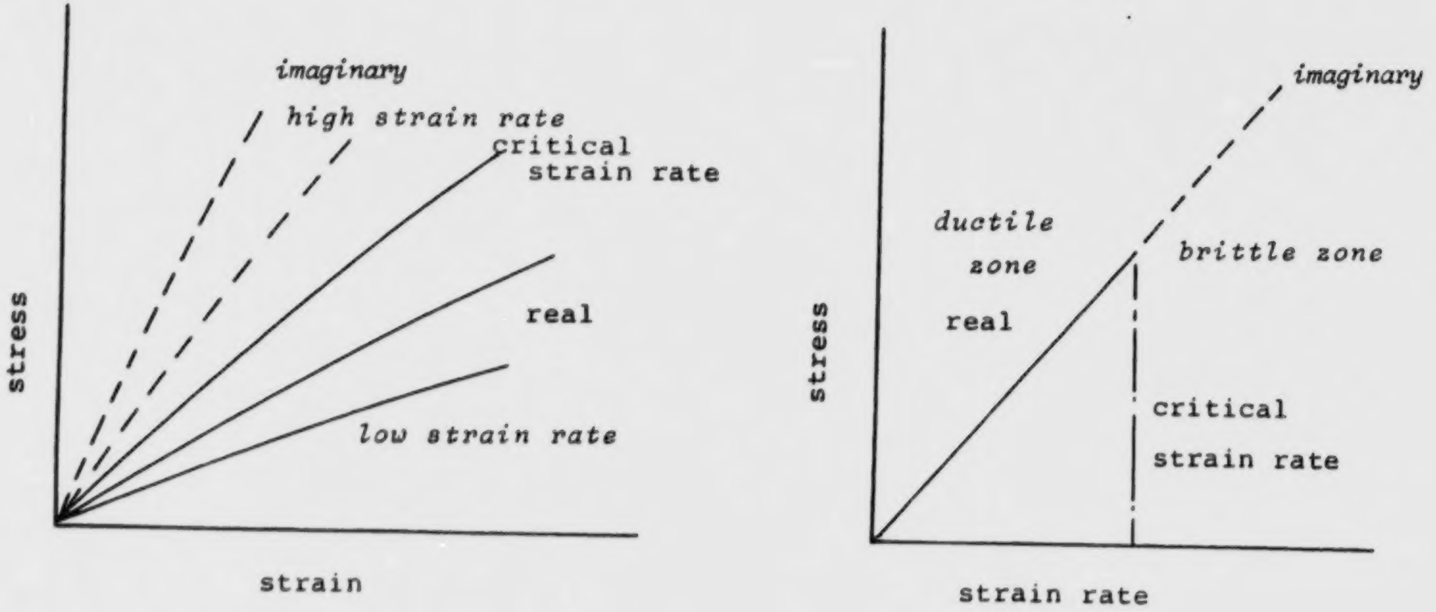
stress
imaginary
high strain rate
critical
strain rate
real
low strain rate
strain
stress
ductile
zone
real
imaginary
brittle zone
critical
strain rate
strain rate

(a) Stress-strain relationship

(b) stress-strain rate relationship

Fig.7 Real and imaginary stress-strain and stress-strain rate relationships of initially granular snow in confined compression.

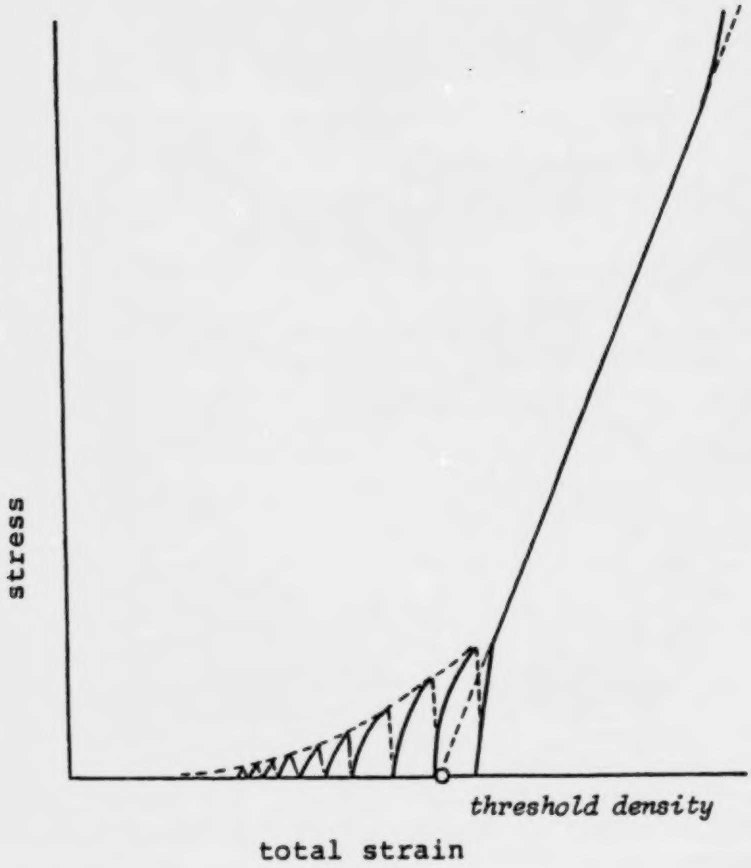

Fig.8 Stress-strain curve of initially granular snow in confined compression, at a high strain rate.

pectively, similar to dead load confined compression.

(4) Mechanical properties of granular snow under other types of loading

The mechanical properties and behaviour of granular snow in a single dead load confined compression, strain controlled confined compression and direct shear performance were described on the basis of the adhesion theory. As mentioned earlier, it is of primary importance that viscous strains provide strain hardening even if it is very small. Therefore, under other types of loading such as incremental load and stress controlled compression, the mechanical behaviour can also be described in terms of strain hardening resulting from the increase in contact area and number.

For example, the compressibility of granular snow under incremental dead load confined compression is considerably low in comparison to single dead load confined compression, for corresponding loads (Fukue, 1979). This is because strong strain hardening takes place under each load increment in the incremental dead load compression.

(5) Mechanical properties of bonded snows

The initial bonding between particles resulting from age hardening, refreezing of melt-water and previous strain hardening may weaken the strain hardening effects on the mechanical properties and behaviour under an application of external force because of the initial contact area already developed. Therefore, the critical strain rate of bonded snows depends upon the initial intensity of bonding and generally decreases with intensity. From the experimental result, it is possible to express the critical strain rate of bonded snow as:

$$\dot{\varepsilon}_c = \frac{A_d}{\alpha} - f(\sigma_0) \qquad (21)$$

where $f(\sigma_0)$ is some function concerned with initial intensity of bonding.

The compressive strength of bonded snows, σ_c, is expressed by a form:

$$\sigma_c = \sigma_0 + \sigma(\varepsilon_v) \tag{22}$$

where

σ_0 = the inherent strength which may depend upon the initial bonds , and

$\sigma(\varepsilon_v)$ = the strain hardening component which is less compared to that of granular snows.

Equation (22) can be applied in both confined and unconfined compressions for snows where the initial density is less than the critical value (Fukue, 1979). Note that snows for which the density reaches critical value, and where compression shear failure does not occur under laterally confined conditions, it is likely that the stress-strain relationship can be illustrated as shown in Fig. 9. This figure shows that the higher the strain rate, the lower the strength. Although this is not a common trend for most materials, it is one of the most fundamental properties of loose snow. Thus, the minimum compressive strength of loose snow can be obtained at the highest strain rate.

Figure 10 shows the penetration resistance of a thin blade into a bonded snow. It can be seen that the trend is similar to that shown in Fig. 9.

Thus the mechanical properties of bonded snow can also be explicable from the adhesion theory.

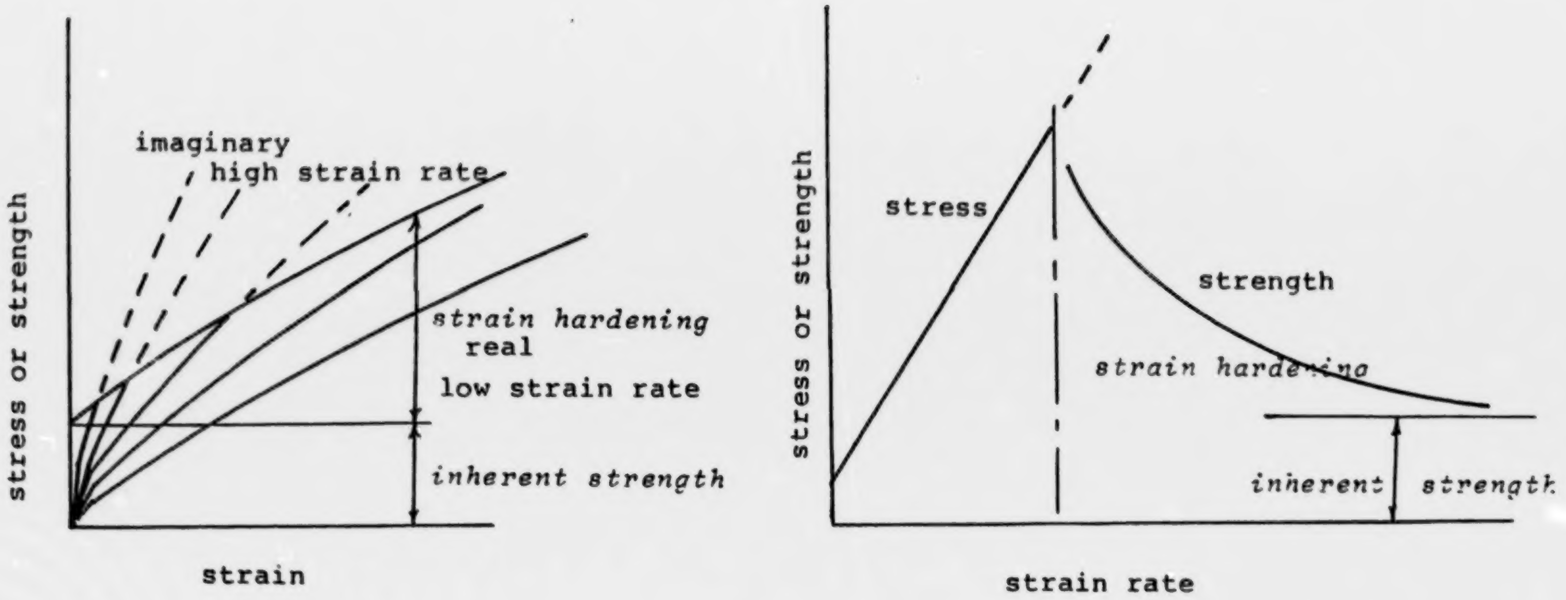
stress or strength
imaginary
high strain rate
strain hardening
real
low strain rate
inherent strength
strain
stress or strength
stress
strength
strain hardening
inherent strength
strain rate

Fig.9 stress-strain and stress-strain rate relationships of bonded snow in compression.

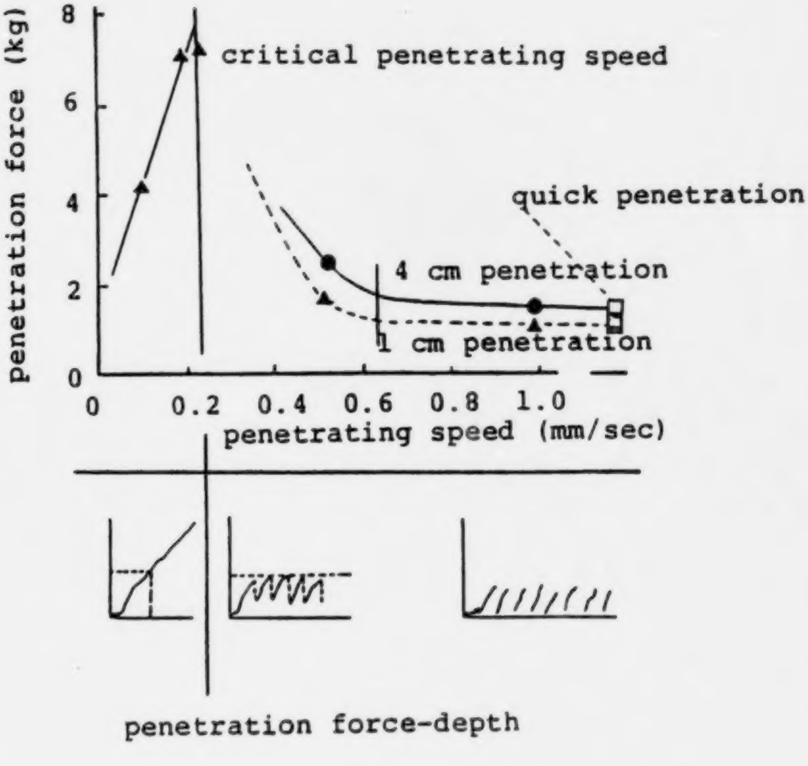

Fig.10 Speed effects on thin blade penetration into age hardened snow.

CONCLUDING REMARKS

It has been shown that the complicated mechanical properties of snow can be simply explained from the adhesion theory. In order to understand the mechanical properties of loose snow, it is necessary to consider the increase in strength and viscosity, resulting from the increase in contact area and number of particles.

In this study, the strain rate effects on snow properties were comprehensively examined by separating the increase in strength from the stress increase under deformation.

The theoretical approach based on the adhesion theory provides good results without any contradiction with the experimental results.

REFERENCES

Fukue, M. (1979) **Mechanical Performance of Snow under Loading,** Tokai University Press, Tokyo. 136 p.

Yong, R.N. and Fukue, M. (1977) **Performance of Snow in Confined Compression.** J. Terramechanics. 14-2:59-82.

AVALANCHE OCCURRENCE AS REVEALED BY TIME LAPSE PHOTOGRAPHY KANANSKIS COUNTRY, ALBERTA

by

F.A. deScally

and

J.S. Gardner

Department of Geography
Faculty of Environmental Studies
University of Waterloo
Waterloo, Ontario
Canada

H.J. McPherson
Department of Geography
University of Alberta
Edmonton. Alberta
Canada

presented at

SNOW PROPERTY MEASUREMENTS WORKSHOP

Lake Louise, Alberta

1-3 April, 1985

TECHNICAL MEMORANDUM 140

Compiled By

P.R. Kry

NRCC 27594

AVALANCHE OCCURRENCE AS REVEALED BY TIME LAPSE PHOTOGRAPHY KANANASKIS COUNTRY, ALBERTA

Introduction

Long term and continuous records of snow avalanche occurrences are difficult to come by. This is especially true for many parts of the mountain west in Canada where population is sparse and habitation, where it does exist, is relatively recent. Outside a few ski areas and sections of highway, such as at Rogers Pass, B.C., systematically accumulated records do not exist. The research reported in this paper tested a system to remotely sense and continuously monitor avalanche occurrence using time-lapse photography. It was thought that such a system could provide a continuous record of avalanches on one or several slopes throughout a winter and spring avalanche season. Repeated year after year, a record could accumulate without the expense and logistical problems of keeping an observer in the field. Such a system would be particularly useful in remote areas. Specifically, it would provide firsthand data on time and frequency of avalanche occurrence and could be used to estimate avalanche magnitude, including the important parameter of runout distance.

Such data are useful in evaluating avalanche hazard and risk in an area. Furthermore, if coupled with meteorological data and information on snowpack conditions , these data would further the understanding of factors which contribute to and initiate avalanches in a particular geographical region, these being different by degree from region to region.

This paper reports some of the results of a time-lapse photography monitoring program directed at two avalanche slopes in Kananaskis Country, Alberta in the winter 1982-83. Kananaskis Country is located to the southwest of Calgary and has long been a favourite summer weekend recreation area (Figure 1). Since 1975, the area has undergone considerable upgrading of recreation facilities for both winter and summer use. In particular, systems of cross-country ski trails have been developed, hiking trails have been upgraded to the point where they are useable for ski traffic, and access roads have been improved. Coupled with a nationwide growth trend in cross-country skiing and ski touring and a concerted advertising campaign these factors have turned Kananaskis Country into a heavily used winter recreation area. The research described here forms part of an overall study of avalanche hazard in Kananaskis Country (McPherson *et.al.*, 1983) conducted in part to provide some baseline information in the face of escalating winter use. Mt. Allen and the Marmot Creek experimental watershed, in the northern part of the area, will be the site of alpine ski events during the 1988 Winter Olympiad. This could well result in a further increase in winter use, including pressure to maintain Highway 40 through Highwood Pass (Figure 1) during the winter. In and of itself this will exacerbate avalanche hazard and risk considerably. Given this socio-economic context, some data on natural avalanche occurrence seemed a necessity.

Photography in Avalanche Research

The use of photography in snow avalanche research is not new. Kahn (1966a) noted that many sequential photographs and movies have been taken of avalanches to record velocities and flow characteristics. Kahn (1966b, 1972) used terrestrial photogrammetry in the Canadian Rocky Mountains and Wasatch Mountains to record avalanche fracture line propagation and avalanche movement and was able to determine the geometry of the avalanches. By photographing slopes before and after avalanche occurrences, VanWijk (1967) was able to estimate volumes of transported snow, velocities, and snow cloud volumes. Shoda (1967), in Japan, photographed avalanche traces from a helicopter and used this information to produce contour maps of the disturbed snow surfaces. Also in Japan, Akitaya (1973) used video pictures to study the dynamics of moving avalanches. Motion pictures were used by Dent and Lang (1982) to record decceleration of scale-model avalanches in the Bridger Range, Montana.

The practicality of time-lapse photography in providing scientific data on time dependent natural phenomena in a severe environment was demonstrated by Banner and van Everdingen (1979). Using time-lapse exposures they were able to record the growth and degradation of frost blisters. Time-lapse photography recently has been used to monitor river ice breakup, floes, and jams in northern Canada (Browse, pers. comm.).

Avalanche Research in Kananaskis Country

Avalanches have been studied as erosional agents and as potential hazards in Kananaskis Country for the past decade. The area around Mt. Rae (Figure 1) was the location of a series of studies which attempted to explain and describe erosion accomplished by snow avalanches (Tarquin, 1977; Gardner, 1983; Gardner et.al., 1983). More important from the viewpoint of this paper is the avalanche hazard research. Early in the 1970's, Brad Geisler, a well-known skier and avalanche expert from Calgary, did a preliminary examination of avalanche hazard in the Highwood Pass area. Gunderson (1978) provided a systematic analysis of avalanche hazard along Highway 40 and the Smith-Dorrien Road. A more detailed analysis of the Smith-Dorrien and Spray Lakes Road became available in atlas form in 1983 (Stethem and Associates, 1983). Avalanche hazard mapping in, and avalanche information systems for, Kananaskis Country have been the focus of recent research (Nieman, 1982; Nieman, Langford and More, 1984; More, Nieman and Langford, 1984).

The research program from which this paper is derived began in 1981. It has involved avalanche path mapping in Kananaskis Country (McPherson, et.al. 1983), detailed studies of selected avalanche paths where frequency and magnitude estimates were made using dendrochronology and vegetation damage (Steel, 1982; Drewry, 1983), and winter monitoring of snowpack conditions, weather and avalanche occurrences (deScally, 1984). Aspects of the time-lapse monitoring system were described previously (McPherson,

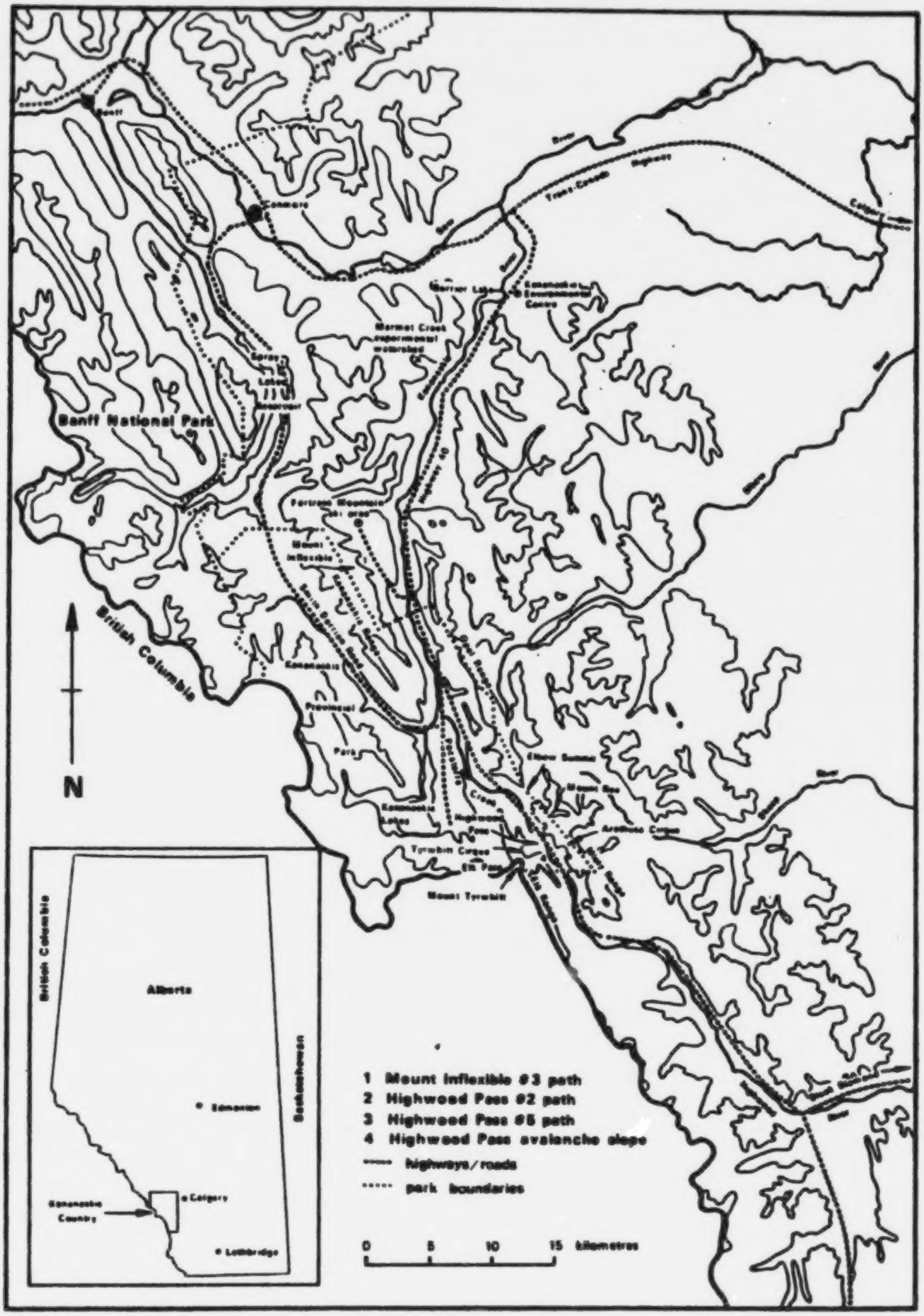
Banff
Canmore
Trans-Canada Highway
Barrier Lake
Kananaskis Environmental Centre
Marmot Creek experimental watershed
Spray Lakes Reservoir
Banff National Park
Fortress Mountain ski area
Mount Inflexible
British Columbia
Kananaskis
Provincial
Park
Elbow Summit
Mount Rae
Kananaskis Lakes
Highwood Pass
Arethusa Cirque
Tyrwhitt Cirque
Elk Pass
Mount Tyrwhitt
N
British Columbia
Alberta
Saskatchewan
Edmonton
Calgary
Kananaskis Country
Lethbridge
1 Mount Inflexible #3 path
2 Highwood Pass #2 path
3 Highwood Pass #5 path
4 Highwood Pass avalanche slope
highways/roads
park boundaries
0
5
10
15
kilometres

Figure 1 Study area

deScally, and Gardner, 1984). Most of the previous research in Kananaskis Country has focussed on identification of avalanche paths and their characteristics and the frequency and magnitude of past avalanches. As yet, relatively little is known about avalanche meteorology and release mechanisms in this area characterized by cold, thin snowpacks and wide fluctuations in winter temperatures.

The Study Sites

Two avalanche paths were chosen for time-lapse photographic monitoring in 1982-83. The prior research, noted above, indicated that both paths avalanche with varying magnitude on a frequent basis. Both paths intersect roads. The first, at Mt. Inflexible (# 1 Figure 1), intersects the heavily used Fortress Mountain ski area road and the second, at Highwood Pass (#4 Figure 1), intersects Highway 40 which is closed during the winter. The first site was readily accessible for frequent checking whereas the second site required a 50 km. round trip by snowmobile for maintenance.

The Mt. Inflexible path is located on the scarp slope of the Kananaskis Range. It is a large north-east facing path which decends 870m vertically to the road. The starting zone is on the lee (downwind) side of the mountain ridge which results in accumulations of wind drifted snow and the development of ridge line cornices. Gradients in the path range from 32 degrees to 50 degrees in the starting zone and upper track to 10 degrees in the runout zone. The starting zone and most of the track are essentially unvegetated while engelmann spruce, subalpine fir, alders and willows become increasingly abundant from the lower track to the runout zone.

The Highwood Pass path is unconfined and forms part of broad avalanche-prone slope to the west of the Pass. Being a lee slope, this too receives added snow loading through wind redistribution. The starting zone is prone to cornice development. Gradients in the path, which has a 520 m vertical drop, range from 37 degrees in the starting zone to 0 degrees in the runout zone. The starting zone and upper track are devoid of all but low tundra vegetation while the krummholz form of subalpine fir and birch and willow shrubs are present in the lower track. A deep snow plant community of heath and sedges attest to the persistence of late-lying snow avalanche deposits in the runout zone.

The Photographic Monitoring System

The cameras chosen for snow avalanche monitoring were Kodak Super 8 Analyst time-lapse cameras equipped with a variable interval setting. These cameras were relatively inexpensive (each $450.) and use standard Super 8 film cartridges. The variable interval setting was modified to an 8 minute exposure interval so that a standard 15 m film cartridge was sufficient to cover a three-week period. An attempt was made to change film every two weeks which left a one week margin in case camera sites could not be reached. The cameras ran continuously, exposing film during the dark hours. Installation of a photo electric cell would permit the cameras to be shut off during the night.

The camera systems were first used in the field during the winter 1981-1982. This experience was filled with frustration but did provide guidance on power supply and siting. The cameras are designed to operate with flashlight batteries but these proved totally inadequate in the cold conditions. Different batteries were tried, including 6-volt fencer batteries, automobile batteries, and rechargeable nickel-cadmium batteries. Eventually, the system was equipped with a transformer and Fulmen generator back up batteries. The batteries were housed in plywood boxes with 10 cm of styrofoam insulation and tin outer sheathing. The tin sheathing and a tough PVC tubing to contain the power lead were necessary to prevent damage by porcupines. Results from 1981-82 indicated that the cameras provided an acceptable and large enough frame to cover starting zone, track, and runout zone when sited at distances between 500 and 800 m from the track.

The camera shelter was also constructed of insulated plywood covered with tin sheathing. A double glass window was built into the shelter in line with the lens. The shelter was mounted on a tree approximately 2 m above the ground while the battery shelter rested atop a free standing frame which could be raised and lowered as the snow depth changed (Figure 2). Small quartz clocks (micronta brand) were used for recording the time of each frame.

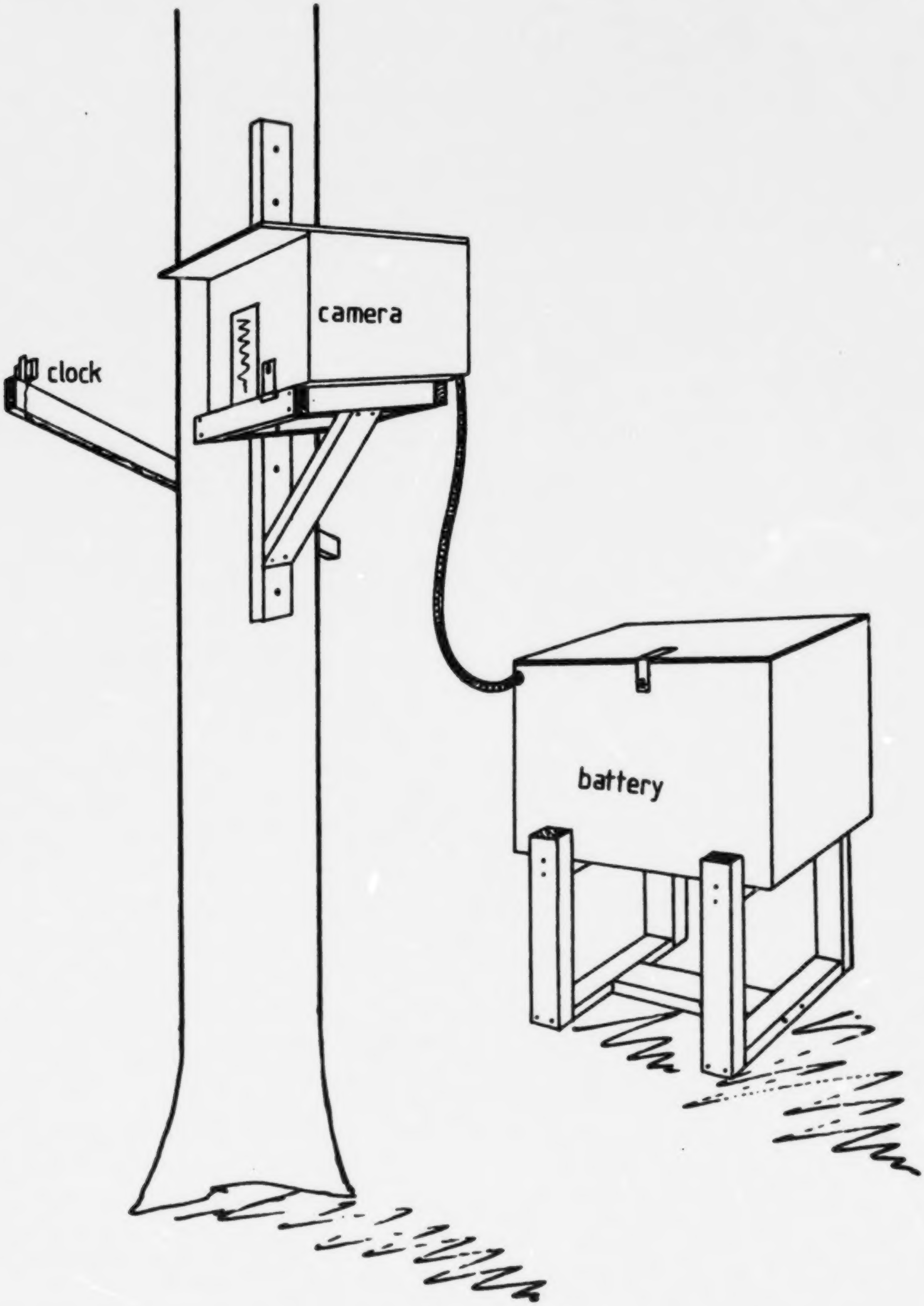
camera
clock
battery

Figure 2 Time-lapse camera system

The clocks were mounted on a boom in front of the cameras so that they would be visible in a corner of the film image. The clocks were powered with rechargeable Nickel- Cadmium batteries.

Several points must be kept in mind when setting up the camera systems. The camera must be mounted on a tree or other object which is large enough not to be greatly disturbed in the wind. The shelters must be located in such a way as to avoid burial by snow and disturbance by avalanche wind blast. If possible the camera should be placed to avoid wet snow adhering to the window.

Results

The time-lapse photographic system operated in the field over a period of five and one-half months and provided some excellent data. The 8-minute exposure interval did not permit the filming of actual avalanche release sequences. Rather, evidence of avalanche release was found in before and after photographs which showed the presence of avalanche debris and other tonal changes in the path. This evidence was most visible when the avalanche paths were in direct sunlight, while the "flat" light of shadow and cloudy days made photo interpretation very difficult. The recording of exact release time for snowfall-triggered avalanches was difficult because of low visibility during storm conditions and the obscuring of debris by subsequent snowfall. Thaw-triggered wet snow avalanches were relatively easy to interpret because of the good visibility and sunlight associated with thaws and the coarse-textured nature of wet snow avalanche debris. A

---

distinction between loose snow and slab avalanches at the Inflexible site was difficult to make because of the distance from the camera to the path (750m). Information on the type of failure was provided by supplementary field investigation. At Highwood Pass proximity of the camera to the path (500m) permitted determination of failure mode in many cases. Also the time-lapse record provided information on snowfall duration and intensity, the latter through rates of snow build up on the clock and nearby trees in calm conditions. In addition, wind direction could be observed by cloud movement and movement of trees. Melt periods could be identified through melting snow on nearby objects.

Given the noted limitations of the time-lapse photographic monitoring system, it is felt that it provides a conservative estimate of avalanche frequency. In 1982-83, 29 avalanches were recorded at the Mt. Inflexible site and 21 were recorded at the Highwood Pass site. All the recorded events at Mt. Inflexible were size 2 (Canadian Avalanche Committee, 1981) or larger while 18 at Highwood Pass were size 2 or larger. Of course, many smaller avalanches may have been missed due to the resolution of the photographic record. The photographic record, supplemented with field observations, biweekly snowpack structure observations, and meteorological data was used as the basis for the data summary displayed in Table 1.

Recognizing that many small, loose snow direct action avalanches may have been missed by the monitoring system, the data indicate that wet snow and soft slab avalanches predominated at

Table 1 Summary of avalanche activity at Fortress Mountain ("Mount Inflexible #3" path) and Highwood Pass area, winter 1982-83.

DATE	PATH	SIZE*	MOISTURE CONTENT	TYPE	POSITION OF SLIDING (BED) SURFACE	LOCATION ON PATH (START TO FINISH)	WEATHER -W.E.=WATER EQUIVALENT	COMMENTS
16/12/82	Mount Inflexible #3	2	dry	slab	surface layers	upper track	heavy wind loading, temp. max. 0°C	
9-10/1/83	Highwood Pass	2-3	dry	slab	surface layers	starting zone → midtrack	67 mm W.E. snow, west wind	- several releases, crowns visible
9-10/1/83	Highwood Pass #5	3	dry	slab	surface layers	reached runout	67 mm W.E. snow	- deposited onto highway
10/1/83	Mount Inflexible #3	2-3	dry	loose	surface layers	starting zone → midtrack	22 mm W.E. snow	- several releases
23-24/1/83	Highwood Pass	3	dry	slab	surface layers	starting zone → runout	23 mm W.E. snow, west wind	
24/1/83	Highwood Pass	2	dry	slab	surface layers	starting zone → midtrack	23 mm W.E. snow, west wind	
27/1/83	Mount Inflexible #3	2	dry?	slab	surface layers	starting zone → upper track	6 mm W.E. snow and wind loading, temp. max. +2 °C	- 3 releases

* Classification of the Canadian Avalanche Committee (1981).

Continued ...

DATE	PATH	SIZE*	MOISTURE CONTENT	TYPE	POSITION OF SLIDING (BED) SURFACE	LOCATION ON PATH (START TO FINISH)	WEATHER -W.E.=WATER EQUIVALENT	COMMENTS
13/2/83	Mount Inflexible #3	3/4	moist	?	surface layers	upper track → mid/lower track	temp. max. +0.5°C, higher previously	- more than one release
28/2-1/3/83	Mount Inflexible #3	2	dry	slab?	surface layers	starting zone → upper track	27 mm W.E.snow, west wind	- new snow slid on melt-freeze crust
9/3/83	Mount Inflexible #3	3	wet	loose	surface layers	upper track → mid/lower track	temp. max. +8.5°C	
9/3/83	Highwood Pass	2	wet	loose	surface layers	starting zone → midtrack	temp. max. 0°C	- path heavily loaded from 45.5 mm W.E. snow on 1-2 March
20-21/3/83	Mount Inflexible #3	1-2	moist	?	surface layers	upper/midtrack	18 mm W.E. snow, temp. max. 0°C	- slid on 2 cm graupel
22/3/83	Mount Inflexible #3	2	moist	loose	surface layers	midtrack	temp. max. - 0.5°C	- slid on 2 cm graupel
24/3/83	Mount Inflexible #3	2-3	wet	slab?	surface layers	midtrack → lower track	6 mm W.E. snow, temp. max. 0°C	
between 16 and 25/3/83	Highwood Pass	1	dry	loose	surface layers	starting zone → upper track	up to 32.5 mm W.E. snow, west wind	- numerous releases. Cornices indicate winds during storm

Continued ...

DATE	PATH	SIZE*	MOISTURE CONTENT	TYPE	POSITION OF SLIDING (BED) SURFACE	LOCATION ON PATH (START TO FINISH)	WEATHER -W.E.=WATER EQUIVALENT	COMMENTS
28/3/83	Highwood Pass	2	dry	loose	surface layers	starting zone → midtrack	32.5 mm W.E. snow 16-25 March, west wind	- though study site temperatures reached only -7°C, the path was in direct sunlight. Cornices indicate winds during storm
3-4/4/83	Highwood Pass - all paths with NE aspect.	2-3	dry	slab	surface layers	starting zone → runout	45.5 mm W.E. snow	- several releases. Cornices indicate winds during storm.
5/4/83	Highwood Pass	1	moist	loose	surface layers	upper track	45.5 mm W.E. snow on 3-4 April	- though study site temperatures reached only -4°C, the path was in direct sunlight
6/4/83	Highwood Pass #5	3/4	wet	slab	surface layers	starting zone → lower track	45.5 mm W.E. snow and heating	- stopped 100 m above highway
6/4/83	Highwood Pass	1-2	wet	loose	surface layers	upper track	45.5 mm W.E. snow, temp. max. +4.5°C	- two releases. Numerous others on slopes with S-SW aspect in Highwood area.
6/4/83	Mount Inflexible #3	3	wet	?	surface layers	upper track → midtrack	23 mm W.E. snow on 2-3 April, temp. max. +13.5 on 6 April	

Continued ...

DATE	PATH	SIZE*	MOISTURE CONTENT	TYPE	POSITION OF SLIDING (BED) SURFACE	LOCATION ON PATH (START TO FINISH)	WEATHER -W.E.=WATER EQUIVALENT	COMMENTS
17/4/83	Highwood Pass	2	wet	?	surface layers	starting zone → upper/midtrack	19 mm W.E. snow on 8-9 April, temp. max. +3.5°C on 17 April	
18/4/83	Mount Inflexible #3	2	wet	?	surface layers	upper track → mid/lower track	temp. max. +13.5°C	- numerous wet releases on slopes of NE aspect in Kananaskis valley near Fortress
18/4/83	Mount Inflexible #3	3	wet	?	surface layers	upper track → lower track	temp. max. +13.5°C	
19/4/83	Mount Inflexible #3	2/3	wet	?	surface layers	upper track → midtrack	temp. max. +14°C	
20/4/83	Mount Inflexible #3	3	wet	?	surface layers	upper track → lower track	temp. max. +16.5°C	
20/4/83	Mount Inflexible #3	2	wet	?	surface layers	upper track → midtrack	temp. max. +16.5°C	
21/4/83	Mount Inflexible #3	2	wet	?	surface layers	starting zone → midtrack	temp. max. +15.5°C	

Continued ...

DATE	PATH	SIZE*	MOISTURE CONTENT	TYPE	POSITION OF SLIDING (BED) SURFACE	LOCATION ON PATH (START TO FINISH)	WEATHER -W.E.=WATER EQUIVALENT	COMMENTS
21/4/83	Path southeast of Mount Inflexible #3	2/3	wet	?	surface layers		temp. max. +15.5°C	
21/4/83	Mount Inflexible #3	3/4	wet	?	surface layers	upper track → lower track	temp. max. +15.5°C	
21/4/83	Mount Inflexible #3	4	wet	?	surface layers	upper track → lower track/runout	temp. max. +15.5°C	
21/4/83	Mount Inflexible #3	3	wet	?	surface layers	upper track → midtrack	temp. max. +15.5°C	
21/4/83	Path northwest of Mount Inflexible #3	3	wet	?	surface layers	reached mid/lower track	temp. max. +15.5°C	
21/4/83	Mount Inflexible #3	3/4	wet	?	surface layers	upper track → mid/lower track	temp. max. +15.5°C	
24-25/4/83	Mount Inflexible #3	3-4	moist	slab	surface layers	reached lower track/runout	50 mm W.E. snow	- several releases, crown fracture on NW side of path
24-25/4/83	Path northwest of Mount Inflexible #3	3	moist	slab?	surface layers	reached lower track	50 mm W.E. snow	

Continued ...

DATE	PATH	SIZE*	MOISTURE CONTENT	TYPE	POSITION OF SLIDING (BED) SURFACE	LOCATION ON PATH (START TO FINISH)	WEATHER -W.E.=WATER EQUIVALENT	COMMENTS
24-25/4/83	Highwood Pass	2-3	dry	slab	surface layers	starting zone → midtrack/runout	40 mm W.E. snow, wind	- 3/4 releases
25/4/83	Highwood Pass #2	4	moist	slab	surface layers	reached runout	40 mm W.E. snow, wind?	- crossed and blocked highway
25/4/83	All slopes in Highwood Pass area	2-4	moist	slab	surface layers/ full depth		40 mm W.E. snow, wind	- crown fractures one metre high on east/ northeast slopes
between 29/4 and 3/5/83	Mount Inflexible #3	2-3	wet	?	full depth	upper track → lower track/runout		- temperatures well above freezing
between 29/4 and 3/5/83	Mount Inflexible #3	3	wet	?	full depth	upper track → mid/lower track		- temperatures well above freezing
4/5/83	Mount Inflexible #3	2	wet	?	surface layers	upper track → mid/lower track	temp. max. +8.5°C	
4/5/83	Mount Inflexible #3	3	wet	?	surface layers	upper track → mid/lower track	temp. max. +8.5°C	
5/5/83	Mount Inflexible #3	2	wet	?	surface layers	upper track → mid/lower track	temp. max. +8.5°C	
6/5/83	Highwood Pass	2	wet	?	surface layers	starting zone → midtrack		- temperatures unknown, but maximum above 0°C

Continued ...

DATE	PATH	SIZE*	MOISTURE CONTENT	TYPE	POSITION OF SLIDING (BED) SURFACE	LOCATION ON PATH (START TO FINISH)	WEATHER -W.E.=WATER EQUIVALENT	COMMENTS
8/5/83	Mount Inflexible #3	3	wet	?	full depth	upper track → mid/lower track	temp. max. +7.5°C	
11/5/83	Mount Inflexible #3	2	wet	?	full depth	upper track → mid/lower track	temp. max. +12.5°C	
15/5/83	Highwood Pass	1-2	wet	loose	surface layers	starting zone → upper/midtrack		- approximately 12 releases; temperatures unknown but above 0°C
17/5/83	Highwood Pass	1	wet	loose	surface layers	midtrack	heavy snow, temp. max. +5.0°C	
21/5/83	Highwood Pass	1/2	wet	loose	surface layers	starting zone → upper/midtrack		- temperatures unknown but above 0°C
23/5/83	Highwood Pass	2	wet	loose	surface layers	starting zone → upper/midtrack		- two releases; temperatures unknown but above 0°C
28/5/83	Highwood Pass	~2	wet	loose	full depth	starting zone → upper/midtrack		- temperatures unknown but above 0°C - mixed snow-debris release, travelled across bare ground

the two sites. Recorded events were most often associated with snowfalls and/or rises in air temperature to or above the freezing point (Figure 3). Wind occurring in conjunction with snowfall at the two sites appears to have been significant because of their lee slope situations. Wind redistribution of snow onto these slopes increased accumulations and soft slab development at temperatures just below freezing. Fracture lines of released slabs were often visible during field visits. Snowfalls, which in this area are generally of a low magnitude, in the absence of wind produced a few small loose snow avalanches.

The snowpack structure at both study sites in 1982-83 was characteristic of a cool, subhumid continental climate. The structure included early winter depth hoar at the base of the snowpack due to cold temperatures and low snowfall. Late winter and spring thaws, sometimes in association with heavy snowfalls, produced complex upper snowpack stratigraphies of melt-freeze snow and crusts with numerous weak interfaces. Field observations indicated that most of the recorded avalanches were initiated at such interfaces rather than within weak strata in the snowpack.

Conclusions

After testing in 1981-82, two time-lapse photographic systems provided continuous monitoring of two avalanche paths throughout the winter of 1982-83. The photographic record provided information on avalanche occurrence, type, size, distance of travel, and

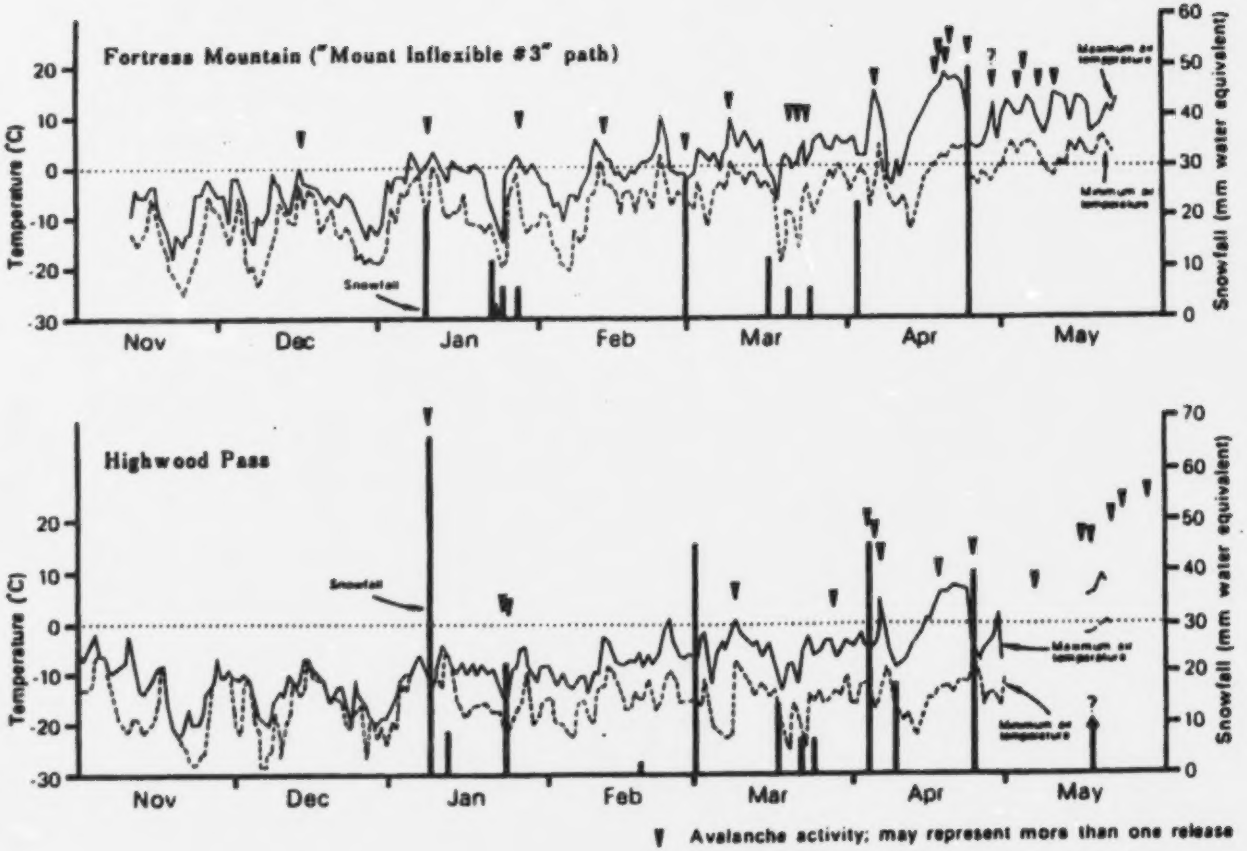

Figure 3 Snowfall, maximum/minimum air temperatures and avalanche activity, 1982-83

weather conditions. Of course, the monitoring system had some limitations such as the obscuring of images during storms and inadequate resolution to pick up minor avalanches while imaging the whole avalanche path. Resolution inadequacies can be overcome by manipulating the technical aspects of the camera system just as power supply problems were overcome through technical adjustments.

Coupled with periodic snowpack observations and various continuous records of meteorological conditions, the time-lapse record provides a useful documentary of avalanche activity over a winter season. The equipment used in this study was relatively inexpensive and at current prices, a system can be purchased, adapted, and assembled for well under $1,000. (Canadian). Based on the experiment described in this paper we believe that such time-lapse photographic systems could be usefully employed in remote areas where day to day observations are not possible and previous data do not exist. The system would be particularly useful in pre-development or pre-construction situations where some baseline data are required on avalanche frequency, magnitude, and release conditions.

Acknowledgement

The research was funded by the Alberta Environment Research Trust in a grant to H.J. McPherson. Manuscript preparation was provided by the Faculty of Environmental Studies, University of Waterloo, Waterloo, Ontario.

References

Akitaya, E., 1973, Observations of avalanches with a video-tape recorder, Teion Kagaku, A, 31:287-289.

Berner, J.A. and van Everdingen, R.O., 1979, Automatic Time-Lapse Camera Systems, National Hydrology Research Institute, Paper No. 4, (Inland Waters Directorate Technical Bulletin No. 112). Environment Canada, Ottawa, 20 pp.

Canadian Avalanche Committee, 1981, Guidelines for Weather, Snowpack, and Avalanche Observations, NRC, Assoc. Comm. on Geotechnical Research. Technical Memo. No. 132, 48 pp.

Dent, J.D. and T.E. Lang, 1982, Experiments on mechanics of flowing snow, Cold Regions Science and Technology, 5(3):253-258.

deScally, F.A., 1984, Snow avalanche hazard in Kananaskis Country, Alberta: The Development of a time-lapse slope monitoring system. M.Sc. Thesis, University of Alberta, Edmonton, Alberta. 190 pp.

Drewery, S.A., 1983, The effect of forest fires on the avalanche frequency of seven sites in Kananaskis Country, Alberta, BES Thesis, Department of Geography, University of Waterloo, Waterloo, Ontario.

Gardner, J.S. 1983, Observations on erosion by wet snow avalanches , Mt. Rae area, Alberta, Canada, Arctic and Alpine Research 15(2):271-274.

Gardner, J.S., Smith, D.J. and Desloges, J.R., 1983. The Dynamic Geomorphology of the Mt. Rae Area: A High Mountain Region in southwestern Alberta. Department of Geography Publication

Series, No. 19, University of Waterloo, Waterloo, Ontario, 237 pp.

Gunderson, B., 1978, Kananaskis Avalanche Site Analysis Phase 1. Smith Dorrien Road and Secondary Road 940, Highwood Summit Section , December 1977 - February 1978. Alberta Department of Highways and Transportation, Edmonton, Alberta.

Kahn, M., 1966a, A study of snow avalanches and their environment by stereophotogrammetric and geophysical methods. *International Conference on Low Temperature Science*, Sappora, Japan, 15 pp.

Kahn, M, 1966b, Interpretation of stereophotogrammetric records of snow avalanches and some consideration on the avalanche flow, *International Conference on Low Temperature Science* Sappora, Japan, 15 pp.

Kahn, M., 1972, Studying the Slide Pattern of Avalanches by Means of Photogrammetric Methods, Cold Regions Research and Engineering Laboratory, Translation 207, Hanover, New Hampshire, 12 pp.

McPherson, H.J., Gardner, J.S., Steel, J., deScally, F., McFarlane, R. and Smith, D.J., 1983, Avalanche Hazard in Kananaskis Country, Alberta, Alberta Environment Research Trust, Internal Report, 143 pp.

McPherson, H.J., deScally, F.A. and Gardner, J.S., 1984, The rise of time-lapse photography to monitor avalanche activity and behaviour. Proceedings of International Snow Science Workshop, Aspen, Colorado.

More, G., Nieman, C., and Langford, G., 1984, Avalanche information systems in Kananaskis country, Alberta, Canada. Proceedings of International Snow Science Workshop, Aspen, Colorado.

Nieman, C., 1982, Observations on snow avalanche activity in the Kananaskis region, Alberta, _Albertan Geographer_ 18:29-42.

Nieman, C., Langford, G. and More, G., 1984, Avalanche hazard mapping integrating Landsat digital data and digital topographic data. _Proceedings 8th Canadian Symposium on Remote Sensing_, 261-271.

Prowse, T.D., National Hydrological Research Institute, personal communication.

Shoda, M., 1967. Aerial observation and their section studies on avalanches. _Physics of Snow and Ice_, Proceedings of International Conference on Low Temperature Science, Sapporo, Japan, 1 (2):1137-1150.

Steel, J., 1982, Frequency and magnitude of avalanche activity on three slopes in the Highwood Pass/Elbow Lake area, Kananaskis, Alberta, B.E.S. Thesis, Department of Geography, University of Waterloo, Waterloo, Ontario. 167 pp.

Stethem and Associates, Ltd., 1983, Avalanche Atlas - Smith-Dorrien Spray Lakes Road. Prepared for Alberta Transportation, 40 pp.

Tarquin, P., 1977, Sediment transport in snow avalanches and the related geomorphic features in the Highwood Pass /Elbow Lake area, Alberta, M.A. Thesis, University of Waterloo, Waterloo, Ontario. 147 pp.

Van Wijk, M.C., 1967 Photogrammetry applied to avalanche studies, _Journal of Glaciology_ 6(2): 917-933.

SNOW MICROSTRUCTURE MEASUREMENTS USING STEREOLOGY

by

J. Dozier and R.E. Davis

Department of Geography
University of California
Santa Barbara, California
U.S.A.

R. Perla

National Hydrology Research Institute
Canmore, Alberta
Canada

presented at

SNOW PROPERTY MEASUREMENTS WORKSHOP

Lake Louise, Alberta

1-3 April, 1985

TECHNICAL MEMORANDUM 140

Compiled By

P.R. Kry

NRCC 27594

Snow Microstructure Measurements Using Stereology

Jeff Dozier and Robert E. Davis
Department of Geography, University of California
Santa Barbara, CA 93106, U.S.A.

Ron Perla
National Hydrology Research Institute
Box 313, Canmore, Alberta TOL OMO

1. Introduction

Snow is a network of ice grains interconnected in a complex structure. Liquid water may also be present, in an intricate configuration. The characteristics of this porous medium govern the response of snow to electromagnetic and mechanical energy and control the movement of heat, liquid water, and water vapor.

Stereology is a branch of mathematics relating three-dimensional parameters defining structure to two-dimensional measurements obtainable on sections of the structure [Weibel, 1979]. A section of the structure represents a planar sample of profiles of the objects of interest. The stereologic relations described here are simple. Although they are based on geometric probability and have been derived by complex mathematical reasoning, we present only the final relations and their necessary assumptions. Complete derivations and discussion can be found in Underwood [1970] and Weibel [1979, 1980].

Some properties of a snow sample can be calculated from a single random section image. Others require three-dimensional topological information, which can only be obtained from serial sections. For some properties detection of anisotropy is crucial, and it is essential to test planes parallel and perpendicular to the macrostratigraphy as observed in the field.

One method previously used to analyze the structure of the air and ice phases is to prepare thin sections, usually less than half a grain diameter in thickness, cut from specially prepared snow samples [Keeler, 1969; Good, 1982]. Preparing a thin section generally consists of cutting a plane in the sample, attaching the sample to a glass slide, and cutting a second plane to obtain the desired thickness. Thin sections using opaque pore fillers or other treatments create a two-dimensional profile

---

Presented at Workshop on Snow Property Measurement, Chateau Lake Louise, April 1-3, 1985.

or section image from which some of the properties of the three-dimensional structure can be calculated. The advantage of thin sections is that the bonds between individual grains can be identified and measured.

If structural properties other than bonding are required, the information may be obtainable from a plane section of a snow sample. Cutting a prepared snow sample with a single plane is less time-consuming and requires less care, provides the same measurements, and allows serial sectioning if topological information is required. Structural measurements of the ice phase in snow have been made from section images using manual analysis [Kry, 1975; Gubler, 1978] and computer-aided analysis [Vallese and Kong, 1981; Good, 1982; Perla, in press].

2. Sample Collection and Preparation

Samples are usually obtained from a snow pit at the same time conventional snow properties are observed. These include several density samples per layer, a detailed stratigraphic description, temperature, liquid water content if present, and preliminary crystal description, noting disaggregated appearance and *in situ* orientation. From this information representative domains are identified for sampling. Blocks of 700 ml or more are carefully cut from the pit wall and packed in containers in an ice chest with snow from the same layers. They are then transported to a cold laboratory, usually within a few hours of sampling. There subsamples are cut from each field sample for section plane preparation and for photography in a disaggregated state (Figure 1a). We prepare orthogonal sections for samples with suspected anisotropy.

The preparation of section planes in snow closely follows the recommendations of Perla [1982] and Perla and Dozier [1984]. A sample of snow is embedded in a supercooled organic liquid that is water-insoluble. Based on the extensive testing done by Perla [1982], we use dimethylpthalate at −5°C. The pore filler is dyed dark blue (oil blue N) to enhance the contrast with the ice grains. Freezing is started with a few grains of dry ice, sprinkled around the corners of the container. The section is then frozen rapidly at (−20°C) or colder.

Once frozen, the original orientation of the sample in the snowpack is marked, and the sample is roughly cut to a block about 3×3×5 cm. The block faces are then

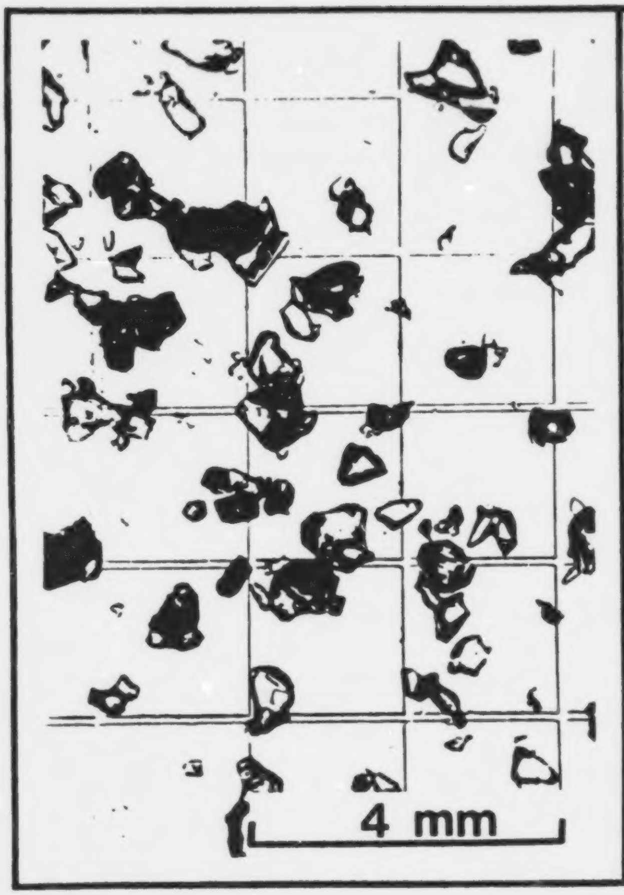

Figure 1a. Photomicrograph of disaggregated grains from a snow sample collected at middepth in a 1.5 m subalpine snowpit at Sunshine, Alberta. Sample density is 375 ± 5 kg/m³. Crystals exhibit faceted and rounded morphology.

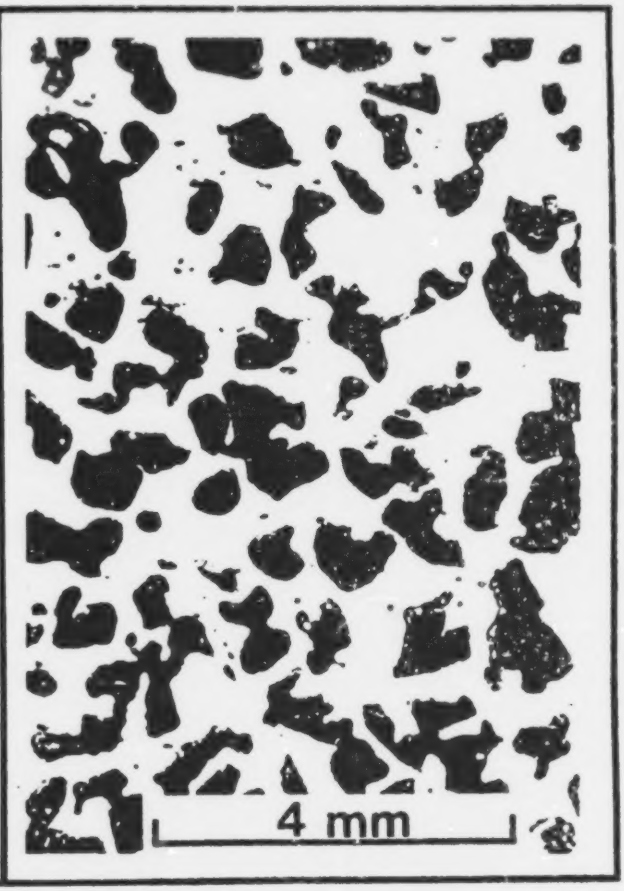

Figure 1b. Photomicrograph of a section-plane prepared from the sample described under Figure 1a. The section-plane was photographed using incident reflected light. Dark profiles represent ice. Some dark specks are probably not ice, and could be misclassified in an objective analysis. Conversely, some white specks may be misclassified as pore space.

planed with a microtome and left for about 10 min before further treatment. The ice grains have a much higher vapor pressure than the pore filler and differentially sublimate, particularly at the ice-pore boundary. The section surfaces are then polished with a find carbon fingerprint powder and high quality lens paper. With a delicate touch the ice grains are left outlined with the powder and the pore filler is smooth and shiny (Figure 1b).

Snow samples with especially fine structure may be difficult to plane and polish without plucking some ice fragments from the surface. In fine snow the ice grains can be allowed to sublimate more completely after initial planing, then planed again a few micrometers deeper. Polishing with lens papers and carbon powder will now fill the cavities left by the grains. The effects of evaporation of the pore filler can be tested by comparing the volume fractions of the object phase, ice, calculated from sections prepared by the two procedures.

3. Measurements from Sections

High contrast photographs are taken with a photomacroscope using a variety of 35 mm films (e.g. Kodak Ektachrome). A ring illuminator with fiber-optic light source provides specular reflection off the pore filler and minimizes sample heating. Generally the ice grains appear darker than the filler because they are more transparent, although occasionally bright reflections are observed from the interior of the ice grains. We get best results with illumination oriented parallel to the optical axis, although oblique illumination can also be used [W. Good, personal communication]. The images are scaled to actual lengths using photographs of a reference grid at various magnifications. Photographs are also taken of the grains in a disaggregated state.

The information contained in the section photographs is digitized and stored. At U.C. Santa Barbara we use a frame-grabber video digitizer, which is part of a Model 70F Image Computer from International Imaging Systems (I^2S). The digital image is then read to a VAX 11/780 from one of the memory channels on the image computer. Each section image is represented by 512×512 pixels with 8-bit brightness levels (0–255) and is classified as two phases: ice and pore space. At N.H.R.I. Canmore we use a Sony video photolab adapter HVT3000 and video camera

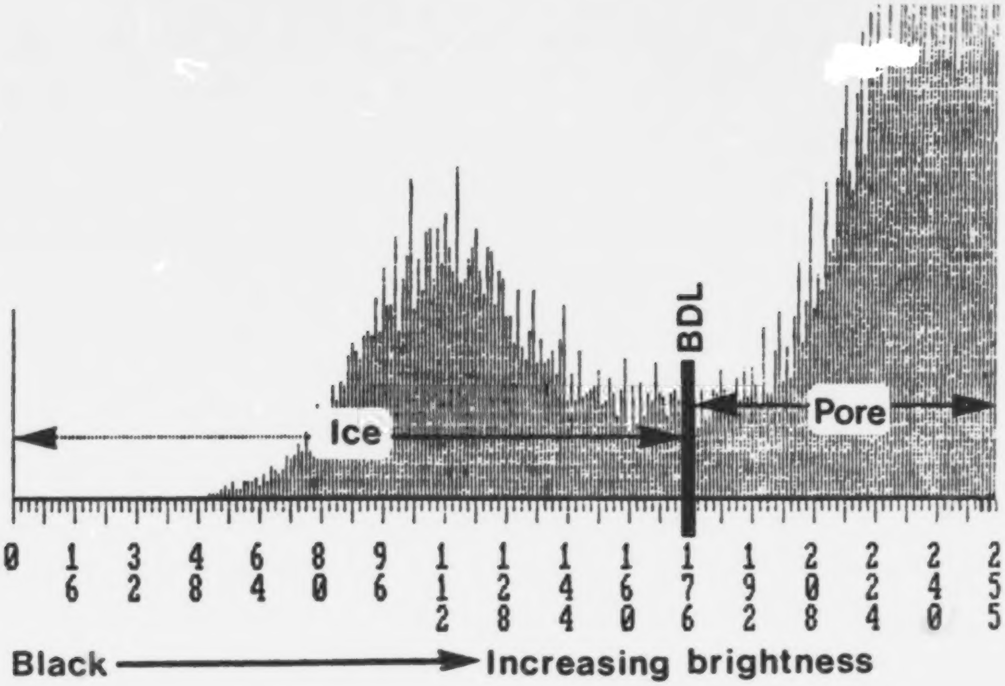

Figure 2. Brightness histogram from a video image of a section-plane photomicrograph. The relative number of pixel are shown at each brightness level from 0 to 225. Note that the histogram is truncated above about 225 because of anomalously high spikes at these higher brightness levels. A brightness discrimination level (BDL) is "guessed" to be at 176 to best separate the ice and pore profiles. This guess for BDL gave a reasonable replication of the qualitative shapes of the ice profile. However, the guess is not unique, and other BDL values in the approximate band 160 to 190 provide reasonable replication of ice shapes and measured sample density.

HVC2800. The digital image is read to an IBM PC. Each image has 240×250 pixels with 8-bit brightness levels.

Discrimination between ice and pore filler in the digitized image is not without problems. Misclassification cannot be avoided using a simple discrimination based on a guess of a brightness level that seems to best separate the histogram into ice and pore areas (Figure 2). Surface flaws, uneven illumination, and spurious reflections from the bottom of the ice crystals are confounding effects. We are currently investigating alternative methods of classifying the digital image into ice and pore filler categories, instead of just using a brightness discrimination level [Haralick and Shapiro, 1985].

Currently the digital date are processed with a sampling technique that results in five measurement parameters and their distributions, but the possibilities certainly have not been exhausted:

(1) Point density P_P, the number of pixels falling on ice particles divided by the total number of pixels.

(2) Intercept number density N_L, the number of ice-pore and pore-ice transitions divided by the number of pixels.

(3) Ice intercept lengths L_i, the distances between pore-ice and ice-pore transitions.

(4) Pore intercept lengths L_p, the distances between ice-pore and pore-ice transitions.

(5) Tangents to the ice-profile boundary T_i, designated as positive or negative depending on local curvature.

The parameter distributions (mean, variance, minimum, and maximum) per line and over all lines are calculated for each image except for the profile tangent sums. For each snow sample two section images are stored: one cut parallel to the snow stratigraphic planes and the other orthogonal to them. This allows testing the assumption that the snow grains are randomly oriented and shows the need for measuring several sections or not. If the variance in the parameters between the orthogonal sections is small, the two may be averaged.

4. Stereologic Relations

Weibel [1979] proposes two general models for deciding the measurements of most value for a particular study. The first considers structural parameters only. The object phase (ice in this study) may have any shape, can be interconnected, and can have many concavities. The second model assumes that the object phase can be adequately described as discrete particles and usually assumes that the particles are convex in shape. Structural parameters can be defined in both models, the difference lying in the difficulty with counting individual grains in the first model. The discrete particle model including a particle shape assumption is needed to measure mean diameter, length of the grains, number of grains per unit volume, and other grain parameters.

Some structure parameters calculated are: (1) volume density V_V, from which the snow density can be calculated, (2) surface density S_V, of which specific surface (surface to volume ratio) of ice phase is a subset, (3) mean curvature density K_V, or mean surface curvature, and (4) mean intercept length L_i, which is related to the mean free path through the ice phase. All these are ratio estimates of statistical parameters and therefore subject to the standard estimates of error [Weibel, 1979, p. 95, p. 137].

Volume density is equal to the point density:

$$V_V = P_P = \frac{P_i}{P_T} \tag{1}$$

P_i is the number of pixels falling on ice, and P_T is the total number of pixels. Snow density ρ_s is

$$\rho_s = \rho_i P_P \tag{2}$$

where $\rho_i = 917$ kg m^{-3} is the density of ice.

Surface density, or surface area per containing volume, is

$$S_V = 2 N_L = 2 \frac{N_i}{L_T} \tag{3}$$

where N_L is the grain boundary intercept density, N_i is the number of profile boundary intersections, and L_T is the length of the line scan. The surface area calculation may be dependent on the magnification used to make the section image, that is, the microscopic resolution. This effect has been known to cartographers for a long time in a lower dimension [Mandelbrot, 1967, 1983] and has been shown in biological studies [Keller *et al.*, 1976]. Volume density remains stable while S_V estimates usually increase with magnification. The effect may also be influenced by the technique, etching *vs.* filling, used to highlight the ice grains against the pore filler background.

Mean surface curvature is determined from the net tangent count:

$$K_V = \pi T_i = \pi \frac{T_{net}}{A_T} \tag{4}$$

T_{net} is the net (positive or negative) tangent count, and A_T is the total area of the section image. The parameter requires that the test grid be regular and equally spaced in orthogonal directions.

Mean intercept length is obtained as a primary measurement from the sections. We can distinguish between mean free path length in ice and in the pores.

5. Application Example

One potential use of plane sections is the measurement of those physical parameters of snow that are important in interpreting its electromagnetic signature. In modeling the reflectance of snow to solar radiation or the emissivity of snow for thermal radiation, to use Mie scattering theory demands the assumption that the scattering properties of the irregularly shaped grains can be appropriately mimicked by some sort of "equivalent sphere" [Wiscombe and Warren, 1980; Dozier and Warren, 1982]. Some proposed equivalences are the sphere of equal volume, equal projected area, equal surface area, or equal volume/surface ratio.

From plane sections it is possible to directly measure these parameters. Thus one could use radiative measurements to choose the spherical radius or radius distribtion that best explains the electromagnetic properties, and then compare these data to the plane section parameters, with the definition of "equivalent" chosen from the candidates listed above.

In the table below we present data from sections made from a snow pit on Mammoth Mountain, California, on February 11, 1985. The pack consisted of 80 cm of new snow, primarily one day old dendrites and needles, above 120 cm of older snow in various stages of metamorphism. Samples from 5–12 cm depth and 39–54 cm depth had the following size properties.

depth (cm)	orientation of section	bulk density ($kg\,m^{-3}$)	digital density ($kg\,m^{-3}$)	volume/surface ratio (mm)	equivalent sphere radius (mm)
5 – 12	horz	196	193	0.182	0.061
5 – 12	horz	196	174	0.176	0.059
5 – 12	vert	196	211	0.193	0.066
39 – 54	horz	170	196	0.172	0.057
39 – 54	horz	170	188	0.174	0.058
39 – 54	vert	170	163	0.169	0.056

We have not yet processed the correlative reflectance measurements, but the grain radii are consistent with snow albedo for new snow [Wiscombe and Warren, 1980].

References

Dozier, J., and S. G. Warren, 1982. Effect of viewing angle on the infrared brightness temperature of snow. *Water Resources Research*. Vol. 18, pp. 1424-1434.

Good, W., 1982. Structural investigations of snow and ice on core III from the drilling on Vernagtferner, Austria, in 1979. *Zeitschrift für Gletscherkunde und Glazialgeologie*. Vol. 18, pp. 53-64.

Gubler, H., 1978. Determination of the mean number of bonds per snow grain and of the dependence of the tensile strength of snow on stereological parameters. *Journal of Glaciology*. Vol. 29, pp. 329-341.

Haralick, R. M., and L. G. Shapiro, 1985. Image segmentation techniques. *Computer Vision, Graphics, and Image Processing*. Vol. 29, pp. 100-132.

Keeler, C. M., 1969. The growth of bonds and the increase of mechanical strength in a dry seasonal snowpack. *Journal of Glaciology*. Vol. 8, pp. 441-450.

Keller, H. J., H. P. Friedli, P. Gehr, M. Bachofen, and E. R. Weibel, 1976. The effects of resolution on estimating stereologic parameters. *Proceedings, Fourth International Congress for Stereology*. E. E. Underwood, R. de Wit, and G. A. Moore, editors, National Bureau of Standards Special Publication 431, pp. 409-414.

Kry, P. R., 1975. Quantitative stereological analysis of grain bonds in snow. *Journal of Glaciology*. Vol. 14, pp. 467-477.

Mandelbrot, B. B., 1967. How long is the coast of Britain? Statistical self-similarity and fractional dimension. *Science*. No. 155, p. 636.

Mandelbrot, B. B., 1983. *The Fractal Geometry of Nature*. W. H. Freeman, San Francisco, CA.

Perla, R., 1982. Preparation of section planes in snow specimens. *Journal of Glaciology*. Vol. 28, pp. 199-204.

Perla, R., in press. Snow in strong or weak temperature gradients. Part II: Section-plane analysis. *Cold Regions Science and Technology*.

Perla, R., and J. Dozier, 1984. Observations of snow structure. *Proceedings, International Snow Science Workshop*. Mountain Rescue, Aspen, CO, pp. 182-188.

Underwood, E. E., 1970. *Quantitative Stereology*. Addison-Wesley, Reading, MA.

Vallese, F., and J. A. Kong, 1981. Correlation function studies for snow and ice. *Journal of Applied Physics*. Vol. 52, pp. 4921-4925.

Weibel, E. R., 1979. *Stereological Methods*, Vol. 1: *Practical Methods for Biological Morphometry*. Academic Press, New York, NY.

Weibel, E. R., 1980. *Stereological Methods*, Vol. 2: *Theoretical Foundations*. Academic Press, New York, NY.

Wiscombe, W. J., and S. G. Warren, 1980. A model for the spectral albedo of snow, 1, Pure snow. *Journal of the Atmospheric Sciences*. Vol. 37, pp. 2712-2733.

DILUTION METHOD FOR MEASURING LIQUID WATER IN SNOW
FIELD TESTS IN A SUBALPINE SNOWPACK

by

R. Perla

National Hydrology Research Institute
Canmore, Alberta
Canada

R.E. Davis and J. Dozier

Department of Geography
University of California
Santa Barbara, California
U.S.A.

E.R. LaChapelle

Department of Atmospheric Sciences
University of Washington
Seattle, Washington
U.S.A.

presented at

SNOW PROPERTY MEASUREMENTS WORKSHOP

Lake Louise, Alberta

1-3 April, 1985

TECHNICAL MEMORANDUM 140

Compiled By

P.R. Kry

NRCC 27594

DILUTION METHOD FOR MEASURING LIQUID WATER IN SNOW: FIELD TESTS IN A SUBALPINE SNOWPACK

by

R. Perla[1/], R.E. Davis[2/], J. Dozier[2/], and E.R. LaChapelle[3/]

ABSTRACT

Several recent studies have revived Bader's (1948) dilution method as an alternative to freezing calorimetry for measuring the liquid water in snow. Laboratory results and field trials (reported elsewhere) were highly promising in terms of speed and accuracy.

The dilution method was used to follow the melting of a subalpine snowpack in the Canadian Rockies from 19 May to 8 June 84. Ten morning and ten afternoon measurements were performed about every third day in vertical pit walls. Additional tests were made along one horizon below the surface. Measurements were taken in sample pairs to check repeatability.

The percent water by mass remained mostly in the band 5% to 15% averaged over the entire profile. Maximums tended to be near the top of the profile. Average error in repeatability was less than 3% in the vertical tests, and less than 1% in the test on one horizon.

One operator can achieve a rate of 10 samples/hour, which is considerably faster than the technique of freezing calorimetry.

1/ National Hydrology Research Institute
Box 313 Canmore, Alberta TOL OMO, Canada

2/ Department of Geography, University of California
Santa Barbara, California 93106, U.S.A.

3/ Department of Atmospheric Sciences, University of Washington
Seattle, Washington 98105, U.S.A.

INTRODUCTION

The dilution method (Bader, 1948; Davis and Dozier, in press) is a fast and accurate measurement of liquid water in a snow sample volume $\sim 10^3$ cm^3. It is also useful for calibrating larger scale measurements of liquid water based on dielectric and/or remote sensing techniques.

A recent variation of the method is described by Perla and LaChapelle (1984), and has been further improved by Davis et al (in press). This latter study also includes an error analysis. The method is as follows: a weak ($\sim 0.01\,N$) stock solution of HCl is mixed thoroughly into a snow sample of unknown wetness, taking every possible precaution to hold the system at 0 °C. About 100 ml is withdrawn from the mixture. The conductivity of the mixture relative to the stock solution determines to a good approximation the unknown wetness in accordance with

$$\frac{W}{M} = \frac{S}{M}\left[\frac{1-(G_x/G_s)^q}{(G_x/G_s)^q-k}\right] \qquad (1)$$

where W/M is the mass of the unknown liquid water per unit sample mass, S/M is the mass of the stock solution per unit sample mass, and G_x/G_s is the ratio of specific conductance of the mixture to the specific conductance of the stock solution. The constant q models the nonlinear relationship between concentration and conductance as

$$\frac{C_x}{C_s} = \left(\frac{G_x}{G_s}\right)^q \qquad (2)$$

where C_x/C_s is the concentration ratio of mixture to stock. For HCl at the concentrations $0.005\,N$ to $0.01\,N$, and at room temperature, $q = 1.0133$, which represents only a small nonlinearity. The numerical constant k models another small correction for the ratio of background impurity concentration of the liquid water in the snow to the impurity concentration of the stock solution C_s. For subalpine snowpacks k is usually less than 0.01 if $C_s \sim 0.01\,N$.

In this paper all W/M measurements are given as percentages. For example, "W/M = 3%" means W/M is 3 g of liquid water per 100 g of total sample mass.

FIELD METHOD

The dilution method was tested at a subalpine (elev. 2300 m) snow study plot near the Sunshine Ski Area, Banff National Park, Alberta. Practice sessions on 14-18 May 84 suggested the following method:

1) Stock samples ($\sim 0.01\,N$ HCl, $S \approx 500$ g) are prepared in polyethylene bottles, and weighed in advance in the laboratory.

2) The bottles are transported to the field site, and stored in an ice bath for several hours in advance of the measurement period in order to reach 0 °C.

3) A vertical pit wall and a work area (shaded from the sun) are excavated in the snow.

4) A 2000 cm^3 wide-mouthed thermos bottle (soup thermos), which serves as the mixing container is set into the snow. A sealed polyethylene bottle filled with ice is stored temporarily inside the thermos to cool the interior of the thermos.

5) A wedge-shaped sample ($\approx 10^3$ cm^3, $M \approx 500$ g) is quickly cut from the pit wall and dumped into the thermos (after removing the cooling bottle). The geometry of the wedge-shaped sample extractor is shown in figure 1.

6) The stock solution ($S \approx 500$ g) is poured into the thermos; the mixture is chopped and stirred.

7) The thermos is quickly sealed, shaken (cocktail-bar style) for ≈30 s, and weighed in an enclosure shielded from sun and wind.

8) The thermos is set back into the snow, opened, and ≈100 ml of solution is sucked out through a pipette fitted with a filter screen on the intake, and a 50 ml syringe to apply suction.

9) This solution is transferred back to the empty stock solution bottle which is transported to the laboratory for conductivity measurements when convenient.

10) The mixing thermos is dryed with towels, and steps 4 through 9 are repeated.

An error analysis of the above and related procedures (Davis et al, in press) demonstrated that the W/M accuracy is better than 2% on the average.

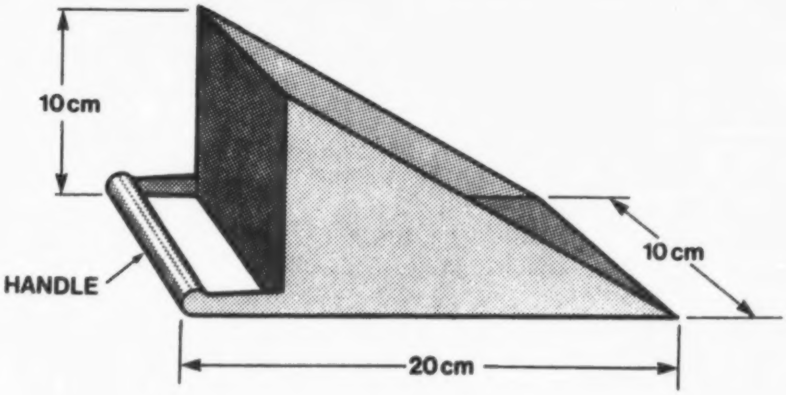

Figure 1. Wedge shaped snow sample extractor (1000 cm^3).

The preceding method was used to follow the melting of the snowpack during the period 19 May 84 to 8 June 84. Measurements were taken on 9 days, with two runs per day (18 runs in all). The first run started at about 1000 h; the second, a few hours later. Each run consisted of 5 pairs, or 10 samples total as illustrated in Figure 2. An attempt was made to collect the left and right members of the pair from the same horizon (Z).

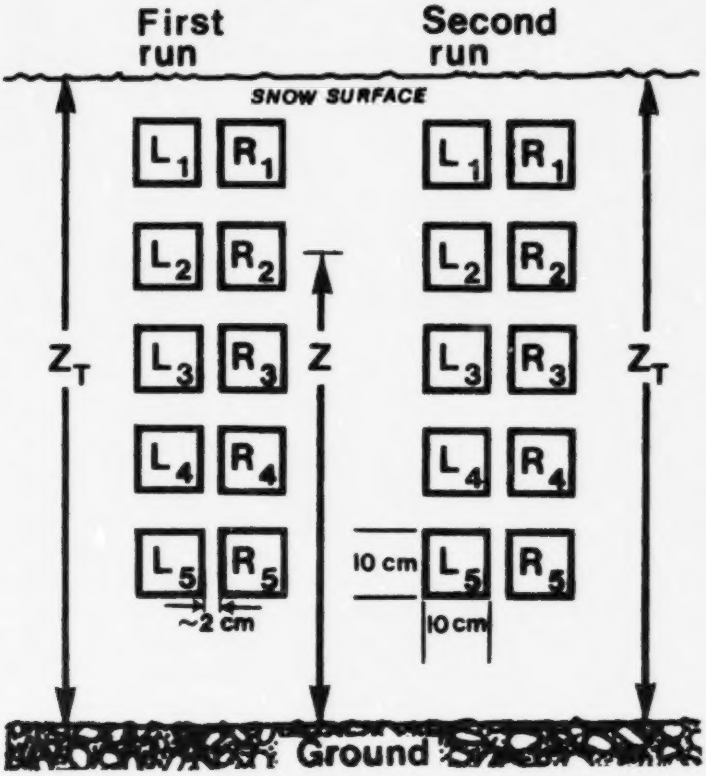

Figure 2. Test geometry used from 19 May to 8 June 84 to measure snow wetness by pairs in a vertical pit wall.

RESULTS: VERTICAL PIT WALL

Table 1 summarizes the 18 runs made in accordance with Figure 2. The mean water W/M is averaged over all 10 samples (5 pairs) in the run. The horizon of the maximum and minimum W/M is expressed as the dimensionless ratio Z/Z_T , thus $Z/Z_T = 0$ refers to the ground, and $Z/Z_T = 1$ refers to the snow surface. The sample rate (minutes) is the total sample time divided by 10. Difference of adjacent samples Δ_A is the average

$$\Delta_A = \frac{1}{5}\sum_{i=1}^{5} |R_i - L_i| \qquad (3)$$

where R_i and L_i are the W/M values (expressed as a percentage) for the respective right and left members of the pair as illustrated in Figure 2. Note that Δ_A is also expressed in %, and that "$\Delta_A = 2\%$" means "Δ_A is 2g per 100 sample grams".

Table 1. Summary of snow wetness profiles measured in vertical pit walls at Sunshine, Alberta, 19 May to 8 June 1984.

				Maximum		Minimum			
Hour	Date (Year = 1984)	Z_T (cm)	$\overline{W/M}$ (%)	W/M (%)	Z/Z_T —	W/M (%)	Z/Z_T —	Rate (min)	Δ_A (%)
1000	19 May	123	7.4	11.9	.93	1.9	.15	7.0	2.0
1230	19 May	124	7.9	13.9	.93	4.9	.58	7.6	0.9
1030	21 May	125	7.9	14.3	.92	3.6	.05	7.5	2.8
1300	21 May	129	7.5	11.3	.90	5.9	.52	7.6	1.0
1000	23 May	130	11.5	15.1	.85	8.3	.50	6.4	3.0
1230	23 May	140	8.3	13.7	.82	4.0	.14	6.5	0.9
1330	25 May	130	6.0	9.1	.70	2.0	.12	4.8	1.8
1530	25 May	123	8.8	13.8	.85	3.0	.12	3.6	1.8
1200	27 May	120	8.0	12.6	.72	4.4	.58	4.3	1.2
1530	27 May	125	9.4	16.2	.92	2.5	.16	4.2	1.1
1000	1 June	115	6.4	9.9	.83	3.0	.22	7.5	0.6
1300	1 June	114	9.0	12.1	.85	6.6	.40	5.4	0.8
1000	3 June	100	6.1	7.7	.67	0.8	.80	6.2	1.2
1330	3 June	101	9.2	10.9	.68	7.3	.85	5.6	0.7
930	6 June	87	8.3	12.9	.84	4.1	.11	6.0	0.7
1430	6 June	85	13.9	17.4	.88	11.9	.56	4.6	1.3
1000	8 June	80	10.4	13.3	.88	7.0	.53	5.0	1.4
1400	8 June	79	11.9	14.3	.86	8.8	.47	5.3	0.9

Z_T = Total thickness of pack

$\overline{W/M}$ = Average liquid water in pack (average of 10 samples)

Z/Z_T = Relative horizon (0=ground, 1=snow surface)

Rate = Average time to measure one sample

Δ_A = Difference of adjacent samples (average of 5 pairs)

As a rough summary of the response of the Sunshine snow study plot during the sample hours (1000 h to 1600 h) and during the sample period late May to early June, we found that $\overline{W/M}$ varied between 5% and 15%, and that the overall $\overline{W/M}$ was roughly 10%. Maximum W/M tended to occur near top layers of the pack ($Z/Z_T \rightarrow 1$). The exception on 3 June was due to a thick surface crust that formed during the clear, cold evening that preceded those runs. More important exceptions (not part of this study) were observed beginning on about 8 June when water started to pool over frozen ground and saturated the lower layers. Until this time, the position of minimum Z/Z_T tended to vary from about 0.5 to 0.1 (with the exception of the 3 June anomaly).

The sample rate was strongly determined by test conditions, with the fastest rates achieved during clear, windless conditions, and the slowest rates during snow or rain storm periods when considerable time was required to shield the equipment from the elements. However, it is reasonable to assume that one operator can achieve a rate of $\approx$10 samples per hour.

Δ_A varied up to 3%. Some of this variation was due to real differences in wetness since the samples were not "identical", and alignment in the Z-direction was only approximate. Hence, the real error in "repeatability" of the method can be assumed less than 3% (less than 3 g/100 sample g), on the average. This is confirmed by the horizontal test run, described next.

HORIZONTAL RUN

On 14 June 84, 20 measurements were made on the same horizon just above an ice crust in accordance with the geometry illustrated in Figure 3. The purpose of this test run was to check Δ_A along a well defined horizon. Here, Δ_A is computed using

$$\Delta_A = \frac{1}{19}\sum_{1}^{19} |R-L| \tag{4}$$

where the 19 pairs are {1, 2} , {2, 3} , {3, 4} ··· {18, 19} , {19, 20}. The result of this computation was Δ_A = 0.7%; the range of individual pairs was 0% to 2.4%, which was considerably better than the results obtained in the vertical pits.

It is possible to check "repeatability" by computing a second statistic Δ_B as

$$\Delta_B = \frac{1}{20}\sum_{i=1}^{20} \left| (W/M)_i - (\overline{W/M}) \right| \tag{5}$$

where $(W/M)_i$ are each of the 20 measurements and $\overline{W/M}$ is their average, in this case 11.6%. It turned out that Δ_B is almost identical to Δ_A at 0.7%. Hence, we conclude that errors in "repeatability" are no higher than 1%, on the average, in this horizontal run.

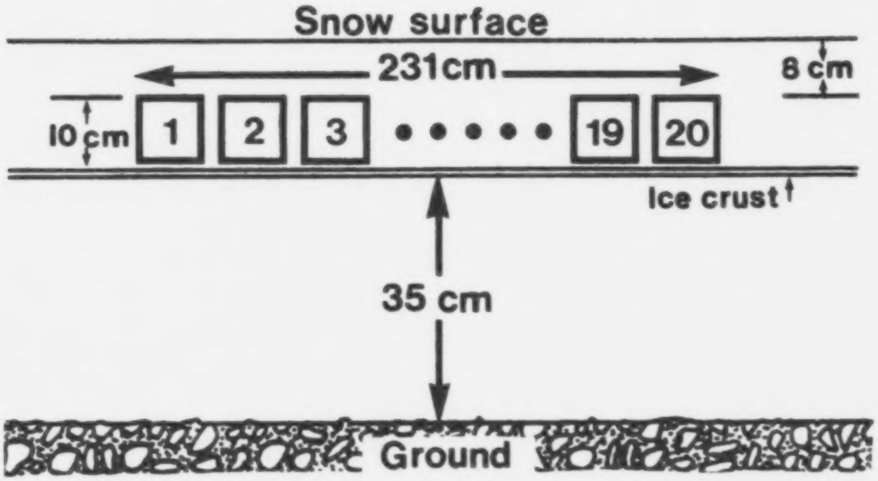

Figure 3. Test geometry used on 14 June 84 to measure snow wetness along one horizon above an ice crust.

DISCUSSION: COMPARISON WITH FREEZING CALORIMETRY

The dilution method is considerably faster than freezing calorimetry. According to Jones et al (1983), three operators using two freezing calorimeters can measure four samples per hour. Using the dilution method in the field, one operator can measure 10 samples per hour. The accuracy of the methods are comparable (2% or 2 g per 100 sample g, using either method).

Average error of repeatability using the dilution method was better than 3% in the vertical tests, and better than 1% in the horizontal test. To our knowledge, there are no data available on repeatability of freezing calorimetry under realistic field conditions.

Our experiences to date indicate that the dilution method is the preferred calibration tool for larger scale measurements of snow wetness.

REFERENCES

Bader, H., 1948. Theory of non-calorimetric methods for the determination of the liquid water content of wet snow. *Schweizerische Mineralogische und Petrographische Mitteilungen*, Bd. 28, Ht. 2, pp. 355-361.

Davis, R.E. and J. Dozier, 1984. Snow wetness measurement by fluorescent dye dilution. *Journal of Glaciology*. Vol. 30, No. 106, pp. 362-363.

Davis, R.E., J. Dozier, E.R. LaChapelle, and R. Perla, 1985. Field and lab measurements of snow liquid water by dilution. *Water Resources Research*. Vol. 21, No. 9, pp. 1415-1420.

Jones, E.B., A. Rango, and S.M. Howell, 1983. Snowpack liquid water determinations using freezing calorimetry. *Nordic Hydrology*, pp. 113-126.

Perla, R. and E.R. LaChapelle, 1984. Dilution method for measuring liquid water in snow. *Proc. Western Snow Conference*, Sun Valley, Idaho, April 17-19, 1984, pp. 80-85.

ABNORMALLY ENRICHED ELEMENTAL CONCENTRATIONS IN URBAN SNOW

by

J.J. Drake and S. Vermette

Department of Geography
McMaster University
Hamilton, Ontario
Canada

S. Landsberger and A. Simsons
Nuclear Reactor
McMaster University
Hamilton, Ontario
Canada

presented at

SNOW PROPERTY MEASUREMENTS WORKSHOP

Lake Louise, Alberta

1-3 April, 1985

TECHNICAL MEMORANDUM 140

Compiled By

P.R. Kry

NRCC 27594

ABSTRACT

Using two multi-elemental techniques (instrumental neutron activation analysis and inductively coupled plasma-atomic emission spectroscopy) we have been able to characterize upwards to eighteen trace elements in the soluble fraction of urban snow. Quality control was achieved by using an NBS certified water standard. Enrichment factor calculations have shown that many trace elements show abnormally high values which can be attributed to short and long-range transportation of either polluted or naturally occurring aerosol composition. In particular we have shown that elemental analysis of urban snow can act as a very good environmental monitor.

INTRODUCTION

Investigation of trace elemental contaminants in snow has not received a great deal of attention for the obvious reason that snowfall does not occur often enough in many places to warrant useful environmental studies. However, investigations of snow composition can be just as informative as that from rainfall. In the last decade several groups throughout the world (1-5) including several in Canada (6-8) have studied the elemental composition of snow. Many other scientists have studied polar snows in great detail (9-11). In general little has been done in studying trace elemental pollutants in urban snowfall (6).

We would like to report on the analytical results as well as environmental intrepretations of snow collected in an industrialized city (Hamilton, Ontario). In particular, we clearly demonstrate how instrumental neutron activation analysis (INAA) and inductively coupled plasma-atomic emession spectroscopy (ICP-AES) have proved to be very complimentary multi-elemental methods in such an environmental program. Both methods have unique advantages.

The preliminary results of this urban snow study is part of a greater on-going investigation of trace elemental pollutants in precipitation (both rain and snow) in a city wide network.

A. Snow Collection And Preparation For Analysis

The frozen state of snow allowed us to use a simple and flexible method where snow could be collected insitu. After a significant snowfall samples were collected from six predetermined sites. These sites were chosen because of their proximity to summer rain collection sites (representing a cross-section of the study area), distance from immediate sources of pollution and in areas with minimum vertical snow movement. Using a plastic scoop, sheathed in a clear polyethylene bag, the first few centimeters of snow were removed and placed into a 29 cm × 34 cm clear polyethylene bag. Extreme caution was used to collect snow as to avoid contamination. Cross-contamination between sites was minimized by replacing, after collection, the clear polyethylene bag in which the plastic scoop was wrapped.

The samples were kept frozen prior to filtering. The filter housing, consisting of a Millipore Swinex water filtration apparatus and Erlenmeyer flasks were washed with soap and distilled water, rinsed thoroughly with distilled water, left soaking in an acid bath of 5% HNO_3, rinsed with deionized-distilled water and dried in an oven. The snow to be filtered was removed from the centre of the collected snow sample and thus was not contaminated by the sides of the polyethylene bag and subsequently packed into the filter housing by a plastic scoop. The snow was allowed to melt passively through a pre-cleaned 0.4 µm. Nuclepore filter paper into an Erlenmeyer flask. The liquid sample was then acidified with one mL of ultrapure nitric acid (Ultrex) and stored prior to irradiation. Approximately 100 mL was collected.

B. INAA

An aliquot of about 5 mL of filtered snow was placed in an acid washed vial, closed, placed in a "rabbit carrier" and then thermally neutron activated at the Neutron Activation Facility at the McMaster Nuclear Reactor. Once the "rabbit" returned the liquid sample was transferred to a pre-weighed acid washed vials and presented to a hyperpure germanium detector for counting. The resolution of the counting system, including a 21% efficient APTEC detector coupled to Canberra 2020 amplifier and thence a Series 90 Canberra analyzer, was 2.2 KeV full width half-maximum at the 1332 KeV cobalt peak.

Typically a 5 minute irradiation at a flux of $\sim 5 \times 10^{12}$ $n \cdot cm^{2} \cdot sec^{-1}$, a 2 minute delay time and a 5 minute counting time was sufficient to get good precision. Upwards to ten elements including (Al, Br, Ca, Cl, Cu, I, Mg, Mn, Na, and V) were readily determined. After the counting period was over the vial was weighed again to determine the exact weight transferred. Synthetic standards were used to calibrate the procedure while quality control was ensured by analysing a NBS certified water reference standard.

Determination of the concentrations was done by using an in-house versatile program employing strict statistical parameters.

C. ICP-AES

The remainder of the snow samples were then analyzed using an ARL 34000 at ICP-AES system at the Institute of Environmental Sciences at the

Table 2: Results for NBS 1643b Certified Water Standard

Element	INAA[1] (ppb)	ICP-AES[1] (ppb)	NBS Value[2] (ppb)
Al	18±3	—	—
B	—	93±1	(94)
Ba	—	43±1	—
Br	13±2	—	—
Ca	35.2±1.4 (ppm)	37±1 (ppm)	(35) ppm
Cl	4.8±0.3 (ppm)	—	—
Cr	—	—	—
Co	—	28±1	26±1
Cu	19±3	24±3	21.9±0.4
Fe	—	104±1	99±8
I	1.7±0.1	—	—
Mg	9.3±0.5 (ppm)	9.9±0.2 (ppm)	(15) ppm
Mn	30±2	30±1	28±2
Na	8.0±0.4 (ppm)	—	(8) ppm
Ni	—	49±4	49±3
S	—	390±14	—
V	44±3	47±1	45.2±0.4
Zn	—	64±1	66±2

1. All results represent on average value of 5 replicates and standard deviation.
2. All NBS values certified except those in parenthesis. Several other elements have no provided values.

University of Toronto. A complete description of the system including typical detection limits have been previously published (12). Concentrations for eight elements including B, Ba, Cr, Co, Fe, Ni, S and Zn were determined.

RESULTS AND INTERPRETATIONS

The concentration values for eighteen elements from six different sampling sites are presented in Table 1. Mean concentrations, typical detection limits, precision of the methods used and enrichment factors are also shown. As can be seen several of the elements, notably aluminum,

Table 1: Range of Concentrations, Mean Values and Average Enrichment Factors in the Snow Soluble Portion.

Element	Range of Concentrations (ppb)	Mean (ppb)	Detection Limit (ppb)	Precision (%)	Average E.F. Value
Al	20-95	48	2 (INAA)	5	=1
B	15-44	20	14 (ICP)	1	6990
Ba	4-6	5	1 (ICP)	2	17
Br	4-26	12	2 (INAA)	10	9660
Ca	511-4676	1374	85 (INAA)	8	86
Cl	837-2407	1360	20 (INAA)	3	10,750
Cr	6-8	7	7 (ICP)	10	210
Co	<10	<10	10 (ICP)	5	<970
Cu	<5-46	19	6 (INAA)	20	1380
Fe	18-36	30	4 (ICP)	1	2
I	2-6	4	0.7 (INAA)	5	19,100
Mg	<140-424	196	140 (INAA)	15	28
Mn	6-29	15	1 (INAA)	5	56
Na	309-2306	1022	15 (INAA)	3	100
Ni	8-13	11	5 (ICP)	8	542
S	683-1042	723	40 (ICP)	4	5530
V	0.6-1.4	0.8	0.1 (INAA)	4	20
Zn	12-51	25	12 (ICP)	2	770

calcium, chlorine, magnesium and sodium have a relatively wide range of reported concentrations. Most of the other elements exhibited much less of a variation.

To help distinguish naturally-occurring elements in precipitation or aerosols from those arising from various types of pollution elemental enrichment factors (EF) can be employed. An element's enrichment factor is defined as follows:

$$EF = \frac{(X/C)\ \text{atmosphere}}{(X/C)\ \text{earth's crust}}$$

where X and C are the concentrations of the elements of interest and reference element, respectively. An EF value greater than unity would suggest that the element arises predominantly from one or more anthropogenic or natural sources. Average EF values are shown in Table 1. Concentrations for the earth's crust are taken from Taylor (13) while aluminum was used as the reference element.

One of the most revealing results is the very high enrichment factors of boron, bromine, chlorine, iodine and sulphur. Also very significant are the EF values for nickel, copper and zinc. Only iron has a value close to unity, while barium, calcium, magnesium, manganese, sodium and vanadium have values moderately enriched. All these values are comparable to those found in another major snow study done in Montreal (6).

Of particular importance is the result for sulphur. Sulphur's contribution to acid precipitation is now very well documented. Boron has been suggested to be a strong indication of fossil fuel burning (14).

Ratios of certain elemental concentrations can also aid in "fingerprinting" either anthropogenic or natural-occurring source emissions. Ratios for Cl/Na gave an average of 1.4 which is close to those found in marine environments of between 1.8-2.2. The Br/Cl ratios gave average values of 8.8×10^{-3} which is about of factor 2.6 times greater than found in sea-water of 3.42×10^{-3}. This can be attributed to the release of bromine from leaded gasolines. The halogen ratio of I/Cl had a value of 2.9×10^{-3} which is about 1,100 times higher than that found in sea-water of 2.63×10^{-6}. This result agrees well with the I/Cl ratio calculated in rainfall in Hawaii (14). The high enrichment of the halogens on the atmosphere is a very complex phenomenum which is covered in a detailed review article by Ciercone (16).

It is interesting to point out that INAA is unique in that Br, Cl, I can all be quantatively determined. Other ratios including Mn/S, Mn/V and Cu/Zn are presently being investigated in a wider range of snow samples.

CONCLUSIONS

Upwards to eighteen elements have been determined with good precision and accuracy in urban snow. We have demonstrated in this pilot project that both instrumental neutron activation analysis and inductively coupled plasma-atomic emission spectroscopy offer a unique combination of determining many environmentally important elements in a totally non-destructive fashion. The one disadvantage is that both INAA and ICP-AES do not the capability of determining either lead or cadium at the levels found in precipitation. Either a freezing technique employing ICP-AES or a graphite furnace atomic absorption spectrophotometry can be used to determine these two elements.

REFERENCES

1. Struempler, A.W. (1976). Atmos. Environ. 10, 33-37.

2. Zajac, P.K. and Grodzinska, K. (1982). Water, Air and Soil Pollut. 17, 269-280.

3. Thornton, J.D., Eisenreich, S.J., Munger, J.W. and Gorham, E. (1981). In "Atmospheric pollutants" (S.J. Eisenreich, ed.) Chap. 14. Ann Arbor Science, Ann Arbor, Michigan.

4. Schrimpff, E., Thomas, W. and Hermann, R. (1979). Water, Air and Soil Pollut. 11, 481-497.

5. Forland, E.J. and Gjessing, Y.T. (1975). Atmos. Environ. 9, 339-352.

6. Landsberger, S., Jervis, R.E., Kajry, G. and Monaro, S. (1983). Int. J. Environ. Anal. Chem. 16, 95-130.

7. Concord Scientific Corporation. (1981). "Snow Core Sampling on the Canadian Shield-Water 1980-81". Report prepared for the Atmospheric Environment Service, Downsview, Ontario, by Concord Sci. Corp., 2 Tippett Road, Downsview, Ontario, Canada.

8. Barrie, L.A. and Walmsley, J.L. (1978). Atmos. Environ. 12, 2321-2332.

9. Boutron, C.F. and Patterson, C.C. (1983). Geochim. Cosmochim. Acta 47, 355-368 (and all references therein).

10. Ng, A. and Patterson, C.C. (1981). Geochem. Cosmochem. Acta 45, 2109-2121.

11. Boutron, C. (1982). Atmos. Environ. 16, 2451-2459.

12. Landsberger, S., Jervis, R.E. and Balicki, A. (1985). Int. J. Environ. Anal. Chem. (in press).

13. Taylor, S.R. (1964). Geochim. Cosmochim. Acta 28, 1273-1285.

14. Gladney, E.S., Wangen, L.E., Curtis, D.B. and Jurney, E.T. (1978). Env. Sci. and Tech. 12, 1084-1085.

15. Duce, R.A., Winchester, J.W. and Van Nahl, T. (1965). J. Geophys. Res. 70, 1775-1799.

16. Cicerone, R.J. (1981). Rev. Geophys. and Space Phys. 19, 123-139.

ACKNOWLEDGEMENTS

We thank the National Research Council of Science and Engineering of Canada for research grants. The co-operation of the staff and operators of the McMaster Nuclear Reactor is gratefully appreciated. We also thank A. Balicki at the Institute of Environmental Sciences, University of Toronto for analysing the samples by ICP-AES.

FIELD STUDIES ON STRESS WAVES IN NATURAL SNOW COVER

by

R.L. Brown and A. Hansen

Department of Civil Engineering and Engineering Mechanics
Montana State University
Bozeman, Montana
U.S.A.

presented at

SNOW PROPERTY MEASUREMENTS WORKSHOP

Lake Louise, Alberta

1-3 April, 1985

TECHNICAL MEMORANDUM 140

Compiled By

P.R. Kry

NRCC 27594

FIELD STUDIES ON STRESS WAVES IN NATURAL SNOW COVER

By

R. L. Brown*
A. Hansen**

ABSTRACT

Field stress wave experiments were performed on medium density snow for the purpose of providing data to evaluate a new constitutive theory for snow. Explosives (0.115 kg - 0.45 kg) were used to generate the stress waves. The pressure waves where spherical waves which were recorded by an array of semiconductor strain gauge pressure transducers. These transducers had flat responses from DC up to 100 kHz. The transducer array was placed within 0.5 m of the explosive, so that the pressure waves were plastic waves with pressures varying between 0.1 MPa and 10 MPa. One transducer was a miniature model which was used to measure the pore pressure associated with the stress wave. The remaining two were larger and were used to record stress wave attenuation.

The results indicate that pore pressures are not negligible and may be responsible for a significant part of the stress wave attenuation. Numerical trigometric series were used to approximate the transducer output in order to determine the frequency content of the stress wave. Results indicate that the stress wave quickly loses its high frequency content. However, it was shown that the wave impulse, which is the time integral of the wave pressure, remained nearly constant as it propagated through the distance of 5 cm between the two large transducers.

---

*Professor, CE & EM Department, Montana State University, Bozeman, MT 59717

**Ph.D. Student, CE & EM Department, Montana State University, Bozeman,MT 59717

INTRODUCTION PROBLEMS ASSOCIATED WITH STRESS WAVE EXPERIMENTS

Stress waves in snow is an important topic for several reasons. Aside from the obvious relevance to military interests, the application of stress waves to avalanche initiation is probably the most quoted reason for studying stress waves in snow. In addition to this, carefully executed measurements of stress wave propagation in snow can provide data which can be used to evaluate material properties. These measurements normally would be restricted to evaluating the high strain-rate properties rather than quazi-static mechanical properties.

A number of problems require knowledge of the high rate mechanical properties of snow. The evaluation of the effect of explosives in snow cover is one such example. Also avalanche impact on structures, terminal ballistics, and vehicle mobility over snow cover all involve strain rates which can vary from as low as 1/s to as high as 10^5/s. These strain rates must all be considered to be large. Normal laboratory testing machines cannot generate strain rates of this magnitude. Consequently experiments involving stress waves are necessary.

Unfortunately, stress wave experiments are difficult to run and to obtain reliable data from. They are also sometimes exorbitantly expensive. For instance, shock tube experiments utilizing a 20 cm diameter tube to produce plastic shockwaves in snow samples can cost as much as $4000 per shot. In view of this, other techniques of generating shock waves must be tried.

One method of generating stress waves is to use an electromagnetic stress wave generator (Bowles and Brown 1981). This system utilizes a high voltage capacitor to discharge a large current (as large as 500,000 amperes) in different directions along two adjacent conducting plates. The repelling electromagnetic force between these two plates throws one plate into a snow sample, thereby generating a stress wave in the sample. This system is substantially less expensive than a shock tube, but has less overall capability. It was found, however, to be an extremely reliable system.

A third method would involve the use of explosives, and this is the method which is used to obtain the data discussed in this paper. The use of explosives results with a large amount of scatter, but tests can be repeated with relative ease, and there is no practical limit on the specimen size that can be tested. In addition, it is the only practical procedure to use for field experiments.

Aside from the technique used to generate the stress wave, the method of monitoring the stress wave presents another set of problems. Since snow is a highly porous material, monitoring stress wave characteristics is more difficult than for nongranular materials such as metals, polymers or even fluids.

There are a number of methods for measuring stress waves which have been found to be successful for various materials. This includes surface capacitors, laser interferometers, accelerometers, pressure transducers, embedded wire coils, and others. Some of these are not suitable for snow or for field testing. For instance, a laser interferometer system would be difficult to use under field conditions, and the capacitor surface system would be unsuitable for a material which has a highly irregular surface.

Imbedded wire coil systems are now being used at Los Alamos and this system might prove useful for testing snow. At the time of the writing of this paper, the authors were not well acquainted with the details of this system, so no further comments will be made.

Accelerometers have been successfully used by Gubler (1977) to measure stress waves in natural snow cover. Impedance matching is a problem with this system. To solve this problem, Gubler first imbedded the accelerometer in a polystyrene container so that the effective density of the system matched that of the snow. Consequently, the accelerometer package would tend to move with the surrounding snow when the stress wave arrived at the location of the accelerometer package. For the experiments reported by Gubler, this appeared to be a workable system. For large amplitude plastic waves which produce large density increases, the container size and accelerometer-container interaction may create problems which would preclude its use. This merits further consideration.

In this study, pressure transducers are used in preference to the other systems. They were chosen, since for intense plastic waves studied in the field, they offered the best combination of cost effectiveness, ease of use, reliability, and repeatability. In studying shock waves, it is essential that the measuring unit have a wide frequency range, since frequencies in excess of 50 kHz may be contained in the pressure wave, and to accurately record the wave, the transducer should have a frequency capability well above this. Generally stress waves attenuate quickly, and the higher frequency component of the wave will quickly become insignificant, so for the type of stress waves considered by Gubler (1977), such frequency capabilities are not necessary. For the study considered here, characteristics of the wave very near bomb crater are evaluated, and a high frequency wave content is quite possible.

The attenuation of a stress wave can be evaluated in several ways. The standard procedure has been to merely evaluate the attenuation of the peak pressure. This is probably not the best way to characterize the stress wave. One reason is that if a transducer of limited frequency response capability (say less than 5 kHz) is used, it won't respond to the high frequency wave and consequently give a wrong measure of the wave intensity. A second reason is that the peak pressure may attenuate much more rapidly than the wave impulse, which is the time integral of the pressure. Consequently the peak pressure may not be a good measure of the ability of a wave to damage a structure or initiate an avalanche.

One method of evaluation of wave attenuation would be to determine the wave structure and then to determine how the wave structure changes. By wave structure is meant the frequency content of the pressure signal generated by the wave. This can be done in a number of different but related ways. The method chosen here is harmonic analysis in which a numerical Fourier expansion of the pressure signal is developed. The distribution of the Fourier coefficients then gives a measure of the frequency content of the wave. This can also be used to quickly evaluate the wave impulse.

STRESSWAVE EXPERIMENTS

The experiments described here were conducted in the Bridger Mountains near Bozeman, Montana. The tests were conducted in a site where the snowfall and wind characteristics lends itself to a fairly uniform snow cover. In addition, since the propagation distances that were being used were on the order of 0.05 m, it was felt that the influence of inhomogeneous conditions were minimized.

The pressure transducers were semiconductor strain gage transducers manufactured by Entran Devices, Inc. These transducers have a full semiconductor strain gage bridge fused to a stainless steel diaphragm. Flexure of the diaphragm then generates a bridge imbalance proportional to the applied pressure. Two of the transducers used in these experiments had an upper limit of 34 MPa and a flat frequency response from DC to 100 kHz. The pressure sensitive area was a circular area about 8.0 mm in diameter. The transducer sensitivity was 0.8 mv/bar (8 mV/MPa). This sensitivity was lower than desired but proved to be acceptable.

A third transducer was used to measure the pore pressure in the stress wave. This transducer was much smaller (a 3.3 mm diameter pressure sensitive area) and had a sensitivity of 4.0 mv/MPa).

These transducers are mounted on the frame shown in Figure 1. Each transducer is attached to the end of a long stainless steel tube which is fixed to a plate. The tubes are approximately 0.5 m long. This gives the pressure transducer sufficient time to measure the incoming stress wave profile before the wave can propagate down the tube and be reflected back to the transducer. The rod itself is stiff enough such that the transducer is rigidly restrained from any significant motion relative to an inertial frame.

The small transducer was shrowded in an 80-mesh screen. The mesh on the screen was small enough to keep any ice particles out of the cavity formed around the transducer, but would allow the pore pressure

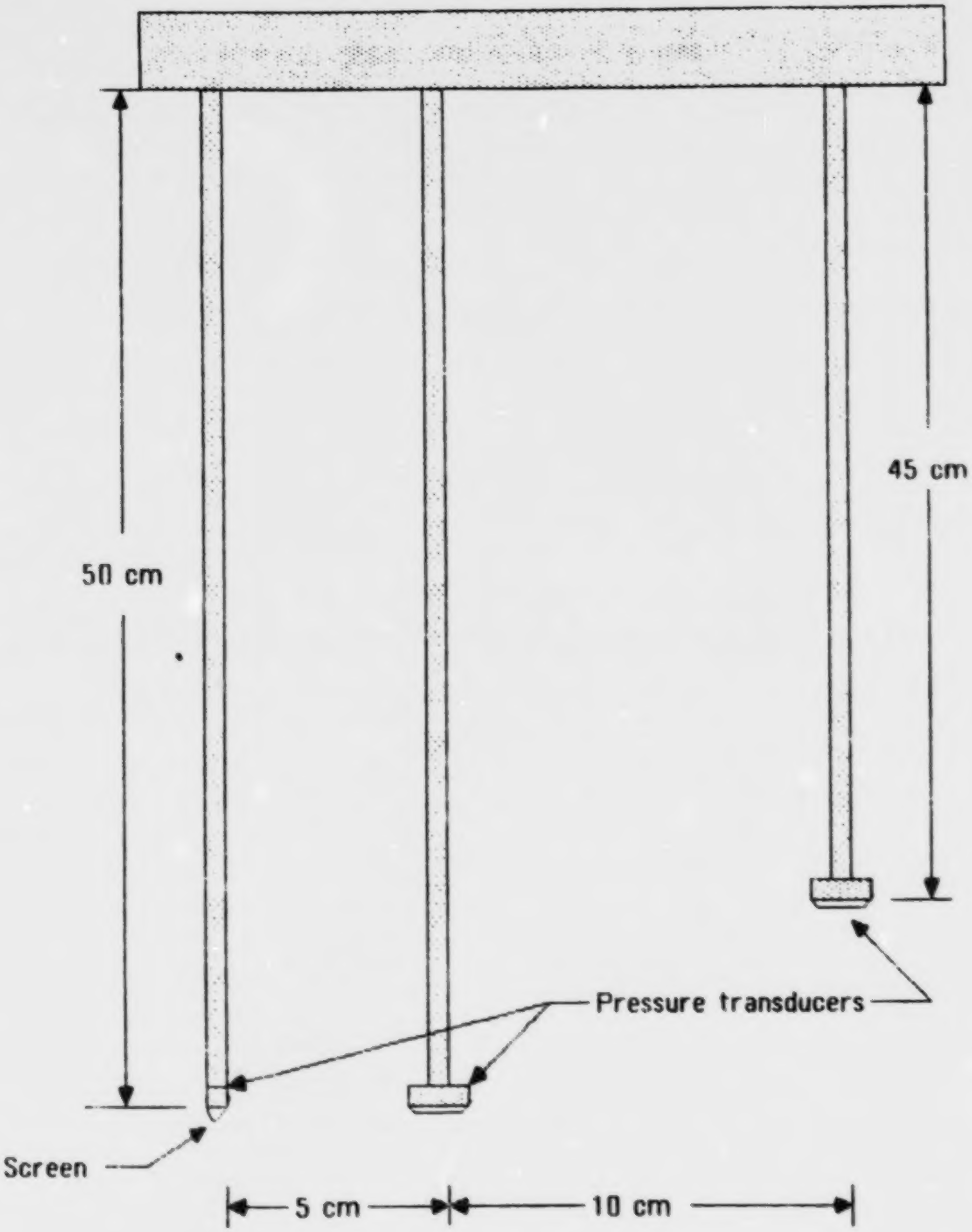
50 cm
45 cm
Pressure transducers
Screen
5 cm
10 cm

Figure 1. Schematic of frame used to hold pressure transducers

wave to pass through the mesh to the transducer. In this way, it was hoped that a good measure of the actual pressure transmitted through the pore space could be measured.

Only two channels of data could be measured in any single shot, since a dual trace oscilloscope was used to record transducer output.

Initially small (0.125 kg) bombs of kine-pac were used. This explosive has a burn speed of about 6400 m/s. The placement of the bombs and transducers are illustrated in Figure 2. two pits were dug so that the pit walls were about 1.0 m apart. The transducer frame was inserted into one pit wall so that the transducers were approximately 0.5 m from the 2nd wall. This first pit was then filled in to isolate the frame from any disturbances other than the stress wave. The bomb was inserted into the other wall so that it was the desired distance (0.3 - 0.5 m) from the lead transducer.

A photocell was situated about 5 m from the bomb to trigger the oscilloscope. The final test set up is shown in Figure 2. Prior to the shot, density and temperature were measured, and a snow sample was taken for a surface section to evaluate snow microstructure. After the shot, another snow sample was used for a second surface section. This sample was taken from snow adjacent to the pressure transducers. The purpose of these surface sections were to evaluate the effect of deformation on a large set of microstructural parameters. Since this is not central to this paper, no more will be said of this, other than to indicate the final density was determined from the surface sections. This proved to provide a more precise measurement of density than using a 200 cc or 500 cc density kit.

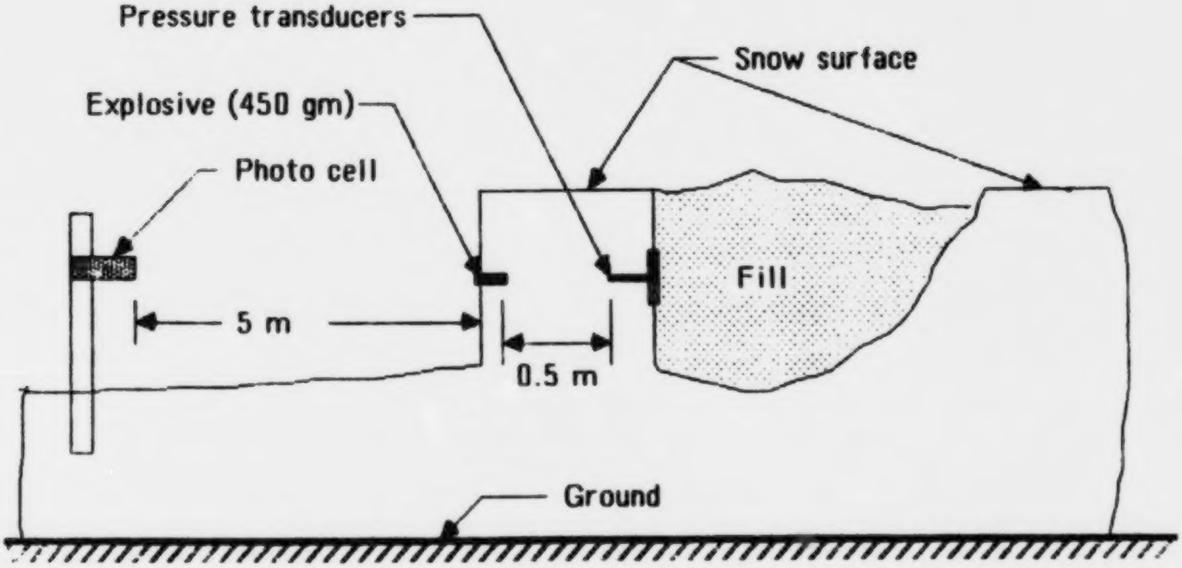
Pressure transducers
Snow surface
Explosive (450 gm)
Photo cell
Fill
5 m
0.5 m
Ground

Figure 2. Field stress wave experiments

ANALYSIS

The stress wave characteristics can be conveniently analyzed by harmonic analysis, i.e. by developing a trigometric series which approximates the actual stress wave curve. The coefficients in the series than allows one to determine the frequency distribution of the signal and the wave impulse.

Suppose we have a signal which is broken into 2N+1 points in the time interval$[-\pi,\pi]$, as indicated in Figure 3(a). The signal is assumed to be periodic of period 2π. The harmonic series approximation of f(t) is

$$f(t_r) = A_o + \sum_{m=1}^{N-1}(A_m \cos mt_r + B_m \sin mt_r) + A_N \cos N\, t_r \tag{1}$$

where

$$A_o = (1/N) \sum_{r=-N+1}^{N} f(t_r)$$

$$A_m = (2/N) \sum_{r=-N+1}^{N} f(t_r) \text{ Cos } m\, t_r \quad m = 1,..N-1$$

$$B_m = (2/N) \sum_{r=-N+1}^{N} f(t_r) \sin m\, t_r \quad m = 1,...,N-1$$

$$A_N = (1/N) \sum_{r=-N+1}^{N} f(t_r) \text{ Cos } N\, t_r$$

This formulation needs to be modified somewhat for the purposes of our study. We assume the stress wave signal is an even function of period 2T, as indicated in Figure 3(b). This is accomplished by producing a "time reflected curve" identical to the actual pressure curve of period T. Then making the time transformation

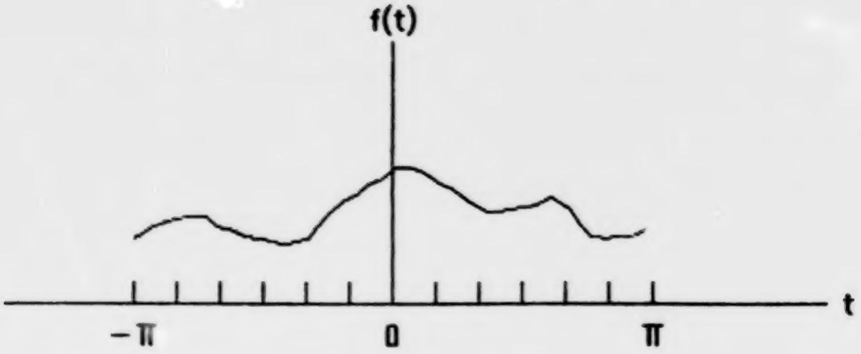

(a) Time function of period T = 2π

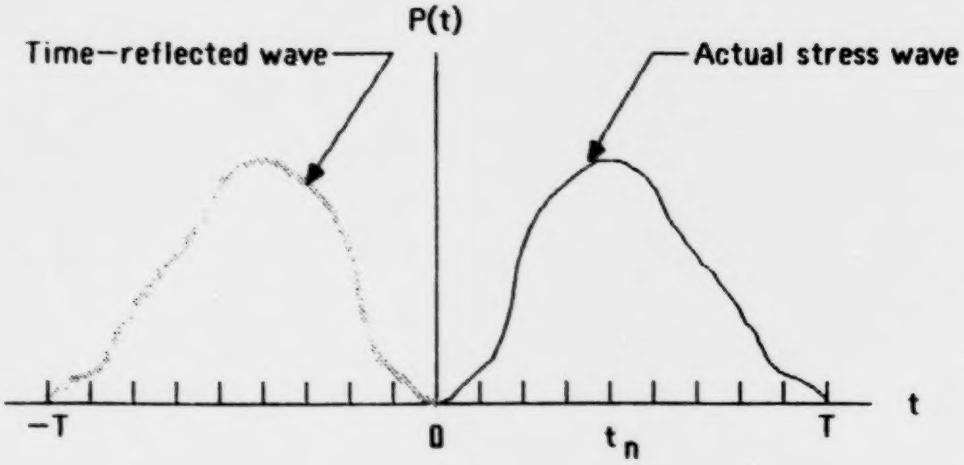

(b) Stress wave signal with reflected signal

Figure 3

$$\tau = Tt/(2\pi) \qquad (3)$$

and realizing that the signal is now an even function of time, we obtain our series

$$f(tr) = A_o + \sum_{r=1}^{N} A_m \text{ Cos } 2m\pi\tau_r/T \qquad (4)$$

where

$$A_o = (1/N) \sum_{r=0}^{N} f(\tau_r)$$

$$A_m = (2/N) \sum_{r=0}^{N} f(\tau_r) \text{ Cos } 2m\, N\, \tau_r/T \qquad (5)$$

$$A_N = (1/N) \sum_{r=0}^{N} f(\tau_r) \text{Cos } 2\, N\tau_r/T$$

This series will match the data points exactly. The first coefficient A_o gives a measure of the wave impulses I,

$$I = \int_o^T f(t)\, dt \qquad (6)$$

which gives

$$I = A_o\,(T/2) \qquad (7)$$

The other coefficients A_1 through A_N can then be used to determine the frequency content of the wave. The above will be used to characterize some of the stress wave properties.

The total wave pressure consists of two parts, that due to the pressure transmitted through the ice structure and the pressure transmitted through the pore space. Mixture theory may be used to study the problem. The momentum balance principles for these two phases are

$$- \partial P_a / \partial x + \hat{p} = \ddot{x}_a$$

$$- \partial P_I / \partial x - \hat{p} = \ddot{x}_I \qquad (8)$$

In the above a plane wave is assumed. $\hat{p}$ is a momentum supply term which characterizes the interaction between the constituents. P_a and P_I are the pressures in the air phase and ice phase, respectively, measured as force per unit mixture area. The mixture area on a surface element is the total area, with part of it containing the air phase and the remaining part containing the ice phase. If we denote as p_a and p_I the pressures per unit phase area, then we have

$$P_a = (1 - 1/a)\, p_a$$

$$P_I = (1/a)\, p_I \qquad (9)$$

where

$$a = \rho_I / \rho_s \qquad (10)$$

is the ratio of the density of ice and the density of snow. These equations are due to stereology theory (Underwood, 1970). The total pressure is

$$P = P_a + P_I$$

$$P = (1 - 1/a)p_a + p_I \qquad (11)$$

During the test, P and p_a are measured, so with the use of Eq. (9) - (11), the portion of the stress wave due to the ice, P_I, can be calculated if the density ratio a(t) can be determined as a function of time. This would require a rigorous solution of the governing momentum balance equations with appropriate constitutive equations.

An approximate determination of the relative magnitude the air wave and ice wave can be made with previous results obtained by Brown (1980). In that study he substituted a volumetric constitutive law for snow into the momentum balance equations and then integrated these equations to perform a detailed analysis of inelastic waves in medium density snow. Those results show that a(t) can be approximated as a linear function of time during the interval that the wave pressure is increasing. This will suffice for the purposes of this study.

If we denote the rise time for the stress wave as T_R, then

$$a = \rho_I/\rho_s = \rho_I/(\rho_o + (\Delta\rho)t/T_R) \qquad (12)$$

where ρ_o is the initial snow density and $\Delta\rho$ is the density jump due to the stress wave. This,then, with Eq. (11) allows an estimate of the relative magnitudes of the air wave and ice wave.

TEST RESULTS

The stress wave program is still in progress, and a full evaluation must await the completion of the winter testing program. However, some preliminary results can now be discussed.

First, it has been observed that the use of explosives in itself produces more scatter than other methods such as the electromagnetic stress wave generator. However, with the use of two staggered pressure transducers as shown in Figure 1, this problem is partially alleviated, since stress wave attenuation characteristics can be evaluated, based on the stress wave characteristics at the front transducer.

The pressure wave associated with the pore space was found to be significant. Figure 4 shows a typical profile recorded by the small pressure gauge with the screen placed over it. Normally, the screen had to be replaced after every three or four shots, since with each shot, the screen was partially flattened. In all about six shots were

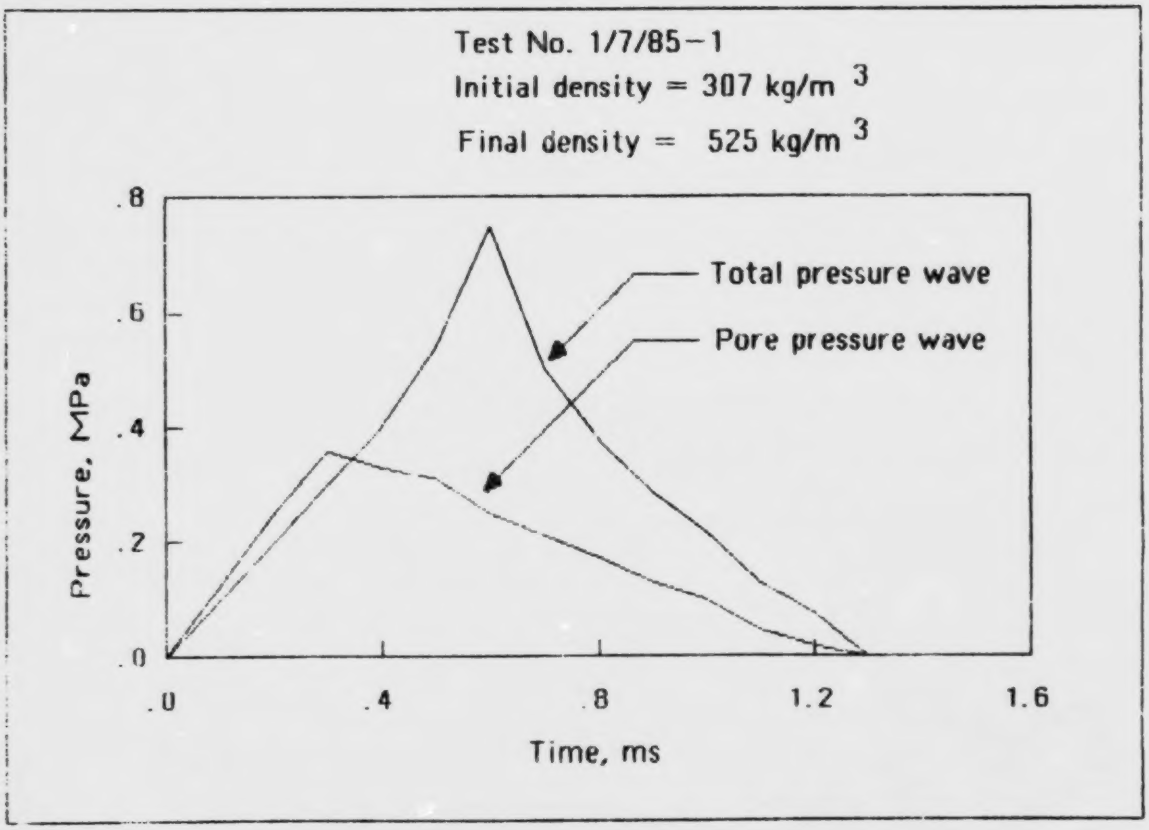

Figure 4. Transducer traces for total pressure wave and pore pressure wave

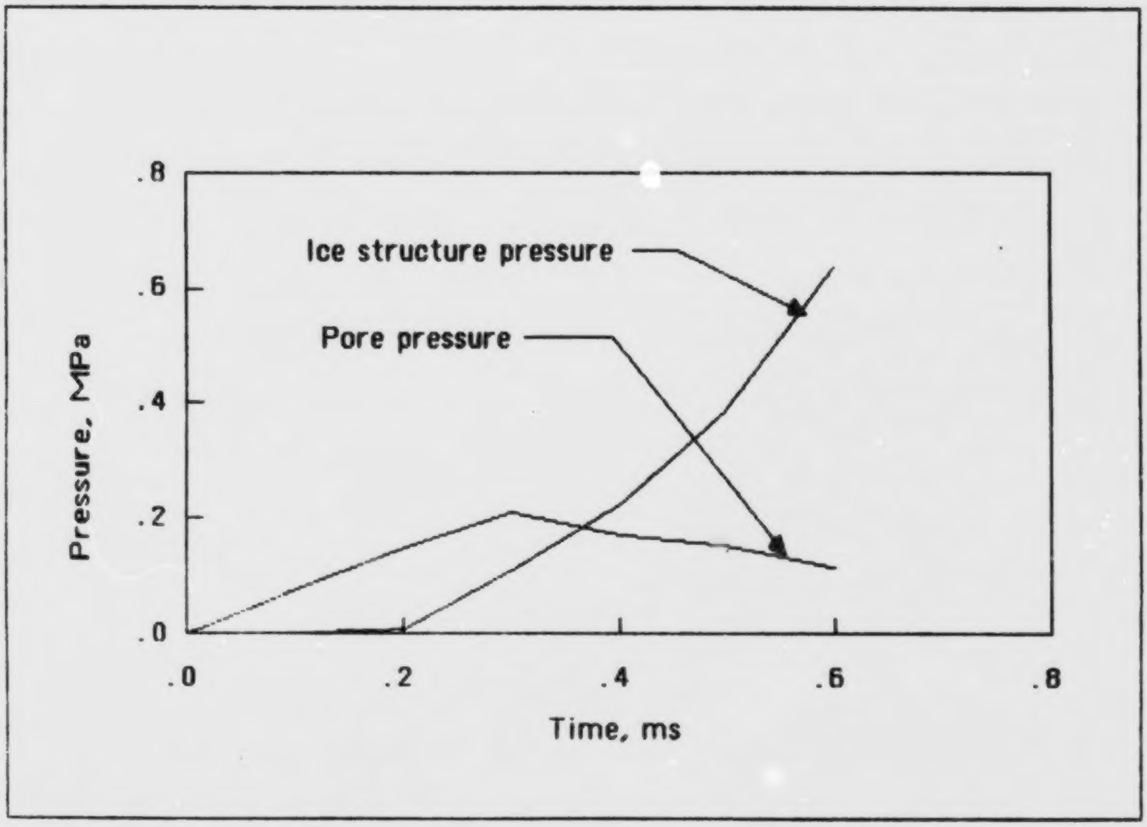

Figure 5. Comparison of pressures produced in the pore space and in the ice structure

obtained to compare the total stress wave pressure with the pore pressure. For one particular test, Figure 5 shows the variation of actual pressures produced by the waves in the ice structure and in the pore space. Due to the assumptions used to arrive at these curves, details of these curves cannot be considered to be accurate, but they do give a good qualitative measure of the importance of the air wave. The sum of these two curves (P_a and P_I) would give to total pressure, as indicated by Eq. (11). This figure indicates that the first part of the wave pressure is produced by the pressure wave propagating through the pore space and that the wave in the ice structure follows closely behind. As indicated the air wave does generate a significant portion of the total wave pressure. The particle velocities thus produced in these two waves will be on the order of:

$$U_a = P_a/\rho_a V \sim 300\text{-}1000 \text{ m/s}$$

$$U_I = P_I/\rho_I V \sim 1 - 10 \text{ m/s}$$

and the magnitude of the difference between these velocities indicate that the momentum supply term in Eq (8) may indeed be very significant and account for some of the wave energy dissipation. The momentum supply term contains a number of effects, including a Stokes drag term and a diffusive force term (Bowen, 1976). Both terms are dependent on the velocity difference ($U_a - U_b$).

Figure 6 illustrates typical transducer outputs for the two large pressure transducers staggered by a distance of 5 cm. The two curves have been time shifted to start at the same time for more convenient comparison, and the output of the rear transducer has been adjusted to account for effects of geometric wave front spreading. Consequently what is shown in figure reflects attenuation due to material

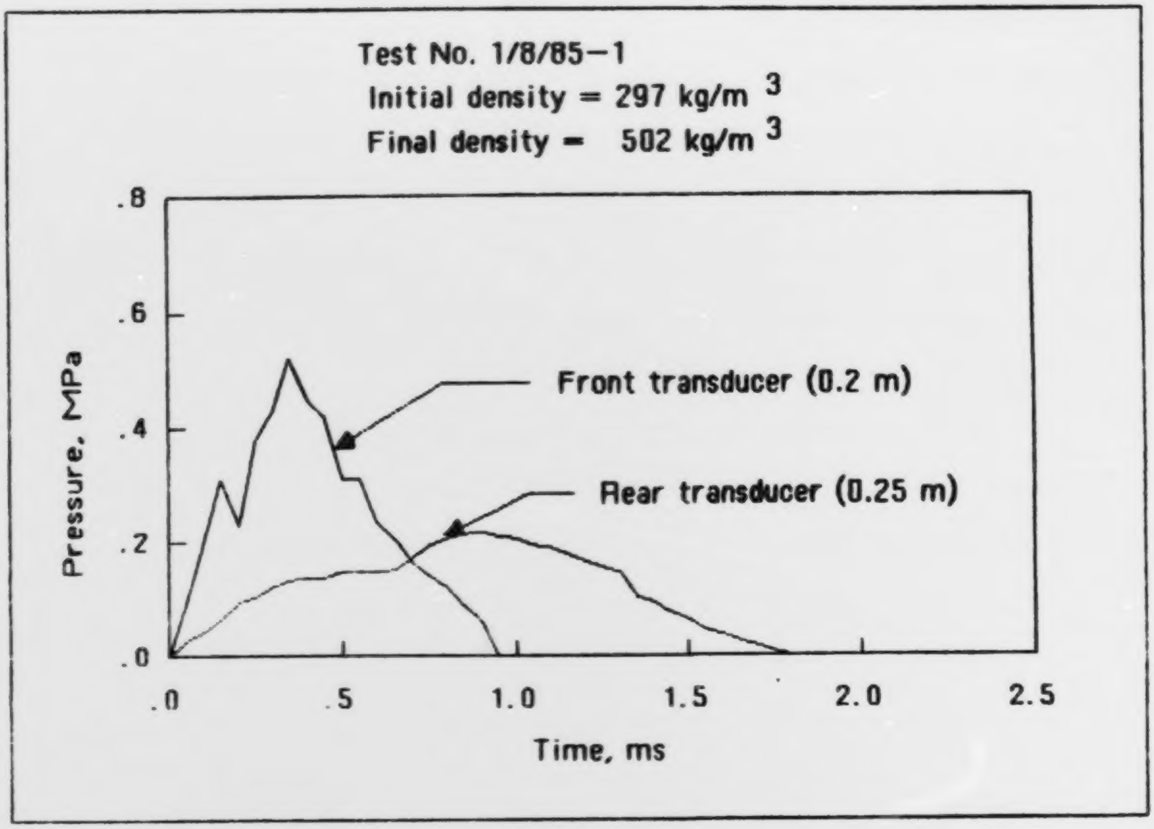

Figure 6. Pressure signals at front and rear transducers

dissipative effects. Based on the difference in arrival times of the two waves, the wave speed was determined to be 88 m/s.

These results were compared with results of laboratory stress wave experiments and theoretical calculations (Brown, 1980). It is noted that the attenuation rates in peak stress observed here compared quite well with those calculated theoretically and measured experimentally in the laboratory for waves of similar amplitude and snow of similar densities. However, there were differences in the stress wave speed. Brown's 1980 calculations indicated wave speeds of 65 m/s as compared to the value of 88 m/s measured here.

Figure 7 illustrates the frequency distribution of the two transducer signals, as determined by the harmonic analysis described by Eqs (4) and (5). The absolute values of the coefficients A_m are plotted in terms of their corresponding frequencies

$$W_m = 2m\pi/T$$

as can be seen there is a definite degradation of the frequency content over the 5 cm interval separating the two transducers. The peak amplitude has shifted to 250 Hz from a value of 1000 HZ. In addition, after propagating an additional 5 cm, there is virtually no frequency content in the wave above 4000 Hz, whereas at the front transducer the wave had significant frequency cotnent up to 12,000 Hz. However, the wave impulse has retained 99% of its value, dropping from an impulse of 234 Pa-s to 232 Pa-s over this interval. This serves to indicate that calculations and measurements used in the analysis are valid.

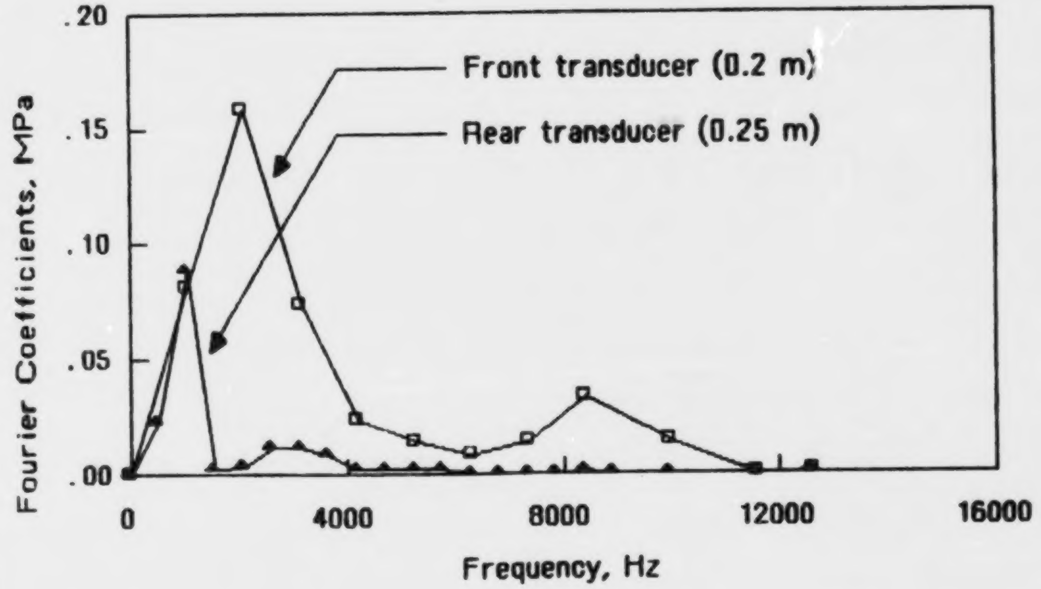

Figure 7. Comparison of frequency content of stress wave after two propagation distances.

CONCLUSIONS

Stress wave propagation in porous media is a topic which is difficult to model analytically and which is not well understood. Stress wave experiments such as described here offers a convenient way of adding to the scarce data now available. The equipment described here seems to work well for conducting field experiments. However, other measuring systems need to be considered. Most granular materials are difficult to work with, and snow is no exception. But, given the funds and time to develop reliable and accurate measuring systems, good data on stress wave propagation in snow will be forthcoming.

More in the line of mathematical modeling of wave propagation is also needed. In the authors' viewpoint, use of mixture theory offers the best potential for conclusive results. To do this, the details of the air-ice structure interaction needs to be determined before the wave equations (Eqs 8) can be integrated. Stress wave studies such as the ones described here may be of use for determining these relations.

ACKNOWLEDGMENTS: The work reported here was supported by Army Research Office Grant No. DAAG29-82-K-0127

REFERENCES

Bowen, R. M. (1976) Theory of Mixtures, Continuum Physics III, Academic Press, New York, N.Y.

Bowles, D. and R. L. Brown (1981) A Stress Wave Generator for Snow and Ice Studies. Journal of Glaciology, Vol. 27, No. 97.

Brown, R. L. (1980) Propagation of Stress Waves in Alpine Snow. Journal of Glaciology, Vol. 26, No. 94.

Gubler, H. (1977) Artificial Release of Avalanches by Explosives. Journal of Glaciology, Vol. 19, No. 81.

Underwood, E. E. (1970) Quantitative Stereology, Addison Wesley Publishing Co., Reading, Mass.

SNOW PROPERTIES IN ACTUAL FIELD CONDITIONS AND STABILITY ANALYSIS

by

M. Fukue
Tokai University
Shimizu, Japan

presented at

SNOW PROPERTY MEASUREMENTS WORKSHOP

Lake Louise, Alberta

1-3 April, 1985

TECHNICAL MEMORANDUM 140

Compiled By

P.R. Kry

NRCC 27594

SNOW PROPERTIES IN ACTUAL FIELD CONDITIONS AND STABILITY ANALYSIS

by

Masaharu Fukue[*]

ABSTRACT

It has been found that under regional conditions there are al-almost unique relationships between density and time, and between strength and time for seasonal snow covers, if snow layers are distinguished by melted-refrozen or unmelted. By using the relationships obtained in this study a stability analysis on snow slopes was made. The analysis of an avalanche which occurred on the northern slope of Mt. Fuji, in 1960, provided good results.

INTRODUCTION

In relatively warm regions, multiple and distinctive snow layers are usually formed through the profile. The formation process of a distinctive layer seems to be very complicated in terms of temperature change, time and other weather conditions.

By this process, snow properties vary widely. For example, the lationship between density and strength of seasonal snow cover varies considerably even if obtained at the same site. In fact, estimation of snow strength from density can lead to considerable error.

---

[*] Tokai University, Shimizu, Japan.

Thus, it is obvious that the restriction of the mechanical analysis on snow engineering problems results from -

1. wide-variation of snow properties in field conditions,
2. time and temperature dependence on snow properties,
3. annual variation of snow profile, and
4. difficulty of measuring in situ snow properties in relation to testing technique.

Therefore an attempt was made to predict the density and strength of snow covers, based on observation of snow profiles made in the winter periods from 1978 to 1982. Furthermore, a stability analysis on snow slope was made as an application in snow engineering problems.

REFROZEN AND UN-MELTED SNOW LAYERS

Figure 1 shows the change in atmospheric temperature and snow temperature, observed at the northern slope of Mt. Fuji, on March 15, in 1980. As can be seen in the figure, the melted layer has a limited thickness in relation to the thermal conduction under the regional conditions.

Most of the melted water may diffuse to which the surface energy of snow skeleton is relatively high, though gravity may cause the excess water to move downward along the surface of snow skeleton. Note that the surface energy is usually high at weak parts of snow skeleton.

Therefore, the refreezing of melted water rebuilds the snow structure which, in turn, usually strengthens the skeleton.

The thickness of the melting-refreezingzone depends mainly upon temperature, radiation and the thermal properties of snow.

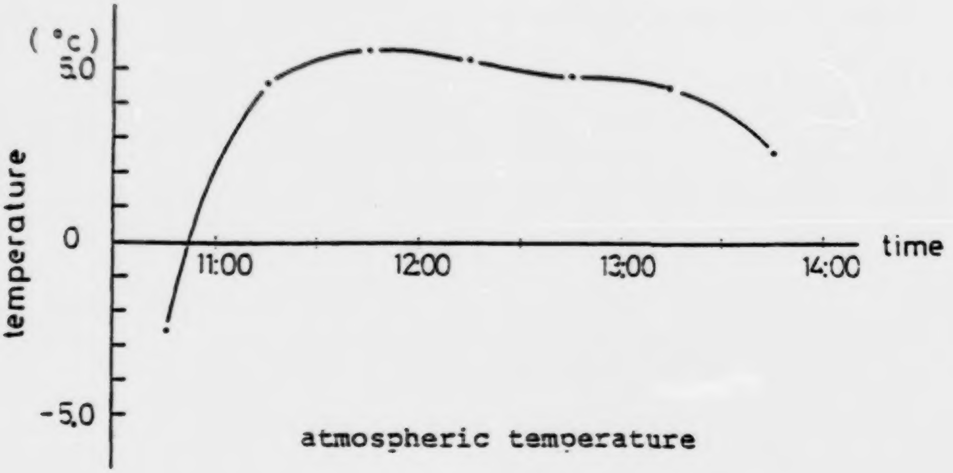

atmospheric temperature

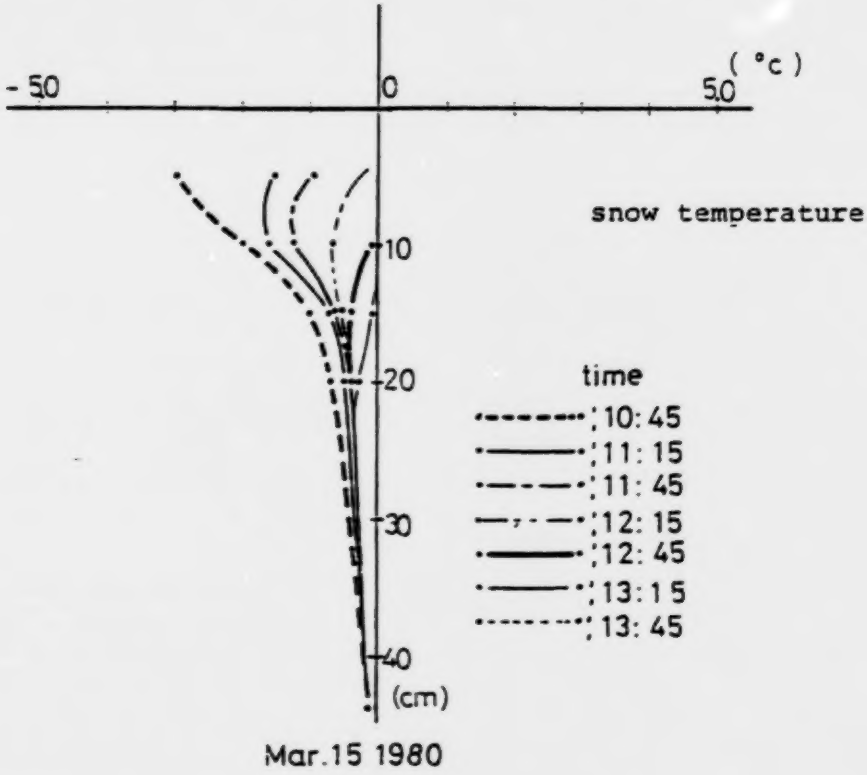

Fig.1 The change in snow temperature in the field condition of Mt.Fuji, observed in March 15, 1980.

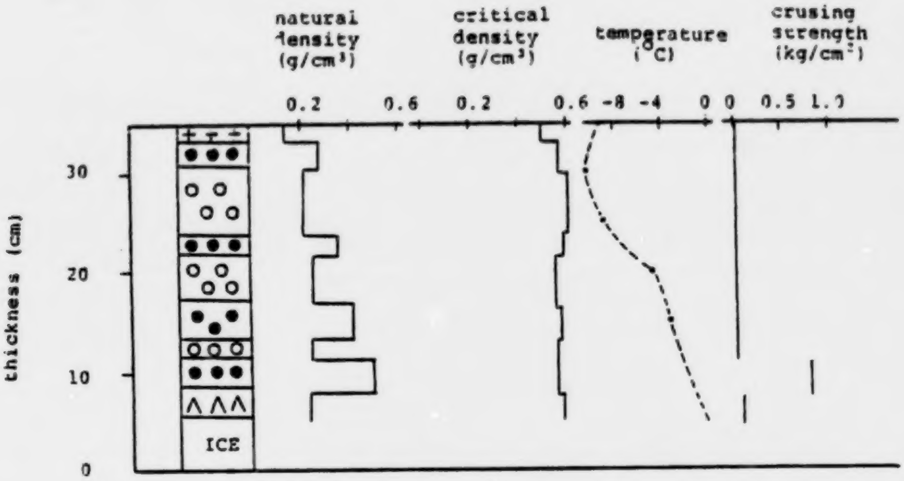

Fig.2 Snow slope with several distinctive layers, observed at Mt.Fuji, in March 11, 1981 (Fukue *et al*, 1982).

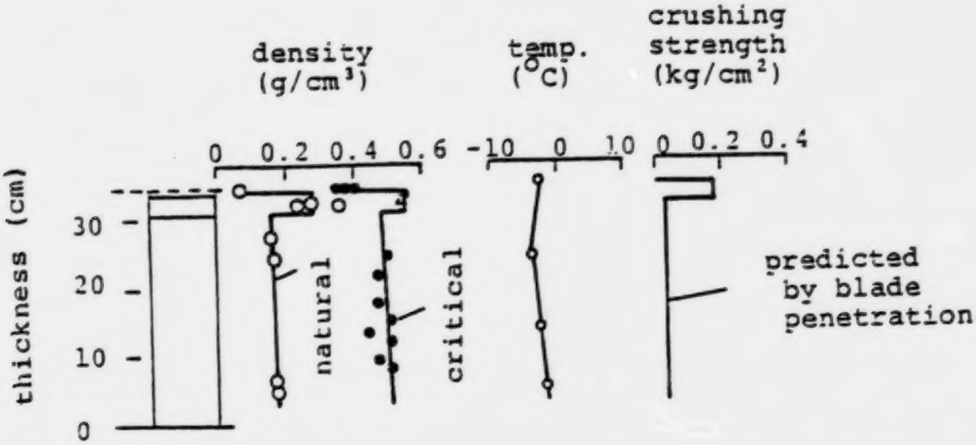

Fig.3 Snow profile with single hardened layer observed at Mt.Fuji, in December 31,1978.

If the temperature mode is relatively low, the thickness becomes less. Thus regular heating and cooling cycles would possibly cause the melted-refrozen snow layer. However, it is noted that the thickness influenced by daily heating and cooling cycles varies because of the day-to-day variation in temperature and the change in the thermal properties of snow.

Figure 2 shows a snow profile observed at Mr. Fuji on March 11, 1981. The snow cover consists of high and poor metamorphic (densified) layers. These two types of snow layers are considered to be melted-refrozen and un-melted, respectively. Since the melting-refreezing thickness is limited from the top surface, Fig. 2 indicates that there were five snowfalls. The existence of an ice layer at the bottom indicates that the melted water percolated through the snow cover by gravity. Therefore, it must be considered that the un-melted snow layer as defined above, melts in late winter or early spring at relatively warm regions, apart from rainfall.

A typical snow profile which has single melted-refrozen layer is shown in Fig. 3. The snow cover accumulates instantly, except for the upper fresh snow.

Thus it is seen that the snow layer is divided into two types, i.e. highly melted-refrozen and poorly melted or un-melted layers. The mechanical and physical properties of these two types can be distinguished as shown in Figs. 2 and 3.

DENSITY-TIME RELATIONSHIPS OF SNOW LAYER IN FIELD

Figure 4 shows the density-time relationships obtained on snow layers for which the precipitation dates are known. The relation-

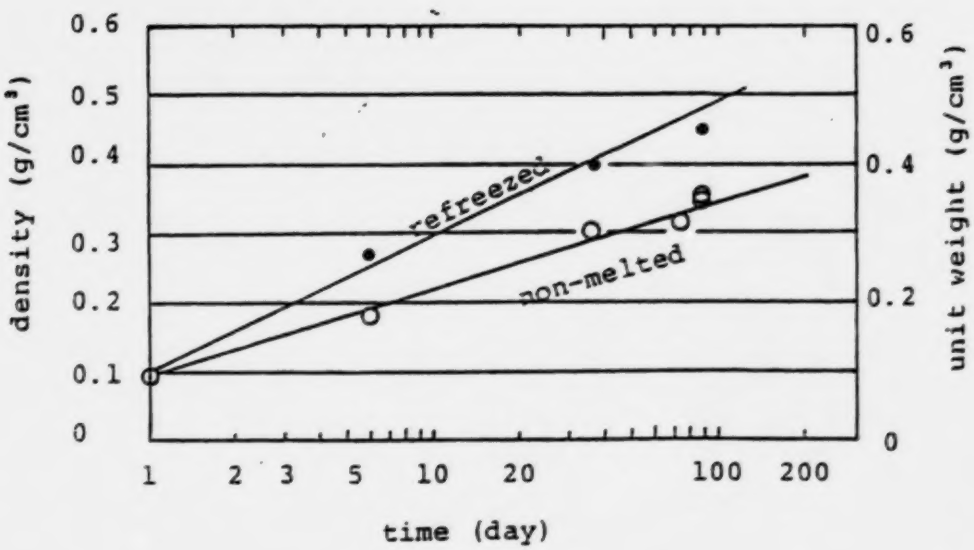

Fig.4 Density-time relationships for melted-refrozen and un-melted snow layers, under the regional conditions of Mt.Fuji.

ships include all the effects of densification due to snow weight, temperature, sintering and other factors under the regional conditions at Mt. Fuji.

The comparison between the density-time relationship at Mt. Fuji and Greenland, shown in Fig. 5, indicates that the increasing rate of density for un-melted snow layer at Mt. Fuji is slightly higher than that of Greenland. This is because the temperature at the slope of Mt. Fuji is higher than that of Greenland. The increasing rate for the melted-refrozen layer is more rapid because of mass transfer due to the downward movement of excess melt-water, (Fig. 6).

The density-time relationships for un-melted and melted-refrozen snow layers would be expressed possibly by:

$$\rho = \rho_0 + c \log(t/t_0) \qquad (1)$$

where

ρ = density,

ρ_0 = density of fresh snow,

t = time (day) from t_0(= one day), and

c = constant.

As shown in Fig. 4, at the slope of Mt. Fuji, ρ_0 is approximately 0.09 g/cm^3 and c is 0.124 and 0.2 g/cm^3 for un-melted and melted-refrozen layers respectively.

SNOW STRENGTH

Snow strength depends upon many factors, i.e. temperature, loading (strain) rate, and snow type (Fukue, 1979); therefore, the definition of 'strength of snow' is obscure at the present time.

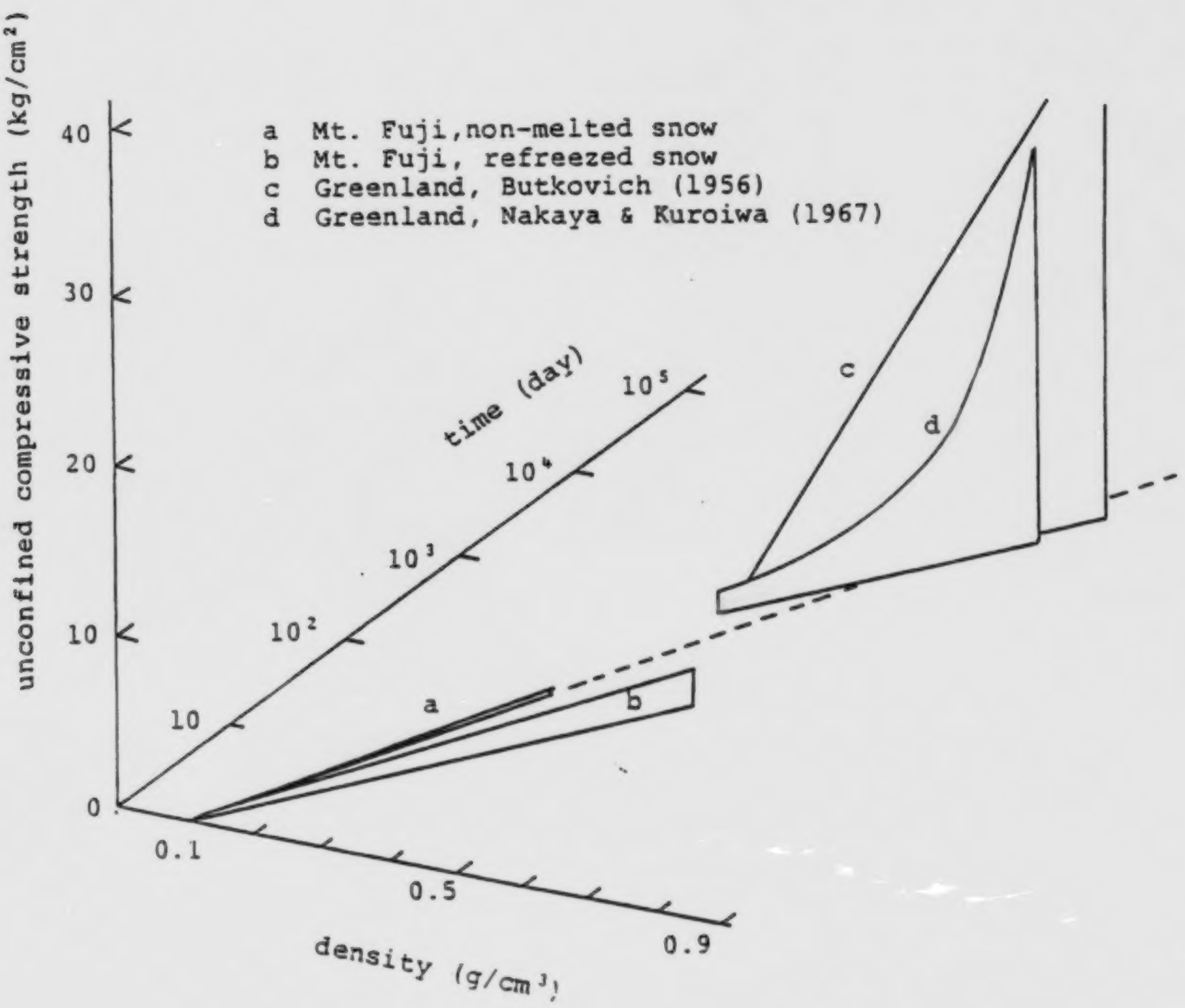

Fig.5 Comparison between density-time relationships, for Mt.Fuji and Greenland.

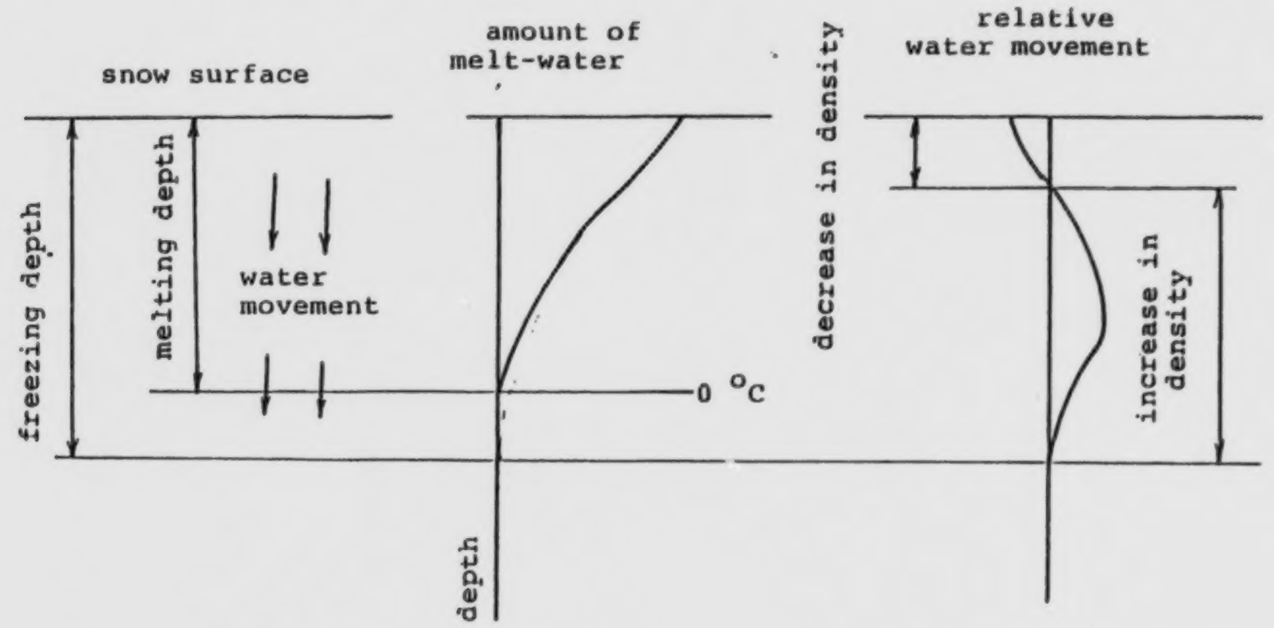
snow surface
amount of melt-water
relative water movement
freezing depth
melting depth
water movement
0 °C
depth
decrease in density
increase in density

Fig.6 General illustration of density change under a melting-refreezing cycle.

However, under a condition which yields a brittle behaviour of snow, snow strength is defined as the maximum stress at failure. Since seasonal snow is so loose that the conventional shear stress theory cannot be applied, the direct shear and compression shear as failure types, should be considered (Fukue and Yong, 1985).

In compression shear the unconfined compressive strength of snow can be expressed by:

$$\sigma_c = \sigma_0 + \sigma(\epsilon_v) \qquad (2)$$

where

σ_0 = the inherent unconfined compressive strength, and

$\sigma(\epsilon_v)$ = the component of strain hardening as a function of volumetric strain (ϵ_v). (Fukue and Yong, 1985).

Similarly, in shear performance of snow, the shear strength can be expressed by:

$$\tau_f = \tau_0 + \tau(\gamma_v) + \sigma \tan \phi' \qquad (3)$$

where

τ_0 = the inherent shear strength,

$\tau(\gamma_v)$ = the component of strain hardening as a function of volumetric strain (ϵ_v).

σ = the normal stress acting on a shear plane, and

ϕ' = the angle of internal friction which is strongly influenced by shear strain rate.

SNOW STRENGTH IN THE FIELD

The evaluation of snow strength in the field becomes difficult when the snow cover is very soft, or when the snow layer is very thin. In such cases, special techniques for measuring the density and strength of snow are used, as shown in the Appendix.

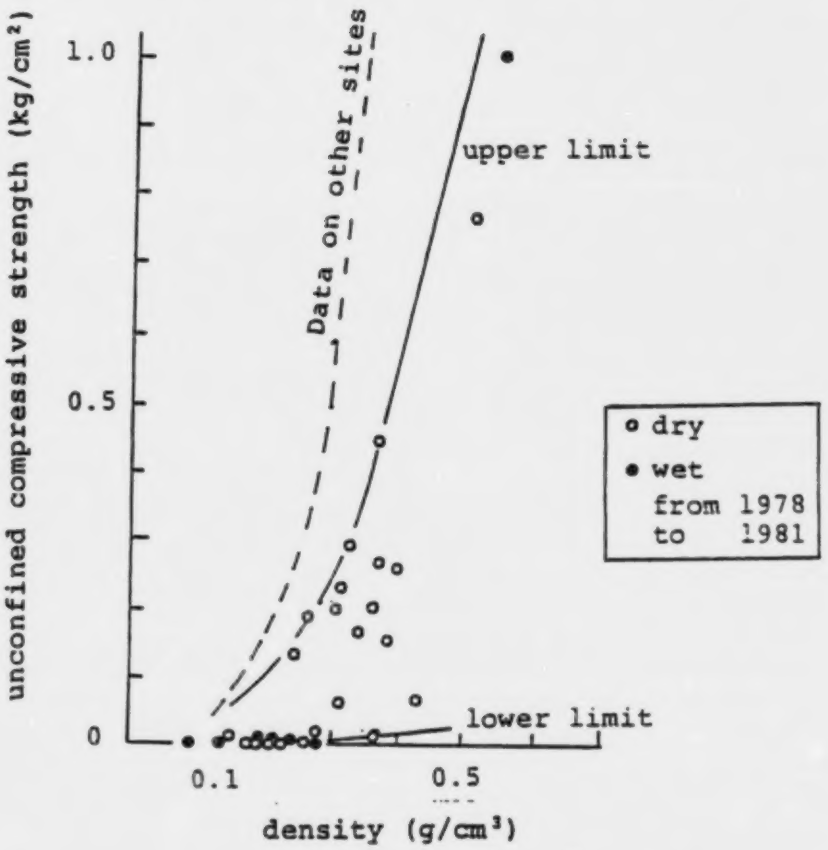

(Fukue *et al*,1982)

Fig.7 Unconfined compressive strength of snow layers at Mt.Fuji.

Snow strength data which have been obtained in the field include, more or less, strain-hardening and temperature effects. However, if data were obtained at a relatively high strain rate, the measurements would be approximate inherent strength, (Fukue and Yong, 1985).

The unconfined compressive strength, obtained at a high strain rate, varies considerably between the upper and lower limits, as shown in Fig. 7. This indicates that the estimate of in situ snow strength from density provides a considerable error. The large variation in the density-strength relation may result from the day-to-day variation of the melting-refreezing process, as was described earlier.

Figure 8 shows the relationships between strengths and time for un-melted snow layer obtained at Mr. Fuji, using a technique shown in the Appendix. Note that the plots indicated in the figure are the mean value for several specimens. Since the relationship between unconfined compressive strength and log t, at a constant temperature, is almost linear, the relationships of the un-melted snow layer shown in Fig. 8 would be true. Note that the un-melted snow layer is formed at a certain depth, where the change of temperature may not be large because of low thermal conductivity of snow.

Therefore, the strength with time for un-melted layer is empirically expressed by:

$$\sigma_0 = \sigma_0^* + b \log(t/t_0) \qquad (4)$$

for compression, and

$$\tau_0 = \tau_0^* + d \log(t/t_0) \qquad (5)$$

for shear.

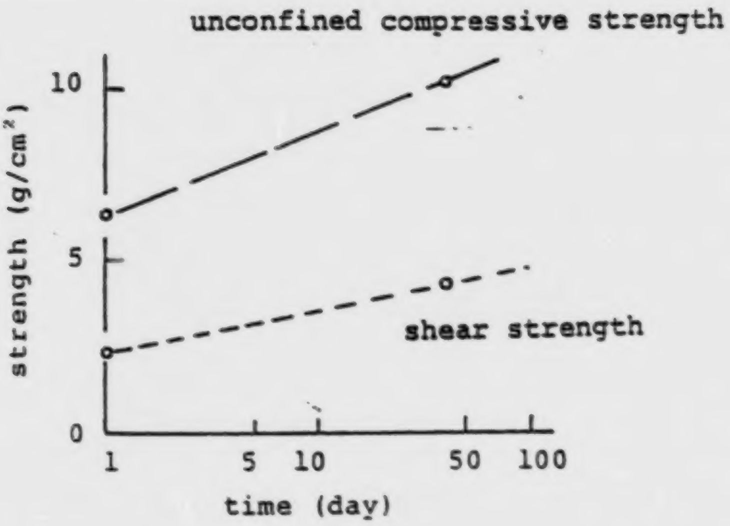

Fig.8 The increase in unconfined compressive strength and shear strength resulting from age hardening, for un-melted snow layers of Mt.Fuji.

where

σ_0 and τ_0 = the inherent unconfined compressive and shear strengths of un-melted aged snow, respectively,

σ_0^* and τ_0^* = the inherent unconfined compressive and shear strengths of fresh snow, i.e., one-day old snow, respectively, and

b and d = the constant.

From Eqs. (2) and (5), the unconfined compressive and shear strengths can be expressed by:

$$\sigma_c = \sigma_0^* + b \log(t/t_0) + \sigma(\varepsilon_v) \tag{6}$$

and

$$\tau_f = \tau_0^* + d \log(t/t_0) + \tau(\gamma_v) + \sigma \tan \phi' \tag{7}$$

respectively.

STABILITY ANALYSIS OF SNOW SLOPE IN DRY CONDITION

In mid-winter the melting of snow may not provide the instability of slope because the melting thickness is strictly limited to the top surface, as was described earlier. Therefore dry snow conditions are examined here.

In the stability analysis, infinite snow slope is more realistic for the following reasons:

(a) Before sliding occurs, the tensile crack which is not always visible would possibly develop in the upper cross-section of the slope. Therefore, the tensile resistance at the upper cross-section should be neglected.

(b) The sliding layer or block is relatively thin compared with the width and length for actual avalanches.

In an infinite snow slope as shown in Fig. 9, the vertical force acting on a weak plane with a depth of h is given by:

$$G = \Sigma\gamma_j h_j \cos i \qquad (8)$$

where

γ_j = the unit weight, and

h_j = the thickness of jth layer.

The normal force is given by:

$$\sigma = G \cos i = \Sigma\gamma_j h_j \cos^2 i \qquad (9)$$

The sliding force is given by:

$$T = G \sin i = \Sigma\gamma_j h_j \cos i \sin i \qquad (10)$$

Since the existing snow slope is statically stable, the condition is given by:

$$\tau_f > T$$

or

$$F_s = \frac{\tau_f}{T} = \frac{\tau_0 + \tau(\varepsilon_v) + \sigma \tan \phi'}{\Sigma\gamma_j h_j \cos i \sin i} > 1 \qquad (11)$$

for shear, where F_s is the safety factor.

Under new precipitation or external force, the critical condition at equilibrium can be given by:

$$\tau_f = T + f \qquad (12)$$

where f is the new snow load or external force acting along the slope.

If snow fails by compression shear, expressions similar to Eqs. (11) and (12) are given by:

$$F_c = \frac{\sigma_c}{\sigma} = \frac{\sigma_0 + \sigma(\varepsilon_v)}{\Sigma\gamma_j h_j \cos^2 i} > 1 \qquad (13)$$

and

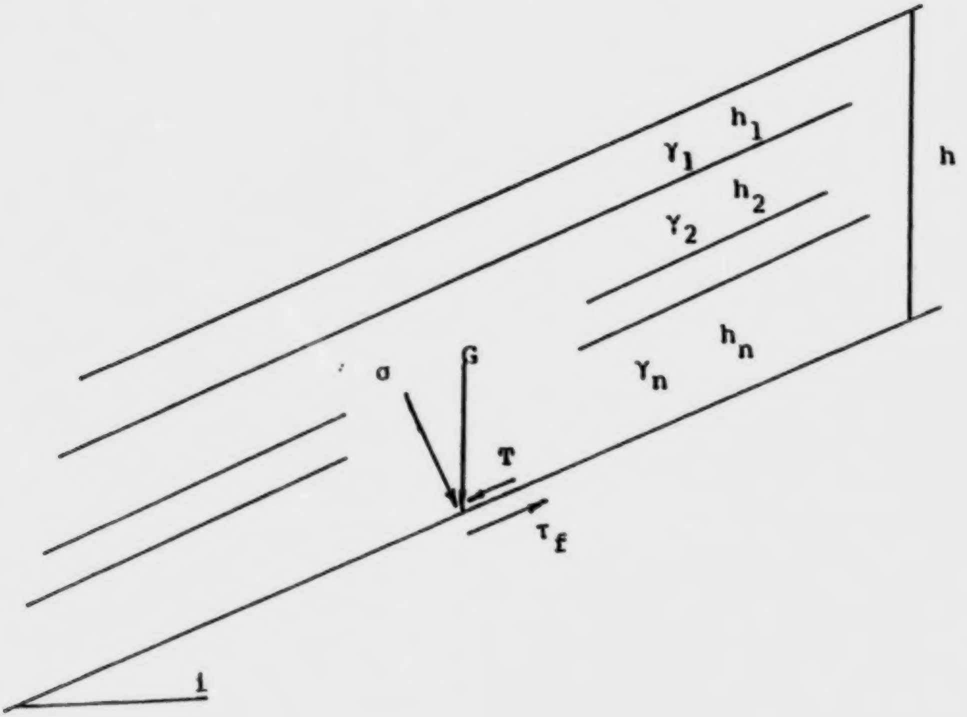
h
h_1
γ_1
h_2
γ_2
h_n
γ_n
σ
G
T
τ_f
i

Fig.9 Forces acting on a plane in infinite snow slope.

$$\sigma_c = \sigma + p \qquad (14)$$

where

p = the additional normal force due to new snow or external force, and

F_c = the safety factor for compression shear.

For an avalanche to occur after shear failure or compression shear failure, the following condition is needed as:

$$\tan i > \tan \phi^* \qquad (15)$$

where

i = the slope angle, and

ϕ^* = the angle of internal friction under a dynamic condition.

Note that the value ϕ^* is approximately equal to the angle of internal friction for granular snow at a high strain rate because the bonding between particles is completely destroyed on the failure plane leading to a dynamic condition.

From the statistical study of avalanches, the minimum slope angle at which avalanches occurred is about 19 degrees. Therefore, the value should be taken as the ϕ^* for the conservative evaluation.

STABILITY ANALYSIS AT Mt. FUJI

On November 19, 1960 a surface snow avalanche occurred on the northern slope of Mt. Fuji, Yoshida Osawa, which involved 41 climbers climbers who were on a training expedition. Unfortunately, eleven of the victims were killed by the avalanche.

According to the description given by the rescued victims, the avalanche had a thickness of about 50 cm, a width of about 30 cm and an ultimate length of more than 2 km. However, the thickness of each of the two layers is not known.

From the meteorological observation at the top of Mt. Fuji, it is deduced that the upper and lower snow layers were one day and seven days' old, respectively. In addition, the temperature records previously observed at Mr. Fuji station indicated that the snow covers were un-melted and poorly metamorphic. Therefore the density and inherent strength of the layers can be predicted using Eqs. (1), (4) and (5).

Figure 10 shows the change in the safety factors until the avalanche occurs, assuming that the initial precipitation is equal for the different aged snows. In the calculation, the values τ_0 and σ_0 were used instead of τ_f and $\sigma_c{}'$, respectively, because the frictional resistance was not predictable. Therefore the actual F_s may be a little higher than that indicated in the figure.

The strain-hardening components appearing in Eqs. (6) and (7) must not be taken into account for the stability analysis of a single snow layer because τ_0 and σ_0 contain the component in terms of time in field. However, if external forces act on the slope, the strain-hardening components should be properly added.

It is seen from Fig. 10 that an existing slope is statically stable without the external force until new snow falls. The new accumulation causes the rapid decrease in the safety factor. It is important that the F_s decreases to 1.15 at the date of avalanche, although the main cause for the avalanche exists in the snow disturbed by climbers.

Thus, stability analysis of dry snow slope becomes possible if the density and strength of snows are properly predicted. In particular, fresh snow avalanche can be easily predicted using the

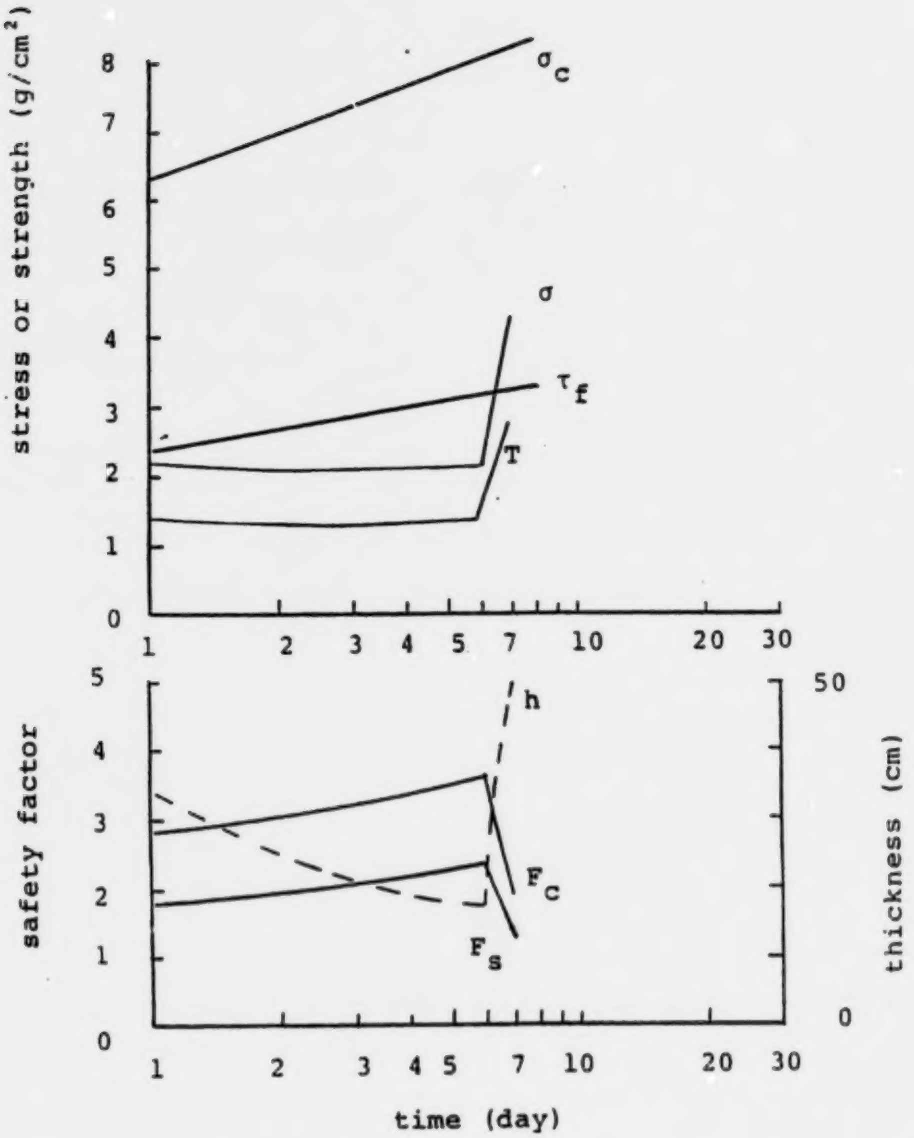

Fig.10 Example of stability analysis for the avalanche which occurred at Mt.Fuji, in November 19, 1960.

density and strength of fresh snow.

Figure 11 shows the critical height for fresh snow at Mt. Fuji. In the calculation, the strain-hardening effects were neglected. The figure indicates that at slope angle greater than $^{\bullet}$, say 20 degrees, the compression shear hardly causes avalanches.

However, an external force of only a few gram per square centimenter decreases the critical height as shown in Fig. 12. Therefore, it is likely that avalanches caused by gust, gun report, explosion of aircraft or other dynamic forces were due to the compression shear.

CONCLUDING REMARKS

The field observation on snow profiles at the same site indicated that there were almost unique relationships between density and time, and between strength and time, for melted-refrozen and un-melted snow layers.

By the time-dependence on the density and strength, which differs for melted-refrozen and un-melted snow layers, there is no unique relationship between density and strength in field condition.

The melting-refreezing in snow cover occurs from the top surface by the regular heating and cooling cycles under the field condition. In seasonal snow covers, the melted-refrozen thickness is restricted by the low thermal conductivity and the effect of latent heat, except in the thawing term. The refreezing process rebuilds and strengthens the structure of snow independently whether the density increases or not. This also provides no unique relationship between density and strength in snow.

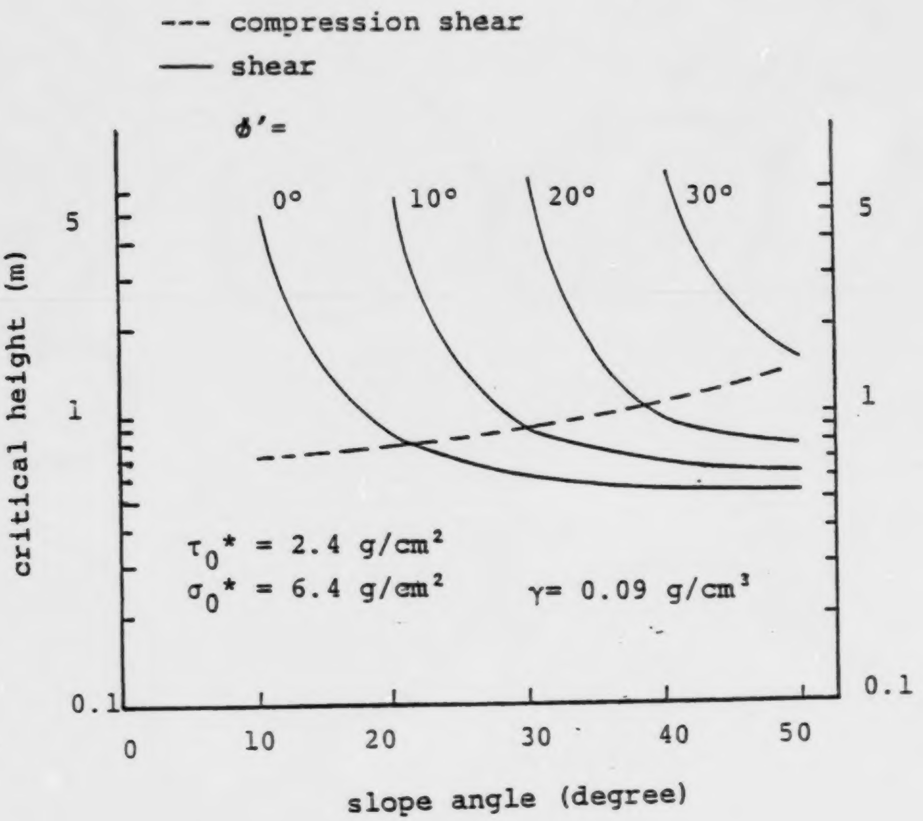

Fig.11 Prediction of fresh snow avalanche at Mt.Fuji.

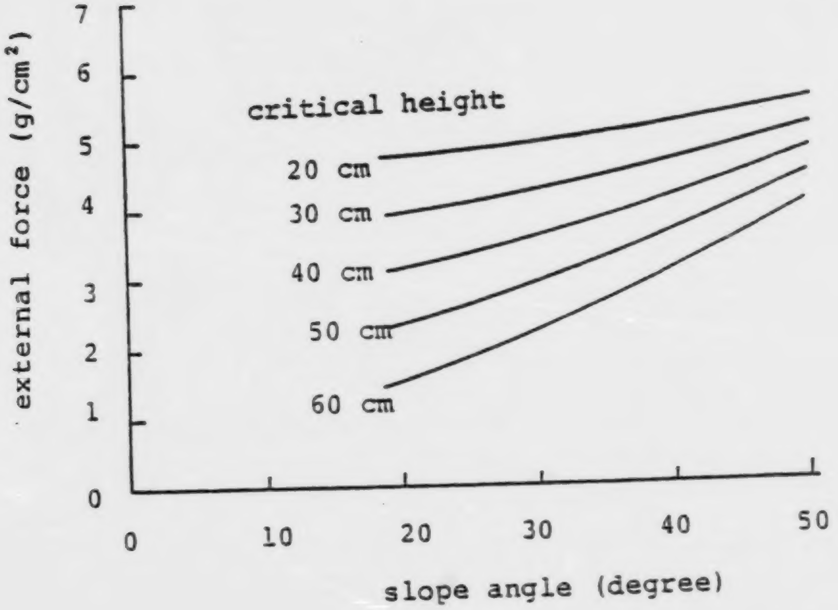

Fig.12 Critical height of fresh snow cover under normal forces applied externally.

By using the density-time and strength-time relationships, which can be obtained as regional properties under a regional condition, the stability analysis based on geometric statics can be achieved, though some consideration on the strength characteristics of snow is required, as was made in this study.

For the stability analysis, two different failures, i.e., shear and compression shear, should be examined for their distinctive mechanical behaviour under loading.

ACKNOWLEDGEMENTS

The field observation made was helped by Messrs. K. Yamashita and K. Emoto. The author is grateful to them for their assistance.

REFERENCES

Butkovich, T.R. (1956) Strength studies of high-density snow. USA CRREL Research Report #18.

Fukue, M. (1979) Mechanical performance of snow under loading. Tokai University Press, p.136.

Fukue, M., Yamashita, K. and Emoto, K. (1982) Physical and mechanical properties of seasonal snow cover with multiple layers at the foot of Mt. Fuji. J. Marine Sci. and Technology, Tokai University, No. 15, pp.181-193.

Fukue, M. and Yong, R.N. (1985) Mechanical and physical properties of snow, prepared for NRC Workshop on Snow Property Measurement, Chateau Lake Louise, Alberta.

Nakaya, U. and Kuroiwa, D. (1967) Physical properties and internal structure of Greenland snow. Physics of Snow and Ice, Proc.Int. Conf. on Low Temp. Sci., Vol.1, Part 2. Ed. Oura, H., The Inst. of Low Temp. Sci., Hokkaido University, pp. 953-971.

APPENDIX

If snow layers are very soft or thin, the unconfined compressive and shear strengths can be obtained by techniques shown in Figs. A-1 to A-4.

In Fig. A-1, the compressive failure plane would be perpendicular to the direction of applied force. Therefore, the effect of variable specimen height is not very important.

It is noted that quick loading in every technique shown in the figures should be used for obtaining the inherent strength.

When the snow layer is very thin, the blade penetrating technique may be useful (Fukue, 1979). The technique shown in Fig. A-2 has been well-examined in laboratory and field conditions (Fukue et al., 1982) and good correlation between blade penetrating resistance and unconfined compressive strength has been obtained.

The evaluation of shear strength is of primary importance for the stability analysis of snow slopes. If snow specimens can be easily formed, the technique shown in Fig. A-3 is applicable, though there are some difficulties in cutting the snow block and for the testing operation.

The most practical and reliable technique for evaluating the inherebnt shear strength is to apply a force on a large cut specimen as illustrated in Fig. A-4.

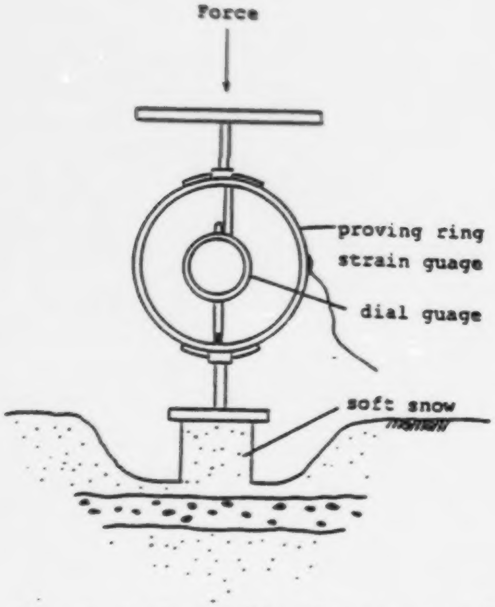
Force
proving ring
strain guage
dial guage
soft snow

Fig.A-1 Unconfined compression test on soft snow (Fukue *et al*,1982).

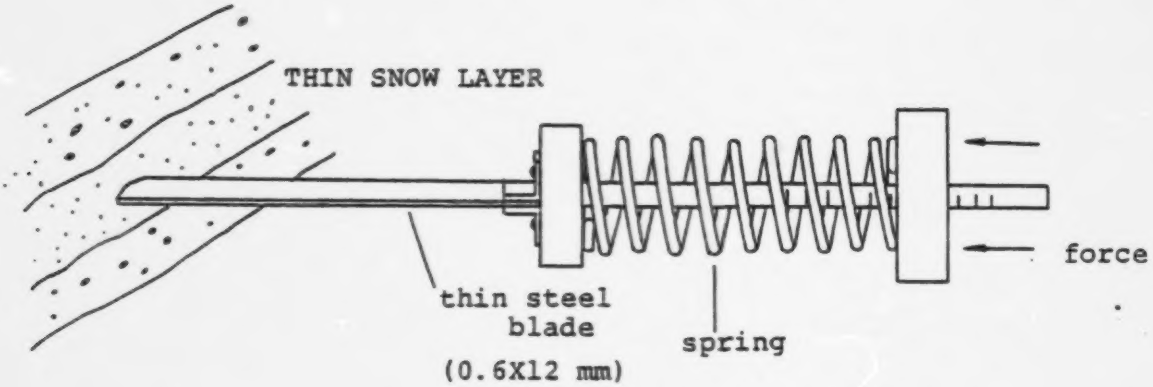
THIN SNOW LAYER
thin steel blade
(0.6X12 mm)
spring
force

Fig.A-2 The blade penetrating technique for evaluation of the compressive strength of thin snow layer (Fukue,1979 and Fukue *et al*, 1982).

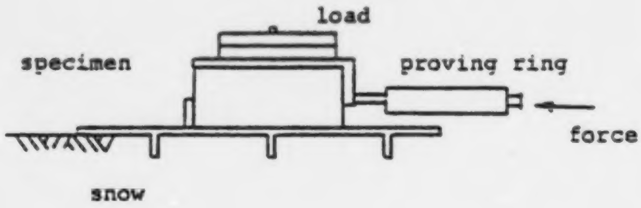
load
specimen
proving ring
force
snow

Fig.A-3 Direct shear test on snow block.

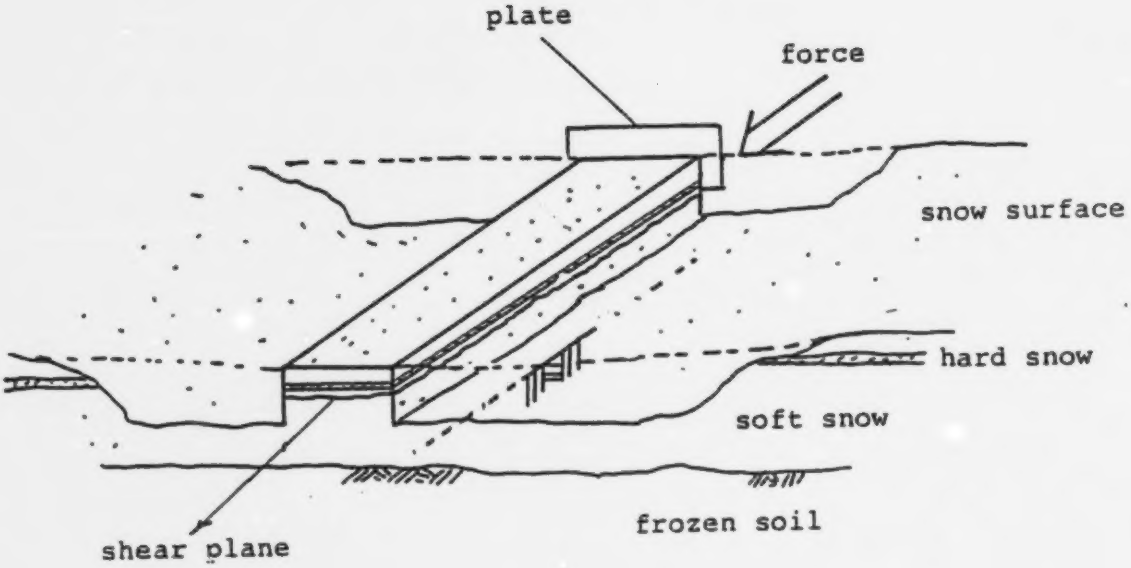
plate
force
snow surface
hard snow
soft snow
frozen soil
shear plane

Fig. A-4 Direct shear test on large specimen (Fukue *et al*,1982).

USE OF INDEX MEASUREMENTS IN STUDIES OF SNOW UNDER VERTICAL LOADING

by

G.J. Irwin

Defence Research Establishment
Suffield, Alberta
Canada

presented at

SNOW PROPERTY MEASUREMENTS WORKSHOP

Lake Louise, Alberta

1-3 April, 1985

TECHNICAL MEMORANDUM 140

Compiled By

P.R. Kry

NRCC 27594

USE OF INDEX MEASUREMENTS IN STUDIES OF SNOW UNDER VERTICAL LOADING

G.J. Irwin
DEFENCE RESEARCH ESTABLISHMENT SUFFIELD, ALBERTA

ABSTRACT

Interest has recently been focussed upon deformation processes in deep snow for the purpose of predicting vehicle performance in known environmental conditions. Of particular interest is the identification of environmental factors that control sinkage of vehicles. To aid in identifying these factors, use has been made of the plate penetrometer to produce deformation zones or pressure bulbs. These can easily be brought into contrast by a technique of spray paint deposition. It has been found that resistance to snow indentation or sinkage at a slow continuous and uniform rate under moist conditions may be dependent on several factors. These are listed as densification, resistance to bulb spreading along layer boundaries, reaction of snow layer boundaries obstructing bulb development in the downward direction, and shear resistance at the bulb periphery. Index properties of snow such as development of pressure bulb geometry under a loading plate penetrometer, plate pressure versus depth profile in initially undisturbed snow, bulb hardness and bulb density serve as reliable indicators of snowpack behaviour under vertical loading. With greater precision in measurement of these indexes, an improved understanding of resistance of snow under mechanical load in the natural environment should be feasible.

Presented at Workshop on Snow Property Measurement
Lake Louise, Alberta, 1-3 April 1985

INTRODUCTION

The index properties of snow provide not only a convenient basis for classification, but also an important means of making correlations between snow quality and response to mechanical loading in applications to the study of oversnow vehicle mobility. In the present study, indexes considered to represent snow properties that control vehicle sinkage have been identified. Focus is placed on observations of mechanical deformation of deposited snow which was initially in an undisturbed state. If properly utilized the indexes should in the particular application envisaged allow for prediction of vehicular sinkage with a minimum of manually obtained field input data.

METHODS

The indexes of interest are snow hardness, snow density, and snow strength. Hardness and density in a deep snowpack were measured in accordance with conventional snow pit methods. Thus the implements used were respectively a Canadian Snow Hardness Gauge and a cylindrical snow sample cutter of volume 0.25 liters. Strength was measured mainly by recording the resistance to snow deformation by vertical loading of a manual plate penetrometer. The latter device was equipped with exchangeable circular platens of diameter 10 and 15 cm. The displacement rate employed was about 2 cm/second while the snow ambient temperature was close to 0°C.

The application of the plate penetrometer to a hitherto undisturbed snowpack usually produces a zone of deformation below the platen. The zone is often referred to as a pressure bulb. It is the nature of this bulb which is the focus of our attention.

RESULTS AND DISCUSSION

As can be seen in the following sequence of slides (Figures 1a to 1j) increasing penetrometer plate indentation in deep snow causes generally increasing dimensions of the pressure bulb. For this slide

FIGURE 1

Series of indentations by a vertically loading manual penetrometer with plate diameter 0.1 m into a deep snowpack. Plate loading produced pressure bulbs over a range of pressures from 4.4 to 38 kPa.

Note in Figure 1a indentation pressures in kPa are from right to left 4.4, 8.7, 17, 13, 21 and 26.

In Figure 1b indentation pressures in kPa are from right to left 21, 26, 30, 34, 38.

Figures 1c to 1j are close-up views of the pressure bulbs resulting from the above penetrometer indentations.

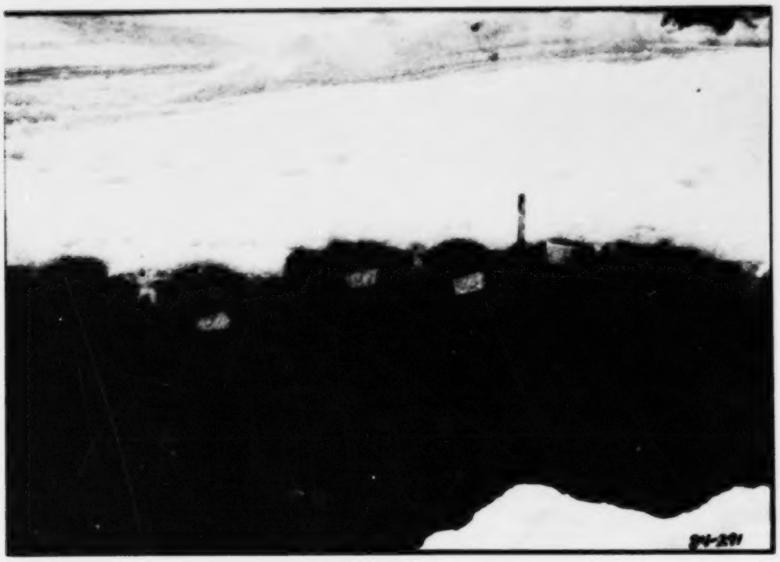

Figure 1a

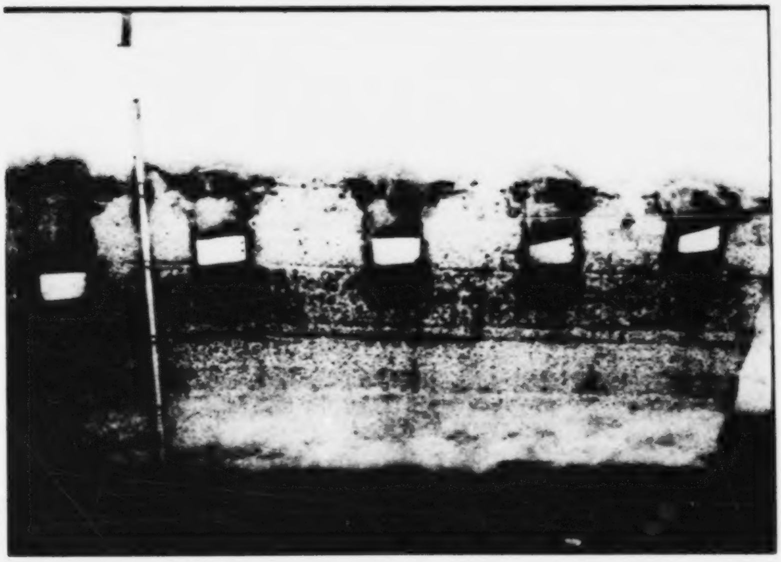

Figure 1b

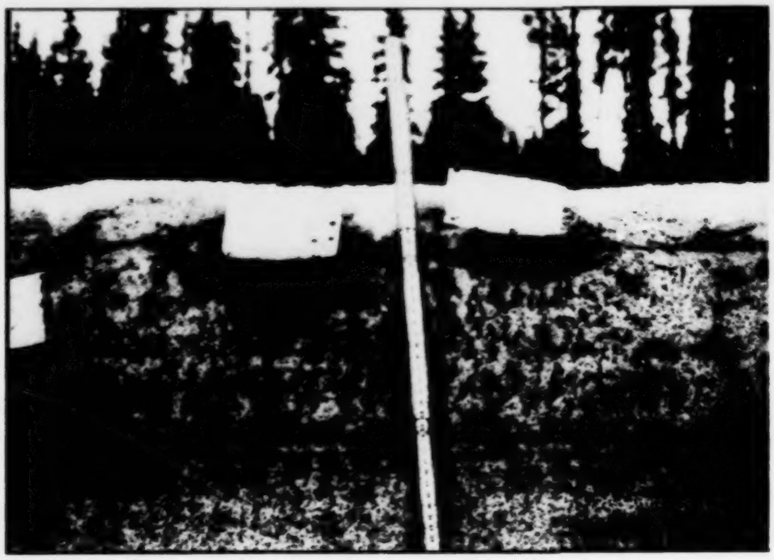

Figure 1c

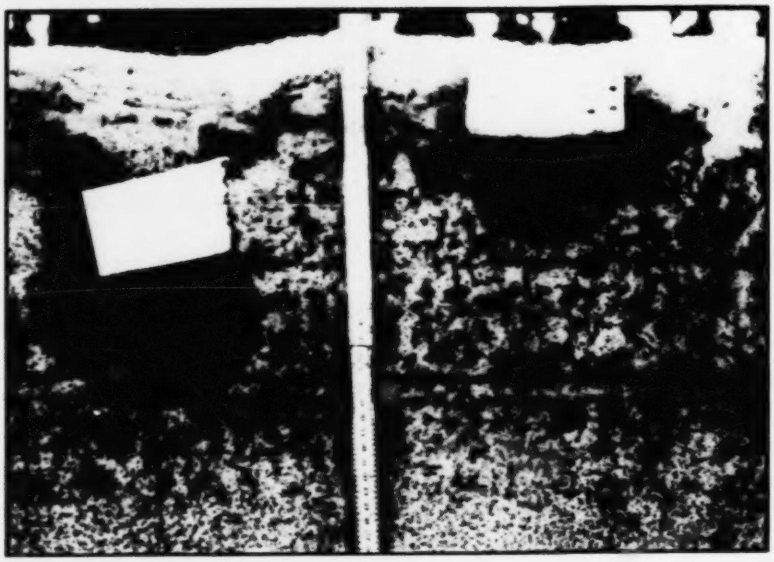

Figure 1d

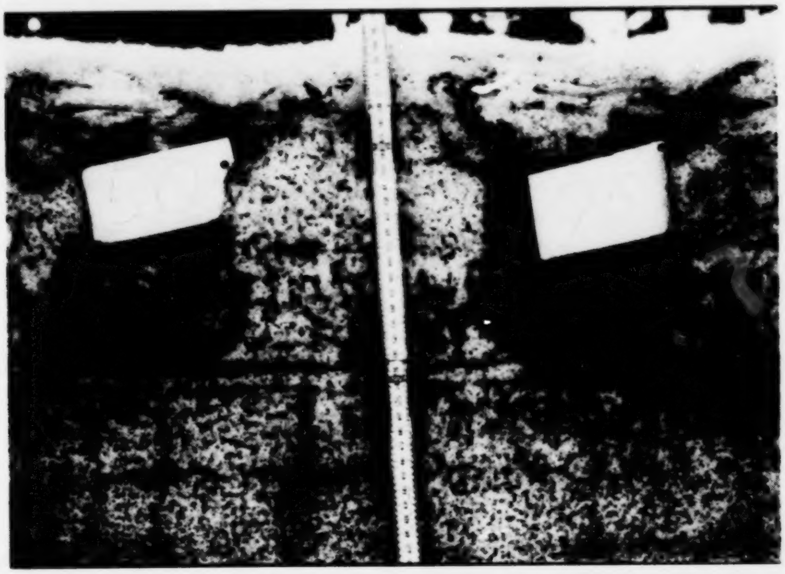

Figure 1e

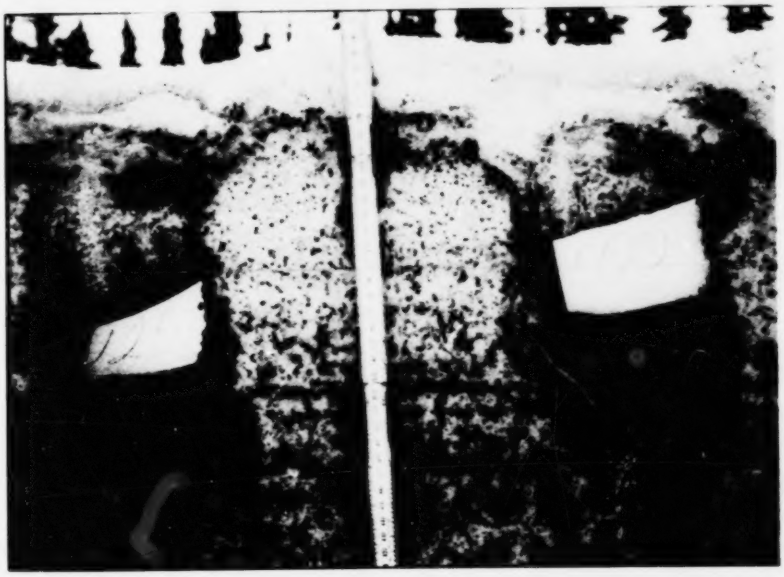

Figure 1f

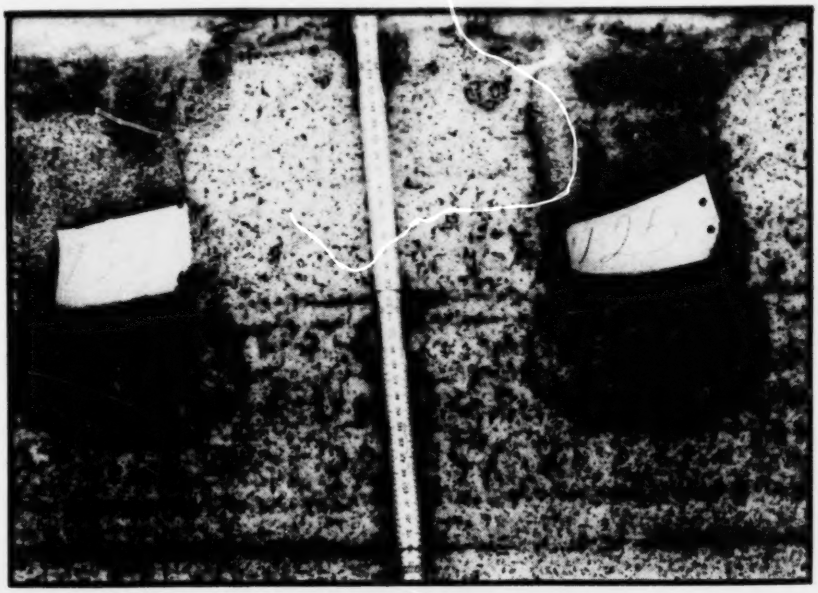

Figure 1g

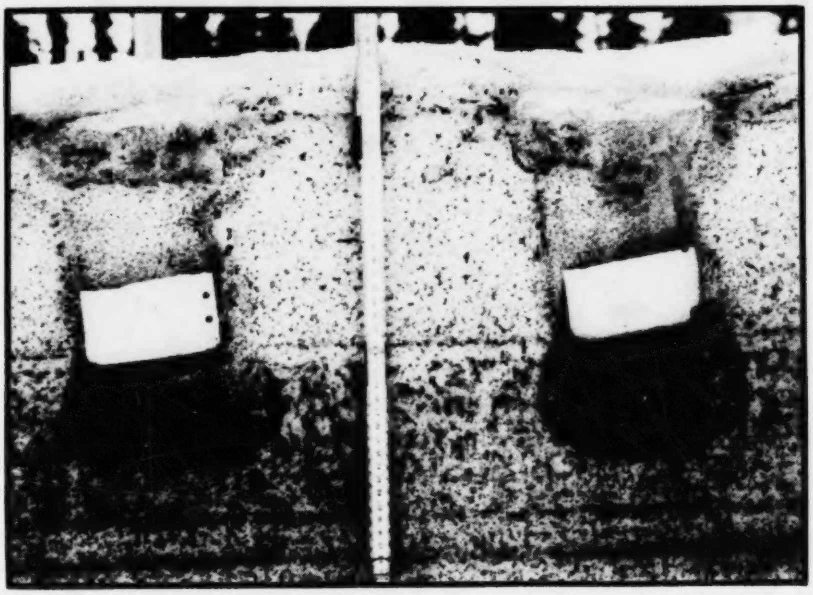

Figure 1h

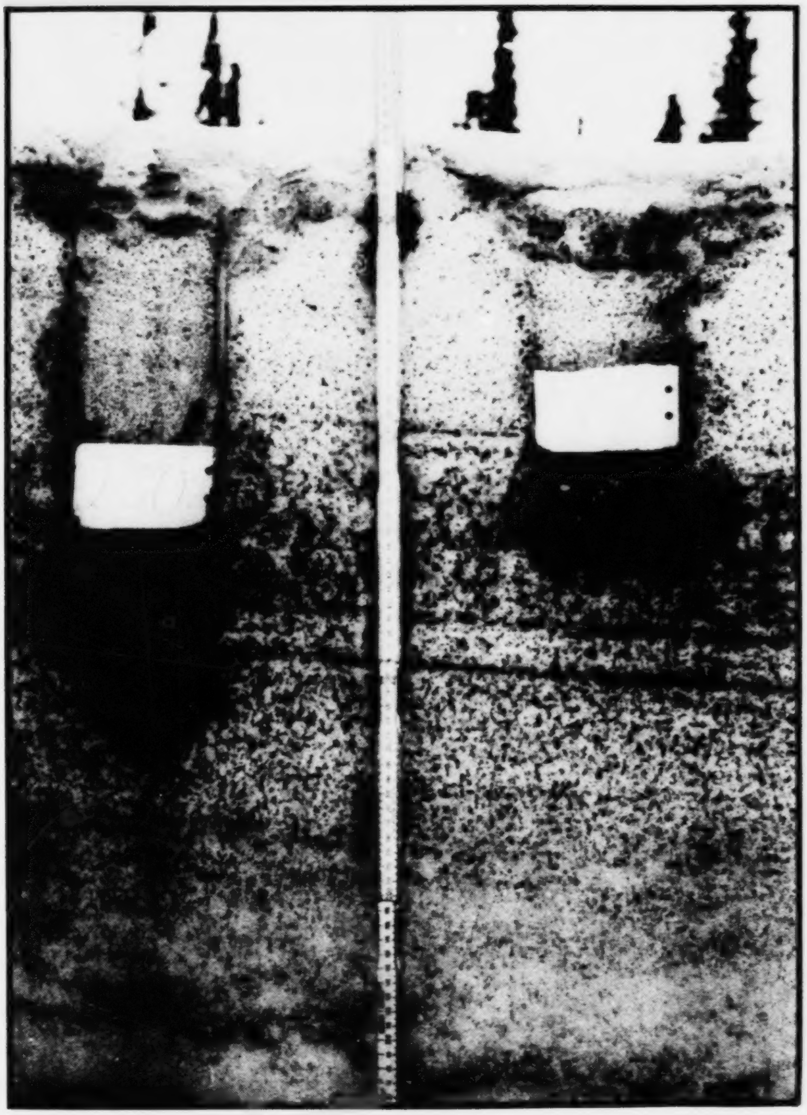

Figure 1j

sequence a snow pit was excavated so as to section the indentation left by the plate penetrometer. A uniform application of black spray paint around pressure bulb zones followed by a period of contrast development (usually a few hours in natural sunlight at air temperatures of about 0°C) produced the vivid features shown here. The labels at each indentation refer to meter readings which are proportional to applied penetrometer load.

By the concentration of spray paint globules in discrete zones the snowpack is seen to consist of multiple layers. It is apparent that by the application of penetrometer load, the downward progression of the pressure bulb is intermittently halted at layer boundaries. A given boundary evidently offers a resistance to puncture by the pressure bulb. With the build up of pressure against the boundary, the pressure bulb tends to spread out along the plane of the layer boundary. Puncture eventually takes place and the cycle is repeated as the lower extremity of the bulb approaches the next lower layer boundary. A source of resistance to indentation is evidently that due to pressure bulb compression against at least some layer boundaries of the snowpack. The phenomenon probably accounts for irregularities in a typical pressure-sinkage relation. Such a relation is best recorded by a bevameter plate penetrometer the results of which are exemplified in Figure 2. Superimposed on the bevameter trace is a smooth curve fit line. It should be noted that an extensive review of snow mechanics including properties of pressure bulbs was carried out by Bader and Kuroiwa (1962). The present report provides some additional illustration of those properties.

It is believed that the pressure bulb could offer a useful medium for assessment of the above mentioned indexes. At the same time bulb and index phenomena together offer additional insight on the nature of snow resistance to vertical loading.

Let us look at some of the classification profiles of undisturbed snow covering the period in which pressure bulb observations were made. Profiles of density and hardness are consistent in revealing local maxima at a depth of about 0.2 m in a 0.8 m cover of warm snow which is on a warming

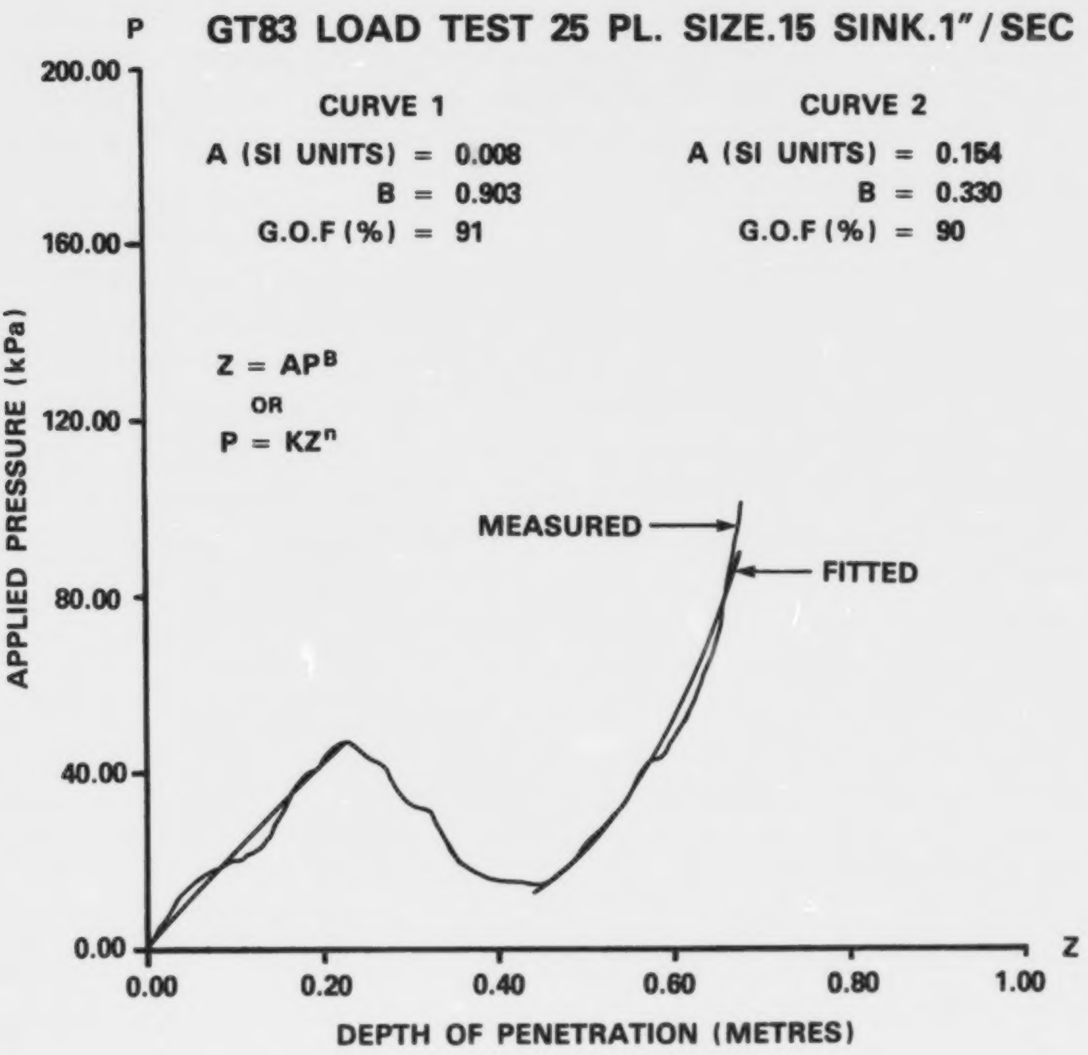

Figure 2

Pressure-depth profile with bevameter

trend (see Figure 3). Yet at or near this level the snow structure contained no ice crusts but only a progression of settled to granular condition with depth. The previous figure (Figure 2) of the bevameter loading profile confirms in terms of strength this undisturbed profile of snow structure. The local maximum of pressure occurs at a depth of about 0.2 m. Thus resistance to plate penetration increases with sinkage to a point of snow collapse. The pressure-sinkage relation is renewed with an even steeper rise as the plate approaches the base of the snowpack.

To study details of pressure bulb development index measurements were taken below separate indentations of two sizes of manual plate penetrometer. For this, tables (I and II) were drawn up listing sinkage, bulb density by calculation and measurement, bulb volume, work or energy consumed in quasistatic indentation by the penetrometer, energy per unit total deformed volume of snow, and applied penetrometer pressure. Calculations were based on geometric measurements of pressure bulbs. The data in Tables I and II are the result of three sets of penetrometer tests using plate diameter as parameter.

Graphs taken from the tables (Figures 4 to 7) indicate that:

(1) pressure (P) and energy per unit volume (E/V) are strongly in parallel when plotted against sinkage,

(2) with respect to P there appears to be very little plate size effect,

(3) energy (E) shows greater than an order of magnitude increase with sinkage,

(4) density (G) and volume of the bulb (Vol) show a decidedly slower rate of increase with sinkage than does energy,

(5) there is a gap in the data set of the larger penetrometer plate between 0.1 m and 0.2 m sinkage,

(6) though no gap in data is apparent with sinkage of the smaller plate, bulb density shows a distinct drop (Figure 6) near 0.1 m sinkage before density again increases with further sinkage.

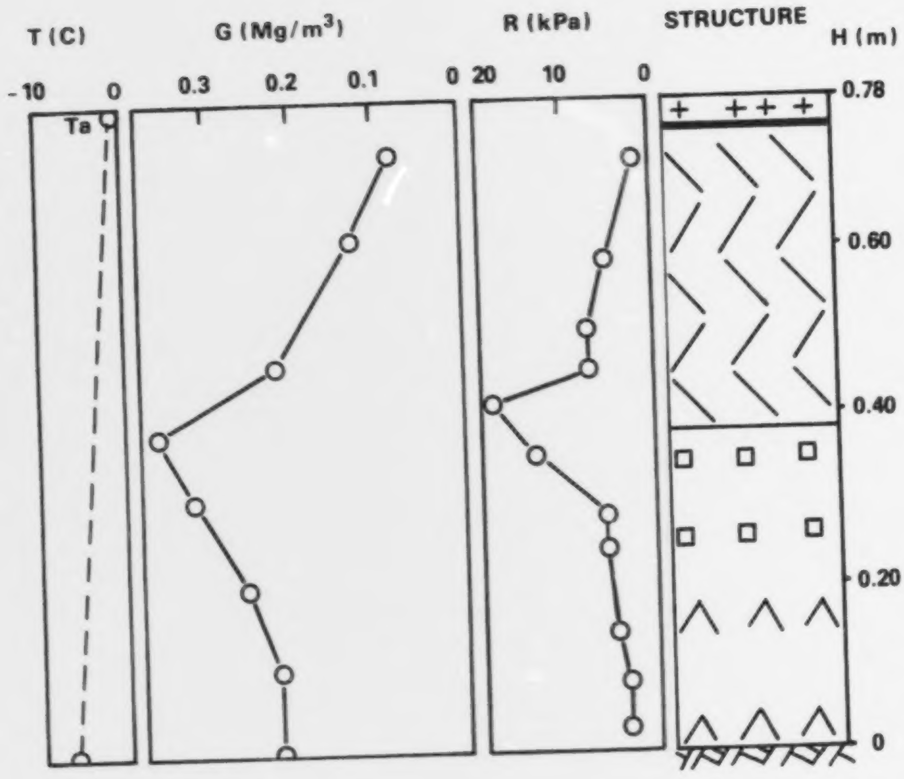

Figure 3

Classification of the snowpack in its initial state

TABLE I

Index Estimates and Measurements at Pressure Bulb

(Penetrometer Plate Diameter: 0.15 m)

z $(10^{-3}m)$	G_{calc} (Mg/m^3)	Vol $(10^{-3}m^3)$	E (N.m)	E/V (kN/m^2)	P (kPa)
18	0.36	0.44	0.34	0.44	2.1
37	0.37	0.83	1.9	1.3	6.0
43	0.37	0.99	1.9	1.1	6.0
93	0.39	1.90	8.0	2.8	9.7
110	0.38	2.40	17	3.8	17.0
200	0.51	2.40	43	7.4	25.0
200	0.46	3.10	57	8.8	32.0
220	0.50	2.90	71	10.5	36.0
190	0.37	4.30	68	8.8	40.0
(Penetrometer Plate Diameter: 0.10 m)					
38	0.45	0.26	0.62	1.2	4.4
64	0.50	0.36	2.2	2.5	8.7
130	0.56	0.61	6.5	4.0	13.0
140	0.34	1.80	9.3	3.2	17.0
160	0.44	1.20	14	5.5	21.0
190	0.45	1.30	19	7.0	26.0
210	0.45	1.40	24	8.0	30.0
220	0.48	1.30	29	9.5	34.0
280	0.57	1.30	42	12	38.0

Symbols: z is penetrometer plate sinkage

G_{calc} is bulb density by estimation

Vol is bulb volume

E is work of indentation

E/V is work per unit of total volume of disturbed snow

P is applied plate pressure

TABLE II

Index Measurements at Pressure Bulb

(Penetrometer Plate Diameter: 0.15 m)

z	G_{meas}	Vol	R	E	E/V	P
(10^{-3}m)	(Mg/m^3)	($10^{-3}m^3$)	(kPa)	(N.m)	(kN/m^2)	(kPa)
40	0.23	4.9	22	1.4	0.25	4.0
90	0.23	2.2	20	4.7	1.2	5.9
120	0.38	1.0	15	10	3.2	9.7
160	0.36	2.5	54	20	3.6	13.0
160	0.39	2.1	54	24	4.9	17.0
240	0.44	1.9	49	55	7.9	24.0
240	0.40	2.3	54	59	9.2	28.0

Symbols:

G_{meas} is bulb density by measurement

R is hardness of pressure bulb

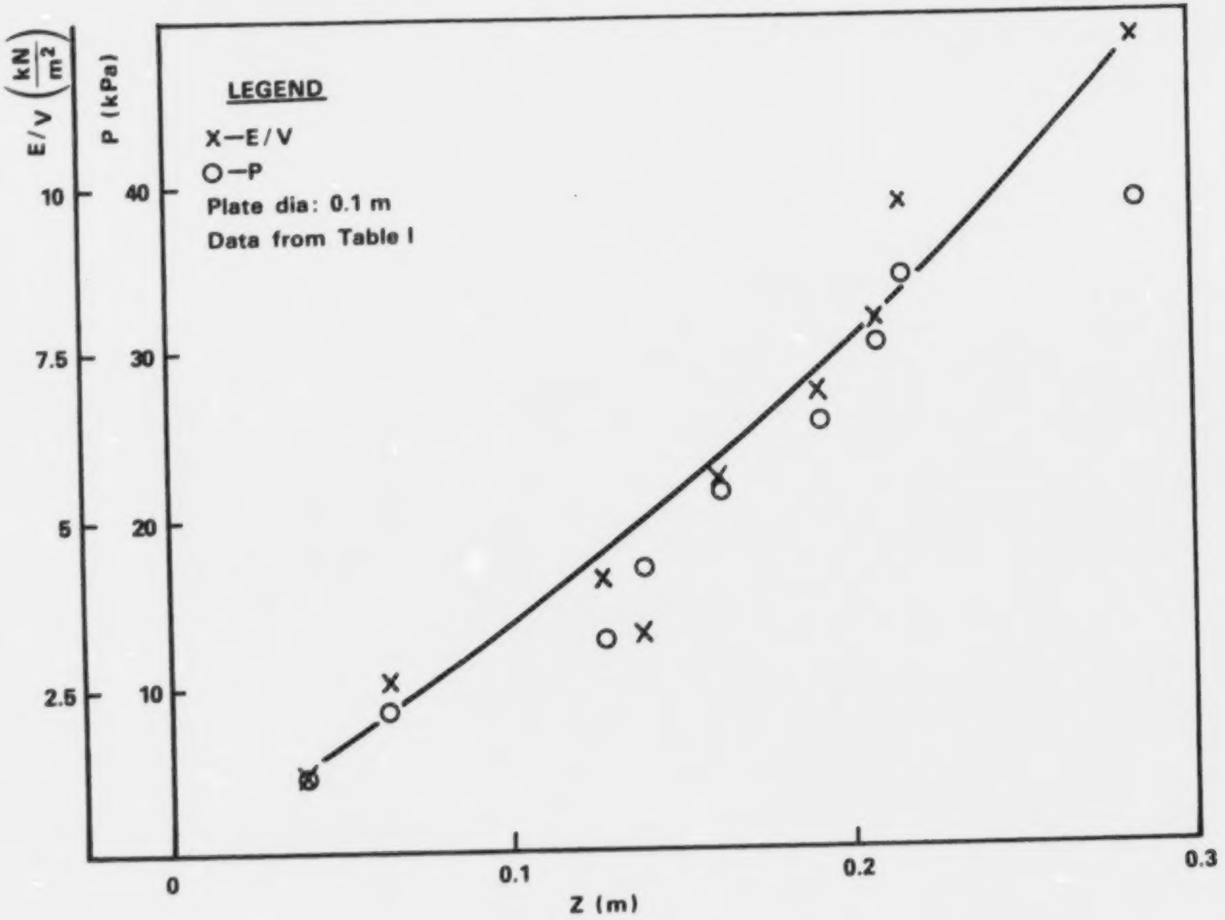

Figure 4

Comparison of manual penetrometer plate pressure and work of penetrometer indentation per unit volume both as a function of sinkage (based on plate diameter of 0.1 m).

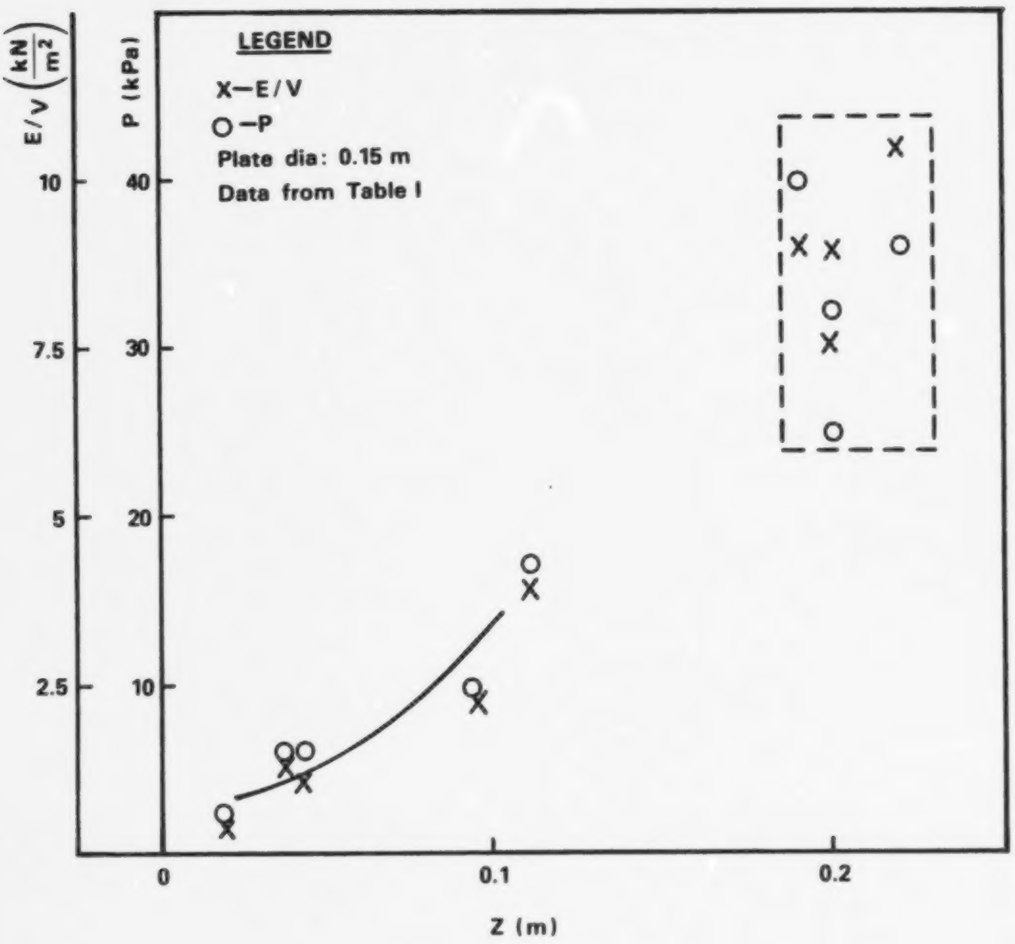

Figure 5

Comparison of manual penetrometer plate pressure and work of penetrometer indentation per unit volume as a function of sinkage (based on plate diameter of 0.15 m).

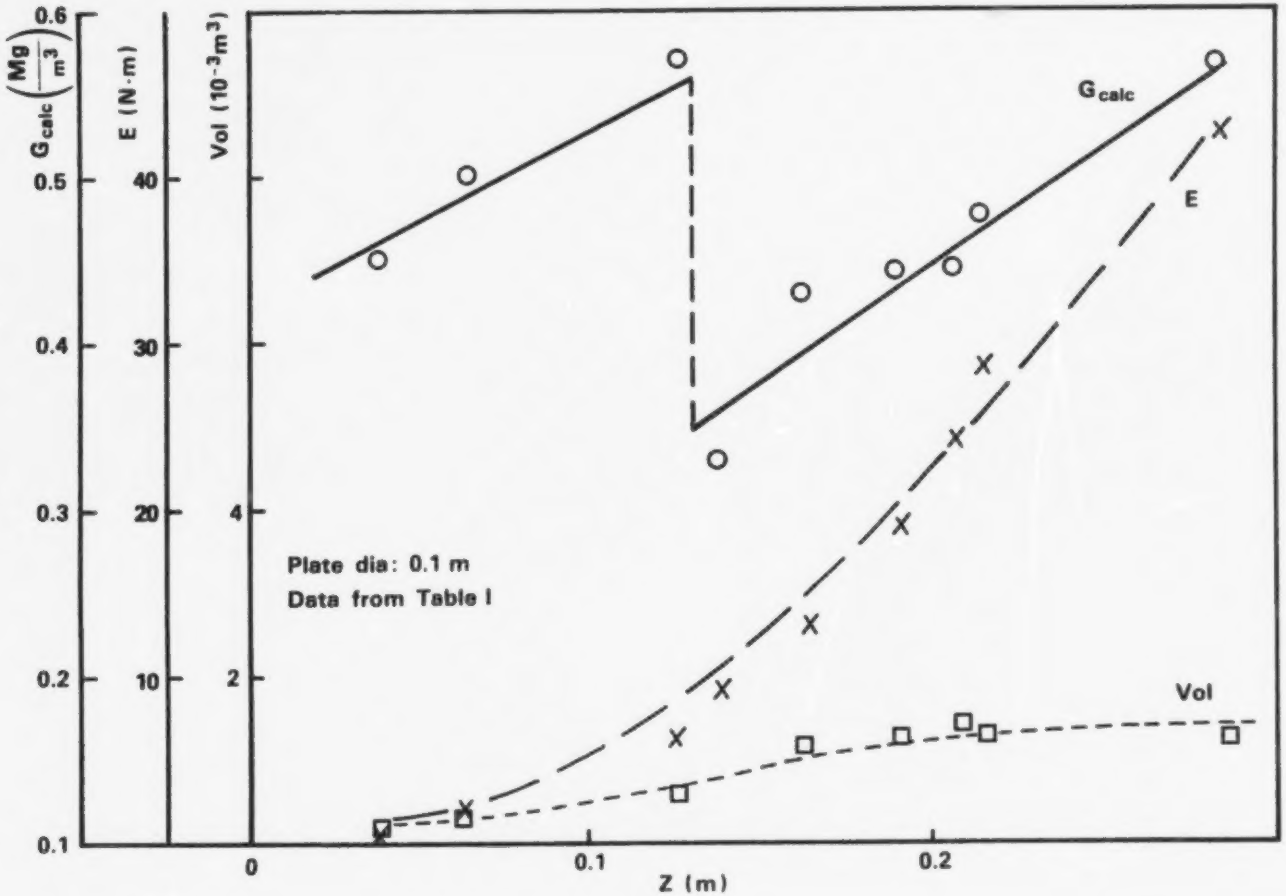

Figure 6

Relationships of estimated bulb density, work or energy of manual penetrometer indentation, and bulb volume to penetrometer plate sinkage (based on plate diameter of 0.1 m and geometric measurements of pressure bulbs).

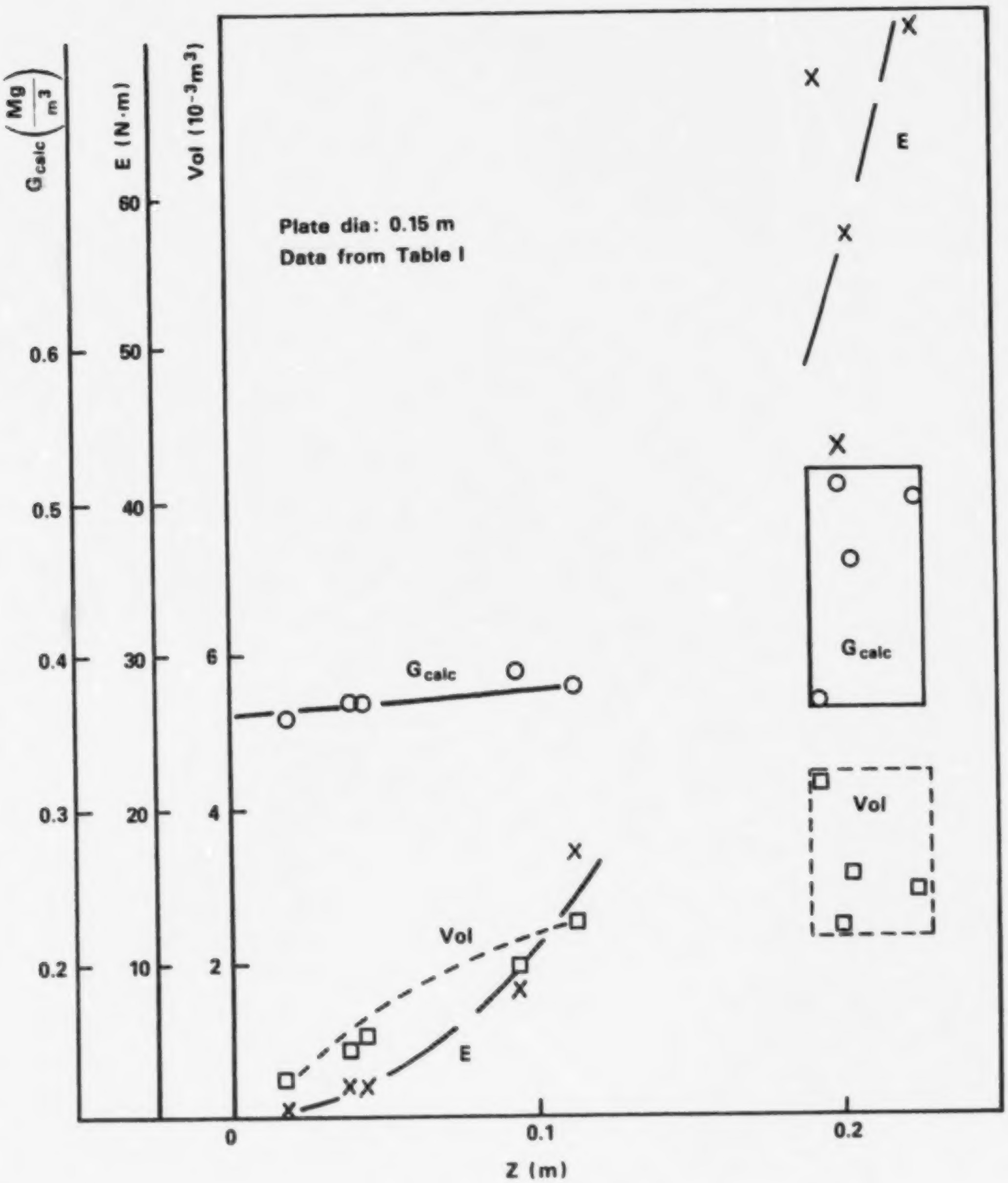

Figure 7

Relationships of estimated bulb density, work or energy of manual penetrometer indentation, and bulb volume to penetrometer plate sinkage (based on plate diameter of 0.15 m and geometric measurements of pressure bulbs).

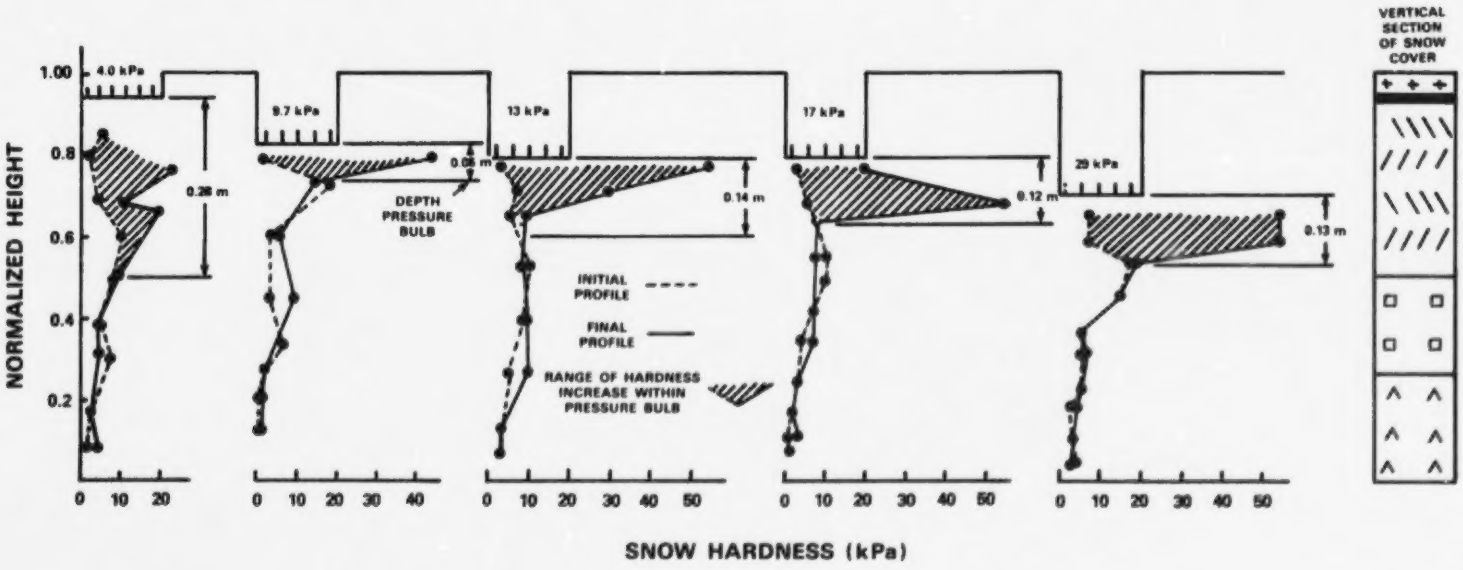

Figure 8

Range of hardness increase due to snow deformation below a penetrometer plate

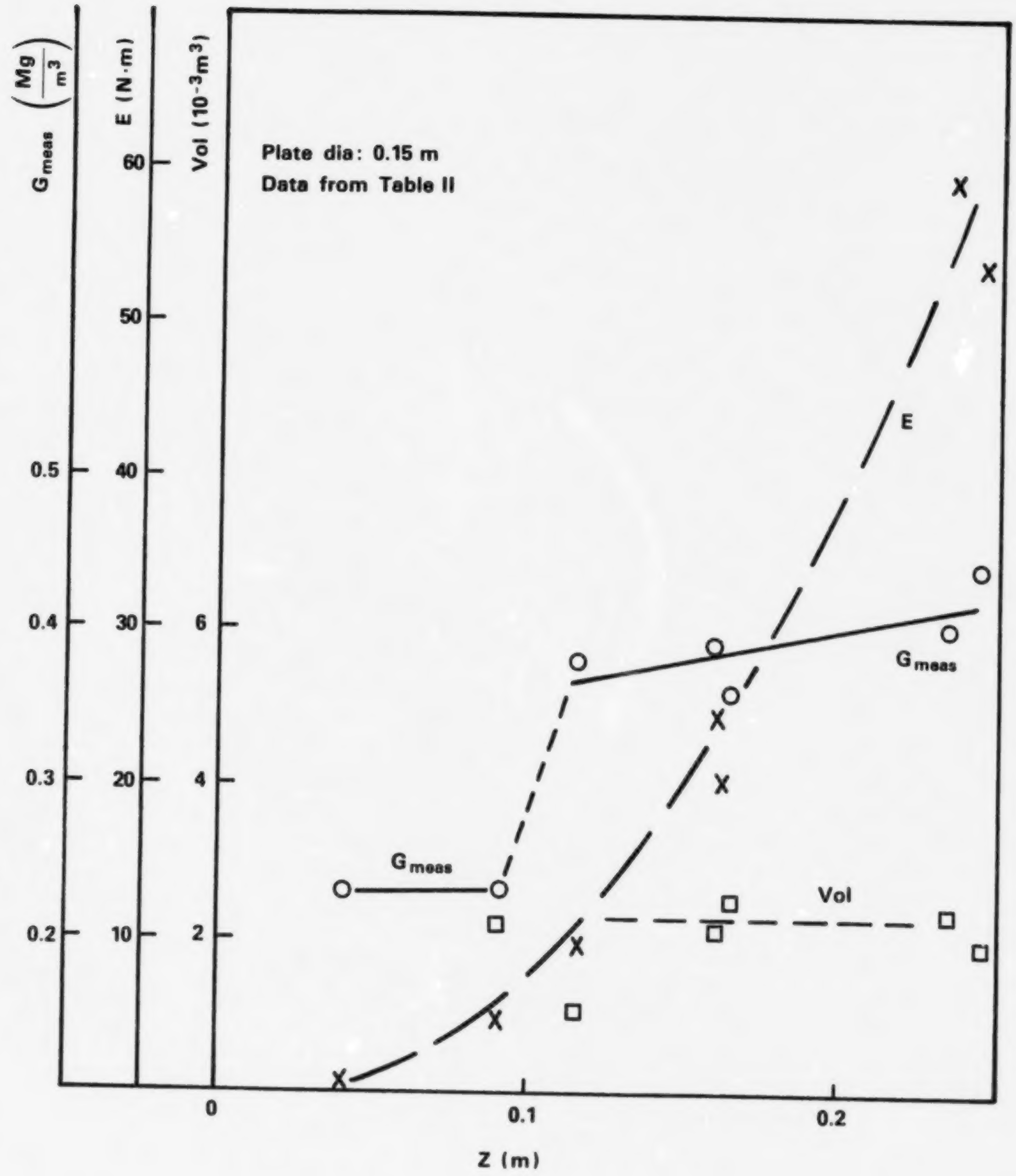

Figure 9

Relationships of measured bulb density, work or energy of manual penetrometer indentation, and bulb volume to penetrometer plate sinkage (based on plate diameter of 0.15 m).

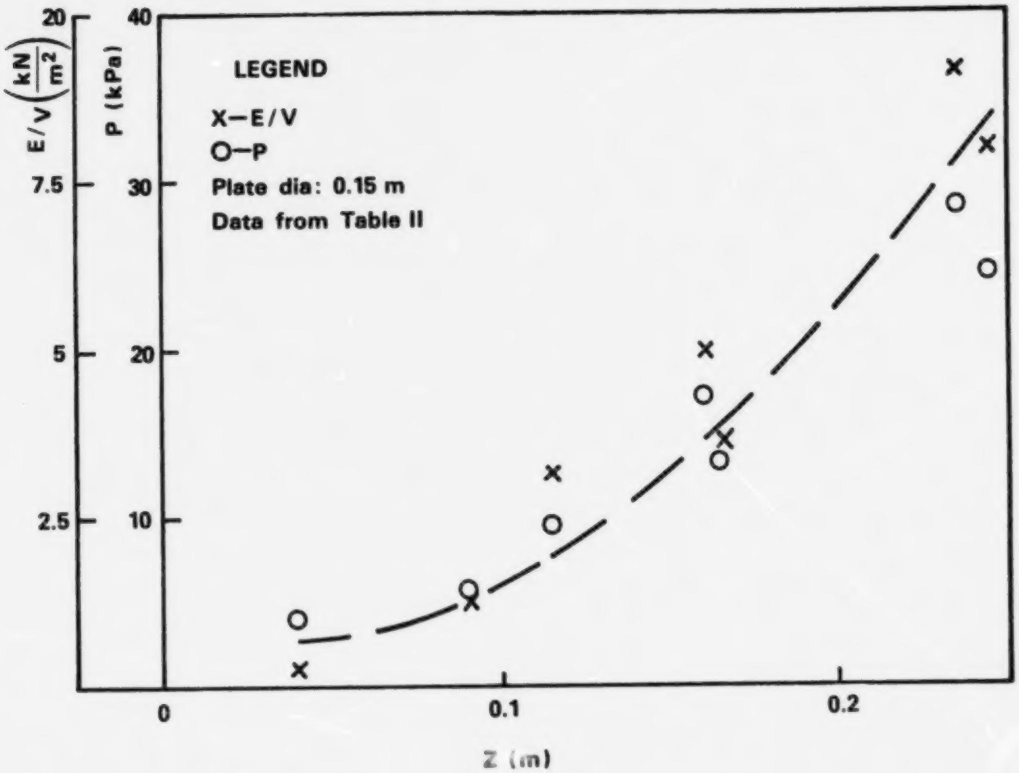

Figure 10

Comparison of manual penetrometer plate pressure and work of penetrometer indentation per unit volume as a function of sinkage (based on a plate diameter of 0.15 m).

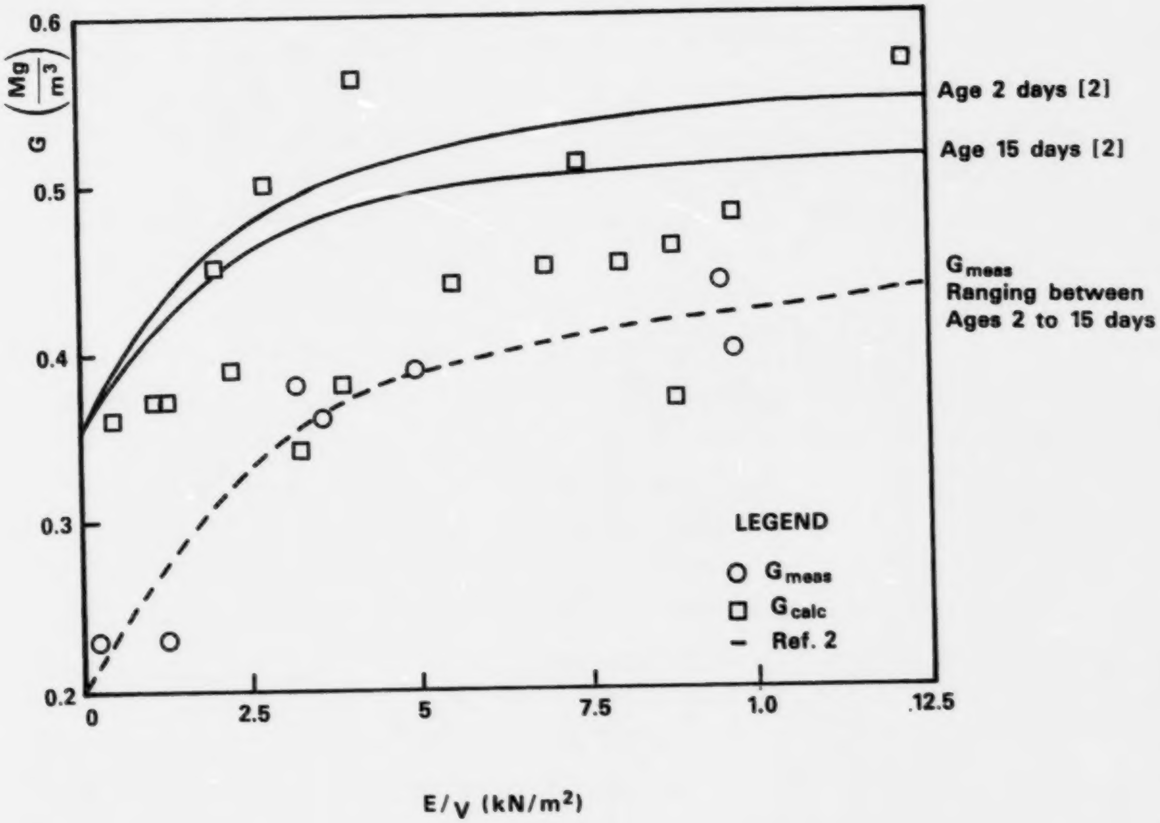

Figure 11

Comparison of laboratory measurements of bulb density vs energy per unit volume to field measurements and estimates of bulb density vs energy per unit volume.

Thus P is a consistent indicator of snow strength and sinkage energy consumption per unit of total deformed volume. The bevameter, for precision in P, is to be recommended over the manual penetrometer however. The latter often will not detect snow collapse effects. Furthermore pressure readings do not strictly correspond to sinkages because of a lack of adequate control. This is seen in Figure 1j where in manual operation applied penetrometer pressure increases from 34 kPa (175 units) to 38 kPa (200 units). The breakthrough strength of the resisting layer boundary is 38 kPa. The corresponding sinkage value should be that for the lower load. A correction would be appropriate but is difficult to apply to manually obtained data.

The relatively slow rise in bulb density and volume with sinkage as compared to energy E, may indicate either that resistance is only slightly controlled by densification or that changes in E are very sensitive to changes in G. At a given sinkage the bulb, if compressed against a layer boundary, is forced to spread out into a snow medium that is denser and hence stronger at that level than is the medium at an upper level. In this way densification and resistance to bulb spreading may both be contributing factors to increases in sinkage resistance during plate indentation. Related to bulb compression is the reaction transferred through the bulb structure from a layer boundary, not yet perforated, to the plate or platen of the loading penetrometer. In addition shear resistance at or near the bulb periphery may be taking place. This derives from the displacement of a high density (bulb) medium past a low density undisturbed medium. The concavity of layer boundaries within the pressure bulbs of Figure 1 are probably a consequence of a normal plate pressure distribution from maximum at center to a low value at the plate edge. It should be noted that Brown (1981) has made theoretical predictions of vehicular power requirements in deep snow based on a model of shear at the pressure bulb wall and within the bulb. However, the idealized rectangular cross section of the bulb on which his model operates, deviates substantially from the shapes observed here.

Measurements of density within the pressure bulb were made directly along with snow hardness in a series of pressure-sinkage measurements using a manual (large plate) penetrometer (see Table II). Hardness in Figure 8 is seen to initially increase rapidly with pressure sinkage then level out. Measured density behaves in a similar manner (Figure 9) while energy of sinkage rises through two orders of magnitude. Again it would appear that sinkage resistance is, at least in part, due to densification of the pressure bulb. Other workers (Abele and Gow, 1975; Brown, 1981; Yong and Metaxas, to be published) have indicated that sensitivity to density change exists and critically depends on initial snow density. Such a sensitivity may be corroborated in Figure 9 in which E rises substantially after a plate sinkage of 0.1 m. Snow possibly collapses from an interim high density value during sinkage at 0.1 m. A densification process recurs beyond 0.1 m sinkage and E correspondingly rises exponentially. Note in Figure 10 that P again parallels development of E/V with sinkage.

Yong and Metaxas have reported a three dimensional laboratory based relationship between G, snow age, and E/V using a deformation rate of 0.58 cm/second and a snow temperature of -13°C. The relationship is considered in principle to serve as an interim step toward a practical application to vehicular sinkage prediction. Given that the snowpack in the field is of an approximate age of 2 to 15 days, a plot of Gcalc and Gmeas vs E/V (Figure 11) provides a scatter of results displaced from the G vs E/V relationship observed in a more controlled manner by Yong and Metaxas. The initial density in the field is much lower than that employed in the laboratory. Furthermore the snow temperature is relatively warm and the displacement rate is much higher. Such differences probably account for the disparity between field and laboratory results. The scatter in field results particularly where G was estimated may be related to the fact that age and initial density profile are not uniform.

To gain further insight on pressure bulb behaviour, refinements should be made in hardness and density sampling methods. We may thus learn whether densification is uniform and synonymous with increasing loading resistance in a deep snowpack. Refinement in hardness sampling may be more easily achieved technically than density sampling and should serve as an indicator of density behaviour provided sintering effects are not immediately significant. Laboratory methods should be developed to isolate and quantify the various factors contributing to load resistance.

SUMMARY

In summary the following comments may be made:

1. Mechanical indexes have been used in a study of pressure bulb development.
2. The indexes employed have been snow strength (i.e. resistance to a manual plate penetrometer), hardness, and density.
3. Snow strength, P(z), consistently parallels the energy per unit volume relationship, E/V(z), with penetrometer sinkage (z). The parallel between P and E/V may be a key element for the prediction of vehicular sinkage. As a predictor P(z) would serve as a useful index.
4. With plate sinkage, pressure bulb density and hardness approach stable values. It is not clear from the indexes however, as to the relative importance to sinkage resistance that the mechanisms of densification, reaction, resistance to shear and the resistance to lateral spreading offer. This problem may be resolved through greater precision of index measurement and through laboratory studies of simulated snowpack structures.
5. Some aspects of pressure bulb behaviour under penetrometer loading have been observed through the use of spray paint contrast. Photographic evidence shows that snow layer boundaries contribute to loading resistance by obstructing downward progression of the pressure bulb and forcing it to densify to some small degree and to spread laterally. It is noteworthy also that layer boundaries are contoured within pressure bulbs. Such contouring probably mirrors loading pressure distribution below the plate of the penetrometer.

ACKNOWLEDGEMENT

The author expresses his thanks to Mr. J. Fitzgerald of Defence Research Establishment Suffield for photography and some assistance in photographic interpretation.

REFERENCES

1. Bader, H. and Kuroiwa, D., "The Physics and Mechanics of Snow as a Material", CRREL Report II-B, editor F.J. Sanger (1962).

2. Brown, R.L., "An Analysis of Vehicle Power Requirements in Deep Snowpack", J. of Terramechanics 18, No. 3 (1981).

3. Abele, G. and Gow, A.J., "Compressibility Characteristics of Undisturbed Snow", CRREL Research Report 36 (1975).

4. Yong, R.N. and Metaxas, I., "Influence of Age Hardening and Strain-Rate On Confined Compression and Shear Behaviour of Snow", To be published.

ENERGY ANALYSIS OF CONFINED COMPRESSION AND SHEAR BEHAVIOR OF SNOW

by

R.N. Yong

Geotechnical Research Centre
McGill University
Montreal, Quebec
Canada

presented at

SNOW PROPERTY MEASUREMENTS WORKSHOP

Lake Louise, Alberta

1-3 April, 1985

TECHNICAL MEMORANDUM 140

Compiled By

P.R. Kry

NRCC 27594

ENERGY ANALYSIS OF CONFINED COMPRESSION AND SHEAR BEHAVIOUR OF SNOW

by

Raymond N. Yong*

ABSTRACT

The problem of assessing the response performance of snow under load is often complicated by the high volume change characteristics of the material. To consider energy transfer from the loading surface to the supporting snow cover or snowpack, and snow behaviour under load in terms of energy of deformation and shear, it is necessary to describe confined compression and shear performances of the snow - recognizing that a large density increase occurs under tractive forces. This study provides experimental input and energy surfaces describing confined compressive and shear effects - related to snow age and initial density.

INTRODUCTION

In the normal compression testing of materials for evaluation of stress-strain relationships, the general procedures used include unconfined compression or triaxial testing of representative test samples. Because loose snow cannot be readily handled without significant disturbance and local shear or collapse, it is generally difficult to assess the shear strength of snow in conventional laboratory testing systems. To minimize or avoid the problems of local collapse, field testing has generally been performed. However, control of pertinent

---

*Director, Geotechnical Research Centre, and William Scott Professor of Civil Engineering and Applied Mechanics, McGill University, Montreal, Quebec, Canada.

boundary and initial conditions in addition to problems of application of load, and proper determination of snow properties in the field have all contributed to hampering the progress of knowledge of snow performance under load.

Observations in the field combined with plate load tests in the laboratory have recently confirmed that except in the case of densely packed snow, plate loading of snow causes a vertical shear zone development - as has been shown by Yong and Fukue [1], (see Figure 1). Following on the work reported previously [1], this study (a) continues the investigation of the mechanical response behaviour of snow under confined compression as shown by element B in Figure 1, and (b) the shear performance of the material, as represented by element A in the same Figure. Particular attention is paid to the effects of (a) ageing of the snow, and (b) rate of load application.

The motivation for the study recognizes the fact that the characteristics and properties of snow change as time progresses after initial snow deposition, which in turn will affect the stability of the material. A better knowledge and understanding of the response behaviour of the snow in confined compression and in direct shear - as represented by the response performance of Elements B and A respectively in Figure 1 - would contribute further to the analysis of snow behaviour under tractive forces. The results reported herein have been taken directly (with minor modifications) from the paper recently prepared by Yong and Metaxas, (1985).

EXPERIMENTATION

Snow Material

Because of the critical need to test replicate samples of snow, the basic snow material used in the study was artificially

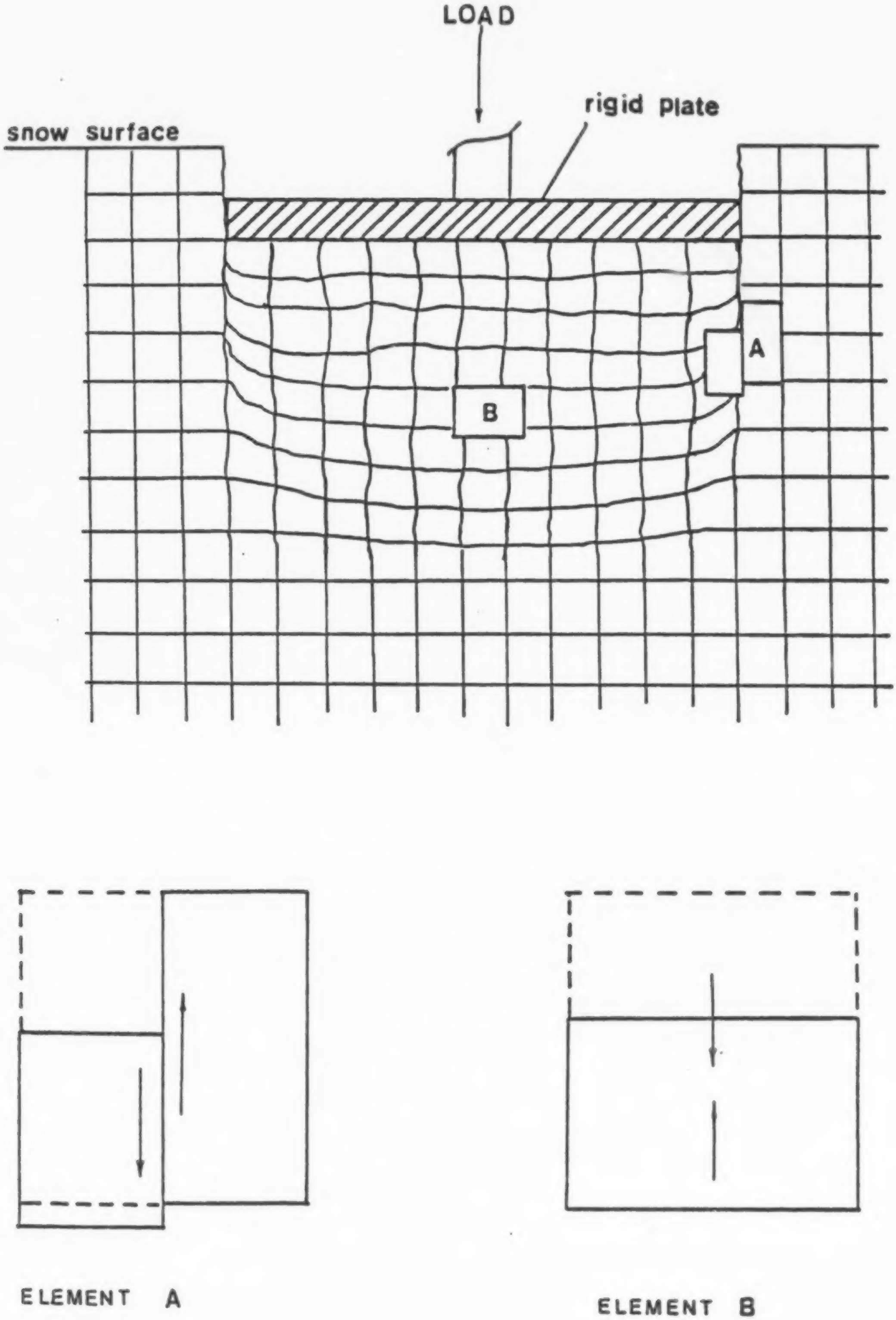
LOAD
rigid plate
snow surface
A
B
ELEMENT A
ELEMENT B

FIG. 1

Failure modes in snow during the penetration of rigid plate.

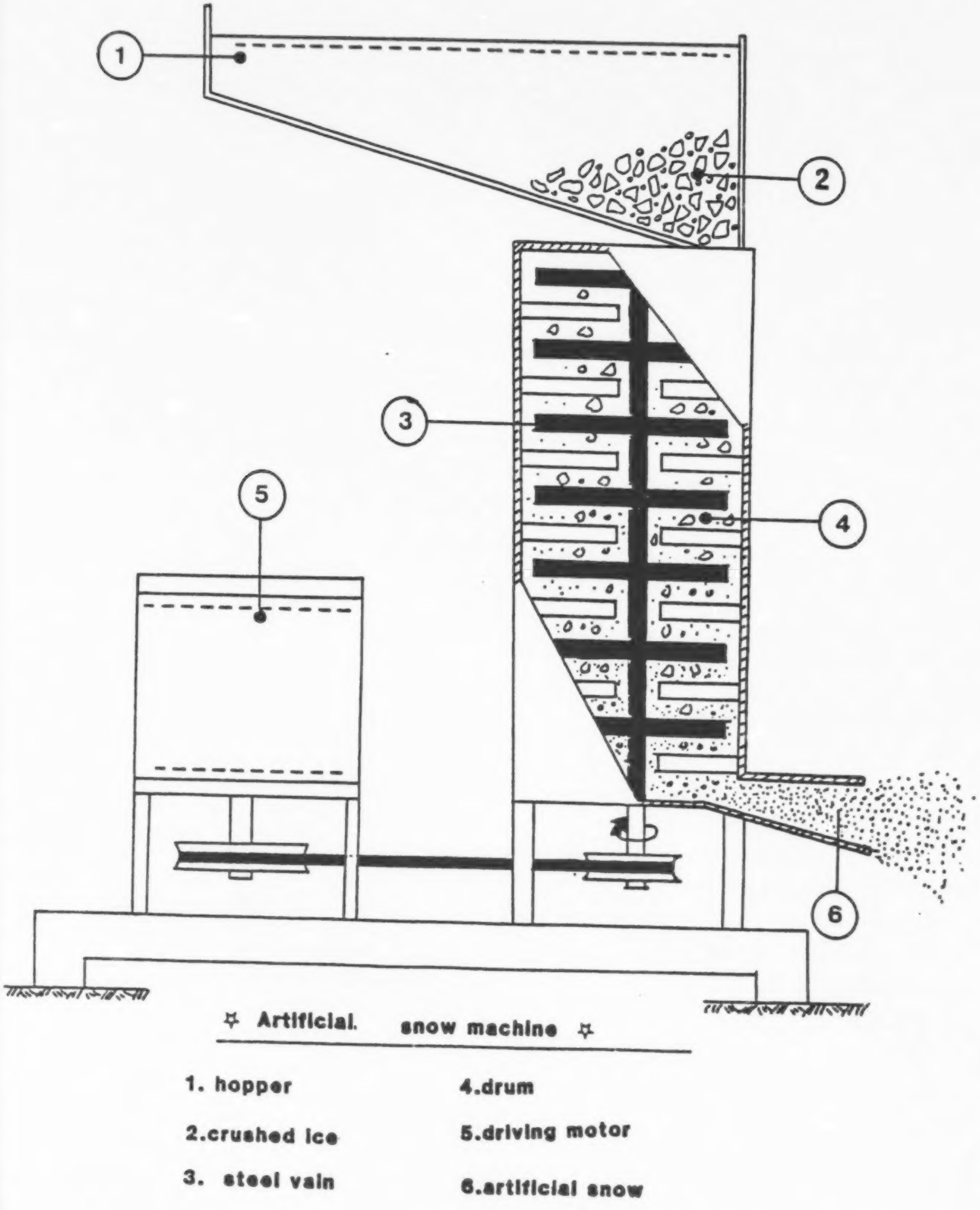
1
2
3
4
5
6
☆ Artificial. snow machine ☆
1. hopper
2.crushed ice
3. steel vain
4.drum
5.driving motor
6.artificial snow

Fig.2 Schematic diagram of snow pulverizer.

made in the laboratory by crushing 3-day old ice with a pulverizer (Fig. 2). This is the same technique used by Yong and Fukue [1]. The grain size distribution of the snow, labelled as ***fresh artificial snow*** (Figure 3) compares favourably with natural and Peter snow. With this procedure for production of snow, control on the production of initial densities of the test snow samples was achieved, at a level of ±0.003 g/cm.^{3}.

The freshly produced artificial snow served as basic snow material for all tests. In all, the seven snow types used in the experimental program were distinguished by the number of days of ageing after production of the basic snow. The seven types were identified as: (a) fresh snow - series 0, (b) 2-day aged snow - series 2, (c) 4-day aged snow - series 4, (d) 8-day aged snow - series 8, (e) 22-day aged snow - series 22, and (f) 30-day aged snow - series 30. To obtain the aged snow samples, freshly produced snow samples were kept in isolation boxes in the cold room which was maintained at a temperature of -13°C. After the prescribed number of days of ageing, the samples were removed for testing. The grain size distribution curves for the freshly produced and aged snows are shown in Figure 4.

From studies of the densities of fresh natural snow obtained from the field, it was observed that ageing of the natural snow for one month at a constant temperature of -13°C. ±1°C., produced a density of about 0.30 g/cm^3. of the aged natural snow. Further ageing to 50 days after snow deposition produced snow densities of about 0.40 g/cm^3. Based on this information, it was decided that an initial density of about 0.35g/cm^3. for the test snow material could be used as a reasonable initial snow density test condition.

Test System

The experimental test system used for confined compression studies is shown in Figure 5. The confined compression apparatus is connected to a switch box which controls the loading rate. Load is sensed by a load transducer and displacements resulting from load application are measured via a DCDT displacement transducer. Density samples were obtained from the test material using thin-walled brass tube samplers.

For confined compression tests, the samples were contained in lucite cylinders with common heights and inside diameters of 17.8 cm. and 3.8 cm. respectively. The wall thickness of the cylinders was 1.3 cms.

Compression Testing

All the snow samples (fresh and aged) were tested under three different rates of load application - denoted in terms of the loading velocities applied to the samples. The lowest loading velocity v_1 was 0.058 cm./sec. whilst the intermediate and highest velocities v_2 and v_3 were 0.158 cms./sec. and 0.216 cms./sec. respectively. Three tests were performed at each loading velocity for each test sample.

Direct Shear Tests

The samples used for direct shear testing were similar to those used for the confined compression tests. The test samples were contained in lucite cylinders with dimensions and shear collar system as shown in Figure 6. Prior to shear testing, the lucite shear cylinder was placed in the shear casing shown in the Figure. Note that the actual test shear casing was rigidly supported laterally by design clamps fixed to the left system rod, and that the right shear sleeve casing was also rigidly fixed to the piston. For direct shear testing, the lucite cylinder containing the snow to be tested was positioned into

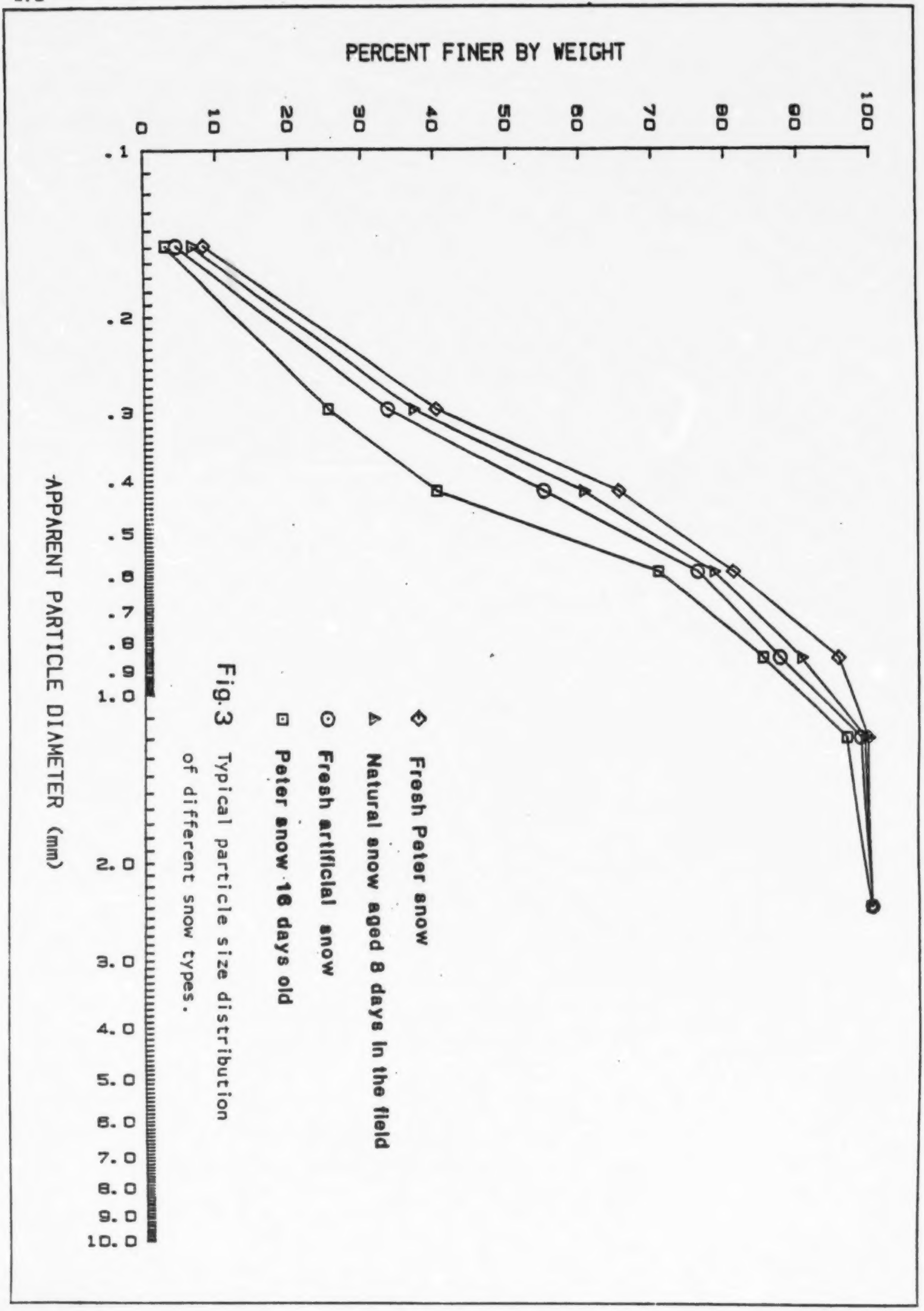

Fig.3 Typical particle size distribution of different snow types.

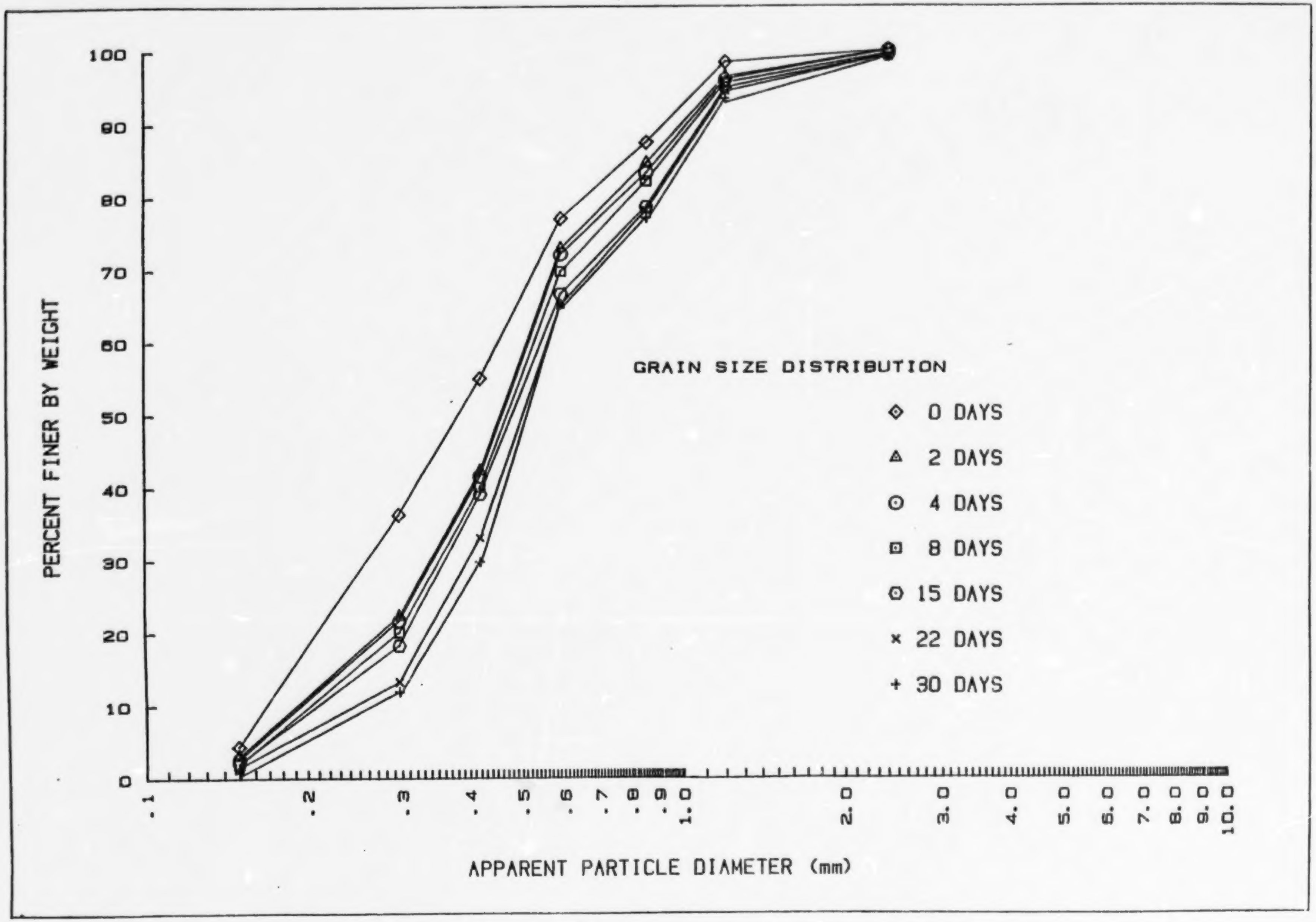

Fig. 4 Particle size distribution of snow types used in the experimental program.

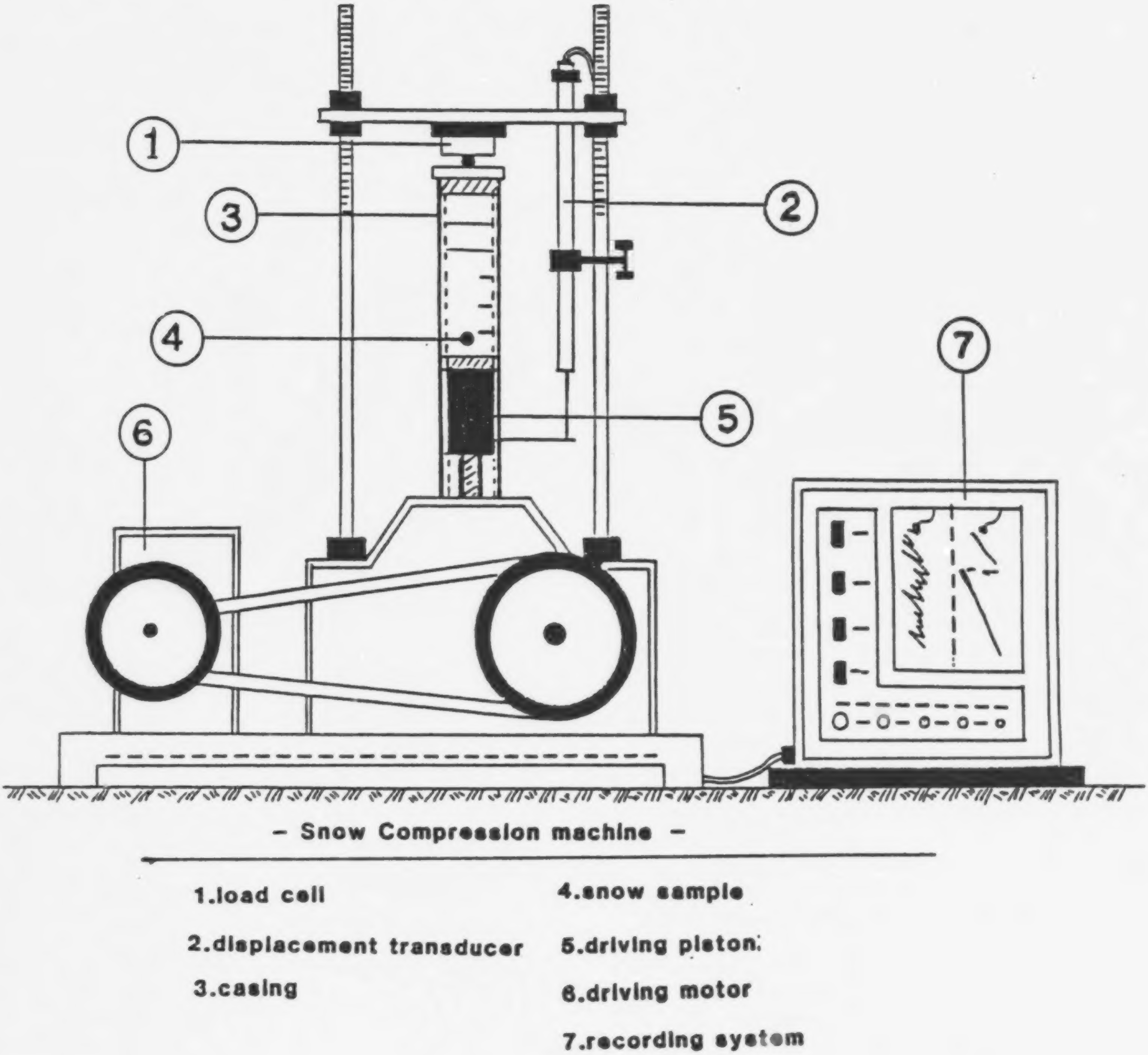
1
2
3
4
5
6
7
- Snow Compression machine -
1.load cell
2.displacement transducer
3.casing
4.snow sample
5.driving piston
6.driving motor
7.recording system

Fig. 5

Confined compression apparatus.

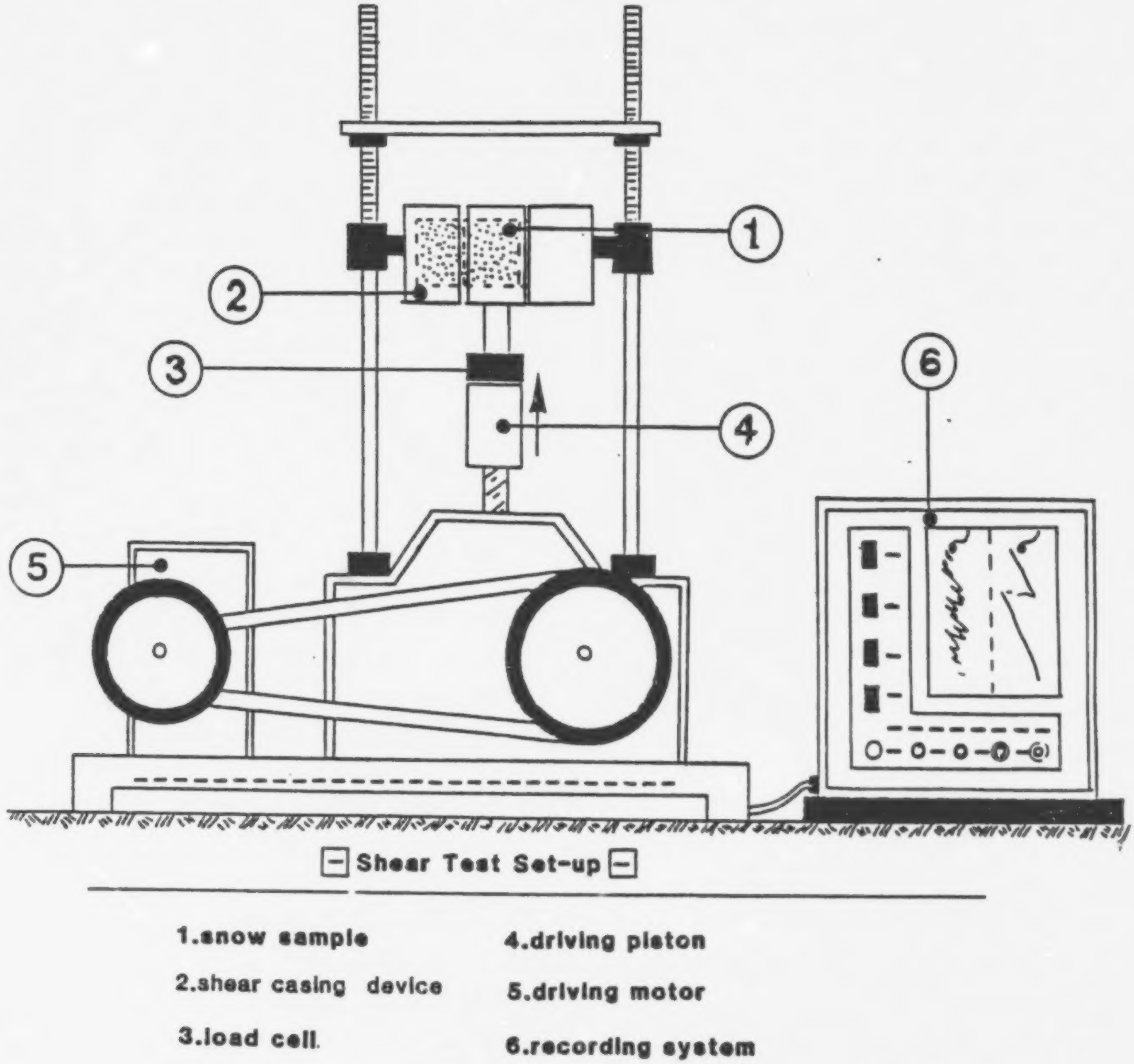
1
2
3
4
5
6
Shear Test Set-up
1.snow sample
2.shear casing device
3.load cell.
4.driving piston
5.driving motor
6.recording system

Fig. 6 Direct shear apparatus.

the shear casing so that the shear plane in the lucite cylinder was coincident with the shear plane of the fixed shear casing. As in the case of the confined compression tests, the same three velocities were used in application of the direct shear loads.

The samples tested in the shear cylinders were prepared at densities of 0.35 gm/cm^3. to 0.60 gm/cm^3. in 0.05 gm/cm^3. increments. These densities were obtained after ageing of the samples and with the aid of the confined compression device. From predetermined total height requirements, control on final density of the test samples was obtained by compressing the test sample with known initial density to a specified height which would yield the desired test density.

RESULTS AND DISCUSSION

Confined Compression Behaviour

A typical test result for the confined compression test is shown in Figure 7. Load application to the test sample is represented on the ordinate. This is achieved by applying a constant-velocity downward motion of the loading head as represented on the ordinate. As the sample compresses (in the confined condition exercised by the sample casing), the density of the test sample obviously increases. Since the cross-section area of the sample is constant, the decreasing height of the sample is a direct registration of the increasing density of the sample. Figure 7 shows the typical density increase (arising from sample compression) in relation to load application - for one loading velocity. The "chattering" load characteristic developed at a specific density range of the test sample is reflective of the continuous local load transfer and fracture of bonds occurring throughout the sample. One can speculate that as one local bond fractures, load transfer to other bonds occur. The continuous load transfer process serves to change and

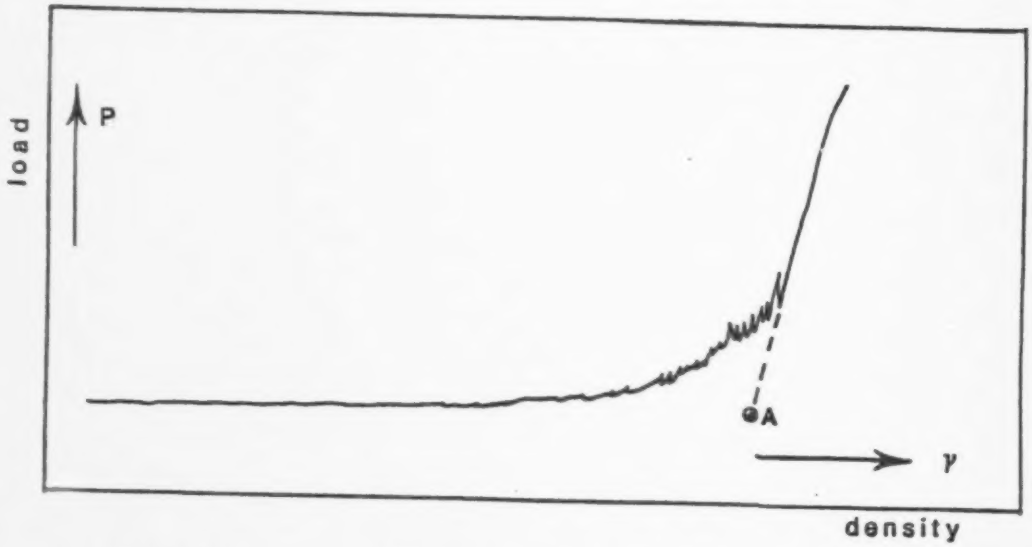

Typical confined compression curve illustrating microfractures and brittle performance.

A : Likely point of threshold density. (intersection on absciss)

Fig. 7
Typical confined compression curve illustrating microfractures and brittle performance.

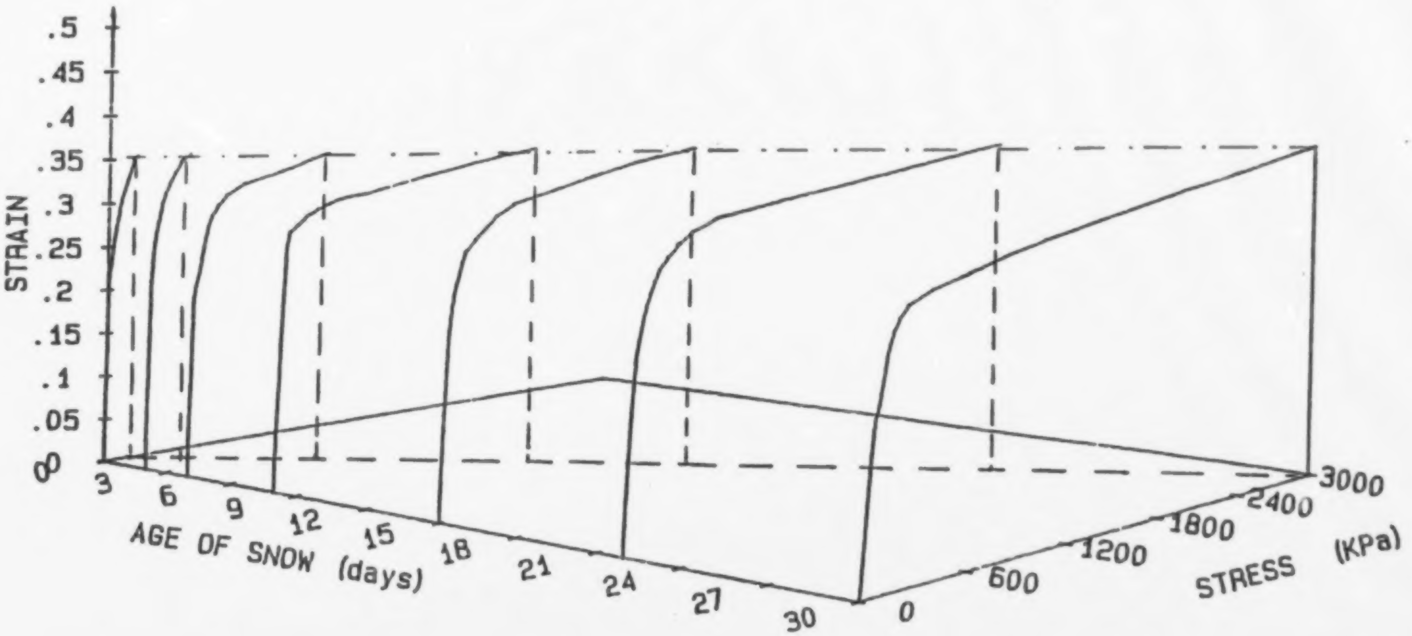

- CONFINED COMPRESSION ON SNOW

AGE EFFECT.

V1 : 0.58mm/sec

Fig. 8 Stress vs strain relationships for different ages of snow in confined compression.

increase the packing of the snow grains, to the threshold density (point A shown in Fig. 7) identified previously by Yong and Fukue [1]. By and large, this point is at the end of the highly visible "chattering" zone. Minor "chattering" continues beyond the threshold density - but with lesser magnitudes of load fluctuation.

Figures 8 to 10 show the compression stress-strain results for the confined compression tests at the three loading velocities, - in terms of days of ageing - plotted as a "state surface". The third axis identifying the age of the snow samples, 0 to 30 days, provides the 'state parameter'. As might be expected, the effect of ageing can be seen in the increases in compression strength (resistance) of the test samples. The differences in strength (resistance) for the same strain developed are significantly larger when the loading velocity is lowest - as seen by comparing the shapes of the surfaces shown in Figures 8 through 10.

It is useful to note that as the velocity of load application increases, the confined strength of the snow decreases for brittle performance. This can be attributed to the fact that as loading velocity increases, the ability for the sample to resist shear distortion via bonding between snow grains becomes considerably diminished. In slow distortion, load transfer to unbroken bonds coupled with a type of "healing" process permits the snow to carry apparently higher loads - in contrast to higher rates of loading which obviously cause correspondingly higher rates of shear distortion. Figure 11 shows this effect well. It is observed that as the snow ages, the influence of rate of load application is much greater - in contrast to the zero-day aged snow which shows very little strength degradation due to increased loading rates.

Bond strength contribution to shear resistance is also a vital issue in the development of higher strengths in aged

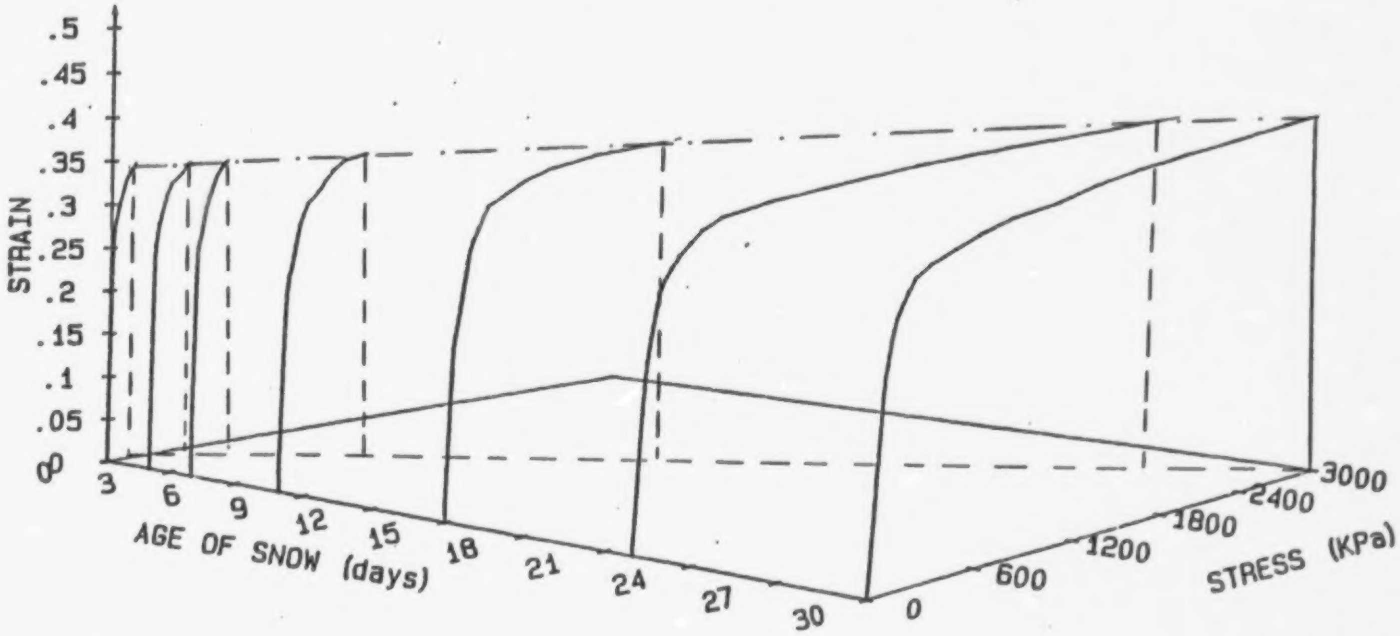

- CONFINED COMPRESSION ON SNOW.

AGE EFFECT.

V2 : 1.57mm/sec

Fig. 8 Stress vs strain relationships for different ages of snow in confined compression.

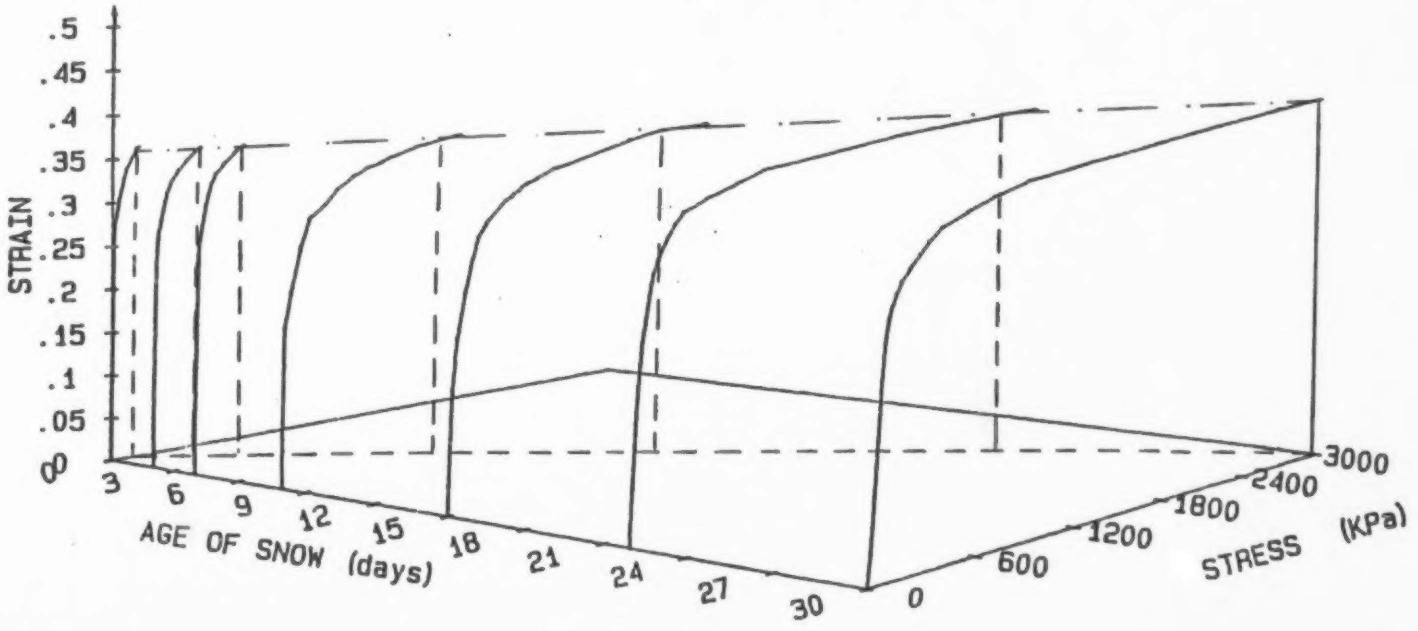

- CONFINED COMPRESSION ON SNOW.

AGE EFFECT.

V3 : 2.16mm/sec

Fig. 10 Stress vs strain relationships for different ages of snow in confined compression.

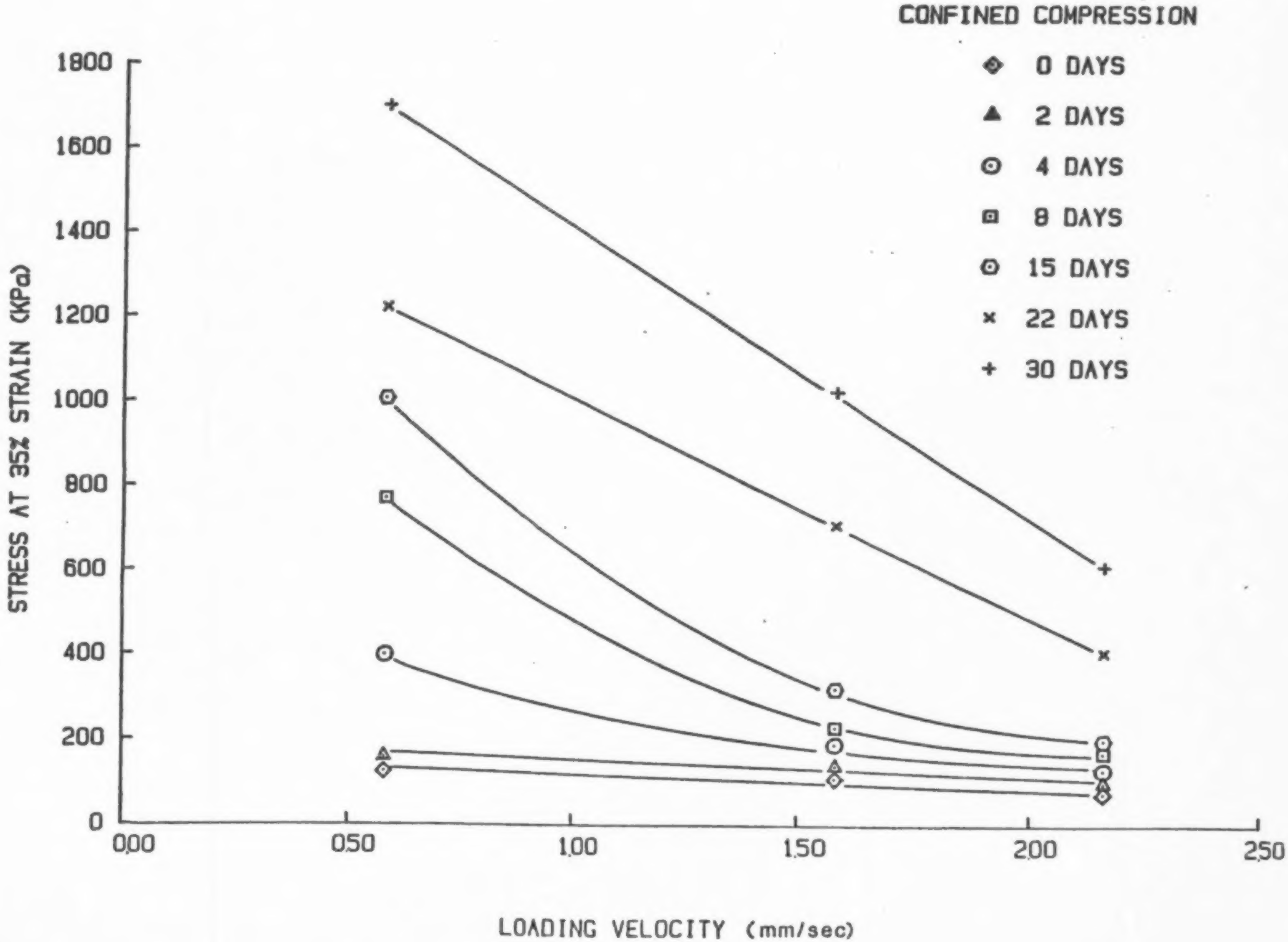

Fig.11 Stress vs loading velocity relationships in confined compression tests.

samples, - as seen in Figure 11. The increase in strength at the lowest rate of loading is significantly large as the period of ageing is increased. As has been noted in many previous studies by various researchers, (e.g. Wakahamia [2], Keeler [3], Hobbs and Mason [4], Colbeck [5,6], Yong and Fukue [1], and Perla [7]) the transformations occurring in the ageing process which lead to the creation and enhancement of bonds between snow grains, would serve to provide a higher resistance to shear application. This has been confirmed in Figures 8 to 11. Under ordinary field conditions, increases in the density of natural in-situ snow will occur with increased ageing, thus providing another reason for higher strengths with aged samples. However, in the laboratory ageing process, because the samples were aged in the isolation box, the density increases with ageing were relatively small - less than 2% increase in density. Fukue [8] notes that below a density of 0.4 gm./cm^3. the strength of snow is quite small and that in the low density range, the strength of the snow depends more on grain structure than on density.

Direct Shear Test Performance

The test results obtained in direct shear testing, using the system described previously are shown in Figures 12 to 14. These highlight the effects of ageing and density on the developed shear strength of the snow samples. These same Figures can be viewed in terms of strain-rate effects. As was the case for the confined compression tests, the higher strain rates caused some degradation in strength of the samples - for the same physical reasons. This strength degradation was common for the various aged snows - as seen in Fig. 15. As in the confined compression study, the zero-day snow is relatively insensitive to the effects of loading rate. At longer periods of snow ageing, the effects of loading velocity become more pronounced. The trends are similar to those shown for confined compression tests.

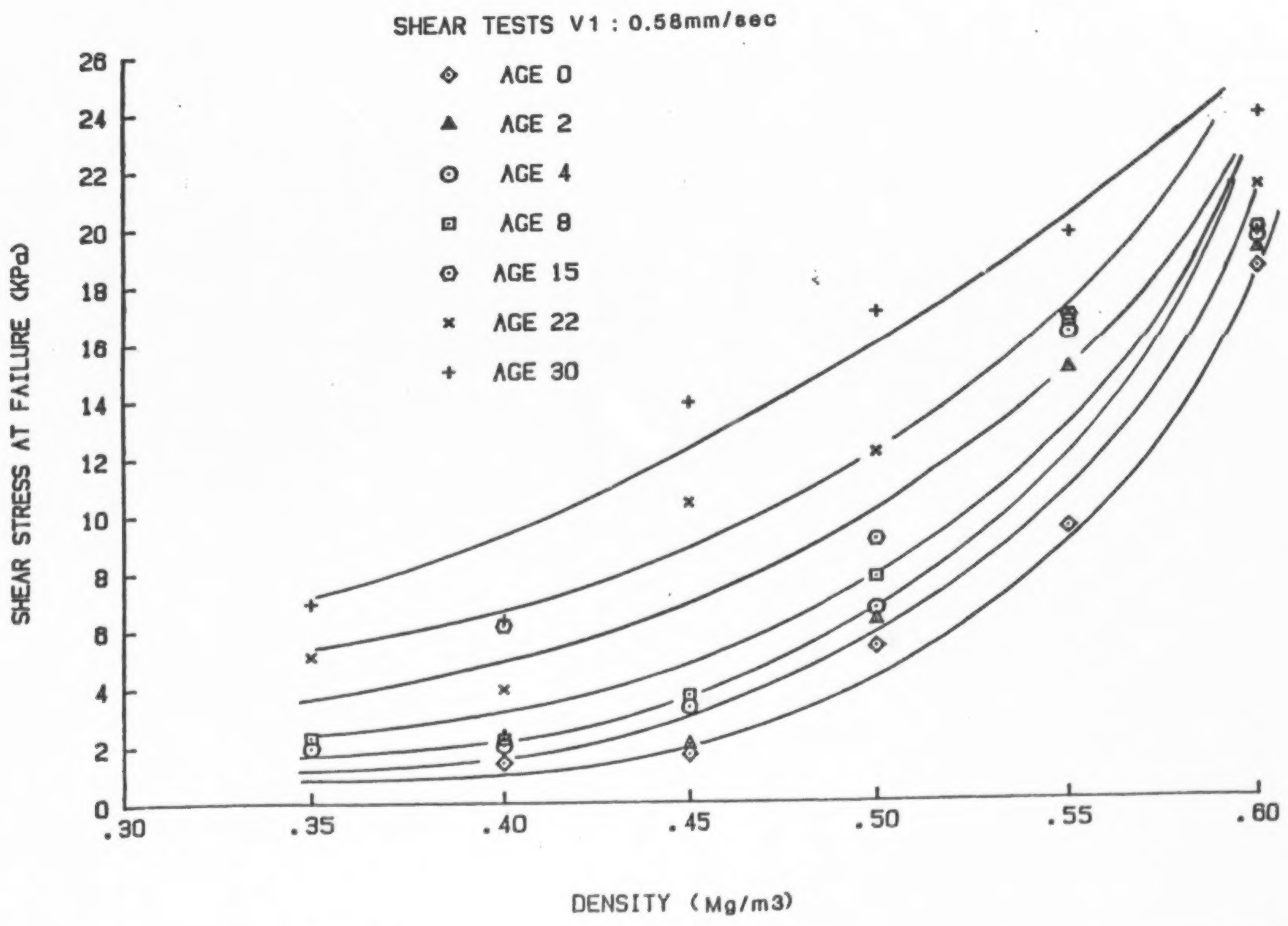

Fig.12 Shear stress vs density relationships for different ages of snow.

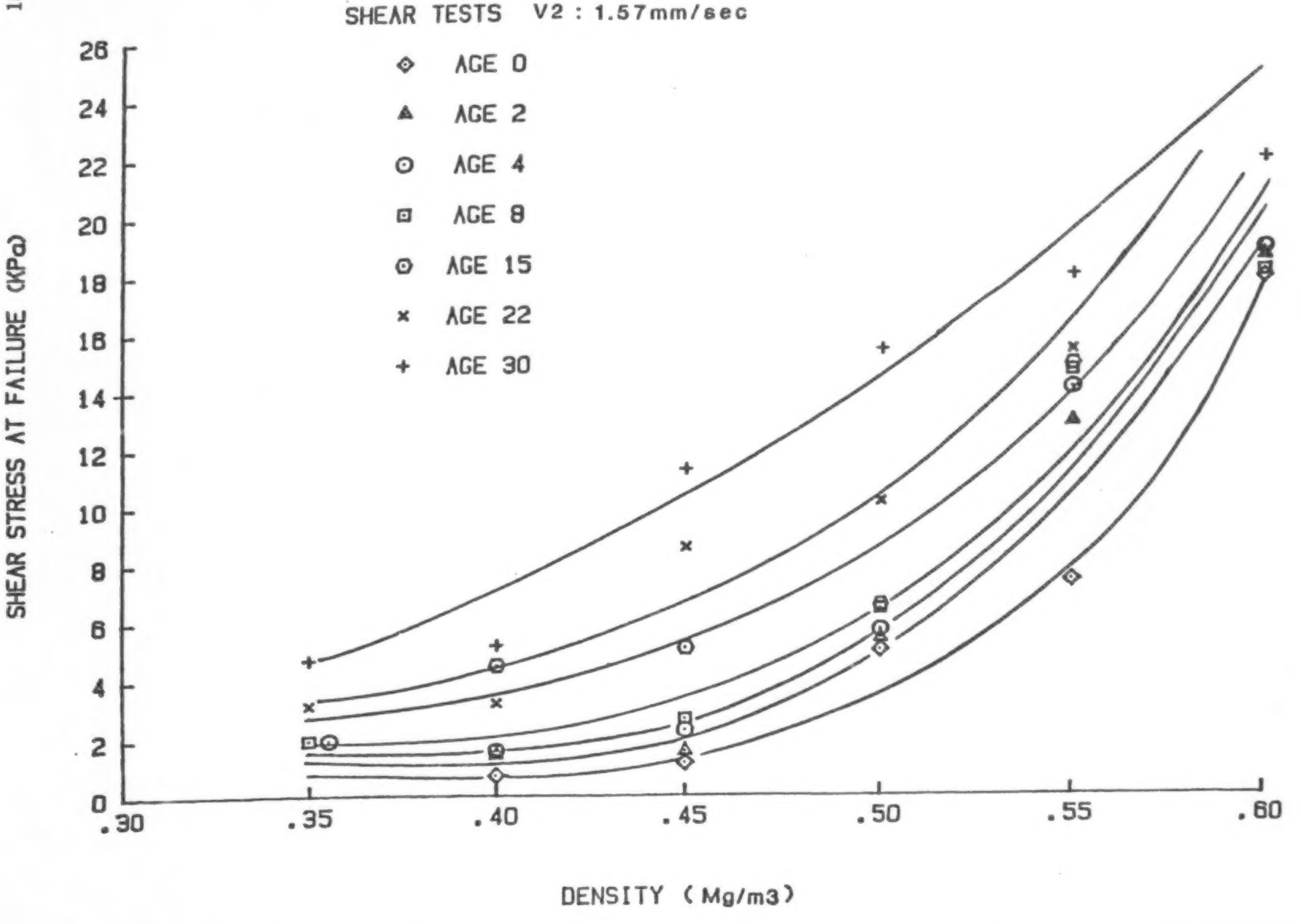

Fig.13 Shear stress vs density relationships for different ages of snow.

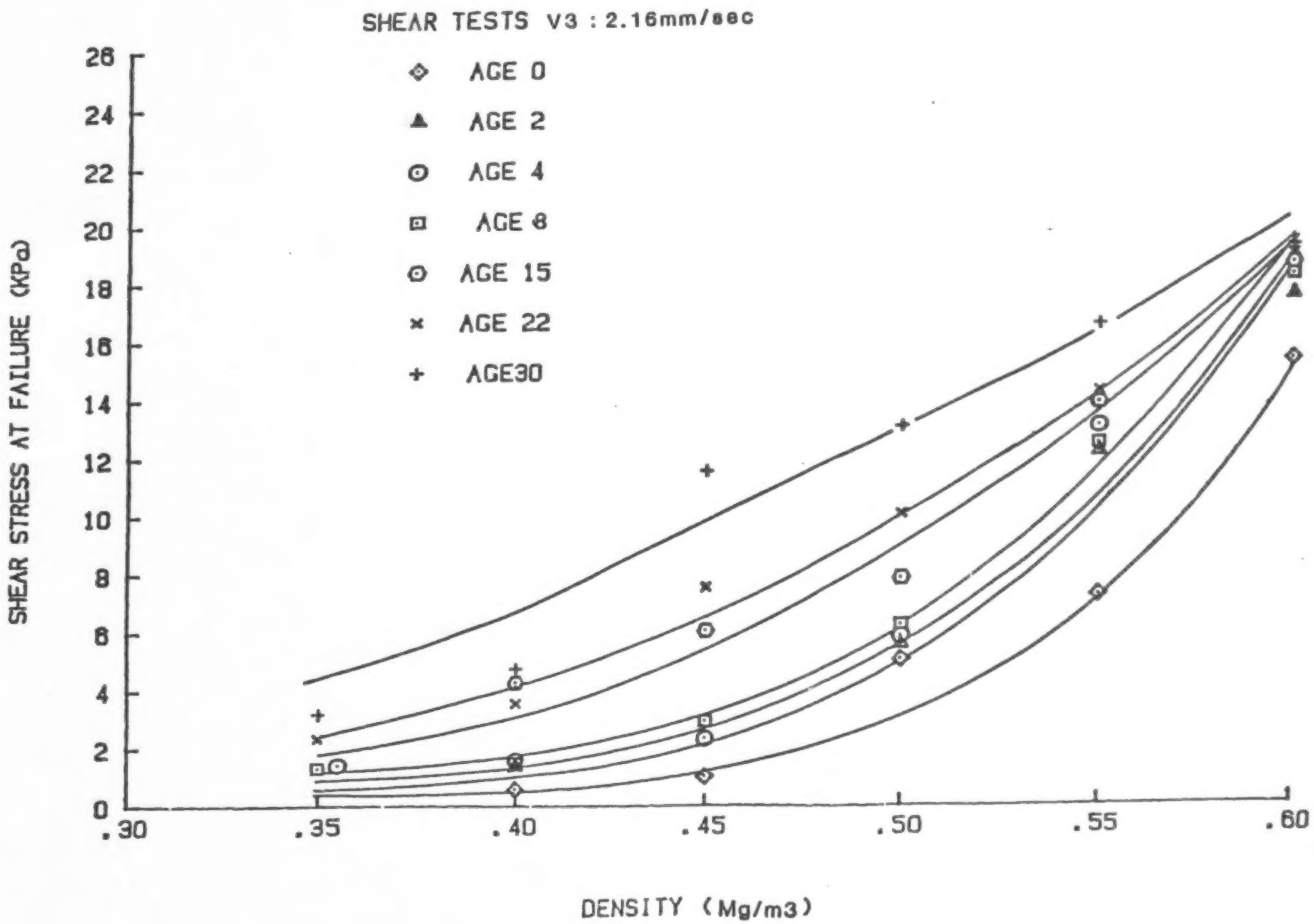

Fig. 14 Shear stress vs density relationships for different ages of snow.

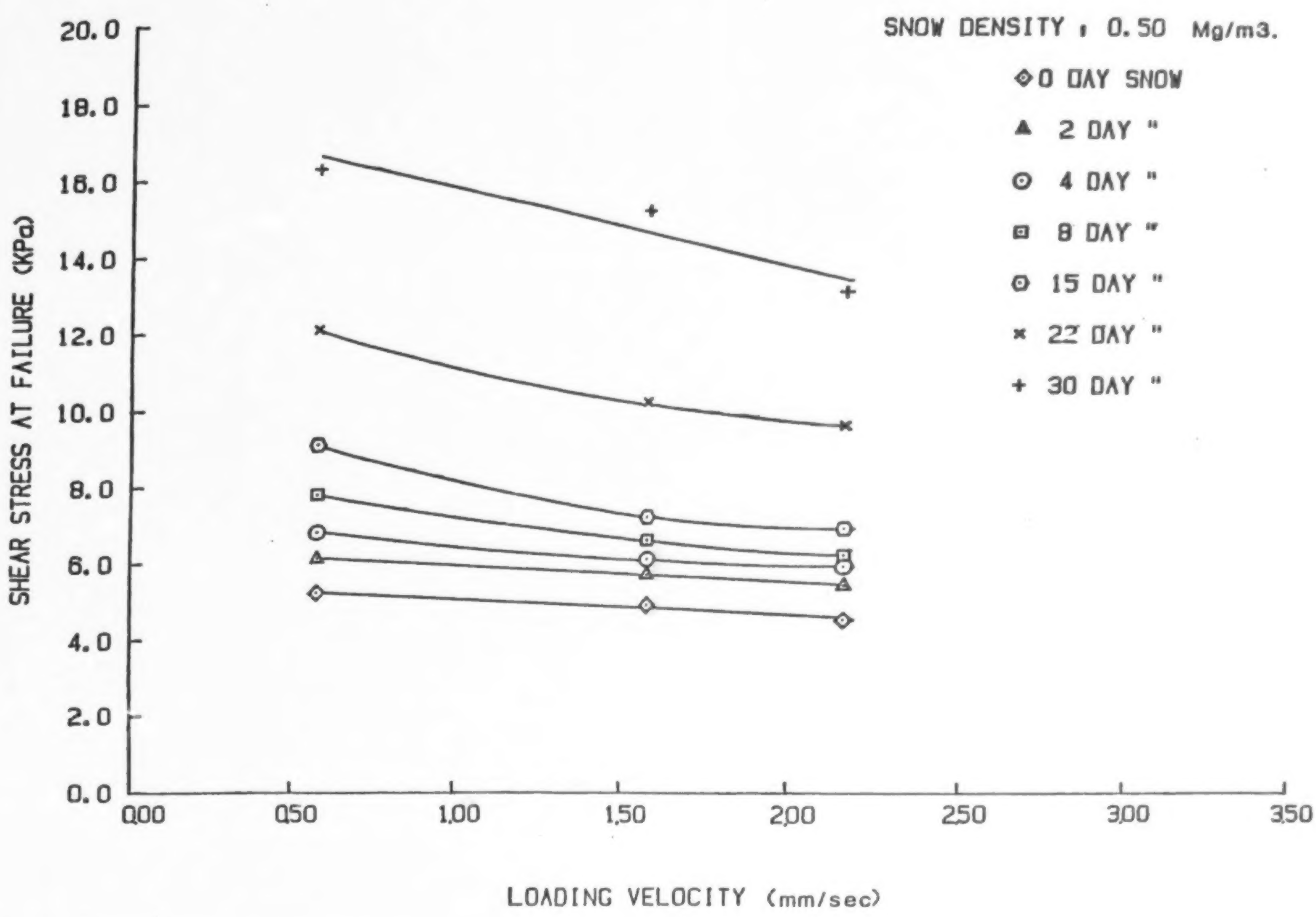

Fig. 15 Shear stress vs loading velocity relationships for different ages of snow.

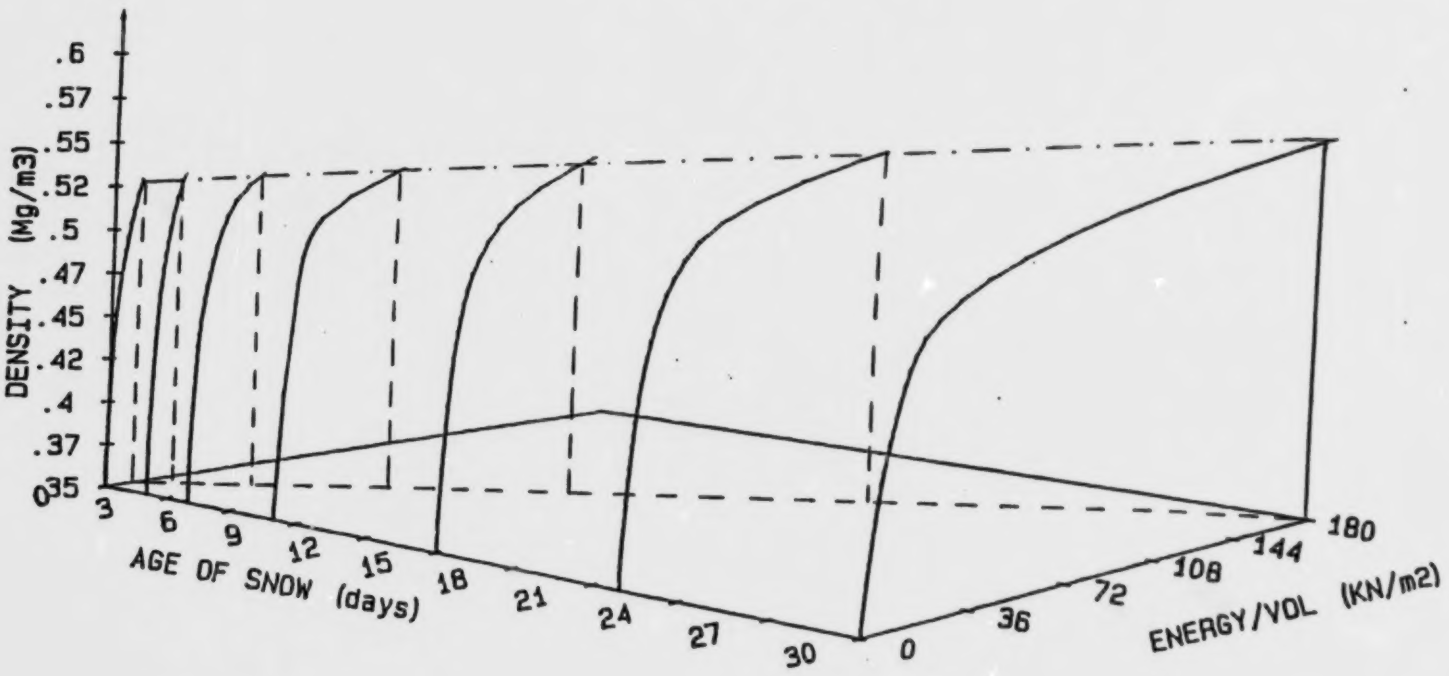

- Energy per unit volume required to create compaction in confined compression.

AGE EFFECT

V1 : 0.58mm/sec

Fig. 16 Energy vs density relationships for different ages of snow in confined compression.

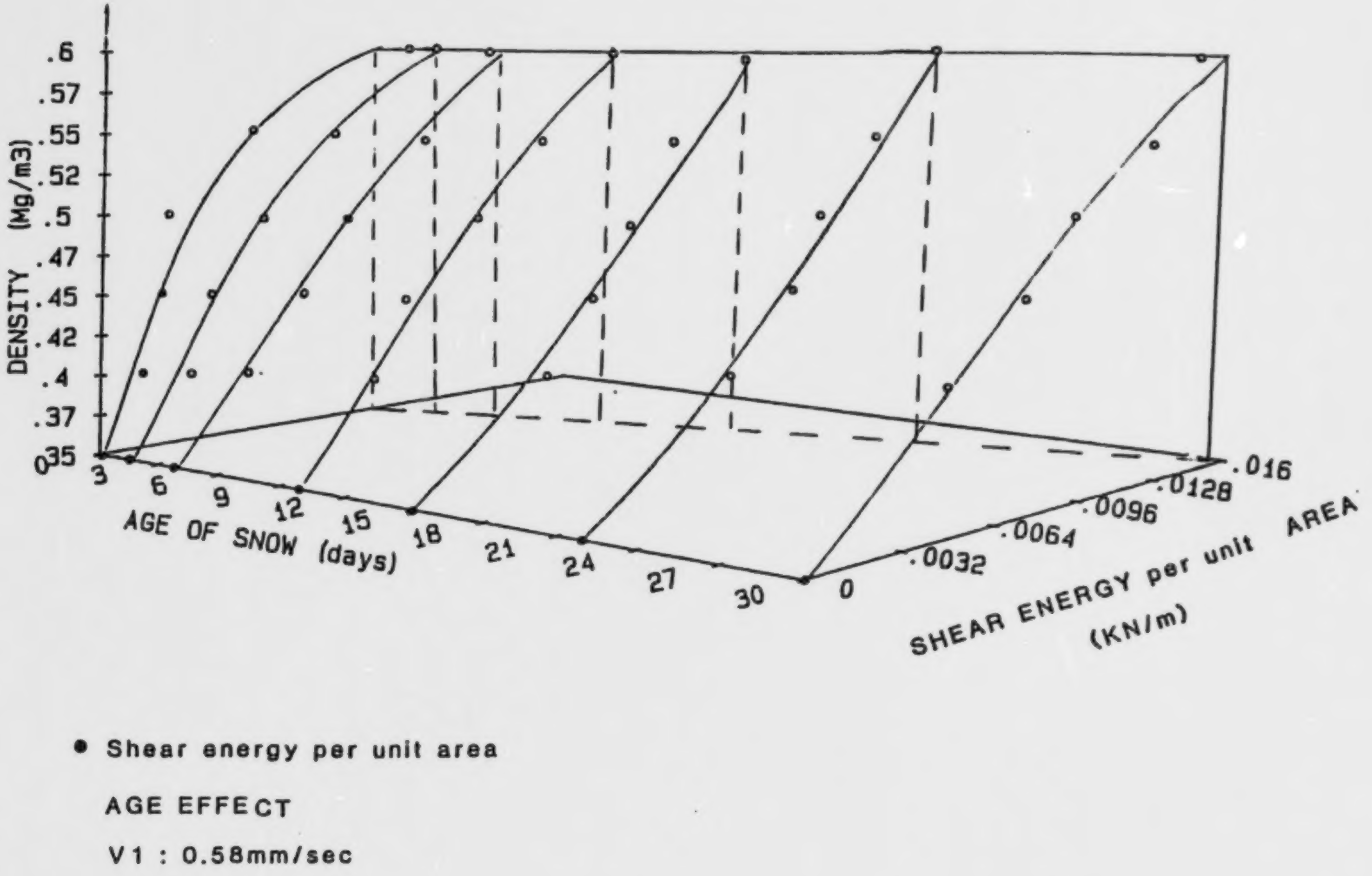

Fig. 17 Shear energy vs density relationships for different ages of snow.

Energy Expenditure

The energy expended in compression and shear constitutes a useful method in examining the response compression/shear behaviour of the snow material. Since the applied load is known, and since the distance of travel of the applied load is measured, the total work expenditure involved in compressing the initial snow in the confining container to the final density under the load can be easily calculated. The energy state surface shown in Figure 16 depicts the energy expenditure for confined compression - for the lowest rate of loading. Similar surfaces can be generated for the other rates of loading. Note that the energy per unit volume which should actually be expressed in terms of kilo newtons per cubic meter, is reduced to kilo newtons per square meter through algebraic cancellation. As might be expected, the energy surface shown in Fig. 16 matches closely the confined stress-strain surface shown previously in Figs 8 to 10, - due obviously to the direct relationship between (a) strain and density, and (b) stress and energy. With Fig. 16, and other similar energy surfaces, we can now establish the amount of energy required to produce compaction at a particular initial snow density, - and for a specific period of snow maturation (age). This is useful information for estimation of the capability of the snow to support load.

In the case of the direct shear tests, the maximum shear stress generated and the displacement of the shear sleeve are known values. The shear energy surface shown in Figure 17 for the same lowest rate of shear application bears some similarity to the compression surface shown in Fig. 16. The preceding not withstanding, these are two distinctly different types of surfaces. In Fig. 17, the surface shows the energy required to shear a snow sample of a particular age and density. On the other hand, the surface shown in Fig. 16 indicates the amount of energy required to compress a snow sample of a particular age, from an initial density of 0.35 g/cm^3.

CONCLUDING REMARKS

The two elements shown in Figure 1 which demonstrate the actual mechanisms of snow performance under load are indicative of the bearing stability of the snow. The tests performed in this study have attempted to provide preliminary information leading to the application of energy transfer mechanics for analysis of snow load bearing capability. The generation of state energy surfaces for compression and shear are indeed preliminary and necessary for the further continuing studies which analyze the problem of energy transfer from surficial load application mechanisms.

ACKNOWLEDGEMENTS

The work which was performed in this study as partial fulfilment of the study requirements for DRES under contract arrangement with DSS, Canada, has been reported recently in the publication prepared by Yong and Metaxas, scheduled to appear in the Journal of Terramechanics (1985).

REFERENCES

1. Yong, R.N. and Fukue, M. (1977) *Performance of snow in confined compression* J. Terramechanics, Vol.14:2, pp. 59-82.
2. Wakahama, G. (1965) *Metamorphisms of wet snow*, Low Temp. Sci., Ser. A, 23, pp.51-66.
3. Keeler, C.M. (1969) *The growth of bonds and the increase of mechanical strength in a dry seasonal snowpack*, J. Glaciology, Vol.8:54.
4. Hobbs, P.V. and Mason, B.I. (1964) *The sintering and adhesion of ice*, Phil. Mag., Eight Ser., Vol.9:98, pp. 181-197.
5. Colbeck, S.C. (1980) *Thermodynamics of snow metamorphism due to variations in curvature*, J. Glaciology, Vol.29:94, pp. 291-301.
6. Colbeck, S.C. (1982) *An overview of seasonal snow metamorphism*, Reviews of Geophysics and Space Physics, Vol.20:1, pp.45-61.
7. Perla, R.I. (1969) *Strength tests on newly fallen snow*, J. Glaciology, Vol.8.
8. Hobbs, P.V. (1965) *The effect of time on the physical properties of deposited snow*, J. Geophysical Research, Vol.70:16, pp. 3903-07.
9. Yong, R.N. and Metaxas, I. (1985) *Influence of Age-Hardening and strain-rate on Confined Compression and Shear Behaviour of Snow.* J. Terramechanics. IN PRESS.

EXPERIENCE GAINED OPERATING SNOW PILLOWS ON A NEAR REAL-TIME BASIS IN THE MOUNTAINOUS AREAS OF ALBERETA

by

G.A. Coles

Water Survey Section
Alberta Environment
Edmonton, Alberta
Canada

D.R. Graham

River Forecast Centre
Alberta Environment
Edmonton, Alberta
Canada

R.D. Allison

Water Survey Section
Alberta Environment
Lethbridge, Alberta
Canada

presented at

SNOW PROPERTY MEASUREMENTS WORKSHOP

Lake Louise, Alberta

1-3 April, 1985

TECHNICAL MEMORANDUM 140

Compiled By

P.R. Kry

NRCC 27594

Experience Gained Operating Snow Pillows on a near Real-Time Basis in the Mountainous Areas of Alberta

by

G. A. Coles, P. Eng.[1], D. R. Graham, P. Eng.[2], R. D. Allison[3].

Introduction

From a water management point of view, the South Saskatchewan River Basin (Figure 1) is probably the most important basin in Alberta. Limitations due to the availability of a reliable water supply are already placing constraints on the development of the industrial and agricultural potential of the basin which covers an area of approximately 111,000 sq. kilometres in Alberta. The water management problems have wider ramifications as an apportionment agreement exists between the Federal Government and the Prairie Provinces which requires Alberta to pass on to Saskatchewan fifty percent of the natural flow originating in the Province.

The South Saskatchewan River Basin is made up of three major sub-basins: the Red Deer, the Bow and the Oldman. All three of these rivers originate in the Eastern Slopes of the Rockies. These mountainous headwater areas have long been recognized as the key to the water supply and flood forecasting in Southern Alberta. However, until recent years, the collection of real-time water related data in the headwaters was extremely difficult due to the remoteness of the area, and the ruggedness of the terrain. For many years, most of the precipitation stations that existed in the area were storage gauges which were visited twice a year and only provided a winter and summer total accumulation of precipitation.

Presented at Workshop on Snow Property Measurement, Lake Louise, Alberta, 1985.

Mention of trade or company names in this paper is solely for the benefit of the reader.

1. Section Head, Water Survey Section, Alberta Environment, Edmonton.
2. Section Head, Procedures & Networks, River Forecast Centre, Alberta Environment, Edmonton.
3. Snow Surveyor, Water Survey Section, Alberta Environment, Lethbridge.

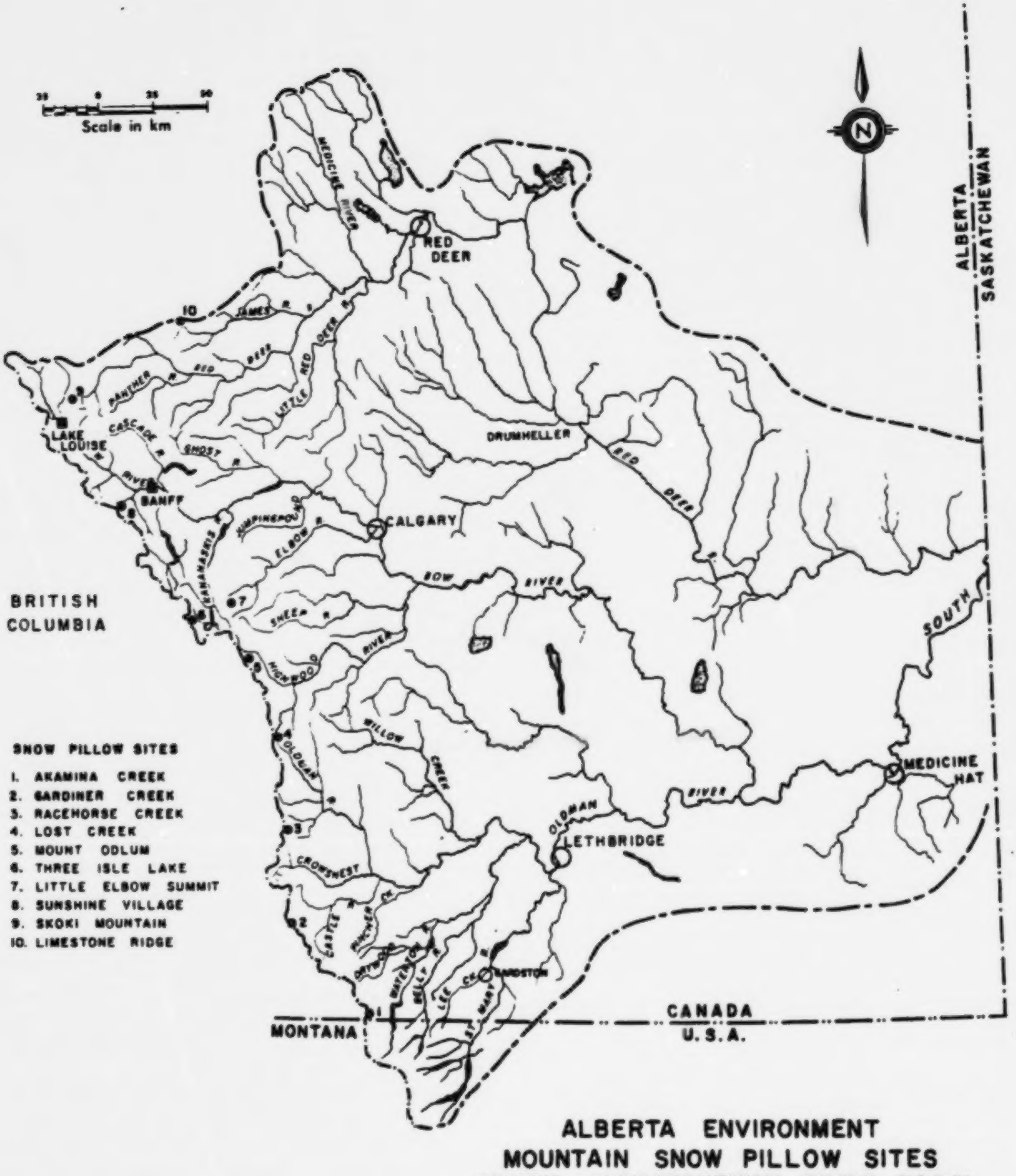
25 0 25 50
Scale in km
N
ALBERTA
SASKATCHEWAN
RED DEER
MEDICINE RIVER
JAMES R.
RED DEER R.
LITTLE RED DEER R.
PANTHER R.
LAKE LOUISE
CASCADE R.
GHOST R.
BOW RIVER
BANFF
DRUMHELLER
RED DEER R.
CALGARY
JUMPINGPOUND
ELBOW R.
KANANASKIS R.
SHEEP R.
HIGHWOOD RIVER
BOW RIVER
BRITISH COLUMBIA
SOUTH
WILLOW CREEK
OLDMAN R.
MEDICINE HAT
RIVER
OLDMAN
LETHBRIDGE
CROWSNEST
CASTLE R.
PINCHER CK.
DRYWOOD
WATERTON
BELLY R.
LEE CK.
ST. MARY R.
CARDSTON
CANADA
U.S.A.
MONTANA
1
2
3
4
5
6
7
8
9
10
SNOW PILLOW SITES
1. AKAMINA CREEK
2. GARDINER CREEK
3. RACEHORSE CREEK
4. LOST CREEK
5. MOUNT ODLUM
6. THREE ISLE LAKE
7. LITTLE ELBOW SUMMIT
8. SUNSHINE VILLAGE
9. SKOKI MOUNTAIN
10. LIMESTONE RIDGE

ALBERTA ENVIRONMENT
MOUNTAIN SNOW PILLOW SITES
SOUTH SASKATCHEWAN RIVER BASIN
(ALBERTA)

MARCH, 1985

FIGURE 1

In addition to the precipitation network there were a number of snow survey sites in the mountain parks which were established and run by the water agencies of the Federal Government. Some of these sites were established as far back as the 1930's. In 1978 Alberta Environment took over the mountain snow survey network and added a number of courses to get better coverage with respect to area and range in elevation. The development of data collection platforms (DCPs) and satellite communication in the 1970's provided the means of obtaining data on a near real time basis from virtually any point in the Province. In 1978, the Alberta Environment River Forecast Centre (Graham and Kuhnke, 1978) produced a major proposal to upgrade the precipitation and climate network of the headwaters of the South Saskatchewan Basin. As the main purpose of the new network is to support flood and water supply forecasting needs, all 26 precipitation stations and the 12 climate (multi-parameter) stations are equipped with telemetry capable of transmitting data on a near real-time basis. In the case of the remote mountain sites telemetry could be provided most economically by the use of satellite communications. In 1979 the network upgrading proposal was accepted and work began immediately.

Instrumentation used to monitor snow

For any snow data collection system to be useful for forecasting purposes, the data must be available in near real time. Conventional snow courses are very expensive to operate particularly in remote mountain areas where helicopters are the only means of access. It is not economically feasible to carry out snow surveys more frequently than once per month. Therefore, it was decided to include snow monitoring equipment at ten climate (multi-parameter) sites. The locations of the sites were chosen taking into account exposure and local ground conditions. It was considered important to have an even geographical distribution of stations from north to south throughout the basin. Some of the sites are located along the continental divide with others along the front and middle ranges. The elevation of the sites varies between 1800 and 2300 metres. See table 1 and figure 1 for locations and further details. As of March 1985, eight of the stations were in full operation and the other two are expected to be completed this summer.

Nine of the ten proposed stations were located in the mountains far from telephone lines or observers. After careful study of the communication alternatives it was decided to use the Geostationary Orbital Environmental Satellite (GOES) system . The first data collection platforms (DCPs) using the GOES system were installed in 1980 and have been extremely reliable. In 1981 for example, eight precipitation stations operated for the full twelve months. Of the 209,646 pieces of data expected for the period, 98.7% were received. The missing data included all losses due to failure of sensors, equipment and line losses between Edmonton and Wallops Island, Virginia (Coles and Graham, 1983). The tenth station located at Sunshine Village ski resort near Banff was installed in cooperation with Parks Canada and forms part of their avalanche warning system. This station uses telephone lines to transmit the data from Sunshine Village to Banff.

TABLE 1

ALBERTA ENVIRONMENT

INVENTORY OF MOUNTAIN SNOW PILLOWS

NAME	BASIN	LOCATION		ELEVATION (metres)	ADDITIONAL SENSORS	YEAR TELEMETRY ESTABLISHED
		LATITUDE	LONGDITUDE			
Akamina Pass	Oldman	49^{0} 01' 40"	114^{0} 03' 10"	1800	P.T.W.H.	1981
Gardiner Creek	Oldman	49^{0} 21' 40"	114^{0} 30' 57"	1920	P.T.W.H.R▼R▲.	1983
Limestone Ridge	Red Deer	51^{0} 53' 19"	115^{0} 23' 04"	1950	P.T.W.H.	1982
Little Elbow Summit	Bow	50^{0} 42' 20"	114^{0} 59' 20"	2120	P. & T.	1979
Lost Creek	Oldman	50^{0} 10' 26"	114^{0} 42' 36"	2130	P.& T.	1985 (Sept)
Racehorse Creek	Oldman	49^{0} 49' 17"	114^{0} 37' 19"	1920	P.& T.	1983
Skoki Mountain	Bow	51^{0} 32' 26"	116^{0} 03' 23"	2040	P.& T.	1981
*Sunshine Village	Bow	51^{0} 04' 43"	115^{0} 46' 48"	2200	P.& T.	1981
Three Isle Lake	Bow	50^{0} 37' 53"	115^{0} 16' 46"	2240	P.T.W.H.	1983
Odlum	Bow	50^{0} 29' 10"	114^{0} 54' 26"	2060	P.T.H.	1985 (Sept)

P - Precipitation
T - Temperature
W - Wind direction & velocity
H - Relative humidity
R▼ - Radiation (Incoming) R▲ Radiation (outgoing)
* Located at Parks Canada Installation

The data collection platforms are powered by twelve volt batteries, recharged by vertically mounted solar panels. Mounting the panels vertically minimizes the build up of ice and snow and guarantees a power source even during the coldest parts of the year.

Each of the ten climate sites are equipped with sensors to monitor precipitation, temperature, and the water equivalent of snow on an hourly basis. Some of the sites also have wind and humidity sensors (See table 1).

The instrument used to measure melt rate and snow water equivalent is the snow pillow. The pillows used by Alberta Environment are 3 metre diameter hypalon pillows manufactured by the Water Saver Company of Denver (See figure 2). The pillow is filled with approximately 1200 litres of a solution consisting of 50% water and 50% methyl alcohol. The pillow is connected directly to a stilling well by means of 19 mm diameter polyethylene tubing. The level in the 20 cm diameter stilling well varies in direct proportion to the amount of pressure exerted on the pillow by the weight of the snow. The changes in level in the stilling well are monitored continuously by a Leupold & Stevens A71 water level recorder. The readings after adjustment for specific gravity provide a continuous historic record of the snow water equivalent. A Baldwin optical encoder working in parallel with the Stevens recorder translates the hourly readings (measured to the nearest millimetre) into binary coded decimal data (BCD). The data are then transmitted every three hours to Wallops Island, Virginia via the GOES system. The data are retrieved automatically by phone at pre-determined intervals which can be changed as required.

Siting and Installation Problems Associated with Snow Pillows.

Siting is the single most important factor to be considered when installing snow pillows. Because the cost of the hardware and its installation is so high, the site chosen should be close to ideal. The 1985 capital cost of a snow pillow with telemetry and sensors to measure precipitation, temperature, humidity and wind is approximately $25,000.00. The cost of installing the station depends on the difficulty due to the individual site and the amount of helicopter time required. Installation costs in Alberta including wages, expenses and miscellaneous materials have ranged between $10,000.00 and $20,000.00.

General guidelines are available (Farnes, 1978) on locating a single snow pillow in a basin. The snow pillow should be installed in a sheltered area near the mean water-producing elevation of the basin. If the pillow is located too low in the basin the snow on the pillow will be depleted before the peak runoff in the basin occurs. Also the amount of snow accumulated on the pillow will be much less than the average snow water equivalent for the basin. On the other hand if the pillow is located at too high an elevation in the watershed, melt will not occur until after the main runoff has taken place at lower elevations. Several pillows located at various elevations within a sub-basin would be ideal, however, the cost of installing several pillows could not be justified.

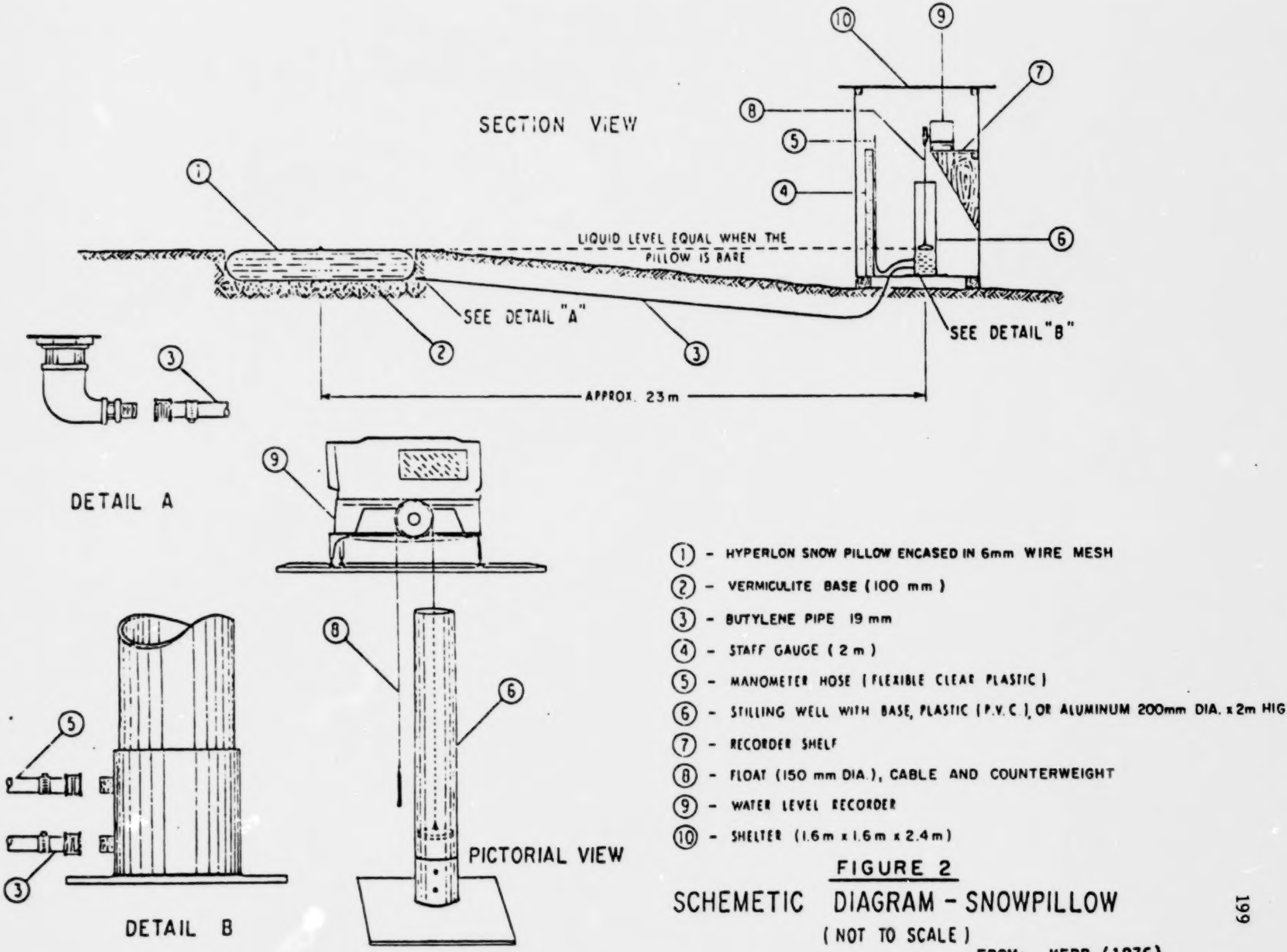
SECTION VIEW
LIQUID LEVEL EQUAL WHEN THE PILLOW IS BARE
SEE DETAIL "A"
SEE DETAIL "B"
APPROX. 23m
DETAIL A
DETAIL B
PICTORIAL VIEW
1
2
3
4
5
6
7
8
9
10

① - HYPERLON SNOW PILLOW ENCASED IN 6mm WIRE MESH
② - VERMICULITE BASE (100 mm)
③ - BUTYLENE PIPE 19 mm
④ - STAFF GAUGE (2 m)
⑤ - MANOMETER HOSE (FLEXIBLE CLEAR PLASTIC)
⑥ - STILLING WELL WITH BASE, PLASTIC (P.V.C.), OR ALUMINUM 200mm DIA. x 2m HIG
⑦ - RECORDER SHELF
⑧ - FLOAT (150 mm DIA.), CABLE AND COUNTERWEIGHT
⑨ - WATER LEVEL RECORDER
⑩ - SHELTER (1.6m x 1.6m x 2.4m)

FIGURE 2

SCHEMETIC DIAGRAM - SNOWPILLOW

(NOT TO SCALE)

FROM: KERR (1976)

Once the general location of the site has been selected the specific site must be chosen. The State of California (1976) and Cox (1978) provide detailed guidelines on this topic. The main points to be considered are the following:

1. Snow pillows should be located in a clearing in the trees, small enough to minimize drifting. However, the trees should not be so close that they influence the snow accumulation by forming a canopy or cause melt due to long wave radiation.

2. Pillows should be located on level ground to prevent creep and drainage problems, but the pillow should be at a slightly higher elevation than the instrument house (see figure 2).

   Extreme care when installing pillows is imperative. If the pillow is not properly installed, malfunctions will occur and no useful information will be obtained for the season. Once the pillow is covered by snow it is virtually impossible to make repairs to the system.

   The most common problems to be aware of are as follows:

1. Leaks in pipes and fittings: Even the smallest leak can drain the pillow and cause complete loss of record.

2. Puncturing of pillows: The ground beneath the pillow must be flat, and clear of any debris which might puncture the pillow. The base should be covered with a clean material such as sand which can be levelled with ease.

3. Damage to the installation by rodents: Rodents tend to eat the pipe fittings and even the pillow itself. Damage can be minimized by covering the pillow with 6 mm hardware cloth.

4. Air locks in the system: A certain amount of air may be introduced into the system when filling with the methyl alcohol solution. A vacuum pump is used to remove all air from the pillow. Care must also be taken to avoid any air locks between the pillow and the stilling well.

5. Destruction of pillows by wildlife: The sharp hooves of deer, moose or elk can easily puncture the pillow. Sites should be fenced to deter such animals. (Unfortunately fencing is not always effective, as the Little Elbow pillow was punctured earlier this winter). In Montana and British Columbia, where bears are a major problem, pillows are completely covered with a light gauge metal sheeting.

Operational problems associated with snow pillows

Most problems associated with the operation of snow pillows can be eliminated by the use of proper installation techniques and careful maintenance. However, there are some problems inherent to the system which should be recognized, otherwise serious errors can be made in the interpretation of the data obtained from the pillow.

Bridging of the pillow commonly occurs when precipitation falls as rain or when a melt period is followed by a severe cold spell. The bridge formed by ice layering in the pack prevents the full weight of snow on the pillow from being transmitted to the stilling well and results in an undermeasurement of the snow water equivalent. Checking the accumulation in the precipitation gauge against the snow pillow indicates if such a condition exists. In Alberta, bridging has been found to be a common phenomenon in the shallow plains snow pack, but seldom occurs in the mountains. The condition can sometimes be relieved by walking around the perimeter of the pillow, thereby breaking the "bridge" that has formed.

Several studies (State of California, 1976) have indicated that there is a lag between the time the snow falls, and the time the recorder fully registers the event. Careful comparison with precipitation gauge data in Alberta has revealed that lags do occur after major snow falls, but they have been usually measured in hours rather than days.

Just before melt occurs quite drastic diurnal fluctuations often occur in many snow pillow plots. A sudden drop in pressure is indicated around mid-morning and the trace in the pillow then recovers slowly reaching a maximum around mid-night. The reasons for these diurnal fluctuations are not fully understood. The fluctuations are not solely temperature dependent, but occur only in the early part of the melt season. It appears the fluctuations are due to structural changes that take place in the pack caused by variations in temperature and short wave radiation. It is interesting to note that when melting has relieved the internal stresses, the diurnal fluctuations disappear and the pillow operation returns to normal. Diurnal fluctuations are much more common in shallow snow packs on the plains then they are in the mountains. They are also more prominent on clear sunny days. The problem of interpreting the data when diurnal fluctuations occur is overcome by using a reading at a time when the pillow is stable. The Alberta Environment River Forecast Centre uses the 6:00 a.m. reading as the value for the day.

At higher elevations drifting due to winds is difficult to predict. At Gardiner Creek, the site was selected in the late spring and the station was installed the same summer. It did not appear that wind would be a problem. However, high winds this winter have caused serious drifting and the results from the pillow have been erratic. The policy now is to run a conventional snow course for at least one full winter before deciding on a pillow installation site. In this manner, it should be possible to detect potential problems before committing to a permanent installation.

Comparison of snow water equivalence data collected from snow pillows and standard snow courses

One of the reasons for installing snow pillows is to reduce or eliminate the number of costly visits that have to be made to measure the standard courses, the eventual goal being to eliminate the need for certain snow courses all together. At some snow pillow sites there are adjacent snow courses which have many years of record. Data from these courses are often used as indices in streamflow forecast models. For this reason it is necessary to relate snow course data to that obtained from the snow pillow.

The method used in Alberta to calibrate the pillow to the snow course is a method suggested by the United States Soil Conservation Services (1972). Over a period of at least three years the ratio of snow course to snow pillow reading for concurrent dates is obtained and a mean value calculated. As long as the variation from the mean of the ratios is not more than plus or minus 0.05, the pillow record is considered to duplicate the snow course record. In the Alberta experience, the relationship between the pillow and the courses does not always meet the criteria described above, and it has been necessary to develop a new index based solely on continuous pillow readings. This may be due to the fact that the snow courses (comprising the average of ten separate point measurements) were established before the snow pillow location was determined. It is now standard practice at each site visit to obtain a reading from the old snow course and readings adjacent to the pillow. Figure 3 illustrates the relationship between pillow and snow course readings in 1982/83 at Little Elbow Summit.

Comparison of precipitation data collected by snow pillow sensors and the Fisher Porter precipitation gauges.

It has been well documented (Goodison & McKay, 1972) that the Fischer Porter automatic gauge under catches snow particularly in areas exposed to wind. As mentioned previously the Alberta snow pillow sites are for the most part well sheltered. Generally, the accumulation of precipitation measured in the Fischer Porter gauges and that measured by the pillow compare favourably. The two values are plotted throughout the winter, and any significant deviation from one to the other usually indicates a problem has occurred or that the precipitation is falling as rain.

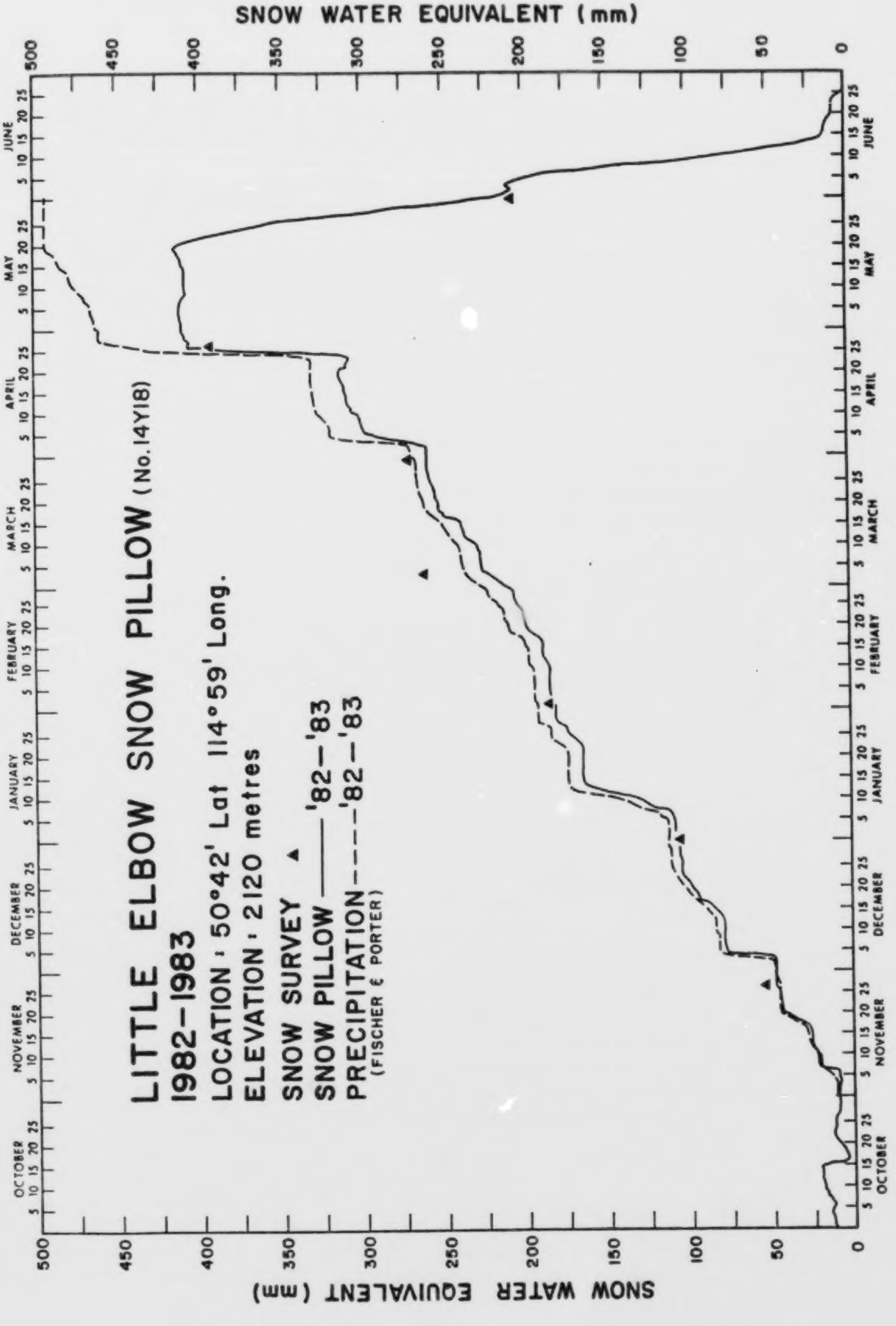
LITTLE ELBOW SNOW PILLOW (No. 14Y18)
1982–1983
LOCATION : 50°42' Lat 114°59' Long.
ELEVATION : 2120 metres
SNOW SURVEY ▲
SNOW PILLOW ——— '82–'83
PRECIPITATION - - - - '82–'83
(FISCHER & PORTER)
SNOW WATER EQUIVALENT (mm)
0
50
100
150
200
250
300
350
400
450
500
OCTOBER
NOVEMBER
DECEMBER
JANUARY
FEBRUARY
MARCH
APRIL
MAY
JUNE
5 10 15 20 25

FIGURE 3

An example of the type of problem that has been noted on several occasions is "capping" of the Fischer and Porter gauge. When the snow fall is wet and sticky (condition that occurs quite often in Southern Alberta), the snow clings to the side of the gauge eventually forming a cap. The cap prevents any more precipitation from entering the gauge. If the temperature should rise above freezing, the cap falls into the gauge and normal operation resumes. It is only with telemetry, the presence of a snow pillow, and a Fischer Porter gauge that this undercatchment can be quantified. In the standard networks which do not have telemetry this phenomenon can go undetected, as the period between visits is often several months.

Heavy rain on snow often results in a dramatic (although sometimes short lived) drop in pressure (Buer et al, 1984) on the snow pillow. Comparison of the snow pillow data with the Fischer Porter data and temperature often confirms that a rain event had taken place. The form in which precipitation falls, snow or rain, is extremely significant to the forecaster, for rain on snow can cause rapid melt.

The primary purpose of the snow pillow is to measure snow accumulation and melt rates whereas the main reason for the Fischer Porter gauge is to measure summer rainfall. However, the experience gained operating both types of sensors in real time during the winter indicates that inconsistencies in performance is due to specific physical conditions and the operation of the dual system of sensors in the winter is well worth while.

How snow pillow data have been used

1. Snow melt rates during the critical spring and early summer period can be fed directly into runoff simulation models. A modified version of the Streamflow Synthesis and Reservoir Regulation (SSARR) model is used to predict mountain runoff in Alberta. A melt rate index is necessary to simulate snow melt runoff with the model. Melt rates from snow pillows are calculated for individual basins. Studies by Ferner & Wigham (1985) have shown that snow pillows in the Marmot Research Basin provide better melt rate estimates for application to SSARR than indirect methods that use temperature and other parameters.

2. To carry out long range water supply forecasts, the daily accumulation of snow obtained from pillows is input to simulation models which are constantly updated. Snow pillows provide a method to constantly update this information, particularly after major storms.

3. Snow pillows provide a reliable estimate of snow accumulation from the start of the runoff season throughout the active period. If the models are deviating too much from the observed snow available, they can be corrected as needed.

4. For flood forecasting in the spring, data from the pillows are used to detect if precipitation is falling in the form of snow or rain.

5. Snow pillows can be used to estimate the date of the peak flow for specific streams. For example, a straight forward way of predicting peak dates using snow pillow data in the Western U.S. has been described by Farnes, (1984).

In the Western United States (Farnes, 1985) where extensive snow pillow networks have been used for many years, pillows are being used for purposes other than those related to water resources. Snow pillows can be used in the management of parks and wildlife. For example, they can give useful information with respect to back country travel, can be used to tell how much snow is on the ground at higher elevations, and whether the snow conditions are ripe for avalanches. Pillows can also be used to help predict when bears may emerge from hibernation, for a good correlation appears to exist between the start of melt and the beginning of bear movements.

In Montana the pillows are also used to help manage remote mountain highways. From a base camp, managers can determine if they need to plough roads and in what order the work should be done. It is believed that in the future, further applications for snow pillow data will be found.

Conclusions

1. Snow pillows in the mountainous areas of Alberta monitored in near real-time and used in conjunction with other meteorological sensors provide valuable information for streamflow forecasting.

2. The successful operation of snow pillows depend on good installation and maintenance practices. Data from the pillow and other sensors must be inspected and evaluated on a ongoing basis to obtain maximum benefit from the information provided.

3. Since winter precipitation may fall either as snow or rain, it is desirable to run a precipitation and temperature gauge in conjunction with the snow pillow at key sites. Anomalies in the performance of these sensors that may normally go undetected can be found by closely monitoring the data from the two different types of sensors.

4. Snow pillows are not the ideal snow monitoring device for they are expensive to install, and they have inherent weakness in operation which are sometimes difficult and even impossible to overcome. They are also prone to destruction by several forms of wildlife. New devices such as the nuclear snow gauge look promising and their performance should be investigated for the forecasting networks of the future.

5. Melt rates provided from strategically placed snow pillows give an index that when used in the SSARR model results in better forecast estimates than using an index based solely on temperature.

6. There are potential uses for snow pillows that go beyond the water resource management field. Some of these are avalanche prediction, wildlife management, and general park management.

REFERENCES

Buer, S.M., et al, 1984, "The Impact of Automated Hydrometeorological Instrumentation upon Data Quality for the Feather River Basin, California," Proc. 52nd. Western Snow Conference.

Coles, G.A., Graham, D.R., 1983, "Alberta Environment Real Time Hydrometeorologic Network Current Status (February, 1983)," Proc. 7th Annual Workshop, Alberta Climatological Association.

Cox, L.M. et al, 1978, "The Care and Feeding of Snow Pillows, "Proc. 46th Western Snow Conference, pp 40-47.

Farnes, P.E., 1978, "Future Snow Survey Operations with Snotel" Proc. 46th Western Snow Conference., pp 15-20.

Farnes, P.E., 1984, "Predicting time of Peak Snowmelt Runoff from Snow Pillow Runoff." Proc. 52nd Western Snow Conference, pp 132-138.

Farnes, P.E., 1985, Personal Communication

Ferner, S.J., Wigham, J.M.,1985, "The Use of Snow Pillow Data for Melt Rate Input to the SSARR Model." 7th Canadian Hydrotechnical Conference (In print).

Goodison, B.E., McKay, D.G., 1978, "Canadian Snowfall Measurements: Some Implications for the Collection and Analysis of Data from Remote Stations." Proc. 46th Western Snow Conference, pp 48-57.

Graham, D.R., Kuhnke, W, 1978, "Hydrometeorological Network Proposal for the Headwaters of the South Saskatchewan River," Alberta Environment, Technical Services Division, Edmonton, Alberta.

Kerr, W.E., 1976, "Snow Experiences in a Prairie (Alberta) Environment", Proc. 43rd Western Snow Conference, pp 39-47.

State of California, Department of Water Resources, 1976, "Snow Sensor Evaluation in the Sierra Nevada, California."

United States Department of Commerce, Soil Conservation Service, 1972 "Snow Survey and Water Supply Forecasting, Section 22, SCS National Engineering Handbook".

REMOTE MONITORING OF DEPTH OF SNOW ON GROUND WITH A MICROLOGGER

by

S.N. Edey

Agrometeorology Section
Land Resource Research Institute
Ottawa, Ontario
Canada

D.J. Buckley, M.J.L. Lalond and C.F. Nicholls

Engineering and Statistical Research Institute
Ottawa, Ontario
Canada

presented at

SNOW PROPERTY MEASUREMENTS WORKSHOP

Lake Louise, Alberta

1-3 April, 1985

TECHNICAL MEMORANDUM 140

Compiled By

P.R. Kry

NRCC 27594

Remote Monitoring of Depth of Snow on Ground with a Micrologger

S.N. Edey
Agrometeorology Section
Land Resource Research Institute
Ottawa, Ontario

D.J. Buckley, M.J.L. Lalond, C.F. Nicholls
Engineering and Statistical Research Institute
Ottawa, Ontario

Summary

A system for automatically monitoring snow depth at remote locations is described. Snow depth is sensed by an ultrasonic transducer which combines a reference target and a microprocessor to compensate for changes in atmospheric temperature, humidity and pressure. Snow depth data is sampled and temporarily stored on a micrologger at the remote site. The micrologger is linked via telephone to a personal computer thus the stored data can be accessed daily.

Introduction

There is a rapid and ever-increasing demand for "real-time" agroclimatic data to be used in agricultural-oriented programs. In conjunction with this demand is the high cost of taking such observations particularly over weekend and holiday periods. This problem is most serious and research managers find it more and more difficult to allocate adequate funds to cover such ongoing and labor intensive activities. For these reasons, a fully automated observational and recording system appears very attractive at this time.

In the past such systems have been expensive, somewhat unreliable, and therefore unacceptable for use in agroclimatic data acquisition networks. Because of the requirements for special data by agriculture, most agricultural establishments observe more than the basic climatic elements of daily maximum and minimum air temperature and precipitation. A well established agroclimatic station usually observes the following items on a daily basis:

1. Maximum temperature
2. Minimum temperature
3. Grass minimum temperature
4. Rainfall
5. Total precipitation (rain plus snow)
6. Depth of snow on ground
7. Duration of bright sunshine
8. Run of wind
9. Maximum wind speed for one hour with direction
10. Evaporation
11. Wetting duration
12. Soil Temperature

As originally agreed to in 1958, Agriculture Canada (Research Branch) follow an observing and reporting procedure established by the Atmospheric Environment Service (AES), Environment Canada. Many of the current agroclimatic observations (AES standards) still rely on mechanical sensors or manual methods of a past era. Depth of snow on the ground is one such observation. Although a wide range of dependable electronic sensors for monitoring of some elements have evolved over the years, point measurement of snowcover in Canada is still limited to the snow ruler, snow stake or similar snow marker systems. Other such climatological events still monitored by mechanical means include hours of bright sunshine, evaporation and daily snowfall amounts.

Within the agricultural industry, real-time snowcover information is extremely important for many reasons. The determination of future plant water availability, irrigation potentials, evaluation of the well-being of overwintering crops, survival rate of pests, mechanical damage to plants due to frost penetration and soil temperature regimes are but a few such reasons. The need for a reliable sensor to monitor snowcover is thus well established. Such a sensor must be readily acceptable to current and future generations of microloggers and the cost must be low in order to lend itself to network application (Gubler, 1981). Although the role of the micrologger appears promising in the provision of high quality and readily available agroclimatic data, the major obstacle at this time is the lack of suitable electronic sensors to monitor certain environmental events significant to agriculture.

System Description

The monitoring system consists of three main parts - the field sensing unit, the micrologger for temporary data storage, and the host computer for access, processing and permanent data storage. In essence, the field unit or sonic snow gauge emits a sonic pulse through the air which is reflected back to the transducer by a reflective surface, in this case snow. The elapsed time is then used to calculate the distance from emitter to snow surface. The digital depth measurement is converted to a millivolt analog output for sampling and storage in the micrologger. The micrologger, in turn, is interrogated by a computer using a telephone modem and line. The computer ultimately formats and stores the measured snowcover data in permanent memory.

The heart of the sonic snow gauge is an ultrasonic ranging device manufactured by the Polaroid Corporation. This transmitter/receiver unit is mounted in a 50 cm long PVC tube or guide which is suspended on a 9-foot tripod, as shown in Figures I and II. The PVC guide can be positioned at any height up to 200 cm above the ground. Average snowcover for the area is used to reference the field height. The tripod itself is anchored by 30 cm pins driven into the soil.

The controller of the unit is a microprocessor chip (Intel 8748) which determines the interval and duration of the sonic burst, measures the time required for the echos to return, filters noise, calculates the snow depth, displays the snow depth on a digital LCD display and generates an analog output via a digital-to-analog converter. A 55 khz sonic burst is transmitted every 50 ms. Two echos are received by the transducer; one (Echo 1) from the fixed reference target located 50 cm from the transducer and the second (Echo 2) from the snow surface. The reference echo is used to compensate for changes in air temperature,

Figure 1. PVC SONIC GUIDE (CROSS SECTION)

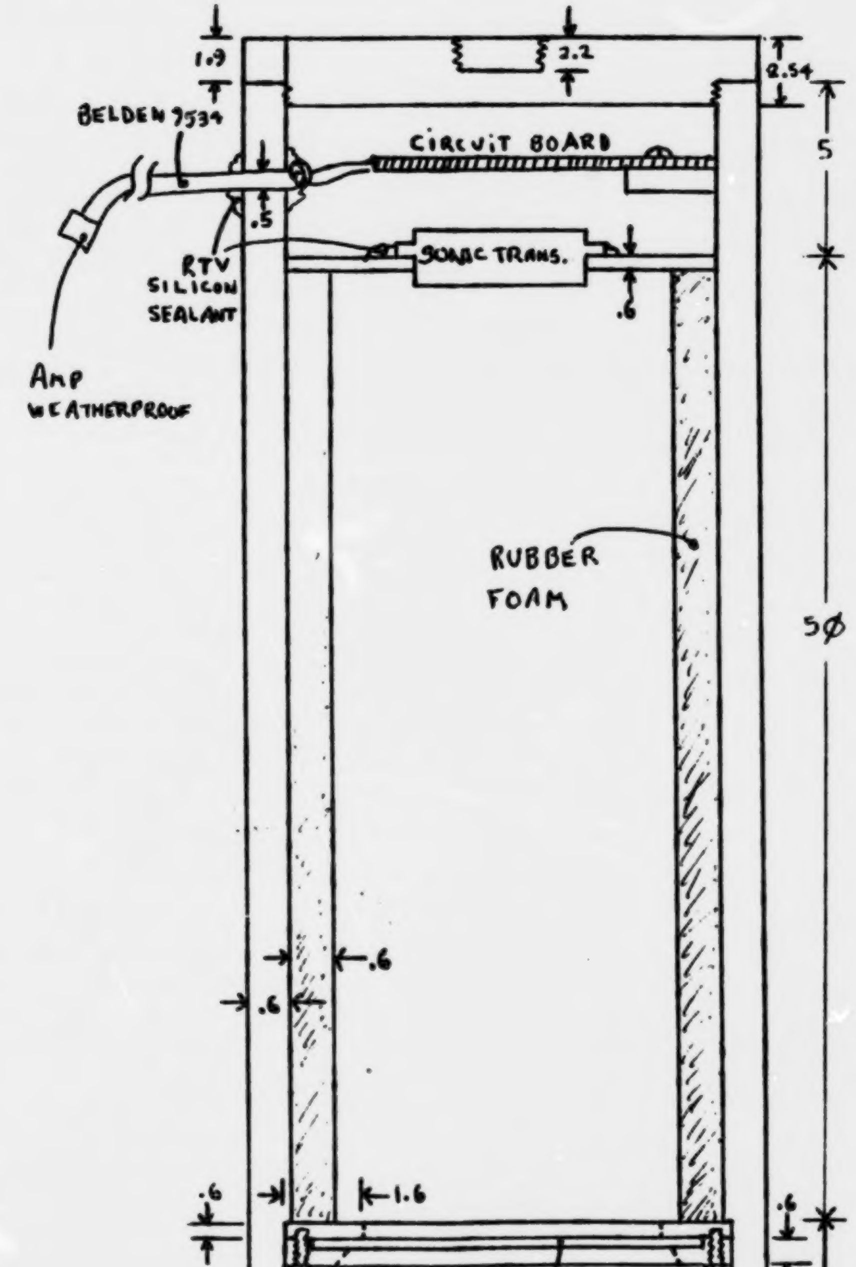
1.9
2.2
2.54
BELDEN 9534
CIRCUIT BOARD
.5
RTV
SILICON
SEALANT
SONIC TRANS.
.6
AMP
WEATHERPROOF
5
RUBBER
FOAM
50
.6
.6
.6
1.6
.6
.6
.6
.8
STAINLESS STEEL
MESH SCREEN
(5.5 sq./cm)
.5
5
11.3

*ALL DIMENSIONS IN CENTIMETERS
(NOT TO SCALE)

Figure 2. Tripod and Sensor

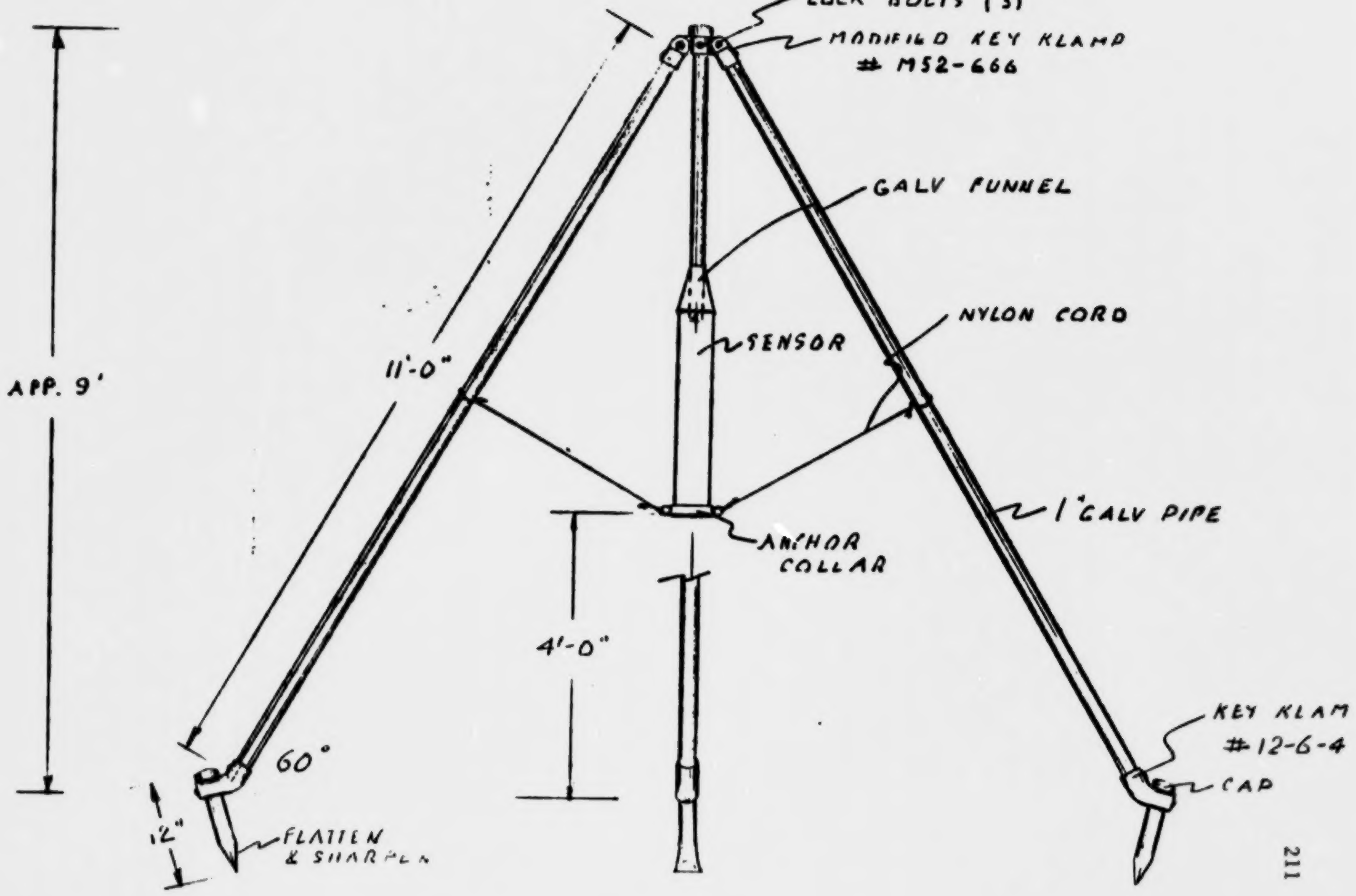
LOCK BOLTS (3)
MODIFIED KEY KLAMP
# M52-666
GALV FUNNEL
NYLON CORD
SENSOR
1" GALV PIPE
ANCHOR
COLLAR
APP. 9'
11'-0"
4'-0"
60°
12"
FLATTEN
& SHARPEN
KEY KLAM
#12-6-4
CAP

humidity and pressure. The distance from the transducers to the snow surface is determined by the equation,

$$x = \frac{tr}{50} (ts)$$

where x is the distance to the snow surface in cm., tr is the transit time for reference echo 1 and ts is the transit time for echo 2 from the snow surface. Since the distance from the transducer to the ground level (zero snow) is known, the snow depth is then calculated by the microprocessor.

After the emission of a sonic burst (4 cycles at 55 khz), the system waits for the first echo to return within 6 ms. If a timeout occurs, it waits for another 50 ms before sending another sonic burst. On the successful return of the first echo, an event counter reads and stores to transit time for future calculations. The sequence is repeated for the second echo. If unsuccessful in reading either echo, the last current measurement for snow depth is displayed along with a double negative sign on the LCD display to indicate that an echo was missed.

Sixteen transit time readings are accumulated in buffers for both echos. An average is made and stored as Echo 1 and Echo 2, respectively which is then used to calculate distance or snow depth. The use of the PVC guide may create a lag response to the velocity of Echo 1 due to a rapid change of air temperature. The portion of the echo travelling beyond the PVC guide, i.e. Echo 2 - Echo 1, responds immediately to any change in air temperature. Thus, a filter (approximately 15-min time constant) is used to minimize the effect of abrupt changes in ambient air temperature. The calculated distance term is unaffected by up to a 5 degree C change of temperature over a 15-min period of time. It is unlikely the air temperature would change more rapidly than this.

A second component of the field sensor is the processing/display unit which in this situation was housed in a nearby instrument dugout. This unit contains the microprocessor, support circuitry, the LCD display and the analog output circuit (10 mV/cm of snow).

The micrologger (Campbell Scientific Model CR21) was used to record and process the measurements from the sonic snow gauge. The CR21 is a miniaturized nine-channel, battery powered micrologger which can handle inputs from a variety of sensors. Once each minute the micrologger samples the input signals according to the input programs specified in a user-entered input table then processes the data and stores according to user-entered output programs. In this case an hourly average for snow depth was calculated and stored for later access by the host computer. Most CR21's have standard input and output programs, however, some may contain non-standard PROM relative to special applications. The stored data may be read later using a dial-up telephone line, telemetry, cassette recorder, portable printer or the digital display.

The third and final component of the system is an IBM-PC host computer which automatically accesses the CR21 via a telephone line and modem. The accessed data is then formatted and stored for data interpretation and final archiving.

Results and Discussion

Performance trials of the snow depth sensor were made in the laboratory prior to the installation of a field unit. No problems were encountered under a wide range of simulated situations. In October, 1984, a prototype sonic snow gauge was installed in the weather compound at the Central Experimental Farm, Ottawa, officially listed as Ottawa CDA. This is a 20 m x 20 m site surrounded by an 8' chain link security fence. A small instrument dugout is contained within the fenced area.

In order to validate the readings from the sonic snow gauge, two metal snowrulers (1 metre) were positioned on the west and east side of the tripod area. These rulers were read once a day by the regular weather observer. A 10-stake snow course over a distance of 1 kilometre in the general area of the weather site was also monitored on a daily basis and an average value recorded. This snow course average provides the official snow-on-ground observation for Ottawa CDA.

The 1984-85 winter season proved to be near ideal for test purposes. A wide variety of weather was experienced which provided the necessary field evaluation conditions. A large number of erroneous observations were encountered initially due to low reflectivity from freshly fallen snow, blowing and drifting snow and very heavy snowfalls. Remedial action consisted of changes to the signal amplification and filtering processes. Eventually a good sensitivity was obtained which could cope with the various snow surface situations and snowfall conditions. No other hardware problems were encountered.

By mid-January, the system appeared operationally acceptable. Table 1 shows the observed values as recorded at the Ottawa CDA weather site. Scouring around the snow rulers due to strong winds was noted and undoubtedly helps to account for the disparity between some of the earlier readings between gauge and snowruler.

Conclusions

Measurement of snowfall and snow on ground is extremely difficult at the best of times. The representativeness of a point observation is questionable considering the extreme variation found on an areal basis. However, the sonic snow gauge does appear to be acceptable as a means of automatically monitoring point depth of snow on ground. The sensor works well over a wide variety of conditions although extreme situations may cause signal attenuation or loss. This is not considered a major drawback since only one daily reading is required for this particular agroclimatic parameter.

Further refinement of the system may provide a basis for monitoring daily snowfall amounts. The relatively low cost of the device is particularly appealing and most suitable for network applications such as those found in Agriculture Canada.

Table 1: Snowfall observations at Ottawa CDA, January 15-31, 1985

Day	Snowfall (cm)	Sonic Snow Gauge	Snow Ruler	Depth of Snow on Ground (marker)
15	0	45	38	28
16	T	45	38	26
17	3	50	41	26
18	2	50	45	26
19	4.6	54	45	28
20	.8	57	54	29
21	1.8	57	56	28
22	T	59	56	29
23	1	59	55	25
24	2.8	62	55	26
25	3.8	66	60	29
26	1.9	67	65	32
27	2.4	64	66	33
28	.7	66	66	34
29	0	64	65	33
30	0	64	66	33
31	1.6	63	64	32
change	26	18	26	4

N.B.: During January 15-22, drifting snow was quite pronounced during the entire period.

Acknowledgements

Thanks to J.C. Lacasse for his contribution as to the logistics of data capture, retrieval and preparation.

References

Gubbler, H. 1981. An inexpensive remote snow depth gauge based on ultrasonic wave reflection from the snow surface. J. Glaciology, Vol. 27, No. 95, pp 157-163.

EXTRAPOLATING SNOW MEASUREMENTS ON THE MARMOT CREEK EXPERIMENTAL BASIN

by

P.Y. Bernier

Northern Forest Research Centre
Edmonton, Alberta
Canada

presented at

SNOW PROPERTY MEASUREMENTS WORKSHOP

Lake Louise, Alberta

1-3 April, 1985

TECHNICAL MEMORANDUM 140

Compiled By

P.R. Kry

NRCC 27594

EXTRAPOLATING SNOW MEASUREMENTS ON THE MARMOT CREEK EXPERIMENTAL BASIN

Pierre Y. Bernier
Northern Forest Research Centre

INTRODUCTION

Hydrological research in Alberta dates back to the early 1960's when the Alberta Watershed Research Program (AWRP) was initiated. The goal of the AWRP was to provide the forest management agency (then the Eastern Rockies Forest Conservation Board) with tools for managing and enhancing the water supply of the East Slopes. Marmot Creek Experimental Basin was the first of three gauged basin set up in the headwaters of the Saskatchewan River under the auspices of the Program.

Located in the Kananaskis valley, 100 km west of Calgary, Marmot Creek basin ranges in elevation from about 1585m at the outlet to 2805m at the peak of Mt. Allen (Figure 1). It is adjacent to the site of the alpine events for the 1988 Calgary Winter Olympics. The basin is divided into 3 sub-basins, Cabin, Middle and Twin, and a confluence area between the sub-basins weirs and the main Marmot Creek weir. A few topographic characteristics of the sub-basins are listed in Table 1.

Forest cover is mainly old spruce-fir (Picea spp. and Abies lasiocarpa (Hook.) Nutt.) with a scatter of trembling aspen (Populus tremuloides Michx.). The lower tip of the basin is covered with even-aged lodgepole pine (Pinus contorta Dougl. var. latifolia). Alpine larch (Larix lyalii Parl.) occupies a narrow band just below tree line.

Snow measurements have been carried out on the basin for over twenty years. This snow data has already found applications in the evaluation of treatment effects in a forest cutting experiment, and in the developemnt and testing of snow melt simulators and water yield estimation procedures. The purpose of this particular exercise was to produce estimates of snow depths and water equivalent for any winter months and for any forested portion of the basin.

TOPOGRAPHIC CLASSIFICATION	CABIN SUB-BASIN	MIDDLE SUB-BASIN	TWIN SUB-BASIN	CONFLUENCE AREA
Total area (km^2)	2.2	3.0	2.8	2.0
Maximum elevation (m)	2750	2805	2600	1870
Minimum elevation (m)	1730	1760	1765	1585
Area above tree line (%)	24.0	74.8	43.4	0
Length of streams (km)	6.7	5.7	5.5	1.9

Table 1. Physiographic characteristics of the sub-basins within Marmot Creek basin (portions of the table from Stevenson, 1967).

SNOW MEASUREMENTS

Snow pillows

The seven large polygonal snow pillows used on the basin are made of butyl rubber and filled with a methyl alcohol solution. The pillows are installed horizontally on the ground or on a low platform. Variations in the pressure exerted on the pillows by the varying snowpack are recorded continuously on strip chart recorders via a stilling well arrangement. Figure 1 shows the location of the four pillows used in the analysis. Description of the individual sites is as follows:

No.1- Installed Fall 1969 in a 20 m (1 H) man-made opening ; 1787 m of elevation on a gentle east-facing slope; mature spruce, lodgepole pine and alpine fir, 20 m tall.

No.2- Installed in Fall 1972 in undisturbed forest; 1950 m of elevation on an east-facing slope; mature spruce, lodgepole pine and alpine fir, 15-20 m tall.

No.3- Installed Fall 1972 in undisturbed forest; 2153 m of elevation on an east-facing slope; mature spruce and alpine fir.

No.4- Installed Fall 1972 in a small natural clearing near tree line; 2153 m of elevation on a broad east-facing ridge; alpine fir and alpine larch, 3 m tall.

Snow courses

Twelve long term snow courses of Marmot Creek Basin are sampled monthly, from February until March, many of them since 1963. In each course, 10 fixed points marked with stakes are sampled for snow depth and snow water equivalence (SWE). Six of these were retained for the analysis. Their locations are shown in Figure 1. The description of the individual sites is as follows:

No.3- Gentle south slope; mature spruce, lodgepole pine and alpine fir; partially logged in the forties.

No.6- Gentle north-east slope; mature spruce, lodgepole pine and alpine fir; partially logged in the forties.

No.8- South slope; lodgepole pine, 6 m tall.

No.11- South-east slope; mature spruce, lodgepole pine and alpine fir.

No.14- North-east slope; mature spruce, lodgepole pine and alpine fir, with small natural openings.

No.18- East slope; 50% mature and 50% newly regenerated spruce, lodgepole pine and alpine fir.

The snow grid consists of parallel sampling lines, 200 m apart, covering the entire forested portion of the basin, along which snow depth and SWE were sampled every 20 m. Every five consecutive readings centered around a fixed marker or "pin" were averaged and expressed as the reading for that particular pin. There are 258 such pins on the basin. Measurements were taken once a year, the third week of March from

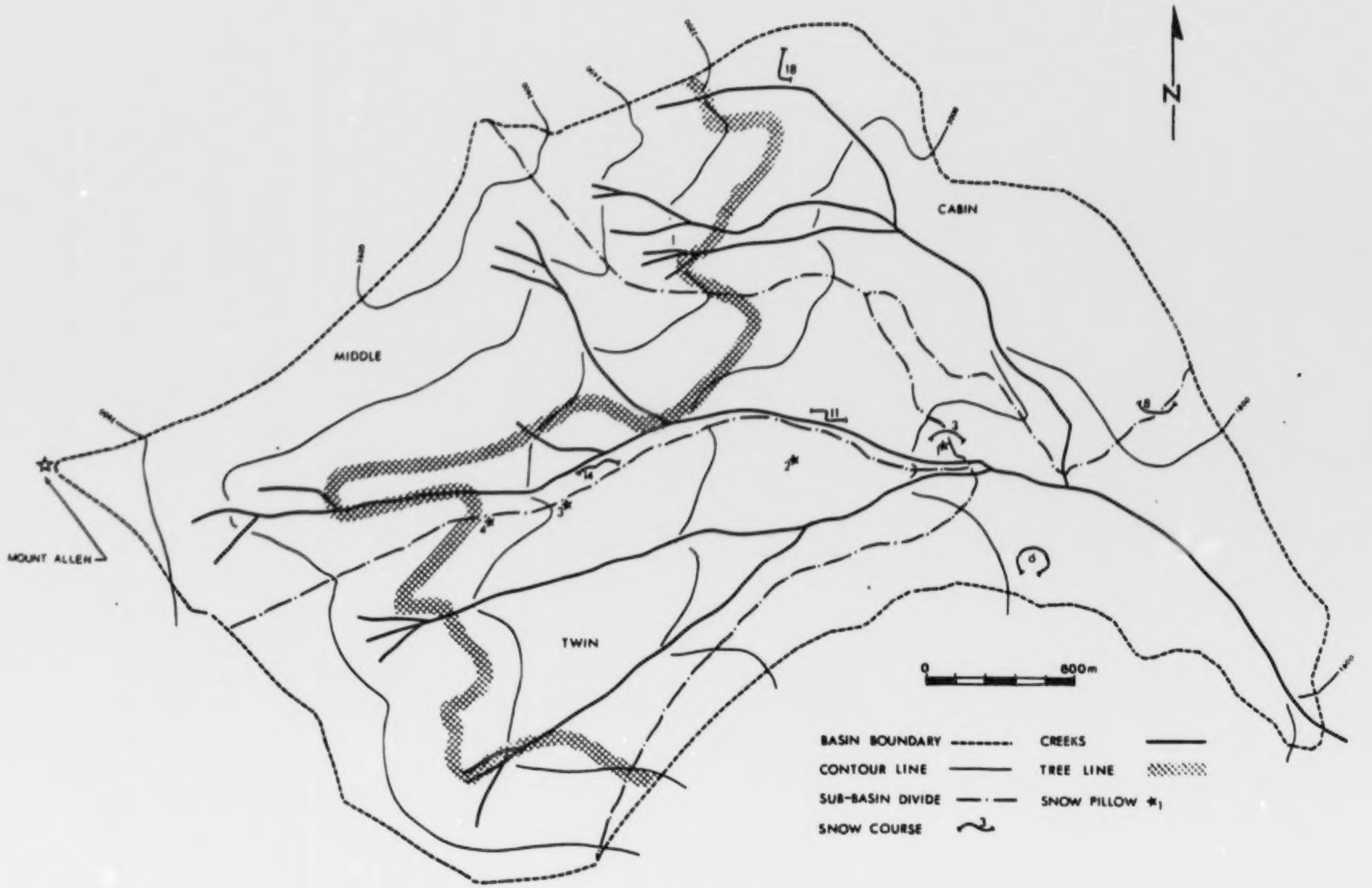
N
CABIN
MIDDLE
TWIN
MOUNT ALLEN
18
11
14
1
2
3
4
0
800m
BASIN BOUNDARY
CONTOUR LINE
SUB-BASIN DIVIDE
SNOW COURSE
CREEKS
TREE LINE
SNOW PILLOW

Figure 1. Map of Marmot Creek Experimental Basin. The contours are in meters

1969 to 1980 (no survey was done in 1979) for a total of 11 readings per pin. Pin locations are shown in Figures 3, 4 and 5.

Snow stakes

An other type of snow measurement whose results will be used later in this paper is the snow stake reading. Snow stakes are markers placed above the tree line where regular sampling is impossible. The snow depth at the stake is read from a convenient vantage point with a telescope. There are over 40 such stakes in the alpine portion of Marmot. Sampling is done monthly from February until June since 1974.

ANALYSIS OF THE DATA

The task of estimating snow depths and water equivalents meant somehow to combine the spatially intensive snow pin data with the temporally intensive snow pillow or snow course data. Previous work done by Golding (1974) showed that topographic and forest-related variables could account for no more than 48% of the variation in SWE at snow course locations. Accordingly, such variables were not included in the present analysis.

The basic concept for the extrapolation of the pin data is simple. A regression is fitted between the measured SWE or snow depth of each pin of the snow grid and the corresponding March readings from a snow course or snow pillow. These equations are then used to estimate pack characteristics at the pin locations for the winter months where pin data is unavailable.

The production of these snow estimates requires the answering of a number of fundamental questions on snow distribution and measurement.

Can a prediction equation based on March data be extended to the rest of the winter? Should the analysis be based on snow course or snow pillow data? Finally, is the pillow or course "most similar in elevation and aspect" to a particular pin the best choice for the extrapolation of the pin data?

To answer the first question, regressions were developed between the March SWE readings of paired snow courses. The pairs were chosen according to the highest R^2, all values obtained being above 0.95. These equations were then used to "predict" snow water equivalent at snow courses locations for the other winter months. Figure 2, a typical result of the test, shows actual versus predicted readings at snow course 18 for February, April and May, from 1969 to 1980. The predictor is, in this case, course 11. The good grouping around the 1:1 line indicates the validity of the March-derived equation.

To answer the second question, three sites were chosen where a snow pillow was adjacent to a snow course. A covariance analysis was run between readings from these instruments and the average reading of 10 to 15 adjacent snow pins. The correlation coefficients (Table 2) showed no significant difference ($\alpha=0.05$) between goodness of fit obtained with snow courses or pillows. A similar analysis (results not shown) was run

	Course 3	Pillow 1	Course 11	Pillow 2	Course 14	Pillow 3
R^2	0.96	0.96	0.98	0.87	0.99	0.97

Table 2. Coefficient of determination (R^2) between snow water equivalent at snow courses or snow pillows and at adjacent snow pins at three different sites on Marmot basin.

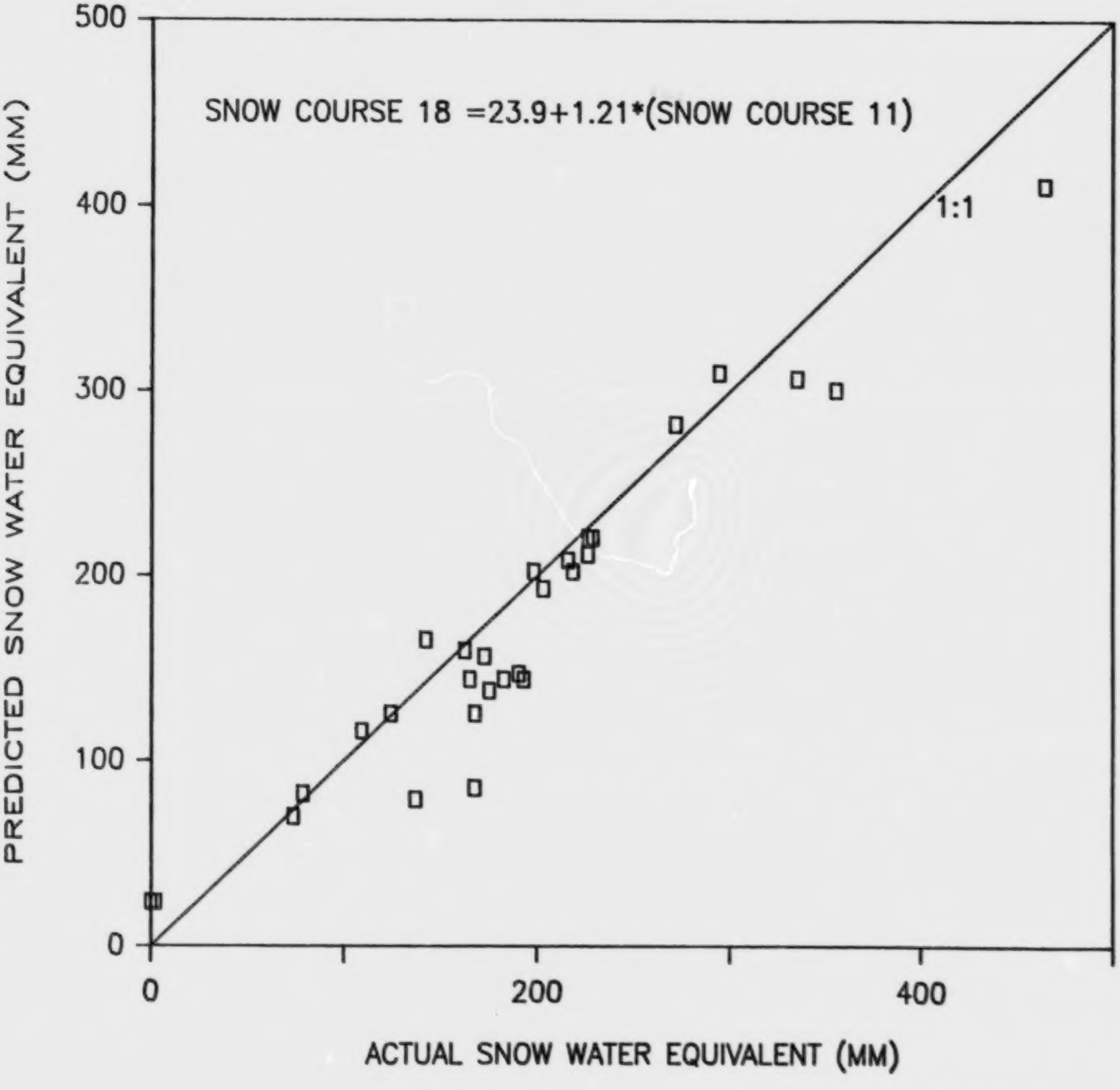

Figure 2. Predicting snow water equivalent at snow course 18 from snow course 11 for the winter months other than March, 1969-1980. The regression is based on March readings for those years

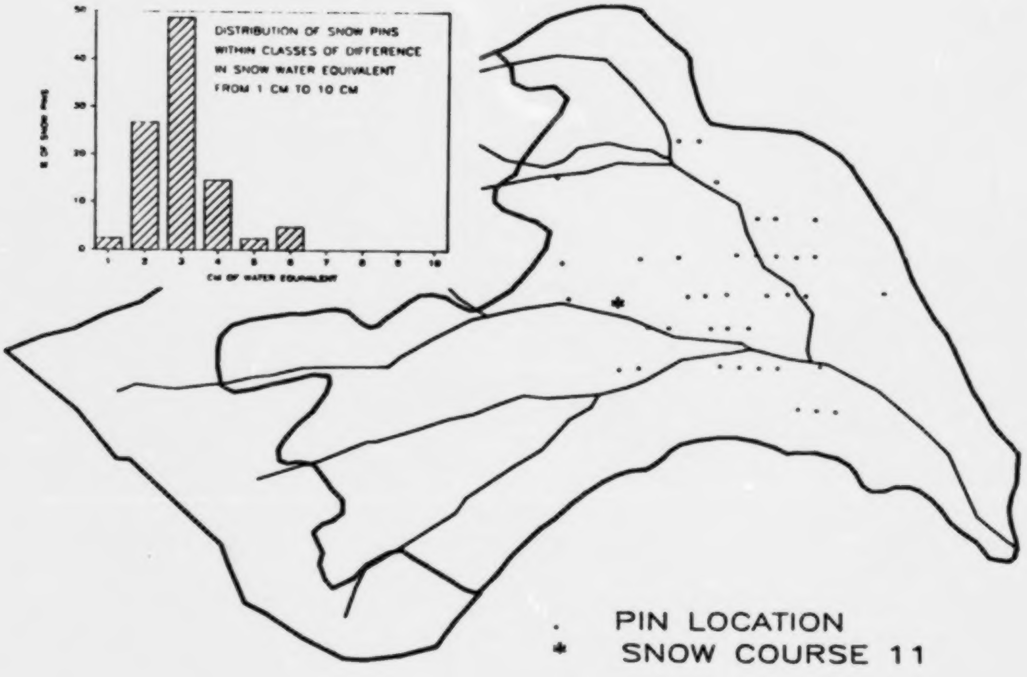
DISTRIBUTION OF SNOW PINS
WITHIN CLASSES OF DIFFERENCE
IN SNOW WATER EQUIVALENT
FROM 1 CM TO 10 CM
0
10
20
30
40
50
1
2
3
4
5
6
7
8
9
10
CM OF WATER EQUIVALENT
. PIN LOCATION
* SNOW COURSE 11

Figure 3. Pairing of pins and snow course 11 according to the smallest average absolute difference in snow water equivalent between the pins and the snow courses. The graph refers to mapped pins.

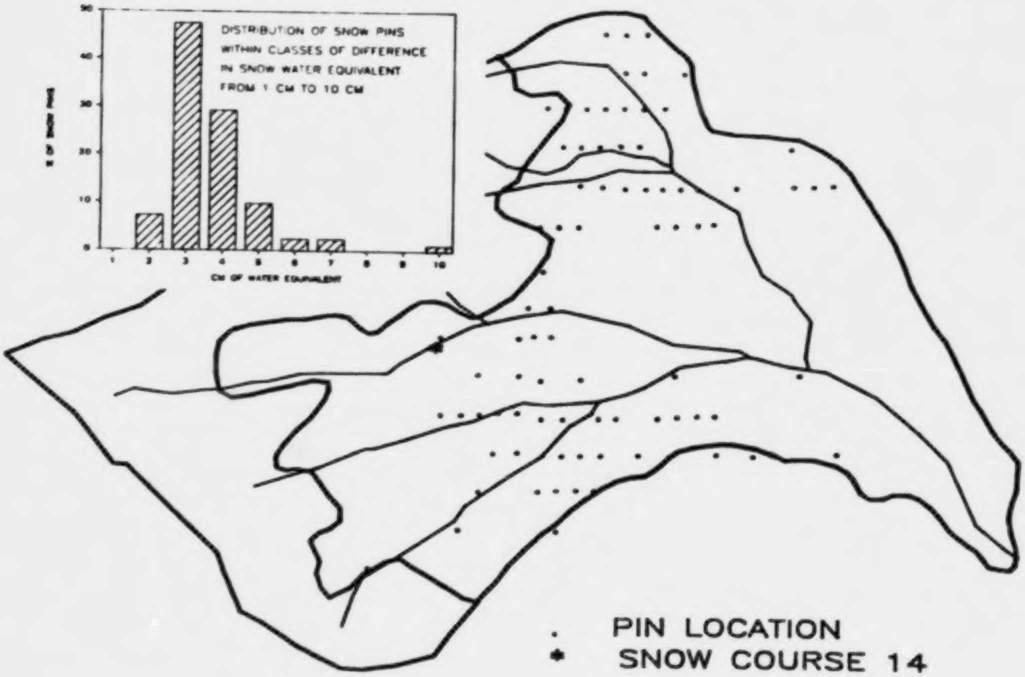
DISTRIBUTION OF SNOW PINS
WITHIN CLASSES OF DIFFERENCE
IN SNOW WATER EQUIVALENT
FROM 1 CM TO 10 CM
0
10
20
30
40
50
1
2
3
4
5
6
7
8
9
10
CM OF WATER EQUIVALENT
. PIN LOCATION
* SNOW COURSE 14

Figure 4. Pairing of pins and snow course 14 according to the smallest average absolute difference in snow water equivalent between the pins and the snow courses. The graph refers to mapped pins.

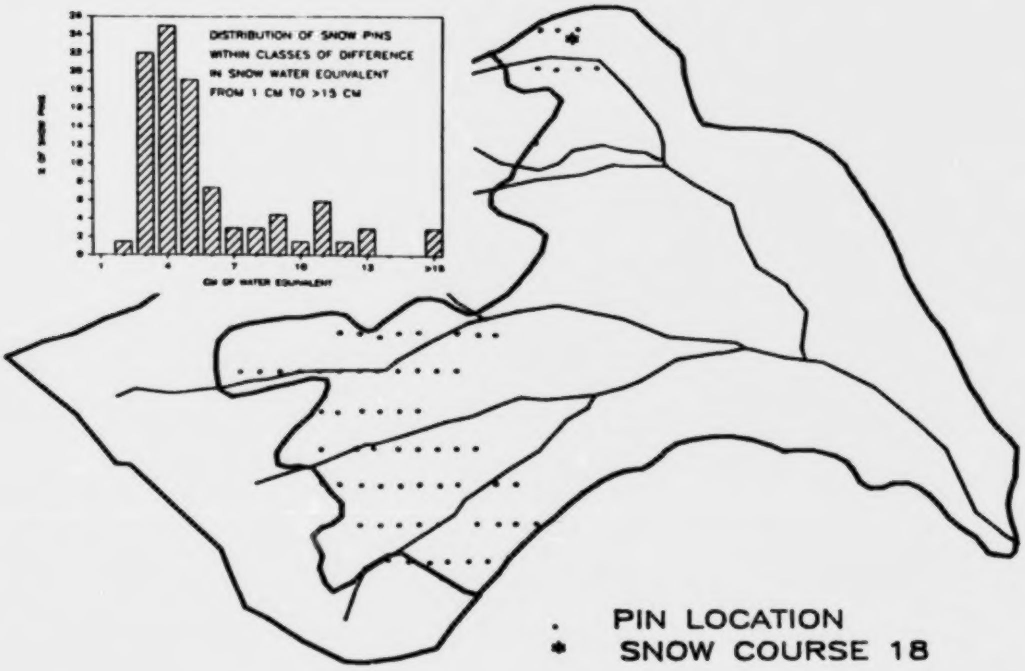
DISTRIBUTION OF SNOW PINS
WITHIN CLASSES OF DIFFERENCE
IN SNOW WATER EQUIVALENT
FROM 1 CM TO >15 CM
# OF SNOW PINS
0
2
4
6
8
10
12
14
16
18
20
22
24
26
1
4
7
10
13
>15
CM OF WATER EQUIVALENT
. PIN LOCATION
* SNOW COURSE 18

Figure 5. Pairing of pins and snow course 18 according to the smallest average absolute difference in snow water equivalent between the pins and the snow courses. The graph refers to mapped pins.

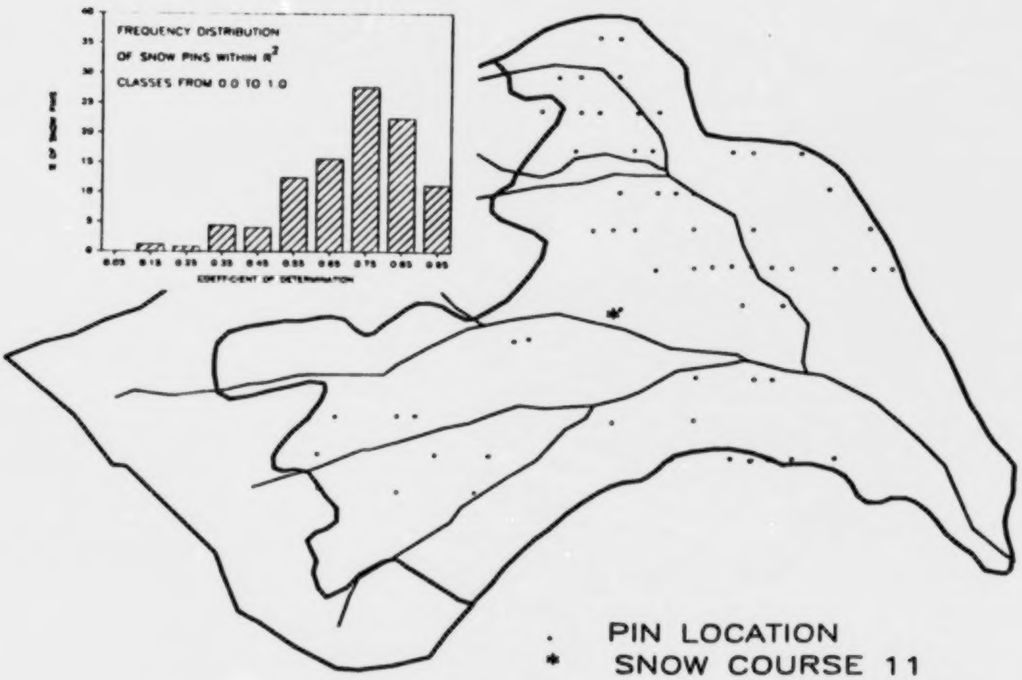
FREQUENCY DISTRIBUTION
OF SNOW PINS WITHIN R²
CLASSES FROM 0.0 TO 1.0
# OF SNOW PINS
0
5
10
15
20
25
30
35
40
0.05
0.15
0.25
0.35
0.45
0.55
0.65
0.75
0.85
0.95
COEFFICIENT OF DETERMINATION
. PIN LOCATION
* SNOW COURSE 11

Figure 6. Pairing of pins and snow course 11 according to the highest R^2 between March snow water equivalent at pins and snow courses. The inset graph refers to all pins of the basin.

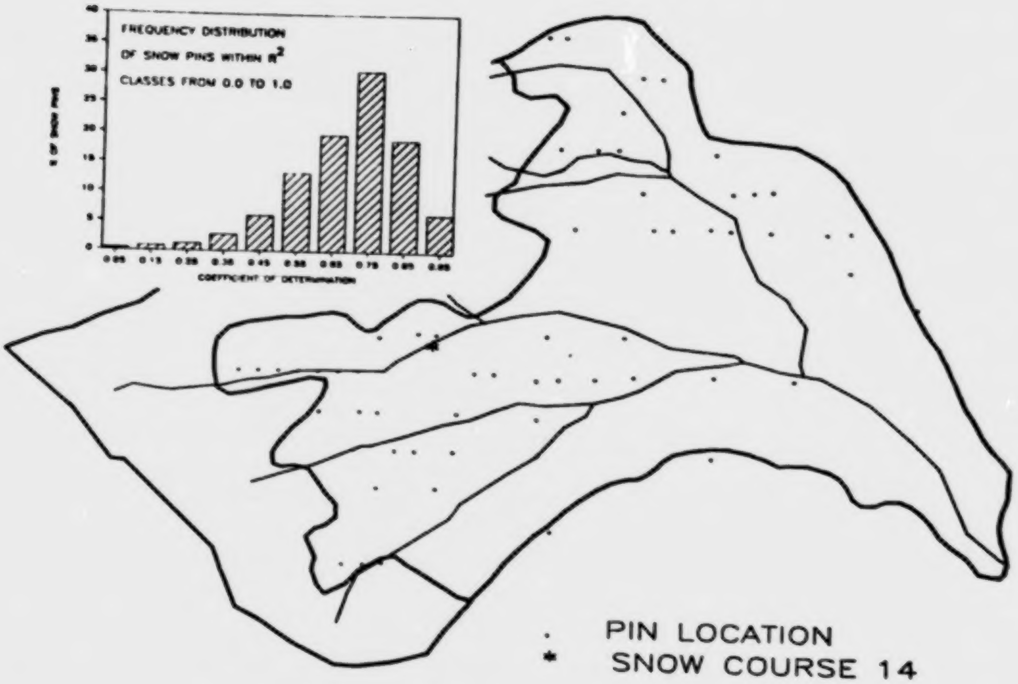
FREQUENCY DISTRIBUTION
OF SNOW PINS WITHIN R^2
CLASSES FROM 0.0 TO 1.0
% OF SNOW PINS
0
5
10
15
20
25
30
35
40
0.05
0.15
0.25
0.35
0.45
0.55
0.65
0.75
0.85
0.95
COEFFICIENT OF DETERMINATION
. PIN LOCATION
* SNOW COURSE 14

Figure 7. Pairing of pins and snow course 14 according to the highest R^2 between March snow water equivalent at pins and snow courses. The inset graph refers to all pins of the basin.

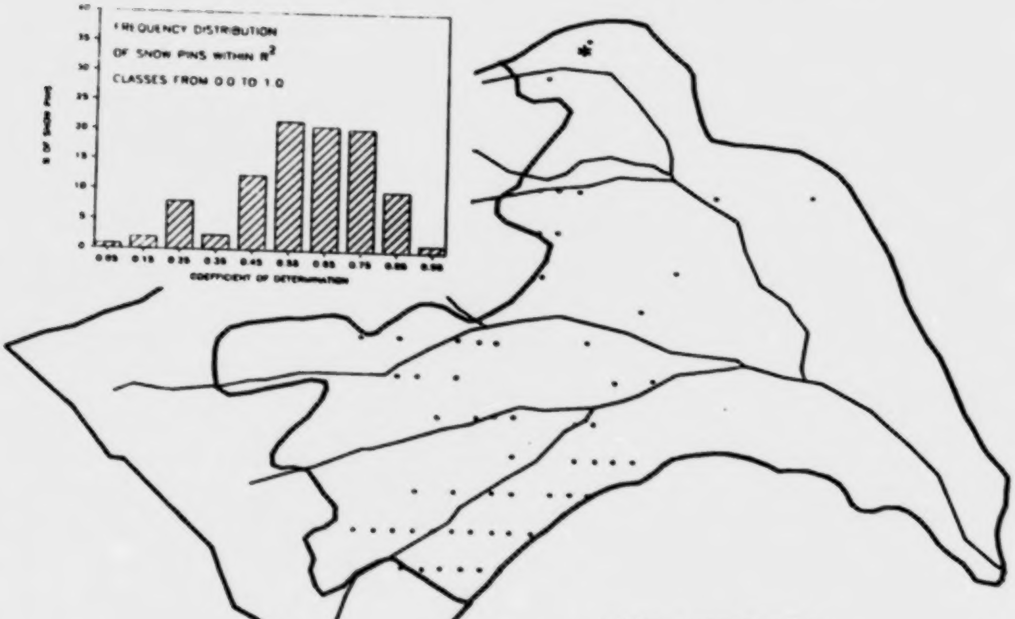
FREQUENCY DISTRIBUTION
OF SNOW PINS WITHIN R^2
CLASSES FROM 0.0 TO 1.0
% OF SNOW PINS
0
5
10
15
20
25
30
35
40
0.05
0.15
0.25
0.35
0.45
0.55
0.65
0.75
0.85
0.95
COEFFICIENT OF DETERMINATION
. PIN LOCATION
* SNOW COURSE 18

Figure 8. Pairing of pins and snow course 18 according to the highest R^2 between March snow water equivalent at pins and snow courses. The inset graph refers to all pins of the basin.

with individual pin measurements from other portions of the basin, and included the data from the three other snow courses and the fourth snow pillow. This time, for many of the pins, the snow course network provided a better fit, probably simply because of the higher number, thus more diverse locations, of the snow courses.

The decision being made to use snow course data to extrapolate the pin measurements, the next question was how to assign one of the six snow courses to each pin. The first obvious way was to pair pins and snow courses on the basis of similar depth or water equivalent of snow. The exact choice criteria was the smallest possible sum of absolute differences between the 11 March readings at each pin and the corresponding readings from snow courses. The pairing acheived in this way is shown in Figures 3, 4 and 5 for the three most "representative" snow courses along with the frequency distribution of the differences in SWE between the pins shown and the particular snow course. It is not surprising to find a good grouping by elevation, as it is well known that depth of snow fall does increase with elevation in the forested portions of the basin.

To make sure that such a grouping was the best one for prediction, a new pairing exercise was done where, this time, the choice criteria was the highest coefficient of determination (R^2). The pairing acheived in this way is shown in Figures 6, 7 and 8, again for the three most "representative" courses. Also shown in these figures is the frequency distribution of all pins within R^2 classes when fitted to the particular snow course. The difference with the results of the first pairing exercise is quite striking. The by-elevation arrangement shown in

Figures 3 to 5 has now given place to a seemingly random pairing. This means that pin readings are approximately equal to the reading from a snow course of similar elevation. But the year to year variations in the pin readings might be better tracked by readings of an other snow course either higher up of lower down the slope. This second pairing method was retained and regression equations were developed for each pin.

Snow contour maps

From these equations, one can now extrapolate pin readings to any month where snow course readings are available. As an example of what such extrapolations might be used for, Figure 9 shows a computer generated contour map of snow water equivalent on Marmot basin for an "average" month of February. Above tree line contours are based on snow stake measurements and do not represent the extreme variability of the alpine snow cover. The curves were smoothed to improve readability.

CONCLUSION

This exercise demonstrates the feasibility of obtaining winter-long detailed data on snow distribution from a once-a-year intensive sampling campaing linked to a once-a-month sampling of a few snow courses. The technique relies on two apparent properties of snow distribution. Predictive equations developed with data from one winter month only can be used to predict snow pack properties for other winter months with little error. Pairing of points on the basis of goodness of fit ensures the best possible predictive relation. But, since in most cases, the best fit pairing is unknown *a priori*, the pairing by proximity is a reasonable alternative. One last remark on pairing, from Figures 6, 7

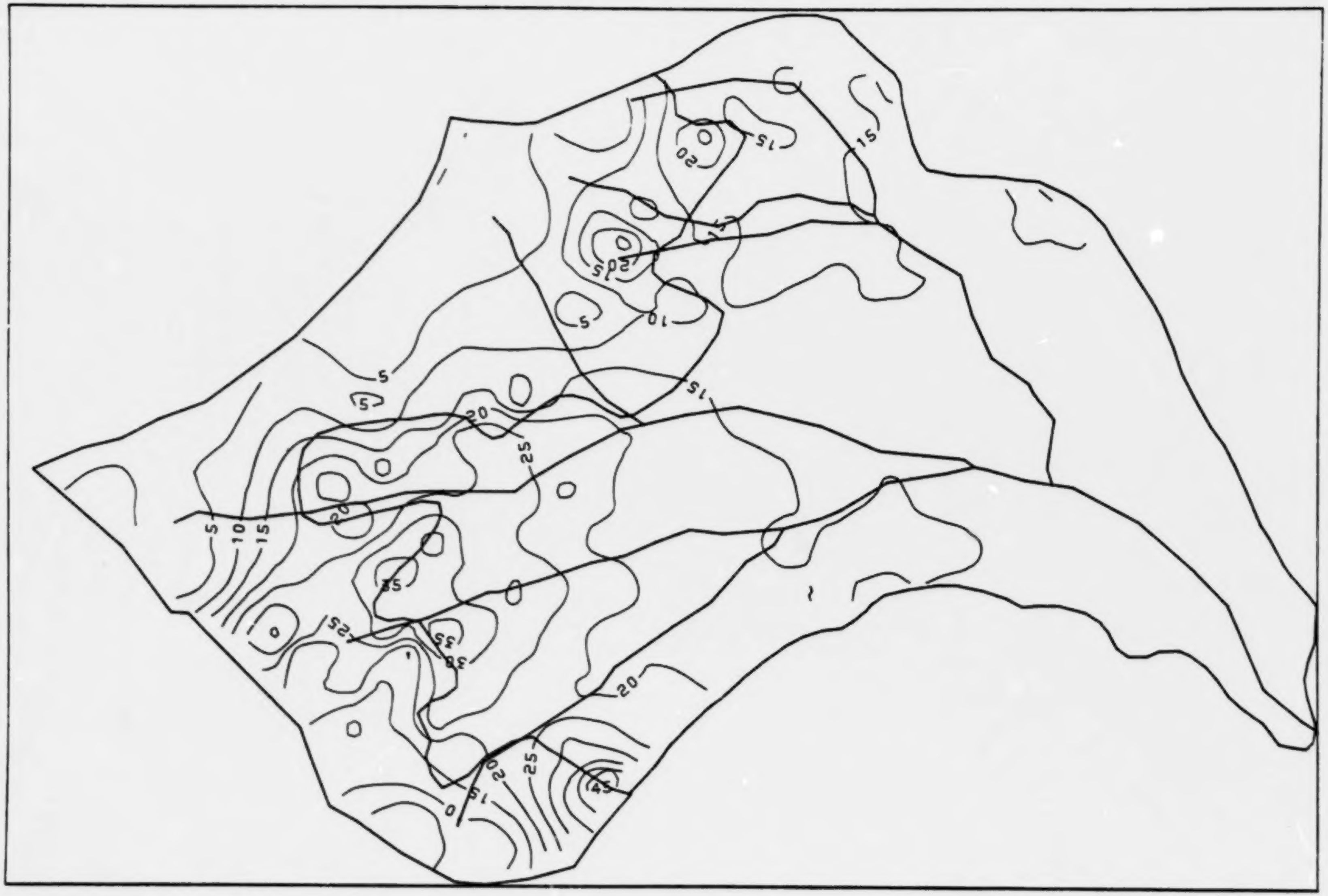
15
15
20
15
25
10
5
5
15
5
20
25
5
10
15
20
35
25
35
30
20
25
20
15
0
45

Figure 9. Distribution of snow water equivalent (in cm) on Marmot Creek basin for an average month of February, as computed from the extrapolated pin measurements.

and 8, we see that had all pins been paired with only one of these three snow courses, over 50% would have had fits with $R^2>0.65$, a surprising fact in such varied terrain.

BIBLIOGRAPHY

Golding, D.L., 1974. The correlation of snowpack with topography and snowmelt runoff on Marmot Basin Creek, Alberta. Atmosphere 12(1): 31-38.

Stevenson, D.R., 1967. Geological and groundwater investigationsin the Marmot Creek experimental basin of southwestern Alberta, Canada. Unpubl. M.Sc thesis, Univ. of Alberta, Edmonton.

TRENDS IN SNOW SURVEYING IN CANADA

by

B.E. Goodison

Canadian Climate Centre, Atmospheric Environment Service
Downsview, Ontario
Canada

J.E. Glynn

National Hydrology Research Institute
Inland Waters Directorate
Hull, Quebec
Canada

D. Harvey and J.E. Slater

Water Resources Branch, Inland Waters Directorate
Hull, Quebec
Canada

presented at

SNOW PROPERTY MEASUREMENTS WORKSHOP

Lake Louise, Alberta

1-3 April, 1985

TECHNICAL MEMORANDUM 140

Compiled By

P.R. Kry

NRCC 27594

TRENDS IN SNOW SURVEYING IN CANADA

by
B.E. Goodison[1], J.E. Glynn[2], D. Harvey[3], J.E. Slater[3]

[1] Canadian Climate Centre, Atmospheric Environment Service
4905 Dufferin Street, Downsview, Ontario M3H 5T4

[2] National Hydrology Research Institute, Inland Waters
Directorate, Environmental Conservation Service,
Place Vincent Massey, Hull, Québec

[3] Water Resources Branch, Inland Waters Directorate,
Environmental Conservation Service,
Place Vincent Massey, Hull, Québec

INTRODUCTION

Snow courses have formed the basis of the Canadian snow survey network for over fifty years. However, recent advances in remote sensing technology offer the potential for significant changes in snow survey procedures in Canada. A combination of ground based, airborne and satellite information, or ultimately remote sensing methods alone, may be the most effective and efficient means of snow survey data collection to meet a variety of user needs, which include streamflow/flood forecasting, water management, irrigation, hydro-electric power, wildlife management, acid snowmelt shock potential assessment, recreation and building design. Although snow surveys have a history in hydrology, many of the current users of these data are other than hydrologists.

This paper will review the snow survey programs of the Atmospheric Environment Service (AES) and the Water Resources Branch (WRB) of Inland Waters Directorate, examine the status of the National Hydrology Research Institute's gamma-ray snow survey program in Canada, and summarize initial results of the Prairie passive microwave research project. Errors and problems with these methods will be discussed.

NATIONAL SNOW SURVEY PROGRAM

Canadian Snow Survey Network

Water Resources Branch has been collecting and publishing snow survey data in some Canadian regions since 1922 (Water Survey of Canada, 1968). By 1964, it was surveying 122 of the nation's 674 snow courses, or 18.1%. At that time, AES (formerly Meteorological Branch, Department of Transport) had only 11 snow courses. Their active participation in taking snow surveys began in 1961-62 following a decision to include regular snow surveys at principal weather stations, where observers were full time employees of the Meteorological Branch (DOT) or Department of National Defence (DND). The data obtained would be of value in estimating the spring runoff potential, agricultural productivity and fertilizer requirements, water-fowl populations, livestock and wildlife survival, snow load calculation and provide information on the physical character of the snow, which would be of interest to the Department of National Defence. Whether the snow course network of AES has successfully met the needs of these users is not really clear.

Table 1 outlines the growth of the snow course network by province from 1963-64 to 1982-83 and includes the totals for WRB and AES, the only agencies operating national snow survey programs. By 1973, 13.6% of all courses were being operated by WRB. The number of WRB snow courses appears to have peaked in 1976, when 175 courses were surveyed out of some 1,200 across Canada. By the winter of 1982-83 the number of stations reporting had dropped to 94, split between the Atlantic Region and the Winnipeg office of the Western and Northern Regions.

Another substantial reduction was made in 1984-85 by the Atlantic Region with the retirement of all but 9 snow courses. These 9 courses are located in the Saint John River Basin and continue to be surveyed as part of the WRB commitment to the Saint John River Forecast Centre. The Winnipeg office is maintaining its 13 snow courses, all located within the Lake-of-the-Woods watershed, by agreement with the Lake-of-the-Woods Control Board. Hence, WRB is currently surveying only 22 snow courses nation wide. It has recently been decided, however, that the 13 courses operated in the Lake-of-the-Woods basin will be eliminated in 1985-86.

AES expanded its network of snow courses, as planned, and currently there are 130 courses operated at principal observing stations across Canada. This represents 10% of the total network. All stations take observations twice monthly and many make weekly observations.

Snow Courses : Problems in Measurement and Analysis

The development of a snow survey network and the frequency and accuracy of associated measurements must be related to its purpose. In hydrology, most snow courses are established to obtain an index of snow water equivalent over an area. For this purpose, the equipment, procedures and siting of the course should remain consistent over time. Unfortunately, some or all of these factors may change over the years; yet, the data continue to be used in the same manner, with users ultimately questioning their validity. Absolute estimates of areal water equivalent can be only obtained after allowance is made for instrumental, observational and siting biases and the sampling network has been designed to reflect areal snowcover variability.

a) Instrument Errors:

Our knowledge of the instrument errors associated with snow samplers used in North America is now well documented (Work et al., 1965; Goodison, 1978; Farnes et al., 1983). In particular, Farnes et al. (1983) document

TABLE 1

Number of Snow Courses in Canada

Province/Territory	Network Size			Operated By: Water Resources Branch			AES		
	1963-64	1972-73	1982-83	1963-64	1972-73	1982-83	1963-64	1972-73	1982-83
British Columbia	139	219	265	0	0	0	2	9	9
Alberta	34	64	54	33	26	5	3	18	20
Saskatchewan & Manitoba	149	258	228	3	14	0	2	19	23
Ontario	125	201	278	15	14	13	0	20	17
Quebec	104	192	183	0	0	0	1	18	22
New Brunswick	38	52	67	14	26	22	1	4	6
Nova Scotia	30	42	32	19	33	23	0	6	3
Prince Edward Island	3	8	4	3	3	3	0	4	1
Newfoundland & Labrador	42	81	74	25	31	28	2	5	5
Yukon & Northwest Territories	10	40	106	10	10	0	0	25	24
TOTAL	674	1157	1291	122	157	94	11	128	130

Note: 1 - Totals were determined from Snow Cover Data and internal WRB reports and correspondence

TABLE 2

OVERMEASUREMENT OF SNOW WATER EQUIVALENT AND CORRECTION FACTOR FOR VARIOUS SNOW SAMPLERS

Type	Cutter Area, cm^2	Overmeasurement (Percent)	Correction Factor[1]
Glacier	81.9	0	1.00
Standard Federal	11.2	10.0	0.91
Broken-tooth Federal	11.2	12.1	0.89
Leupold and Stevens	11.2	8.0	0.93
Sharpened Federal	11.2	6.2	0.94
Bowman	11.2	5.1	0.95
BUNG	11.2	4.2	0.96
McCall	11.2	4.0	0.96
Rosen	11.2	3.5	0.97
Utah	11.2	5.1	0.95
1978 Metric (short)	10.0	7.6	0.93
1978 Metric (long)	10.0	4.0	0.96
1979 Metric	10.0	7.6	0.93
1980 Metric	10.0	4.5	0.96
1981 Metric	10.4	3.8	0.96
ESC 30	30.0	-0.3	1.00
ESC 40	40.0	0.2	1.00
ESC 50	50.0	-0.1	1.00
PVC Tubing	20.9	0.0	1.00
Adirondack	35.7	0.1	1.00
MSC	39.1	5.7	0.95
Aluminum Tubing	77.1	0.6	0.99
CRREL Tubes (Volume = 500 cm^3)	26.5	7.1[2]	0.93

[1] To obtain true SWE with various samplers, multiply measured SWE by the correction factor.

[2] All tests in shallow snow in Alaska

Based on data obtained by Metrication Committee and other studies of snow sampler accuracy. Comparisons made with glacier sampler when data available; otherwise, comparisons made with standard Federal or combination of glacier and standard Federal.

the field tests, methods and results from the studies on the accuracy and design of existing and recommended metric manual snow sampling equipment. Table 2 gives the mean measurement error for various snow samplers, based on data obtained by the Metrication Committee of the Western Snow Conference and other studies of snow sampler accuracy. These results show that small diameter cutters (i.e. areas of 10-12 cm^2) overmeasured by up to 10%, while large diameter samplers measure closer to true.

Figure 1 shows the snow water equivalent measured using the standard Federal snow sampler, which is the sampler used in deep snowpacks in North America, compared to the Glacier snow sampler (reference sampler). The Federal overmeasures by an average 10% based on samples taken in Ontario, British Columbia, Montana and California. Up to this point in time, agencies have not corrected their data for this measurement bias, although it is now realized that it is significant, particularly in deep snowpack regions.

Work et al. (1965) and Freeman (1965) also found that the relative errors caused by inner cutter point diameter, individual scale accuracy through normal field temperature ranges, and scale reading errors associated with different observers were small. The most important factor in determining the absolute accuracy of a sampler was felt to be its ability to cut and hold an accurate snow core. This is assuming, of course, that equipment is properly maintained - tubes are waxed, cutters are kept sharp, and spring balances are checked regularly for accuracy (Atmospheric Environment Service, 1973)

b) Metrication of Snow Samplers:

The Western Snow Conference established a Metrication Committee in 1978 to review, test and recommend equipment and procedures for the metrication of snow surveys and manual snow sampling equipment. Their report (Farnes et al., 1983) recommended two metric samplers - one for deep snowpacks, another for shallow snowpacks. The WSC metric snow sampler, with cutter area of 10.6 cm^2 and with scales that read in true weight (i.e. 1 gram weight equals 1 mm water equivalent), is proposed for deep snowpacks. The principles of design are similar to the Federal sampler now in use. Results of tests with this sampler are given in Figure 2. Figure 3 shows the results using the ESC-30 sampler, proposed for use in snowpacks up to 1 m deep. It has a cutter area of 30 cm^2 and uses clear plastic instead of aluminum for the snow tube. For snow depths less than 1 m, this sampler shows no significant overmeasurement. Detailed design information on both samplers is provided in Farnes et al., 1982, 1983.

Three phases could be used in the conversion to metric units. First, a soft conversion would be applied to data obtained with existing equipment. AES started doing this with the 1978-79 **Snow Cover Data** publication. Secondly, existing equipment can be modified by changing the markings on the tube and scale to metric units. British Columbia Water Resources Service converted their Federal samplers in this manner in 1977. Changing the cutters on these samplers to the metric ones would complete the conversion; this step has not yet been taken by B.C. The final step in conversion would

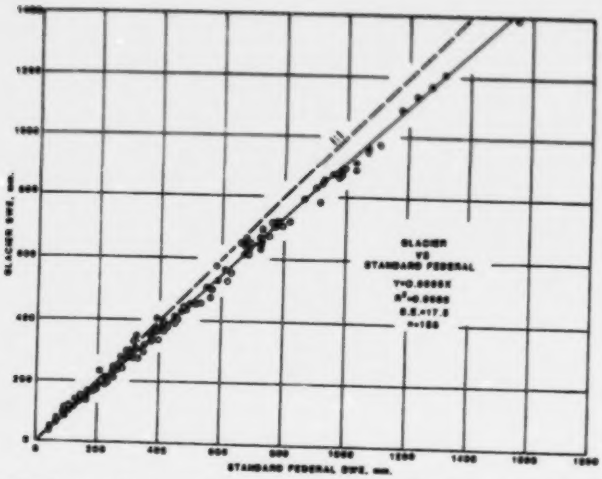

FIGURE 1. Snow water equivalent (SWE) for the Glacier snow sampler compared to the standard Federal snow sampler

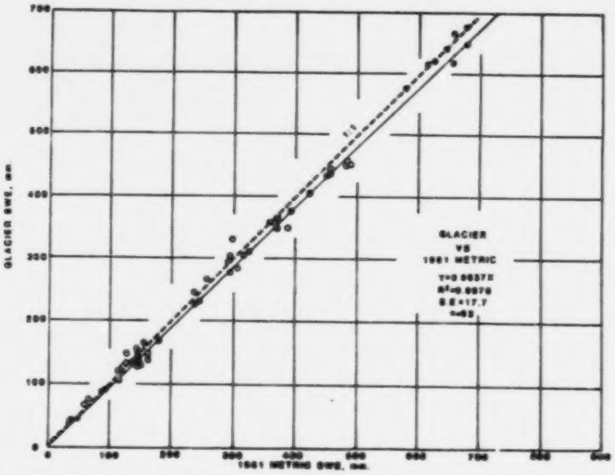

FIGURE 2. Snow water equivalent (SWE) for the Glacier snow sampler compared to 1981 WSC metric snow sampler

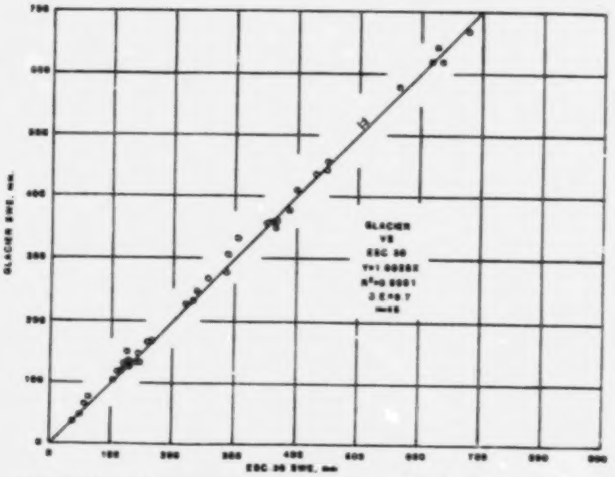

FIGURE 3. Snow water equivalent (SWE) for the Glacier snow sampler compared to the ESC 30 snow sampler

be implementation and use of the new metric equipment. In Canada, for shallow snowpack sampling, the MSC sampler would be replaced by the ESC-30 sampler.

AES has initiated the changeover of its equipment. Blueprints for the new metric samplers have been completed. The first order of small diameter metric samplers, including new spring balances, calibrated in metric, have been received, passed inspection and put into operation at stations requiring new equipment. The cutter design has not yet been changed and it is still that of the old Federal sampler. Cutters will be changed when other snow survey agencies change their cutters. The first 15 ESC-30 samplers have been acquired, but not deployed, as new spring balances are not yet available. AES proposed using a more sensitive spring balance for the ESC-30 than proposed by the WSC Committee. AES would like to replace all MSC samplers with ESC-30 samplers at the same time so that there is minimum disruption and confusion in data acquisition, processing, archiving and analysis.

No decision has been made whether historical data will be corrected to eliminate instrument error. The U.S. Soil Conservation Service and California Department of Water Resources plan to correct historical data files for sampler overmeasurement and convert to metric when they convert existing equipment to metric. This decision is extremely important for users, particularly those involved in flow forecasting, since forecast procedures will have to be adjusted to account for any change in snow measurement related to the change in equipment. This is particularly true for models which use snow survey data as an index. A 10% reduction in measured snow water equivalent caused by equipment changes will certainly affect the flow volume forecast. Index models may have to be recalibrated. This problem could be accentuated even more if some agencies change their equipment and others do not. The goal of the WSC Metrication Committee was for all agencies to convert equipment at the same time to minimize discrepancies in data analysis.

c) Representativeness of Snow Survey Data:

As noted above, instrument errors are now well documented. However, there remains the problem of using snow course data to represent areal snow cover conditions. Terrain, land use, and vegetative cover are important factors affecting snowcover distribution, and ultimately melt. Are our snow courses really representative of the surrounding area?

This question alone is one that can be debated by many, but it has been clearly demonstrated that accurate basin snow cover estimates of depth, density and water equivalent can be obtained from a snow course network or survey sampling scheme specifically designed to represent local landscape characteristics, i.e. vegetation and terrain variations (Steppuhn and Dyck, 1974; Adams, 1976; Goodison, 1981; Woo et al., 1983). This concept is fundamental in the accurate determination of basin snow storage; the sampling of only one type of land use or terrain condition results in a biased estimate useful, at best, as an index of regional snow cover. Unless one knows the site characteristics of snow courses used in an analysis, it is difficult to develop climatological or synoptic maps of snow cover water equivalent. By using known vegetative and physiographic parameters, objective techniques such as multiple regression, trend surface or proximity analysis can then be tested for the development of basin maps of snow distribution (Trivett and Waterman, 1980). Table 3 is one example of the difficulty in making effective use of standard snow survey data. It compares data from three "snow courses" at Sioux Lookout. They are at three different sites, each with a different number of sampling points, operated by three different agencies, and possibly using different equipment. Needless to say, the measured water equivalent varies considerably. Which is "right" or "wrong"? Each may in fact be correct for the land cover and terrain characteritics that it represents.

TABLE 3

Comparison of Snow Course Water Equivalent Measurements (mm)
Sioux Lookout 1975-1979

March (first week)	AES[1] (mm)	% change	Ontario Hydro (mm)	% change	WRB (mm)	% change
1975	183		102		130	
1976	134	-26%	84	-18%	97	-25%
1977	117	-13%	99	+17%	112	+15%
1978	154	+32%	106	+ 7%	112	0
1979	108	-30%	76	-28%	99	-12%

[1] Means of survey on March 1 and 8

It is important to eliminate or minimize our errors of measurement and to standardize our methods not only to assist current users of these data, but it is these measurements which form the "ground truth" for developing algorithms for the determination of snow cover using remote sensing. The accuracy of snow data determined from satellite remote sensing will very much be a function of the accuracy of the "ground truth" data against which it is calibrated.

DATA PUBLICATION AND ARCHIVING

Atmospheric Environment Service publishes **Snow Cover Data**, which is an annual summary of snow course (depth, water equivalent) and, for some stations, snow depth observations across Canada. Nineteen agencies currently contribute data to the publication, but there is no national digital archive of the data. Spatial and temporal analyses are hindered by the fact that an easily accessible national archive does not exist. Each agency, however, may have their own data archived in a format suited to their own use.

AES is currently investigating the feasibility of changing the method and format of publication in line with the recommended format suggested by Findlay and Goodison (1978). A computer compatible archive would be created, from which a hard copy could be directly produced for publication. This would create a permanent data storage facility which may be readily accessed and will grow in usefulness, particularly for statistical purposes, over a number of years. It would provide a standardized format for data collected by a variety of agencies for differing reasons and would facilitate use of the data over broad regions. Finally, the proposed format allows for the inclusion for publication of additional physical information, such as snow crusts, ice layers, environmental characteristics, sampler types, etc., which are recorded by many agencies, but not regularly published. This type of information is becoming even more important in our environmental investigations. We know stratigraphy is an important factor in avalanching, so it is carefully monitored. However, stratigraphic information is extremely important for the study of snow cover properties using microwave techniques and is useful in the study of acidic snowmelt shock potential. Traditionally, such information is not readily available, and use of historical data for algorithm or model development is hindered.

FUTURE OF THE SNOW SURVEY NETWORK

It is not unreasonable to expect that the number of snow courses operating in Canada will decline in the future. In particular, what has caused the apparent decline of the snow survey program within Environment Canada's Water Resources Branch? It is likely that the reductions in the number of snow courses surveyed by WRB in recent years are the combined result of increased resource constraints, a diminishing profile of the snow survey program relative to the national hydrometric data collection program, a lack of clearly identified users and benefits of the data, and uncertainty as to whether the collection of snow survey data is within the WRB mandate. Within the WRB, snow survey data have traditionally been collected as a secondary hydrometric parameter, with the surveys being incorporated into normal operational plans. However, no formal commitment has ever been made to the program and it has always been a discretionary item of the budget. In recent years, the snow surveys have become the target of belt-tightening measures, a trend which could be attributed to at least two major events which occurred in the last ten years. The first was the drafting of the federal-provincial Water Quantity Survey Agreements in 1975, which reinforced the hydrometric data collection role of the Branch, but did not include snow data collection. The second event was a nation-wide survey and subsequent report which reviewed the national hydrometric data collection program (Environment Canada, 1980), but which did not directly address the collection of snow data. Hence, within WRB, the profile of the snow survey program seems to have diminished considerably while more emphasis has been placed on the national hydrometric data collection program.

The Water Resources Branch is definitely interested in a snow survey program, but recognizes the deficiencies of the present decentralized system of snow data collection in Canada. Currently, agencies are independently operating snow courses across Canada. This fragmented approach has led to a disparity in methods and procedures which, in turn, has yielded data of questionable comparability. As well, non-standard analytical procedures and models, used to relate snow data to runoff potential, give inconsistent results. There is little doubt that the lack of a more comprehensive network providing accurate estimates of snow properties has inhibited progress in basic research and in the development of improved measurement and analysis techniques

AIRBORNE GAMMA RAY SNOW SURVEYS

One very viable alternate snow survey procedure which deserves close examination is the airborne gamma ray method. The airborne snow survey method is based on the attenuation by a snowpack of gamma radiation emitted by natural radioactive decay in the ground. This technique has been used in Canada on an experimental basis since 1972. In the last three years gamma ray snow surveys have been performed in Southern Saskatchewan, around the north shore of Lake Superior, and in the Saint John River Basin. These surveys involved flying two airplanes, operated by the Geological Survey of Canada (GSC) and the U.S. National Weather Service (NWS), each with different types of spectrometers.

Canada/US Prairie Snow Cover Runoff Study

In February 1982 a major snow survey experiment was conducted in southern Saskatchewan. Background and details of the experiment are given in Goodison et al., 1984. One of the three objectives of the multi-stage remote sensing component was to provide a direct comparison of airborne gamma radiation snow water equivalent measured made by the GSC system and the NWS system with each other and with ground observations. The flight line network developed for the experiment is shown in Figure 4. Intensive ground snow surveys on calibration lines 101C, 103C, 105C were specifically designed to be representative of the areal land use so that the best estimate of ground snow cover could be obtained using standard snow surveys. Ground data on other calibration lines were not specifically collected on the strict basis of area land cover.

A comparison of the two gamma ray systems with each other and with ground data is described in Carroll et al. (1983). These results indicate that the two systems agree with each other with an RMS error of 4.5 mm. The GSC system agreed with the ground data to an RMS error of 4.6 mm (4.0 mm on line 100) and the NWS system agreed with the ground data with an RMS error of 7.5 mm (6.0 mm on line 100). These results are over flat farmland with snow water equivalent (SWE) ranging from 60 to 80 mm; they probably indicate the closest possible agreement of the gamma ray technique with ground based measurements. It is interesting that the two gamma ray systems agree more closely with each other than with the ground data, indicating the good repeatability of the technique.

A serious problem encountered during this survey was the extremely high level of atmospheric radon gas, which occurred on the first day of the experiment. Radon gas is a heavy radioactive daughter product of the uranium series and is released into the atmosphere when a low pressure system moves through an area. The calibration procedure must filter the data collected by the aircraft system to reduce the effect of radon before the snow water equivalent can be calculated. The GSC system corrects for radon in the

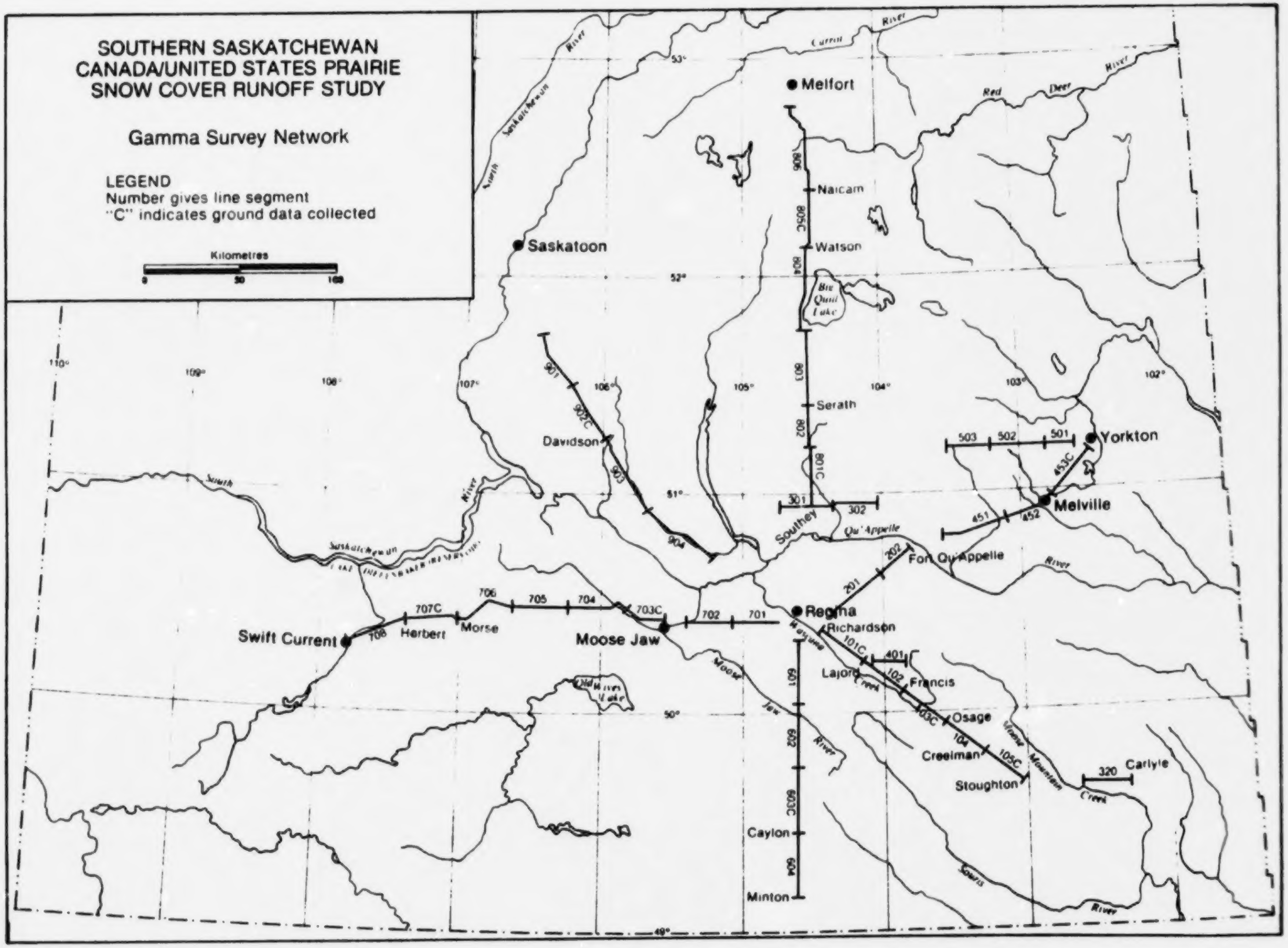
SOUTHERN SASKATCHEWAN
CANADA/UNITED STATES PRAIRIE
SNOW COVER RUNOFF STUDY
Gamma Survey Network
LEGEND
Number gives line segment
"C" indicates ground data collected
Kilometres
0
50
100
Melfort
Naicam
Watson
Big Quill Lake
Serath
Saskatoon
Davidson
Yorkton
Melville
Fort Qu'Appelle
Regina
Richardson
Lajord
Francis
Osage
Creelman
Stoughton
Carlyle
Swift Current
Herbert
Morse
Moose Jaw
Caylon
Minton
Southey
Old Wives Lake
Red Deer River
Current River
South Saskatchewan River
Qu'Appelle River
Moose Jaw River
Wascana Creek
Moose Mountain Creek
Souris River
806
805C
804
803
802
801C
301
302
901
902C
903
904
503
502
501
453C
451
452
201
202
101C
401
102
103C
104
105C
320
708
707C
706
705
704
703C
702
701
601
602
603C
604
110°
109°
108°
107°
106°
105°
104°
103°
102°
53°
52°
51°
50°
49°

Figure 4: Flight lines for airborne gamma and microwave surveys

atmosphere by flying the aircraft over a lake to measure the background atmospheric radiation. The lake results are then subtracted from the terrestrial flight line data to obtain the net gamma radiation from the ground. This method poses a problem in the prairies because there are very few lakes and radon conditions near a lake may not be representative of conditions near the flight lines. In addition, radon conditions may change during the time it takes the airplane to fly from the lake to the flight lines. NWS uses a different technique to correct for radon. It involves placing a smaller detection package above the main package. The main detection package will then shield the small one from terrestrial radiation, so the small package will only measure atmospheric radiation. A problem with this method is that the heavy radon gas often lies between the ground and the aircraft so it is invisible to the upward looking detector. Despite these differences, the two systems agreed remarkably well.

Lake Superior Surveys

In March 1982 and again in March 1983 GSC and NWS gamma ray snow surveys were conducted over the Lake Superior Basin (Fig. 5). The surveys were funded by Environment Canada and the US Army Corps of Engineers. These surveys have provided valuable experience in flying over hilly forest covered terrain with highly variable radiometric ground concentration.

This type of environment provides many more sources of error than the prairies, the most important one being the variability in the soil moisture. Soil moisture absorbs part of the natural gamma ray signal in the ground and hence the airborne data must be corrected for it. The usual method of correction is to take 20 to 40 soil samples along several so called "calibration" lines, determine the gravimetric moisture content, and then extrapolate these data to the other flight lines. Although this technique may be justified in an agricultural environment where the soil moisture is largely determined by the land use, problems may arise in a region where terrain plays a major factor in soil moisture variability. Another factor influencing the results is the problem of flight line replication. The analysis of the gamma ray data relies on a pre-snow survey to correct for background terrestrial radiation. In the prairies, the flight lines followed conveniently spaced straight country roads. However, in most wooded areas the pilots must rely upon transmission lines, pipeline rights-of-way, winding roads and occasionally rivers and streams as navigational aids. This problem is magnified in the Lake Superior region where granitic outcrops cause high spatial variability in the radioelement concentrations. As well, the radiometric signal reaching the aircraft spectrometer is weakened by the high SWE in the area (up to 250 mm).

In spite of these problems the GSC system and the NWS system agreed with the ground data with a 19 mm RMS error. In addition, the systems agreed with each other with a 4.5 mm. RMS error (Gauthier et al., 1983). These results confirm the high degree of repeatability of the gamma ray technique. Statistical errors arising from the ground sampling procedure account for about half of the 19 mm RMS difference.

Saint John Basin Survey

The latest airborne gamma ray survey was performed in March 1984 in the Saint John River basin in a project funded by IWD of Environment Canada and the US National Weather Service. The GSC and the NWS aircraft each flew over fifty one flight lines in the basin. Intensive ground snow and soil moisture surveys were carried out along eight of these lines (Fig. 6).

A comparison of the GSC and ground measurements revealed an overall RMS error of 62 mm. The high discrepancy was due to large errors along three of the flight lines. Each of these lines had more than 300 mm SWE and one had 460 mm SWE. When these lines were excluded from the calculations the RMS error dropped to 20 mm. The large error in deep snowpack areas appears to be the result of systematic underestimation of the ground based measurements by the aircraft. Some possible reasons for this underestimation are:

> **Forest Cover.** Trees emit relatively low levels of radiation, so they are usually assumed to be pure absorbers. However, in a very deep snowpack with few gamma rays escaping through the snow, the radioactive emissions from trees become a significant portion of the total signal. The erroneously high counts detected by the spectrometer will result in an underestimation of SWE.
>
> **Variability in the Snow Cover.** The SWE is computed from the count rate along a flight line rather than the average of the SWE computed at each point along the line. The count rate decreases exponentially with increasing SWE and the nonlinearity of this relationship results in a systematic underestimation of SWE.
>
> **Overestimation of Ground Surveys.** The calibration flight lines always follow roads and in hilly terrain the roads usually follow the valleys. Therefore, the ground based sampling of SWE usually takes place in the valleys. However, the aircraft flies 150 metres away from the road closer to ridges and the tops of hills. If these ridges are windswept this could result in an apparent underestimation of the SWE by the aircraft.
>
> **Radon emanating from the ground.** Radon gas could escape into the snowpack and cause the snow to become an emitter of gamma rays. This would result in more gamma rays escaping into the snow resulting in an underestimation of the integral value (Glynn and Grasty, 1980) of SWE.

Surveys performed in these three areas have indicated that the airborne gamma ray technique gives repeatable and accurate estimates of snow water equivalent under a variety of terrain types and snow conditions. More work must be performed in regions where the snow water equivalent exceeds 300 mm. In addition, it would be useful to test the accuracy of the method in a mountainous area in Western Canada. Such a survey would, however, be expensive since a helicopter would be required.

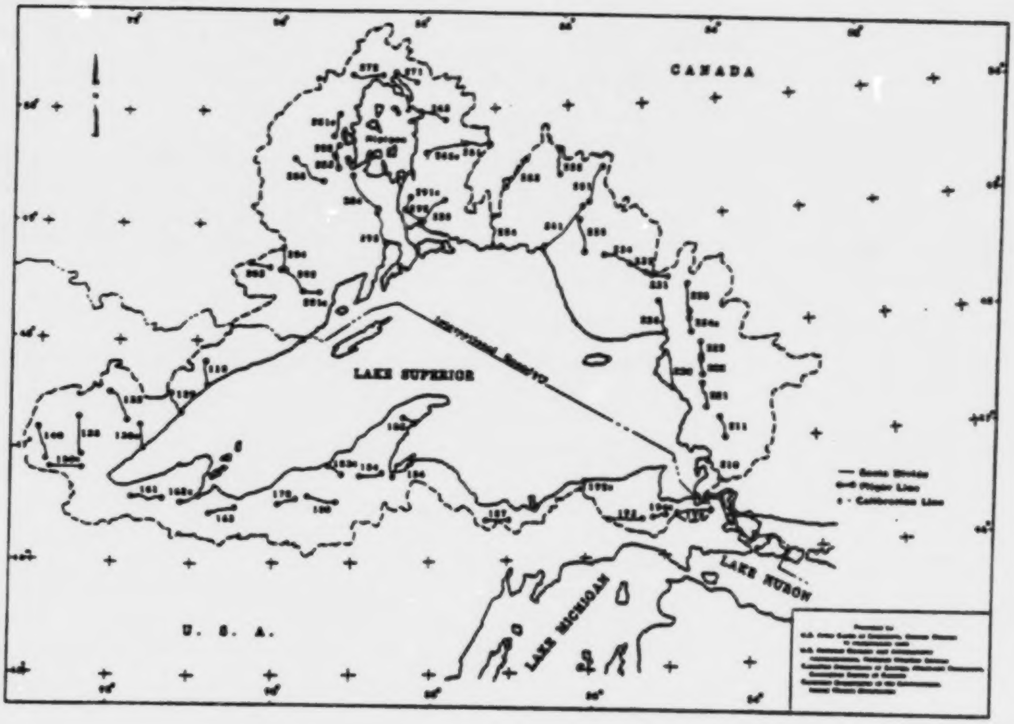
CANADA
LAKE SUPERIOR
U. S. A.
LAKE MICHIGAN
LAKE HURON

Figure 5. Flight line network and map of the Lake Superior basin

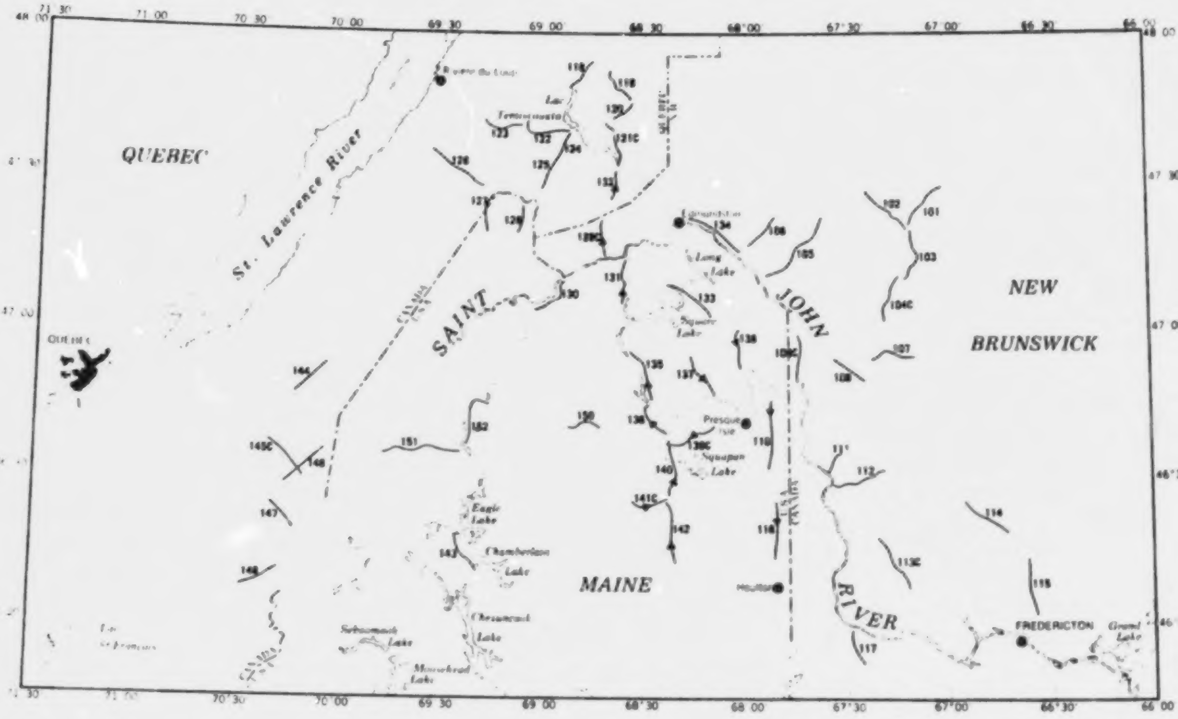
QUEBEC
St. Lawrence River
SAINT
JOHN
RIVER
NEW
BRUNSWICK
MAINE
Lac Temiscouata
Long Lake
Square Lake
Presque Isle
Squapan Lake
Eagle Lake
Chamberlain Lake
Chesuncook Lake
Moosehead Lake
Houlton
FREDERICTON
Grand Lake
71 30
71 00
70 30
70 00
69 30
69 00
68 30
68 00
67 30
67 00
66 30
66 00
48 00
47 30
47 00
46 30
46 00

Figure 6. Saint John River Basin airborne gamma ray snow survey

Operational Gamma Ray Snow Survey Programs

Airborne gamma ray snow survey programs have been conducted in most of the northern latitude countries. Operational snow survey programs exist in Finland, Norway and USA. Finland has just completed a three year pilot program to assess the technique as an aid to reservoir regulation for hydroelectric projects. The surveys were conducted over relatively flat forested land in northern Finland; the results indicate that the gamma ray method can be beneficial in the regulation of reservoirs where the average residence time is about one year. They intend to continue with their program. In Norway, airborne gamma ray snow surveys have been conducted for over ten years in a program funded by the Norwegian Electricity and Water Resources Board. The surveys have taken place in mountainous regions of the country over nine basins ranging in size from 100 to 2000 km^2. Helicopters and fixed-wing aircraft have been used for the surveys and the results have been used by the Electricity Board as an aid to reservoir regulation for hydroelectric power generation. The United States has the most ambitious gamma ray snow survey program. The US National Weather Service has an airplane dedicated to airborne snow surveys on a year round basis. Their operational coverage area currently extends from Montana to Maine. Data from these surveys are used primarily as an aid to flood forecasting.

Pilot studies are also underway in Sweden and Denmark. The Swedish hydro-electric authority has funded a five year pilot study over an 1100 km^2 regulated basin in the northern part of the country. A water balance study was performed in which the gamma ray data were compared with data from three precipitation stations in the basin as predictors of runoff from snowmelt. The conclusions will be released shortly by the Swedish Meteorological and Hydrological Institute. This year the Danish government will begin funding the Greenland Technical Organization to fly gamma ray snow surveys over small basins on the west coast of Greenland. The surveys will be flown by helicopter and the results will be used to determine the suitability of these basins for small scale hydro-electric projects. The USSR, where the method was first developed (Vershinina and Dmaksyan, 1972), has conducted operational airborne snow surveys in the past, but it is difficult to determine the current state of its program.

At a workshop in Finland in October 1984, representatives from the four Scandinavian countries and Canada discussed the current state of airborne gamma ray snow surveys. The official conclusions were that:

1. Airborne gamma ray snow surveys can be used operationally and they provide improved estimates of snow water equivalent.
2. Other remote sensing techniques, such as passive microwave radiometry and ground-based impulse radar, should be investigated.
3. The gamma ray results should be verified by performing a water balance analysis of the basin.
4. The development of models which use the results of gamma ray surveys as well as other remotely sensed data should be encouraged.

FEASIBILITY OF A CANADIAN GAMMA RAY SNOW SURVEY PROGRAM

The National Hydrology Research Institute (NHRI) of Environment Canada is conducting a feasibility study to determine the costs and user interest in an operational airborne gamma ray program in Canada. The cost of operating an airborne snow survey program is primarily determined by the type of aircraft used and by the number of crew members required to run the survey. In Canada, the GSC uses a Skyvan with a three man crew and the charges for this operation are $2,500 per day. If the aircraft flies fifteen flight lines a day (20 km each) the cost per flight line is about $170. The United States NWS uses a smaller aircraft, a Grumman Aero-Commander, and they estimate their costs to be somewhat less. As the preceding discussion indicates, the accuracy of the gamma ray system is within 10 mm in flat farmland and within 20 mm in forest terrain provided the SWE is less than 300 mm. A detailed ground based survey could take two persons a full day to cover a 20 km flight line provided that the line is accessible by road. If salaries, transportation costs, and occasional overnight accommodation are included, a detailed ground based survey averages about $300 per flight line. Thus, the cost effectiveness ratio for the gamma ray technique works out to be roughly 300/170 = 1.76. This rough analysis excludes ferrying cost of the aircraft to the survey site, but these costs would be minimized in a large scale airborne program since several surveys could be performed along the route. In addition, the benefit to cost ratio will improve in regions where the survey sites are inaccessible by road.

A questionnaire was circulated by NHRI to over 300 users and collectors of SWE data in Canada. The survey results have not been completely tabulated at this time, but a preliminary conclusion indicates widespread user interest in the gamma ray technique. Of approximately 100 responses, over 30 organizations have indicated interest in providing financial support for surveys in their regions. However, several questions remain to be answered regarding the future of the gamma ray method in Canada. The technique has been shown to give accurate results in different types of terrain and snow conditions commonly found in Eastern Canada. The technique has therefore moved from the research stage to the level of technology transfer. The results from snow surveys are usually used as indices in runoff models and these models often require lengthy records before the survey data can be used operationally. There is, therefore, the need to justify a new program which might not become truly operational for several years. Another major question is the source of funding for such a program. Should cost recovery from individual users be considered? In that case, an accounting procedure would have to be devised to recover costs on a proportional basis from small and large users of the data. In addition, a priority scheme would be needed since it is likely that several users might want surveys performed at the same time.

There is another general question which should be considered. What economic benefit arises from improved estimation of snow water equivalent? Do improved estimates of SWE lead to improved flood forecast estimates? If so, is it possible to quantify the economic benefits of these improved estimates? The gamma ray method has been used extensively in Scandinavia for predicting runoff from snowmelt as an aid to reservoir regulation for hydroelectric projects. The economic benefits of such an application should be easier to estimate than the benefits to flood forecasting. However, even in this case, no quantitative studies have been performed in Scandinavia. Nevertheless, many of the hydro authorities in these countries believe intuitively that the improved estimates of SWE justify the use of the gamma ray technique. Is the informed intuition of experts a justifiable reason for the further development of this technique in Canada?

SATELLITE REMOTE SENSING OF SNOW COVER

Satellite remote sensing of snow cover is not new - it was the first application of satellite data in the water sector. We should now be at the stage where it is possible to develop, assess and integrate new techniques for snow cover assessment, including the acquisition of point and areal snow measurements by remote sensors. During the WMO Snow Studies by Satellite Project, initiated in 1974, snowcover analyses were carried out on the Columbia, Souris, Lake-of-the-Woods and Saint John River Basins, by different agencies using NOAA and LANDSAT imagery. In most cases, the basic technique was optical-electrical image analysis, but some analysis was conducted using digital satellite data. Satellite snowcover mapping has been continued by AES (Hydrometeorology Division) in the Saint John Basin. A digital processing system using NOAA/TIROS multi-channel data has been developed to determine the areal extent of snowcover in this forested basin (Waterman et al. 1980), and an analogue/digital procedure using NOAA or GOES data has been recently developed (Johnstone and Ishida, 1984). Both techniques are only used to map areal extent of snow cover. In an effort to determine basin water equivalent, Power et al. (1980) tested the use of LANDSAT digital data to delineate various vegetation categories in a basin and then used concurrent snow course data obtained within the given vegetation category to distribute the snow water equivalent over the area within each basin containing that category of vegetation. This is one potential method for combining satellite and ground data for snow cover determination.

From such studies the limitations of satellite data for snowcover studies were identified. In Canada, LANDSAT data cannot be used effectively on an operational basis because the 16 or 18 day temporal coverage is inadequate. The probability of cloud free coverage every 18 days is low and during that time interval the snowpack could disappear entirely. For large basins, such as the Saint John, the increased spatial resolution of LANDSAT means that passes on 4 or 5 successive days are required for coverage of the entire basin and this limits operational application of these data to many snowcover problems. Cloud cover is a real problem in snowcover mapping both in obtaining coverage of the basin and in distinguishing between cloud and snow. Daily coverage of target areas by the weather satellites is an advantage in obtaining usable and timely data.

Currently, only the areal extent of snowcover is operationally derived from satellite data, but there is no centralized system for mapping every basin that might be required by user agencies. For each user to implement their own analysis system would require the receipt of satellite data in near real-time and the development of an objective interpretation system which is affordable and transferable to "non-specialists".

A major challenge in the remote sensing of snowcover is to develop algorithms to determine snow depth, water equivalent, areal extent and liquid water content using sensors having all-weather capabilities. The most immediate promise in this area is the application of passive and active microwave data to snowcover problems. Research at the University of Kansas has been extremely important in advancing our knowledge of active and passive microwave responses to different snowpack conditions (Stiles and Ulaby, 1980; Ulaby and Stiles, 1980).

Goodison et al (1980) reported initial results on the use of airborne synthetic aperture radar imagery (X and L band) for snowcover monitoring. No quantitative determination of snow depth or water equivalent was possible. Assessment of X and C band SAR for the determination of snow depth, state of the ground and snowmelt was proposed as a RADARSAT project. Until the new airborne C-band SAR is operational, further Canadian experimentation will be limited.

At the moment, passive microwave data offer the greatest prospect for the determination of snow cover. Recent investigations (Kunzi et al, 1982; Chang et al., 1982; Foster et al., 1980; Rango et al., 1979) using data from the Scanning Multichannel Microwave Radiometer (SMMR) on NIMBUS-7 and from ESMR on NIMBUS 5 and 6 have shown that there is a potential for using passive microwave sensors to monitor snow cover, notably areal extent, depth, water equivalent and melt.

One of the objectives of the Canada/US Prairie Snow Cover Runoff Study was to assess the utility of passive microwave data for the mapping of prairie snowcover, particularly in relation to areal extent, depth and water equivalent. As part of the experiment, a US Air Force Hercules flew the NASA airborne multifrequency microwave radiometer along the same flight line as the gamma aircraft (see Fig. 4). Microwave data (18 and 37 GH_z, horizontally and vertically polarized) were obtained every 0.5 seconds. Concurrent colour aerial photography was obtained which provided reference imagery to confirm location of the microwave data. NIMBUS-7 SMMR data were obtained for the overflight dates.

Analysis of the airborne and satellite data are still in progress. Efforts have been directed at deriving an initial algorithm to estimate snow water equivalent from microwave radiometer data. Airborne gamma measurements of SWE are being used as one of the "ground true" data sets against which the microwave data are calibrated. Both the gamma data and airborne microwave data were averaged over 20-25 km segments for the analysis. This averaging distance is in line with the 35 x 35 km resolution of 37 GH_z SMMR satellite data which are also being analyzed.

Initial results are very encouraging and are in line with those being reported by European and American investigators. Fig. 7 shows the relation between gamma derived estimates of SWE and 37 GH_z vertically polarized brightness temperature measured by the NASA airborne radiometer. The data are for dry snow regions only. When snow is melting, its structure and electromagnetic behaviour change markedly and a different relation will exist. Work is in progress to test other relationships with snowpack properties and to test the results using satellite data. It should be noted here that information on snowpack structure (stratigraphy, ice layers, grain size, wetness, etc) is very important in the interpretation of the microwave data. Generally, information on snowpack structure is not readily available. In the future, consideration should be given to recording such information at selected snow course sites.

There are many questions yet to be answered in the use of passive microwave data for the derivation of snowpack properties, but recent progress has been positive and research should continue on developing this technique. Since passive microwave resolution from space is about 30 km, the technique would be best applied over large, relatively homogeneous regions, such as the Prairies. Theoretical studies and field experiments involving scientists from different disciplines will be necessary to advance the application of this technique. Co-operation among agencies will be vital just as it was during the airborne gamma experiments. At this time satellite microwave radiometer data are available from NIMBUS-7, which is a research satellite. This sensor is not carried on any of the meteorological or operational earth resources satellites. Data are not currently available to Canadians in near real-time. Operational application of such a technique would require data to be available in near real-time.

OUTLOOK

This paper has attempted to provide an overview of current trends in snow surveying in Canada. Our ground based techniques are being standardized, errors are being quantified. But for various reasons, the number of snow courses will probably decrease. Airborne gamma ray snow surveys offer a viable alternative; however, implementation of an operational system in Canada is yet to be achieved. In the future, satellite data, notably passive microwave, may provide the basis for large scale assessment of snowcover properties.

Yet, where are we today? AES, which operates the only nation wide snow survey network, publishes the data collected by agencies and provides direction on snow survey equipment and procedures. Nonetheless, a more comprehensive and co-ordinated national program is needed. Such a program should ensure the standardization of data collection, analysis and dissemination procedures, while at the same time ensuring the introduction of modern techniques. Such a program should also be responsive to the needs of the water resources community and other users. It should promote the development of the necessary expertise to apply knowledge, gained from basic research, to the analysis and interpretation of snow data and thereby provide the information needed by water resources managers. The identification of all potential users and benefits of snow data and arrangements for cost-sharing and/or cost-recovery are considered essential to the successful implementation of such a program.

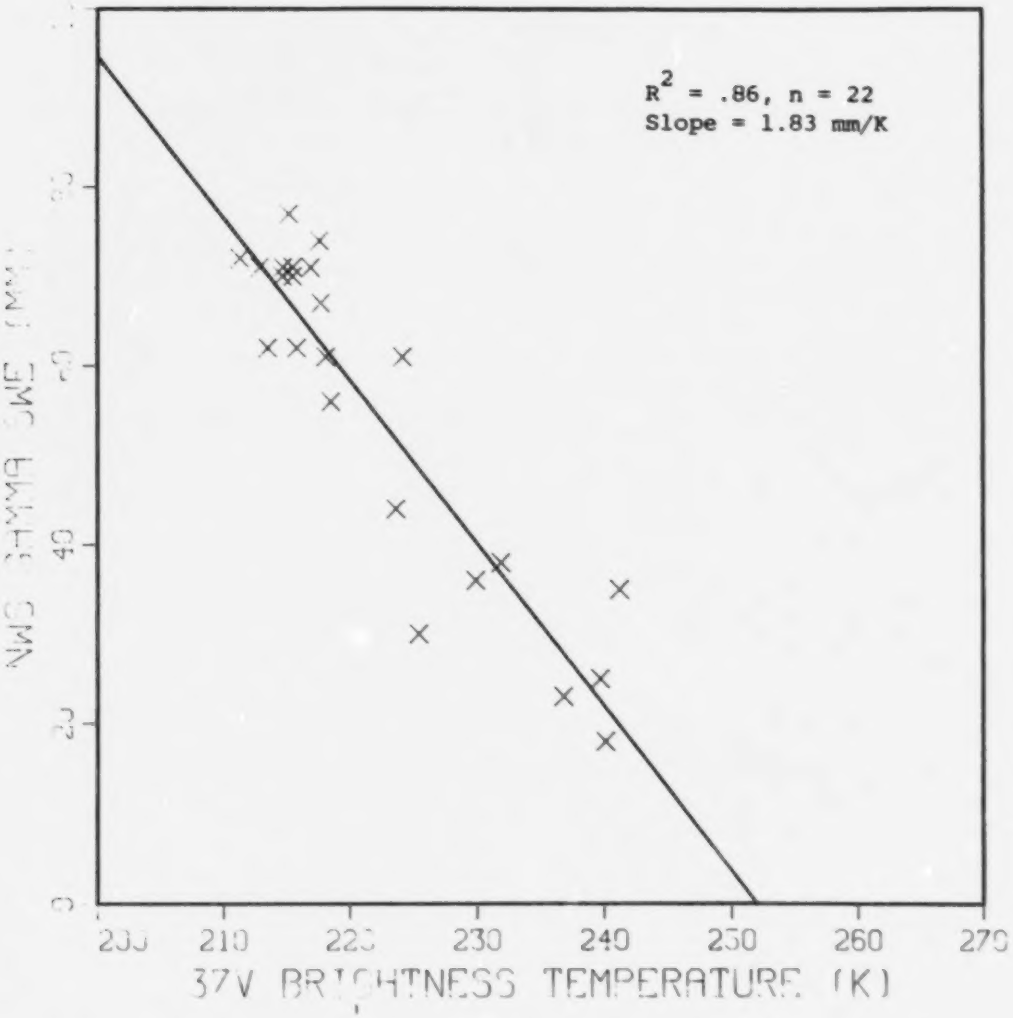

FIGURE 7: Comparison of NWS airborne gamma SWE and 37GHz vertically polarized airborne microwave brightness temperatures for dry snow, February 17-18, 1982, Saskatchewan

REFERENCES

Adams, W.P., 1976: Areal differentiation of snow cover in East Central Ontario. Water Resour. Res., 12, 1226-1234.

Atmospheric Environment Service, 1973: Snow Surveying : Manual of Standards and Snow Surveying Procedures. 2nd ed. Downsview, Ontario, 20 p.

Carroll, T.R., J.E. Glynn and B.E. Goodison, 1983: A Comparison of U.S. and Canadian gamma radiation snow water equivalent measurements. Proc. Western Snow Conf., 51st Annual Meeting, Vancouver, Washington, April 19-21, 1983, 27-37.

Chang, A.T.C., J.L. Foster, D.K. Hall, A. Rango and B.K. Hartline, 1982: Snow Water Equivalent Estimation by Microwave Radiometry. Cold Regions Science and Technology. Vol. 5, 259-267.

Environment Canada, 1980: An Evaluation of the Hydrometric Surveys Component - EMS Water Management Data Program No. 51. Ottawa, Ontario.

Farnes, P.E., B.E. Goodison, N.R. Peterson and R.P. Richards, 1983: Final Report, Metrication of Manual Snow Sampling Equipment. Western Snow Conference, Spokane, Washington, 106 pp.

Farnes, P.E., B.E. Goodison, N.R. Peterson and R.P. Richards, 1982: Metrication of Manual Snow Sampling Equipment by Western Snow Conference Metrication Committee. Proc. Western Snow Conference. Reno, Nevada, pp. 120-132.

Findlay, B.F. and B.E. Goodison, 1978: Archiving and Mapping of Canadian Snow Cover Data. Proc. Workshop on Snow Cover and Sea Ice Data, WDC-A for Glaciology, Report GD-5, Boulder, Colorado, 71-88.

Foster, J.L., A. Rango, D.K. Hall, A.T.C. Chang, L.J. Allison and B.C. Diesen III, 1980: Snowpack Monitoring in North America and Eurasia Using Passive Microwave Satellite Data. Remote Sensing of Environment. Vol. 10, 285-298.

Freeman, T.G., 1965: Snow survey samplers and their accuracy. Proc. Eastern Snow Conference, 1-10.

Gauthier, R.L., T.R. Carroll and J.E. Glynn, 1983: Airborne Gamma Radiation Data Used to Assess Snow Water Equivalent over the Lake Superior Basin. Proc. Seventeenth Intl. Symp. on Remote Sensing of Envr. Environmental Research Institute of Michigan, Ann Arbor, MI (1):415-424.

Glynn, J.E. and R.L. Grasty, 1980: A Calibration Procedure for Airborne Gamma Ray Snow Surveys. Proc. Western Snow Conf. April 15-17, 1980, Laramie, WY, 120-127.

Goodison, B.E., 1981: Compatibility of Canadian Snowfall and Snow Cover Data. Water Resour. Res., Vol. 17, No. 4, 893-900.

Goodison, B.E., 1978: Accuracy of Snow Samplers for Measuring Shallow Snowpacks: An Update. Proceedings of Eastern Snow Conference, 35th Annual Meeting, pp. 36-49.

Goodison, B.E., A. Banga and R.A. Halliday, 1984: Canada - United States Prairie snow cover runoff study. Can. Water Res. J., 9, 1, 99-107.

Goodison, B.E., S. Waterman and E.J. Langham, 1980: Application of Synthetic Aperture Radar Data to Snow Cover Monitoring. Proc. 6th Can. Symp. on Rem. Sens., Halifax, N.S. May 21-23, 1980, 263-271.

Johnstone, K.J. and S. Ishida, 1984: An Analogue/Digital Procedure for the Mapping of Snow Cover from Satellite Imagery. Canadian Climate Centre, Report No. 84-9, Atmospheric Environment Service, Downsview, 28 p.

Kunzi, K.F., S. Patil and H. Rott, 1982: Snow Cover Parameters Retrieved from NIMBUS-7 Scanning Multi-Channel Microwave Radiometer (SMMR) Data. IEEE Trans. Geosc. Rem. Sens. GE-20(4), 453-467.

Power, J.M., C.J. Merry, N.B.A. Trivett and S.E. Waterman, 1980: Snowpack Estimation in the St. John River Basin. Proc. 14th Int. Symp. on Rem. Sens. of Envir. San Jose, Costa Rica, April 23-30, 467-486.

Rango, A., A.T.C. Chang and J.L. Foster, 1979: The Utilization of Spaceborne Microwave Radiometers for Monitoring Snowpack Properties. Nordic Hydrology. Vol. 10, pp. 25-40.

Steppuhn, H. and G.E. Dyck, 1974: Estimating True Basin Snowcover. In Advanced Concepts and Techniques in the Study of Snow and Ice Resources, National Academy of Sciences, Washington, D.C., 314-324.

Stiles, W.H. and F.T. Ulaby, 1980: The active and passive microwave response to snow parameters: I. Wetness. J. Geophys. Res., V. 85, 1037-1044.

Trivett, N.B.A. and S.E. Waterman, 1980: Evaluation of the Spatial and Temporal Distribution of Snowpack Parameters in the Saint John River Basin. Proc. Eastern Snow Conf. 19-35.

Ulaby, F.T. and W.H. Stiles, 1980: The active and passive microwave reponse to snow parameters II. Water equivalent of dry snow, J. Geophys. Res., V. 85, 1045-1949.

Vershinina, L.K. and A.M. Dimaksyan, 1969: Determination of the Water Equivalent of Snow Cover. Israel Program for Scientific Translation, Jerusalem, 1971.

Waterman, S.E., W.D. Hogg, A.J. Hanssen and V.L. Polavarapu, 1980: Computer analysis of TIROS-N/NOAA-6 satellite data for operational snowcover mapping. Proc. 6th Can. Symp. on Remote Sensing, Halifax, N.S., May 21-23, 1980, 435-442.

Water Survey of Canada, 1968: 1968 Annual Snow Survey Report. Western and Northern Region, Inland Waters Branch, Canada Department of Energy, Mines and Resources.

Woo, Ming-ko, R. Heron, P. Marsh and P. Steer, 1983: Comparison of weather station snowfall with winter snow accumulation in high Arctic basins. Atmosphere-Ocean, 21(3), 312-325.

Work, R.A., H.J. Stockwell, T.G. Freeman and R.T. Beaumont, 1965: Accuracy of Field Snow Surveys in Western United States, including Alaska. CRREL Technical Report 163, Hanover N.H., 43 p.

SNOWPACK MEASUREMENTS IN A FORESTED ENVIRONMENT

by

D.A. Daugharty and R.B.B. Dickison

Department of Forest Resources
University of New Brunswick
Fredericton, New Brunswick
Canada

presented at

SNOW PROPERTY MEASUREMENTS WORKSHOP

Lake Louise, Alberta

1-3 April, 1985

TECHNICAL MEMORANDUM 140

Compiled By

P.R. Kry

NRCC 27594

SNOWPACK MEASUREMENTS IN A FORESTED ENVIRONMENT

D.A. Daugharty and R.B.B. Dickison
Department of Forest Resources
University of New Brunswick

INTRODUCTION

Canada is often characterized as a country of abundant snow and expansive forests — not an unfair generalization because, over most of the continent, 20 - 35% of annual precipitation occurs as snow, and 37% of the land mass is forest covered. Substantial snowpacks persist throughout the winter over most of this area, making the measurement of snowpacks in the forest an important facet of the inventory and development of all our water-related resources.

The presence of the forest complicates the estimation of snow reserves simply because trees are taller than the snow is deep. Projecting forest canopies intercept and redistribute falling snow, they absorb and emit radiation, they influence the movement of wind in both canopy and stem space, and may or may not have a second layer, or understory, that occupies the zone of snow accumulation (Jeffrey, 1970). For measurement purposes these canopy effects cannot be negated. If the effect of varying canopy closure is removed by taking measurements in small clearings within the forest, a bias is introduced by the extra snow induced by the clearing itself (Golding, 1982). If the effects of both canopies and small forest clearings are removed by taking measurements in nearby large open areas, a bias resulting from the redistributing effect of wind and greater exposure to melt factors is introduced (Lull and Rushmore, 1960). Thus, we are committed to a process of estimating snow reserves in forests from measurements taken in situ, where snowpack characteristics will have a unique regimen and variability.

Committed to taking measurements in the forest, one needs to know the extent to which a forest cover influences problems related to any sampling strategy. These problems can be generally categorized as follows:

1. Network design: How many snow courses are required to adequately sample the area? How are they to be distributed?
2. Location and design of snow courses: Does the forest create problems in a sampling scheme? Can the snow courses be designed to alleviate these problems?
3. Number of observations within snow courses: How many observations are required to produce a statistically valid measure? This could be restated as - What is the expected variability of the parameter to be measured? Does this variability change with covertype and does it vary as the snowcover season progresses?
4. Selection of individual sampling sites: What guidelines might apply to the selection of appropriate sampling sites?

In this paper, we will address these questions, based on our experiences of snowpack sampling in two small, forested catchments in central New Brunswick. These catchments are the clearcutting treatment (Narrows Mountain Brook Basin - NMBB) and control (Hayden Brook Basin - HBB) basins of the Nashwaak Experimental Watershed Project (NEWP). Snow surveys were carried out in both basins, each winter, during the 1973-78 portion of the calibration period. Five or six surveys spanned the mid-January to late-April period of each year.

The snow depth and water equivalent data that we will discuss have been gathered using Mount Rose (standard Federal) snow samplers. Gravimetric techniques have traditionally supplied the bulk of snowpack data collected by survey agencies. However, for the past decade or so, in the face of rising costs and logistical problems associated with gravimetric surveys, remote sensing methods have been rapidly developed to a point where they provide an alternative in some cases. These relatively new techniques may eventually replace the more conventional techniques but, for the immediate future, ground-based surveys will at least continue to provide calibration data. In addition, forest cover, particularly dense conifer cover, poses a separate problem for remote sensing techniques (Dillard, 1981; Lillesand et al., 1982). Since this is the dominant forest covertype in Canada we can expect conventional snow surveys to be a part of estimating snow reserves in forested areas for an even longer time.

NETWORK DESIGN

The most common purpose of a network of snow courses is to estimate basin snow reserves either in absolute terms or from an index value. The former might be used in operational planning and the latter to indicate flood risk or as an index to winter severity for wildlife. Regardless of purpose, the network must be designed to reflect the interaction of local climate and physiographic conditions (Goodison, 1978); if not, the absolute estimate will be imprecise and the index may not be representative.

The literature contains many snow surveying designs (Gray et al., 1979; Young, 1974; Goodison, 1977; Adams, 1976; Vershinina, 1972; Dickinson and Whiteley, 1972; Steppuhn and Dyck, 1974). These works outline methods that would reduce (or relocate) sampling so that more precise estimates can be obtained for any given level of effort.

The most common technique involves some sort of stratification, using a knowledge of snowpack characteristics as they relate to topography and land use or vegetative cover. Many multi-factor studies have investigated these relationships where the vegetative cover has been a forest (U.S. Corps of Engineers, 1956; Anderson and Pagenhart, 1957; Golding, 1970; Packer, 1962), and the often-quoted review of Meiman (1970) provides an excellent summary. A general ranking of physiographic influences would put the effect of elevation as greatest, followed by aspect and slope, with the effect of variations in forest cover rivaling that of elevation. In fully forested areas, some of the influence of topography may be masked by the effect of vegetation. Swanson (1970) found non-significant, or significant but inconsistent, differences in water equivalent attributable to differences in slope, aspect, and elevation. Daugharty (1984) found slope to be non-significant, and aspect to be consistently significant only to snow depth, and then only late in the season. Variations in forest cover have added importance in areas where covertype ranges from complete hardwood to complete softwood. Snow under leafless hardwoods accumulates and melts in amounts substantially different than snow under evergreens (Lull and Rushmore, 1960; Kuzmin, 1960). In summary, network design for sampling snowpacks in fully forested areas should, therefore, at least consider elevation and forest cover characteristics.

The network we have used has taken these factors into account. Actually, in this part of New Brunswick the two sources of variation are related — there is a strong correlation between forest covertype and elevation, with hardwoods found almost exclusively at the higher elevations and softwoods at lower elevations along streamsides. For NEWP, expressing the hardwood contribution as the percentage of the total basal area that is in hardwood species yields a correlation coefficient with increasing elevation of 0.618. In this case, a network designed to sample variation in elevation will also sample variation in covertype.

Aspect has been previously mentioned as second in importance to elevation as a topographic factor defining landscape classes, and we have included aspect-sampling in our network design.

The network is shown in Figure 1. We established snow courses at regular intervals along four transects of each basin. This number of transects was chosen so that each basin could be surveyed in one day. The two days required to survey both basins was judged to be the longest period that could safely be assumed free of significant accumulation or ablation. The transects are equally spaced from headland to outlet, so that the complete range of elevation is sampled. They are oriented more or less at right angles to the long-axis of each basin so that aspects are sampled roughly in proportion to their occurrence. Headland elevations (and aspects) are sampled by locating the highest transect above the source of each channel.

The transects identified for snow surveying make up approximately one-third of a set of transects used to locate permanent sample plots for a study of forest growth and composition. Along each transect these plots are located at approximately 300-m intervals. An examination of a topographic map and aerial photographs revealed that significant changes in elevation and particularly in forest cover could occur over horizontal distances no greater than a few hundred metres. It was therefore decided to locate snow courses for sampling snow depth and water equivalent in all of the forest growth plots found on each of the four transects in each basin. Two snow courses, for the sampling of depth only, were located at 100-m intervals between each depth and water equivalent snow course. Snow depth can be sampled rapidly, compared to the time required to sample water equivalent or the time required to travel from one plot to the next, so the additional snow courses allowed an increased sampling density without compromising our ability to complete a basin survey within one day. Numbers of snow courses in each basin are summarized in Table 1.

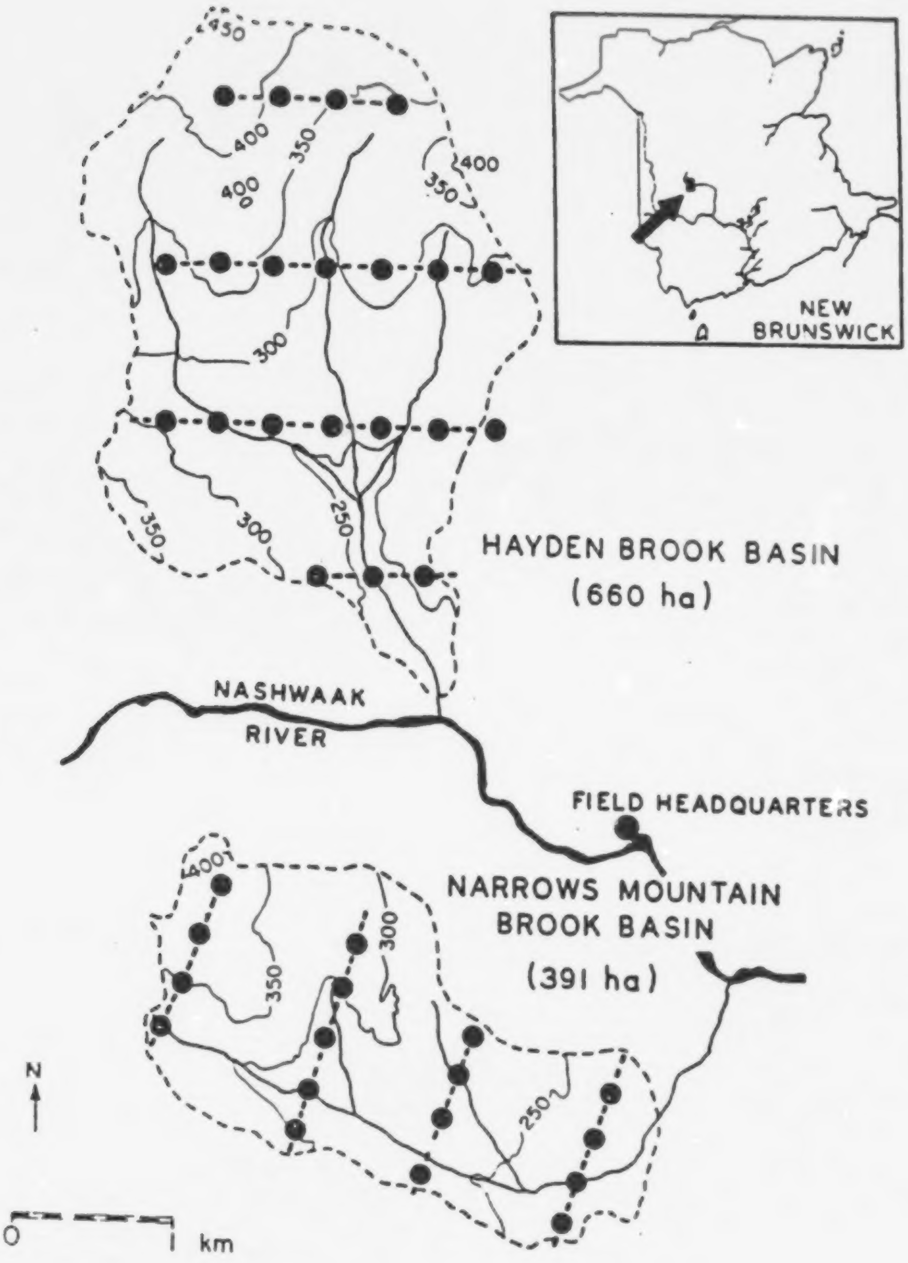
450
400
350
400
350
400
300
350
300
250
HAYDEN BROOK BASIN
(660 ha)
NASHWAAK
RIVER
FIELD HEADQUARTERS
NARROWS MOUNTAIN
BROOK BASIN
(391 ha)
400
300
350
250
NEW
BRUNSWICK
N
0
1 km

Figure 1. Snow course locations in the NEWP basins.

Table 1. Numbers of snow courses in HBB and NMBB.

Measurement	HBB	NMBB	Total
Snow depth	59	47	106
Snow depth and water equivalent	21	17	38

For this network, the correspondence of sampling effort and areal extent of elevation, aspect, and covertype classes has been found to agree closely (Daugharty, 1984); only the steeper slopes were not well sampled. A total of 5.5% of the snow courses occurred on slopes steeper than 20% and yet these slopes occupy 17.3% of the basin areas. This situation could be expected as a general case, for small headwaters basins, where the steeper slopes are strongly associated with the highest elevations that form the height of land, and sampling is carried out over the range of elevations necessarily found in other parts of the basin. Although Young (1974) found slope to be more important than elevation in an elevation-stratified sampling scheme for glaciers, it is generally conceded to be less important than elevation or aspect under forest cover (U.S. Corps of Engineers, 1956; Swanson, 1970; Daugharty, 1984). Therefore, a network design that doesn't consider slope as defining a separate topographic province is not necessarily deficient.

Index Snow Courses

Sampling all of the landscape classes may be a possibility only where landscape classes are few and cover broad areas, or for small basins, or for research purposes. A more realistic situation uses index snow courses to represent mean conditions over some very large area.

Bias is allowable in index measurements as long as it is consistent. At some point in the application of the data, bias may be compensated for by applying empirical coefficients to the index values. However, the use of index snow course data to indicate snow reserves may not be a good practice. Gray *et al*. (1979) offered this comment:

> "Network snow courses have been established on the Prairies primarily to assist in the forecasting of flood flows and water yield. As they are to serve these functions and, in addition, they must suffice the requirement of providing consistent and continuous data from year to year, many courses have therefore been placed in accessible locations that favour maximum accumulations each year. In many years it is found the data from these courses do not provide reliable indices of the areal snow water equivalent."

A somewhat similar situation exists in New Brunswick where a network of snow courses has been developed to provide data to the Saint John River Flood Forecasting Unit. These data are also found published annually in Snow Cover Data (e.g. AES, 1982) and because of the regularity of the surveys and their period of record, an attempt might be made to use these data to estimate snowpack reserves. Some of these snow courses are located in the immediate vicinity of stream gauging stations which have the advantages mentioned by Gray *et al*. of being accessible and being visited regularly. (New Brunswick is not peculiar in this regard — McKay (1970) also noted the bias for snow courses at prime gauging sites.) Two examples of this situation are the snow courses, sampled by Water Survey of Canada (WSC) personnel, located near the stream gauges on Narrows Mountain and Hayden Brooks. Although the WSC survey schedule and ours were not coordinated, several contemporaneous surveys are available for comparison. Snow depth and water equivalent data from these snow courses and basin means of the NEWP transect surveys are shown in Figure 2. The limitations of using the WSC snow course data to estimate basin snow reserves is made obvious by the deviations from the 1:1 line: the WSC snow courses consistently underestimate basin-average depth and water equivalent. It is interesting to note that the Narrows Mountain Brook WSC snow course better estimates basin snow reserves since the basin was clearcut (1980-82 data points).

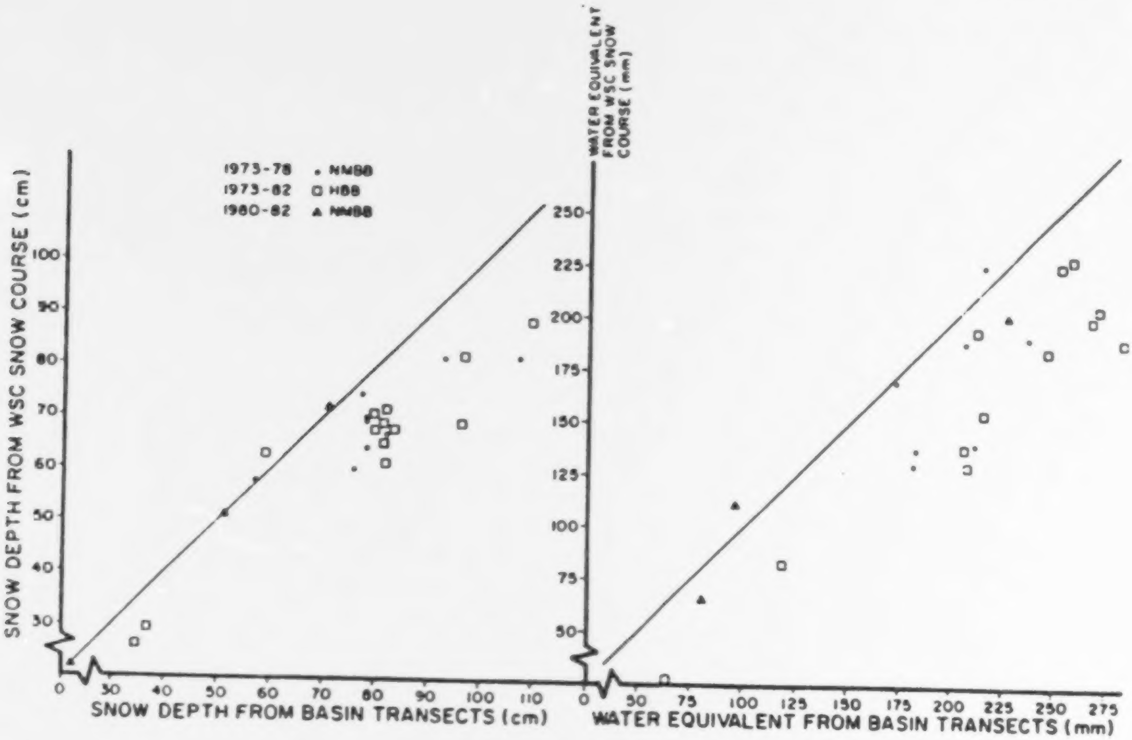

Figure 2. Snow depths and water equivalents from snow courses located at the outlet of HBB and NMBB plotted against mean values from the basin transect surveys.

Stream gauge snow courses combine the biases associated with the lowest elevation and, in this case where softwoods dominate only the lower elevations, an unrepresentative covertype. For the 11 contemporaneous surveys in Hayden Brook Basin, the calculated underestimate of mean basin SWE by using the WSC snow course is 24%. In Narrows Mountain Brook Basin, where the elevation and covetype differences are less, the underestimate using seven available surveys before harvest is 15%.

It is possible to adjust for the biased locations of the WSC snow courses by applying correction factors for elevation and forest cover. To make an adjustment the rate of change of snowpack characteristics for unit changes in elevation and forest cover must be known. For this region, such values are available only for the time of maximum pack. It has been determined that the mean increases in snow depth and water equivalent associated with each 100-m increase in elevation are 6.0 cm and 20.5 mm, respectively; and mean reductions in depth and water equivalent for each 10% increase in canopy closure are 1.8 cm and 4.8 mm, respecively (Daugharty, 1984). The WSC snow course is 97 m lower than the HBB mean elevation and has a canopy closure approximately 35% greater than the basin mean. Of the data shown in Figure 2, six surveys were carried out in the HBB close to the time of maximum pack. Table 2 summarizes the snowpack data and their differences for these six surveys and gives values for the WSC snow course adjusted to basin mean elevation and canopy closure.

Table 2. Snow depth (SD) and water equivalent (SWE) data from the HBB WSC snow course, HBB transect surveys and adjusted WSC snow course.

Date	WSC Snow Course		Basin Mean Snowpack				Transect Survey — WSC Snow Course			
			From Transect Surveys		Adjusted WSC Snow Course					
	SD (cm)	SWE (mm)	SD (cm)	SWE (mm)	(cm)	(mm)	Measured SD (cm)	Adjusted SD (mm)	Measured SWE (cm)	Adjusted SWE (mm)
27-03-73	61.2	195.6	81.8	213.9	73.0	232.2	20.6	8.8	18.3	-18.4
02-04-75	67.6	231.1	79.3	259.3	79.4	267.8	11.7	-0.1	28.2	-8.5
13-04-76	62.7	132.1	58.5	208.0	74.5	168.8	-4.2	-16.0	75.9	39.2
13-03-79	69.3	191.0	96.0	284.5	81.1	227.7	26.7	14.9	93.5	56.8
31-03-80	29.7	83.8	36.2	119.4	41.5	120.5	6.6	-5.2	35.6	-1.1
31-03-82	70.8	186.0	79.1	246.4	82.6	222.5	8.3	-3.5	60.4	23.7
							|78.1|	|48.5|	|311.9|	|147.7|

The improvement in the adjusted data can be seen from the absolute value summations of the differences between transect surveys and WSC snow course values. However, in some cases large deviations still exist.

Two observations might be made from this example. The first is that for snowpacks in forested areas, proximity alone is no assurance of the quality of an index, as might be more the case for liquid precipitation. If only one snow course is to be used to estimate basin snow reserves, it should at least be at mid-elevation and within a covertype representative of the basin as a whole. We have tested each snow course in the HBB with respect to its ability to closely and consistently estimate mean snowpack characteristics for both basins (Dickison and Daugharty, 1978). Not surprisingly, the snow course identified as the most suitable index was located very close to the mean elevation, aspect and covertype for the basins. The second observation is that one snow course, even if adjusted for differences in elevation and covertype, will at times poorly estimate basin snow reserves. Adjustment factors, if available at all, will almost certainly be mean values and will not compensate for between-years variations in accumulation or ablation characteristics. This can be illustrated by comparing mean (rather than absolute) values of differences between transect surveys and the WSC snow courses. From Table 2, the mean difference in depth before adjustment is 11.6 cm; the mean difference after adjustment is -0.2 cm. Mean differences in water equivalent are similarly reduced from 52.0 mm before adjustment to 15.3 mm afterwards.

If a network of snow courses is to produce statistically valid estimates concerning the populations of various snowpack characteristics the snow courses must be randomly located, or if a systematic sampling scheme is used we must assume an areally random snowpack. Steppuhn and Dyck (1974) point out that neither of these conditions is likely to be the case. Random location of snow course sites is not the most realistic alternative because of the logistical difficulties of surveying such a network; on the other hand, it is generally agreed that snowpacks develop in ways that are related to topographic and vegetative cover characteristics. These landscape features are not randomly distributed in a basin and the assumption of an areally random snowpack is therefore not justified.

A systematic sampling scheme that originates from a randomly located baseline or point, nevertheless, has many of the features of random sampling. Although sampling points are fixed after the starting point is chosen, if the starting point is selected at random, every point in the basin initially has an equal chance of being chosen. Additional random components are contributed by micro- and meso-scale factors and these contributions are greater under forest cover (Steppuhn and Dyck, 1974).

Regardless of the sampling scheme chosen, the opportunity for the sampler to introduce bias when locating snow courses is negated by strict adherence to the scheme. The point to be made here is that rigid adherence to any sampling scheme may locate snow courses in some rather odd places. In other words, within the network there will be some snow courses that represent a combination of features quite different from those described by the general features of the landscape unit being sampled.

The representativeness of each snow course in the NEWP network was assessed from a residual analysis. Residual (observed minus estimated) values for the 106 snow courses for the 24 surveys during the 1974-78 period were calculated. For each survey, estimated values were calculated from a multiple linear regression of snow depth and water equivalent on elevation, aspect, slope, and forest canopy closure.

Fifteen snow courses were found to produce large residuals or a seasonal pattern in residual values. Obviously, then, these sites were not adequately represented by factors in the model specification. The physiographic descriptions of these sites were examined in closer detail, and surveyors' notes were studied to discern any obvious peculiarities. In two cases, errors were found in the original physiographic descriptions. In the other cases, based mainly on surveyors' notes, it seemed that they could be grouped into four categories with similar patterns of residual differences: (1) sites influenced by periodic flooding; (2) sites characterized as "softwood thickets"; (3) sites in or near small openings; and (4) sites with extreme aspect exposures. The characteristics of each of these will be discussed in detail.

Snow Courses Influenced by Periodic Flooding

Three snow courses were located in areas subject to periodic flooding. This results in melting of the snowpack from beneath and/or the formation of ice layers if freezing occurs at stages high enough to raise the water level close to the surface of the pack. As an example, the residual values for one of these snow courses are shown in Figure 3.

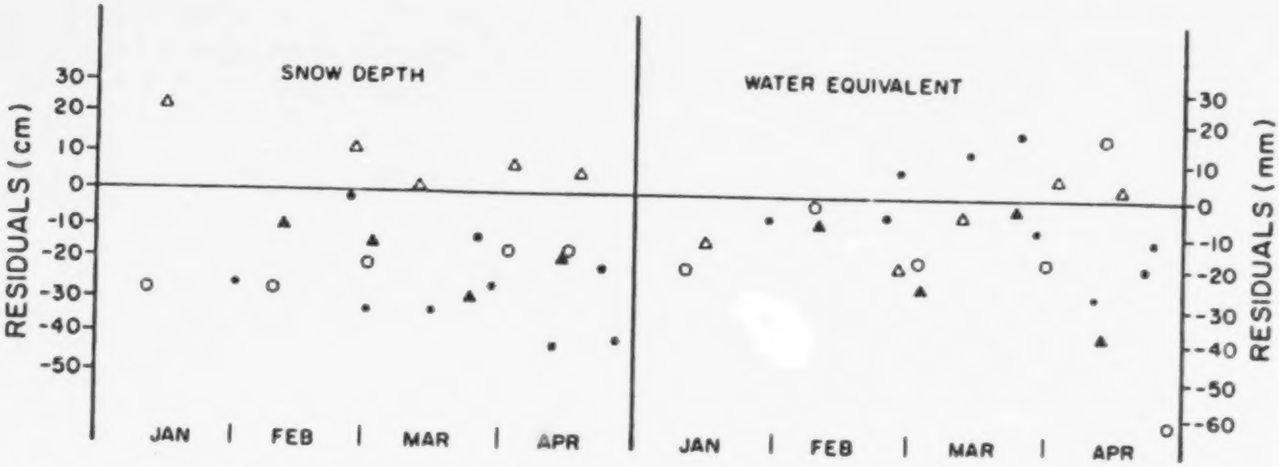

Figure 3. Residual values for a snow course subject to periodic flooding for the surveys of 1974(·), 1975(Δ), 1976(▲), 1977(o) and 1978(*).

Snow depth residuals for these courses are commonly negative (melting from beneath, with subsequent settling) but show some positive values (throughout 1975) believed to result from the greater snow depths found when new snow is supported by ice-bridging. Water equivalent residuals show a wide scatter, some are positive from the added water equivalent of ice layers, but most are negative resulting from melting of the submerged snowpack. The increased sampling difficulties associated with the presence of heavy ice layers will also contribute a larger-than-normal sampling error to these residuals.

Winter rainstorms and periods of mid-winter melt can be expected frequently in this region (Potter, 1965), and snow courses located in certain areas will be flooded regularly. Perhaps of greater importance than the frequency of these events is that the effects, once established in the pack, persist throughout the remainder of the season to influence subsequent surveys and to establish these areas as separate landscape units.

Snow Courses Influenced by Softwood Thickets

Three snow courses were found to have negative residuals throughout the season that show no tendency for change with time. An example is shown in Figure 4. These snow courses were located in areas that have a thick softwood understory and show negative residuals because the overstory forest cover variable in the regression model fails to account for the decreased accumulation resulting from the understory. Cover conditions for these snow courses closely approximate the "dog-hair plots" of Gary and Troendle (1982) where deficiencies in accumulation were also found.

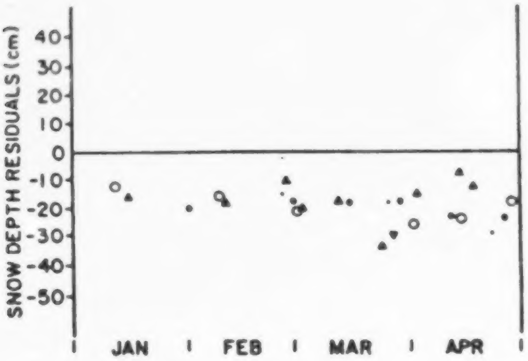

Figure 4. Residual values for a snow course located in a softwood thicket for the surveys of 1974(·), 1975(Δ), 1976(▲), 1977(o) and 1978(*).

Within the forest, areas of abundant advanced regeneration can be expected frequently under some conditions. These areas will be found in locations where natural succession is replacing an intolerant, pioneer overstory species with a more tolerant climax species, or where insect or disease is removing a mature to over-mature overstory and the same species is (are) regenerating in the openings created. This latter case is common throughout many areas of the boreal forest where mortality from spruce budworm is prevalent.

The consistency and magnitude of the residuals indicates that these areas are separate landscape units that should be sampled, and yet their presence may not be apparent on aerial photographs or may develop over the life of a snow course. Therefore, the original definition of landscape units, if accomplished using aerial photos, should be made with great care and should be periodically reassessed.

Snow Courses Influenced By Small Openings

Five snow courses with residual patterns are associated with openings in the forest. One of these snow courses is located about three metres to the north of an old haul road (residuals shown in Figure 5a); three others are located on the north sides of beaver ponds (an example of the residual pattern is shown in Figure 5b) and one is located in the opening left by an old haul road (Figure 5c).

A consensus exists as to the effect of small openings on snow cover (Gary, 1974; Golding, 1982; Golding and Swanson, 1978; Swanson and Stevenson, 1971). Excesses are found in the opening, with deficiencies found in the adjacent (often downwind) forest. The excesses can be attributed to two mechanisms: a reduction in interception losses, and an increase in accumulation because of modified wind patterns over the opening. The latter mechanism deposits snow in the clearing that would otherwise have been deposited in an area nearby.

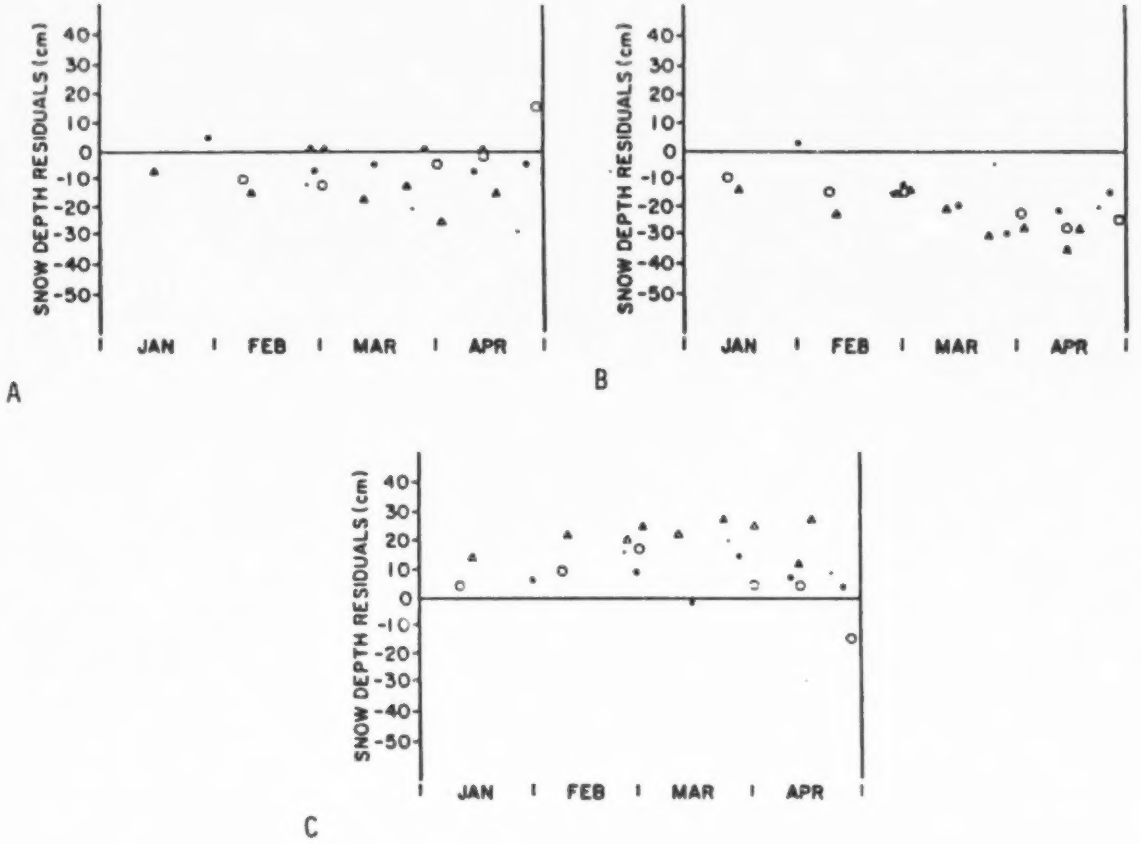

Figure 5. Residual values for snow courses influenced bysmall openings in the forest canopy for the surveys of 1974(·), 1975(Δ), 1976(▲), 1977(o) and 1978(*).

In this way the excess is associated with an adjacent "source" area. Some authors suggest that this is an equal-sized area downwind (Gary, 1974; Leaf, 1975), but Golding (1982) noted deficiencies in a variety of locations and calculated the area of adjacent forest required to satisfy the excess in the opening to be from 2-55 times the opening for clearings of diameter 4H (where H represents the height of the surrounding forest) and smaller. Clearing sizes do not have to be large to exhibit the effect. Swanson and Stevenson (1971) reported excesses in natural clearings as small as 0.5H and Golding (1982) found increases in circular clearings of diameter 0.25H.

The snow courses located on the north sides of openings exhibit negative residuals because they are located in the "source" areas associated with the adjacent openings. The residuals for the snow course shown in Figure 5a are smaller than those of the snow course shown in Figure 5b because 5a is associated with a smaller opening (Golding, 1982; Troendle and Leaf, 1980). Residuals in both cases show some tendency to increase as the season progresses because of greater snowpack losses associated with excesses in energy on the north sides of clearings (Golding, 1982).

Another snow course (Figure 5c) shows positive residuals that have a tendency to reach a maximum at the end of March, approximately the time of maximum pack. This pattern is consistent with what would be expected given this course's location in a "clearing".

The snow courses associated with small openings exhibit varying effects according to the respective location of snow course and openings, and the size of the opening. The deficiencies noted on the north sides of beaver ponds might have been expected, but the effect of the old haul roads is surprising. Prior to these surveys, there had been no harvesting activity in the basins for more than 20 years, and the roads were for the most part overtopped by the canopies of trees at their edges. Even the roadways had grown over considerably, although the stems were smaller than those in the surrounding forest.

Snow Courses Influences by Extreme Aspect Exposure

Two snow courses are characterized by consistently negative residuals which are small throughout most of the season but show an increasing trend in March and April. An example is shown in Figure 6. This pattern indicates accumulation which initially compares favourably with that estimated by the regression model but exhibits unexplained late-season reductions in the snowpack. Both of these courses are located in open hardwood stands, on relatively steep slopes, facing east-southeast; none of these are common factors which might help explain higher-than-predicted rates of melt. These courses do, however, have low estimates of canopy closure in the southerly direction, similar to some of the courses in the previous group which were located on the north edges of clearings and exhibited melt effects from the penetration of solar radiation. In the cases of this group, low southerly canopy coverage results from their topographic position; although the predominant aspect is east-southeast, the land also slopes away steeply to the south, allowing only the open tops of the hardwood crowns to impede penetration of the solar beam. Negative residuals throughout the year suggest that the increased topographic exposure of these courses results in small deficiencies in accumulation which are added to increases in melt late in the season.

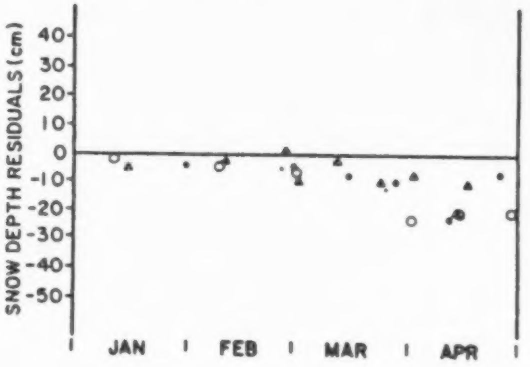

Figure 6. Residual values for a snow course influenced by extreme aspect exposure for the surveys of 1974(·), 1975(Δ), 1976(▲), 1977(o) and 1978(★).

To summarize, 13 of 107 snow courses in this network are influenced by peculiarities not associated with a landscape type that would have been defined by topography and forest cover. The effect of these influences is substantial. In snowpacks that rarely exceed mean snow depths of 100 cm, residuals are frequently 20 to 30 cm different than would have been expected.

Users of these data are therefore faced with deciding whether or not the affected snow courses are representative. If the purpose of the network is to determine topographic and forest cover influences on snowpack characteristics, data from these courses can be considered to have come from a population other than the one it was intended to sample and are therefore seriously compromised. But the more common purpose of a snow course network is to provide estimates of basin snow reserves. Vershinina (1969) after carefully examining Russian snow survey data, rejected some snow courses as unrepresentative. However, the definition of what is unrepresentative must be approached with care. The effects we have noted are common occurrences in any forested environment — even the openings associated with old logging roads simulate the type of opening that could occur from blowdown in a purely undisturbed situation. These areas would contribute data to the basin-wide sample only in proportion to their frequency of occurrence and should be included in the determination of aerial snowpack characteristics.

The number of snow courses to be located in any landscape unit is a function of the expected variability within the unit. Snowpacks in forested areas are responding to factors that may well be unforeseen at the time a sampling scheme is adopted. In addition to underlining the dangers of using a single snow course to index an area, the effect of the unforeseen influences may result in greater variability than indicated by a preliminary survey unless the survey is comprehensive.

Snow Course Design

The snow courses we have used are very short in comparison with most other designs. Sampling is completed over a distance of about 10 metres with samples spaced about two metres apart. The spacing is adequate to ensure that a point-peculiarity is not repeated and the short length allows isolation of a particular combination of slope, aspect, and forest cover density in a region where these features remain constant only over small areas.

Although short snow courses may fit physiographic variation very well, their use results in an increase in the probability that all the samples will be influenced by factors such as those discussed in the previous section. In longer snow courses, there would likely be only a single observation influenced by an opening in the forest canopy, for instance, and excesses found at one point would be balanced by deficiencies at another. The problem of representativeness would change to one of increased variability within the snow course.

VARIABILITY OF SNOWPACK CHARACTERISTICS

One of the first considerations in planning a snow survey is the number of observations on each snowpack property that will be required to achieve a chosen level of confidence. Most statistics texts give the relationship between sample size, variance of the measured parameter, and the desired confidence interval (e.g. Steel and Torrie, 1960; 86). Interval length is chosen according to the precision of estimate required from the survey but, at the outset, population variance will probably be unknown.

A review of the literature will give some indication of the range of variances of commonly measured snowpack characteristics. A brief review is given in Table 3. These data are most frequently reported in terms of the coefficient of variation which allows direct comparison among various studies and relative comparison among depth, water equivalent and density. In most cases, mean values of snowpack characteristics are also given, making the computation of sample variability and sample size for a given confidence interval straightforward.

From Table 3 and a review of the studies cited, some general observations regarding variability can be made. Firstly, water equivalent is more variable than snow depth and density varies less than either water equivalent or depth; secondly, variability may change as the season progresses; and thirdly, there is an association between variability and vegetative cover with the more complete covers having decreased variabilities.

Each generalization listed above was investigated using the NEWP snow survey data. Standard deviations and coefficients of variation for snow depth, water equivalent and density were determined for all the surveys of 1973-78 with the exception of 1974. This year was not included because successive rain storms and mid-winter thaws held the pack at less than 40 cm of depth, and few surveys were carried out. Hardwood and softwood covertypes were examined separately. Standard deviations and coefficients of variation for each covertype were calculated by averaging the individual values for four snow courses in each covertype.

Standard Deviations

Standard deviations plotted against date of survey show similar patterns for both forest covertypes. Figure 7 shows the standard deviations for depth, water equivalent, and density for the hardwood covertype. Although there is some variation between years, particularly in snow depth, and in water equivalent at about the time of maximum pack, standard deviations are remarkably similar from one year to the next considering the great between-years differences in meteorological conditions. For example, the winter of 1976 included two heavy mid-winter thaws, one of which reduced snowpack depth by approximately 40 cm; on the other hand, the winter of 1977 had one light mid-winter thaw and the winter of 1978 had none.

The correlations between date and standard deviations were consistent enough to suggest that standard deviation could be estimated from a regression relationship using date (specifically, Julian day number) as the independent variable. Polynomial regressions were found to fit the data best and are given in Table 4. Data from a 10-point snow course, in the open, at the NEWP Headquarters exhibited similar relationships, and is included for comparison. Solutions to the polynomial equations are given in Figure 8.

Table 3. Coefficients of variation for various snowpack characteristics.

Source	Date	Covertype	Coefficients of Variation (%)			Location	Remarks
			Snow Depth	Water Equivalent	Density		
Bray (1973)	27 Jan	Field	12	20		New Brunswick	Variability increased after ice layers formed in the pack.
	13 Feb		13	16			
	10 Mar		19	35			
Adams and Barr (1979)	21-27 Feb	Lake	66	127	23	Labrador	Interaction of wind and sparse cover contribute to variability
		Open lichen woodland	40	61	30		
		Close lichen woodland	28	41	27		
		Tundra	78	76	29		
Mathers (1980)	@ maximum pack	Deciduous forest	11	13		Southern Ontario	
		Coniferous forest	13	25			
		Mixed forest	11	28			
		Pasture	17	15			
Goodison (1978)	@ maximum pack	Mixed forest		37		Southern Ontario	Average of seven years, range 31-37% with an observation of 57%
		Long grass	25[a]	26			Average of seven years, range 22-34%
		Short grass	55[a]	57			Average of seven years, range 40-79%
		Deciduous bush	18[a]				
Vershinina (1969)	@ maximum pack	Forests	10-20		3-9	European USSR	
		Fields	20-40		12-14		Level land, northern regions.
			30-80				Level land, central and southern regions.
Granberg (1978)	@ snow depths of 20 cm	Forest-tundra	45[b]			Northern Quebec	
	40		50				
	60		67				
	80		71				
	100		74				
Dickinson and Whiteley (1972)	31 Jan	Open	40[c]	43	14		
	28 Feb		33	38	24		
	30 Mar		52	67	22		
	31 Jan	Cedar forest	23	26	8		
	28 Feb		23	27	6		
	30 Mar		33	31	13		

[a] Data approximated from Figure 3 of Goodison (1978), average of three snow courses.

[b] Data approximated from Figure 3 of Granberg (1973).

[c] Data approximated from Figures 10 and 11 of Dickinson and Whiteley (1972).

NOTE: Values for snow depth and density are given by Steppuhn and Dyck (1974) for snow courses in Saskatchewan and the Yukon. These values are classified by several landscape classes and are not included in this Talbe only because of the large number of values given.

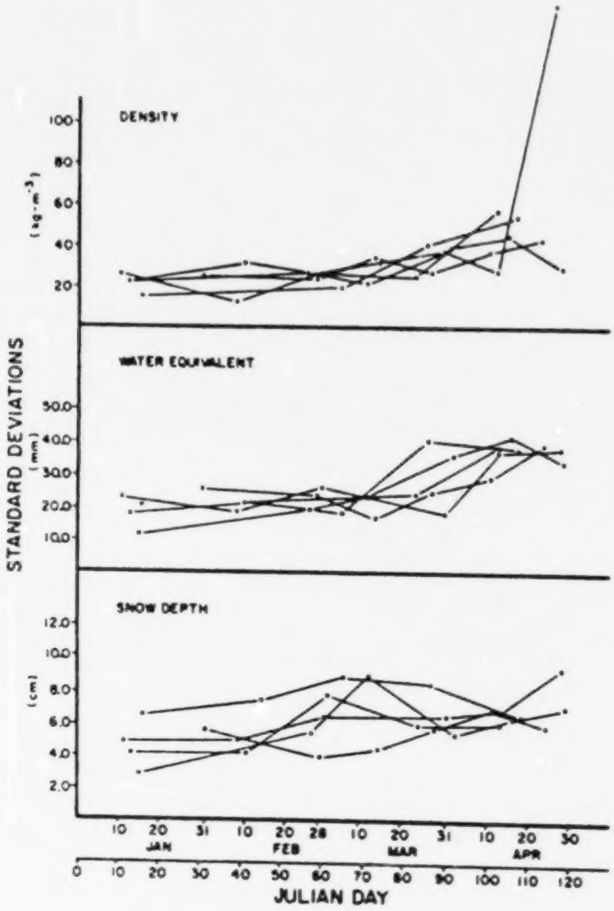

Figure 7. Scatter diagrams of standard deviations for snow depth, water equivalent and density under hardwood cover for the surveys of 1973 and 1975-78.

Largest differences in standard deviations, among the three cover types, exist for snow depth. Standard deviations of depth in the open showed very little scatter from one year to another (lowest S.E.), but also showed no

Table 4. Polynomial regression equations of standard deviation versus Julian day number.

SNOW DEPTH	
HARDWOOD	Std. Dev. = 4.231 + 0.0423 Day # - 0.0001634 Day #^{2} S.E. = 1.40 cm, F(2,25) = 3.75*
SOFTWOOD	Std. Dev. = 3.999 + 0.1086 Day # - 0.0004914 Day #^{2} S.E. = 2.17 cm, F(2,25) = 7.36**
OPEN	Std. Dev. = 3.272 - 0.0046 Day # + 0.0000192 Day #^{2} S.E. = 1.08 cm, F(2,23) = 0.05^{ns}
WATER EQUIVALENT	
HARDWOOD	Std. Dev. = 20.185 - 0.0985 Day # + 0.002210 Day #^{2} S.E. = 5.47 mm, F(2,25) = 21.00***
SOFTWOOD	Std. Dev. = 11.383 + 0.1970 Day # + 0.0003217 Day #^{2} S.E. = 6.40 mm, F(2,25) = 22.21***
OPEN	Std. Dev. = 9.569 + 0.3464 Day # - 0.00234 Day #^{2} S.E. = 3.88 mm, F(2,23) = 5.06*
DENSITY	
HARDWOOD	Std. Dev. = 28.428 - 0.5468 Day # + 0.007577 Day #^{2} S.E. = 21.52 kg-m^{-3}, F(2,25) = 7.69**
SOFTWOOD	Std. Dev. = 32.628 - 0.4777 Day # + 0.006126 Day #^{2} S.E. = 9.84 kg-m^{-3}, F(2,25) = 22.10***
OPEN	Std. Dev. = 20.859 - 0.2345 Day # + 0.003092 Day #^{2} S.E. = 8.08 kg-m^{-3}, F(2,23) = 20.49***

ns - non-significant

* - $\alpha = .05$

** - $\alpha = .01$

*** - $\alpha = .001$

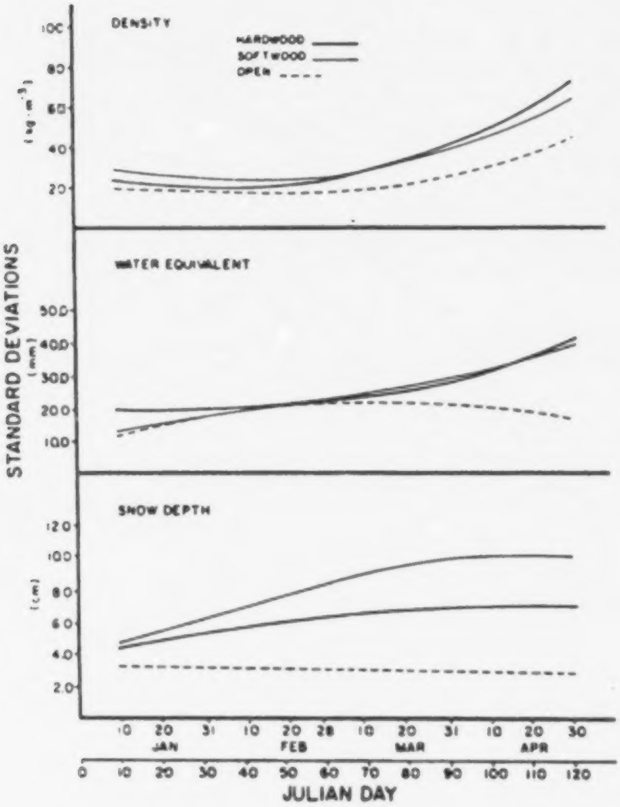

Figure 8. Polynomial regression relationships between standard deviation and Julian day for snow depth, water equivalent and density.

tendency to change over time (non-significant relationship with Julian day). The open snow course is located on level ground close to the centre of a large clearing (6H). Therefore all points along its length are equally influenced by effects that might result in variations in depth from one point to another. The higher standard deviations under the forest covertypes indicate a less uniform snowpack. This would be expected considering the effect of the forest on wind and radiation. The snowpack is least uniform under the softwood cover where the influence of canopy elements is greater. This has been associated with dense conifer crowns creating a "ridge and hollow" effect in the pack (Gray, 1978). Although this term describes a more pronounced condition than we have noticed, it helps create an impression of the processes at work. Differences in standard deviations between softwood and hardwood covertypes are not great, reaching a maximum of about 3 cm. The softwood stands sampled here are mature to over-mature spruce and fir. The canopies are frequently tightly closed (80-100% canopy closure) and there is no foliage throughout much of the stem space. This separates the canopy and the snowpack with a distance of close to 10 m. The effect of the evergreen canopies is lessened by this separation resulting in development of a more uniform pack than would be found in stands where canopies extend closer to the ground. The increased variability within the forest is, in part, a function of an increase in roughness of the forest floor. Soil displaced by the overturned roots of blown-down trees helps develop a hummock and hollow configuraton that lasts a long time in this zone of little erosion. In addition, fallen trees and large branches contribute to an increase in surface roughness. In softwood stands, we have frequently observed a bit of moss and a small amount of rotted log forming the plug in the end of the sampler.

After the approximate time of maximum pack there is no further increase in standard deviations of depth for either forest covertype. This would appear to support the hypothesis that after a certain accumulation, the ability of "rough" surfaces to trap differential amounts of snow diminishes and the pack becomes more smooth (Granberg, 1978). However, we have not found a similar levelling off in the standard deviations in water equivalent.

The standard deviations in water equivalents observed for the open snow course reach a maximum in mid-winter and decline to approximately early-season levels at the end of the season. This mid-winter maximum variability is likely associated with sampling errors that result from sampling a pack that contains heavy ice layers. It is common to have more than one ice layer in these packs and is not uncommon for at least one of these to be hard blue ice as much as 50 mm thick. Early in the season the ice layers may not be present, and late in the season their quality has deteriorated so they interfere less with precise sampling. Standard deviations of water equivalent under both types of forest cover are similar and show steady increases throughout the season. Drip and mass-release patterns of intercepted snow, which are more concentrated than snow throughfall — especially during the warmer weather — are likely contributors to increases in the variability of water equivalent under forest cover.

Standard deviations for density show very similar relationships with Julian day for all three covertypes: little change through January and February, with marked increases thereafter. In the forested areas variability in density would result from differential wind and radiation effects, and from the drip and mass-release patterns mentioned previously, but these factors cannot provide an explanation for the late-season increase in standard deviations for the open snow course. Although we have no substantiating observations, the late-season increase in variability in the open may be linked to a deterioration in the association of depth and water equivalent. Instead of the greatest depths being associated with the greatest water equivalents, as had been the case earlier in the season, movement of melt-water within the pack may result in greater depths associated with a variety of water equivalents.

Coefficients of Variation

Coefficients of variation provide a measure of variability that allows direct comparison among snowpack properties and with other studies. These data were calculated in the same way as were the standard deviations and solutions to polynomial regressions of coefficients of variation versus Julian day are given in Figure 9. Each curve exhibits a characteristic broad U-shape, similar to those shown by Dickinson and Whiteley (1972), with minimum values occurring at about the middle of February for all cases. At mid-season, standard deviations have not increased much over early-season values but mean values of snowpack characteristics have: their quotient is therefore a minimum. Early in the season, variabilities are less but so are the mean values of snowpack characteristics. Late in the season, deviations increase as mean snowpack depth and water equivalent begin to decrease.

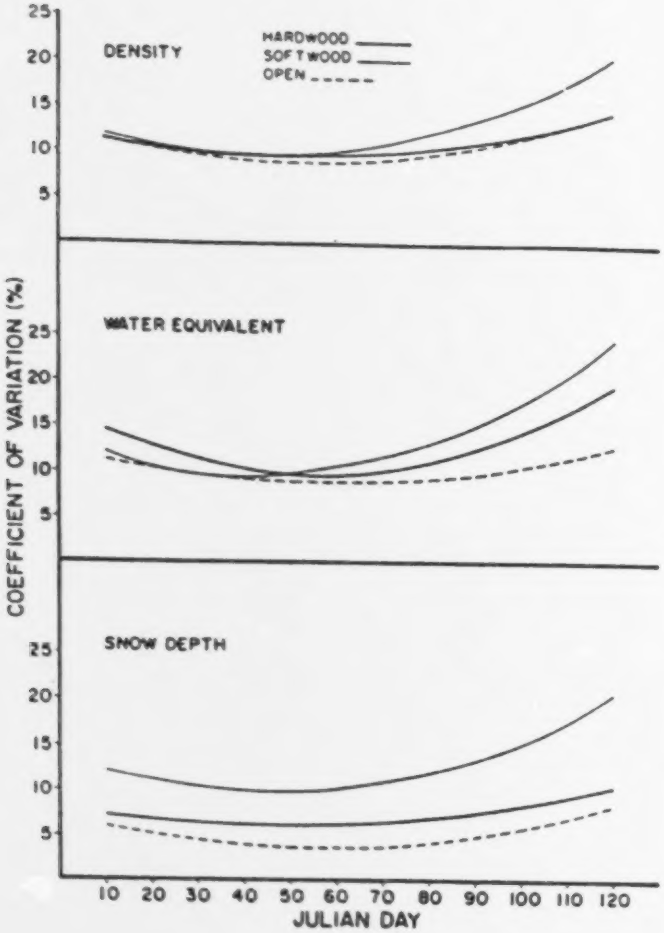

Figure 9. Polynomial regression relationships between coefficients of variation and Julian day for snow depth, water equivalent and density.

Coefficients of variation of water equivalent and density for all three cover types, and of snow depth for the softwood covertype, are quite similar throughout the year: before mid-winter, they range from 8-15% increasing to 20-25% by late-season. The very uniform snow depth at the open snow course and the intermediate variability of depth under hardwood cover result in smaller coefficients of variation that range from 5-10% throughout most of the winter for these cases. Values for density are quite similar to those reported under forest cover by Dickinson and Whiteley (1972) but they show greater variability for water equivalent and depth.. The forest cover in their study was dense cedar which tends to retain foliage throughout the stem space even under fully stocked conditions. The intercepting and redistributing effects of the canopy are therefore extended right down to the pack, which is quite different from the condition of our mature spruce-fir forest, where the stem-space was largely free of branches.

Table 4 gives mean values for coefficients of variation for depth, water equivalent and density at the approximate time of maximum pack (the end of March). These can be compared with values listed in Table 3. Good agreement is found for some cases — e.g. values for depth and water equivalent under deciduous and coniferous covertypes given by Mathers (1980) for the Kawartha Lakes region in Ontario and values for depth and density found in forested areas of the European USSR (Vershinina, 1969).

Table 4. Coefficients of variation (%) at approximately the time of maximum pack for NEWP snow courses.

Cover Type	Snow Depth	Water Equivalent	Density
Hardwood	7.5	12.5	11.0
Softwood	13.5	15.0	13.5
Open	5.0	9.5	10.5

The effect of wind, in increasing snowpack variability under more open stand conditions, can be readily seen by comparing NEWP coefficients of variation with those given by Adams and Barr (1979) and Granberg (1980) for the northern tundra-fringe of the boreal forest.

Snowpack Variability in Harvested Areas

After the forest cover is harvested it might be presumed that snow would accumulate in more uniform manner, much as it might in a sheltered field. This is, however, not the case. The presence of slash, residual trees and regeneration contribute to a snowpack that is at least as variable as it is under full forest cover.

Figure 10 compares standard deviations for harvested snow courses that had been located under softwood and hardwood covertypes with those given in Figure 8 for the open snow course. The post-harvest data were obtained in 1982, three years after the NMBB had been clearcut.

Early in the season, the surveyors were impressed by the variability of snow depth. Areas adjacent to slash piles, in the vicinity of clumps of residual trees that had been too small to harvest, and around regeneration — which by 1982 had reached a height of about one metre and was quite uneven in distribution — were areas of excess accumulation. By mid-season, the snowpack in some of these areas was consolidated so that it would support the weight of a man without snowshoes, while in others the snow was of low density and the surveyors sank to a considerable depth. The more protected areas were those of least density and it is believed that the areas of increased density were those that accumulated snow after it had been transported for some distance by wind. This observation corresponds, in time, to that portion of Figure 10 that shows marked increases in standard deviations of density and water equivalent. Prior to this time the surface had been too rough for snow to be transported for any distance before it was trapped, but continued accumulation resulted in a smoothing of the surface and transport over greater distances (Granberg, 1980).

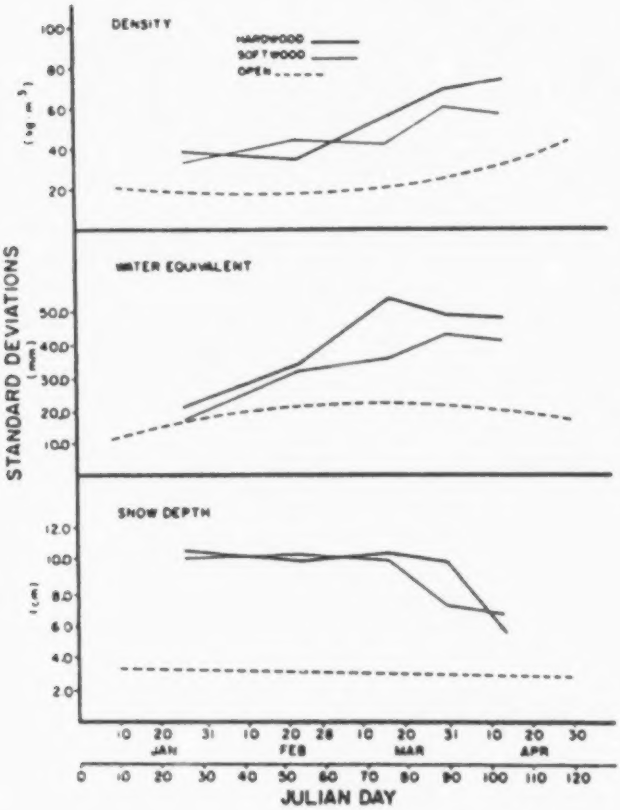

Figure 10. Standard deviations for harvested snow courses that had been under hardwood and softwood covertypes compared to polynomial regressions of standard deviation for the open snow course.

SELECTION OF SAMPLING SITES

There are as many variations in snow course design for forested areas as there are snow surveyors. These range from the very long landscape snow courses used in the USSR to the very short ones we have used. Each design has been chosen to suit the particular needs of an investigator or agency, but common to all are the difficulties faced in choosing sampling sites within the snow course.

Effects of Individual Trees

In stands where evergreen canopies extend down to the snowpack, significantly greater amounts of snow accumulate around the periphery of the canopy than beneath its branches. Under these circumstances the snow surveyor is faced with the problem of deciding where the sample should be taken so that the mean for the snow course properly estimates the snowpack at that location. Granberg (1980) has called the failure to include these areas of low accumulation "lazy sampling" and estimates the bias to be approximately + 10%. Systematic variations in the snowpack were also described by Smith (1974) where snow intercepted by conifer crowns melted in the canopy and could form a "drip-ring" of excess water equivalent at some point around the base of the tree.

We have not encountered differential accumulations such as those described The softwood stands we have sampled were described earlier as closely stocked with a considerable distance separating canopy and snowpack. In late-season surveys conducted soon after a storm, we often noted craters in the surface of the pack partially filled with a lump of snow. These have been made by intercepted snow that has slid from the canopy and fallen to the pack. These lumps of snow are seemingly everywhere, distributed in a random pattern.

The tree boles themselves occupy part of the stand space and deduct from the total snow reserve of the site. Granberg (1980) substituted a zero for depth and water equivalent when sampling these sites was dictated by a very dense sampling scheme to determine "true" snowpack characteristics. In most cases such an adjustment is unnecessary as the effect of ignoring this volume is inconsequential. In one representative 400 m^2 plot, for example, we calculated the reduction in water equivalent resulting from the space occupied by tree boles to be only 0.2% at the time of maximum pack. A further consideration is the reduction in water equivalent in the melt rings associated with each bole (Timmer and Weetman, 1969). These were surveyed extensively on one plot on Arpil 11, 1979 when melt-rings were well developed. Melt-ring depths and diameters were measured for a variety of bole diameters, and the relationships applied to the plot as a whole. Given the snow depth of 87.4 cm and density of 0.324 on that occasion, the combined tree bole + melt-ring effect was only slightly greater than 0.3%. This effect would vary directly with the stocking of the area but would have to increase by more than an order of magnitude even to approach the size of instrumental errors.

Effects of Vegetation Hidden in the Pack

The presence of regeneration or herbaceous undergrowth interferes with water equivalent measurement in three ways. Firstly, their stems and foliage occupy space that would otherwise be filled with snow and may be included with the sample; secondly, the sampler, when it encounters a hidden stem, may push it through the remainder of the pack rather than cut through it; thirdly, coniferous regeneration may be associated with partial voids under its foliage.

These problems are listed in ascending order of importance; fortunately, they are also in order with respect to ease of detection. The first effect is very difficult to detect, but very small, determined by the difference in density between vegetation and snow, multiplied by the volume of included vegetation. Vershinina (1969) reported that the error involved is within the limits of instrumental error and results in no detectable bias. The second effect will result in shortened cores and differences in the "feel" of the penetration of the tube. Vigilant surveyors will not miss these situations and will replace the samples. The third situation represents a genuine reduction in the snow reserve and such a sample is valid as long as the snow above the void is adequately sampled. The presence of voids is readily detected as it is associated with rapid penetration of the sampler through a considerable depth.

Areas of dense undergrowth offer little opportunity for replacement sampling. These areas should be identified by a snow-free season inspection of the snow course and alternate sampling sites chosen. It is inadvisable to clear a site where undergrowth is a problem. Many undergrowth species reproduce by sprouting or suckering so that when a single stem is cut, it is replaced by many others from the same root. The new stems can easily grow to a height of one metre before the next snow surveying season, so that the problem becomes worse, instead of better, unless an elaborate maintenance program is undertaken.

Effects of the Forest Floor

The organic material — either leaves or needles — found on the forest floor provides an excellent plug to hold a snow core inside the sampler. This is most often not frozen and has a consistency quite different from the snowpack. Thus, surveyors can easily detect when they have taken a complete sample without introducing more than a few centimetres bias to the measurement of snow depth. The presence of rocks is also easily detected, and although this alone does not constitute a reason for rejecting a sample, surveyors must be careful to note losses from the tube in this instance. In forests there is no need to artificially prepare a surface by spreading straw (Soil Conservation Service, 1972).

The condition of the forest floor may contribute to variability between samples. In areas where large-diameter litter has fallen, there may be several centimetres difference between the depth of one sample and another. This situation is most prevalent in spruce and fir stands that have been affected by insect damage. The decaying boles of large-diameter trees may litter the ground in this case, and because of natural resistance to decay the effect remains for many years. Large-diameter hardwood litter is less frequently encountered, tends to decay more rapidly, and therefore contributes less to between-sample variability. The forest floor in stands that have originated after fire tend to be smoothest.

For the NEWP snow courses, we have been fortunate in not having had to deal with some of the more problematic situations described — for instance, the effect of "lazy sampling" noted by Granberg (1980)— and have therefore been able to adopt less rigorous methods for locating sampling sites. We have permanently marked start- and end-points for each snow course, but have not marked points for intermediate sampling. Surveyors are instructed to sample at approximately two-metre intervals which sometimes results in passing the end-point if replacement samples are required. As many as six surveys of each snow course are made in one season. To avoid the bias of sampling the area compacted during a previous survey, the first is carried out between the markers, with each subsequent sampling moving to the right of the previous survey by about one metre. The presence of large boulders, softwood regeneration or blown-down trees is often made noticeable by the configuration of the surface of the pack and these areas are avoided. A full core is the main criterion used in accepting a sample.

SUMMARY

The presence of a forest cover complicates the measurement of snow properties by adding another factor that significantly influences development of the snowpack. Any sampling strategy must consider variations in the snowpack resulting from variations in topographic features, particularly elevation, and variations in forest canopy density. The location of index snow courses benefits from the same consideration; those located at mean basin elevation and under a representative covertype will better index basin snow reserves than those biased by neglect of these features.

The data from each snow course in a network should be subjected to some comparative examination. The heterogeneous nature of forest cover may result in some snow courses being influenced by factors, such as thickets or openings, that were not foreseen in the original survey design.

The variability of snowpack properties is remarkably consistent from one year to the next considering the between-years differences in meteorological conditions. Variabilities in snowpack properties, expressed either in terms of standard deviations or coefficients of variation, are greatest for a softwood covertype throughout much of the season. However, the tightly closed canopies of a mature to over-mature softwood cover resulted in a fairly uniform snowpack that was not much more variable than that found under hardwood cover. Snowpack properties in harvested areas are more variable than under forest cover and much more variable than found for snowpacks in the open.

Snowpacks in forested areas are more variable than those in the open, and some snow courses may be influenced by subtle features of this cover, but these have not been our greatest problems. The greatest problem we have faced in sampling snowpack properties has been the accurate determination of water equivalent — and hence density — from a gravimetric survey of a pack that contains ice layers. At times, we have had problems resulting from snow freezing in the tube when air and snowpack temperarures differed widely but these instances are less common than the presence of ice layers. Excerpts from the surveyors' notes, covering the worst sampling conditions found in each of several years, elucidate these problems rather well:

> March 6, 1973. Three ice layers are present in the pack at the HQ snow course site, two of these are thin (1 cm) but the third, at 60 cm depth, is made up of 50 mm of solid blue ice and was easily able to carry a man's weight. The surveyors noted about 55 cm of snow above a heavy crust throughout both basins with sampling conditions very poor and core lengths only fair.
>
> February 25, 1974. The surveyors report a discontinuous layer of ice at the bottom of the pack, a thick ice layer (50 mm) at 10 cm depth and a thin ice layer 3 cm from the surface.
>
> March 12, 1975. It was very cold (-24°C at 0600) early in the morning but warmed rapidly to about freezing shortly after the survey began. Problems were encountered with snow freezing to the inside and outside of the tube making tare weights variable. Efforts were made to keep the tube clear.
>
> The core depths vary between 30 and 70 cm and many samples were rejected. The pack is made up of 25 cm of light, low density snow on top of a 50 mm ice layer which is underlain by 15 cm of coarse granular snow.
>
> February 10, 1976. The surveyors reported a thick crust in both basins under all cover types. At HQ, there were two thick crusts (approximately 50 mm thick), one at 15 cm depth and the other at 35 cm depth. Core depths in HBB averaged approximately 35 cm from a 75 cm pack.

March 1, 1977. There was an ice layer on the surface in NMBB and a heavy crust in HBB. The crust noted Jan. 11, is now 40 mm thick and at 75 cm depth. Liquid water, perched above the crust, froze in the tube blocking entrance of the snow below that depth. Sampling conditions were extremely bad with cores averaging 30 cm from a 100 cm pack.

March 15, 1978. Sampling problems were encountered in HBB when the sampler contacted heavy wet snow at about three-quarters of pack depth with little of the lower portion entering the tube. Snow freezing to the inside and outside of the tube caused tare weights to vary from 615 to 711 mm. It was impossible to clear all of this snow between samples so tare weights were taken for each one.

For most of these instances, the presence of ice layers or crusts simply slowed sampling. These layers had to be penetrated slowly so that a sheet of ice was not broken out of the layer and pushed through the remainder of the pack blocking the entrance of the tube. Even though care was taken, short cores were more frequent and sampling was slowed further by the need to take replacement samples. For these cases, the accuracy of the survey is heavily dependent on the skill and patience of the surveyors.

In four cases (March 12, 1975; February 10, 1976; March 1, 1977; and March 15, 1978) the problems encountered were almost insurmountable — cores of adequate length could not be obtained even after several replacements were taken. Sampling problems for these cases are more related to the instrument itself than to individual technique and surveyor skill cannot overcome them.

Given the fact that water equivalent in these snowpacks is frequently difficult and sometimes extremely difficult to sample accurately, what is the best sampling strategy for estimating basin snow reserves in these cases? The least compromising approach may be to sample snow water equivalent only at a number of carefully selected index snow courses, while maintaining the regular network of snow depth measurements. Ice layers may be sampled independently from the layers of more permeable snow above and/or below, rather than risk having them block the sampler.

REFERENCES

Adams, W.P. 1976. Areal differentiation of snow cover in East Central Ontario. Wat. Resour. Res. 12: 1226-1234.

Adams, W.P. and D.R. Barr. 1979. Vegetation-snow relationships in Labrador. Proc. A. East. Snow Conf. 36: 1-25.

Anderson, H.W. and T.H. Pagenhart. 1957. Snow on forest slopes. Proc. A. West. Snow Conf. 25: 19-23.

Atmospheric Environmant Service. 1982. Snow Cover Data, Canada. Winter 1981-82. A.E.S., Env. Can., Downsview, Ontario, 51 pp.

Bray, D.I. 1973. A report on the variability of snow water equivalent measurements at a site. Proc. A. East. Snow Conf. 30: 20-31.

Daugharty, D.A. 1984. Topographic and forest cover influences on snowpacks. MScF Thesis, University of New Brunswick, 256 pp.

Dickinson, W.T. and H.R. Whiteley. 1972. A sampling scheme for shallow snowpacks. Bull. Int. Ass. Hyd. Sci. 3(10): 247-258.

Dickison, R.B.B. and D.A. Daugharty. 1978. A square grid system for modeling snow cover in small watersheds. Pp. 71-76 In Colbeck, S.C. and M. Ray, eds. U.S. Army, CRREL. Hanover, N.H.: Proc. Meeting on Modeling Snow Cover Runoff, 26-28 Sept., 1978, Hanover, N.H., iv + 432 pp.

Dillard, J.P. 1981. Applications Systems Verification and Transfer Project Vol. 5. Operational applications of staellite snow cover observations: Northwest United States. Washington, D.C., U.S. NASA Tech. Paper 1826, Dec. 1981, 77 pp.

Gary, H.L. 1974b. Snow accumulation and melt along borders of a strip cut in New Mexico. U.S. Dept. Agric. For. Ser. Res. Note RM-279, 8 pp.

Gary, H.L. and C.A. Troendle. 1982. Snow accumulation and melt under various stand densities in lodgepole pine in Wyoming and Colorado. U.S. Dept. Agric. For. Serv. Res. Note RM-417, 7 pp.

Golding, D.L. 1970. Computer mapping of the Marmot Creek snowpack and the influence of topographic and forest stand variables on the pack. Pp. 76-83 In Powell, J.M. and C.F. Nolasco, eds. Can. For. Serv. Edmonton, Alta.: Proc. Third For. Microclimate Symp., 23-26 Sept., 1969, Seebe, Alta., 232 pp.

Golding, D.L. 1982. Snow accumulation patterns in openings and adjacent forest. Pp. 91-112 In Natn. Res. Coun. Ottawa: Hydrologic processes of forested areas. Proc. Can. Hyd. Symp. 82, 14-15 June, 1982. Fredericton, N.B., v + 670 pp.

Golding, D.L. and R.H. Swanson. 1978. Snow accumulation and melt in small forest openings in Alberta. Can. J. For. Res. 8(4): 380-388.

Goodison, B.E. 1977. Snowfall and snow cover in Southern Ontario: Principles and techniques of assessment. Ph.D. Thesis, Univ. of Toronto, 403 pp (Cited in Goodison, 1978).

Goodison, B.E. 1978. Compatibility of Canadian snowfall and snow cover data. Pp. 34-43 In Colbeck, S.C. and M. Ray, eds. U.S. Army CRREL. Hanover, N.H.: Proc. Meeting on Modeling Snow Cover Runoff, 26-28 Sept., 1978, Hanover, N.H., iv + 432 pp.

Granberg, H.B. 1978. Snow accumulation and roughness changes through winter at a forest-tundra site near Schefferville, Quebec. Pp. 83-92 In Colbeck, S.C. and M. Ray, eds. U.S. Army, CRREL. Hanover, N.H. Proc. Meeting on Modeling Snow Cover Runoff, 26-28 Sept., 1978, Hanover, N.H., iv + 432 pp.

Granberg, H.B. 1980. Snow sampling bias in the boreal forest. Proc. A. East. Snow Conf. 37: 66-75.

Gray, D.M. and Others. 1978. Snow accumulation and distribution. Pp. 3-33 In Colbeck, S.C. and M. Ray, eds. U.S. Army, CRREL, Hanover, N.H.: Proc. Meeting on Modeling Snow Cover Runoff, 26-28 Sept., 1978, Hanover, N.H., iv + 432 pp.

Gray, D.M., H. Steppuhn and F.L. Abbey. 1979. Estimating the areal snow water equivalent in the Prairie environment. Pp. 302-322 In Natn. Res. Coun. Ottawa: Cold Climate Hydrology. Proc. Can. Hyd. Symp. 79, 10-11 May, 1979, Vancouver, B.C., v + 597 pp.

Jeffrey, W.W. 1970. Snow hydrology in the forest environment. Pp. 1-19 In Can. Natn. Com. Int. Hyd. Decade. Ottawa: Workshop Seminar on Snow Hydrology, 28-29 Feb., 1968., Fredericton,N.B., xiii + 82 pp.

Kuzmin, P.P. 1960. Snowcover and snow reserves. (English Transl. by Isreal Prog. Sci. Transl., Transl. 828), 140 pp.

Leaf, C.F. 1975. Watershed management in the Rocky Mountain sub-alpine zone: The status of our knowledge. U.S. Dept. Agric. For. Serv. Res. Pap. RM-137, 31 pp.

Lillesand, T.M., D.E. Meisner, A.L. Downs, and R.L. Deuell. 1982. Use of GOES and TIROS/NOAA satellite data for snow-cover mapping. Photogrametric Eng. and Remote Sensing 48: 251-259.

Lull, H.W. and F.M. Rushmore. 1960. Snow accumulation and melt under certain forest conditions in the Adirondacks. U.S. Dept. Agric. For. Serv. Stn. Pap. NE-138, 16 pp.

Mathers, T.S. 1980. The role of vegetation in the disposition of snowfall on a mixed forested watershed in the Kawartha Lakes region of east central Ontario. Pp. 36-50 In Roulet, N.T. ed. Studies in Snow and Ice, Trent University Geographical Society, Trent University, Peterborough, Ont., 192 pp.

McKay, G.A. 1970. Problems of measuring and evaluating snowcover. Pp. 49-62 In Can. Natn. Com. Int. Hyd. Decade. Ottawa: Workshop Seminar on Snow Hydrology, 28-29 Feb., 1968. Fredericton, N.B. xiii + 82 pp.

Meiman, J.R. 1970. Snow accumulation related to elevation, aspect and forest canopy. Pp. 35-47 In Can. Natn. Com. Int. Hyd. Decade. Ottawa: Proc. Workshop Seminar on Snow Hydrology, 28-29 Feb., 1968. Fredericton, N.B., xiii + 82 pp.

Packer, P.E. 1962. Elevation, aspect and cover effects on maximum snowpack water content in a western white pine forest. For. Sci. 8(3): 225-235.

Potter, J.G. 1965. Snow cover. Clim. Studies No. 3. Can. Dept. Trans. Meteor. Br., Toronto, 69 pp.

Smith, J.L. 1974. Hydrology of warm snowpacks and their effects upon water delivery-some new concepts. Pp. 76-89 In Natn. Acad. Sci. Washington, D.C.: Proc. Symp. on Advanced Concepts and Techniques in the Study and Snow and Ice Resources, 2-6 Dec., 1973, Monterey, Calif., x + 789 pp.

Soil Conservation Service. 1972. Snow survey and water supply forecasting. SCS Natn. Eng. Handbook, Section 22, Washington, D.C.: U.S. Dept. Agric. Soil Cons. Serv., 195 pp.

Steel, R.G.D. and H.J. Torrie. 1960. Principles and procedures of statistics. New York: McGraw-Hill Inc., xvi + 481 pp.

Steppuhn, H.W. and G.E. Dyck. 1974. Estimating true basin snowcover. Pp. 314-328 In Natn. Acad. Sci. Washington, D.C. Proc. Symp. on Advanced Concepts and Techniques in the Study of Snow and Ice Resources, 2-6 Dec., 1973, Monterey, Calif., x + 789 pp.

Swanson, R.H. 1970. Local snow distribution is not a function of local topography under continuous tree cover. J. Hyd. (N.Z.) 9(2): 292-298.

Swanson, R.H. and D.R. Stevenson. 1971. Managing snow accumulation and melt under leafless aspen to enhance watershed value. Proc. A. West. Snow Conf. 39: 63-69.

Timmer, V.R. and G.F. Weetman. 1969. Humus temperatures and snow cover conditions under upland black spruce in northern Quebec. Woodl. Pap., Pulp Pap. Res. Inst. Can., No. 11, February, 1969, 28 pp.

Troendle, C.A. and C.F. Leaf. 1980. Effects of timber harvest in the snow zone on volume and timing of water yield. Pp. 231-242 In Baumgartner, M., ed. Coop. Ext. Wash. State Univ.: Interior West Watershed Management Symp., 8-10 April, 1980. Spokane, Wash., 288 pp.

U.S. Army Corps of Engineers. 1956. Snow hydrology. North Pac. Div., Portland, Ore., xxv + 437 pp.

Vershinina, L.K. 1969. Assessment of the accuracy in determining water equivalent of snow cover. Pp. 100-127 In Vershinina, L.K. and A.M. Dimaksyan, eds. Determination of the Water Equivalent of Snow Cover. Trudy No. 178 (English Trans. by Israel Prog. Sci. Transl.)

Vershinina, L.K. 1972. Ratios between the water equivalents of snow in the field, forest and ravine-gully network in river basins. Sov. Hyd. 5: 421-438.

Young, G.J. 1974. A data collection and reduction system for snow accumulation studies. Pp. 304-313 In Natn. Acad. Sci. Washington, D.C. Proc. Symp. on Advanced Concepts and Techniques in the Study of Snow and Ice Resources, 2-6 Dec., 1973, Monterey, Calif., x + 789 pp.

SNOWMELT AND RUNOFF DURING RAIN-ON-SNOW IN FOREST AND ADJACENT CLEARCUT

by

P.G. Beaudry

British Columbia Forest Service
Prince Rupert Forest Region
Smithers, B.C.
Canada

D.L. Golding

Faculty of Forestry
University of British Columbia
Vancouver, B.C.
Canada

presented at

SNOW PROPERTY MEASUREMENTS WORKSHOP

Lake Louise, Alberta

1-3 April, 1985

TECHNICAL MEMORANDUM 140

Compiled By

P.R. Kry

NRCC 27594

INTRODUCTION

Abundant precipitation during late fall and winter is a predominant characteristic of the Coastal mountains of British Columbia. At high elevations snowfall is the dominant process, while at low elevations precipitation may fall almost exclusively as rain. The zone referred to as the transient snow zone, located between the high and low elevation, receives a mixture of snow and rain, with many successive snow-accumulating and melting periods throughbout the season. For southwestern British Columbia this transient snow zone extends from about 400 to 1000 meters above sea level.

The heavy winter rainfall that coincides with the presence of snow in this transient snow zone is often the source of peak flows for many coastal watersheds. The combination of large amounts of rainfall and rapid snowmelt has the potential for initiating debris torrents, floods and headwater erosion. Harr (1981) documented the potential hazards naturally occurring from this type of event and indicated that 85% of landslides studied in western Oregon were associated with snowmelt during rainfall.

Many of the present forest-harvesting activities are located in this transient snow zone. Recently the question has been raised by forestry and fisheries managers, forest companies, and the public as to how does forest harvesting affect snowmelt and subsequent runoff during rain-on-snow events. Of concern is the possibility of much higher runoff generated from large clearcut areas, compared to the uncut forest, resulting in higher peak flows.

The U.S. Army Corps of Engineers (USACE) 1956 snowmelt equations suggest that clearcut harvesting could increase runoff during rain-on-snow, largely due to the higher snowmelt rates caused by increased transfer of sensible and latent heat to the snow surface. However, some authors suggest that clearcut logging has little or no effect, or even decreases runoff (Harr *et al*. 1975, Harr and McCorrison 1979, Rothacher 1973, Anderson 1970).

This study was initiated with two main objectives:

1. To compare the energy and water balances of a melting snowpack during rain-on-snow for the forest and for a recent clearcut, and

2. To determine the applicability of the USACE snowmelt equations for coastal rain-on-snow situations in both forest and open sites.

SITE

The study site is located on the Jamieson Creek experimental watershed near Vancouver British Columbia (Figures 1 and 2). This coastal watershed extends from 300-1300 meters above sea level, has a southerly aspect and an average slope of 48%. Mean annual precipitation is 3300 mm with the wettest months being October-December. The mean annual temperature measured at the watershed outlet (305 m) is 4.9°C. The forest is composed of mature and over-mature stands of western hemlock, Douglas-fir, and red cedar. The open snowmelt plot is located in a 16-ha clearcut, harvested in 1979, with the forest edge 142 m from the plot center. It has a southwestern aspect, average slope of 29°, and elevation of 730 m. The

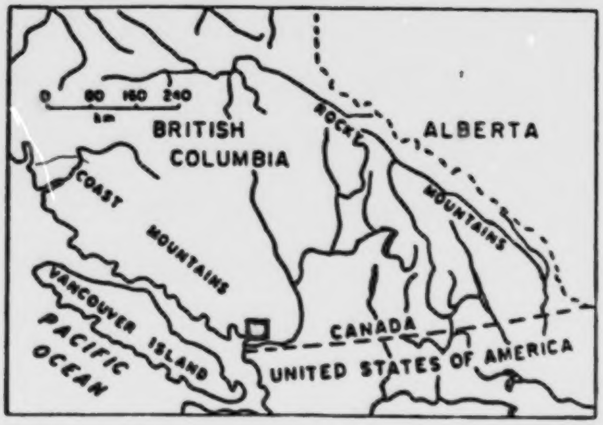
0 80 160 240
km
BRITISH COLUMBIA
ALBERTA
ROCKY MOUNTAINS
COAST MOUNTAINS
VANCOUVER ISLAND
PACIFIC OCEAN
CANADA
UNITED STATES OF AMERICA

Figure 1. Location of Study Watershed (Cheng, 1975).

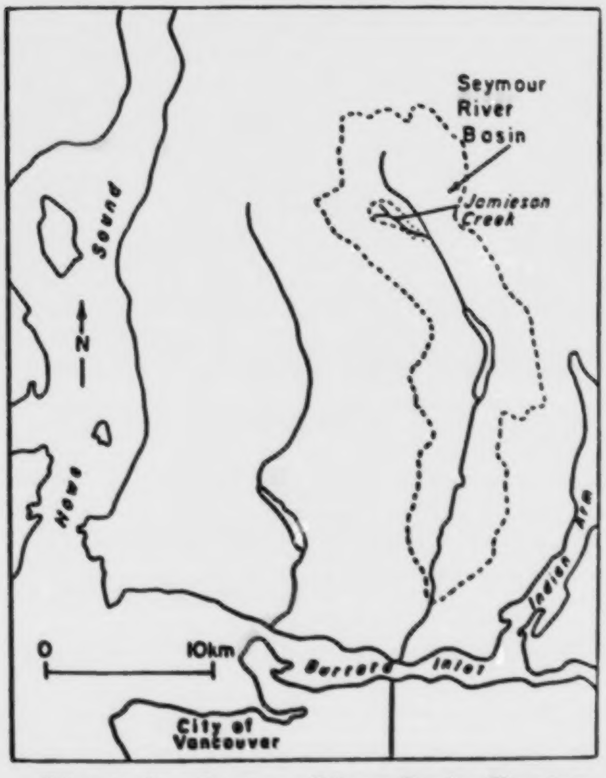
Seymour River Basin
Jamieson Creek
Howe Sound
N
0
10km
Burrard Inlet
Indian Arm
City of Vancouver

Figure 2. Seymour River Basin Showing Jamieson Creek Location (Cheng, 1975).

forest plot is at 655 m, average slope of 26°, southwestern aspect and approximately 500 m from the clearcut plot.

METHODS AND MATERIALS

Data was collected for three winters (1981-82, 82-83, 83-84). During the first winter, measurements consisted exclusively of air temperature, snowpack description and snowmelt lysimetry. Specific results were minimal, but general field observations of the processes involved during rain-on-snow were useful.

In 1982 both sites were intensively instrumented to estimate energy balances above the snowpack and to collect the data required by the USACE point snowmelt equations. This equation is expressed as follows:

$$M_{tot} = M_{rs} + M_{rl} + M_c + M_e + M_r + M_g \qquad (1)$$

where:

M_{tot} = Total snowmelt (mm/day)

M_{rs} = Melt from shortwave radiation (mm/day)

M_{rl} = Melt from longwave radiation (mm/day)

M_c = Melt from the turbulent transfer of sensible heat to the snow (mm/day)

M_e = Melt from the turbulent transfer of latent heat to the snow (mm/day)

M_r = Melt from rain heat (mm/day)

M_g = Melt from ground heat (mm/day)

The radiation melt ($M_{rs} + M_{rl}$) was measured directly with the use of Fritchen-type net radiometers, with three in the forest and one in the open, at 1.5 m above the snowpack. M_c, M_e, and M_r were evaluated with the following equations.

$$M_c = 0.957(P/P_o)(Z_a Z_b)^{-1/6}(T_a - T_b)v_b \qquad (2)$$

$$M_e = 0.2007(Z_a Z_b)^{-1/6}(e_a - e_s)v_b \qquad (3)$$

$$M_r = 0.00125{*}T_r{*}P_r \qquad (4)$$

Where P and P_o are the air pressure at the location and at sea level respectively; Z_a and Z_b are the measurement heights in cm above the snow surface, of air temperature and wind speed respectively; T_a is air temperature in °C; T_s is the snow surface temperature in °C (0°C when melting); v_b is the wind speed in m/sec; e_a is the vapour pressure in mb (6.11 mb for a melting snow surface); P_r is the daily rainfall in mm and T_r is the temperature of the rain (assumed to be air temperature) in °C. Vapour pressure of the air, e_a, was evaluated using Teten's (1930) empirical formula:

$$e' = (0.6108) \text{ antilog}_{10} (7.5{*}T_a/(T_a + 237.3)) \qquad (5)$$

and $\text{R.H.} = 100 (e_a/e')$ (6)

where e' is the saturated vapour pressure (kPa) at T_a, and R.H. is the relative humidity (%) at the study site.

A series of five Campbell Scientific model 101 thermistor probes measured temperature at 5 and 10 cm below the ground surface, at the snow-ground interface, and at two levels in the snowpack. These temperature profiles served to estimate the ground energy available for melt and the cold content of the snowpack. Wind, air temperature, and relative humidity (Campbell Scientific model 201 humidity probes) were measured at 60 cm and 150 cm above the snowpack at one-minute intervals.

M_g was not directly measured. However, ground temperature data suggests that this heat input would be relatively small because ground temperatures close to the snow remained close to 1°C. The USACE (1956) suggests that under these conditions the melt caused by ground heat can be taken as a constant of 0.5 mm/day.

In the summer of 1981 both sites were instrumented with a pair of lysimeters with total surface area of 0.5 m^2. They were buried with a lip of 3-5 cm protruding above the soil to prevent surface runoff from entering the lysimeter. Snowmelt runoff was piped to a tipping-bucket connected to an Esterline Angus 20-channel strip chart event recorder. The 1981-82 data showed little correspondence between the amount of runoff from the lysimeter and snowmelt estimated from snow surveys. The problem lay with the very small area of the lysimeters. As water flows through the snowpack it concentrates in preferential pathways (Smith 1974). If a small lysimeter is situated directly under one of the pathways the resulting runoff flowing through the lysimeter would be much greater than that calculated for the area it represents. On the other hand, melt originating on the lysimeter may be channeled off the lysimeter. Also, ice lenses may form within the pack impeding the free flow of water to the underlying lysimeter. During the summer of 1982 larger lysimeters were installed at both the forest and the open sites. These were constructed of a 22 m^2 triangular-shaped fiberglass-reinforced plastic placed directly on the ground surface with a 50-80 cm lip around the perimeter. The lip reduced the chance of melt water entering the lysimeter from outside or of water leaving the lysimeter by overtopping. The slope from the lysimeters to the instrument shelters provided a constant downward gradient to prevent water laying in the pipe and eventually freezing. Metal screening was placed on the orifice of the lysimeter to prevent blockage by litter. The screening was easily accessed and was cleaned frequently.

Instruments were connected to four Campbell Scientific CR-21 data loggers, programmed to register samples, maximums, minimums and averages every 30 minutes. Data loggers and tape recorders were housed in insulated boxes, heated with propane heat exchangers and kept dry with silica gel. Snowpack depth, density, and water equivalent (w.e.) were measured weekly on a 30-point snow survey in both the forest and open. Precipitation intensities were obtained from a recording rain gauge at the opensite.

During preliminary analysis it was observed that certain values of the net radiation exchange over the melting snowpack, measured with the net radiometer, provided some unrealistic results when compared with the literature. The net radiometers were then calibrated under controlled laboratory conditions. They performed well under high intensity radiation, but errors became quite significant under low intensity conditions. This was attributed to the construction of the radiometers, principally to their low sensitivities, and the difficulty of the CR-21 to monitor such low electrical signals. Unfortunately the radiometers were not calibrated under rain conditions during which time the field measurements seemed to be the most erroneous. These periods of high relative humidities, low clouds and rainfall over wet snow correspond to low net radiation and consequently very low signals to the CR-21. Water on the radiometer domes has an unknown effect but it would be reasonable to assume that it contributes at least partially to the erroneous results. Thus it was decided that, during precipitation events, an alternate method of estimating net radiation at the snow surface would be used. Two recent rain-on-snow studies (Harr and Berris 1983; Zuzel _et al_. 1983) used empirical equations to evaluate the net longwave radiation exchange at the snow surface and obtained good results. Several authors (USACE 1956, Gray and Male 1981) have suggested that under 100% low cloud cover the net longwave radiation exchange is simply a function of air and snow temperature and can be estimated as:

$$R_{lw}{*} = \sigma(T_a{}^4 - T_s{}^4) \qquad (7)$$

where σ is the Stephan-Boltzmann constant ($5.67*10^{-8}$ W/(m^2°K^4)) and T_a and T_s are air and snow temperatures respectively.

USACE (1956) has suggested that the net shortwave radiation exchange during rain-on-snow is relatively small. Using the plotted data presented in Gray and Male (1981) and assuming an albedo of 0.6 for wet snow several days old, a latitude of 50° north and a southwest facing slope of 25 degrees, an average 24-hour net shortwave radiation value for rain events occurring in January was estimated at 1.8 mm snowmelt per day.

The total net radiation available for snowmelt at the surface of the snowpack is the sum of the net longwave radiation plus the net shortwave radiation. During non-rain events this total net radiation was obtained directly with the net radiometers. However, the total net radiation during rain events was calculated as the results from equation (7) plus the constant value for shortwave radiation.

The R.M. Young model No. 6001 anemometers, with a threshold velocity of 0.7 m/s were mounted at 60 and 150 cm above the snowpack to estimate the wind profile above the pack. There were very few occasions when the wind within the forest exceeded the threshold velocity of the anemometers. Because calculation of the turbulent transfer of sensible and latent heat is a direct function of windspeed, the absence of measurable wind resulted in these two terms being zero in the forest. However, this assumption of negligible transfer of sensible and latent heat was not totally erroneous as Hendrie and Price (1978) demonstrated. They showed that turbulent exchanges over a melting snowpack under a leafless deciduous hardwood canopy were so damped that they could be considered quantitatively insignificant.

RESULTS AND DISCUSSION

Only results of the 1984 season are reported in this paper as preliminary results (1981-82, 1982-83) have been published in Beaudry and Golding (1983). The 1984 results are the most significant, as they represent a variety of conditions and reflect the experience gained through the first two years of the study.

Three rain-on-snow events have been chosen to illustrate differences in runoff patterns between the forest and open sites during rain-on-snow. These events seem to be typical of observations throughout the study. Each event will be subdivided to facilitate discussion of the processes involved.

For each event a description of the micro-climatic conditions that prevailed during the event will be followed by analysis of the measured and calculated runoff data. The measured runoff is what is produced from the lysimeters, while the calculated runoff is: M_{tot} + measured rainfall. For the forest site M_c and M_e were considered negligible due to the absence of measurable wind. Thus for the forest site $M_{tot} = M_{rs} + M_{rl} + M_r + M_g$. Because of the absence of an intense network of precipitation gauges at the forest site, P_r was estimated at 85% of the rainfall measured in the open site. The interception loss value of 15% is only an estimate, but is based on results reported in the literature (Zinke 1966, Patric 1966, Rutter 1963, Thom and Oliver 1977, McMinn 1960).

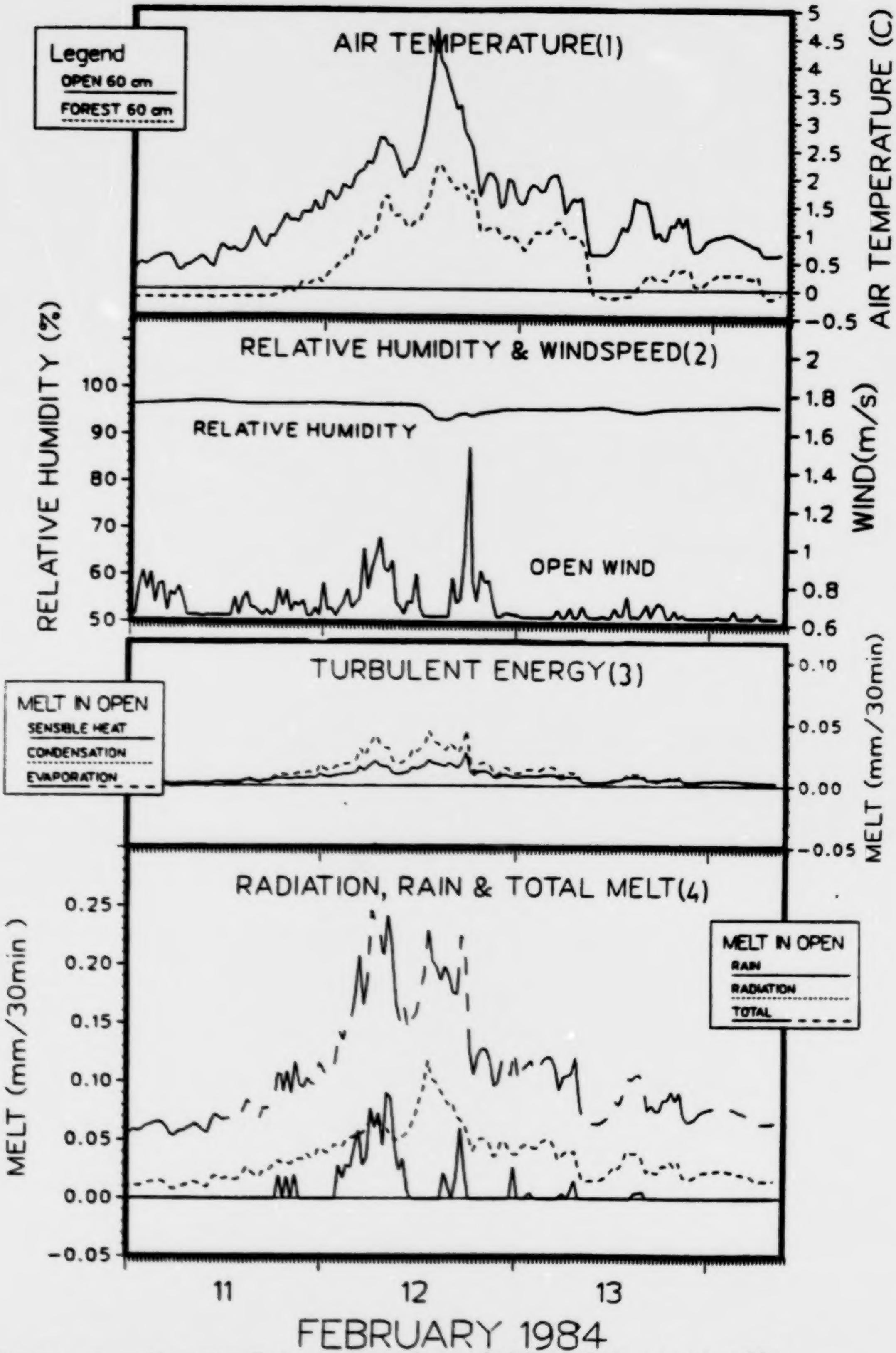

Figure 3 - Measured & computed variables, Feb. 11-14, 1984

For each event described, graphs are presented showing air temperature; relative humidity and wind speed; melt due to turbulent energy; melt due to radiation, and rain; total melt, precipitation intensity; lysimeter runoff; calculated and measured snowmelt runoff from both open and forest sites.

EVENT 1: FEBRUARY 11-14, 1984 (4 subevents)

Weather patterns at our study site, during January and February, generally bring precipitation in the form of snow followed by increases in air temperature and the snow changing to rain. This process, illustrated by this three day event, seems to be characteristic of the transient snow zone.

The five-day period, February 9-13, saw temperatures fluctuating around 1°C (Figure 3-1), resulting in a succession of rain and snow events (Figure 4-1). Although the highest runoff peak was recorded at the open site (Figure 3-2), the difference between this and the highest recorded peak in the forest is small.

There are two distinct periods when runoff from the forest is greater than that from the open (subevents a and d, Figure 4-2). The common characteristic of these is that they were immediately preceded by snowfall (Figures 4-1 and 4-2). When snowfall occurs, much of the snow gets trapped in the canopy where it is temporarily stored, or it may be melted by canopy heat. As temperatures rise and rainfall begins (e.g., evening February 11) the snow, distributed through several layers of the canopy, quickly melts and falls as canopy drip on a shallow snowpack. This results in almost instantaneous high runoff rates from the forest site. In the clearcut the process is slower because the snowpack is generally much deeper and the liquid water deficiency of the new snow (61 mm w.e. for this event) must be satisfied before percolation can begin. Also, it has often been observed that while canopy drip, and consequently runoff, are occurring in the forest, snow is accumulating in the open and there is no runoff.

Runoff rates during rain-on-snow depend on antecedent weather and snow and rainfall intensities. Peak flows may be generated from either the forest or open depending on these antecedent conditions. Five snowmelt situations have been identified from field observations (Table 1). Each of the sub-events presented in Table 2 are identified, in the last column, by one of these conditions.

Measured runoff rates are compared to the calculated rates (Figures 4-3 and 4-4). For the open site the correspondence is generally good. The time lag between measured and calculated runoff is due to the time it takes for the lysimeter to respond to the instantaneous changes of energy and water inputs at the surface. For the forest site the correspondence is generally poor during those periods when there is snow in the canopy because the USACE equations use micro-climate data obtained at the forest floor, when much of the melting, and energy exchanges, are occurring in the canopy.

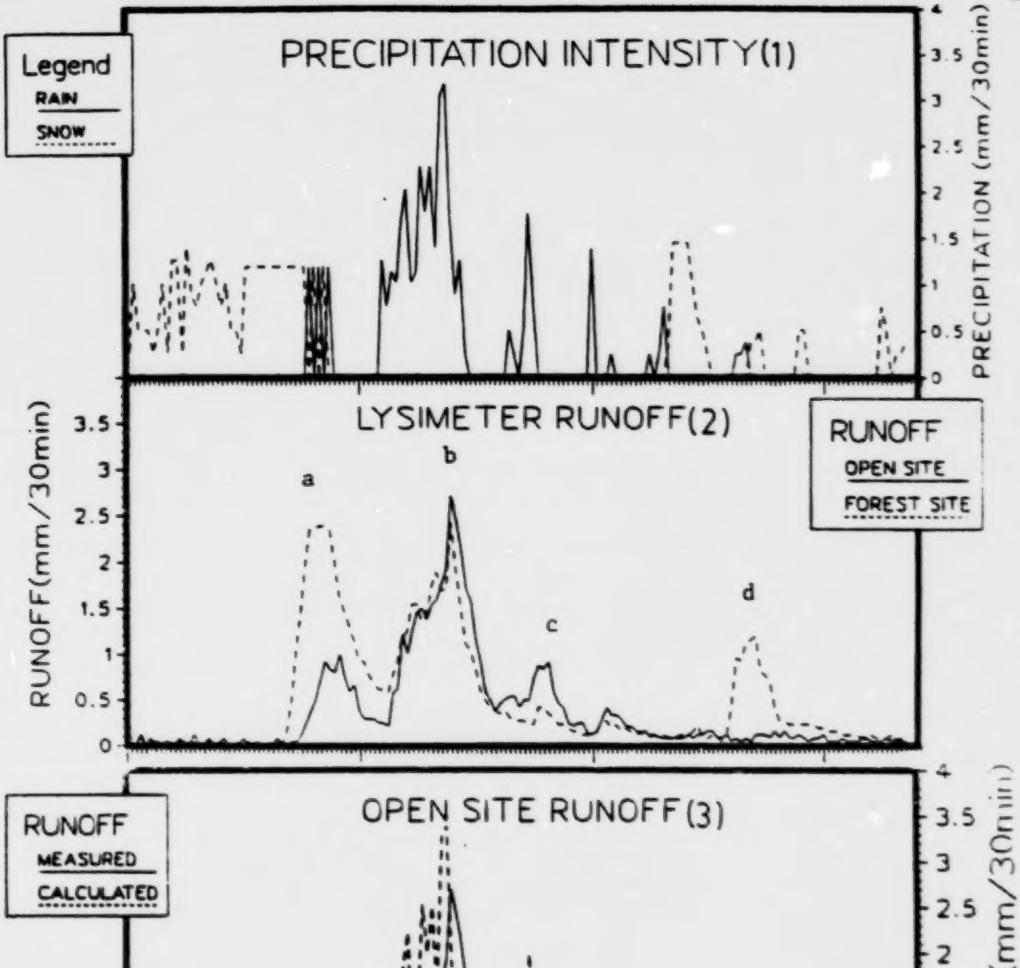

Figure 4 - Precipitation and runoff, Feb.11-14,1984

Table 1. FIELD OBSERVATIONS.

Condition	Open	Forest
1) Snowing T° = -.5 to 1.5°C very wet snow	- Accumulation of snow - No runoff	- Snow trapped in canopy, falls through as rain - Some runoff
2) Light rain when snow in canopy T°≥1.5°C	- Rain primes snowpack - Runoff minimal	- Rain on wet warm snowpack - Drip from canopy - Runoff greater in forest
3) Light rain no snow in canopy T°≥1.5°C	- Rain primes pack or gets stored as free water - Depends on snow quality	- Rain caught in canopy; lost by evaporation and drip
4) Heavy constant rain no snow in canopy T°≥1.5°C	- Deeper snow more stored water - No interception - Air T°≥ forest - Runoff is important	- Absence of turbulent energy - Air T°≤open - W.E.≤ open - Canopy interception
5) Snowing T°≤.5°C	- Snowfall is stored water - Colder snow, greater energy deficit	- Snow stored in trees, will leave as: a) evaporation b) canopy drip c) fall in heavy balls

Table 2. SUMMARY OF THE 1984 RESULTS.

Event	Duration (hours)	Peak Runoff Intensity (mm/30 min)		Total Runoff (mm)		Condition[1]
		Open Site	Forest Site	Open Site	Forest Site	
1a	8.5	1.00	2.70	7.5	24.5	(2)
1b	11.5	2.90	2.60	31.0	29.0	(3)
1c	14.0	0.90	0.40	11.4	5.0	(3)
1d	12.0	0.10	1.20	2.4	11.1	(2)
2	60.0	3.38	2.80	136.8	94.0	(4)
3a	8.5	0.00	2.61	0.0	20.0	(2)
3b	18.0	1.15	0.85	11.6	16.3	(3)
3c	12.0	0.10	1.90	2.3	19.8	(2)
3d	18.0	1.90	1.15	26.3	16.2	(4)
3e	8.5	2.70	1.20	26.7	12.5	(4)
3f	22.0	2.20	1.30	33.4	18.5	(4)

[1] The numbers in this column correspond to one of the five conditions described in Table 1.

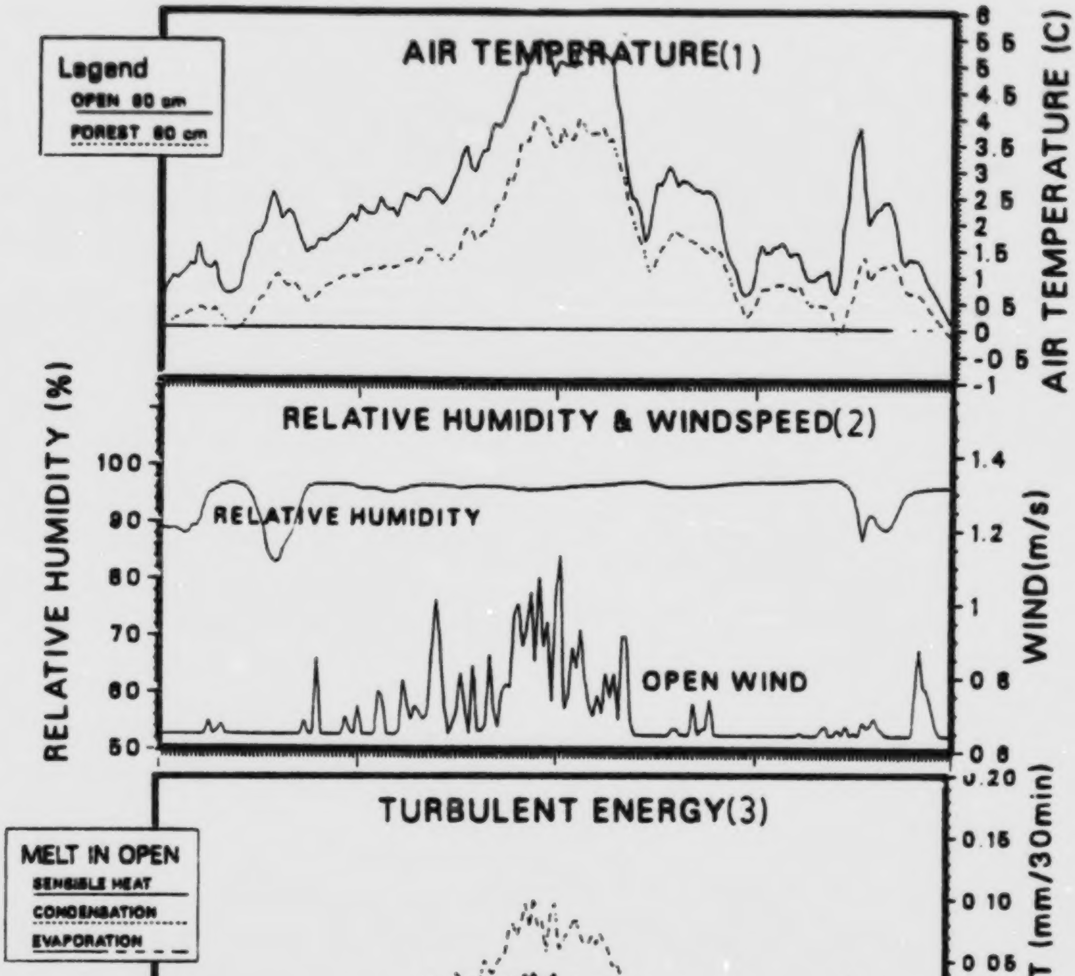

Figure 5 - Measured & computed variables, Feb. 18-22, 1984

EVENT 2: FEBRUARY 18-21, 1984

This is an excellent example of condition 4 (Table 1). The climatic conditions, and thus the lysimeter runoff pattern, differ from the previous event, but still represent a frequently occurring situation.

Prior to this rain-on-snow event the forest canopy was dry and devoid of snow, with canopy storage capacity near maximum, contrary to the previous described event. Air temperature rose to an average daytime high of 5°C on February 19 and 20, with mean windspeeds remaining at about 1 m/sec (Figure 5-2). Precipitation intensities peaked at 2.8 mm/30 min, with a total rainfall for the two days of 102 mm (Figure 6-1).

Substantial energy was provided for snowmelt by these atmospheric conditions. Calculated M_{tot} for the open site peaked at 0.51 mm/30 min, which is 15% of the measured peak runoff (3.38 mm/30 min, Table 2). Total runoff for this 60-h event was 136.8 mm for the open site compared to 94 mm for the forest site (Table 2). These results, i.e. greater total and peak runoff from the open site, are typical of rain-on-snow events when the forest canopy is devoid of snow. The factors that account for this are:

1) Higher snowmelt rates due to more available energy (i.e. more convection, condensation, radiation, and rain melt) in the open than on the ground under the forest canopy;
2) No interception loss in the open, thus more rainfall to the snowpack there.

For both the open and forest sites the calculated runoff corresponds extremely well to the measured runoff (Figures 6-3 and 6-4), with the expected time lag between the start of rainfall and measured runoff. This time lag is about four hours for the open site and decreases to 1.5 h as the snowpack satisfies its liquid water deficiency. At the forest site, the time lag is about 6-7 h between the start of the rain and a significant increase in runoff rates (Figure 6-4). This suggests that the storage capacity of the forest canopy was satisfied during this period.

This event demonstrates that the USACE snowmelt equations provide adequate results for both forest and open sites during rain-on-snow events with no snow in the forest canopy.

EVENT 3: JANUARY 22-25, 1984 (6 sub-events)

This four-day event combines several different situations in a succession of six sub-events of 8-22 h duration (Figure 8-2, Table 2). Among these sub-events two show forest runoff far exceeding open runoff. These two events (Figure 8-2, a and b) occurred immediately after snowfall and were accompanied by a rapid rise in air temperature, causing canopy drip (Figures 8-4 and 7-1). After the second forest peak there was a sequence of three short duration events, all of which had greater peak runoff from the open site (Figure 8-2, d, e, f). During this four-day event the highest runoff peaks in the open are not much greater than those from the forest. Of importance is the distribution of the peaks; where the highs from the forest are desynchronized in relation to the highs from the open (Figure 8-2).

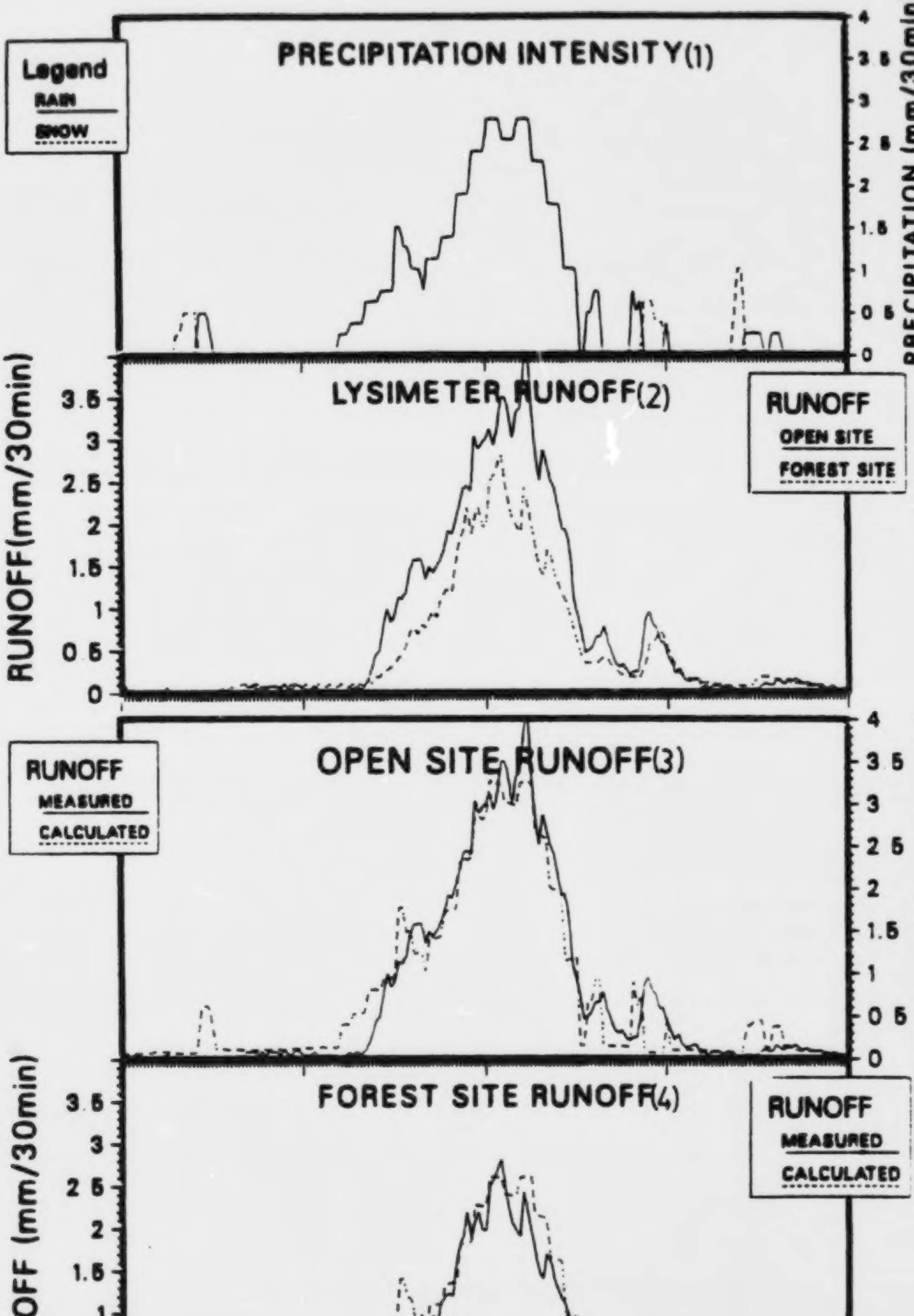

Figure 6 - Precipitation and runoff, Feb.18-22,1984

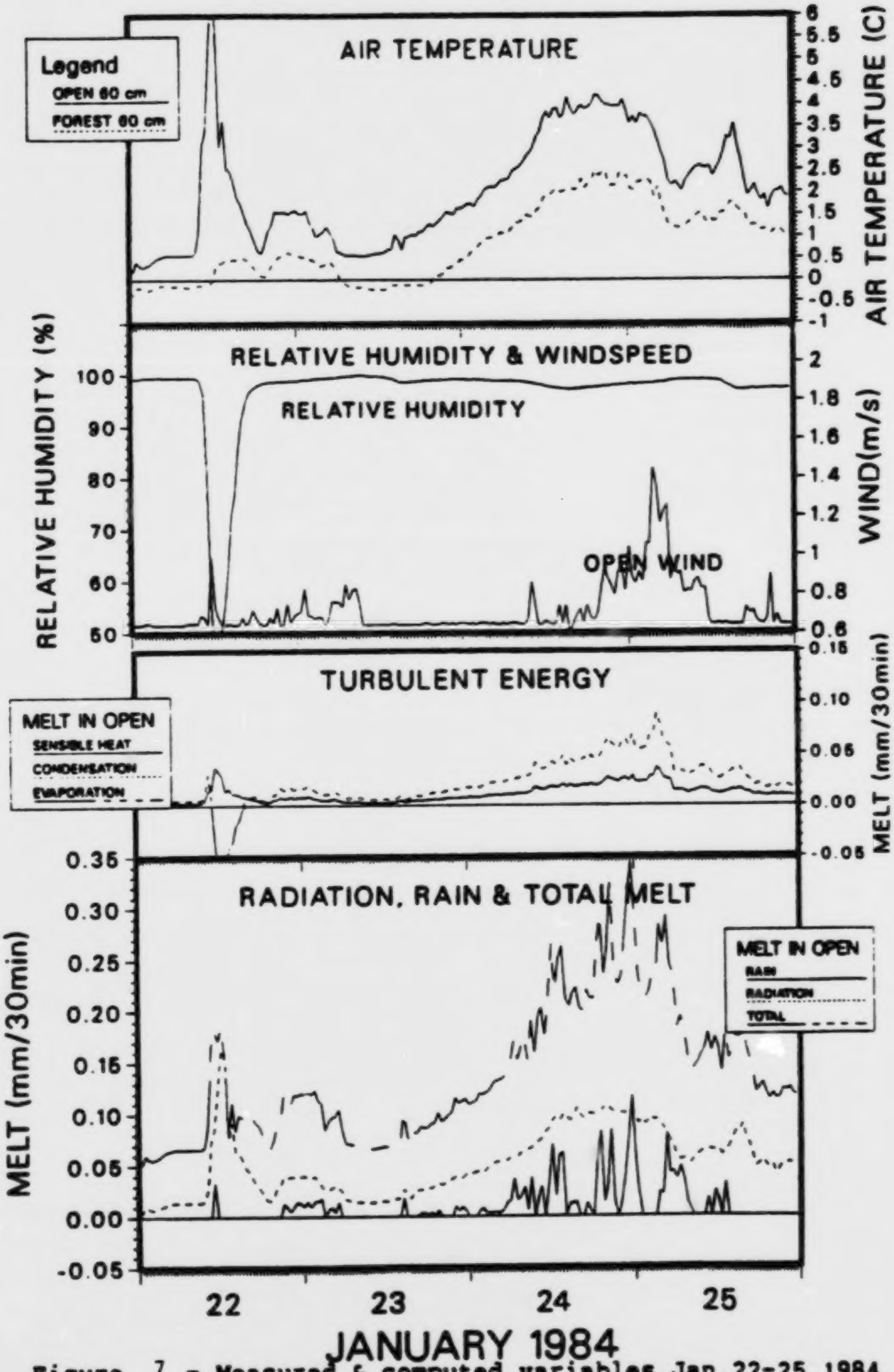

Figure 7 - Measured & computed variables,Jan.22-25,1984

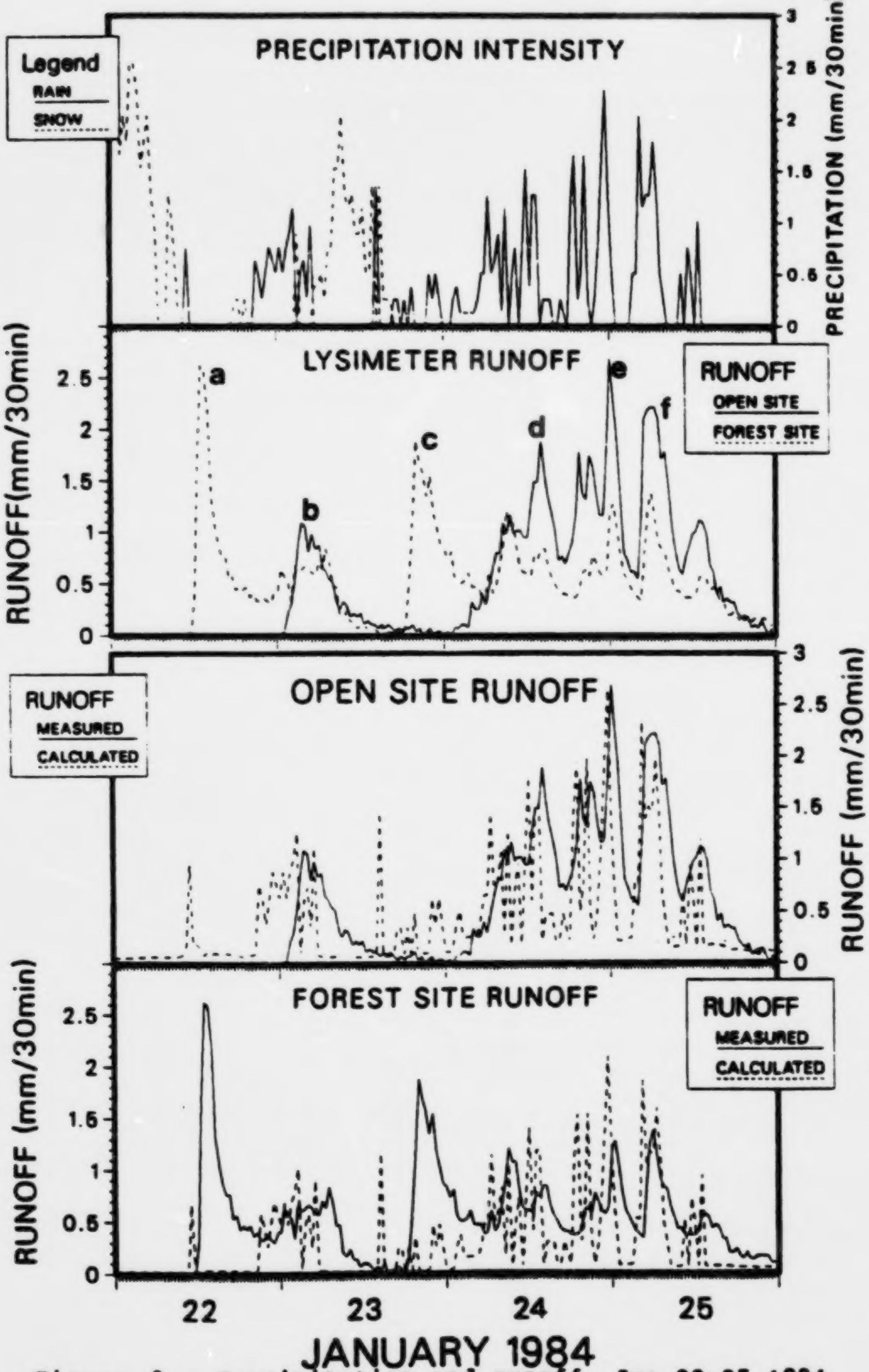

Figure 8 - Precipitation and runoff, Jan.22-25,1984

Again, in the open site calculated runoff corresponds well to measured runoff. The initial time lag is important (Figure 8-3) because of the time required to satisfy the liquid water requirements of the 58 mm w.e. of freshly fallen snow (January 21 and 22). The USACE snowmelt equations do a poor job of predicting measured runoff for the forest site, especially during canopy drip (Figure 8-4, a and c).

SUMMARY AND CONCLUSIONS

The results of this study have provided us with much useful information on the processes that occur in a forested and harvested environment, during rain-on-snow. The precipitation, snowmelt and runoff intensities are greatly influenced by the presence of the forest canopy, thus its removal (forest harvesting) will have definite effects on these. However, these effects are not necessarily negative. We have shown that peak runoff intensities may be generated from either the forested or open sites, depending on climatic conditions during and prior to the rain-on-snow event.

Observations of several storms at our study site suggest that precipitation often begins in the form of snow, filling the interception capacity of the forest canopy, followed by rising air temperatures with snow changing to rain. During the first hours of this rainfall, the liquid water requirements of the freshly fallen snow are being satisfied at the open site, while massive canopy drip occurs in the forest. This results in intense peak runoff rates in the forest, while very little runoff occurs from the open. As rainfall continues, the forest runoff decreases due to the absence of snow in the canopy and open runoff increases and surpasses the forest runoff. Thus, we conclude that the single most important factor that explains the differences in runoff, between forest and open sites, is the interception and the redistribution of the precipitation by the forest canopy.

The results of the 1983 and 1984 winters have shown that the measured runoff in the open agrees well with the calculated runoff using the USACE (1956) snowmelt equations. However, because of the phenomenon of canopy drip, and the difficulty in quantifying interception losses, it is difficult to predict runoff in the forest. The snowmelt equations generally performed well when no snow was in the canopy. However, during canopy drip, these equations performed poorly because climate measurements were made near the forest floor, while the important energy exchanges were occurring in the canopy.

These results seem to offer some important forest management possibilities. We have shown that rain-on-snow generated runoff from a clearcut may peak at a different time than that of an adjacent forest. It would thus seem possible to set out harvesting patterns that would desynchronize runoff peaks, resulting in lower peak streamflows. Thus, with proper planning and management the presence of clearcut "patches" in a watershed could be beneficial in the regulation of rain-on-snow generated flows.

REFERENCES

Anderson, H.W. 1970. Forest and meteorological influences on snow and snowmelt and their management. In Proc. FAO/USSR International Symposium on Forest Influences and Watershed Management, Moscow, USSR. pp.41-54.

Beaudry, P.G. 1984. Effects of forest harvesting on snowmelt during rainfall in Coastal British Columbia, Unpublished M.F. thesis, University of British Columbia. 185pp.

Beaudry, P.G. and D.L. Golding. 1983. Snowmelt during rain-on-snow in coastal British Columbia in Proc. 51st Western Snow Conference, Vancouver, Washington. pp.55-66.

Cheng, J.D. 1975. A study of streamflow hydrology of a small forested watershed in the Coast Mountains of southwestern British Columbia. Unpublished Ph.D. thesis, Faculty of Forestry, University of British Columbia. 157pp.

Gray, D.M. and D.H. Male. 1981. Handbook of Snow. Pergamon Press. 776pp.

Harr, R.D. 1981. Some characteristics and consequences of snowmelt during rainfall in Western Oregon. J. Hydrology 53:277-304.

Harr, R.D. and S.N. Berris. 1983. Snow accumulation and subsequent melt during rainfall in forested and clearcut plots in Western Oregon. Proc. 51st Ann. West. Snow Conf., Vancouver, Wash. p.38-45.

Harr, R.D., R.L. Fredriksen and J. Rothacher. 1975. Changes in stream flow following timber harvest in South Western Oregon. USDA Forest Service, Research Paper PNW-249, 22pp.

Harr, D.R. and F.M. McCorison. 1979. Initial effects of clearcut logging on size and timing of peak flows in a small watershed in Western Oregon. Water Resources Research 15(1):90-94.

Hendrie, L.K. and A.G. Price. 1978. Energy balance and snowmelt in a deciduous forest. In Modeling Snow Cover Runoff, U.S. Army Cold Regions Research Engineering Lab, Hanover, New Hampshire, U.S.A. p.211-221.

McMinn, R.G. 1960. Water relations and forest distribution in the Douglas-fir region of Vancouver Island. Div. Forest Biol., Dept., Agr. Can. Pub. #1091.

Patric, J.H. 1966. Rainfall interception by mature coniferous forests of southeast Alaska. J. Soil and Water Conserv. 21(6):229-231.

Rothacher, J. 1973. Does harvest in the west slope Douglas-fir increase peak flows in small forest streams? USDA, Pacific Northwest Forest Range Experimental Station, Forest Service Research Paper PNW-163, 13pp.

Rutter, A.J. 1963. Studies in the water relations of Pinus Sylvestris in plantation. J. Ecol. 51:191-203.

Smith, J.L. 1974. Hydrology of warm snowpacks and their effects upon water delivery - some new concepts. In Advanced Concepts and Techniques in the Study of Snow and Ice Resources. National Academy of Sciences, Washington, D.C. p.76-85.

Tetens, O. 1930. Mber einige meteorologisch Bergriffe. Z. Geophy. 6:297-309.

Thom, A.S. and H.R. Oliver. 1977. On Penman's equation for estimating regional evaporation. Quart. J. Roy. Met. Soc. 103:345-357.

Toews, D.A. and D. Wilford. 1978. Watershed management considerations for operational planning on T.F.L. #39 (Blk.64). Graham Island. Fisheries and Marine Service Manuscript report No. 1473. Fisheries and Environment Canada, 32pp.

USACE. 1956. Snow Hydrology. U.S. Army Corps of Engineers, Portland, Oregon, 437pp.

Zinke, P.J. 1966. Forest interception studies in the United States. In Forest Hydrology (W.E. Sopper and H.W. Lull, eds) p.137-161. Pergamon, Oxford.

Zuzel, J.F., R.N. Greenwalt and R.R. Almaras. 1983. Rain-on-snow: transient snowpacks with frozen soils. Proc. 51st Ann. West. Snow Conf., Vancouver, Wash. p.67-75.

OBSERVATIONS ON FLOATING SNOWPACKS: LAKES, RIVERS AND THE SEA

by

P. Adams

Watershed Ecosystems
Trent University
Peterborough, Ontario
Canada

T. Prowse

Cold Regions Section, National Hydrology
Research Institute, Environment Canada
Ottawa, Ontario
Canada

H. Granberg
Department of Geography
McGill University
Montreal, Quebec
Canada

presented at

SNOW PROPERTY MEASUREMENTS WORKSHOP

Lake Louise, Alberta

1-3 April, 1985

TECHNICAL MEMORANDUM 140

Compiled By

P.R. Kry

NRCC 27594

OBSERVATIONS ON FLOATING SNOWPACKS, LAKES, RIVERS AND THE SEA

by

Peter Adams, Watershed Ecosystems, Trent University

Terry Prowse, Cold Regions Section, National Hydrology
Research Institute, Environment Canada, Ottawa

Hardy Granberg, Department of Geography,
McGill University.

Introduction

A remarkable proportion of the total global snowpack which exists at any particular time is afloat. Canada, with its huge expanses of seasonally and perennially ice-covered sea, and its thousands of seasonally ice-covered lakes and rivers, including its share of the Great Lakes, is particularly well endowed with floating snowpack. Indeed, in Canada, at certain times of the year, it is not unusual for more than 50 per cent of the snowpack of large 'land' areas (eg. the Mackenzie Delta, many parts of the Shield) to be on water. Percentages such as these are low in that they do not include the wetland case but rather focus on 'open' water.

And yet, the term 'snowpack' conjures in most minds a land or glacier-based phenomenon. Snow courses, the principal organizational devices for monitoring snowpack, are, with rare exceptions, land-based. Aerial snow survey techniques, such as gamma ray spectrometry, are used almost exclusively for land snowcovers. It is rare, in the literature, to find a discussion of snow stratigraphy which deals with something other than a land - or glacier-based profile.

This is a remarkable state of affairs when it can be argued that the floating snowpacks are of disproportionate importance and interest from various points of view. Water bodies, including the sea, are a focus for Man and animals year-round. In winter they are major highways which are sought out by small and large animals and by humans. Given a bearing thickness of ice (sensu-stricto), it is the condition of the snowpack upon it which generally determines travel conditions. The snowpack which develops on water represents the atmospheric inputs to the waterbody of a more or less extensive period. At ice break-up, these inputs, including both nutrients and pollutants, unlike the land-based contributions, pass rapidly, directly and completely into the water body. This same snowcover plays important roles in the winter and spring hydrology of the water body including roles in the evolution of the 'ice' sheet upon which it is located. Even before melt, the snowpack on a water body affects the biology of the underlying water, particularly through its control of the amount and type of light available for photosynthesis under the cover but also through its effects on other aspects of the water body's energy balance.

The albedo and other properties of the snow cover of oceans and seas are now known to be important factors in the global energy balance and key features of the surface-atmosphere linkages which control circulation of the atmosphere and the oceans. It should be borne in mind that at the global scale, floating snowpacks cover a greater area than glacier snowpacks which cover a greater area than land snowpacks. The cover of the seas and oceans is largely monitored by remote sensing techniques which are focussed on the sea 'ice' rather than the sea 'snow' despite the fact that the amount and type of snow is often a critical complicating factor for the remote sensing technique as well as being a key facet of the floating 'ice' system which is being studied.

One of the problems here has been that the study of the winter cover of water bodies has deliberately focussed on the 'ice' sheet. At sea, for example, the focus has been on the implications of the cover for ships or for aircraft landings. Similarly on lakes and rivers, the measuring programs have been designed to assess the bearing capacity of the ice or to measure flow, or other water column features, beneath the ice sheet. As a result, snow data (usually snow depth only) have been gathered only as an extra. Until relatively recently, most winter limnological studies tended to ignore the winter cover more or less entirely. The exceptional studies tended to gather snow depth at a single site.

Thus those working on land tend to ignore the floating snowpack, despite its potential importance for their work. Those working on the water bodies also tend to ignore the snow component of the winter cover, focussing their attention on the ice beneath the snow or on the unfrozen water beneath that ice. This is unfortunate as, in most situations, it is particularly difficult to generalize from land sites (where snowpack information is available) even to floating snowpack situations which are nearby.

The purpose of this paper is to detail the special character of floating snowpacks and to elaborate, in a selected number of examples, on their significance. Examples have been chosen, from our experience and the literature, which demonstrate the broad range of implications associated with floating snowpacks and which will best stimulate thought about additional situations. The cases considered are lake snowpacks, river snowpacks and, to a lesser extent, sea snowpacks.

The nature of floating snowpacks

Land snowcover often begins to accumulate before local rivers and lakes become ice covered. Thus early winter snow may fall into open water and be lost to the waterborne pack. In the case shown in Figure 1, for example, the river snowpack lacks some sixteen per cent of the possible inputs for this reason. In Figure 2, on the other hand, this effect is negligible. In some situations, this loss might be considered as being compensated for by the persistence of a waterborne pack in the spring, after the snow on land has gone. Snow falling directly into open water may be important through the processes of nucleation and agglomeration in the formation of the floating ice sheet.

The snow which does fall on a water body after an ice sheet has formed is particularly prone to redistribution by wind, as the ice provides a surface which is often extremely smooth and flat in comparison to other natural surfaces. This redistribution results in a general compaction and some deflation (see Kuusisto 1984) of the surface snowcover. In some situations, snow blown from the ice cover is deposited in adjacent open water. The loss of windblown snow to leads in sea ice is a notable example of this.

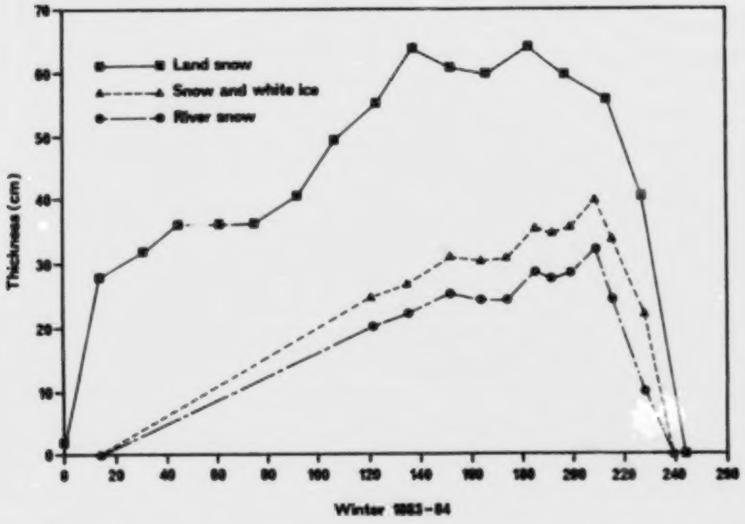

Figure 1 Development of snowcover on land and on river ice within the Mackenzie River Delta, NWT. Values for river snow represent the mean of eighteen point measurements made at six different channels in an east-west profile across the delta. The land measurements are from standard snow course measurements near the Inuvik airport. "Snow and white ice" represents the combined depths of these two layers.

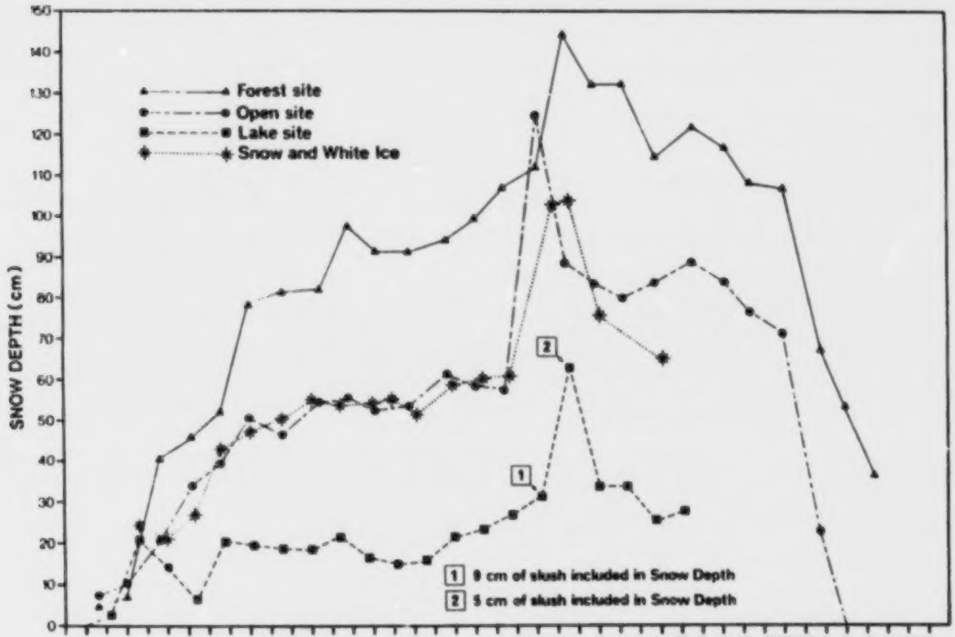

Figure 2 Development of snowcover on Knob Lake, Quebec (mean of 3 sites) and at two points on the McGill snowcourse adjacent to the lake. The lake sites 'represent' more than 20% of the landscape. In this situation, the difference between snow depth at the open land site and that on the lake is roughly equal to the thickness of white ice (see "snow and white ice" plot). The official measuring sites on this lake are treated in a zone which, for the lake, is a relatively deep snow zone (see Adams, 1984, Fig. 1.)

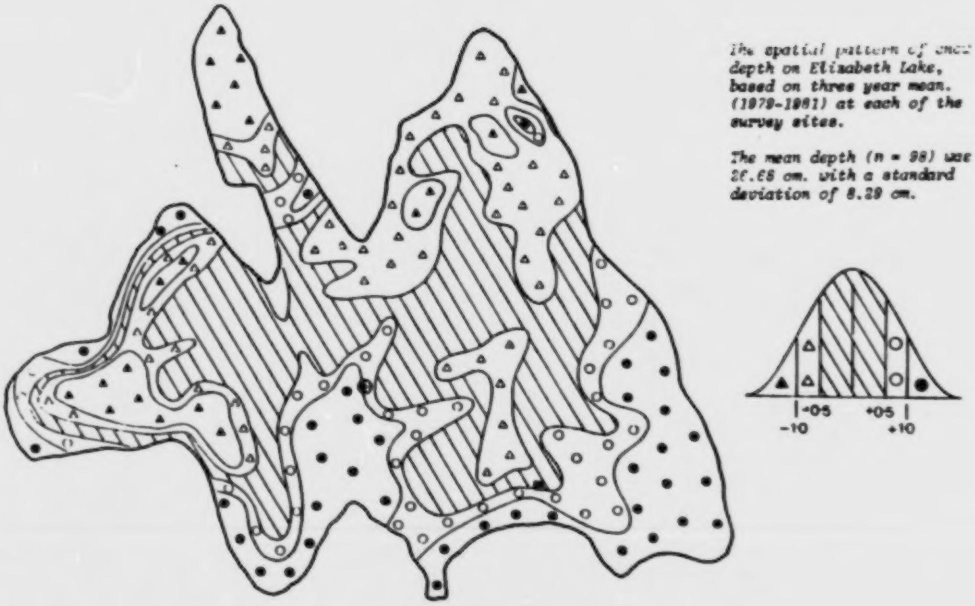

The spatial pattern of snow depth on Elizabeth Lake, based on three year mean. (1979-1981) at each of the survey sites.

The mean depth (n = 98) was 26.65 cm. with a standard deviation of 8.29 cm.

Figure 3a The spatial variation of late February snow depth on Elizabeth Lake, Labrador, expressed as standard deviations from a three-year mean (n= ca. 100), see Adams and Roulet 1984.

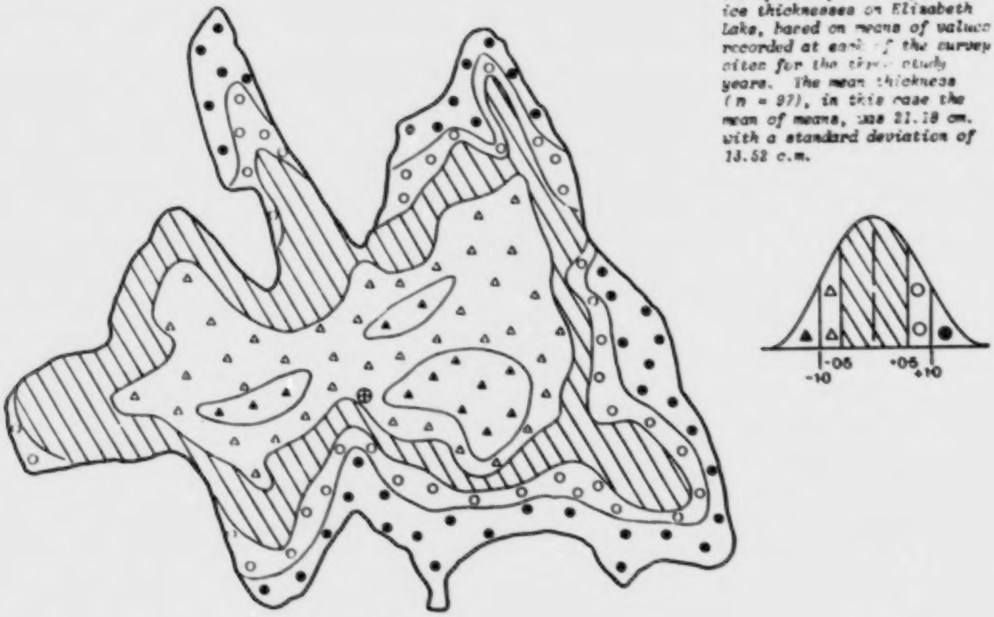

The spatial pattern of white ice thicknesses on Elizabeth Lake, based on means of values recorded at each of the survey sites for the three study years. The mean thickness (n = 97), in this case the mean of means, was 21.18 cm. with a standard deviation of 13.52 c.m.

Figure 3b The spatial variation of late February white ice thickness on Elizabeth Lake, Labrador expressed as in Figure 3a. It can be argued that the late winter pattern of white ice is a good indication of the winter-long tendency for snow to accumulate in certain patterns.

One result of the redistribution of snow on the ice surface is the marked spatial patterns which develop throughout the entire snow and ice cover. As found on lakes, which is the best documented case e.g. Adams and Roulet 1980, 1984; Adams and Prowse, 1981; Prowse, 1978, snow is deep at lee and downwind locations, and is shallow or non existent, in exposed and upwind locations. Equivalent patterns have been demonstrated in the spatial variability of water equivalence and density of lake snowpacks (Adams, 1984). The nature of these patterns naturally varies with the size, shape, orientation and shoreline character of the lake but in general there is a concentration of snow in relatively narrow marginal zones at the expense of relatively large, exposed, offshore areas. This effect is apparent from Figure 3a,b, (see also Kuusisto, 1984, Figs. 118, 119).

In the case of narrower or smaller water bodies (e.g. Fig.4 a,b.), the marginal zones become relatively more important. In deeply incised rivers, the bank effect can be conceived as dominating the distribution completely as the channel, or even the valley, becomes a snowtrap, gaining snow from, rather than losing snow to, the surrounding land area.

In the case of young sea ice, the formation of frost or salt flowers (Fig.4c) and the upmigration of brine greatly affect the distribution of snow (Crocker, 1984a). The flowers are "a form of surface hoar or

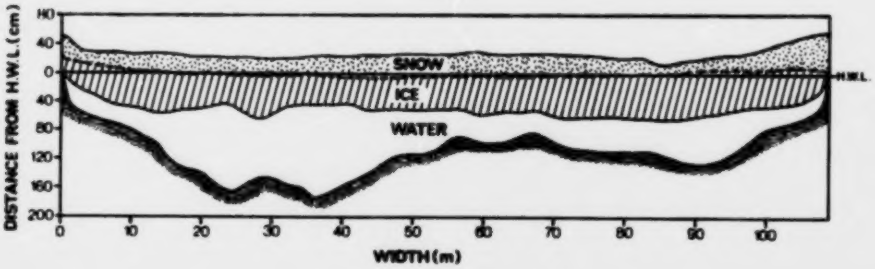

Figure 4a Transect of snow and ice on a Finnish River (12 December 1973) after Kuusisto (1984), Figure 122. Note marginal drifts and positive hydrostatic water levels at the sides.

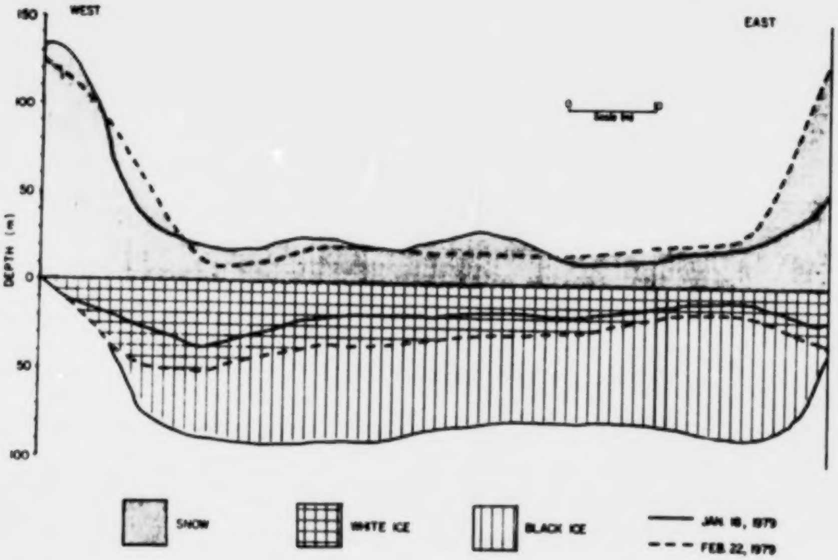

Figure 4b Transect of a narrow bay on Elizabeth Lake, Labrador. (see Adams and Roulet 1980).

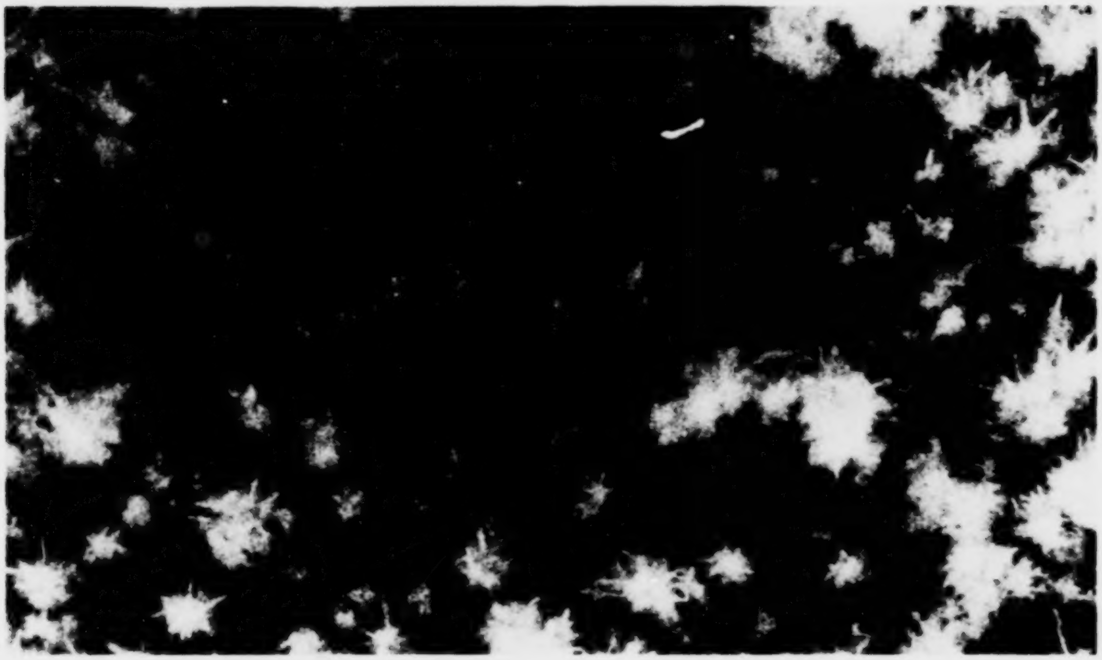

Figure 4c Close-up of "frost flowers" on young sea ice, November 1982, Resolute Passage, NWT (from Crocker, 1984a).

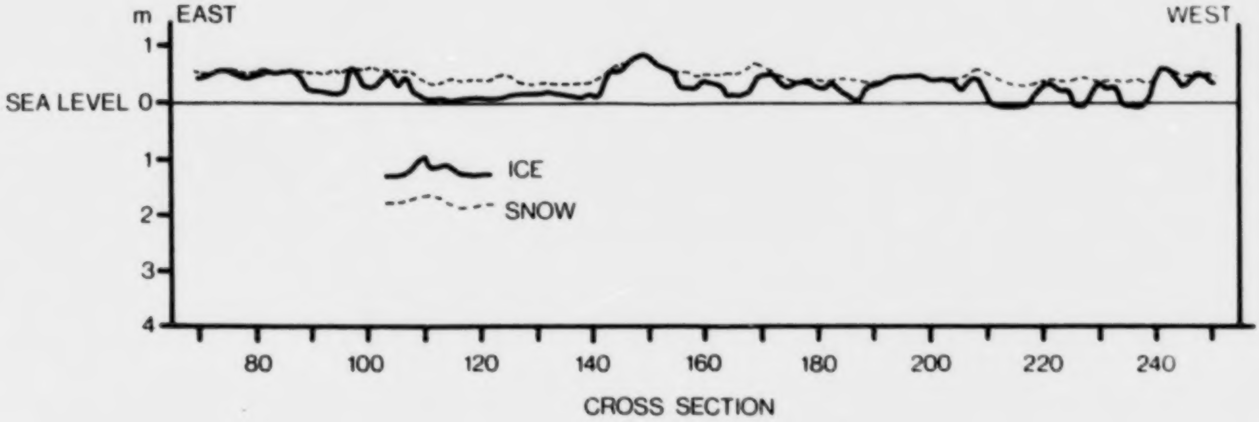

Figure 4d Profile of sea ice topography and snow distribution (after Hibler et al. 1972).

rime" which may form a layer of "snow" which is centimetres thick before real snow begins to accumulate. When snowfall does occur, the increase in aerodynamic roughness which the flowers represent produces a thin snowcover over huge areas which would otherwise be effectively snow-free in such a windy environment. The surface layer of slushy brine, characteristic of young sea ice, has a similar effect. Accumulation of a thin layer of snow has the effect of decreasing surface roughness again! At later stages of sea ice development, when ridges and hummocks are common, snow has a similar effect on a macro scale (Fig.4d), as it often does for irregular terrain on land. Reductions in the surface roughness of sea ice are especially important because it is the wind which is usually the main driving force in sea ice drift.

Another factor affecting the development of pronounced spatial patterns in waterborne snowpacks is the occurrence of slush. Slush does occur on land and on glaciers but it is less commonly an important annual feature of snowpack evolution in those situations. On waterborne ice sheets, snowpacks may be slushed in various ways. Water may rise into the pack from below (see Figure 5); in the sea ice case it may involve tidal or other pumping; rain-on-snow events (on the impermeable ice substrate) may slush the entire snowcover or melt or ground-water may flow onto the

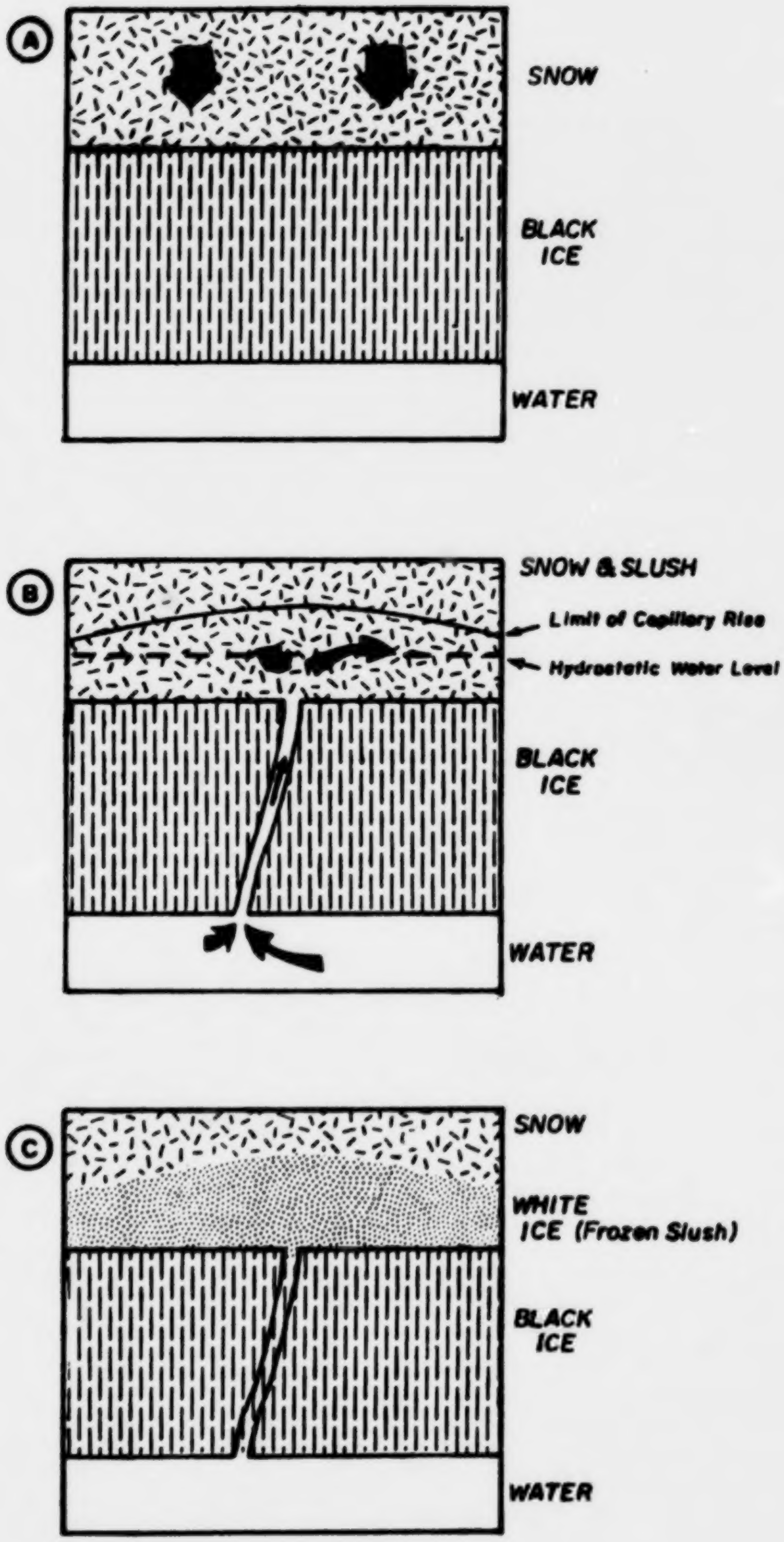
A
SNOW
BLACK ICE
WATER
B
SNOW & SLUSH
Limit of Capillary Rise
Hydrostatic Water Level
BLACK ICE
WATER
C
SNOW
WHITE ICE (Frozen Slush)
BLACK ICE
WATER

Figure 5 The process of white ice formation when slushing is from below. This mode of formation has particular implications for the evolution of snowpack on the lake. Among other things, it produces distinctive chemical profiles in the cover (see Adams and Lasenby 1985).

floating ice-sheet from adjacent land. The case of water flowing onto river ice sheets to produce icings (which may encompass adjacent land snowpacks, e.g. Grey and MacKay, 1979), is one of these slushing mechanisms. Slush so formed, upon refreezing, becomes the snow ice or white ice which is a prominent feature of ice sheets in various parts of Canada. Where the slushing is the result of water rising from below as in Fig.5, slushing and refreezing may be a periodic feature of the evolution of waterborne packs, occurring whenever cracking occurs while the ice surface is depressed below the hydrostatic water level by its burden of snow. In this case and in others, slush develops in definite spatial patterns (most slush where the ice sheet is most depressed).

The refreezing of slush results in the incorporation of snowpack into the floating 'ice' sheet, and in this sense it represents a loss of snow to the pack. It has, for example, been suggested that the pattern of white ice on lakes which are prone to the type of slushing illustrated in Fig. 5 is, towards the end of the winter, the best indication of the winter-long tendency of snow to accumulate in certain patterns. It is not uncommon, in the snowier parts of Canada, for most of a lake ice sheet to be white ice and for that ice to contain most of the winter's snow receipts.

In the case of all water bodies, but especially rivers, appreciable amounts of snow can be incorporated into the ice sheet during its initial period of formation (Jones, 1969; Michel 1970). This is but one example of the great potential for slush formation on rivers. The relatively greater influence of marginal drifting, the potential for ice cracking in the flowing water situation, the potential for flooding as a result of fluctuation of river levels (including those fluctuations which occur as a result of ice formation and jamming) all combine to increase the scope for conversion of snow to white ice in the river case. This is especially true on regulated rivers where rapid increases in stage due to releases from upstream reservoirs and powerplants are common. Kuusisto (1984) reports that the thickness of white ice on a sample of regulated rivers in Finland is approximately 15 per cent greater than that for unregulated rivers.

The slushing of surface snowcover on some rivers, especially in arctic and subarctic regions, often results from the formation of surface ice accumulations referred to above as icings, also known as aufeis. Icings form from the seepage of water onto the surface ice cover. Seepage occurs where the flow beneath the intact ice cover encounters some form of obstruction or resistance, such as that created by a thickening ice cover or by the accumulation of frazil and anchor ice. At these points, the river velocity decreases, the stage rises and a pressure head develops forcing water up through cracks and holes into the ice cover, often resulting in a complete slushing of the surface snow cover. Depending on the flow rate and temperature conditions, the exposed water and snow mixture will refreeze as a large ice mound or hummock near the point of seepage, or as a large sheet of ice, spreading some distance downstream. Where the process continues throughout the winter, icings can grow to be two to three times the maximum thickness of thermal ice covers formed on nearby lakes. Icings are most common on shallow, braided streams with poorly defined surrounding flood plain and incorporate much of the land snowcover in an 'extended' river ice cover.

We are not aware of discussions of slushing of the types discussed above for sea ice although there is a small literature on snowmelt and slush as a part of the annual mass balance of arctic pack. However, liquid brine is a normal feature of snowpack on young sea ice (Crocker, 1984a, and references).

The greater importance of the mechanical alteration of crystals by wind movement is one example of differences in stratigraphic evolution between waterborne snowpacks and those on adjacent land. The compaction (lower depths, higher thermal conductivity) in the waterborne case produces relatively steeper temperature gradients within the pack which are often enhanced by the presence of the waterbody as a steady heat source, beneath the snow. Steeper temperature gradients within the snowpack favour temperature gradient metamorphism thus promoting the development of constructive crystal forms, culminating in the production of depth hoar (see Adams and Prowse, 1978). It should be noted that, by keeping the waterborne packs relatively shallow, slushing has a similar effect. It is interesting that some of these processes affecting the evolution of waterborne packs appear to be self-cancelling. For example, redistribution by wind results in compaction and an increase in density to levels appreciably higher than those on 'equivalent' land areas, (Fig.6; as demonstrated from several years of records in Finland by Kuusisto 1984). However, periodic slushing from below will remove the lower, older snow layers, leaving only lighter, more recent receipts. The pronounced temperature gradients in the typically shallow (Fig.7) floating snowpacks will produce marked constructive crystal forms in the basal layers (producing the distinctive collapsing sound which sometimes greets skiers on otherwise silent lakes) but periodic slushing removes the layers most affected by this, leaving only fresher 'atmospheric' or 'destructive' crystal forms in the near-surface layers. Similarly, it can be argued that the distinctive spatial patterns discussed above are periodically muted by slushing which has greatest effect where the snow is deepest ,thus tending to even out the depth distribution.

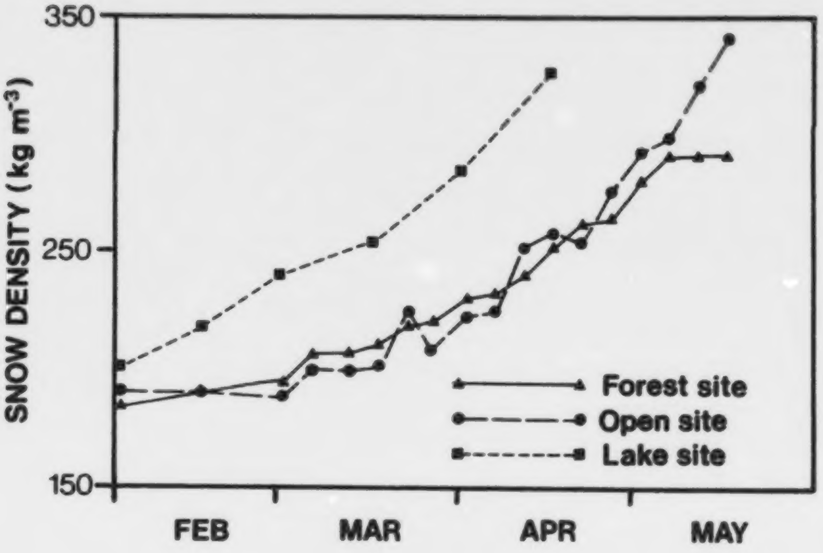

Figure 6 Note the consistently greater density of snow on the lake versus both land locations, even into the spring melt period. Higher densities are the product of wind compaction and the mechanical fragmentation of crystals (after Kuusisto 1984). Lower densities on the lake could be expected in years of persistent shallow snow and extensive depth hoar.

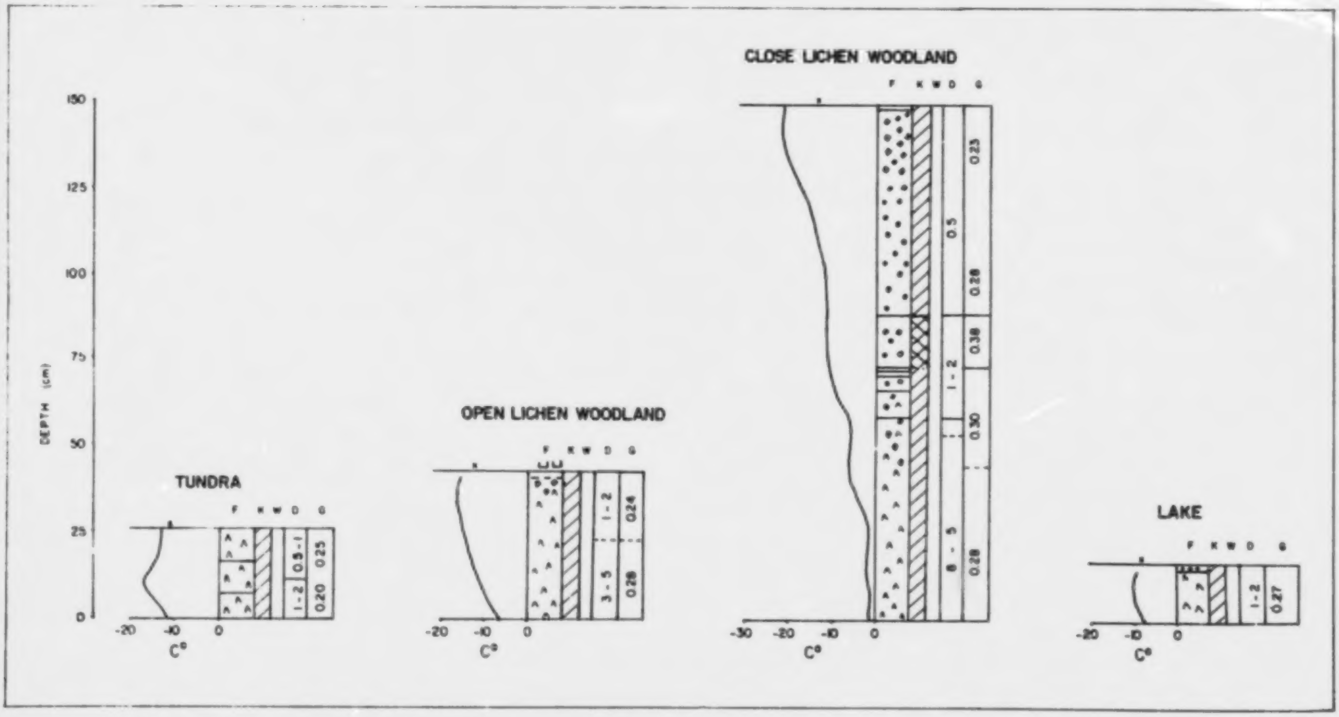
DEPTH (cm)
150
125
100
75
50
25
0
TUNDRA
F K W D G
0.5-1
1-2
0.25
0.20
-20
-10
0
C°
OPEN LICHEN WOODLAND
F K W D G
1-2
3-5
0.24
0.28
-20
-10
0
C°
CLOSE LICHEN WOODLAND
F K W D G
0.5
1-2
8-5
0.23
0.28
0.38
0.30
0.28
-30
-20
-10
0
C°
LAKE
F K W D G
1-2
0.27
-20
-10
0
C°

Figure 7 Examples of snow stratigraphy on and near Elizabeth Lake, Labrador. These pit profiles were obtained along the transect shown in Figure 4b (see Adams and Roulet 1980). Examples of the temporal evolution of snow stratigraphy on a lake and at adjacent land sites are presented in Adams and Prowse (1978).

Indeed, in the case of lakes in snowier regions, it might be argued that the most distinctive feature of the waterborne snowpack is the periodic dramatic reduction of mass associated with slushing. In such cases, the accumulation of the pack and the operation of metamorphic processes in it is markedly variable over time in comparison to the situation at 'equivalent' land sites where the pack can be conceived as developing more or less steadily. This may well present the greatest difficulty for those wishing to generalize from available land snowpack data to the nearby waterborne situation. The timing of such extrapolations, with respect to the timing of slushing events, may well be critical.

Another general point about the stratigraphic evolution of floating snowpacks is that, with the notable exception of the wetlands case mentioned briefly above, they tend to be relatively clean, lacking the soil and vegetation-derived contaminants which are a normal feature of land snowpacks. This cleanliness is shared by glacier-packs. Impurities within the floating packs are largely restricted to atmospheric and wind-blown contaminants and matter introduced from the underlying water body. The sea-borne snowpack, where salt is incorporated into the pack as a result of the up-migration of brine during ice-formation, is an important case of the latter (see Crocker 1984a and references). Salinities are highest in the early stages of pack formation (when the base includes the frost flowers mentioned above), decreasing over time. The basal layers of the pack retain high concentrations. Contaminants have various roles in snowpack evolution, affecting its thermal properties and vapour flow. In the sea case, considerable spatial and temporal variations of the distinctive saline liquid content of the pack are normal.

Thus, with some qualification, it can be said that a waterborne snowpack can be expected to be shallower and, often, more compact than an 'equivalent' land pack. It will contain less evidence of atmospheric crystal forms in its surface layers and more evidence of vapour deposition forms in its lower layers. Because of losses to open water and the growth of white ice, the water equivalent of the floating snowpack will be markedly less than that on land, even at very open sites (Figs.1 & 2, 4a, 4b, 7). In general, it is a cleaner snowpack contaminated only by substances from the atmosphere, upwelling water and those windblown from adjacent land. Over rough ice surfaces it tends to reduce surface roughness just as on land, but where the water body is 'confined' and margins are an important physical feature, it will often be more spatially variable than open, level, areas on land. However, these distinctive spatial patterns and the distinctive stratigraphic development may, at a particular time, be absent as a result of recent slushing.

Implications - Examples

The transition from open water to winter conditions on most water bodies is accompanied by drastic changes in the local energy regime. Capping of the water surface by even a thin layer of ice immediately reduces the exchanges of sensible and latent heat to negligible levels. Initially, the radiation flux is less affected, because most forms of "thermal ice" are relatively transparent to short wave radiation. However, once a layer of snow accumulates on the ice surface, a large percentage of the incoming short wave radiation is either reflected or attenuated before it reaches the water column. Slushing of the snowpack improves its optical transmissive properties, but even white ice substantially reduces the penetration of radiant energy.

Although surface reflection is primarily responsible for reductions in radiation receipts, the albedo usually decreases as the snow ages and the relative importance of attenuation within the snowpack thereby increases. In the case of a deep melting snowpack, the losses due to attenuation can exceed those due to reflection. The extinction coefficient of snow is related to physical parameters such as density, free water content, and grain size, shape and orientation but, for most practical purposes, the penetration of short wave radiation into snow can be considered to be a function of depth. However, all of these characteristics have been shown to vary substantially between land and floating snowpacks. One would therefore expect the radiation regime between these two snow environments to also be quite different. Examples of the waterborne snow-light literature are Maguire, 1975 a,b; Roulet and Adams, 1984; Stephenson and Prowse, 1983.

By limiting the penetration of radiation into water bodies, floating snowpacks control, to a considerable degree, biological activity beneath the ice cover. For example, the thickness of snow determines the quantity of transmitted light, which in turn controls the level of photosynthetic activity and thus the production of oxygen. During the winter months, photosynthesis within a water body is usually the major source of oxygen supply. For lakes with only a limited throughput of water and a high oxygen demand to support winter productivity, decreases in the photosynthetic production of oxygen can be biologically detrimental. Deep winter snowcovers are often responsible for the oxygen deficits in lakes which lead to the winterkill of fish.

The patterns of snow thickness can also be important to lacustrine life. Figure 8 depicts the percentage of total incoming radiation received at lake surface after accounting for losses due to reflection and attenuation within the overlying snow and ice

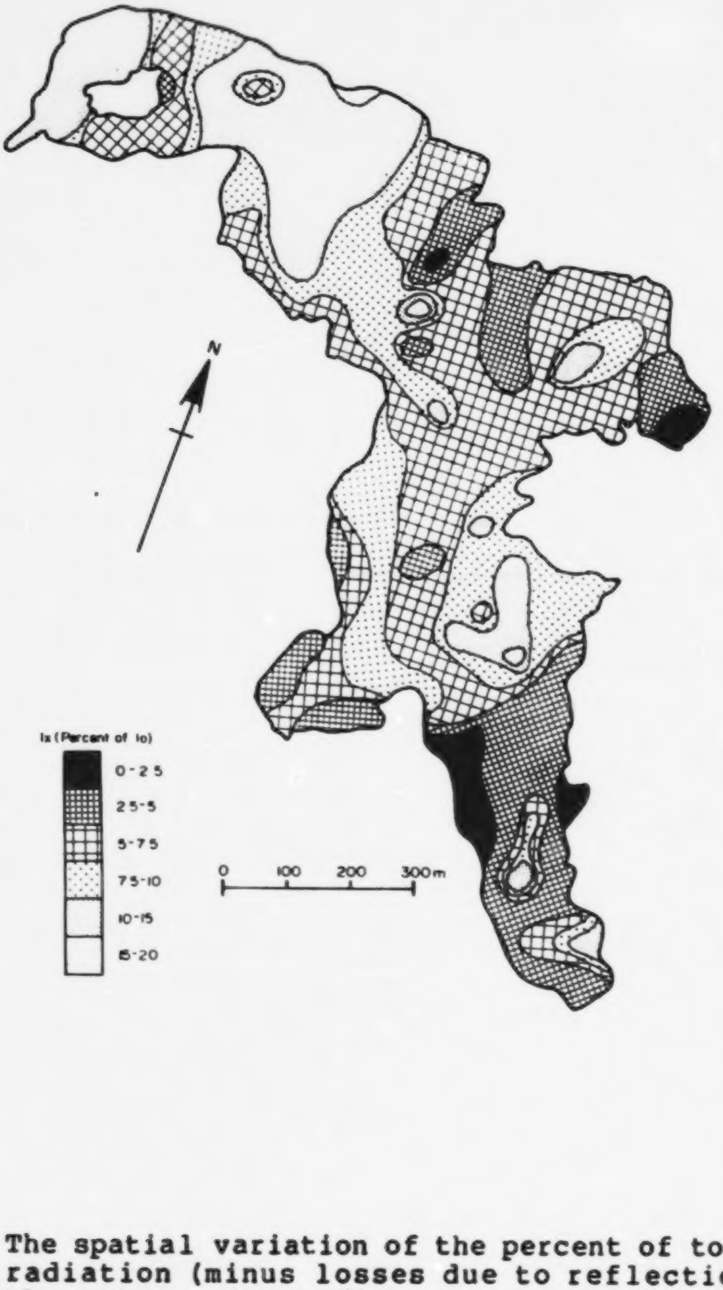

Figure 8 The spatial variation of the percent of total incoming radiation (minus losses due to reflection) reaching the water column after accounting for attentuation within the snow and ice strata (after: Stephenson and Prowse 1983). The lowest light levels are found where snow and white ice thicknesses are greatest, such as in the southern bay. Highest light levels are in the windswept, relatively snow free, middle and northern portions of the lake. The prevailing wind direction is from the north-east. Localized zones of higher light levels are also evident where slushing events have converted snow to white ice.

strata. As might be expected, the radiation receipts are highest in the windswept central portions of the lake and least near the margins where the thicknesses of snow and white ice are greatest. Notably, the margins of lakes usually coincide with the littoral zone, the habitat preferred by many life forms because of the abundance of light during the open water period.

Floating snowpacks also affect the heat balance of water bodies. Snow, as an effective insulator, severely restricts the flow of heat from the water to the atmosphere and, as an optical barrier, controls the radiative warming of the underlying water. The latter effect is most pronounced during the spring period when radiation levels are rapidly increasing and the snowcover begins to abate. Fig.9 is an example of the dependence of water temperature on the depth of snowcover found by Kuusisto (1984) for a Finnish lake. A simple linear regression between the data indicates that a 5 cm decrease in snow depth will increase the water temperature by 0.1 °C. Radiative heating of a water column is most apparent where mixing and turbulence is minimized. In the case of rivers, warming of the underlying water is less noticeable because of the rapid dissipation of heat throughout the cross-section and the greater water to ice heat transfer induced by flow turbulence.

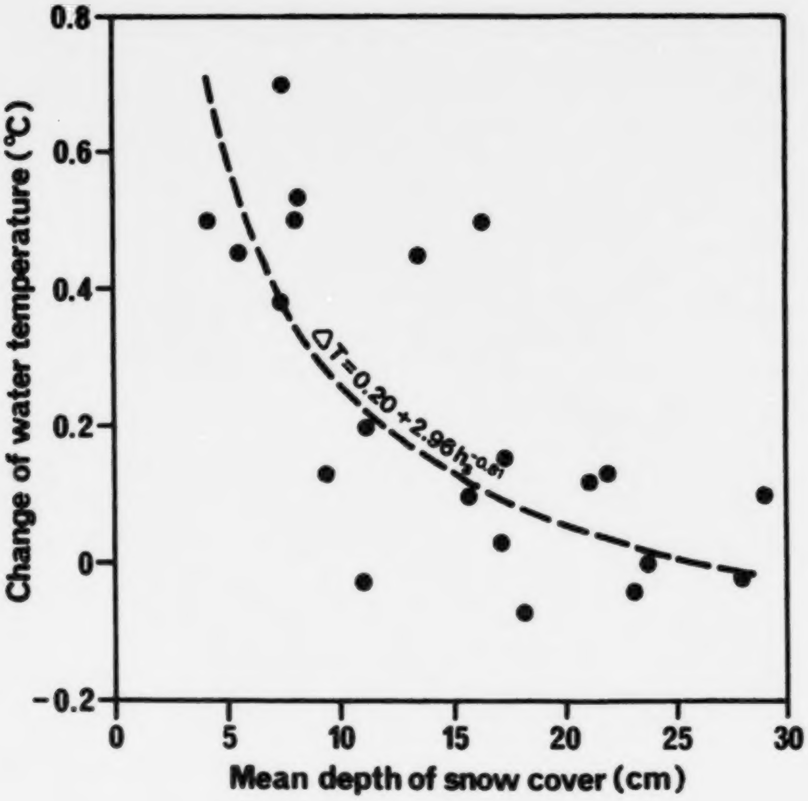

Figure 9 The average change of temperature in the upper 10m of lake water as a function of mean snow depth in April (after Kuusisto 1984). Increased warming occurs because the atmosphere-to-water heat flux (short-wave radiation) increases as the snow cover decreases. Temperatures increase on average 0.1 C for each 5cm decrease in snow depth.

Once appreciable quantities of light penetrate a floating snowpack, deterioration of the underlying ice cover begins. For rivers this has special significance because it greatly influences the type of ice breakup which will occur. In general, two factors control river ice breakup: the forces operating to destroy and convey the ice cover downstream and the ability of the ice cover to resist such forces. This latter factor is largely dependent on the pre-breakup mechanical strength of the ice sheet. The term 'premature' or 'mechanical' is used to describe a breakup in which the ice sheet is relatively competent and has retained much of its original mechanical strength. In contrast, an 'overmature' or 'thermal' breakup occurs when there has been appreciable pre-breakup deterioration of the ice sheet. In extreme cases, the ice sheet may melt *in situ*; a situation not unlike that which occurs on lakes. Of the two types of breakup, a premature event is usually the most dramatic, and the one responsible for the most severe ice jamming and associated backwater flooding.

Most changes in ice strength during the pre-breakup period are related to thermally induced deterioration. Although the transfers of sensible, latent and radiative heat are all important to the ripening and melt of the snow and ice cover, radiation produces the largest and most dramatic changes in the mechanical strength of an ice cover. As the overlying, protective layers of snow and white ice are melted away, increasing amounts of radiation are transmitted into the transparent black ice structure. Some of this radiation is absorbed at inter-crystalline boundaries, resulting in localized melt, a breakdown in crystal bonds, and a decrease in the mechanical strength of the ice. If a river is blanketed by only a thin layer of snow and white ice at the beginning of the melt season, the black ice quickly becomes exposed to large radiation inputs and rapidly deteriorates. Unless a spring flood wave is generated early in the season, an overmature breakup will likely result and the clearance of river ice will be rather uneventful. On the other hand, if the layers of snow and white ice are especially thick, the underlying black ice may remain protected during the entire pre-breakup melt period. The ice sheet, having retained much of its original mechanical strength, will then pose a formidable obstacle to the spring flood wave and be more likely for form numerous and quite large ice jams.

The effects of floating snowpacks on ice decay are somewhat more complex in the case of perennial ice covers, such as multi-year sea ice, where the equilibrium ice thickness is dependent on the seasonal rates of accretion and ablation. During the winter months, ice accretion at the base of thin sea ice is, as is the case for other water bodies, a function of surface snow depth. A thinner snowpack allows a greater water to atmosphere transfer of heat and therefore accelerated ice growth. However, for a perennial ice cover, a thin snowpack also means a prolonging of the summer ablation period because the snow is removed relatively early in the season. Following the removal of snow, ice thinning occurs both at the surface and at the bottom because of the penetration of short-wave radiation. In contrast, a thick snow cover impedes winter ice growth by insulating the waterbody to cold temperatures, but it also reduces the amount of summer thinning by reducing the length of the ablation season. Maykut and Untersteiner (1969) have modelled the effects of varying snow depth on sea ice thickness and have found that for snow depths between 0 and 70 cm. the average ice thickness remains almost unchanged because of a mutual compensation between the thickening and thinning effects. Only when the snow depth exceeds 70 cm do the effects go out of balance. Notably, the greater snow depth results in an _increased_ ice thickness, because decreasing radiation receipts and ablation dominate the balance. This is in direct contrast to the seasonal ice case where one thinks of deep snow being responsible for _decreased_ ice thickness.

It is clear that the thermal and optic roles of floating snow packs, examples of which have been given, cannot be fully understood without an appreciation of the stratigraphy of the pack involved. Depth is often a poor index of the properties which it is used to represent.

One of the reasons for the neglect of snowpacks on freshwater bodies is "mass balance thinking". The floating snow is, from a hydrostatic viewpoint, already part of the system. It has, as it was, been allowed for. However pulses of water from loading lake ice sheets with snow can be a very significant portion of winter flow. Jones (1969) suggests that 14% of his winter flow (i.e. 8 months of the discharge) was produced in this fashion. Kuusisto (1984) found flow of this type to be particularly important in regulated systems (Fig.10). Also, as has been suggested above, lake snow, including that which is incorporated in the white ice, can significantly affect spring melt in terms of the amount and timing of water released and in terms of the quality of water concerned.

Crocker (1984a) clearly develops the point that the implications of the special characteristics of sea borne snow, especially those resulting from its salinity, are still remarkably poorly understood. The thermal properties of snow are particularly affected by brine content. He points out that the presence of brine has a great influence on snow properties such as thermal conductivity. It is possible, for example, to have a temperature gradient in brine slush whereas freshwater slush is isothermal (reducing the thermal conductivity

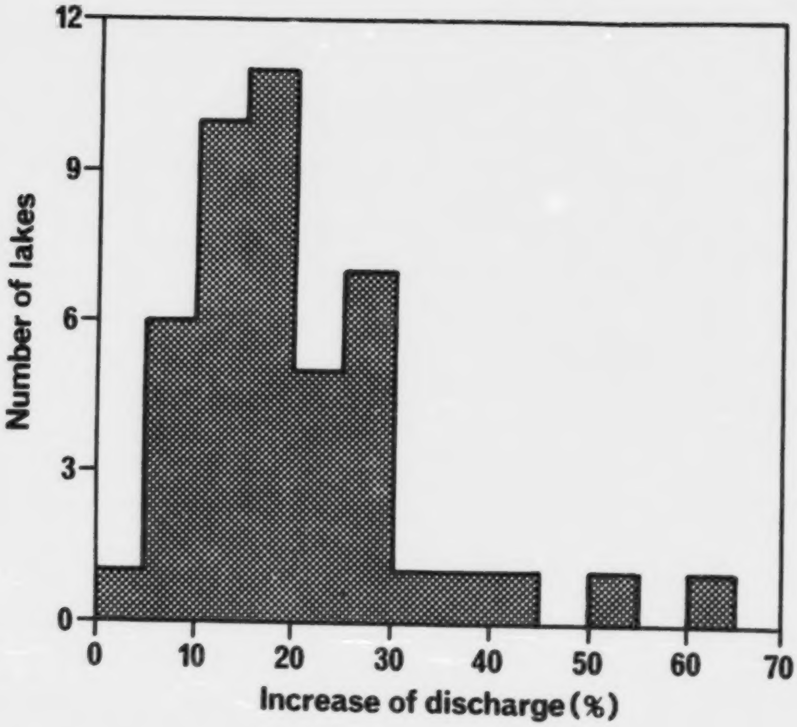

Figure 10 The percentage increase of outflow from a sample of 45 unregulated Finnish lakes in February, assuming a 50mm increase (water equivalent) in the total snow load (after: Kuusisto 1984). Depletion of lake storage is often a major source of winter stream flow. The above effect is greatest during periods of low flow, especially in basins with a high proportion of lakes.

to zero). Crocker (1984b) shows that ignoring brine in sea snowpacks can result in underestimates of thermal conductivity of up to 50%. Further, ignoring distinctive layers in this and other snowpacks is to ignore the fact that in a system of series-connected conductors, the least conducting layers dominate. Thus even where bulk density values are available thermal conductivity is likely to be underpredicted.

Remote sensing techniques have been applied more extensively and intensively to sea ice than to any other floating ice situation. And yet, knowledge of properties of sea borne snowpack (e.g. the typical crust underlain by depth hoar with brine present in the young sea ice case) is very limited. This lack of knowledge directly affects the value of the results of the remote sensing. The implications of the thermal conductivity points, made above, for thermal imagery are one example of this. In the case of active and passive microwave similar points can be made (see Crocker 1984a). The presence of liquid water, throughout the winter at sea, periodically in the freshwater case, with its high dielectric constant compared to that of dry snow, dominates and complicates results. Brine on sea ice, for example, increases the attenuation of synthetic radar (SAR) images.

Concluding remark

One of the reasons for the neglect of floating snowpacks has been interest in the underlying 'ice' and water towards which measuring and observing systems have been geared. It is ironic that lack of knowledge of the snowpacks is now a serious limiting factor in the evolution of remote sensing techniques as a highly promising means of studying floating 'ice' sheets.

Acknowledgements

A number of colleagues and students contributed to this work including D.R. Barr and O. Choulik of the McGill Subarctic Research Station and P. Doran and S. Gardiner of Trent University. Special thanks are due to the Inuvik Scientific Resource Centre, Indian Affairs and Northern Development, particularly Dave Sherstone. We are most grateful to Greg Crocker, Cambridge University, England, for his advice.

References

Adams, W.P. 1984. Improving snow and ice measurements on lakes. Proc. Fifth Northern Research Basins Symposium and Workshop, Finland, 1.1-1.14.

Adams, W.P. and D.C. Lasenby 1985. The roles of snow, lake ice and lake water in the distribution of major ions in the cover of a lake. Annals of Glaciology, 7, (in press).

Adams, W.P. and T.D. Prowse 1978. Observations on special characteristics of lake snowcover. Proc. Eastern Snow Conf. 35, 117-128.

Adams, W.P. and T.D. Prowse 1981. Evolution and magnitude of spatial patterns in the winter cover of a temperate lake. Fennia, 33, 100-116.

Adams, W.P. and N.T. Roulet 1984. Sampling snow and ice on lakes. Arctic, 37,3,270-275.

Crocker, G.B. 1984a. Physical properties of snowcover on sea ice in the central high Arctic. M.Sc. Thesis, McGill University Montreal, P.Q.

Crocker, G.B. 1984b. A physical model for predicting the thermal conductivity of brine wetted snow. Cold Regions Science & Technology, 10, 69-74.

Grey, B.J. and D.K. MacKay 1979. Aufeis (overflow ice) in rivers. Proc. Canadian Hydrology Symposium, Vancouver, 139-163.

Hibler, W.D., S.Ackley, W.F. Weeks and A.Kovacs 1972. Top and roughness of a multiyear ice floe. AIDJEX Bull. No.13. Div. of Marine Resources, University of Washington, Seattle, Washington 98105, 91p.

Jones, J.A.A. 1969. The growth and significance of white ice on Knob Lake, Quebec. Can. Geog. 13, 354-372.

Kuusisto, E. 1984. Snow accumulation and snowmelt in Finland. Publications of the Water Research Institute, No.55, National Board of Waters, Helsinki, Finland, 149 p.

Maguire, P.J. 1975a. Effects of ice and snowcover on transmission of light in lakes. Inland Waters Directorate, Environment Canada, 54, 24p.

Maguire, P.J. 1975b. Light transmission through snow and ice. Inland Waters Directorate, Environment Canada, 91.

Maykut, G.A. 1976. Energy exchange over young sea ice in the central arctic. AIDJEX Bull.31 (Arctic Ice Dynamics Joint Experiment, Division of Marine Resources, University of Washington, Seattle, Washington 98105), 74p.

Maykut, G.A. and N.Unteisteiner 1969. Numerical prediction of the thermodynamic response of arctic sea ice to environmental changes. The Rand Corp., Santa Monica, Calif. RM-6093-PR, 173p.

Michel, B. 1970. Winter regime of rivers and lakes. USA CRREL Mono, 111.BlA.

Prowse, T.D. 1978. Winter cover on temperate lakes. M.Sc.Thesis, Biology-Geography Watershed Ecosystems Program, Trent University, Peterborough, Ontario.

Roulet, N.T. and W.P. Adams 1984. Illustration of the spatial variability of light entering a lake using an empirical model. Hydrobiologia, 109, 67-74.

Stephenson, R. and T.D. Prowse 1983. Variability in winter lake cover: implications for radiation receipts and oxygen deficits in temperate lakes. Proc. Eastern Snow Conference, 40,37-52.

MEASUREMENT OF BLOWING SNOW PROPERTIES USING OPTICAL ATTENTUATION DEVICES

by

J.W. Pomeroy, T. Brown, D.H. Male

Division of Hydrology
University of Saskatchewan
Saskatoon, Saskatchewan
Canada

presented at

SNOW PROPERTY MEASUREMENTS WORKSHOP

Lake Louise, Alberta

1-3 April, 1985

TECHNICAL MEMORANDUM 140

Compiled By

P.R. Kry

NRCC 27594

INTRODUCTION

Blowing or drifting snow can occur frequently over the winter in regions where sufficient snowcover and open terrain permit entrainment of the snowpack by the wind. In the North American prairies, the Arctic, Siberia and Antarctica blowing snow causes widespread relocation of precipitation. Wind transport also enhances the rate of sublimation from the snowpack (Schmidt, 1982). Relocation of and sublimation from snow during wind transport make the phenomenon of importance to hydrology, agriculture, transportation, plant ecology and engineering design. However, there has been limited development of simple devices capable of continuous, rapid monitoring of blowing snow. This is due in part to the variability of blowing snow transport rates with height and windspeed and in part to the severe meteorological conditions under which blowing snow occurs.

The blowing snow measurement system described here simultaneously measures two optical indicators of blowing snow; the proportion of light extinguished while passing through a snow-air flux and the number of pulses caused by blowing snow particles interrupting a narrow beam of light. Using geometrical optics theory, the drifting mass density (drift density) and mean particle size can be determined from these two measurements. The system is relatively inexpensive and suitable for meteorological studies or continuous monitoring.

Properties of Blowing Snow

Blowing snow refers to frozen precipitation mechanically removed from the surface snowpack by the action of wind. It occurs in two modes of transport: saltation and suspension. Saltation involves regular contact and momentum exchange between the particle and the snowpack surface. Snow particles are ejected into the saltating layer by impact from other particles, aerodynamic lift and magnus effect forces (Kobayashi, 1972; Owen, 1964; White, 1982). The particles travel curved trajectories generally less than 0.1 m in height. When vertical turbulent diffusion is sufficient to overcome gravitational and drag effects, the snow particle enters suspension. The suspended layer of snow transport can reach from 0.1 to over 300 m in height (Budd et al, 1965).

The drift density of snow increases logarithmically with height. A maximum of near 500 g/m^3 has been recorded in the saltation layer (Fig. 1). At a 2 m height, values from 0.1 to 10 g/m^3 are common. Transport rates up to 1 kg/sec through an area 1 m wide and 300 m high have been calculated for Antarctica (Budd et al, 1965).

Budd (1965) found that for blowing snow without snowfall, particle diameter distributions match a two-parameter gamma function distribution. The gamma frequency distribution for particle diameters, P_d, as given by Budd is;

$$f(P_d) = \frac{P_d^{(\alpha-1)}}{\beta^{\alpha}\,\Gamma_{(\alpha)}}\, e^{(-P_d/\beta)} \quad , \qquad (1)$$

where α and β are the shape and scale parameters and $\Gamma_{(\alpha)}$ is the gamma function (Haan, 1977). Note that $\beta = \overline{P}_d/\alpha$, where $\overline{P}_d$ is the mean particle diameter. This allows the description of the relative number of particles for any diameter class using two variables; the mean diameter and α from the gamma function. Schmidt (1981, 1984) has confirmed the validity of the gamma distribution for blowing snow and has shown that concurrent snowfall quickly metamorphoses into the expected particle diameter distribution during saltation. Schmidt (1982) has also found that blowing-snow particles are somewhat ellipsoid although they show no preferred orientation while suspended.

EXTINCTION OF TRANSMITTED LIGHT BY BLOWING SNOW PARTICLES

Single Particle Extinction

The effect of a single particle in extinguishing a narrow light beam is the basis for snow particle counters or detectors. These instruments are designed to measure the number and often size of particles by recording pulsed drops in

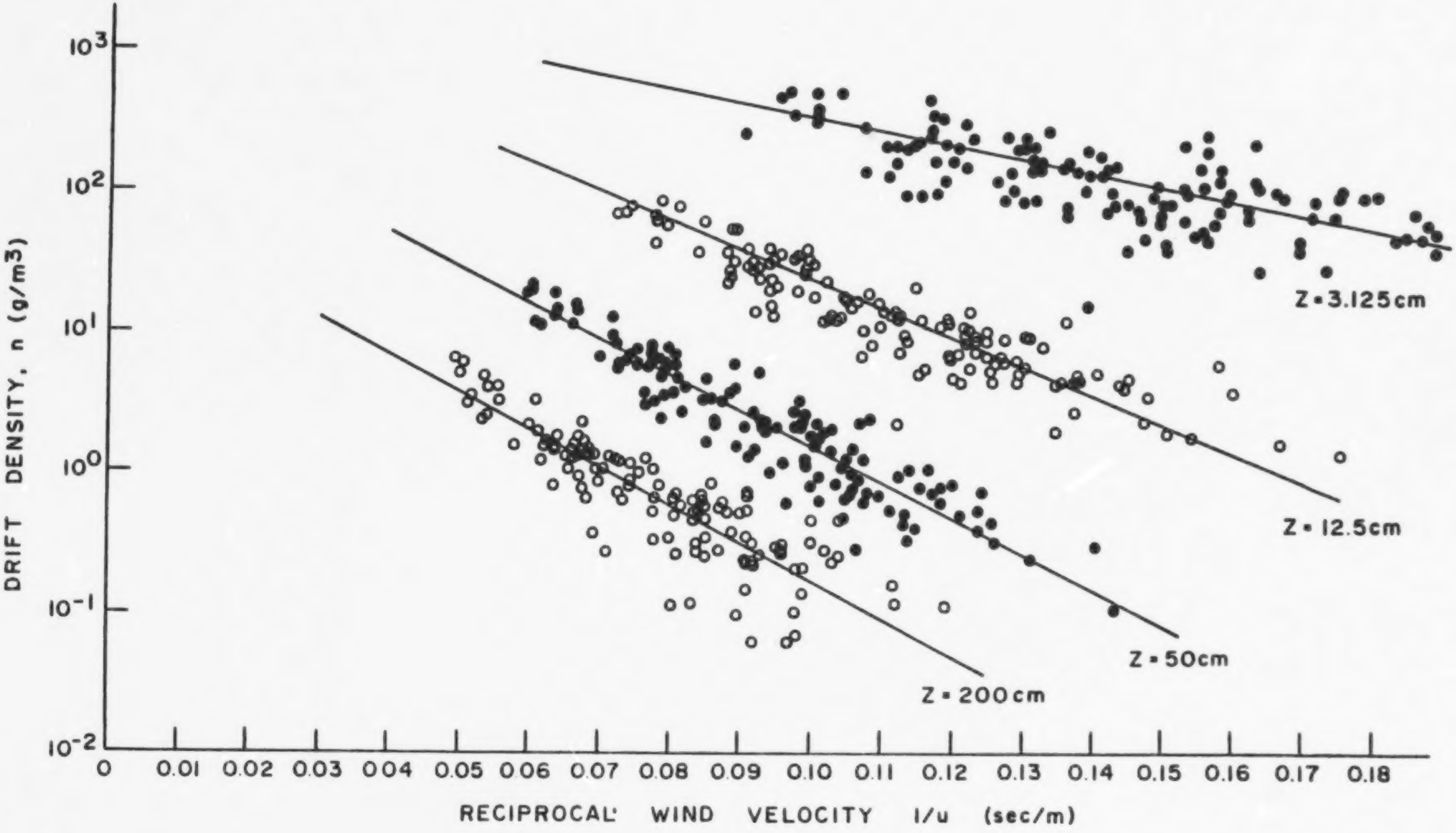

Figure 1. Drift density as a function of wind velocity for a range of heights (z) (after Budd et al., 1965).

beam transmittance. The pulses are caused by a moving particle interrupting the light beam. Geometrical optics approximations can accurately describe the effects of single and multiple particle light scattering and absorption for translucent particles in the size range of blowing snow particles (Ungut, et al, 1981). Geometrical optics theory is therefore used in these calculations.

For a single blowing snow particle, interrupting a uniform beam of parallel light, the transmittance T is found from the expression (Zuev, 1970);

$$T = T_0 - (\pi P_r^2 / \pi B_r^2) E_c \quad . \qquad (2)$$

T_0 is the transmittance before the beam is interrupted, P_r is the radius of a circle of equivalent cross-sectional area to the particle, B_r is the cross-sectional radius of the light beam and E_c is the corrected extinction efficiency of the particle-light beam arrangement. Since blowing snow particles have no preferred orientation (Schmidt, 1984), P_r can be considered the effective particle radius when large numbers of particles are examined.

For a specific light beam geometry and electromagnetic wavelength, the corrected extinction efficiency of a particle is the ratio of the light flux scattered and absorbed to the flux geometrically incident on the particle. E_c is conceived as having four components; the extinction efficiency E, the diffraction correction ΔE_0, the external reflectance correction ΔE_1 and the refraction correction ΔE_2. Where;

$$E_c = E - (\Delta E_0 + \Delta E_1 + \Delta E_2) \quad . \qquad (3)$$

For ice spheres from 20 to 500 μm diameter in visible to near-infrared light $E = 2.0$ (Seagraves, 1984). The extinction efficiency refers to light extinguished by both interception and diffraction by the particle (Van de Hulst, 1957).

The diffraction correction, ΔE_0, is the reduction in extinction due to detection of diffracted light by the sensor. It can be significant for ice spheres in the sizes and wavelengths of interest and is found from the expression (Hodkinson and Greenleaves, 1963; corrections - Seagraves, 1984);

$$\Delta E_0 = 1 - (J_0{}^2\{(2\pi P_r/\lambda)\ \sin(B_r/\ell)\} + J_1{}^2\{(2\pi P_r/\lambda)\ \sin(B_r/\ell)\}) \qquad (4)$$

where J_0 and J_1 are zeroth and first order Bessel functions of the first kind respectively, λ is the electromagnetic wavelength and ℓ is the distance between the particle and beam sensor or detector. For parallel light, the beam radius is assumed equal to the active radius of the detector. Thus, the amount of light diffracted forward into the beam detector is a function of particle radius, light wavelength and the angle of the cone formed by the particle centre and the detector perimeter.

The external reflectance correction, ΔE_1, is the reduction in the extinction efficiency due to detection of externally reflected light. It is a function of the detector-particle geometry and the complex index of refraction, m, for the particles. For ice, m = 1.302 (Liou, 1981). According to Hodkinson and Greenleaves (1963), ΔE_1 reaches a maximum of 0.01 for possible detector-blowing snow particle geometries. Variation in m due to various light wavelengths or ice contamination has little effect on ΔE_1 in this range. For most snow particle-detector geometries, ΔE_1 is much less than 0.01. It will be ignored in this analysis.

The refraction correction, ΔE_2, is the reduction in extinction due to collection of light transmitted from the source then refracted by the particle. It is a function of the particle-detector geometry and the complex index of refraction of the particle. Though often ignored in the analysis of light transmission through air-snow mixtures, ΔE_2 can be as high as 0.45 for ice spheres. ΔE_2 is calculated following Hodkinson and Greenleaves (1963);

$$\Delta E_2 = 4\left(\frac{m}{m^2-1}\right)^4 \int_0^{\theta} \frac{(m\cos\theta/2-1)^3(m-\cos\theta/2)^3(1+\sec^4\theta/2)\sin\theta}{\cos\theta/2(m^2+1-2m\cos\theta/2)^2}\,d\theta\ , \qquad (5)$$

where $\theta = \arcsin(B_r/\ell)$.

If the incident beam is not parallel, the corrected extinction efficiency will drop further, due to a change in the angle of light incident on the particle and the detector. ΔE_0 and ΔE_2 increase by an amount which cannot be readily determined. Approximately parallel beams are therefore necessary for precise theoretical calibrations of particle detectors and extinction meters.

A consequence of the dependence of ΔE_0 and ΔE_2 on $\arcsin(B_r/\ell)$ is that for a given particle, the corrected extinction efficiency varies, dependent on the particle location along the light beam. As well, a single particle whose path does not entirely intercept the beam will cause a drop in transmittance corresponding to the intercepted area of the particle, not its true area. These two effects make theoretical calibration of a device which determines ice particle size from single-particle light extinction unreliable. The effects are enhanced when the light is not collimated and represent a major drawback of particle counters.

Multiple Particle Extinction

The effect of an ensemble of particles in extinguishing light transmittance is the basis for extinction or attenuation meters. These devices are designed to measure the drift density of a snow flux by recording the mean drop in light beam transmittance caused by interception with the particles. Geometrical optics are used to calculate this.

Following Winchester and Gimmestad (1983), for a number of uniformly dispersed blowing snow particles with extinction coefficient σ_λ m^{-1}, located in an optical path of length L m, the transmittance, T for wavelength λ m is;

$$T = \exp(-\sigma_\lambda \cdot L) \quad . \tag{6}$$

The extinction coefficient is a property independent of the length of light transmission, but is a function of the wavelength and particle-detector geometries. Seagraves (1984) notes that for the simplified case of a mono-sized dispersion of snow particles in the atmosphere;

$$\sigma_\lambda = N \pi P_r^2 \overline{E}_c \quad , \tag{7}$$

where $N(\#/m^3)$ is the number of particles per unit volume of atmosphere, P_r is the snow particle radius and $\overline{E}_c$ is the mean corrected extinction efficiency.

Evaluation of $\overline{E}_c$ is similar to E_c for the single particle extinction case, except that the diffraction and refraction corrections are averaged over the beam length. Thus,

$$\overline{E}_c = E - \frac{1}{L}\int_0^L (\Delta E_0 + \Delta E_2) d\ell \quad . \tag{8}$$

ΔE_0 and ΔE_2 are calculated using Eqs. 4 and 5 respectively.

Equation 7 can be expanded to fit snow particle dispersions of various sizes. For some particle radius distribution;

$$\sigma_\lambda = \int_{P_r} n(P_r) \overline{E}_c \pi P_r^2 dP_r \quad , \tag{9}$$

where $\int_{P_r} dP_r$ is the integral of P_r over the expected particle radius range, and $n(P_r)$ is the number of particles of radius P_r per unit volume. Note that $\overline{E}_c$ is a function of the particle radius.

The gamma distribution is the preferred frequency function for blowing snow particle sizes (Budd, 1966; Schmidt, 1984). $n(P_r)$ can be related to the relative frequency of a particle radius, $f(P_r)$, by;

$$n(P_r) = N \cdot f(P_r) \quad . \tag{10}$$

Particle radius frequency is found using the two-parameter gamma distribution of the form

$$f(P_r) = \frac{P_r^{(\alpha-1)}}{\beta^\alpha \Gamma_{(\alpha)}} \quad e^{(-P_r/\beta)} \quad , \tag{11}$$

where α is the shape parameter and β is the scale parameter (Haan, 1977). Note that $\beta = \overline{P}_r/\alpha$, where $\overline{P}_r$ is the mean particle radius. Substituting the gamma distribution into Eq. 9 yields;

$$\sigma_\lambda = \frac{N\,\pi}{\beta^\alpha \Gamma_{(\alpha)}} \int_{P_r} \overline{E}_c \, P_r^{(\alpha+1)} \, e^{(-P_r/\beta)} \, dP_r \quad . \tag{12}$$

To find the extinction coefficient in terms of the drift density C kg/m^3, the drift density must first be defined in terms of indiviudal ice particle volumes and densities. For some distribution of P_r;

$$C = \int_{P_r} n(P_r) 4/3 \pi \rho_i P_r^{\,3} \, dP_r \quad , \tag{13}$$

Where ρ_i kg/m^3 is the density of ice. Substituting the gamma distribution yields,

$$C = \frac{4\pi N \rho_i}{3\beta^\alpha \Gamma_{(\alpha)}} \int_{P_r} P_r^{(\alpha+2)} \, e^{(-P_r/\beta)} \, dP_r \quad . \tag{14}$$

Combining Eqs. 12 and 14 makes it possible to determine σ_λ from the variables L, $\overline{P}_r$, α and C. Thus,

$$\sigma_\lambda = \frac{3C \int_{P_r} \overline{E}_c \, P_r^{(\alpha+1)} \, e^{(-P_r/\beta)} \, dP_r}{4\rho_i \int_{P_r} P_r^{(\alpha+2)} \, e^{(-P_r/\beta)} \, dP_r} \quad . \tag{15}$$

Equations 8 and 15 can be extremely useful in the development of calibration curves for blowing snow detection using light extinction meters. Similar geometrical optics equations used with laser transmissometer outputs have accurately predicted precipitation rate and particle size for falling snow (Seagraves, 1984).

OPTICAL MEASUREMENT OF BLOWING SNOW

Extinction Meters

Orlov (1961) described a gauge which responds to light extinction as snow blows between a collimated lamp and a photocell. Landon-Smith and Woodberry

(1965) describe in detail a similar system using a cadmium sulfide photoconductor detector and a broad-band source. To exclude the effects of ambient light the source and detector are housed in a black rectangular tube whose openings are exposed to the flux of blowing snow. The gauge was empirically calibrated against an anemometer and a mechanical snow trap. The gauge design resulted in incomplete exclusion of ambient light. This factor along with the constantly changing sensitivity of the system necessitated frequent reference measurements. For a reference measurement, incoming snow was blocked and the gauge output signal recorded. Landon-Smith and Woodberry report a systematic error caused by the non-linear relationship between gauge output and drift density. The output was averaged over 30 min. and the drift density calculated from the averaged signal. This error could have been reduced by shorter averaging times. The investigators recognize but make no attempt to correct errors in transmittance caused by varying particle size distribution parameters.

Wishart (1965) improved the electronics and mechanics of the Landon-Smith and Woodberry design. In his instrument light baffles and yellow light limiting filters reduce the effects of ambient light fluctuations. A reference photoconductor monitors fluctuations in the source intensity and photoconductor sensitivity. However significant signal drift still occurred and the tubing and baffles used to protect the detector from ambient light interferred with the snow-air flux.

Sommerfeld and Businger (1965) describe an extinction meter similar in design to Wishart's except that light baffles are not used. The authors did not report how ambient light effects were accounted for. The device was empirically calibrated in a cold room. The authors found its useful range limited due to low sensitivity and inadequate strength in construction of the support arms. At windspeeds below 10 m/s drift densities were too low to elicit an adequate signal from the device. Above 15 m/s vibrations from the support arms introduced signal noise and the snow shielding on the detector housing became inadequate. Advantages of this instrument over other gauges are its rapid response time, large sampling area and reduced interference with the air stream (Hollung et al., 1966).

Particle Counters

Hollung et al. (1966) describe a gauge designed to detect individual blowing snow particles. This gauge employs two rectangular light beams separated by 1 mm and of cross-sectional dimensions 0.62 x 2.75 mm. The beams are arranged so that a snow particle crosses both beams perpendicular to the long dimension. The interruption of the beams by a particle causes a pulse in each beam's output. The velocity of the particle is calculated from the elapsed time between the particle's edge contacting the first beam and the second beam. Hollung et al. estimated the particle diameter from the elapsed time as the particle travels from the midpoint between the two beams to the point where its edge leaves the second beam. The estimate of diameter is dependent upon the accuracy of the velocity estimate.

Two fast response photo-duo-diodes were used as detectors, with a broad-band lamp as the single source. Two rectangular windows in front of the photo-diodes limit the area of light projected on the detectors. The length of the beams exposed to the snow flux is 25 mm. The structure supporting the source and detectors was designed for stability and interferes somewhat with the snow-air flux. The two photodiode signals are presented in opposite polarities, this allows electronic identification of the signal pulses. The signals are amplified twice, increasing voltage by a factor of 10,000. Signal distortion is not reported below particle counts of 60,000 per second. Signals from the device were recorded on magnetic tape and the transmittance record examined on a storage oscilloscope. Data on the extinction pulses were collected manually from the oscillogram.

A problem with this system is that since snow particles are not perfect spheres, a random cross-section of a particle may not be representative of its volume. The pulse shapes shown on the oscillograms vary considerably and suggest that determination of the particle edge from the pulse edge is a subjective procedure. Diffraction effects by the particle edges are not discussed by the authors. Geometrical optics theory states that ideally, as much light is diffracted by the edges of a small particle as is incident on the particle. The authors state that for the same size obstruction, the pulse size dropped as the light beams were interrupted further from the detectors. This indicates that non-parallel light was used which would distort the shadow of a particle with increasing distance from the detector. It is felt that these factors put in question the claims that this device does not require physical calibration.

Schmidt (1977) describes the development of a particle counter based on the design by Hollung et al. The source-detector geometry is almost identical to the Hollung et al. model. However the lamp and phototransister housings are redesigned to maximize stability and minimize interference with the snow-air flux. Amplifier design was improved, with low-impedence current to voltage converters permitting more rapid signal response times. Noise common to both phototransisters was filtered at this stage. The amplified signal is then sent to an analog tape recording unit or strip chart recorder. Schmidt (1984) describes a more recent analog to digital converter which feeds digital signals into a commercial microprocessor. The microprocessor can then dump directly into a desktop computer, which controls the system.

Schmidt (1977) altered the signal analysis procedure from that of Hollung et al. (1966). Particle velocity estimates are made using the time interval between the signal pulse from the first and second phototransister. An electronic time interval counter is triggered at a set voltage. When this voltage threshold is crossed by a signal pulse the timer is triggered. A more recent version utilizes a signal peak detector (Schmidt, 1984) to measure peak amplitude. This technique is dependent on the pulse size and shapes being identical. Particle size estimates are made based on signal pulse amplitude. Schmidt found for his detector that a simple linear relationship between the square of particle radius and pulse amplitude is unworkable. Non-parallel light and non-uniform sensitivity across the detector areas are cited as reasons for this. The variation of extinction efficiency corrections with the distance from particle to detector, noted earlier in this paper, must also be a component of the problem. Schmidt (1984) notes that even if the light beams were perfectly parallel, only a part of some particles will cross the beam. This results in underestimated mean particle sizes and skewed particle size distributions calculated from such data. Schmidt therefore does not attempt an exact calibration of the pulse amplitude to particle sizes.

The calibration Schmidt develops is empirical and complex. From tests with lead shot, sieved sand and sieved snow the author finds a correspondence between particle size and the largest signal pulse it can generate. This pulse occurs when the particle path bisects the beam cross-sections and crosses the beams adjacent to the detector windows. Therefore only a small percentage of pulses (less than 1%) will be significantly related to the snow particle size (Schmidt, 1977). Pulses are classified based on their maximum amplitude. The number of particles in a diameter class is hypothesized to be related to the area under the signal amplitude frequency distribution contributed by that class size (Fig. 2), where

$$n(P_d) = KA\Delta(n(A)) \quad . \qquad (16)$$

$n(P_d)$ is the number of particles in a particle diameter class with midpoint P_d, K is an empirical constant determined from sieved sand and snow tests and is a function of the pulse amplitude, A is the pulse amplitude and $\Delta(n(A))$ is the

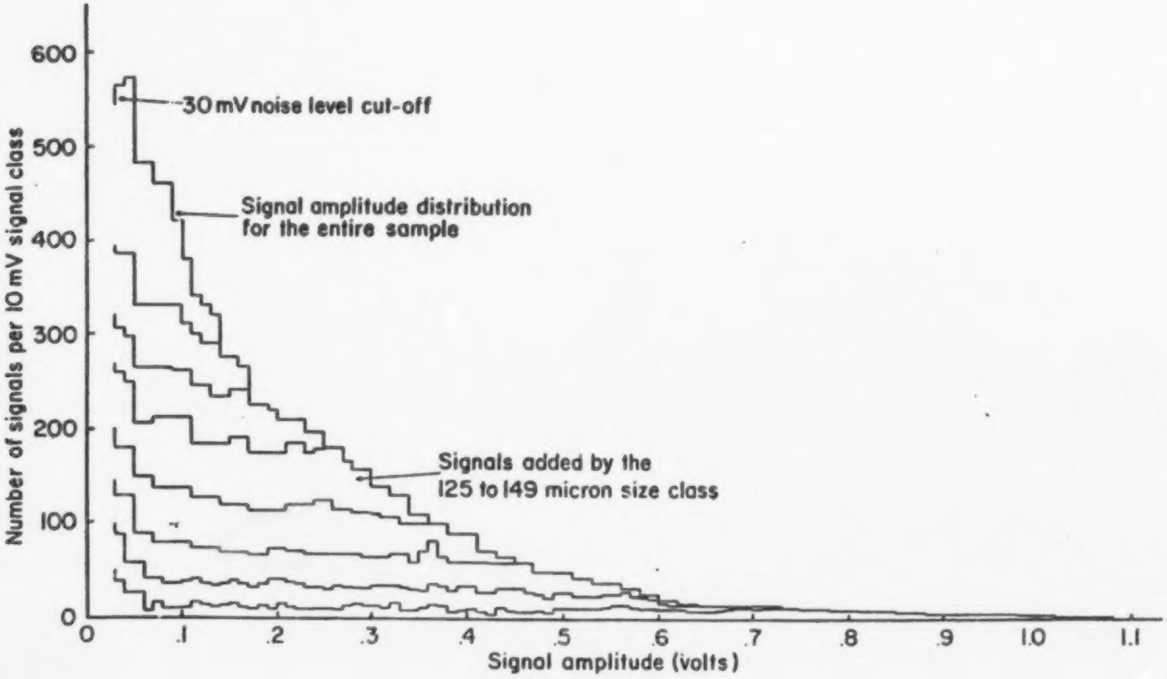

Figure 2. Signal amplitude density distribution showing contributions of particle size classes as measured by Schmidt's particle counter (after Schmidt, 1977).

difference in the number of pulses per 10 mv between class limits at amplitude A. Schmidt's (1977) plot of A against K for known particle diameters shows considerable scatter.

While the type of information calculated from Schmidt's snow particle counter is of scientific interest, its performance and empirical calibration raise several questions. Calculation of particle size is based on less than 1% of collected observations and on an empirical relationship developed primarily using sand particles. Schmidt's (1977) examples of particle diameter distributions found using the snow particle counter vary significantly from the sieved particle diameter distributions used to generate the signals. Actual mean particle diameters vary from estimated means by up to 25%, while no example of close correspondence between actual and estimated distributions is shown for snow particles.

Particle velocity estimations are handicapped by problems similar to diameter estimations. Tests with a spinning wire (Schmidt, 1977) show a 10% variance in particle velocity estimates for various distances from the detector window. This is due to the divergance of the sensitive beam area from the detector windows to the source window. It should be noted that the spinning wire is an ideal case. Actual particles will produce edge diffraction effects which will vary due to irregular shape. Only the particle velocity component perpendicular to the light beams is measured. This presents some problems when compared to windspeeds estimated using cup anemometers. The author notes that the snow particle counter is saturated in the saltation layer, as more than one particle at a time is in the light beams.

Gubler (1981) designed a snow particle counter that uses an infra-red light emitting diode (LED) source and a photodiode detector. The LED source is superior to conventional incandescant sources because of its uniformity of intensity across the beam width, stability with respect to time and low power consumption.

The length of the exposed beam is 0.02 m and the beam cross-section is 0.5 by 1.0 mm. Light is collimated by lenses in front of both the LED and photodiode and by 0.04 m of narrow tubing between each lens and the windows. The combination of the lens to straighten the light and tubing to exclude passage of stray light is apparently sufficient to collimate the beam.

Uniform collimated light simplifies the task of determining particle size from signal pulse amplitude. Gubler develops a linear relationship between signal pulse amplitude and area of the beam obstructed. He bases this relationship on tests with spinning wires of various diameters. However the expression is not presented in the text. An equation to find the mass snow flux, Q kg $m^{-2}s^{-1}$, as a function of the total number of particles counted, N, is given as;

$$Q = N \frac{(1.42\ P_{dl}/2)^3 4/3\ \pi\ 918}{Tn\tau F}, \tag{17}$$

where P_{dl} is the smallest detectable particle diameter in metres, T is the period of time over which count N is taken in minutes, n is the number of samples per minute, τ is the duration of one sample in seconds and F is the sensitive area of the beam in m^2. Equation 17 is based on a "typical" particle size distribution (log-normal) recommended by Pope but unpublished and the results of the spinning wire pulse amplitude calibration.

Gubler notes that non-spherical particle shapes, deviations in the actual particle size distribution, effects from particles just grazing the beam and LED intensity changes with temperature all contribute significant deviations to calculated mass flux using Eq. 17. However even if these effects were compensated for, errors in using an extended linear object (spinning wire) instead of spheroids (snow particles) put the validity of the initial calibration in question. A linear object will have a different edge perimeter than a sphere of the same area and therefore a different diffraction effect. It is felt that the author's estimated accuracy in the mass flux measurement of ± 50% is conservative.

Schmidt et al. (1984) tested four snow particle counters against small filter fabric bag snow traps as described by Takeuchi (1980). Tested are his initial analog system (Schmidt, 1977), his digital system (Schmidt, 1984), a new system similar to the digital system but including particle speed in the flux calculation and Gubler's (1981) particle counter system. Filter fabric bag traps are reasonably accurate and efficient blowing snow traps when emptied frequently. Plots of the mass flux measured by the filter bags and those calculated by the snow particle counting systems show an almost random scatter (Fig. 3). The collection efficiencies of filter bags are not known to change erratically with either drift density or windspeed, and can be compensated for using wind tunnel tests to determine the aerodynamic efficiency of the bags (Takeuchi, 1980). It is therefore most probable that the scatter in the plots is due to inaccuracies in output from the snow particle counters.

It is apparent that after nearly 20 years of development, snow particle detectors are unable to provide reliable estimates of blowing snow mass flux and therefore the parameters of blowing snow transport that determine the mass flux. Factors that still impede the development of accurate snow particle counters are the variation in single snow particle extinction efficiency with distance from the detector, non-representative pulse amplitudes when a particle only grazes the beam, the large number of particles that must be sampled to describe a snow flux with confidence and the small amplitude of the individual pulses created by particles interrupting the detection beam. In both Schmidt's and Gubler's particle counters, pulses are often near the electronic noise level. These factors suggest that pending improvements in opto-electronic technology and optical theory, snow particle counters may not be suitable for use in measuring particle diameters and velocities in blowing snow.

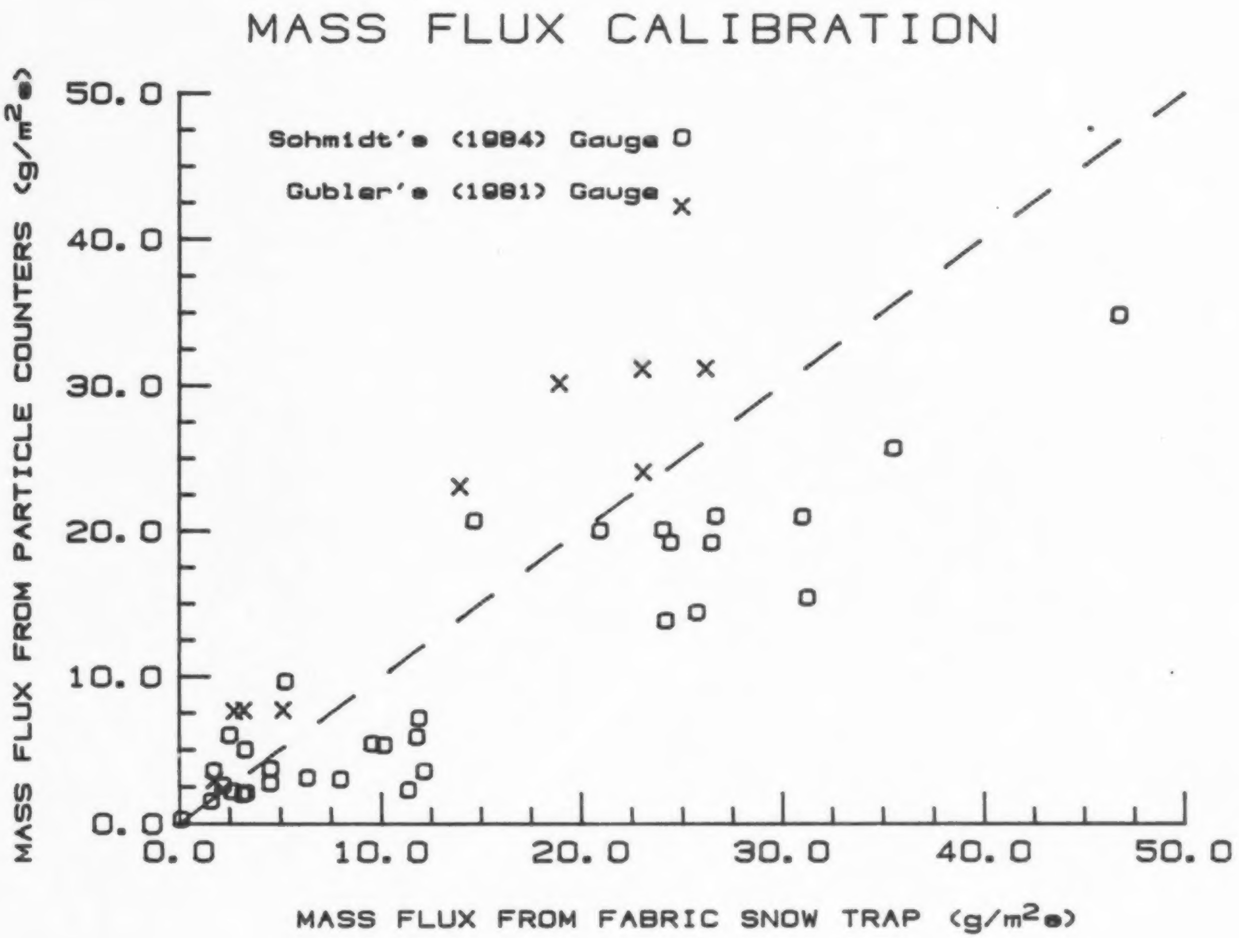

Figure 3. Comparison of the mass flux estimated by Schmidt's (1984) and Gubler's (1981) particle counters with that trapped by a fabric bag snow trap. The dashed line represents a 1:1 correlation (after Schmidt *et al.*, 1984).

BLOWING SNOW DETECTION SYSTEM

Based on the experiences of previous reseachers and considering the implications of geometrical optics theory for snow particles, it was decided that a gauge measuring multiple particle extinction in combination with a gauge measuring the number of single particle light extinction pulses would compose a reliable blowing snow detection system. Advances in opto-electronics since the 1960's have made the development of an accurate light extinction meter possible, however the reduction in transmittance measured by these meters is a function of the drift density and particle size distribution. Single particle detectors can accurately count particles, the number of particles counted can be related to the number density of blowing snow particles. Assuming a particle size distribution shape parameter, output from an extinction meter and particle detector can be used to find the drift density and mean particle radius of blowing snow. It will be shown that variation in α over its range in blowing snow leads to only minor variations in the results.

Infrared Extinction Meter

Desired attributes of a light extinction meter are; capability to detect incoming light accurately, negligible interference with the air-snow flux, capability to compensate for ambient light levels, stable light source intensity and spectral range, stable detector responsivity and signal output, low power consumption and inexpensive components. The gauge described here is an attempt to meet these criteria.

The extinction meter consists of an LED source and a photodiode detector, mounted 0.15 m apart on two supporting arms (Fig. 4). The LED (Motorola MLED 930) is approximately collimated by a convex lens. Beam divergence is less than 10° for irradiances greater than 90% of the maximum irradiance (Technical Information Centre, 1983). The spectral output of the LED reaches a maximum at a wavelength of 900 mm, in the near-infrared range of the spectrum (Fig. 5).

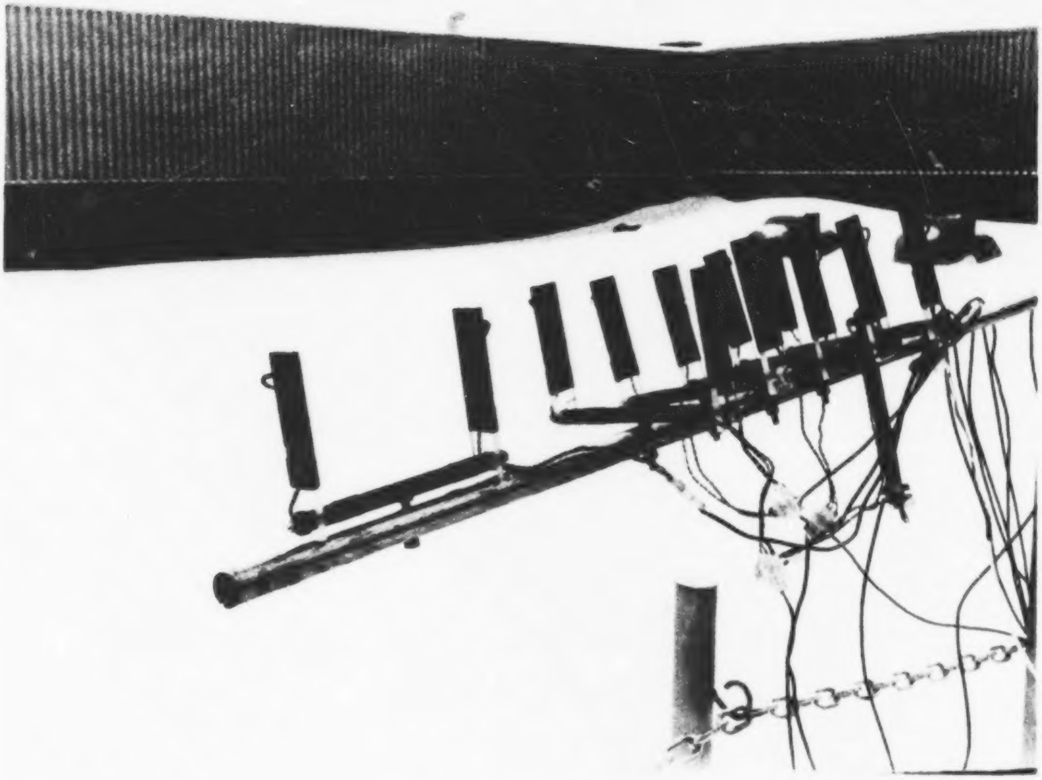

Figure 4. Infrared extinction meter.

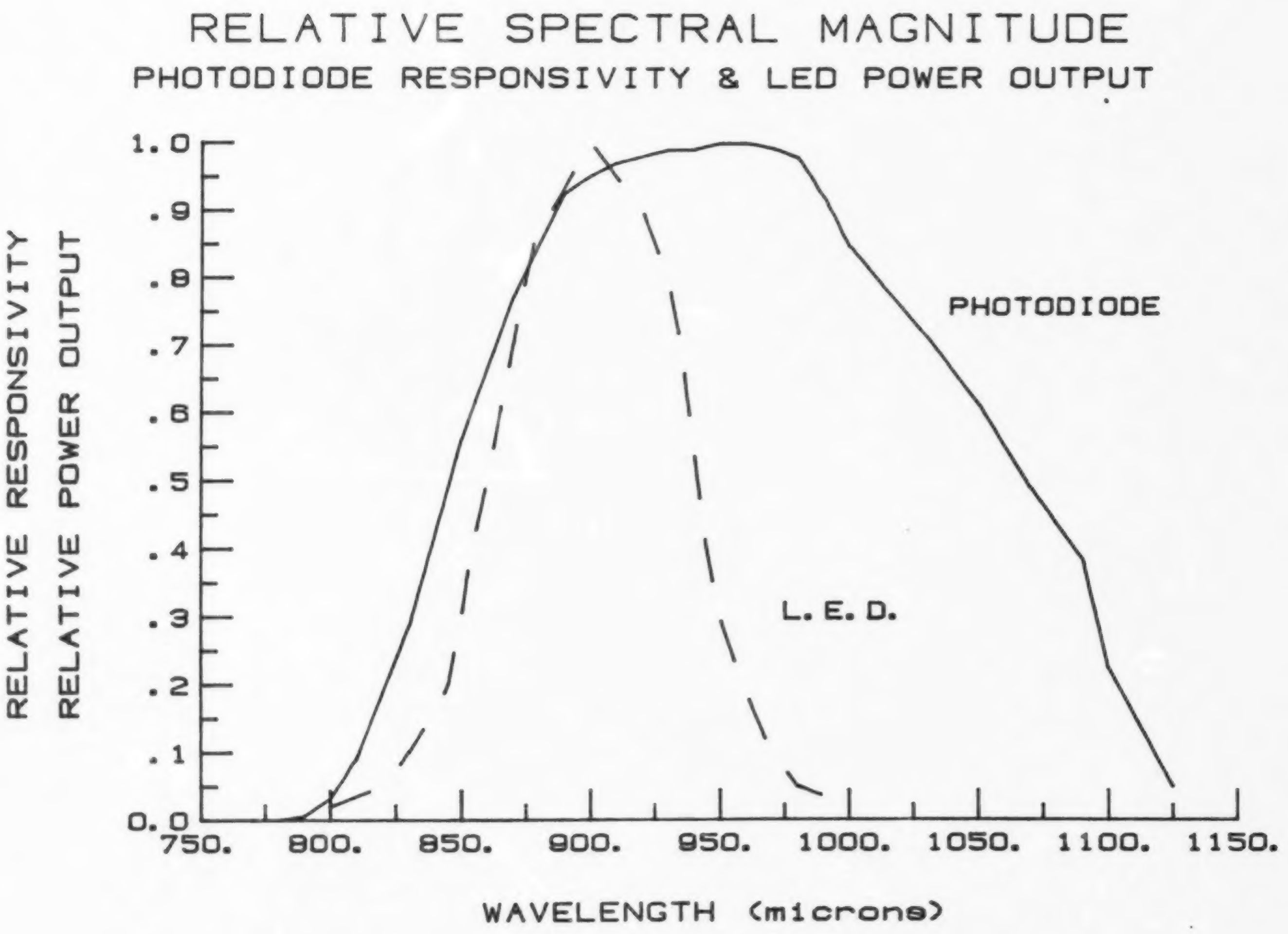

Figure 5. Spectral distributions of the relative photodiode responsivity and LED power output for the extinction meter and particle detector.

Relative power of the LED increases as the temperature decreases, at -32° C the output is twice that at 25° C (Technical Information Centre, 1983). The LED lens is circular with a radius of 1750 µm.

The photodiode (Silicon Detector Corporation SD-100-11-11-021) is operated in the photovoltaic mode, with peak responsivity at a wavelength of 900 nm. Solar radiation is reduced by water vapour absorption in this spectral range (Oke, 1978), resulting in less intense ambient light than levels found in the visible range. The detector is limited in its visible range by a visible light reducing filter (Kodak 87C). The responsivity of the detector with filter across the spectral range is well matched to the LED output (Fig. 5). The optimal frequency response of the photovoltaic detector for an 80% step in received radiation is 100 MHz. Typical response is somewhat slower. The detector is circular, with no optics and has an active detector surface radius of 1270 µm.

To compensate for the level of ambient light detected, the LED is switched. An ambient light reading is taken with the LED off and an ambient plus LED light reading is taken with the LED on. The current output from the detector is fed to an amplifier, which amplifies and converts the current signal to a voltage (Fig. 6). The voltage signal is then sent to an analog to digital converter (A/D converter), which integrates the signal over 33.3 ms, and digitizes the result. To maintain the input voltage for the A/D converter within its acceptable range (± 2V), an opposing "offset" current to offest ambient light is applied to the photodiode signal current before it reaches the amplifier. The magnitude of the offset current is adjusted until the analog signal voltage is within the A/D converters operating range. The offset current is selected on the first reading (LED off).

The pair of digitized voltages are read by a microprocessor which subtracts the voltage corresponding to ambient light from the voltage corresponding to ambient and LED light. The resultant voltage is a linear function of the

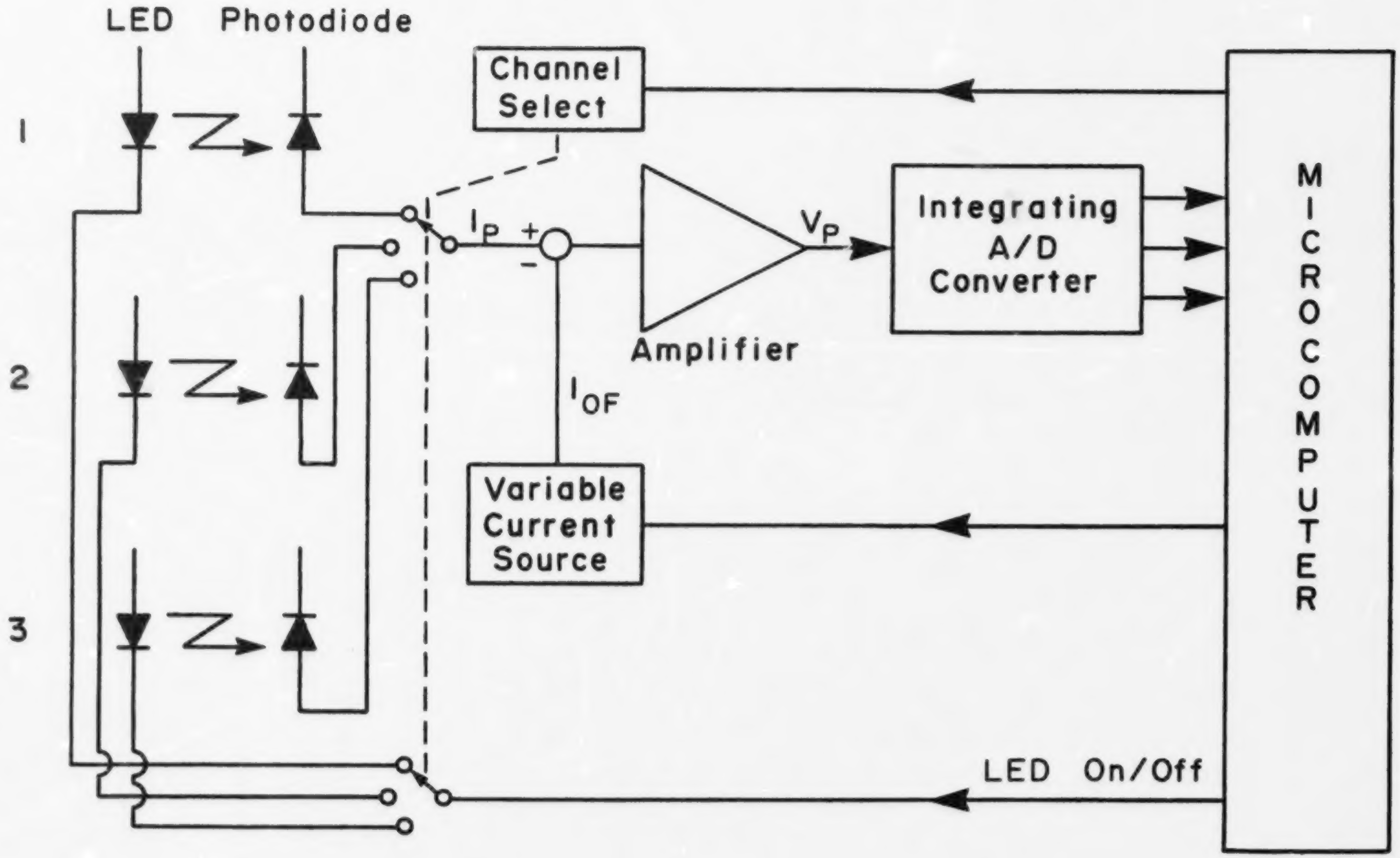
LED
Photodiode
1
2
3
Channel Select
I_P
+
−
I_{OF}
Amplifier
V_P
Integrating A/D Converter
Variable Current Source
MICROCOMPUTER
LED On/Off

Figure 6. Extinction meter signal processing (shown for several gauges).

radiant power received from the LED. A pair of readings is taken in sequence for each extinction meter in use (presently 8). Each meter is sampled every 56.25 sec. At the end of 7 1/2 min. the eight readings are averaged.

The extinction meter output is calibrated theoretically using geometrical optics theory. When extraneous factors affecting detector output are compensated for and the assumptions of geometrical optics theory met, theroretical calibrations of multiple snow particle light extinction gauges can be extremely accurate (Landon-Smith and Woodberry, 1965; Seagraves and Ebersole, 1983; Seagraves, 1984 and Winchester and Gimmestad, 1983). A major requirement of geometrical optics predictions is the use of approximately parallel light. While the extinction meter optics are not perfectly collimated, the maximum deviation of the active beam is only 0.18°. This deviation does not significantly affect the corrections to the extinction efficiency (ΔE_0, ΔE_2).

Equations 6 and 15 are used to calibrate the extinction meter output. In terms of gauge output, transmittance is defined as the ratio of the present output to the unattenuated output. To calibrate the gauge in terms of transmittance the inputs are; $\lambda = 900 \cdot 10^{-9}$m, $B_r = 1.27 \cdot 10^{-3}$m, m = 1.302, L = 0.15 m, $\rho_i = 930$ kg/m^3. Equation 15 is solved for σ using an array of the variables C kg/m^3, $\bar{P}_r$ m and α. Equation 6 is then solved for transmittance, using the extinction coefficient. The variation of transmittance with drift density for $\alpha = 10$ and a wide range of mean particle radii is shown in Fig. 7. Figure 7 demonstrates that for this gauge, a meansof estimating the mean particle radius is necessary for precise determination of the drift density from transmittance. Figure 8 shows the variation of transmittance with drift density for a common mean particle radius and a range of shape parameters of the particle radius distribution (α). The effect of α on the drift transmittance for a drift density is limited for most of the range of α.

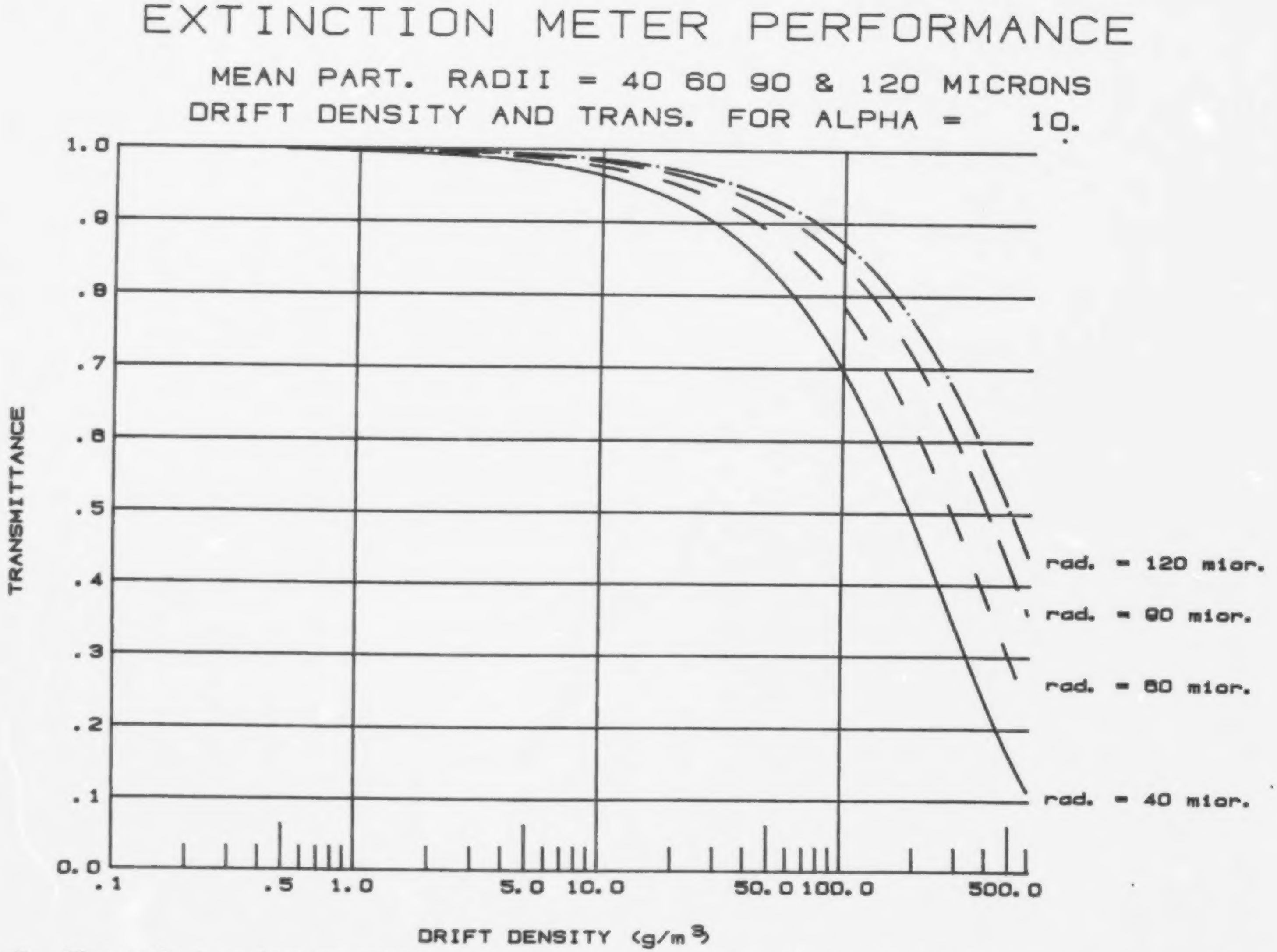

Figure 7. Theoretical extinction meter performance for particle radius distribution parameter, α = 10 and various mean particle radii.

Factors other than infrared extinction in blowing snow that might affect the gauge output are; temperature variations, frost accumulation on the LED and photodiode, changes in ambient light intensity that are faster than a pair of gauge readings (66 ms) and other light attenuating atmospheric phenomena. Since blowing snow is accompanied by a strong degree of atmospheric surface layer mixing, phenomena associated with temperature inversions such as fog and ice crystals are usually not concommitant with blowing snow. Any levels of ambient light not subtracted from the signal will be gaussian in magnitude and will tend to average out. Operator maintenance and the small quantity of heat produced by the LED can control frost and snow accumulation on the gauge during light winds. High winds tend to clear snow and ice crystals from the detector and source windows. Variation with temperature of the LED radiant power, photodiode responsivity and system voltage changes the gauge output. Use of a reference gauge, shielded from blowing snow or a calibration of output against gauge temperature during periods of no blowing can compensate for this effect.

Particle Detector

The particle detector is inspired by Gubler's (1981) model, however it is designed to simply count particles. Construction is similar to the infrared extinction meter, with an LED source and photodiode detector mounted 0.02 m apart on two supporting arms (Fig. 9). The LED (Motorola MLED 930) is identical to that in the extinction meter. However, to insure a light beam of constant cross-sectional area along its length, the LED beam is shone through a 500 μm diameter hole. The hole is precision drilled in a brass shim plate. The light leaving this hole is well collimated.

The photodiode is a smaller version of that used in the infrared extinction meter (Silicon Detector Corp. 50-020-11-11-011), with identical relative responsivity over its spectral range. Ambient light reception is limited by a filter identical to that on the extinction meter. The optimal frequency response of

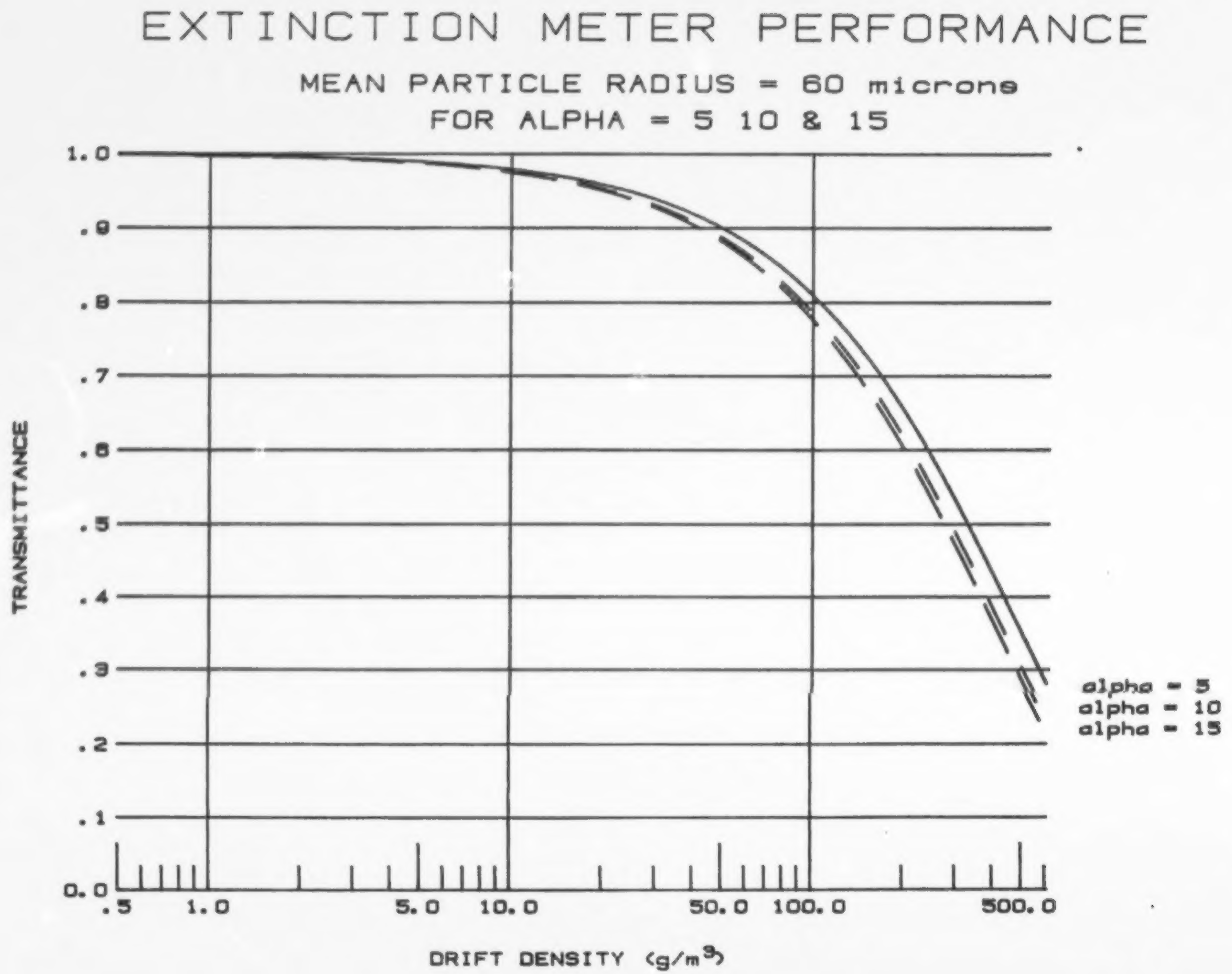

Figure 8. Theoretical extinction meter performance for mean particle radius = 60 μm and various gamma distribution shape parameters.

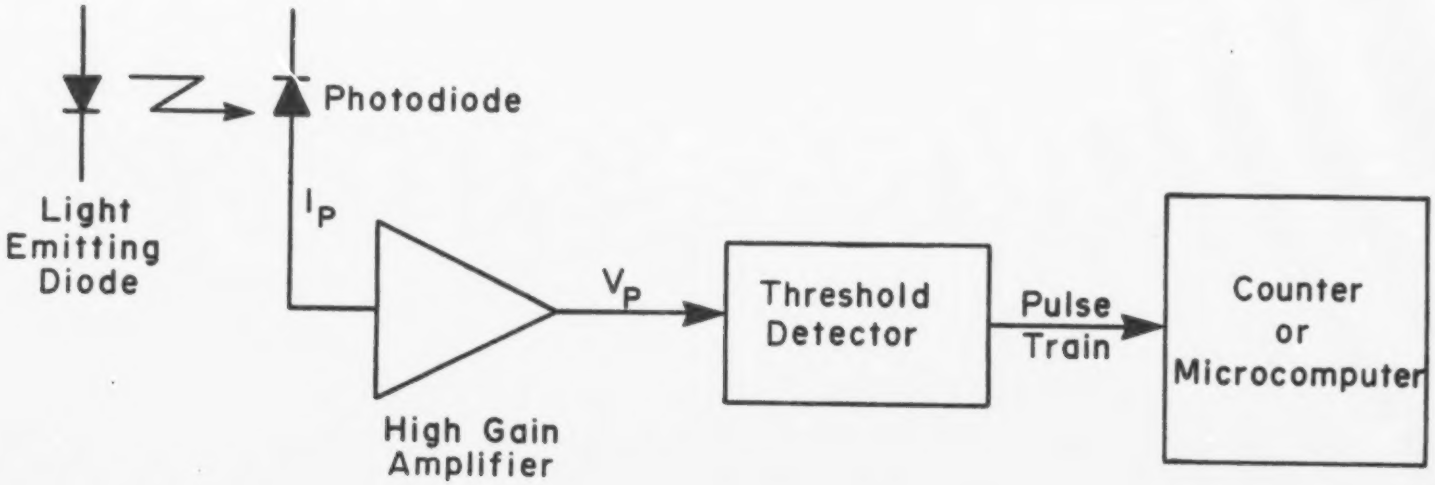
Light
Emitting
Diode
Photodiode
I_P
High Gain
Amplifier
V_P
Threshold
Detector
Pulse
Train
Counter
or
Microcomputer

Figure 10 Particle detector signal processing.

the photovoltaic detector for an 80% step in received radiation is 143 MHz. The active detector surface radius is 254 μm, identical to that of the light exit window of the LED.

When a particle interrupts the light beam, there is a momentary drop in the photodiode output signal. Current from the photodiode is fed to a high gain amplifier which converts the current signal to a voltage signal. This signal is filtered to eliminate low frequency noise (ambient light, AC). The voltage signal is sent to a threshold detector, which produces an output for each pulse whose amplitude is greater than a threshold voltage. This signal is sent to a pulse counter (Fig. 10).

A typical pulse amplitude from a blowing snow particle is in the range of microvolts and therefore difficult to detect electronically. The problem is compounded by the nature of the pulse, it is not with respect to the ground but rides on top of a high level signal caused by the ambient light and the LED output. In practise, the threshold amplitude of detection is determined by the responsivity of the detector, level of electronic noise, limits of the amplifier, speed of response and resolution of the threshold detector. Only those particles eliciting a pulse amplitude above the threshold can be counted.

The pulse amplitude is a function of the particle radius, crossing position between the source and detector, cross-sectional trajectory through the beam, particle velocity, and the electronic system frequency response and electronic noise level at the time of detection. The projected area of the particle in the beam is a function of the cross-sectional area and trajectory of the particle in the beam. The effective radius of the particle is the radius of a circle of equivalent area to the projected area of the particle. The influence of the effective radius and distance from the particle to the detector on the drop in transmittance can be calculated using Eq. 2 and is shown in Fig. 11. The effective radius of the particle E_r, is substituted for P_r in the calculation. The

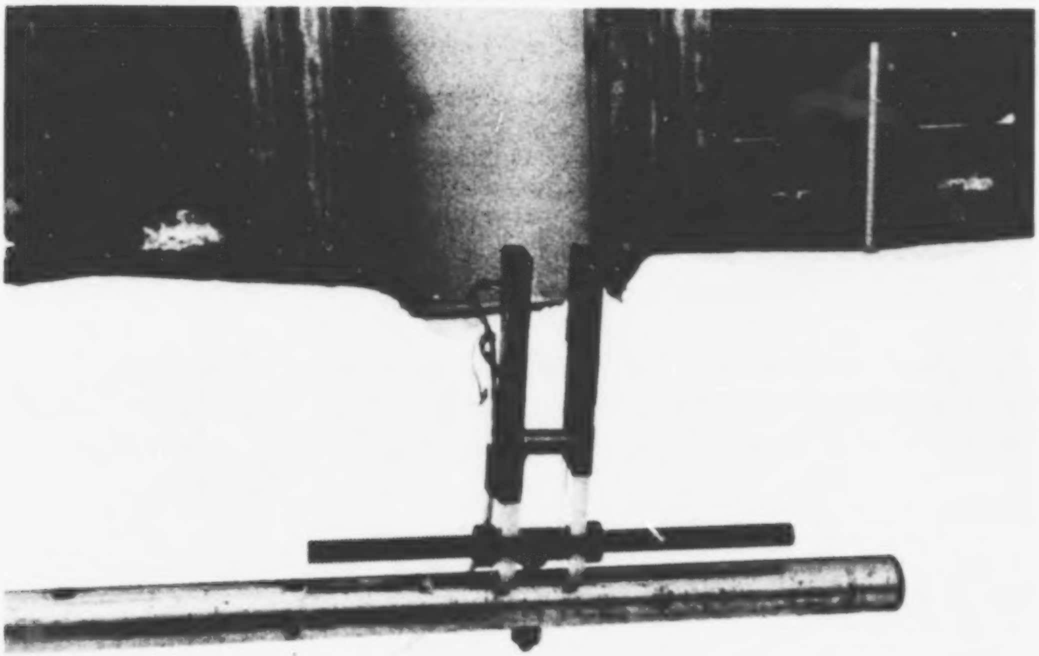

Figure 9. Particle detector.

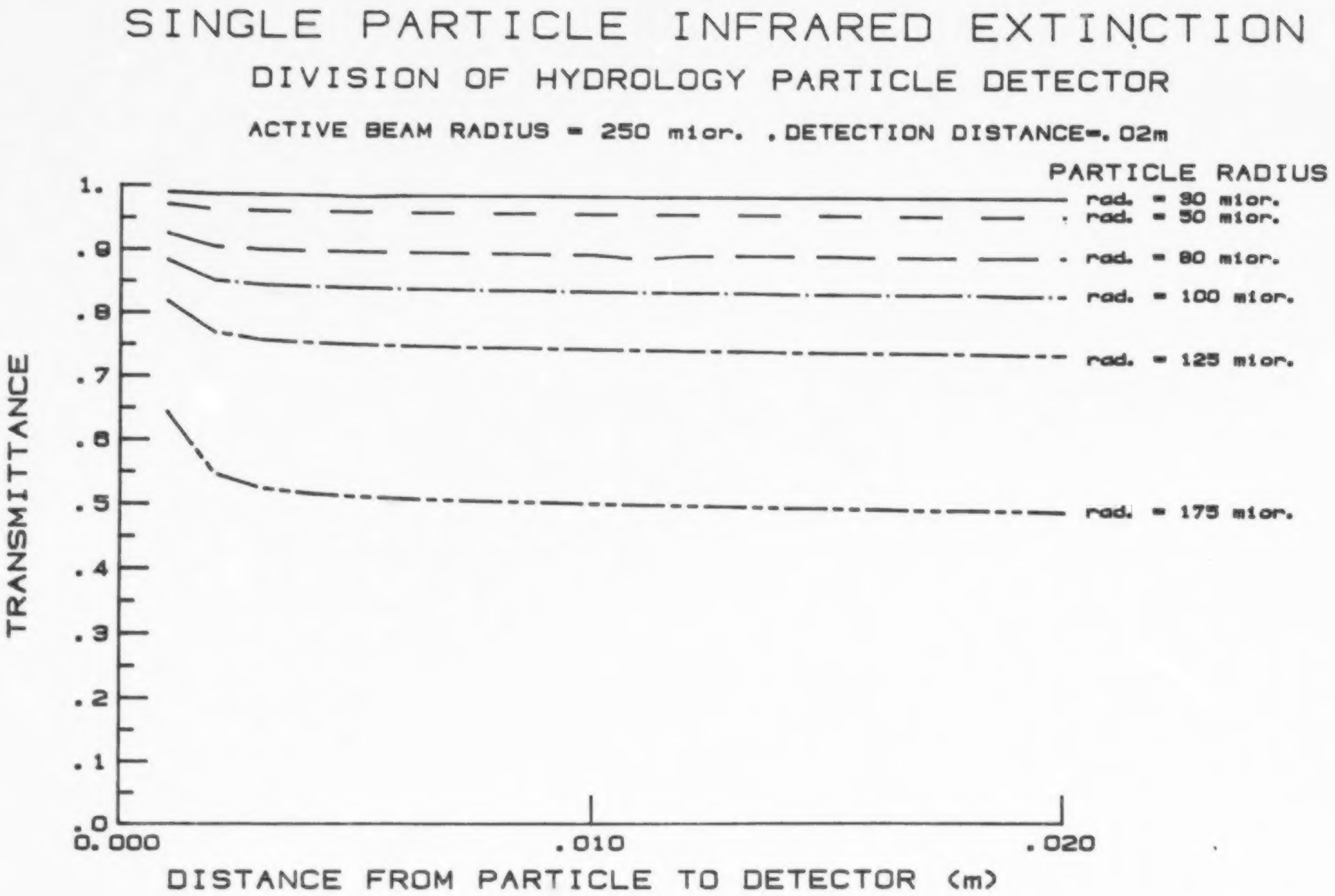

Figure 11. Single particle infrared extinction for several effective particle radii in the particle detector.

small transmittance drop for smaller particles makes it evident that not all particles can be counted.

For a given pulse threshold and frequency response and assuming particle speed and the electronic noise level are constant, a threshold transmittance can be defined. This is the transmittance associated with the smallest detectable pulse. Using Eq. 2, this level of transmittance can be related to the effective radius of a particle. The threshold effective radius E_{tr}, is the radius resulting in a transmittance at the threshold of detection. For a threshold effective radius and some particle radius greater than E_{tr}, there will be a maximum distance from particle centre to beam centre such that the threshold effective radius is exceeded. This distance above and below the beam centre is the vertical component of the detector sampling area, referred to as the sampling height of the detector for that particle radius and velocity.

The sampling height of the beam for a particle size and velocity is found using the geometry of the particle and beam cross-sections. The threshold transmittance (a function of the particle velocity) T_t, can be used to find the threshold effective radius E_{tr}, where;

$$E_{tr} = B_r\sqrt{(T_o - T_t)/E_c} \quad . \tag{18}$$

The projected area of the particle in the beam A_p, is

$$A_p = \pi E_{tr}^{\;2} \quad . \tag{19}$$

The distance G, from the particle centre to the beam centre, must be calculated using two different procedures. For case 1, where $A_p/\pi P_r^{\;2} < \frac{1}{2}$, the projected area is the shaded area of intersection of the beam and particle shown in Fig. 12. This area is calculated using the geometry of the beam and particle cross-sections. Thus,

$$P_r^{\;2}X + B_r^{\;2}Y - P_r\sin(2X) + B_r\sin(2Y) = A_p \quad , \tag{20}$$

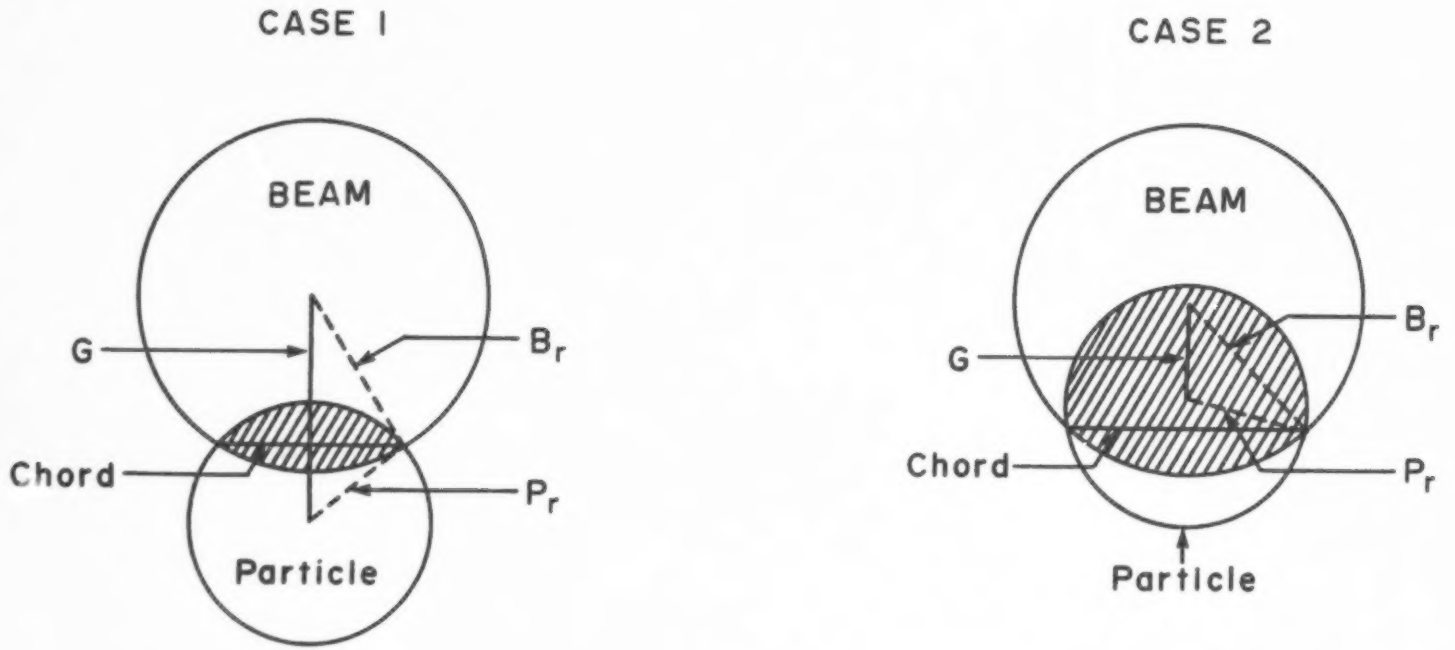
CASE I
BEAM
G
B_r
Chord
P_r
Particle
CASE 2
BEAM
G
B_r
Chord
P_r
Particle

Figure 12. Particle-beam cross-sectional geometry for the particle detector. Shaded areas denote the projected area of the particle, P_r is the particle radius, B_r is the beam radius and G is the distance from the beam centre to the particle centre.

where: $$X = \arccos\left(\frac{G^2+P_r{}^2-B_r{}^2}{2GP_r}\right) ,$$

$$Y = \arccos\left(\frac{G^2+B_r{}^2-P_r{}^2}{2GB_r}\right) .$$

G can be found from Eq. 20 using a trial and error procedure. For case 2 where $A_p/\pi P_r{}^2 \geq \frac{1}{2}$, the projected area is calculated using the somewhat different geometry of the beam and particle as shown by the shaded area in Fig. 12. Thus,

$$\pi P_r{}^2 + B_r{}^2 Y - P_r{}^2\ [1.571 - X] - B_r \sin(2Y) + P_r \sin[2(1.571 - X)] = A_p\ . \qquad (21)$$

Again G can be found using a trial and error procedure. The sampling height H_s, is twice the distance between the beam centre and the particle centre, when that particle is projecting an area possessing the threshold effective radius and the particle is at the closest point to the beam centre in its trajectory.

To find a representative sampling height across the beam length, changes in the corrected extinction efficiency with distance from the detector should be taken into account. For this particle detector the variation is not large and a simple averaging procedure is used. Thus,

$$\overline{E}_{tr} = B_r \int_o^L \sqrt{(T_o - T_t/E_c}\ d\ell \ . \qquad (22)$$

$\overline{E}_{tr}$ is the mean threshold effective radius of the detection width. When $\overline{E}_{tr}$ is used to calculate G, twice G is $\overline{H}_s(P_r,U)$, the mean sampling height for a particle radius and velocity U. The sampling area A_s is

$$A_s(P_r,U) = \overline{H}_s(P_r,U)L \quad . \qquad (23)$$

When numbers of particles are considered in blowing snow conditions, the horizontal wind velocity can be considered equivalent to the horizontal particle velocity.

The number density of blowing snow particles can now be calculated from the number of particles counted per unit time and the windspeed. For a monosized particle distribution with constant windspeed and $P_r > E_{tr}$

$$N = \phi/uA_s \quad . \tag{24}$$

N is the number density of particles in #/m³, ϕ is the number of particles counted per second by the particle detector in #/s, u is the windspeed in m/s and A_s is the sampling area perpendicular to the snow flux, in m². For a gamma density function distribution of particle radii and a windspeed u for which there is a threshold particle radius P_{tr}, N is found by dividing the number density of particles greater than P_{tr} by the cumulative frequency of particles greater than P_{tr}. P_{tr} is defined as the particle radius for which $A_s = 0$, and is a function of the windspeed. For a constant windspeed u, N is found by

$$N = \frac{\int_{P_{tr}}^{\infty} \eta(P_r)/A_s(P_r)\, dP_r}{u\int_{P_{tr}}^{\infty} f(P_r)\, dP_r} \quad , \tag{25}$$

where $\eta(P_r)$ is the number of particles of radius P_r counted per second. Note that P_{tr} is a function of the windspeed u. The output of the particle detector, ϕ is the number of particles per second integrated over the interval from P_{tr} to infinity, not $\eta(P_r)$. For the cumulative frequency of particles greater than some threshold, P_{tr} is given by the cumulative frequency of all particles less the cumulative frequency of particles with radii below the threshold (Haan, 1977). If α is an integer, the cumulative frequency of P_r greater than P_{tr}, where j is an integer (Haan, 1977), is;

$$\int_{P_{tr}}^{\infty} f(P_r)\, dP_r = e^{(-P_{tr}/\beta)} \sum_{j=0}^{\alpha-1} (P_{tr}/\beta)^j/j! \quad . \tag{26}$$

To find $\eta(P_r)$ for any P_r, ϕ is multiplied by the frequency of P_r as given by the gamma density function distribution of particle radii. Thus

$$\eta(P_r) = \frac{\phi P_r^{\alpha-1} e^{(-P_r/\beta)}}{\beta^{\alpha}\Gamma_{(\alpha)}} \quad . \qquad (27)$$

N, as found from the particle detector output ϕ is therefore;

$$N = \frac{\phi \displaystyle\int_{P_{tr}}^{\infty} (P_r^{\alpha-1} e^{(-P_r/\beta)})/\Lambda_s(P_r,U)\,dP_r}{u \displaystyle\int_{P_{tr}}^{\infty} P_r^{\alpha-1} e^{(-P_r/\beta)}\,dP_r} \quad , \qquad (28)$$

where the threshold particle radius and size and shape parameters of the gamma distribution are known. Confidence in N as obtained from this equation depends on the value of P_{tr} in comparison with the distribution of particle radii. If P_{tr} is large with respect to the radius distribution, N will be based on very few observations. However, if P_{tr} is small, the number density of snow particles can be calculated with a high degree of confidence. For a given detector performance level, P_{tr} is a function of windspeed, therefore the accuracy of Eq. 28 will decrease as u increases. The sensitivity of the electronic detection system is therefore an important factor in determining the range of conditions in which a particle detector is useful.

Operation of the Blowing Snow Detection System

The infrared extinction meter, particle detector and an anemometer compose the instruments necessary to determine the mass flux and particle radius distribution of blowing snow. Both the extinction meter and particle detector are sensitive to the particle size distribution, and their separate outputs require knowledge of α and β for correct interpretation. When the outputs of both gauges are used to solve for N, the number density of particles, only α need be assumed. The errors involved in incorrectly characterizing α are small (Fig. 8). A snow particle photography system is presently being used to find characteristic α's for blowing snow conditions in Western Canada. By solving for N by using the outputs of both gauges, β becomes the only unknown.

Recall Eq. 12 which is now solved for N;

$$N = \frac{\sigma_\lambda \beta^\alpha \Gamma_{(\alpha)}}{\pi \int_0^\infty \bar{E}_c \, P_r^{(\alpha-1)} \, e^{(-P_r/\beta)} P_r^2 dP_r} \quad . \tag{29}$$

This is equated to Eq. 28, which is also solved for N. Using trial and error solutions for N, β can be found. With α estimated, the mean particle radius is;

$$\bar{P}_r = \alpha\beta \quad . \tag{30}$$

Equation 14 is then solved for the drift density, C, using the particle radius distribution and the extinction coefficient. Where;

$$C = \frac{4 \, \sigma_\lambda \rho_i \int_{P_r} P_r^{(\alpha+2)} e^{(-P_r/\beta)} \, dP_r}{3 \int_{P_r} \bar{E}_c \, P_r^{(\alpha+1)} e^{(-P_r/\beta)} \, dP_r} \quad . \tag{31}$$

The drift flux is found by multiplying the drift density by the windspeed;

$$q = C \, u \quad . \tag{32}$$

Where q is the drift flux in kg $m^{-2} s^{-1}$. Other values that can be calculated from the gauge outputs include the frequency distributions of particle diameters, masses and surface areas. These variables are useful in determining fall velocities and sublimation rates for the snow particles.

As shown in Eqs. 6, 15 and 30, the transmittance for a particular drift density responds to changes in $\overline{P}_r$ when α is held constant. The wide range of transmittances caused by variation in $\overline{P}_r$ with α held constant is shown in Fig. 7. When compared to the narrow range of transmittances caused by variation in α with $\overline{P}_r$ held constant (Fig. 8), it is evident that most of the uncertainty in calculating C from the extinction meter output is due to β . Solving for β by using the particle detector output with the extinction meter output (Eqs. 28 & 29) allows more precise interpretation of the extinction meter output.

At this time a calibration curve between particle velocity and the threshold effective particle radius is being developed for the particle detectors. It is expected that a separate relationship will be developed for each gauge, as their response varies somewhat. These relationships will allow calculation of the sampling areas of the particle detectors for various particle velocities. This is the only empirical calibration required for interpreting the gauge outputs. A complete test of the detection system involves comparing the particle radius distribution as calculated from the extinction meter, particle detector and anemometer outputs to that measured by photographic techniques. Such a test will be completed in the near future.

CONCLUSION

The blowing snow detection system and data analysis procedure described here are capable, in principle, of giving precise estimates of blowing snow parameters. Such systems depend on the optical properties and the extinction capabilities of small spheres, but the analysis of the optical effects of blowing snow is not straightforward. Using geometrical optics approximations, it has been demonstrated that theoretical calibrations of multiple particle light extinction meters and single particle counters are possible when the optical characteristics of the measuring system are known. Thus, "black box" calibrations are not required. The gauges incorporate improvements in opto-electronic and signal processing design over previous gauges. These improvements lead to enhanced sensitivity, response time, stability and data retrieval characteristics. In addition the resulting gauges are amenable to theoretical calibration.

Potential problems with the system may result from the estimation of particle velocities from wind velocity. This may limit the effectiveness of the present analysis procedure for data collected from the lower saltation layer. At the top of the saltation layer and in the suspended layer, horizontal particle velocities tend to approximate horizontal wind velocities (White, 1982). Of importance to the operation of the system is keeping the smallest detectable particle size for the particle detector low. This is necessary to maintain the accuracy of the calculation of the particle radius distribution.

Because of its minimal interference in the windstream, continuous monitoring capability and detailed data collection it is felt that this blowing snow detection system will increase our understanding of the blowing snow phenomena.

REFERENCES

Budd, W.F., 1965. The drifting of nonuniform snow particles. In M. Rubin (ed.), Studies in Antarctic Meteorology. American Geophysical Union, Antarctic Research Series, 9. pp. 59-70.

Budd, W.F., Dingle, R. and Radok, U., 1965. The Byrd snow drift project: Outline and basic results. In M. Rubin (ed.), Studies in Antarctic Meteorology. American Geophysical Union, Antarctic Research Series, 9. pp. 71-134.

Gubler, H., 1981. An electronic remote snow-drift gauge. Journal of Glaciology, 27(95). pp. 164-174.

Haan, C.T., 1977. Statistical Methods in Hydrology. The Iowa State University Press, Ames, Iowa. 378 p.

Hobbs, P.V., 1974. Ice Physics. Oxford University Press, London. 837 p.

Hodkinson, J.R. and Greenleaves, I., 1963. Computations of light-scattering and extinction by spheres according to diffraction and geometrical optics, and some comparisons with the Mie theory. Journal of the Optical Society of America, 53(5), pp. 577-588.

Hollung, O., Rogers, W.E. and Businger J.E., 1966. Development of a system to measure the density of drifting snow. University of Washington, Dept. of Electrical Engineering, Dept. of Atmospheric Sciences, Joint Technical Report, Seattle. 54 p.

Kobayashi, D., 1972. Studies of snow transport in low-level drifting snow. Contributions from the Institute of Low Temperature Science, A24. pp.1-58.

Landon-Smith, I.H. and Woodberry, B., 1965. The photoelectric metering of wind-blown snow. ANARE Interim Reports, Series A(IV) No. 79. Antarctic Division, Dept. of External Affairs, Melbourne. pp. 1-17.

Liou, K., 1980. An Introduction to Atmospheric Radiation. Academic Press, New York. 392 p.

Mellor, M., 1965. Blowing Snow. Cold Regions Science and Engineering, Part III, Section A3C, Cold Regions Research and Engineering Laboratory. U.S. Army Materiel Command, Hanover, NH. 85 p.

Oke, T.R., 1978. Boundary Layer Climates. Metheun and Co. Ltd., London. 372 p.

Orlov, N.I., 1961. Novyi metod izmereniia perenosa snega (New method of measuring blowing snow). In Rol'snezhnogo pokrova v prirodnykh protsessakh. Institut Geografii, Akad Nauk SSSR. (In Russian).

Owen, P.R., 1964. Saltation of uniform grains in air. Journal of Fluid Mechanics, 20. pp. 225-242.

Schmidt, R.A., 1977. A system that measures blowing snow. U.S.D.A. Forest Service Research Paper RM-194. Rocky Mountain Forest and Range Experiment Station, Fort Collins, CO. 33 p.

Schmidt, R.A., 1981. Estimates of threshold windspeed from particle sizes in blowing snow. Cold Regions Science and Technology, 4. pp. 187-193.

Schmidt, R.A., 1982. Vertical profiles of windpseed, snow concentration and humidity in blowing snow. Boundary Layer Meteorology, 23. pp. 223-246.

Schmidt, R.A., 1984. Measuring particle size and snowfall intensity in drifting snow. Cold Regions Science and Technology, 9. pp. 121-129.

Schmidt, R.A., Meister, R. and Gubler, H., 1984. Comparison of snow drifting measurements at an alpine ridge crest. Cold Regions Science and Technology, 9. pp. 131-141.

Seagraves, M.A. and Ebersole, J.F., 1983. Visible and infrared transmission through snow. Optical Engineering, 22(1), pp. 90-93.

Seagraves, M.A., 1984. Precipitation rate and extinction in falling snow. Journal of the Atmospheric Sciences, 41(11), pp. 1827-1835.

Sommerfeld, R. and Businger, J.A., 1965. The density profile of blown snow. Journal of Geophysical Research, 70(14), pp. 3303-3306.

Takeuchi, M., 1980. Vertical profile and horizontal increase of drift snow transport. Journal of Glaciology, 26(94), pp. 481-492.

Technical Information Centre, 1983. Motorola Optoelectronic Device Data. Motorola, Inc., Phoenix, AZ.

Ungut, A., Grehan, G. and Gouesbet, G., 1981. Comparisons between geometrical optics and Lorenz-Mie theory. Applied Optics, 20(17), pp. 2911-2918.

van de Hulst, H.C., 1957. Light Scattering by Small Particles. John Wiley and Sons, New York. 470 p.

White, B.R., 1982. Two-phase measurements of saltating turbulent boundary layer flow. International Journal of Multiphase Flow, 8, pp.459-473.

Winchester, L.W. and Gimmestad, G.G., 1983. Scattering corrections to extinction coefficients measured in falling snow. Optical Engineering, 22(1), pp. 86-89.

Wishart, E.R., 1965. A new photoelectric drift snow gauge. ANARE Interim Reports Series A(IV), No.79. Antarctic Division, Department of External Affairs, Melbourne. pp. 23-26.

Zuev, V.E., 1970. Propagation of Visible and Infrared Radiation in the Atmosphere. Translation by D. Lederman. Israel Programme for Scientific Translations, London. 405 p.

MEASUREMENTS OF THE CONCENTRATION OF FALLING SNOW

by

J.R. Stallabrass

National Research Council of Canada
Division of Mechanical Engineering
Ottawa, Ontario
Canada

presented at

SNOW PROPERTY MEASUREMENTS WORKSHOP

Lake Louise, Alberta

1-3 April, 1985

TECHNICAL MEMORANDUM 140

Compiled By

P.R. Kry

NRCC 27594

MEASUREMENTS OF THE CONCENTRATION OF FALLING SNOW

Introduction

Because of the lack of data on the mass concentration of falling snow in the atmosphere, a programme of measurement was instituted in the Low Temperature Laboratory. This lack of data first became apparent as a result of engine problems during helicopter flight in falling snow (Ref. 1). However, knowledge of the snow concentration has a wider interest and has application to snow ingestion problems of various sorts (railway locomotives, stationary gas turbine installations, etc.), to the accumulation of wet snow on transmission lines and communication equipment, to obscuration problems of visible and infra-red propagation through falling snow, etc.

This paper presents an update of results that have been presented previously elsewhere.

The mass concentration can, in theory, be derived from the precipitation rate but requires a knowledge of the fall velocities of the spectrum of snow particles comprising the snowfall. Unlike rain, for which the liquid water content may be derived from precipitation rate with some confidence, the derivation of snow mass concentration from snowfall rate is unreliable because of the dependence of the terminal velocities of the snow particles not only on their size but also on their form, their degree of aggregation into flakes, and their liquid water content in the case of wet snow. Add to this the fact that snowfall rates are averages over a period of time (quite customarily six hours), and it is clear that some direct means of measuring the concentration is needed. Further, such measurements might show whether it is possible to estimate the snow concentration using other easily and routinely measured meteorological parameters, such as visibility, temperature and relative humidity.

Snow Measuring Apparatus

After reviewing other possible means of detecting and measuring the snow content of the air, such as capacitance methods, it was decided to use the most basic and absolute method, that of actually sampling the mass of snow in a given volume of air. The sampling device, which was swept through the air at the end of a rotating arm (Fig. 1), employed the principle of inertial separation to capture the snow for measurement of its mass.

The measurements made fell into two phases; first a manual or discrete sampling phase during which various other parameters were measured or observed simultaneously to try to determine any interrelationships. These parameters were air temperature, relative humidity, wind speed and direction, precipitation rate, observed visibility, Videograph* output, and snow crystal type and estimate of mean size. A description of the precipitation gauge is given in the Appendix.

---

* The Videograph is a back-scatter visibility meter developed by Dr. F. Fruengel of Germany and manufactured in Canada by Sperry Inc. Electronic Systems.

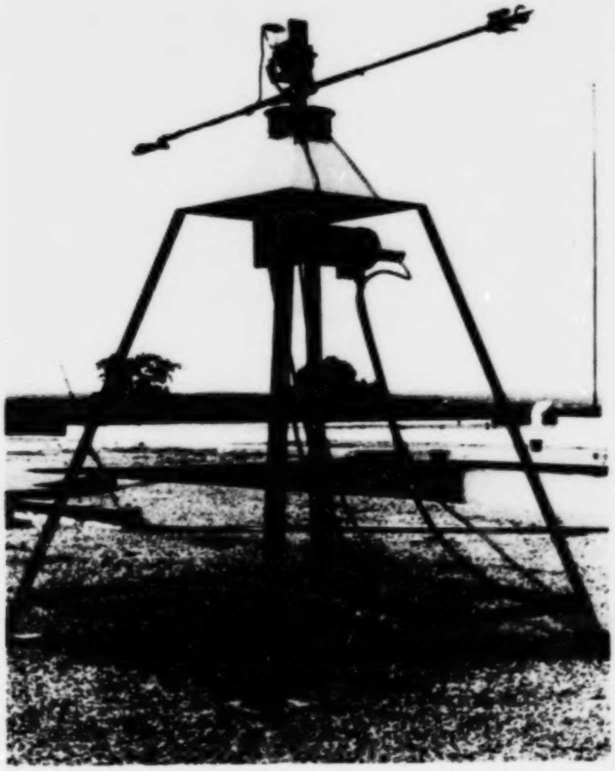

FIG. 1 WHIRLING ARM APPARATUS,
MANUAL CYCLONE SAMPLER ON NEAR ARM,
AUTOMATIC SNOW CONTENT METER ON FAR ARM

The second or automatic phase, in which longer term data on the snow concentration cumulative frequency are being collected, uses a fully automatic sampler or snow content meter (SCM). This instrument takes successive 1-minute average concentration values. A data system records every 10 minutes the last 1-minute average as well as the average over the preceding 10-minute period. Also recorded simultaneously are air temperature, dew point, wind speed and direction, and Videograph output.

Manual Phase. During this first phase of the measurements, a cyclone separator was used as the snow collecting device (Fig. 2). The captured snow was weighed after a given sampling period, usually between 2 and 6 minutes depending on the estimated intensity, and, knowing the area of the sampling inlet and its velocity through the air, the mass concentration was derived. Flow through the separator ensured a high catch efficiency, while both cyclone and centrifugal action ensured efficient separation of the snow from the air with little chance of particle re-entrainment in the exhausting air.

Automatic Phase. The snow content meter, which was developed during the preceding manual phase of the measurements, was initially mounted on the opposite end of the rotating arm from the cyclone separator for comparison purposes. Subsequently, SCMs have been mounted at both ends of the arm. The SCM is a simplified form of inertial separator (Fig. 3) wherein inertia and coriolis forces restrain the snow particles to flow down the back side of the sampling tube, while the air exits by a few small holes in the front of the tube, but is then directed around the tube to finally exhaust in the rear. At the tube's extremity the snow is melted and flows through a squared-off hypodermic needle under the influence of the centrifugal acceleration. The resulting droplet stream is monitored photoelectrically and the pulses so generated are counted over a 1-minute time period to obtain the snow concentration. Using a calibration based on the drop size data of Harkins and Brown (Ref. 2), the resulting performance was found to be in close agreement with the concentration mesurements provided by the cyclone device.

Results of Manual Phase Measurements

Snow Type Classification. Snow crystal type was observed by allowing a number of crystals or flakes to fall onto a velvet covered board. The crystal classification scheme of Magono and Lee (Ref. 3) was used in recording crystal type. However, for the purposes of correlating the data, many of these types were grouped together reducing the individual categories to 9, as shown in Table 1.

Concentration and Visibility. The most significant correlation between the various measured variables was that between the mass concentration and the visibility. It was expected that, since, in the absence of precipitation, the visibility was dependent to a large extent on relative humidity, the introduction of this parameter into the regression analysis would help to resolve some of the scatter in the Concentration-Visibility plot (Fig. 4). However, it was found that the relative humidity was itself influenced by the snow intensity and hence was not an independent variable that could be taken properly into regression.

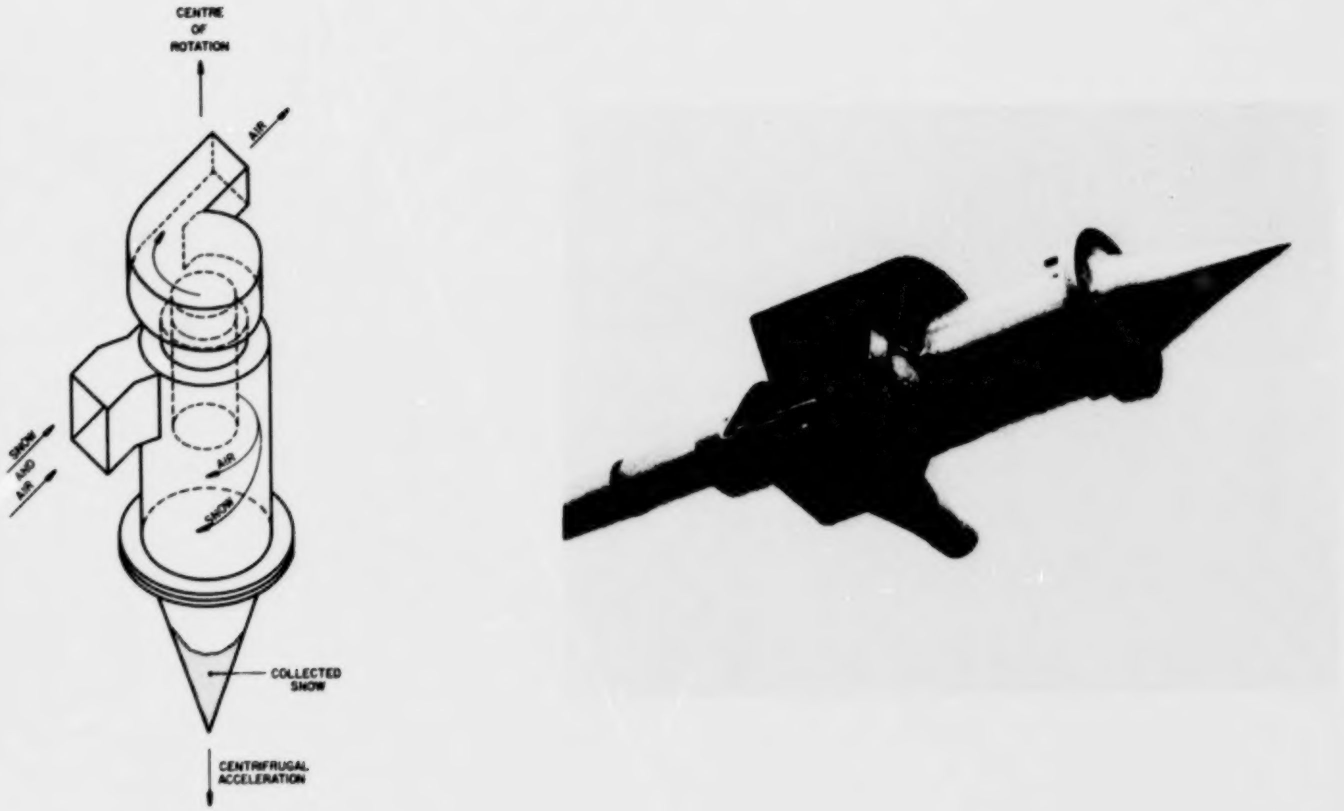
CENTRE OF ROTATION
AIR
SNOW AND AIR
AIR
SNOW
COLLECTED SNOW
CENTRIFRUGAL ACCELERATION

FIG. 2 CYCLONE SEPARATOR USED FOR MANUAL MEASUREMENT OF SNOW MASS CONCENTRATION

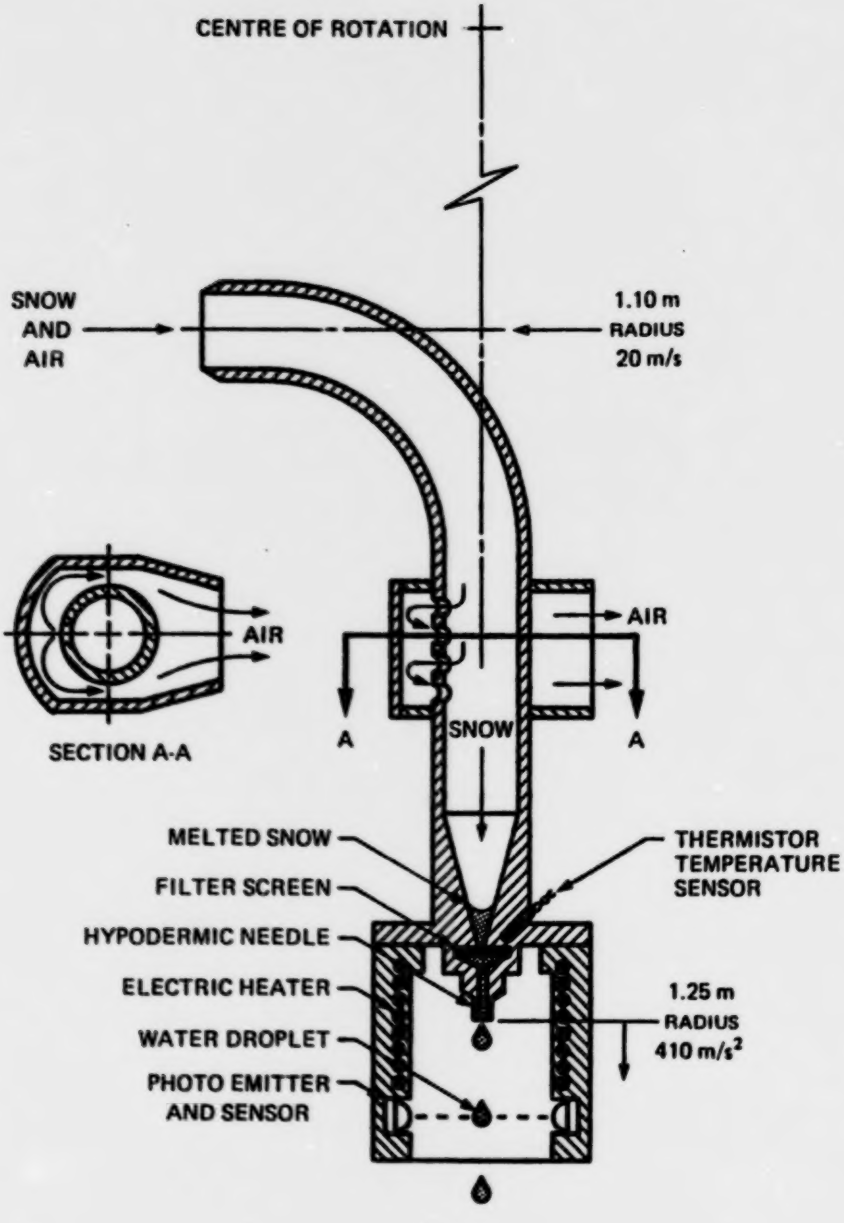
CENTRE OF ROTATION
SNOW AND AIR
1.10 m RADIUS 20 m/s
AIR
AIR
A
A
SECTION A-A
SNOW
MELTED SNOW
FILTER SCREEN
HYPODERMIC NEEDLE
ELECTRIC HEATER
WATER DROPLET
PHOTO EMITTER AND SENSOR
THERMISTOR TEMPERATURE SENSOR
1.25 m RADIUS 410 m/s²

FIG. 3 SNOW CONTENT METER USED FOR AUTOMATIC MEASUREMENT OF SNOW MASS CONCENTRATION

TABLE 1 - SNOW TYPE CATEGORIES

Type Category	Description	Magono and Lee Classification
1	Plates and Broad Branched Crystals	Pla,Plb,Plc,P7a
2	Dendritic and Stellar Crystals	Pld,Ple,Plf,P2a, P2b,P2c,P2d,P7b, CPlb
3	Rimed Plates and Dendrites	Rlc,Rld,R2a,R2b, R3a
4	Graupel	R3b,R3c,R4a,R4b, R4c
5	Needles, etc.	Nla,Nlb,Nlc,Nld, Nle,N2a,N2b,N2c
6	Rimed Needles	Rla,Rlb
7	Columns, Bullets, etc.	Clb,Clc,Cld,Cle, Clf,C2a,C2b,CPla CP2a
8	Multiple Capped Columns, Side Plane Assemblages, etc.	CPlc,S1,S2,S3
9	Miscellaneous, including Broken Crystals, etc.	I1,I2,I3a,I3b, I4

Figure 4 shows all the points measured with the cyclone device over a period of seven winters, and indicates a close approximation to the log-log relationship suggested by physical reasoning. The regression equation is:

$$\mathrm{Log}_{10}C = -0.543 - 1.286 \log_{10}V \qquad (1)$$

or

$$C = 0.286\ V^{-1.286} \qquad (1a)$$

(where C is the mass concentration in g/m_3 and V is the visibility in km), with a correlation coefficient of -0.943. At low concentrations, where the effects of haze are more significant, there is a tenfold total variation in concentration for a given visibility, and about a fivefold variation in visibility for a given mass concentration. At high mass concentrations, which are more significant as far as engineering applications are concerned, these variations decrease to about fourfold and threefold respectively.

As expected, scatter decreases when individual snow types are considered. Snow types exhibiting similar regression equations have been grouped together in the regression results of Table 2. One group comprised the

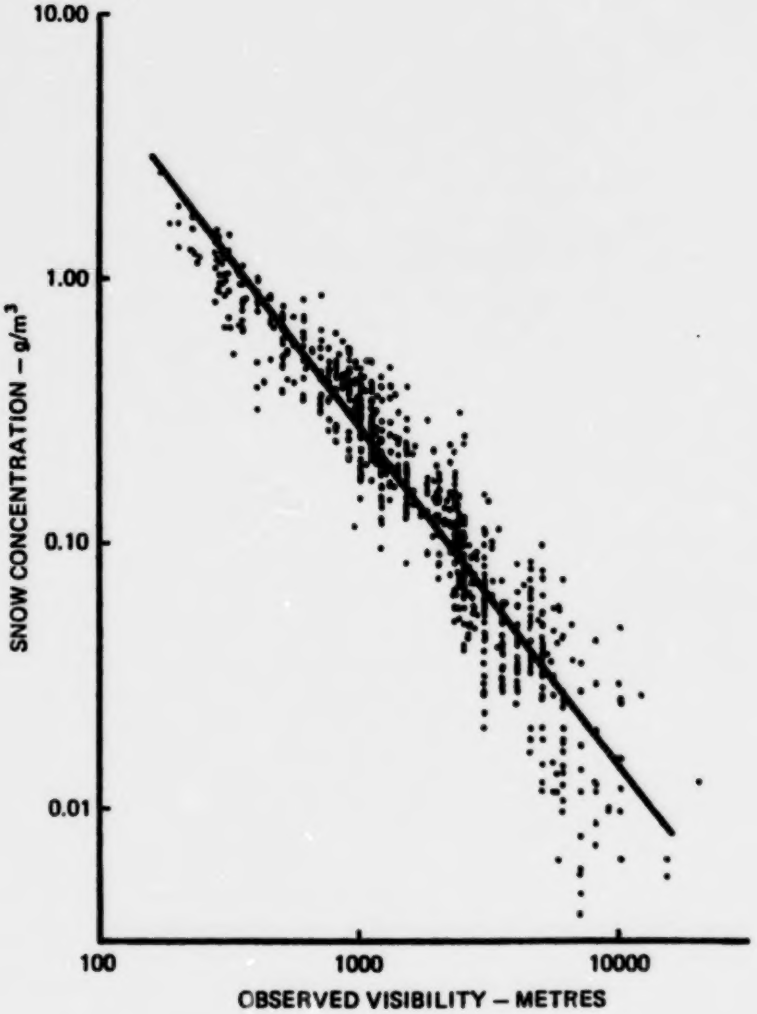

FIG. 4 DATA PLOT OF MANUAL SNOW MASS CONCENTRATION MEASUREMENTS AGAINST OBSERVED VISIBILITY FOR ALL SNOW TYPES, AND SHOWING REGRESSION LINE $C = 0.286\ V^{-1.286}$ (C in G/M^3, V in kM)

three rimed types while the other was composed of plates, columns and side plane assemblages.

TABLE 2

REGRESSION RESULTS, LOG$_{10}$ CONCENTRATION (g/m^3) VS. LOG$_{10}$ VISIBILITY (km), FOR VARIOUS SNOW TYPES AND GROUPS OF TYPES

Snow Type	No. of Samples	Regression Equation	Correlation Coefficient	Std. Error of Estimate
ALL	832	$\text{Log}_{10}C = -0.543-1.286\ \text{Log}_{10}V$	-0.943	0.174
1,7 & 8	312	$\text{Log}_{10}C = -0.522-1.367\ \text{Log}_{10}V$	-0.954	0.130
3,4 & 6	310	$\text{Log}_{10}C = -0.537-1.202\ \text{Log}_{10}V$	-0.949	0.173
2	77	$\text{Log}_{10}C = -0.562-1.564\ \text{Log}_{10}V$	-0.930	0.171
5	6	$\text{Log}_{10}C = -0.774-1.022\ \text{Log}_{10}V$	-0.972	0.114
9	127	$\text{Log}_{10}C = -0.534-1.264\ \text{Log}_{10}V$	-0.930	0.209

Not unexpectedly the miscellaneous category exhibited a low correlation and the highest standard error of the estimate. Snow type 2, the dendritic and stellar crystals, had an equally low correlation, and this is attributed to the higher tendency of these crystal forms to aggregate to form snowflakes, although in none of the other types did this appear to have any marked effect.

Concentration and Videograph Output. The Videograph backscatter visibility meter proved to be a useful instrument for estimating snow mass concentration. Mean values of the instrument's output current were recorded for all concentration samplings. Fig. 5 shows the data points. Again a log-log relationship was found to give the best fit to the data. The regression equation for all snow types was found to be:

$$\text{Log}_{10}C = 0.143 + 4.648\ \log_{10}I_v \tag{2}$$

or

$$C = 1.39\ I_v^{4.65} \tag{2a}$$

(where C is in g/m$_3$, and the Videograph output current I_v is in mA), with a correlation coefficient of 0.97. The scale of a milliammeter has been redrawn in terms of g/m^3 according to eq.(2) and provides a direct indication of the snow concentration.

Like the visibility results, rather better correlation is obtained by considering individual snow types, but with less difference between types, so that all the unrimed types with the exception of type 1 (plates) could be treated as one group, while the rimed types as before formed another group. The regression results are given in Table 3. Type 1 (plates and broad branched crystals) differ significantly in their response, giving a lower

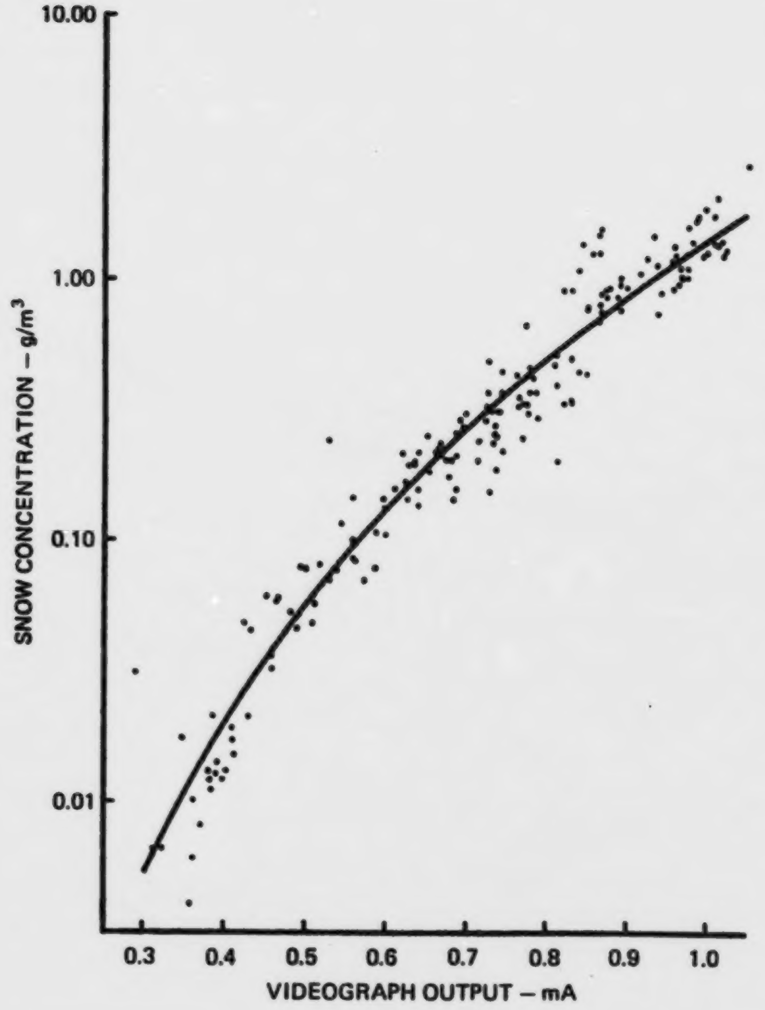

FIG. 5 DATA PLOT OF MANUAL SNOW MASS CONCENTRATION MEASUREMENTS AGAINST VIDEOGRAPH OUTPUT CURRENT FOR ALL SNOW TYPES, AND SHOWING REGRESSION LINE $C = 1.39\ I_v^{4.65}$ (C in G/M^3, I_v in mA)

backscatter return than the other crystal types. This is believed to be because plates tend to fall flat rather than with the more random orientation of less regular crystals. Rimed crystals, conversely, give a larger backscatter than their unrimed counterparts, possibly because orientation effects are less critical.

The usefulness of the Videograph for indicating the snow concentration is illustrated in Figures 6 and 7, where the Videograph estimate of the concentration is compared with the SCM measurements for two different storms. In Figure 6, readings were taken at 1-minute intervals; a three-point smoothing has been applied to the data since the Videograph readings were instantaneous readings, while the SCM values were the average concentration over a 50-second period between Videograph samples. In Figure 7, samplings were made every 10 minutes, the SCM readings being the 50-second average immediately following the instantaneous Videograph reading. This data is unsmoothed. Both examples show good estimation by the Videograph of the snow mass concentration, with estimated values being generally within a factor of two of the measured values.

TABLE 3

REGRESSION RESULTS, LOG_{10} CONCENTRATION (g/m_3) VS. LOG_{10} VIDEOGRAPH OUTPUT CURRENT (mA), FOR VARIOUS SNOW TYPES AND GROUPS OF TYPES

Snow Type	No. of Samples	Regression Equation	Correlation Coefficient	Std. Error of Estimate
All	176	$\mathrm{Log}_{10}C = 0.143+4.648\ \mathrm{Log}_{10}I_v$	0.970	0.154
1	17	$\mathrm{Log}_{10}C = 0.347+4.880\ \mathrm{Log}_{10}I_v$	0.982	0.059
2,7,8&9	94	$\mathrm{Log}_{10}C = 0.152+4.614\ \mathrm{Log}_{10}I_v$	0.968	0.153
3,4 & 6	65	$\mathrm{Log}_{10}C = 0.093+4.773\ \mathrm{Log}_{10}I_v$	0.988	0.110

Concentration and Precipitation Rate. Earlier predictions that precipitation rate was not likely to be a good indicator of mass concentration are not fully borne out by the results obtained during this study. As Figure 8 shows, there is only about a 3-fold variation in concentration for a given precipitation rate. However, the difficulties of accurately measuring the snowfall rate, particularly over short periods of time and under conditions of wind, make this an impractical means of determining the mass concentration.

Figure 6 shows the regression line through the data, having the equation:

$$C = 0.374\ R^{0.697} \qquad (3)$$

(where C is in g/m^3, and R is the water equivalent snowfall rate in mm/h), and a correlation coefficient of 0.92. Also shown for comparison are the results

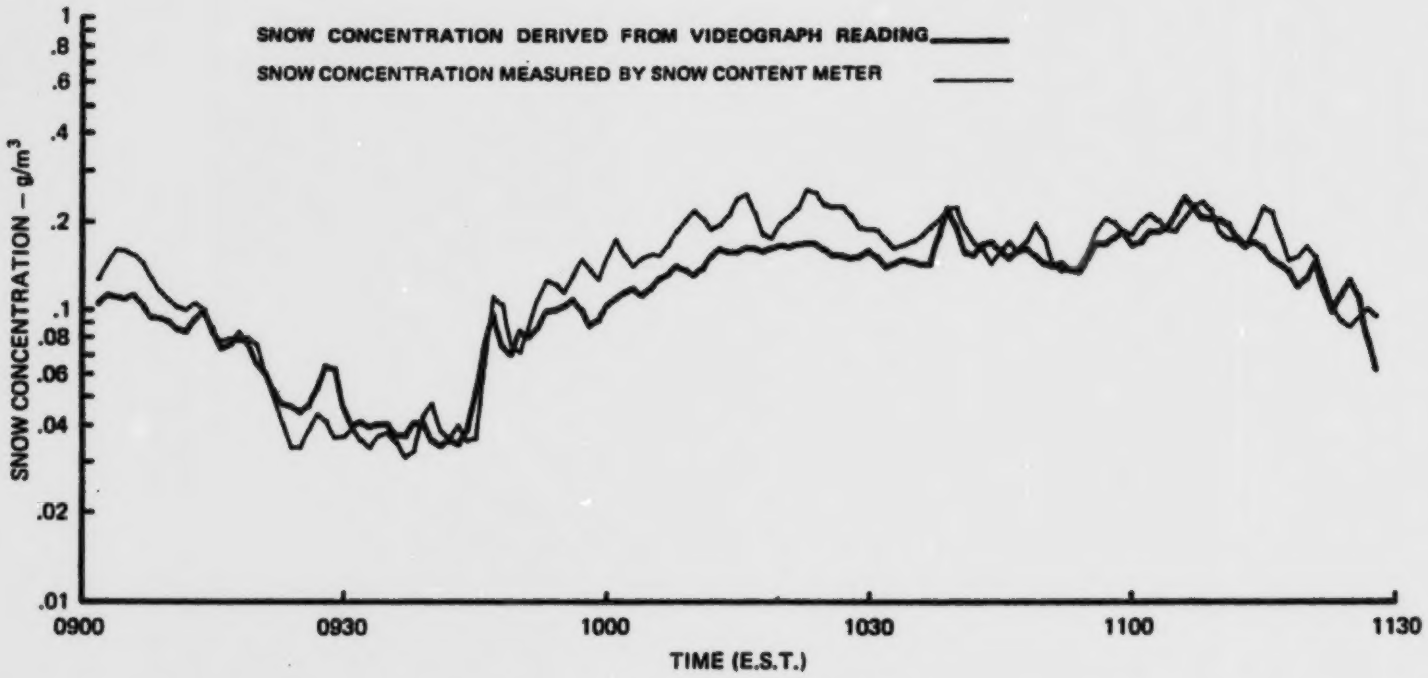

FIG. 6 COMPARISON BETWEEN SNOW MASS CONCENTRATION DERIVED FROM VIDEOGRAPH OUTPUT AND THAT MEASURED BY SNOW CONTENT METER. PORTION OF STORM OF 22 FEBRUARY 1977 SAMPLED AT 1-MINUTE INTERVALS.

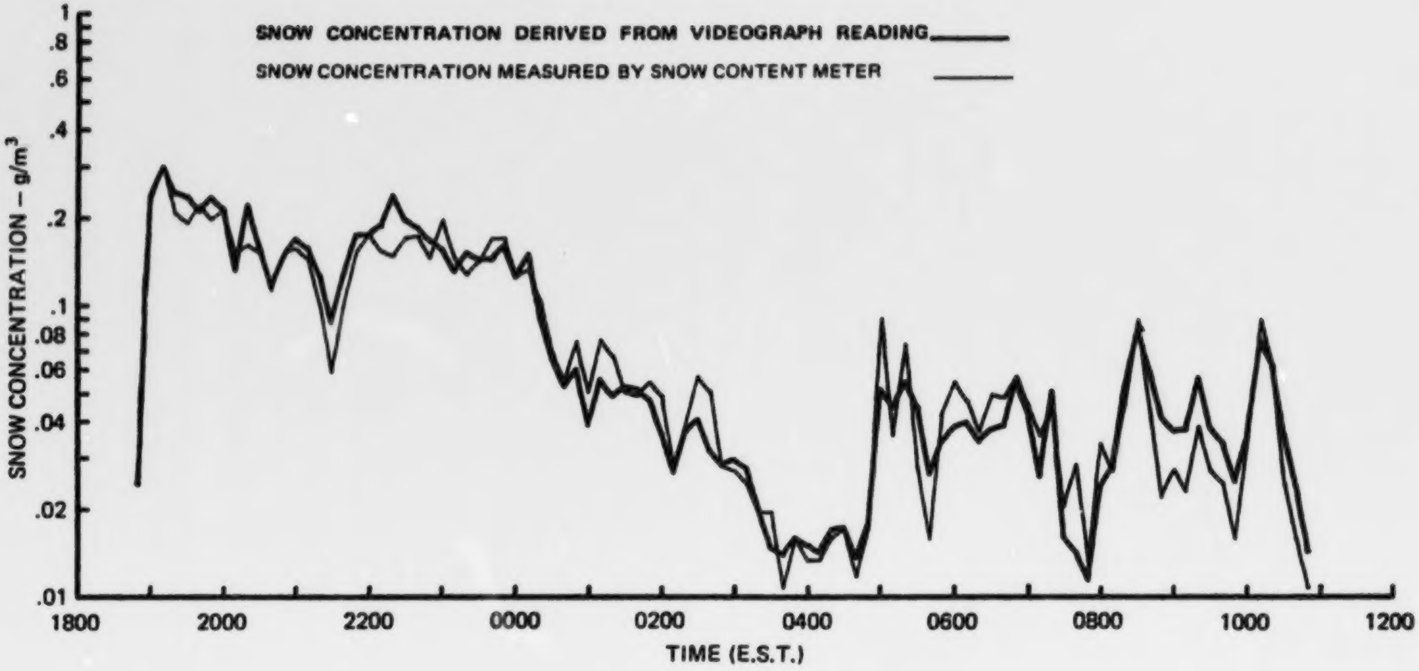

FIG. 7 COMPARISON BETWEEN SNOW MASS CONCENTRATION DERIVED FROM VIDEOGRAPH OUTPUT AND THAT MEASURED BY SNOW CONTENT METER. STORM OF JANUARY 20-21, 1978 SAMPLED AT 10-MINUTE INTERVALS

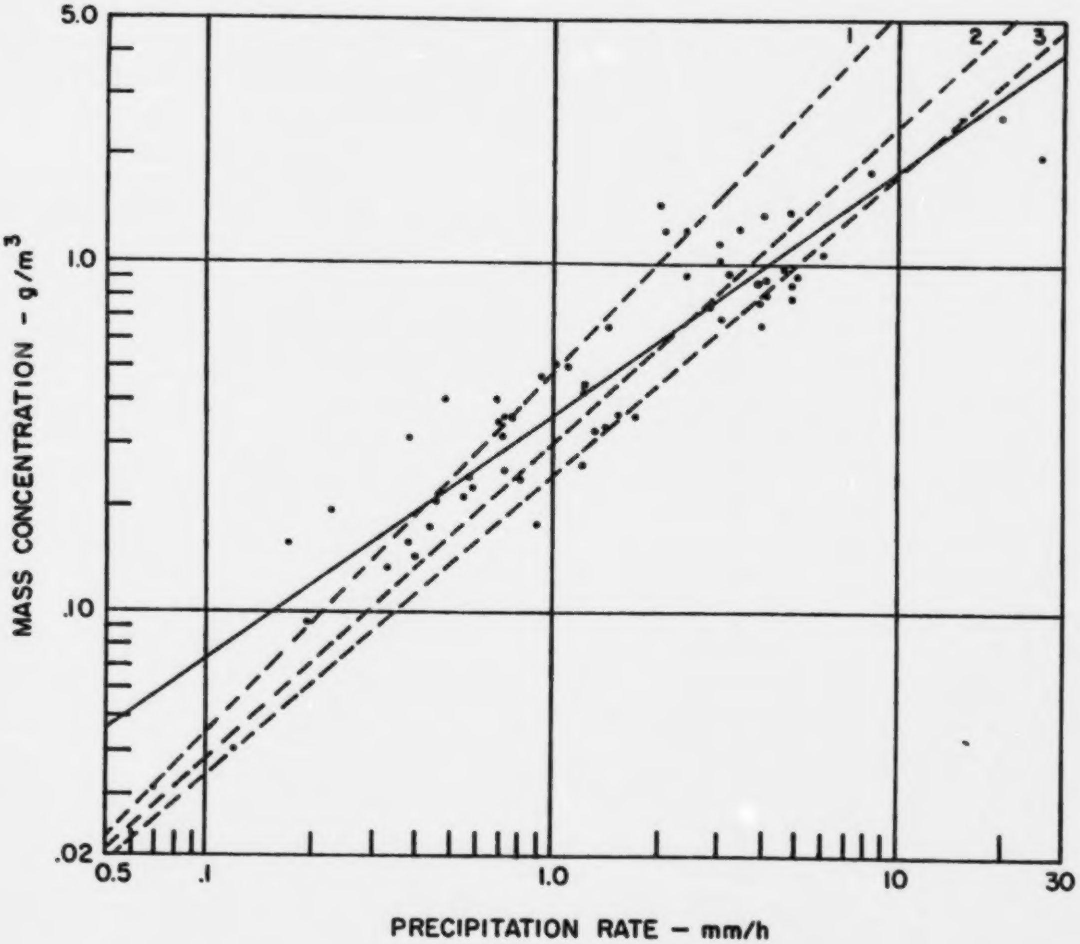

FIG. 8 SNOW MASS CONCENTRATION VERSUS PRECIPITATION RATE. PRESENT DATA COMPARED TO RESULTS FROM OTHER SOURCES. SOLID LINE - REGRESSION LINE ($C=0.374R^{0.697}$) THROUGH PRESENT DATA POINTS. BROKEN LINES: 1. O'BRIEN, $C = 0.502R^{1.03}$. 2. MELLOR, $C = 0.315R^{0.90}$. 3. SEKHON AND SRIVASTAVA, $C = 0.25R^{0.86}$.

from other workers' data (Refs. 4,5 & 6). Of these, the results from Mellor's[4] data agree most nearly with the present data.

Precipitation Rate and Visibility. Similar correlation ($r=0.91$) was observed between the precipitation rate and visibility. Figure 9 shows the data points and the least square fit to them, i.e.

$$V = 0.919\ R^{-0.64} \tag{4}$$

The figure also shows the results of other workers (Refs. 4,5,7 & 8), those of O'Brien[5] agreeing most closely with the present results, although any of them, with the exception of Mellor's, could describe the present results with fair accuracy.

Concentration and Air Temperature. The temperature dependence of the mass concentration at Ottawa is shown in the form of a scatter plot in Figure 10, using SCM readings for the four winters, 1980/81 to 1983/84. As expected, the greatest mass concentrations and the greatest numbers of events occur close to 0°C, with a general, if rather erratic, decrease in both as the temperature decreases, to insignificant amounts below about -25°C (the few events below this temperature being more in the nature of ice fog or ice crystals than snow). Such a relationship is perhaps not entirely to be expected since the temperature at ground level may bear little relation to that at those levels at which formation and growth of the snow crystals took place, and undoubtedly accounts to a large extent for the erratic nature of the plot. The great variety of crystal types falling concurrently on many occasions, the frequent complex crystal forms, and the occurrence of riming all attest to the variations in temperature and saturation of the air encountered by the snow particles during their lifetime.

Probability Distribution of Mass Concentration. The cumulative distribution curve of all measurements made with the SCM during five winters (1978/79, 1980/81, 1981/82, 1982/83, 1983/84) is shown in Figure 11 as curve "A". This shows that, over this period, the median concentration for Ottawa was 0.05 g/m^3, while the probability of exceeding 0.32 g/m^3 was 10% and a concentration of 0.8 g/m^3 was exceeded only 1% of the time.

By using the correlation between mass concentration and visibility presented earlier, another cumulative distribution curve has been derived based on the hourly visibility readings during reported snowfall at Ottawa airport for the 20-year period 1955-1974. This is shown as curve "B" in Figure 11. The 50, 90 and 99 percentiles for this curve are 0.035 g/m^3, 0.19 g/m^3 and 0.55 g/m^3 respectively, i.e. about 0.66 of those from the direct measurements.

There are several possible reasons for this discrepancy. These include the much shorter observation period of the direct measurements, i.e. 5 winters as compared to 20 winters, the different years of the records, i.e. 1979/1984 and 1955/1974, the different sampling frequency, i.e. 10 minutes and 1 hour, possible subjectivity in assessing visibility, the presence of other obstructions to vision, and the loss of SCM data at low concentrations (<0.002 g/m^3) owing to the system being activated only above a threshold value of Videograph output current.

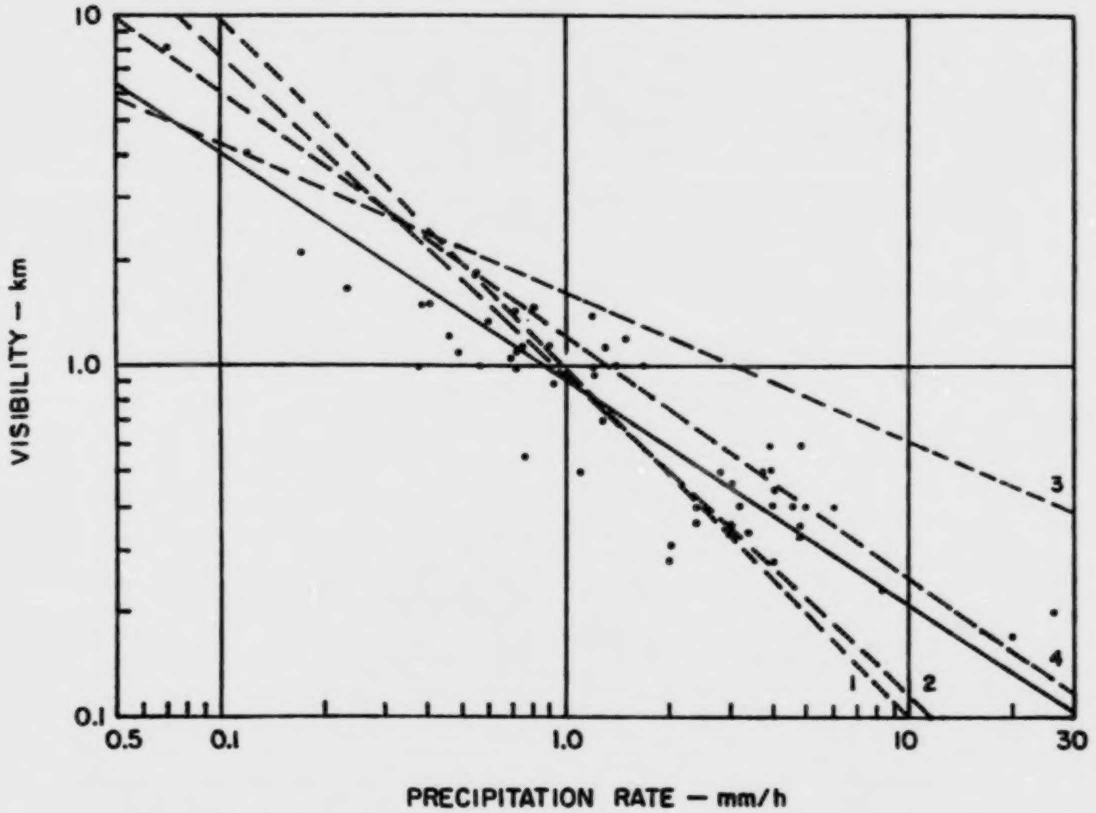

FIG. 9 VISIBILITY VERSUS PRECIPITATION RATE. PRESENT DATA COMPARED TO RESULTS FROM OTHER SOURCES. SOLID LINE - REGRESSION LINE ($V = 0.919R^{-0.64}$) THROUGH PRESENT DATA POINTS. BROKEN LINES: 1. LILLESAETER, $V = R^{-1}$. 2. POLYAKOVA AND TRETJAKOV, $V = 0.94R^{-0.91}$. 3. MELLOR, $V = 1.65R^{-0.42}$. 4. O'BRIEN, $V = 1.25R^{-0.69}$.

SNOW MASS CONCENTRATION - g/m³ \ AIR TEMPERATURE - °C	-30 – -28	-28 – -26	-26 – -24	-24 – -22	-22 – -20	-20 – -18	-18 – -16	-16 – -14	-14 – -12	-12 – -10	-10 – -8	-8 – -6	-6 – -4	-4 – -2	-2 – 0	0 – 2
2.5 – 2.6															1	
2.4 – 2.5																
2.3 – 2.4																
2.2 – 2.3																
2.1 – 2.2																
2.0 – 2.1																
1.9 – 2.0														1	1	
1.8 – 1.9														1		
1.7 – 1.8															1	
1.6 – 1.7																
1.5 – 1.6											1				1	1
1.4 – 1.5																2
1.3 – 1.4											1					1
1.2 – 1.3													1		1	3
1.1 – 1.2											1			2	1	2
1.0 – 1.1						1	1				1			1	3	4
0.9 – 1.0					1	1	1				2			1	2	
0.8 – 0.9						1		1			2	3	1	2	2	7
0.7 – 0.8					2		2		1	1	2	7	3	5	11	2
0.6 – 0.7					2	2	1	2	5	2	4	21	6	3	14	2
0.5 – 0.6					4	3	1	1	5	3	13	31	10	5	34	7
0.4 – 0.5					4	5		3	10	9	35	44	19	18	61	11
0.3 – 0.4					6	4	2	12	19	16	46	55	51	29	87	24
0.2 – 0.3					6	6	8	27	51	28	63	101	74	91	136	35
0.1 – 0.2				9	14	11	47	73	117	52	86	200	150	172	176	94
0 – 0.1	4	4	9	65	103	140	280	322	632	419	413	573	496	691	541	467

FIG. 10 PLOT SHOWING NUMBER OF CONCENTRATION MEASUREMENTS WITHIN EACH 0.1 g/m^3 INTERVAL FOR EACH 2°C INTERVAL OF AIR TEMPERATURE FOR 4 WINTERS (1980/81 to 1983/84)

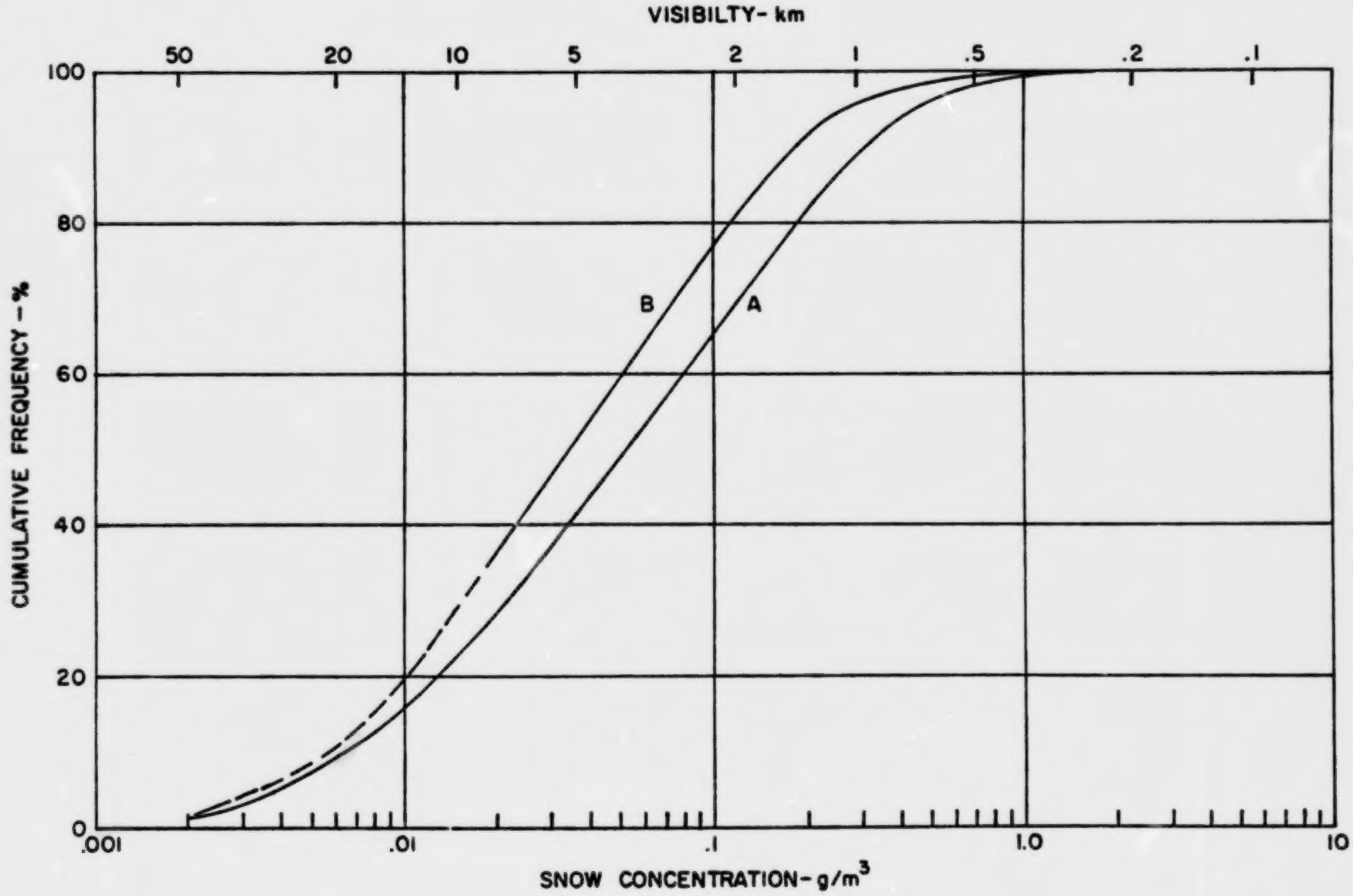

FIG. 11 CUMULATIVE DISTRIBUTION CURVES OF MASS CONCENTRATION FOR OTTAWA. CURVE A: 5 WINTERS OF SCM MEASUREMENTS 1979-84. CURVE B: FROM DIURNAL FREQUENCIES OF REPORTED VISIBILITY DURING SNOW FOR 20 YEARS, 1955-74 AT OTTAWA AIRPORT, USING RELATION $C = 0.286V^{-1.286}$

Concluding Remarks

The maximum snow concentration measured with the manual sampler during this work was 2.66 g/m^3 on 21 December 1977. The temperature was -2.5°C and the visibility 170 metres. The maximum value recorded by the SCM was 2.6 g/m^3 on 3 April 1983 at a temperature of -1.4°C.

The most intense storm recorded was on 10 January 1977 when concentrations in excess of 1 g/m^3 persisted for one period of 1.5 hours and another of 1.3 hours.

Among normally measured meteorological parameters, visibility was found to provide the most reliable estimate of mass concentration by use of the relation:

$$C = 0.286\ V^{-1.286}$$

The standard error of the estimate implies a 95% confidence that the concentration will be within a factor of 2.2 of the estimate given by the above equation. For example, a visibility of 2.5 km gives a concentration estimate of 0.09 g/m^3 with a 95% confidence that the actual concentration lies between 0.04 and 0.20 g/m^3.

A backscatter visibility meter, such as the Videograph, is a useful device for providing a measure of the prevailing snow concentration.

Although the two probability distribution curves presented show some discrepancy, they are perhaps sufficiently similar to suggest that visibility data may be used to provide concentration probability estimates for any station for which such data are available.

References

1. Stallabrass, J.R. Engine snow ingestion in the Bell 206A Jet Ranger helicopter. NRCC, Mech. Eng. Rept. MET-513, 1971.

2. Harkins, W.D. and F.E. Brown. The determination of surface tension (free surface energy), and the weight of falling drops: the surface tension of water and benzene by the capillary height method. J.Amer.Chem.Soc., 41, 1919, 499-524.

3. Magono, C. and C.W. Lee. Meteorological classification of natural snow crystals. Jour. of the Faculty of Science, Hokkaido Univ., Ser.VII (Geophysics), 11, 1966, 321-335.

4. Mellor, M. Light scattering and particle aggregation in snowstorms. U.S. Army, Cold Regions Research & Engineering Laboratory. Res. Rept. 193, 1966.

5. O'Brien, H.W. Attenuation of visible light by falling snow. U.S. Army, Cold Regions Research & Engineering Laboratory. Res. Rept. 242, 1969.

6. Sekhon, R.S. and R.C. Srivastava. Snow size spectra and radar reflectivity. Univ. of Chicago, Laboratory for Atmospheric Probing, Tech. Rept. No. 12, 1969.

7. Poljakova, E.A. and V.D. Tretjakov. Visibility in falling snow. Glavnoi Geofiz. Obs., Trudy No. 100, Leningrad, 1960, 53-57.

8. Lillesacter, O. Parallel-beam attenuation of light, particularly by falling snow. J.Appl.Met., 80, 1965, 607-613.

APPENDIX

DESCRIPTION OF VOLUMETRIC PRECIPITATION GAUGE

To meet the requirements for a precipitation gauge that would accurately measure the snowfall rate, modifications were made to a prototype gauge developed by the Atmospheric Environment Service (AES). This gauge, variously referred to by the AES as the Volumetric Precipitation Gauge (VPG) or the Heated Liquid Surface Precipitation Gauge, was designed to measure precipitation by metering equal volumes of water and recording these volumes with an event recorder and/or display counter.

The principle of operation of the NRC modified gauge is illustrated in Figure A1. The upper section of the gauge contains a water reservoir about 15 cm deep and 20 cm in diameter. The lower section contains an electrically operated three-way valve, electronic control circuitry, and heating systems for both sections.

The water in the reservoir is heated to a few degrees above freezing by a thermostatically controlled electric heater, and is covered with about a 0.5 cm layer of silicone oil to prevent evaporation.

The water level in the instrument is sensed by the cutting of a beam of infrared radiation by a knife-edged blade mounted on a float. The blown glass float and the optical sensor fit inside a stand pipe which communicates with the water in the reservoir through a small tube to minimize the effects of disturbances on the surface of the water reservoir. The sensor mounting block is also heated to prevent the possibility of condensate forming on the sensor optics.

When the water level in the reservoir rises sufficiently to cause the float to cut the sensor beam, a signal is sent to the electronic control circuit which actuates the three-way valve. The valve connects a metering stand pipe of known (and adjustable) volume to either the reservoir or to a drain. Normally the metering stand pipe is connected to drain, and remains empty, but when the valve receives a signal from the sensor circuit, it connects the metering chamber to the reservoir for ten seconds, so that an equilibrium is reached between the water in the metering stand pipe and that in the reservoir, before the valve returns to the drain position.

The volume of water in the metering stand pipe can be adjusted by means of a movable piston. It was normally adjusted to provide a signal for each 0.2 mm of precipitation.

The volumetric precipitation gauge was operated with an Alter shield.

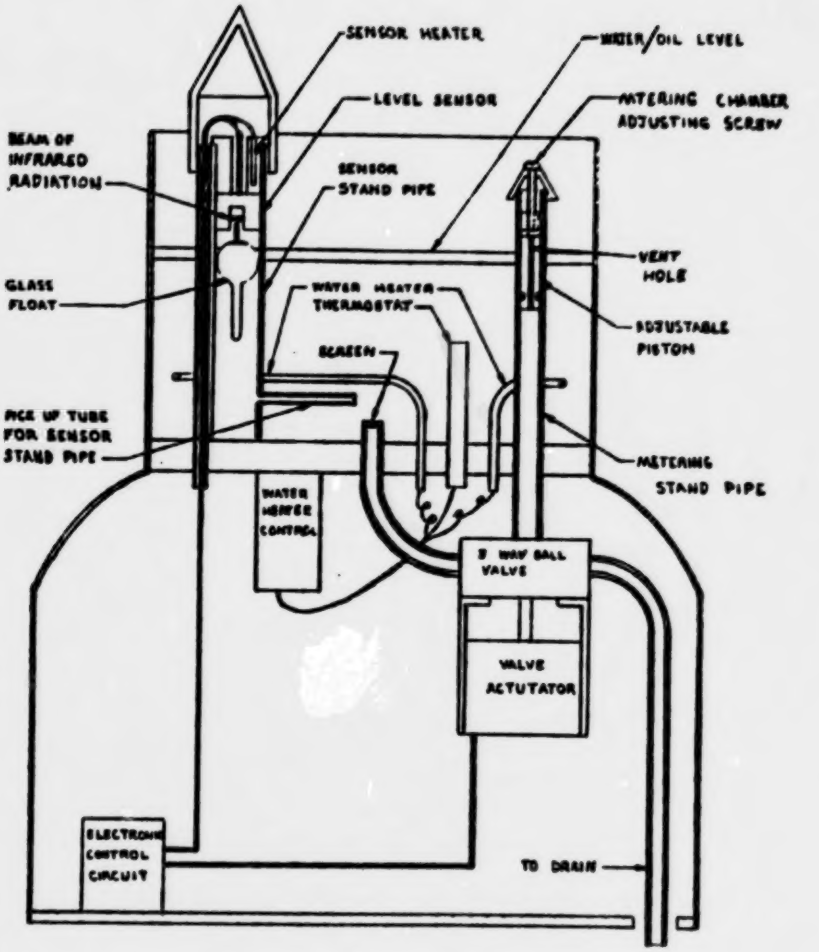
SENSOR HEATER
WATER/OIL LEVEL
LEVEL SENSOR
METERING CHAMBER ADJUSTING SCREW
BEAM OF INFRARED RADIATION
SENSOR STAND PIPE
VENT HOLE
GLASS FLOAT
WATER HEATER
THERMOSTAT
ADJUSTABLE PISTON
SCREEN
PICK UP TUBE FOR SENSOR STAND PIPE
METERING STAND PIPE
WATER HEATER CONTROL
3 WAY BALL VALVE
VALVE ACTUTATOR
ELECTRONIC CONTROL CIRCUIT
TO DRAIN

FIG. A1 - VOLUMETRIC PRECIPITATION GAUGE

SNOW-DRIFTING: A REVIEW OF THE PROCESS AND OF MODELLING METHODS

by

R.J. Kind

Department of Mechanical and Aeronautical Engineering
Carlton University
Ottawa, Ontario
Canada

presented at

SNOW PROPERTY MEASUREMENTS WORKSHOP

Lake Louise, Alberta

1-3 April, 1985

TECHNICAL MEMORANDUM 140

Compiled By

P.R. Kry

NRCC 27594

Snow-Drifting: A Review of the Process and of Modelling Methods

by

R.J. Kind,
Department of Mechanical and Aeronautical Engineering,
Carleton University, Ottawa, Ontario, K1S 5B6.

Summary

The physical process of snow-drifting is briefly described. Saltation is the dominant mode of mass transport. The requirements for modelling of snow-drifting are outlined and it is shown that these cannot all be simultaneously satisfied in practice. A variety of approaches have been used to model snow-drifting and these are reviewed in the light of the requirements. In many modelling situations short saltation trajectories are essential. Short trajectories are readily attainable when modelling is carried out in water flows, using fine sand to represent the snow. This fact, and the convenience of water modelling, make this approach suitable and attractive for most situations even though the saltation process is not dynamically similar to that of real snow in air. This shortcoming is absent when high-density particles (e.g. fine sand) are used in air flows, but this approach has other shortcomings. Modelling can provide valuable design information but results must be interpreted with caution and field experience with snow-drifting is a valuable asset.

1. Introduction

This paper is primarily concerned with snow-drifting, as distinct from snow-fall. In snow-drifting, loose snow lying on the surface is moved by wind action and substantial re-distribution of snow mass can occur. Both wind speed and wind flow pattern are important, as is the condition of the surface snow. The overall process is quite complex and even qualitative prediction of snow-accumulation patterns is often difficult. Physical modelling, at reduced scale, is useful for obtaining predictions but even this approach must be used with caution as the modelling laws cannot all be satisfied in practice.

The objectives of the paper are to provide improved appreciation of the main factors which influence accumulation patterns due to snow-drifting and to outline current modelling methods and their limitations. Pertinent characteristics of the wind near the earth's surface are reviewed and the snow-drifting process is described. The requirements for physical modelling are summarized; it will be seen that these cannot all be satisfied in practice and every modelling method therefore involves some compromises. Current approaches to modelling are reviewed.

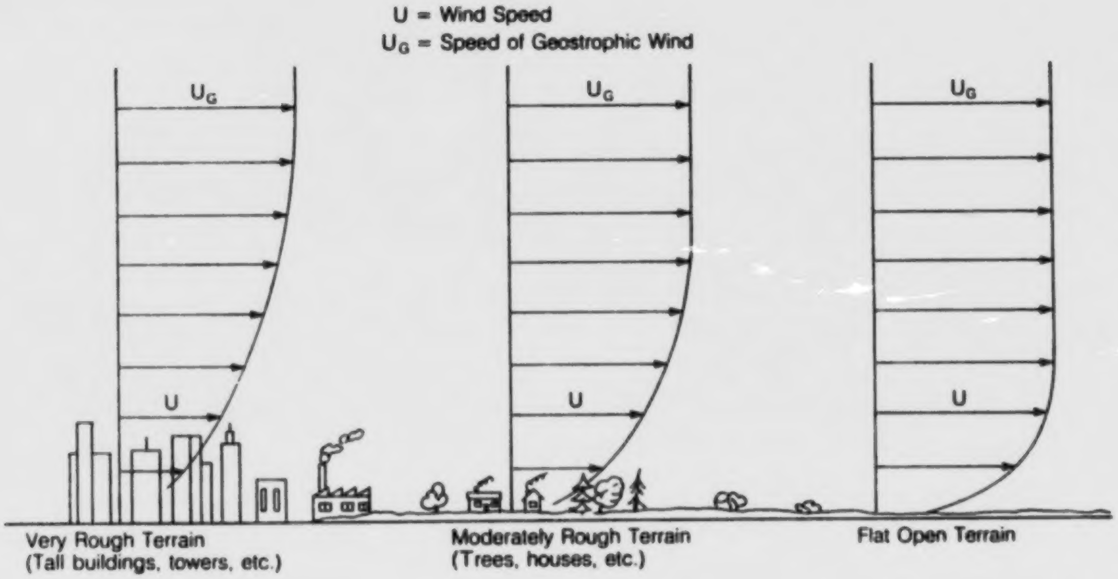
U = Wind Speed
U_G = Speed of Geostrophic Wind
U_G
U
U_G
U
U_G
U
Very Rough Terrain
(Tall buildings, towers, etc.)
Moderately Rough Terrain
(Trees, houses, etc.)
Flat Open Terrain

FIG. 1 - WIND VELOCITY PROFILES OVER TERRAIN WITH DIFFERENT ROUGHNESS

2. Some Characteristics of Winds Near the Earth's Surface

At altitudes above about 500 m the winds are governed by the pressure distributions associated with large-scale weather systems and are independent of surface topography. Right at the earth's surface the wind speed must be zero (no-slip condition). Therefore the wind speed must increase with height above the earth's surface, as illustrated in Fig. 1. The layer across which the speed varies is known as the atmospheric boundary layer. Over relatively rough terrain the boundary layer is thicker and the wind speed increases relatively slowly with height; over flat open terrain the opposite is true (see Fig. 1). The wind in the atmospheric boundary layer is usually turbulent or gusty. The speed distribution and turbulence in the wind are also influenced by thermal stratification of the atmosphere; stratification effects are, however, normally unimportant when significant snow-drifting is occurring since wind speeds are then relatively high.

The wind speed quoted in weather reports is normally measured at a height of 10 m at a local airport site where the terrain is relatively flat and open. As suggested by Fig. 1, this speed will differ from that at other heights and/or over different terrains.

The wind exerts a shear stress, τ_o, on the snow surface and it is this shear stress which causes movement, or drifting, of loose snow. The value of τ_o depends on the velocity gradient and turbulence structure in the wind very near (within, say, 10 cm) the snow surface. Conditions very near the snow surface in turn depend on conditions in the atmospheric boundary layer as a whole. The relation between the surface shear stress, τ_o, and the wind speed at any given height, for example 1 m or 10 m, is thus rather complex. It can, however, be said that for any particular site and wind direction, τ_o will be approximately proportional to wind speed squared. Also, τ_o will be greater when the wind approaches over flat open terrain, as opposed to rough terrain, because the velocity gradient near the snow surface will then be greater.

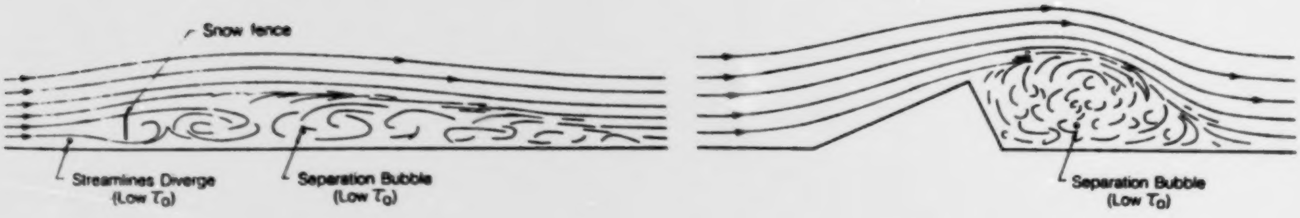
Snow fence
Streamlines Diverge (Low τ_0)
Separation Bubble (Low τ_0)
Separation Bubble (Low τ_0)

(a) Flow over a Slatted Snow Fence

(b) Flow over an Embankment

FIG. 2 WIND FLOW PATTERNS OVER SURFACE FEATURES

Surface features, for example snow fences, buildings, bushes, embankments, highway cuts, etc., have a profound effect on the nearby flow, and thus on the surface shear stress distribution and snow-drifting process near themselves. The most profound effect normally occurs on the leeward side of the features where a low velocity wake or separation bubble is present in the flow pattern (see Fig. 2). The low velocity implies a low surface shear stress, τ_0, and thus a reduced ability to transport snow; snow therefore tends to be deposited in the wake when drifting conditions prevail. Wakes are of order 10 feature-heights long. Surface features can also cause local accelerations of the wind, particularly near their windward faces and lateral edges. In acceleration zones τ_0 is relatively high and snow tends to be eroded. Drift-control devices or strategies are basically man-made surface features which modify the flow pattern and surface shear stress so as to either induce or prevent deposition when drifting conditions prevail. For example, conventional snow fences produce a wake and induce deposition upwind of roadways while blower fences [1]* or raised roadbeds cause local flow accelerations near the road surface and thus prevent deposition.

Wind characteristics pertinent to snow-drifting are discussed in somewhat more detail in [2] while [3] includes extensive information on wind characteristics in general.

---

*Numerals in square brackets denote references listed at the end of this paper.

Table 1

Some Threshold Velocities

Snow Surface Condition	U^*_{th} (m/s)	U at 1 m height (m/s)
loose fresh dry snow at less than -2.5°C	0.15	4.
newly fallen snow at 0°C	0.25	5.5
slightly aged (several hours) snow near 0°C	0.4	8.5

(data from reference [2])

3. Description of the Snow-Drifting Process

Consider wind blowing over a surface consisting of snow particles. When the wind speed exceeds some threshold value, snow particles are caused to move by the drag force (i.e. downwind force) exerted on them by the moving air. The drag force per unit plan area is the surface stress, τ_0, referred to earlier. Thus wind-induced snow movement, or drifting, begins when the surface shear stress exceeds some threshold value which depends on the size, shape and weight of the snow particles and on the strength of any inter-particle cohesive forces which may be present. Threshold conditions are usually correlated in terms of a shear velocity, U^*, defined as $U^* \equiv \sqrt{\tau_0/\rho}$, where ρ is the density of the air; although U^* has dimensions of velocity it is not a true velocity. Cohesive forces are negligible in newly-fallen snow at temperatures below about -2°C. After a little movement the large snow particles are broken into smaller ones of roughly similar shape and size; nominal diameter of the dominant mass-fraction of particles is then roughly 0.5 mm. The threshold shear velocity, U^*_{th} is about 0.15 m/s for these conditions. Threshold values are substantially higher in wet, aged or wind-hardened snow because substantial inter-particle cohesive forces are then present. Because τ_o is approximately proportional to wind speed squared, the actual threshold wind speed at any given height above the snow surface is approximately proportional to the threshold shear velocity, U^*_{th}. Table 1 gives some representative values of U^*_{th} and of threshold speed at a height of 1 m.

Provided that the wind speed is not too far above the threshold value (say $U^* \tilde{<} 5\ U^*_{th}$), the moving snow particles bounce along close to the surface in a mode of motion called "saltation". The mean wind velocity is approximately horizontal (parallel to the surface) and particles can only rise to substantial heights above the surface if vertical velocities in turbulent eddies are at least equal to U_{TER}, the terminal velocity of the particles in free fall. Bagnold [4] points out that this only happens when $U^* \tilde{>} 5\ U^*_{th}$ ($U_{TER} \cong 10\ U^*_{th}$ for particles larger than 0.5 mm [5] and root-mean-square vertical air velocity $\cong 2\ U^*$ [6]). Thus, unless the wind speed at 1 m height exceeds 14 m/s, corresponding to $U^* \cong 0.75$ m/s, the main mass of snow particles cannot be lifted to any substantial distance above the surface. Rather, these particles saltate, propelled by aerodynamic drag forces. A small mass fraction of the surface snow may consist of very fine particles ("snow dust") whose terminal velocity is relatively low; when saltation is occurring the larger (saltating) particles no longer protect the snow dust from wind action and it is carried to considerable heights by the turbulent eddies in the wind. The bulk of the mass transport is, however, by saltation of the relatively large particles except in the relatively rare instances when wind speeds exceed about 14 m/s at 1 m height. Figure 3 shows a typical mass flux distribution as a function of height above the surface.

Figure 4 is a sketch of a typical saltation trajectory. The trajectories are 5 to 10 times longer than their height, which is of order 1 cm. The particles rise more or less vertically from the snow surface and are accelerated in the downwind direction by aerodynamic

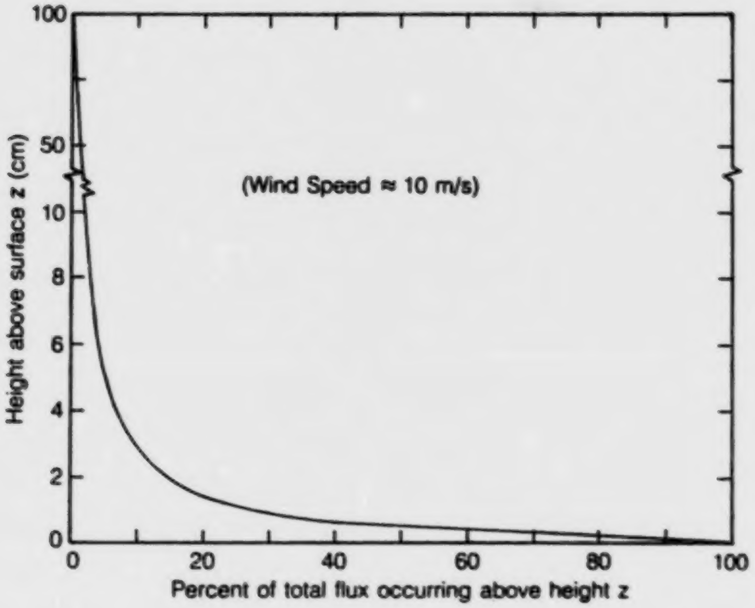

FIG. 3 DISTRIBUTION OF MASS-TRANSPORT RATE OF BLOWING SNOW WITH HEIGHT (BASED ON DATA FROM [7] and [8]).

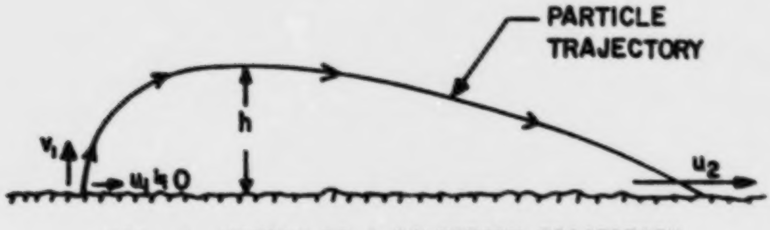

FIG. 4 SKETCH OF A SALTATION TRAJECTORY

drag forces. Gravity eventually causes each particle to splash back into the surface, thus terminating the trajectory; most of the momentum of the impacting particle is dissipated into the snow surface but one or two new particles may be ejected, thus maintaining the saltation process. The acceleration/impact process transfers momentum from the wind to the snow surface and this is equivalent to a shear stress between the wind the and snow surface; in fact, when saltation is occurring, this is the mechanism responsible for most of the surface shear stress, τ_o. The rate of mass transport by saltation thus depends on the ability of the wind to exert shear stress on the snow surface. As the wind speed increases its ability to exert shear stress also increases and an increased particle acceleration/impact rate can be sustained; that is more particles can participate in the saltation process. Moreover the saltation trajectories increase in length since the particles acquire greater horizontal velocities.

A theoretical analysis based on these concepts shows that the particle transport rate increases approximately as shear or wind velocity to the third power [5]. Figure 5 shows a comparison of the results of saltation theory with field data of Kobayashi [8]. The agreement is seen to be quite good. The rapid increase of mass transport rate with increasing wind speed is noteworthy. Kobayashi [8] also presents photographs which clearly show that most of the snow moves in the saltation mode. One of these photographs is reproduced in [2].

Since the mass transport rate is very sensitive to local shear stress or wind speed (Fig. 5), drift-control devices only need to produce moderate changes in the latter parameters to be effective.

4. Modelling Principles

If physical modelling is to give valid results, modelling procedures and interpretation of results must satisfy certain requirements. Strictly speaking, correct modelling requires that geometry, flow patterns and snow-particle trajectories are all scaled by the same ratio; then flow patterns and particle trajectories have the same shapes in both the model and the prototype situations — they are just smaller in the model. The modelling requirements are outlined below.
For correct flow patterns we require:

- geometric similarity (geometric scaling) of both the model and nearby upwind terrain (1)
- correct velocity profile in the approach wind (2)

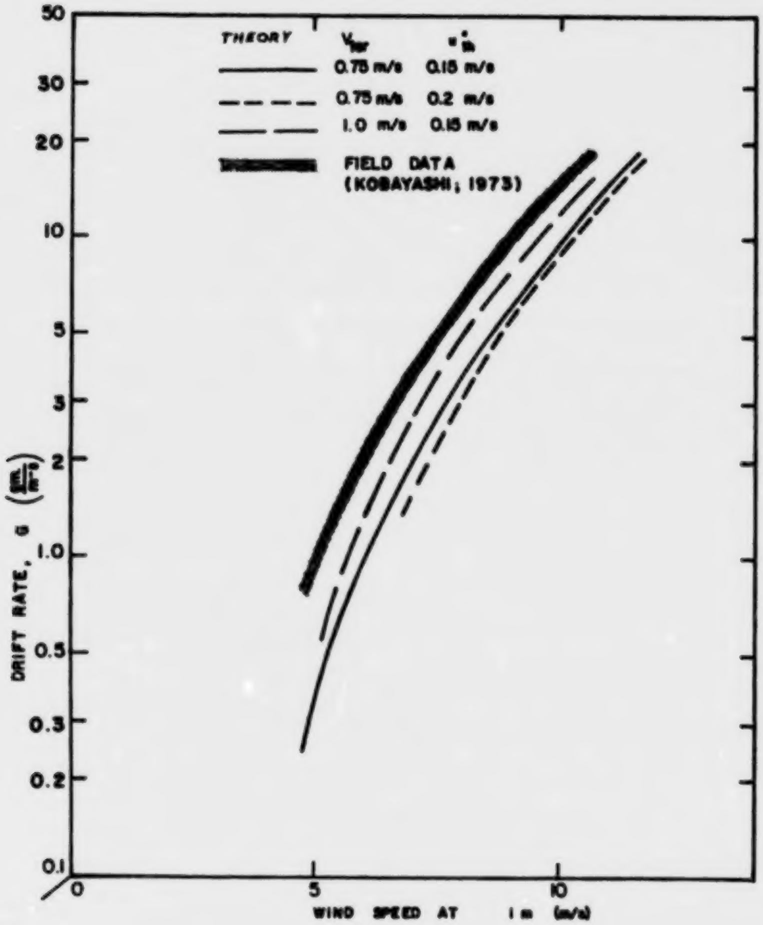

FIG. 5 COMPARISON BETWEEN RESULTS OF SALTATION THEORY AND FIELD DATA (FROM [5])

For correct particle trajectories we require:

$$\circ \quad \left[\frac{\text{inertia force}}{\text{gravity force}}\right]_M = \left[\frac{\text{inertia force}}{\text{gravity force}}\right]_P \qquad (3)$$

$$\circ \quad \left[\frac{\text{drag force}}{\text{inertia force}}\right]_M = \left[\frac{\text{drag force}}{\text{inertia force}}\right]_P \qquad (4)$$

- correct modelling of ejection of particles from surface (5)

The subscripts M and P denote the model and prototype, respectively.

Requirement (3) leads to the relation:

$$\left[\frac{V^2}{Lg}\ \frac{\sigma}{\sigma-\rho}\right]_M = \left[\frac{V^2}{Lg}\ \frac{\sigma}{\sigma-\rho}\right]_P \tag{6}$$

where V = reference wind velocity
L = reference length dimension
g = gravitational acceleration
ρ = density of the fluid (air in the prototype case)
σ = density of the particles

Requirement (4) leads to the relation:

$$\left[\frac{U_{TER}}{V}\right]_M = \left[\frac{U_{TER}}{V}\right]_P \tag{7}$$

Requirement (5) can be expressed as

$$\left[\frac{v_1}{V}\right]_M = \left[\frac{v_1}{V}\right]_P \tag{8}$$

where v_1 is the 'ejection velocity' which the particles have when they rise from the surface

The ejection process is not well understood but v_1 is most probably dependent on d, σ, ρ, ν and U^*, where d is the nominal diameter of the particles, ν is the fluid's kinematic viscosity and other symbols are as defined earlier. Indications are [5,9] that the ejection process is modelled satisfactorily if:

$$\left[\frac{U^*}{U^*_{th}}\right]_M = \left[\frac{U^*}{U^*_{th}}\right]_P \tag{9a}$$

or

$$\left[\frac{V}{V_{th}}\right]_M = \left[\frac{V}{V_{th}}\right]_P \tag{9b}$$

$$\left[\frac{U_{th}^{*\,3}}{2g\nu}\right]_M \gtrsim 30 \qquad (10)$$

and

$$\left[\sigma/\rho\right]_M \gtrsim 600 \qquad (11)$$

Requirement (9) is also necessary to ensure correct shear stress distribution over the surface, and hence correct erosion/deposition patterns.

Ideally then, one must satisfy requirements (1, 2, 6, 7, 9, 10 and 11). Of these, (1, 2, 7, 9 and 11) can be satisfied without undue difficulty. Reference [5] outlines procedures for selecting particles which simultaneously satisfy (7) and (9). In practice there is, however, a conflict between requirements (6) and (10). Assuming that air is the model fluid (wind-tunnel or outdoors modelling), requirement (6) would require $V_M << V_P$ because $L_M << L_P$ in practice. Then requirement (9) implies $\left[U_{th}^*\right]_M << \left[U_{th}^*\right]_P$, meaning that requirement (10) is violated because, as it happens, $(U_{th}^{*\,3}/2g\nu)$ has a value of only about 30 for the prototype case of real snow. Thus requirements (6) and (10) cannot both be satisfied by wind-tunnel or outdoors modelling at reduced scale. If water is used as the model fluid (water-flume modelling), requirement (11) is not satisfied because (σ/ρ) typically has a value near 3 (sand particles in water); furthermore, requirement (6) still would require $V_M << V_P$ and requirement (10) still could not usually be satisfied, despite the fact that ν of water is about 10 times less than that of air. It is certainly open to question whether requirements (10) and (11) should be considered at all for water-flume modelling, but it is generally acknowledged that saltation in water is considerably different from saltation in air [4,10,11]. Water-flume modelling offers great advantages of convenience.

A number of other authors have also considered the modelling requirements, notably Strom et.al. [12], Odar [13], Isyumov [14], and Iversen [15,16,17,18,19]. There is agreement that requirements (1,2,6, 7 and 9) should, in principle, be satisfied, but requirements (10) and

(11) must be considered controversial at this time. Other parameters relating to the ejection and fluid/particle interaction processes have been proposed in lieu of those of (10) and (11).

In summary, many of the requirements for modelling of snow-drifting can be satisfied without undue difficulty in both wind-tunnel and water-flume modelling. In practice, however, some of the requirements must be compromised in either modelling approach. Consequently a variety of approaches have been tried by various investigators. A number of the more recent of these are reviewed in the next section of this paper.

5. Approaches to Modelling

5.1 Modelling of Snow-fall Situations

When snow falls in windy conditions, snow accumulations can be rather non-uniform in built-up areas or in areas of complex topography even if the wind speeds are too low to cause drifting of the fallen snow. This is because the snow particles must fall through the non-uniform wind flow patterns resulting from the buildings, topography, etc. Physical modelling of such conditions is relatively easy because saltation does not occur so requirements (5,8,9,10 and 11) of Section 4 are irrelevant. Only requirements (1,2,6 and 7) need to be satisfied and this can be accomplished without undue difficulty in either wind tunnels or water flumes. References [20,21] are examples of such model tests. The only real shortcoming of such tests is the inability to model the cohesive and sintering properties of real snow.

5.2 Modelling of Situations with Snow-Drifting

For situations involving snow-drifting or both snow-drifting and snow-fall, the modelling requirements are as outlined in Section 4 of this paper. It was seen that the requirements cannot all be satisfied in practice and some compromise is inescapable. The physical implications of possible compromises are first discussed in general terms and then approaches which have been tried by various investigators are briefly reviewed.

5.2.1 Physical Implications of Compromises

It is necessary to violate either requirement (6) or requirement (10), and possibly also (11) of Section 4. The parameter in (6) is known as the 'densimetric Froude Number' and violation of (6) is violation of 'Froude scaling'. The violation usually is in the sense that velocities are too high in the model and this means inertia forces acting on the saltating particles are too high in comparison with gravity forces. The saltation trajectories are then too high and too long. The consequences of this are probably not serious if the saltation trajectories in the model are still much shorter than the smallest significant snow-drift dimension. The other alternative is to violate requirement (10), and possibly also (11). These requirements relate to the interaction between the wind flow and the particle bed and to the particle ejection process [5]. The consequences of violating them are not clear at this time, but some experiments by Kind & Murray [9] indicate that the consequences can be significant and that violation of Froude scaling is preferable where trajectory lengths are relatively short.

5.2.2 Low-Density Particles in Air

Low-density particles have relatively low terminal and threshold velocities, U_{TER} and U^*_{th}, respectively. Velocities, V, in the model tests therefore are relatively low which works in favour of satisfying Froude scaling, requirement (6). On the other hand, requirement (10) cannot be satisfied by such particles.

Finney [22] was probably the first to use this modelling approach. He tested drift-control devices for highways in a wind tunnel, using balsa sawdust to model the snow. He worked on an intuitive basis and did not do an analysis of modelling requirements.

Kind and Murray [9] did wind tunnel experiments on snow-fences using expanded polystyrene particles to represent the snow. These particles were particularly light, with $\sigma/\rho = 130$. Froude scaling, requirement (6), was approximately satisfied as were requirements (1,2,7 and 9); requirements (10) and (11) were, however, violated, the parameter of (10) having a value of only 2.0. The model snowdrift profiles were significantly different from field data; furthermore the saltation trajectories were unusually high and long considering the low wind speeds involved in these experiments and it was concluded that the saltation process with these light particles was not dynamically similar to that of real snow in the field. Complementary experiments using sand ($\sigma/\rho = 2200$) to represent the snow gave drift shapes in good agreement with field data despite the fact that the Froude number (requirement (6)) was about 20 times too large. Particle trajectory length is approximately proportional to the Froude number. It should be noted that even in the model cases, the snow-drifts formed by the fences are long compared to the saltation trajectory lengths. These experiments suggest that when significant drift dimensions are long compared with saltation trajectories, it is preferable to use high-density particles (e.g. 0.2 mm diameter sand) to represent the snow in wind-tunnel modelling. Trajectory lengths for 0.2 mm sand are of order 5 cm.

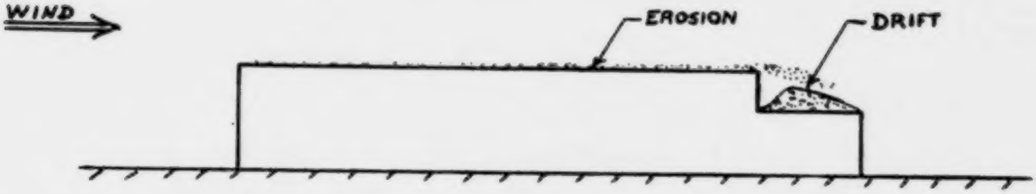

FIG. 6 STEPPED-ROOF BUILDING

da Matha Sant'Anna [23] is using fine sawdust in a wind tunnel to model snow-drift formation on the lower roof level of a stepped-roof building (see Fig. 6). This is a difficult modelling problem because the entire building model can only be of order 30 cm. long if it is not to cause excessive blockage in a wind tunnel of modest size. The lower roof is then only about 10 cm long and it is imperative that model particles blown off the upper roof follow correctly scaled trajectories so that they land and accumulate on the lower roof as they do in the prototype situation. Model and prototype Froude numbers should therefore be equal. This is very difficult to achieve since the length scale ratio L_P/L_M is typically about 400:1 in these situations, so that the wind speeds, V, in the model would have to be very low, well below the threshold velocity required to initiate saltation of even small low-density particles. The use of low-density particles seems to be virtually essential if situations such as this are to be modelled in air, despite the anomalous saltation behaviour observed by Kind & Murray [9] with such particles. Some form of artificial enhancement of the particle-ejection process might also be considered.

5.2.3 High-Density Particles in Air

This modelling approach has been tried by many workers. The threshold velocity of particles varies with size and is minimum for a nominal diameter of about 0.1 mm [24]. For high density particles ($\sigma/\rho \cong 2000$) in atmospheric air the minimum threshold velocity is about the same as that of real dry cohesionless snow. Therefore, when high-density particles are used, Froude scaling (requirement (6)) must be violated if the velocity ratio (V/V_{th}) is to be properly scaled (requirement (9)). Of course one can compromise, and choose particles and wind speeds to violate both requirements (6 and 9) to some degree. In any case the particle size should be chosen in the range 0.05 to 0.2 mm so that the threshold velocity is near the minimum possible. This minimizes the necessary compromises of the modelling requirements.

Strom et.al. [12] examined a variety of particle materials and finally chose 0.1 mm dia. borax for tests at 1/10th scale. Their values of (V/V_{th}) were several times less than in the prototype case so that their Froude numbers were essentially correct. They obtained realistic-appearing drift shapes around model buildings, storage tanks and snow fences.

Kind & Murray [9] used 0.2 mm silica sand particles in wind tunnel experiments on snow fences. The Froude number was about 20 times too high but all other modelling requirements were satisfied. As already mentioned, these experiments gave good results for drift shapes.

Drift shapes were found to be insensitive to the value of (V/V_{th}), requirement (9).

Iversen [16,17,18] uses 0.05 to 0.1 mm diameter glass beads in a wind tunnel. Iversen agrees that, in principle, the modelling requirements (1,2,6,7 and 9) should be satisfied and he introduces a roughness parameter and a Reynolds number requirement in lieu of requirement (10). Recognizing that compromise is essential, he takes the following approach. Extensive measurements of particle mass-transport rates in saltating flows are expressed in terms of a non-dimensional parameter and correlated in terms of other non-dimensional parameters like those appearing in requirements (6,7 and 9). Prototype values of the non-dimensional parameters are matched (equated) as closely as possible in the model tests. Imperfect matching is accounted for by using the mass-transport rate correlation to scale the model results up to prototype conditions. In this way the most crucial parameter, the mass-transport rate, is scaled reasonably precisely even though modelling of the actual saltation process is not precise. The inherent assumption is that the same transport-rate correlation applies in both model and full-scale situations; high-density particles are therefore essential since low-density particles follow a substantially different correlation [9]. Iversen has obtained realistic results for snow accumulations near highway facilities.

Tabler [25] has made the interesting suggestion that essentially correct modelling, at reduced scale, is possible outdoors in real drifting snow conditions. For example,a scale model would be placed on the snow surface outdoors and snow erosion/deposition patterns and rates near the model would be monitored. This approach is essentially the same as wind-tunnel modelling with real snow particles representing the snow. As such, one might expect the same difficulties mentioned earlier regarding conflict between Froude scaling and other modelling requirements. Specifically, since $U^*_{thM} = U^*_{thP}$ in this case, the Froude number would apparently be too high in the model situation. However Tabler argues that in real snowdrifting a natural sorting action takes place such that the predominant size of saltating snow particles is determined by the prevailing value of the surface shear stress, τ_o, or shear velocity U*. That is, he argues that the predominant size of saltating particles is always such that their threshold shear velocity, U^*_{th}, is always equal to the prevailing shear velocity, U^*; in other words, $(U^*/U^*_{th}) \cong 1$ regardless of the wind speed (above some minimum value). If this is the case, prototype situations with $U^* = 0.6$ m/s could for example be correctly modelled at 1/16 scale when the wind speed is such that $U^* = 0.15$ m/s; model and prototype Froude numbers would then be equal as required, and (U^*/U^*_{th}) would have a value of about 1 in both model and prototype situations. This is an interesting idea and it may offer an escape from the seemingly inevitable compromise discussed earlier. It should also be noted that outdoor modelling is not really a necessary feature of this idea. In the above example, the model test could equally correctly be carried out in a wind tunnel using sand with a value of 0.15 m/s for U^*_{th} and running the tunnel such that $U^* \cong 0.15$ m/s.

Tabler conducted some 1/30 scale model tests outdoors and obtained saturation drift profiles in good agreement with corresponding profiles measured in the full-scale installations. One of the experiments involved fairly complex terrain which had a marked effect on the snow accumulation pattern. Length dimensions were such that saltation trajectories would have been relatively small in both the model and full-scale experiments.

Anno and Anno & Konishi [26,27,28] have used very fine (1-10 μm) activated clay particles in a wind tunnel to model snowdrift accumulations. The particles are injected into the air-stream using compressed air and dispersed by turbulent diffusion. Therefore the saltation process which is dominant in actual snowdrifting is not represented and this approach must rely heavily on judgement. The activated clay particles have the advantage of a relatively high angle of repose (40° to 50°). Anno [27] finds that the approach-wind profile shape can be varied widely with little effect on 'snow' accumulation produced by the model snow-fence. He obtains reasonable accumulation patterns.

5.2.4 Sand in Water

Water flumes are very convenient for snow-drifting experiments. There is no dust problem and the model is readily accessible via the open top of the flume. These reasons alone amply justify this modelling approach for many cases. Like the other approaches, modelling in water involves compromises. Perhaps the most important compromise is that the saltation process in water is considerably different from that in air, as mentioned earlier. The detailed mechanics responsible for the differences are not understood at this time.

Because the ratio σ/ρ is relatively low in water, the situation is similar to that of low-density particles in air. It is possible to attain quite low threshold velocities so that Froude scaling can be approximately satisfied even at much reduced model scales while still satisfying the velocity-ratio requirements (7) and (9). Only requirements (10) and (11) or alternatives, relating to the particle-ejection process, cannot be satisfied.

Isyumov [14] was perhaps the first to satisfy the main modelling requirements in water flume experiments. He used 0.15 mm silica sand in 1:200 scale experiments on snow accumulations on building roofs. He satisfied requirements (1,2,6,7 and 9) reasonably closely. Isyumov had no field data with which to compare his model results, but the results appeared reasonable and he was able to show comparative effects of wind speed and direction, roof geometry and upwind terrain roughness.

Wuebben [29] used 0.12 mm diameter sand ($U_{TER} \cong U^*_{th} \cong 0.01$ m/s) in a water flume for experiments on 1:50 and 1:100 model snow fences. To satisfy requirement (7) this required a relatively low flow velocity V, and the densimetric Froude number (requirement 6) was thus rather low in his experiments. His ratio (V/V_{th}) was appropriate for snow with a small amount of cohesion ($U^*_{th} \cong 0.35$ m/s). Wuebben obtained drift profiles in reasonable agreement with Tabler's [30] field data. Rather pronounced ripples were however present on the drifts.

Irwin and Williams [21] describe an approach pioneered by Theakston and used for many years for commercial studies of possible snow accumulations around projected buildings, highway facilities, etc. They use 0.12 mm diameter silica sand which is precipitated into the water flow such that sand falls over the area of the flume floor occupied by the model and its surroundings. The flow speed is adjusted such that (V/V_{th}) is slightly above unity($V \cong 0.1$ m/s) at the model so that the sand particles are moved along the surface in regions of relatively high velocity but remain stationary in low-velocity regions. The saltation trajectory length is very short (only a few grain diameters in length) and Irwin & Williams argue that this allows the complexities of what determines the details of the path itself to be sidestepped. This author is inclined to agree with them. It should however also be noted that with $V \cong 0.1$ m/s and $U_{TER} \cong 0.01$ m/s, in the typical 1:500 scale model the Froude and velocity scaling requirements (6), (7) and (9) are reasonably well satisfied for a prototype wind speed, V, of 5 m/s and snow with $U_{TER} = 0.5$ m/s and $V_{th} \cong 5$ m/s. The latter are reasonably typical of real snow. The Froude number tends to be somewhat too low, rather than too high, and this is probably advantageous as it tends to keep particle trajectories short relative to significant drift dimensions. Long experience with the technique has demonstrated that it can give predictions which agree well with subsequent field observations.

6. Discussion

It is generally accepted that fully correct, reduced scale modelling of snowdrifting is not possible in practice. All of the modelling approaches consequently involve some compromise and each one of the three main approaches reviewed in Section 5.2 has something to offer. It is important to recognize that, whatever approach is used, particles tend to settle in zones of low velocity and to erode from zones of high velocity. Reasonably representative erosion/deposition patterns will therefore be obtained in most situations provided that the wind flow patterns are reasonably well simulated.

This requirement is relatively easy to satisfy as it requires only a reasonably correct approach-flow velocity profile and a geometrically scaled model and surroundings (modelling requirements (1) and (2)). If only these requirements are satisfied, however, no attempt should be made to scale transport rates or accumulation rates up to prototype values; even scaled-up drift dimensions should be regarded as very approximate. Moreover, misleading results are possible. Most of the approaches reviewed in Section 5.2 allow the majority of the modelling requirements to be satisfied without undue difficulty and it would be preferable to adopt one of these approaches. Quantitative scaling of model results would then often be appropriate and the liklihood of misleading results would be reduced. The approach used should be appropriate to the situation being investigated. For example, wind-tunnel modelling using high density particles is not appropriate if particle trajectory lengths are apt to be comparable to significant drift dimensions. Caution is always called for when interpreting results and field experience with snowdrifting phenomena is a valuable asset.

The most attractive modelling approach for most purposes would appear to be sand in water. This approach has great advantages of convenience. Moreover, the saltation trajectories are short so that it is appropriate for most situations. The main shortcoming is that the detailed dynamics of the saltation process apparently differ substantially from those for real snow in air. For most situations, as discussed by Irwin & Williams [21], this shortcoming is rendered insignificant by the shortness of particle trajectories.

In situations where detailed saltation dynamics are judged to be significant, an appropriate modelling approach is the use of a wind-tunnel with high-density particles. Model Froude numbers will tend to be substantially greater than prototype values, however, and particle trajectories must therefore be short relative to significant drift dimensions.

7. Conclusions

Saltation is the most important mass-transport process in snowdrifting for wind speeds below about 15 m/s.

Fully correct modelling is feasible for snow-fall but not for snow-drifting situations. Compromise is therefore essential and a variety of modelling approaches are available for snow-drifting; they can give very useful results but must be selected and used with some caution.

Modelling with sand particles in water is very convenient and allows most of the requirements to be satisfied. Saltation trajectories are short which makes this approach suitable for most situations. Detailed saltation dynamics differ from those of real snow in air but this is not important in most situations.

Saltation dynamics of high density particles in air are dynamically similar to those of real snow in air. Wind tunnel modelling with such particles is therefore appropriate where detailed saltation dynamics are judged to be significant, provided that particle trajectory lengths in the model are not comparable to significant drift dimensions. This approach is suitable in any situation where the trajectory-length condition is satisfied.

References

1. Wang Zhonglong and Chen Yuan, "Research on Prevention of Snow Drifts by Blower Fences", J. Glaciology, Vol. 26, No. 94, pp. 435-445, 1980.

2. Gray, D.M. and Male, D.H. (eds.), Handbook of Snow-Principles Processes, Management & Use, (Chapter 8), Pergamon Press Canada Ltd., Toronto, 1981.

3. Plate, E. (ed.), Engineering Meteorology, Elsevier Scientific Publishing Co., Amsterdam, 1982.

4. Bagnold, R.A., "The Nature of Saltation and of Bed-Load Transport in Water", Proc. R. Soc. Lond. A.332, pp. 473-504, 1973.

5. Kind, R.J., "A Critical Examination of the Requirements for Model Simulation of Wind-Induced Erosion/Deposition Phenomena Such as Snow Drifting", Atmos. Environment, Vol. 10, pp. 219-227, 1976.

6. Counihan, J., "Adiabatic Atmospheric Boundary Layers: A Review and Analysis of Data from the Period 1880-1972", Atmos. Environment, Vol. 9, pp. 871-905, 1975.

7. Oura, H., "Studies of Blowing Snow I", in Physics of Snow and Ice"(H. Oura ed.), Proc. Int. Conf. on Low Temp. Sci., Hokkaido University, Sapporo, Vol. 1, part 2, pp. 1085-1097, 1967.

8. Kobayashi, D., "Studies of Snow Transport in Low-Level Drifting Snow", Inst. of Low Temp. Sci., Sapporo, Japan, Report No. A31, pp. 1-58, 1973.

9. Kind, R.J. and Murray, S.B., "Saltation Flow Measurements Relating to Modeling of Snowdrifting", J. Wind Eng. and Indust. Aero., Vol. 10, pp. 89-102, 1982.

10. Bagnold, R.A., The Physics of Blown Sand and Desert Dunes, Methuen, London, 1941.

11. Yalin, M.S., Mechanics of Sediment Transport, Pergamon Press, Oxford, 1972.

12. Strom, G., Kelly, G.R., Keitz, E.L. and Weiss, R.F., "Scale Model Studies on Snow Drifting", Research Report 73, U.S. Army Snow, Ice and Permafrost Establishment, 1962.

13. Odar, F., "Simulation of Drifting Snow", Research Report 174, U.S. Army Cold Regions Research and Engineering Laboratory, 1965.

14. Isyumov, N., "An Approach to the Prediction of Snow Loads", Ph.D. thesis, University of Western Ontario, 1971.

15. Iversen, J.D., "Drifting Snow Similitude", J. Hyd. Div., ASCE, Vol. 105, No. HY6, pp. 737-753, 1979.

16. Iversen, J.D., "Drifting Snow Similitude - Drift Deposit Rate Correlation", proc. Fifth Int. Conf. on Wind Engineering, Ft. Collins, Colorado, July 1979, Pergamon Press Ltd., pp. 1035-1047, 1980.

17. Iversen, J.D., "Drifting Snow Similitude - Transport-Rate and Roughness Modeling", J. Glaciology, Vol. 26, No. 94, pp. 393-403, 1980.

18. Iversen, J.D., "Small-Scale Modeling of Snow-Drift Phenomena", proc. Int. Workshop on Wind Tunnel Modeling Criteria in Civ. Eng. Applications, Gaithersburg, Maryland, April 1982, Cambridge Univ. Press, pp. 522-545, 1982.

19. Iversen, J.D., "Comparison of Snowdrift Modeling Criteria: Commentary on "Application of Anno's Modeling Conditions to Outdoor Modeling of Snowdrifts", Cold Regions Sci. and Technol., Vol. 9, pp. 259-265, 1984.

20. Kind, R.J. and Irwin H.P.A.H., "Study of Snow Accumulation on the Removable Roof of the Montreal Olympic Stadium", National Research Council of Canada report LTR-LA-239, Dec. 1979.

21. Irwin, H.P.A.H. and Williams, C.J., "Application of Snow-Simulation Model Tests to Planning and Design", proc. Eastern Snow Conf. Vol. 28, 40th Annual Meeting, pp. 118-130, June 1983.

22. Finney, E.A., "Snow Control on the Highway", Bulletin, Michigan Engineering Experiment Station (East Lansing), No. 57, 1934.

23. da Matha Sant'Anna, F., private communication, National Research Council of Canada, Division of Building Research, 1984.

24. Iversen, J.D. and White, B.R., "Saltation Threshold on Earth, Mars and Venus", Sedimentology, Vol. 29, pp. 111-119, 1982.

25. Tabler, R.D., "Self-Similarity of Wind Profiles in Blowing Snow Allows Outdoor Modelling", J. Glaciology, Vol. 26, No. 94, pp. 421-434, 1980.

26. Anno, Y. and Konishi, T., "Modelling the Effects of a Snowdrift-Preventing Forest and a Snow Fence by Means of Activated Clay Particles", Cold Regions Sci. and Technol. Vol. 5, pp. 43-58, 1981.

27. Anno, Y., "Requirements for Modelling of a Snowdrift", Cold Region Sci. and Technol., Vol. 8, pp. 241-252, 1984.

28. Anno, Y., "Applications of Anno's Modeling Conditions to Outdoor Modeling of Snowdrifts", Cold Regions Sci. and Technol., Vol. 9, pp. 179-181, 1984.

29. Wuebben, J.L., "A Hydraulic Model Investigation of Drifting Snow", U.S. Army Cold Regions Research and Engineering Laboratory Report 78-16, 1978.

30. Tabler, R.D., "Geometry and Density of Drifts Formed by Snow Fences", J. Glaciology, Vol. 26, No. 94, pp. 405-419, 1980.

WINTER PRECIPITATION, SNOWPACK AND ATMOSPHERIC CONDITIONS IN THE SOUTHERN CANADIAN ROCKIES

by

N.H. Thyer

Division of Survey Engineering
University of Calgary
Calgary, Alberta
Canada

F.D. Barlow and F.E. Robitaille

Atmospheric Sciences Department
Alberta Research Council
Edmonton, Alberta
Canada

presented at

SNOW PROPERTY MEASUREMENTS WORKSHOP

Lake Louise, Alberta

1-3 April, 1985

TECHNICAL MEMORANDUM 140

Compiled By

P.R. Kry

NRCC 27594

Winter Precipitation, Snowpack and Atmospheric Conditions in the Southern Canadian Rockies

N.H. Thyer

Division of Survey Engineering
University of Calgary
Calgary, Alberta

F.D. Barlow and F.E. Robitaille

Atmospheric Sciences Department
Alberta Research Council
Edmonton, Alberta

ABSTRACT

The snow climate of the southern Canadian Rockies is being examined by the Alberta Research Council to determine the modification potential of clouds. This effort includes analyses of cloud and snowfall characteristics. The results to date of the climatological analyses of precipitation data and their relationship to features of the atmosphere are discussed.

A summary of results of the analyses and examples are presented in three sections. The first examines frequencies of occurrence of various daily snowfall amounts over the season for selected climate stations. A seasonal distribution index is presented that suggests different regimes exist on each side of the continental divide. The fractional contribution of daily precipitation amounts to the total winter precipitation is presented. The second aspect of this study examines the relationship of daily snowfall amounts to meteorological characteristics of the atmosphere. These characteristics are interpolated from rawinsonde observations at the 700 millibar and 500 millibar levels and include temperature, wind speed and direction, vorticity and lapse rate. General results are summarized and examples of relationships are given. Finally, the relationship between snowpack observed at mountain stations and precipitation measured at climate stations is examined. Results indicate a good correlation in some cases but not in others.

1.0 INTRODUCTION

The meltwater from winter snowpack of the southern Canadian Rockies provides the principal water source for irrigation agriculture in southern Alberta. Future agricultural expansion and accommodation of other water-based requirements depends on careful management of this region's water resources (Environment Council of Alberta, 1982). Supplementing this water resource by increasing the snowpack storage may assist in such management.

The Alberta Research Council initiated a preliminary project to examine the feasibility of supplementing the snowpack through the controlled use of cloud-seeding techniques. This projects's initial aim is to measure and analyze precipitation processes of snow-producing orographic clouds. The project study area straddles the Alberta-British Columbia border and includes the Oldman River basin (Figure 1).

As part of this analysis, a study of the long-term precipitation data of the region was initiated. Snowpack and daily precipitation data selected from climate stations, snow survey stations and upper air measurements were used. This paper reports on some of the results.

There are three sections to the climatological examination presented here: a) seasonal snowfall characteristics, b) snowfall/upper air relationships and c) snowfall/snowpack relationships. Each of these sections presents highlights and examples of the analysis.

2.0 SEASONAL SNOWFALL CHARACTERISTICS

Analyses discussed in this section were carried out for 24 stations in the study area (Figure 2 and Table 1). Periods of record for these stations range from 11 to 33 years, with varying degrees of completeness. Days with missing data were not included.

2.1 Procedures

For the selected stations, three analysis steps were carried out:

(1) total snowfall measured for each month of record was determined;

(2) the number of occurrences for each month of daily snowfall exceeding 0, 2, 4, 8, 16, and 32 centimetres were found;

(3) the number of occurrences for each month were summed over all years of record.

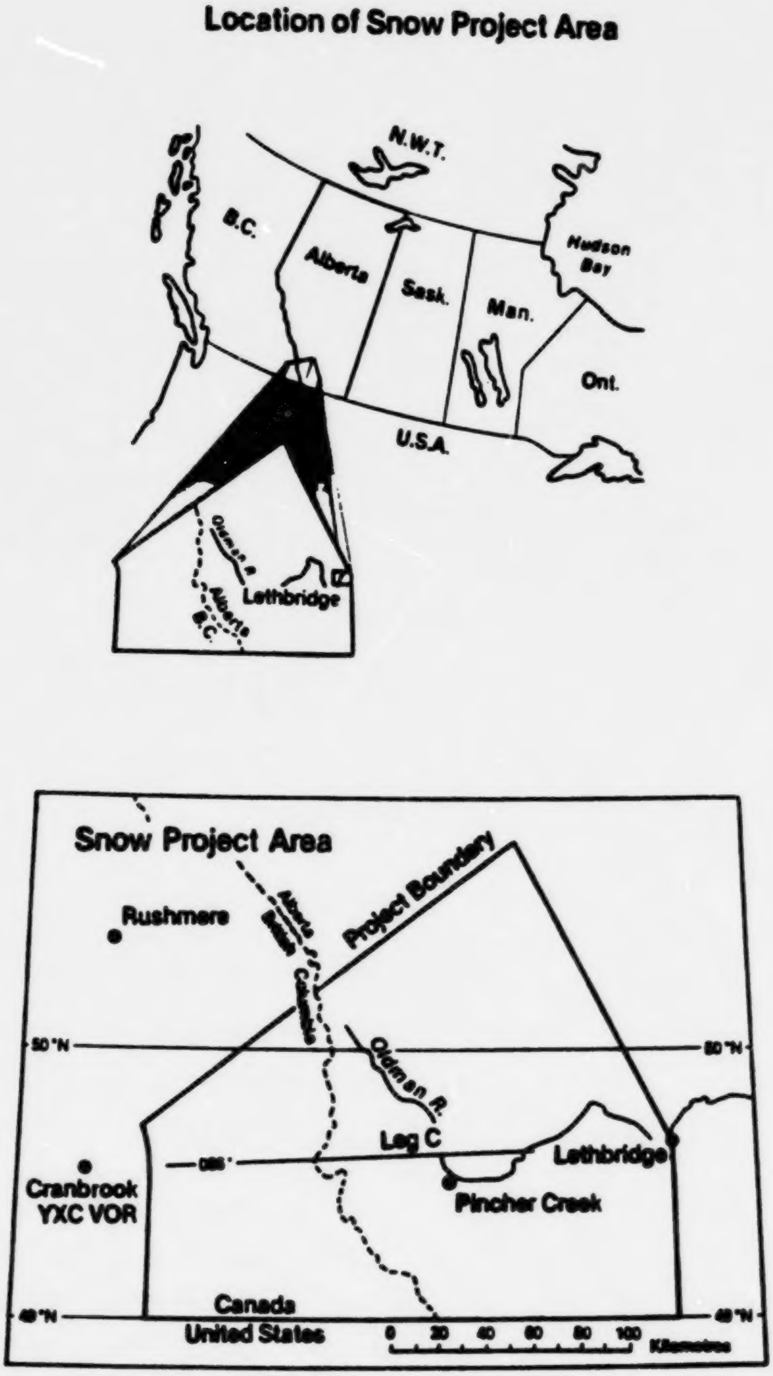
Location of Snow Project Area
N.W.T.
B.C.
Alberta
Sask.
Man.
Hudson Bay
Ont.
U.S.A.
Oldman R.
Lethbridge
Alberta
B.C.
Snow Project Area
Rushmere
Alberta
British Columbia
Project Boundary
50°N
Oldman R.
Leg C
095°
Lethbridge
Cranbrook
YXC VOR
Pincher Creek
Canada
United States
49°N
0 20 40 60 80 100
Kilometres

Figure 1. The Alberta Research Council Snow Project Area.

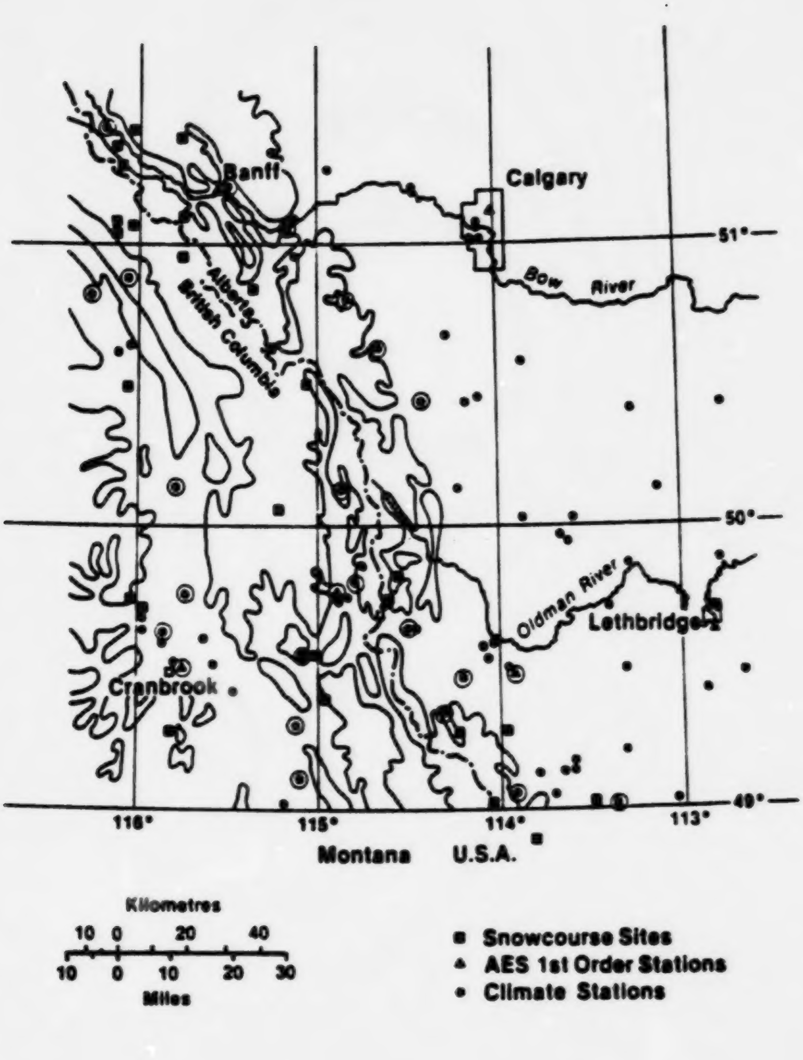
Banff
Calgary
51°
Bow River
Alberta
British Columbia
50°
Oldman River
Lethbridge
Cranbrook
116°
115°
114°
113°
49°
Montana
U.S.A.
Kilometres
10 0 20 40
10 0 10 20 30
Miles
■ Snowcourse Sites
▲ AES 1st Order Stations
● Climate Stations

Figure 2. Location of precipitation measurement sites used in the study. Climate stations selected for analysis are circled and the 2000 metre contour is shown.

Table 1. Climate stations selected for the snowfall analysis.

Station Name	Station Number	Elevation (meters)	Latitude	Longitude
Canal Flats RS	1151288	817	50-09	115-49
Cranbrook A	1152100	920	49-32	115-46
Elko	1152670	939	49-18	115-06
Fernie	1152850	1007	49-30	115-03
Fording R	1152899	1658 1702	50-11	114-52
Grasmere	1153282	869	49-06	115-05
Kimberly A	1154200	919	49-44	115-47
Kootenay NP	1154400	1170	50-52	116-03
Natal Harmer	1155402	1890	49-46	114-50
Natal Kaiser	1155403	1128	49-45	114-53
Wasa	1158730	930	49-49	115-38
Brisco	1171020	830	50-49	116-15
Carway	3031400	1359	49-00	113-22
Pincher Creek	3035201	1155 1190	49-30	113-57
Banff	3050520	1397	51-11	115-34
Beaver Mines	3050600	1286	49-28	114-10
Castle RS	3051430	1364	49-24	114-20
Coleman	3051720	1341	49-38	114-35
Elbow RS	3052270	1433	50-54	114-42
Kananaskis	3053600	1390	51-02	115-03
Lake Louise	3053760	1529	51-25	116-10
Pekisko	3055120	1439	50-22	114-25
Sheep RS	3055883	1494	50-39	114-39
Waterton Cabin	3057243	1280	49-07	113-51

Where two elevations are listed the station was relocated during the period of record.

2.2 Results

Graphs showing the percentage frequency of occurrence of snowfall exceeding given values as a function of month were prepared for each station. The curves for Lake Louise are shown in Figure 3. For Lake Louise and all stations in the study area, the percentage frequencies for September are lower than those for April. This difference is much greater for stations in the Alberta foothills than for British Columbia stations. Low September snowfall is due to higher temperatures in that month. In April, snowfall is infrequent at stations west of the Continental Divide, whereas, at most stations east of the Divide, snowfalls of a given size are just as likely to occur during mid-winter.

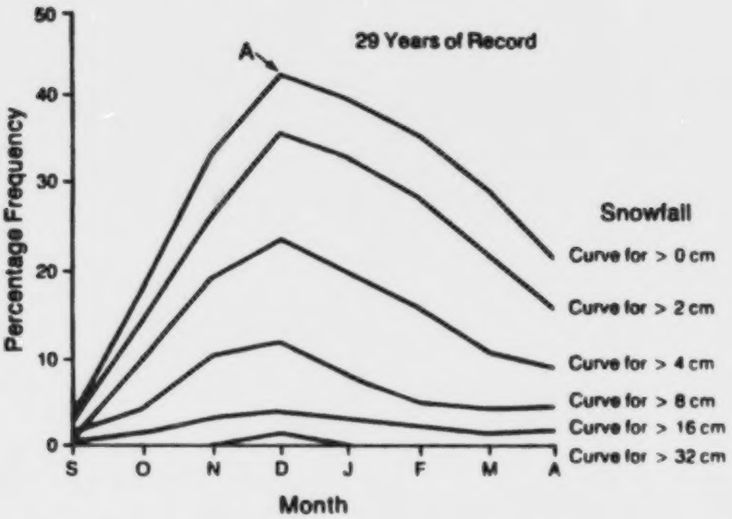

Figure 3. Percentage frequency of occurrence of snowfall exceeding given values as a function of month for Lake Louise. "A" indicates there was snowfall greater than zero centimetres 43% of the time in December.

To demonstrate differences in seasonal snowfall between stations east and west of the Divide, a seasonal distribution index is used. For a given daily snowfall, this index is equal to twice the sum of its percentage frequencies for March and April, minus the sum of the percentage frequencies for November, December, January, and February. Thus, this index is positive for stations which experience more of the given snowfall event in the spring, and negative for stations which experience these events in late fall and mid-winter. A contoured map of this index for daily snowfall exceeding eight centimetres is shown in Figure 4. The index areal pattern for events exceeding 16 centimetres per day (not shown) is similar. Apparently, seasonal distribution of moderate to heavy daily snowfall in the southern Canadian Rockies has two principal forms. West of and over the Continental Divide, such snowfalls occur mainly in midwinter; while east of the Divide, these snowfalls occur more frequently in spring.

The contribution of daily snowfall amounts to the total snowfall from September through April for Lake Louise is shown in Figure 5. Plots of this kind were produced for all 24 climate stations. When the shapes of such curves differ from station to station, differences in snowfall climatology are implied.

Figure 6 presents the percentage contribution of daily snowfall events exceeding eight centimetres to the total September through April snowfall. Daily snowfalls of more than eight centimetres per day are responsible for less than 40% of the seasonal total in the Rocky Mountain Trench but more than 60% over mountainous areas near the Continental Divide. Similarly, events exceeding 16 centimetres per day indicate only a 10% contribution in the Trench and a 20 to 30% contribution over higher terrain near the Divide.

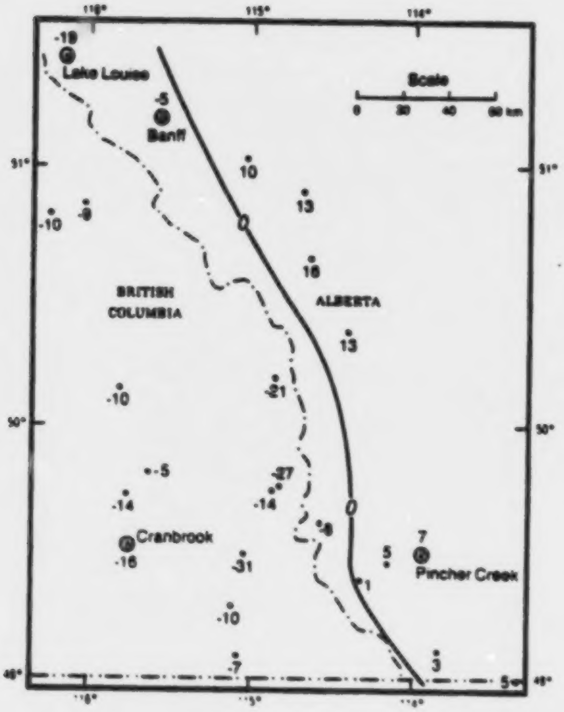
116°
115°
114°
51°
50°
49°
-19
Lake Louise
-5
Banff
Scale
0
20
40
60 km
10
13
-10
-9
0
16
BRITISH
COLUMBIA
ALBERTA
13
-10
-21
-5
-27
-14
-14
0
-8
Cranbrook
-16
-31
5
7
Pincher Creek
1
-10
-7
3
5

Figure 4. Seasonal distribution index for daily snowfalls exceeding eight centimetres. Negative values indicate moderate to heavy snowfall was more frequent in mid-winter and positive values indicate more frequent moderate to heavy snowfalls in the spring.

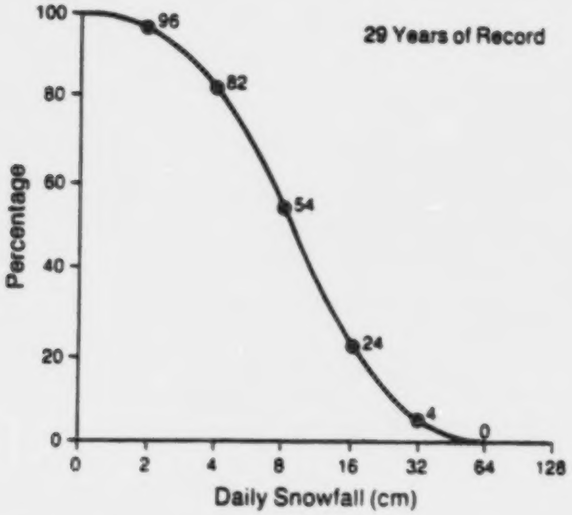

Figure 5. Percentage of season's daily snowfall events which occurred in amounts exceeding the snowfall values for Lake Louise.

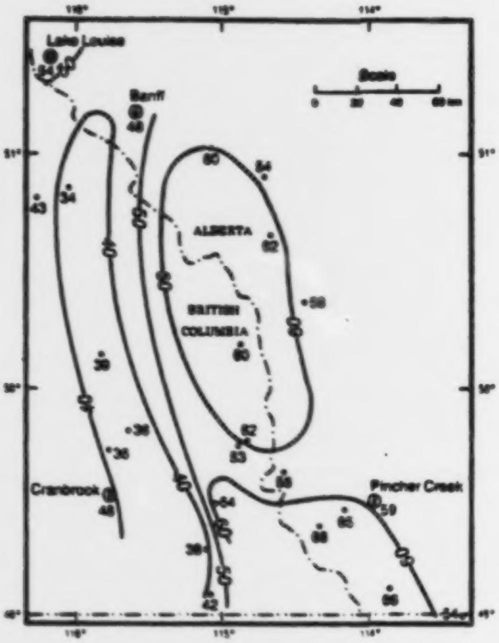

Figure 6. Percentage contribution to total winter snowfall of daily snowfall exceeding eight centimetres. For example snowfalls of eight centimetres or more account for 54% of the total snowfall at Lake Louise.

3.0 SNOWFALL RELATIONSHIP TO UPPER AIR CONDITIONS

Precipitation in the mountains is a complex combination of the effects of convergence, convection, and orography. The relative importance of orographic effects on precipitation is difficult to assess but it may be a major contributor to winter precipitation. Reinelt (1970), estimated that the orographic component accounts for over 50% of the September to April precipitation in the Alberta Rocky Mountains.

The amount of orographic precipitation in mountain regions is related to three different factors: 1) airmass characteristics and the synoptic scale pressure patterns 2) local terrain-induced vertical motions and 3) microphysical characteristics of the clouds (Barry, 1981). These three factors vary widely in scale and importance.

This section examines the possible impacts of the first factor. These synoptic aspects can be described qualitatively by airmass type or circulation systems. A more accessible approach is by quantitative description using the physical and dynamic characteristics of the measured upper air conditions. The latter approach is used here.

3.1 Procedures

Daily measured snowfall at selected climatological stations was compared to daily upper air conditions interpolated above each station. These upper air conditions were derived using measurements from daily rawinsonde releases and interpolating to the geographic location of the stations. The joint occurrence of various upper air quantities to station snowfall is interpreted in light of the synoptic conditions. While both daily precipitation and snowfall records were examined, only snowfall cases were used in results reported in this section.

Daily snowfall data were obtained for the period September through May. These measurements are made at 0800 local time and represent the accumulated precipitation for the previous twenty-four hour period. The eight stations selected with relatively long and complete records were: Banff, Beaver Mines, Brisco, Carway, Coleman, Elko, Lake Louise and Pekisko.

Upper air variables measured by rawinsonde are pressure, temperature and humidity; derived variables include wind speed and direction, and the height of various isobaric surfaces. Important quantities that can also be derived from these measurements include vorticity and lapse rate. Vorticity can be used as an indicator of synoptic development and lapse rate gives a measure of atmospheric stability. Some of the variables examined were temperature, wind speed and direction, height, vorticity and lapse rate. Two standard reported pressure surfaces, the 700 and 500 millibar levels, were used. For the standard IACO atmosphere, these two levels correspond to heights of 3012 metres (9882 feet) and 5574 metres (18,289 feet) respectively. The height of the 700 millibar level is thus generally just above the mountain barrier. The upper range of the 500 millibar level represents a general upper limit to winter orographic precipitation activity (Hjermstad, 1975).

The 0000 UCT rawinsonde sounding was used to calculate upper air parameters which were associated with the day's snowfall. This sounding is closest in time to the mid-point of the daily snowfall measurement "day". Analyzed data consisted of the period from February, 1966 to December, 1982 which had both snowfall measurements and 700 and 500 millibar values.

Since, upper air data is not available within or near the study area, it was necessary to interpolate values for the selected climate station comparisons. This was done using rawinsonde data from stations closest to the study area: Edmonton (northeast), Great Falls (southeast), Spokane (southwest) and Vernon (west-northwest) and Prince George (northwest). Prince George was used prior to October, 1971 when Vernon was established. The analysis was restricted to cases since February, 1966 when Edmonton commenced operations, since there is no appropriate substitute.

Upper air parameters were derived using an interpolation procedure based on the relative position of each of the stations to the upper air stations. A quadratic function was selected to express the heights (H) of the 700 and 500 millibar levels and the 700 millibar temperature:

H = A + Bx + Cy + D(x**2) + E(y**2) + F(x*y)

where x and y are the cartesian coordinates of the rawinsonde stations and A to F are constants for a given time. A linear function was used to express the 500 millibar temperature field. Geostrophic wind components were obtained from space derivatives of the height values.

A parametric least squares optimization procedure was used to derive the coefficients for the expressions on a daily basis. The upper air characteristics over a selected climate station were then interpolated from the derived expressions by substituting its location coordinates into the expression. Daily values of temperature, wind, and vorticity for the two pressure levels were then matched with the recorded snowfall quantities.

3.2 Results

The results of the analysis are presented in the form of two-way frequency tables. Each of the parameters: temperature, wind speed, wind direction, vorticity and 700- 500 millibar temperature differences were divided into eight equal-interval classes. Each class included its upper limit and excluded the lower. Frequency of occurrence for each class were cross-tabulated with each of the nine snowfall amount classes previously noted. The frequency of occurrence of a given parameter class over the total occurrence of the daily snowfall amount classes was then calculated. This procedure was completed for each of the eight climate stations on both a monthly and a seasonal basis for the entire period from February, 1966 to December, 1982 inclusive.

The general results for days with relatively heavier snowfalls (greater than eight centimetres) were noted. Generally, wind directions for both 700 and 500 millibar levels were the expected westerlies, with a slight southerly component present in the spring, for stations east of the Rockies. Wind speeds at 700 millibars were approximately 10 metres/second in autumn and spring, and 15 metres/second in mid-winter. The 500 millibar wind speeds were, in comparison, an above average 20 to 30 metres/second in the winter and 10 metres/second in spring and autumn periods. Temperatures ranged from -10 C to -15 C at 700 millibars while 500 millibar temperatures varied from -20 C to -30 C.

Both 7C0 and 500 millibar vorticities were similar to average values, and showed no obvious trend. The average temperature lapse rate for the heavier snowfall conditions was about 15 C. This lapse rate approximates the expected saturated adiabatic lapse rate between the two pressure levels and is consistent with the occurrence of a cloud layer.

Tables 2 and 3 show the seasonal results for the 700 millibar wind direction variables at Lake Louise and Beaver Mines. The relative frequency of occurrence of a given snowfall amount distributed among the eight wind direction classes is displayed. Also given are the relative directional frequencies for both snowfall days in general and the overall expected wind distribution for all cases. The percentage contribution of each snowfall class to total snow events is displayed next to the respective class as an indicator of their relative importance.

Table 2. Relative Frequency of daily snowfall amounts for Lake Louise (1966-1982).

		700 MILLIBAR WIND DIRECTION CLASSES (Degrees)							
		0-45	45-90	90-135	135-180	180-225	225-270	270-315	315-360
TOTAL (%)		3	1	2	2	8	30	42	13
SNOW DAYS (%)		<1	<1	<1	1	8	43	42	5
SNOW CLASSES (cm)	(%)								
0-2	27	<1	0	1	1	5	38	46	8
2-4	29	0	<1	0	2	10	43	40	5
4-8	26	1	0	1	1	11	42	42	4
8-16	13	1	0	0	1	8	51	38	3
16-32	5	0	0	0	0	7	47	47	0
32-64	<1	0	0	0	0	0	0	100	0

Lake Louise is at the northern edge of the project area and is within the main mass of the mountain terrain. In contrast, Beaver Mines is at the southern edge near the U.S. Border, and east of the main mountain barrier. The relative importance of any upslope flow on snowfall characteristics was expected to be more apparent for the latter station.

These two tables show the dominance of the 700 millibar westerly flow, which include over 90% of the overall daily values at Lake Louise and Beaver Mines. Westerly dominance is more pronounced for the snowfall days at Lake Louise, while Beaver Mine's snow days follow the general wind distribution. Snowfall occurrences from northerly flows are relatively rare, and easterly flow snow events are very rare for Lake Louise. The tables indicate that any significant differences in snow regime between the two sites are not apparent from the 700 millibar wind directions.

Table 3. Relative Frequency of daily snowfall amounts for Beaver Mines (1966-1982).

		700 MILLIBAR WIND DIRECTION CLASSES (Degrees)							
		0-45	45-90	90-135	135-180	180-225	225-270	270-315	315-360
TOTAL (%)		3	1	1	2	6	28	44	14
SNOW DAYS (%)		2	1	2	2	6	32	45	9
SNOW CLASSES (cm)	(%)								
0-2	22	4	4	2	1	6	35	43	6
2-4	28	1	1	1	3	7	33	41	13
4-8	23	1	1	1	1	7	31	48	9
8-16	18	1	1	1	4	7	34	44	8
16-32	8	2	0	5	2	4	24	56	7
32-64	1	0	0	0	14	14	14	57	0

4.0 RELATION BETWEEN MOUNTAIN SNOWPACK AND VALLEY PRECIPITATION

Estimates of mountain snowpack are of hydrological and climatological importance. If a relation between valley precipitation and mountain snowpack could be found, then estimates of mountain snowpack may be made when direct measurements are not available.

4.1 Hypothesis

To find such a relation, the following assumptions are made:

(1) Up to a certain date in the autumn when precipitation occurs at a valley station, rain or snow falls at higher elevations. Any snowfall at a higher elevation snowpack station soon melts and does not contribute to the snowpack.

(2) After that date and until a certain date in the spring when precipitation occurs at a valley climate station, a proportional amount of snow falls at the snowpack station and contributes to the snowpack. The time between these dates can be called the accumulation period.

(3) After that date in the spring, melting of the snowpack is significant, and the growth of snowpack is no longer proportional to the precipitation at the climate station.

4.2 Details Of Model

If this hypothesis is true, there should be a linear relationship between precipitation accumulated from the beginning of the period, a given date within the period, and the snowpack on that given date. This relation can be determined by linear regression if the beginning of the accumulation period is specified.

Usually, this starting date is not known and a trial and error method must be used. A linear relation for any arbitrary starting date within the accumulation period should exist. Different regression lines corresponding to different starting dates should only differ in their intercepts.

4.3 Interpretation Of Model

As an example, to find the snowpack at station B on February 1, knowing the precipitation at valley station A, an arbitrary starting date such as October 1, is selected. For all winters of record the total precipitation at A from October 31 to January 31 is compared with the snowpack measured at B on February 1. The corresponding pairs of values are plotted on a scatter diagram and a "line of best fit" determined by linear regression (Figure 7). From this regression line, the accumulated snowpack for another winter at station B can be estimated for February 1 based on the the accumulated precipitation at station A for the October 1 to January 31 period.

Similarly, the total precipitation from October 1 to February 28 can be compared with the snowpack measured on March 1 (Figure 8). If October 1 and March 1 lie within the accumulation period, the values of both variables will be greater than in the previous case (Figure 7). A regression line can also be drawn as a "best fit" to the points in Figure 8.

These two regression lines will generally be different. The first can be used only to estimate snowpack on February 1, and the second only for snowpack on March 1. In other words, each of the two regression lines refers to snowpack for an individual month. Nevertheless, if the hypothesis is true, the two regression lines should be similar. If this is the case, the data can be combined to obtain a single regression line which gives the "best fit" for all points (Figure 9). From this new regression line the snowpack on any given date between February 1 and March 1 can be estimated if the cumulative precipitation at valley station A from October 1 to that given date is known. Hence, this regression line can be used not only for the beginning of an individual month, but for an "extended period" ending on March 1.

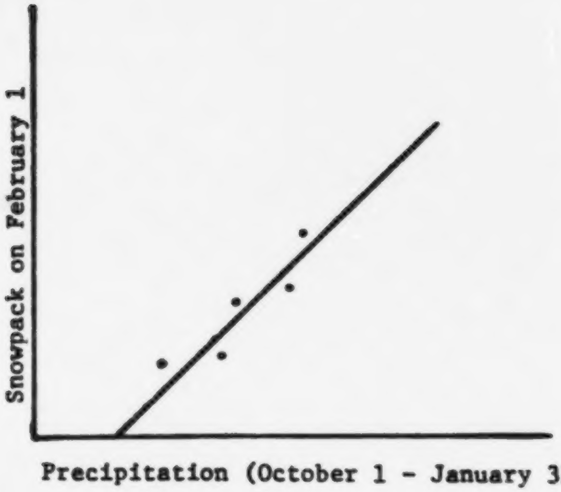

Figure 7. Regression line for an "individual month" (February 1). The five points refer to five different winters.

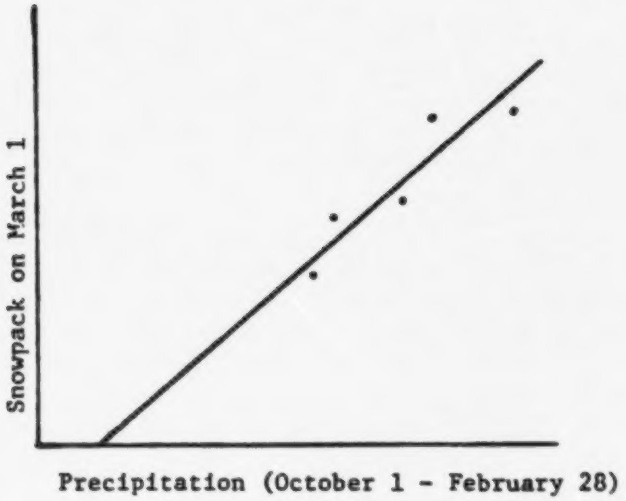

Figure 8. Regression line for an "individual month" (March 1). The five points refer to five different winters.

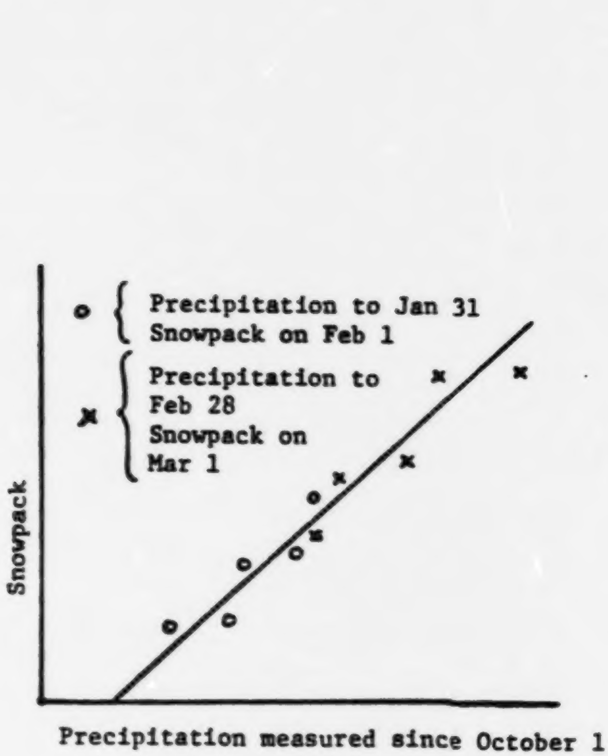

Figure 9. Regression line for an "extended period" (February 1 to March 1).

The October 1 starting date mentioned here is an arbitrary one. Similar analyses can be made using starting dates of September 1, November 1 and January 1.

In each case, the "goodness of fit" of the regression line can be estimated by computing the appropriate correlation coefficient. The best fit, and highest correlation coefficients should occur when the period of cumulative precipitation at valley station A lies within the accumulation period. Therefore, the regression line with the highest correlation coefficient should be selected for making snowpack estimates.

4.4 Sample Of Results

Correlations and regression relations of this type have been found for 23 pairs of snowpack and precipitation measuring stations. The pairs were chosen on the basis of geographic proximity and length of record available, with an observation history of 10 years being considered desirable, but not always attainable.

The correlation coefficients for these 23 pairs of stations have been quite variable ranging from less than zero to as high as 0.996 for 6 data points and 0.977 for 27 data points.

Sample values of the correlation coefficients are presented for Banff (precipitation) and Sunshine Village (snowpack). Figure 10 shows three curves. One represents the correlation coefficients corresponding to an estimate of the Sunshine Village snowpack on March 1 using Banff cumulative precipitation for starting dates from September 1 to January 1. The other two curves are for Sunshine Village snowpack on April 1 and May 1. The curve for the snowpack on February 1 is omitted because the data sample was too small, only 4 observations compared to 9 or 10 for the cases shown. The best correlation occurs when precipitation accumulates at Banff starting October 1. However, some later starting dates give correlations close to 0.9. Therefore, to determine the Sunshine Village snowpack for March 1, April 1 or May 1, a regression relation relating the Banff accumulated precipitation from October 1 to the desired date should be used.

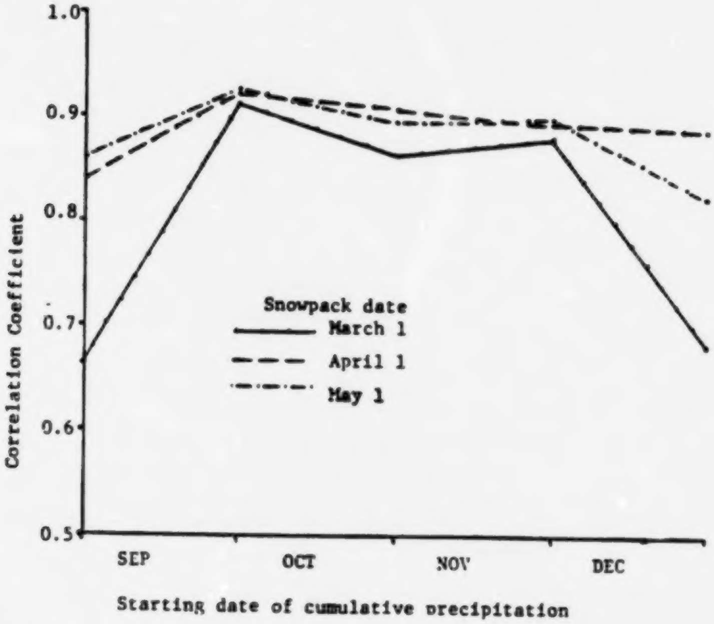

Figure 10. Correlation coefficients for single months. The climate station at Banff and the snowcourse at Sunshine Village were used.

Figure 11 also shows three curves. One is based on Sunshine Village snowpack readings taken February 1 and corresponding Banff precipitation accumulated to January 31, plus snowpack readings taken March 1 and corresponding precipitation accumulated to February 28. Thus, it refers to an "extended period" ending on March 1. The different points on the curve refer to different starting dates from which the cumulative precipitation was computed. The second curve is based on snowpack readings taken February 1, March 1 and April 1 and corresponding precipitation accumulated to January 31, February 28 and March 31 respectively. It refers to an "extended period" ending on April 1. Similarly, the third curve refers to an extended period ending on May 1.

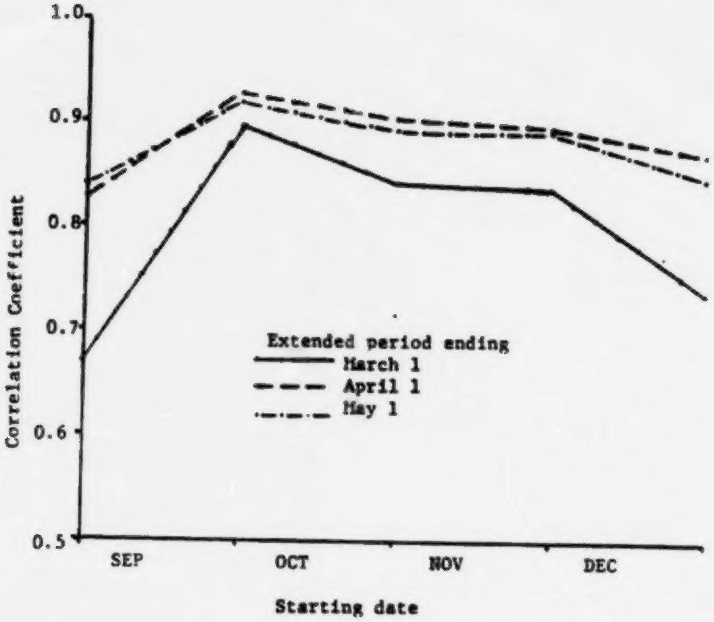

Figure 11. Correlation coefficients for extended periods starting February 1. The climate station at Banff and the snowcourse at Sunshine Village were used.

These curves also show a maximum correlation coefficient for a starting date at the beginning of October, and only slightly smaller values for later starting dates. The correlation coefficients for the extended period ending on May 1 are almost as great as those for the period ending on April 1. Together, these features suggest that the accumulation period at Sunshine Village starts sometime in September and ends after May 1.

Not all station pairs produced such high correlations or consistent results. The reasons for low correlations could be small sample size, differences in weather conditions at the two stations, variation of the starting date of the accumulation period from year to year, and occurrences of irregular midwinter thaws during the normal accumulation period. Examples of correlation coefficients for some pairs are given in Table 4.

Table 4. Examples of correlations for station pairs, using a starting date of October 1 for an extended period ending April 1.

Precipitation Station	Snow Survey Station	Correlation Coefficient
Fernie	Morrissey Ridge	0.944
Banff	Sunshine Village	0.926
Elko	Morrissey Ridge	0.925
Lake Louise	Kicking Horse	0.875
Fernie	Fernie	0.730
Banff	Banff	0.713
Lake Louise	Field	0.478

For those cases where the correlation is not good, it may be appropriate to take into account the prevailing air temperature as well as precipitation.

5.0 CONCLUSIONS

A seasonal index of snowfall frequency indicates that different regimes may be present on each side of the continental divide. The relative contributions of different snowfall intensities indicate a geographic relationship to the divide.

The relationship of snowfall to upper air conditions was not readily apparent. It was postulated that these upper air values would characterize the role of the synoptic conditions in determining snowfall. The results obtained are inconclusive and show that at various sites the synoptic atmospheric conditions for periods of snowfall are similar to the average. While certain synoptic conditions are required for particular snowfall types, their occurrence alone is not sufficient. Additional factors, such as local orographic effects, low level upslope flows, and cloud microphysical characteristics may be necessary for initiating the snow process.

Finally, the correlation of mountain snowpack to snowfall measurements was shown to be high for some cases but not for others. Additional parameters such as rate of change of upper air variables may be required for their successful interpretation.

ACKNOWLEDGEMENTS

The authors would like to gratefully acknowledge the assistance of J.W. Mason, R. Myrick and C.M. Sackiw of the Alberta Research Council in the preparation of this paper. This work has been funded by Alberta Agriculture and the Alberta Research Council.

REFERENCES

Barry, R.G., 1981, Mountain Weather and Climate, Methuen, 313 pp.

Environment Council of Alberta (ECA), 1982, "Irrigation Agriculture in Alberta", ECA81-17/1B8, Edmonton, Alberta, 74pp.

Hjermstad, L.M., 1975, Final Comprehensive Operations Report 1970- 1975 Season, Colorado River Basin Pilot Project, EG and G, (Report A1-1200), New Mexico.

Reinelt, E.R., 1970, On the role of Orography in the Precipitation Regime of Alberta, Alberta Geographer, 6, 45-58.

A COMPARISON OF VARIOUS SNOW GAUGES ON THE CANADIAN PRAIRIES OVER FIVE WINTERS

by

K.H. Jones

Scientific Services, Atmospheric Environment Service
Regina, Saskatchewan
Canada

presented at

SNOW PROPERTY MEASUREMENTS WORKSHOP

Lake Louise, Alberta

1-3 April, 1985

TECHNICAL MEMORANDUM 140

Compiled By

P.R. Kry

NRCC 27594

A COMPARISON OF VARIOUS SNOW GAUGES ON THE CANADIAN PRAIRIES OVER FIVE WINTERS

1. INTRODUCTION

Snow gauge networks are established to measure snowfall at specific locations. These point readings are then, hopefully, a close estimate of the average snowfall over the area. The accurate measurement of snowfall, however, is difficult in a plains environment. The major source of error is turbulent air flow around the gauge causing it to undercatch significantly in high winds. It has been found that unshielded gauges catch from one-third to one-half the amount of a well protected gauge in a forest (Larson, 1971). To eliminate the reduction of snow catch due to wind, various types of shields have been deployed. This makes the comparison of snowfall data from various locations extremely difficult. In fact, it has been shown that under windy conditions the catch of snowfall by precipitation gauges may be as much as eighty percent in error (Rechard et al., 1973).

The objective of this study was to compare the performance of various shields and gauges in an exposed prairie environment over a number of years to determine if any consist catch results could be found.

2. REGINA EXPERIMENTAL SITE

The study site is located near the Regina Airport and is typical of the wide open natural prairie grassland. The closest building is about 160 m away, so that no building eddies influenced snow catch.

The area is flat and treeless. This last year (83-84), however, four aviation fuel tanks were built about 60 metres to the west of the site area. These tanks do not appear to have influenced the results as the data from the winter of 1983-84 has remained consistent with the other winters. The location of the site with respect to the airport is given in Figure 1. It is in proximity to the official ten-point snow course.

3. GAUGES AND SHIELDS USED

The five gauges used for the winter of 1983-84 with their shielding are:

GAUGE	SHIELD
A.E.S. STANDARD	MSC NIPHER
FISCHER AND PORTER	SCALED-UP NIPHER
BELFORT	ALTER INSIDE WYOMING
SACRAMENTO	ALTER
STANDPIPE	ALTER

All five gauges were located in proximity to each other as shown in Figure 2. Most of the gauges were mounted at a height of 2.2 m above ground. Two gauges at the Regina site are, however, at a different height. The A.E.S. standard gauge was mounted at an orifice height of 1.7 m above ground. The Fischer and Porter recording gauge with a scaled up Nipher shield was also mounted at a height of 1.7 m above ground.

The large Nipher shield on the Fischer and Porter was constructed to fit the 20.7 cm diameter found on recording gauges. This scaled up

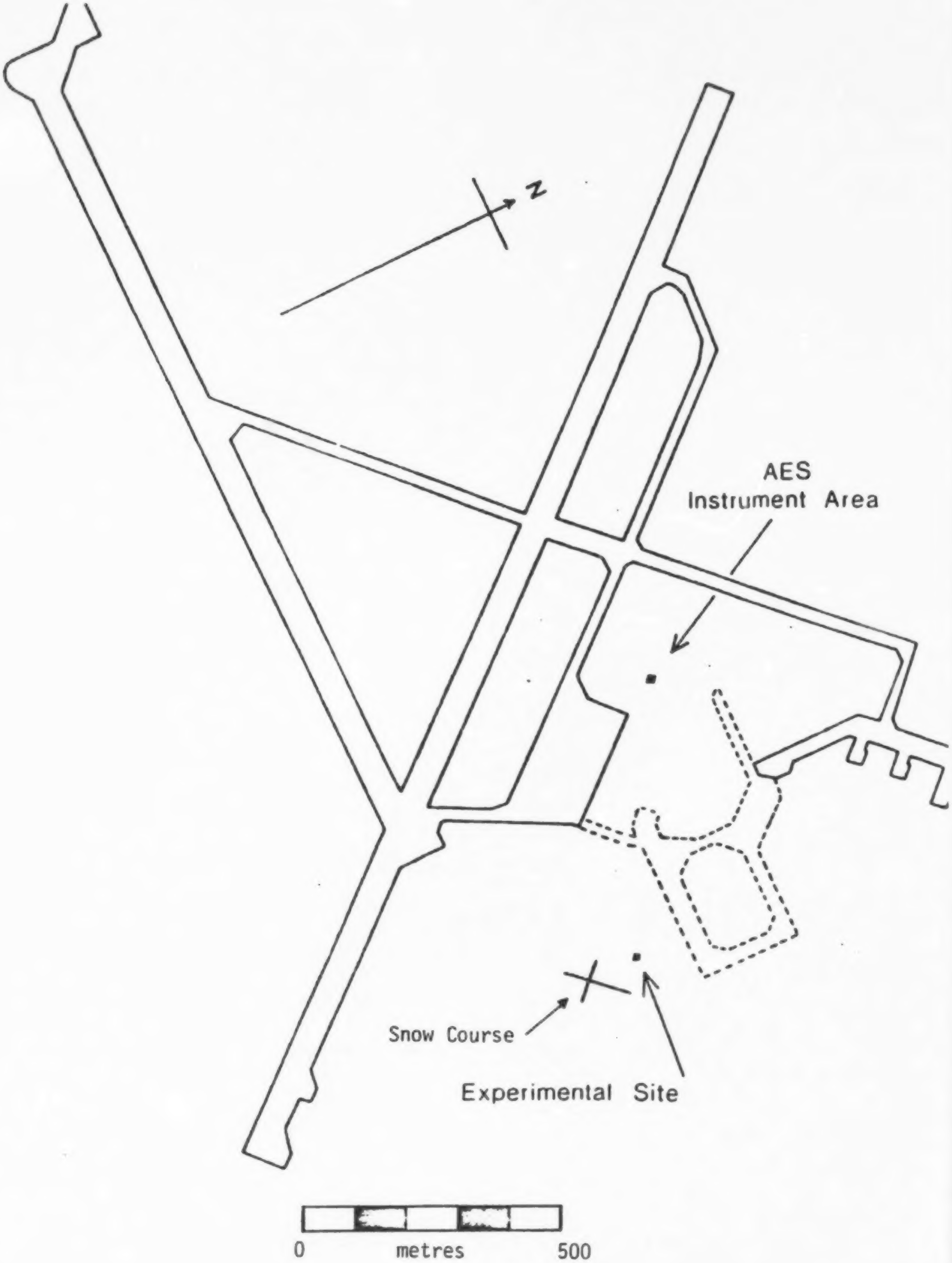
N
AES
Instrument Area
Snow Course
Experimental Site
0
metres
500

Fig. 1 Location of Experimental Site at Regina Airport

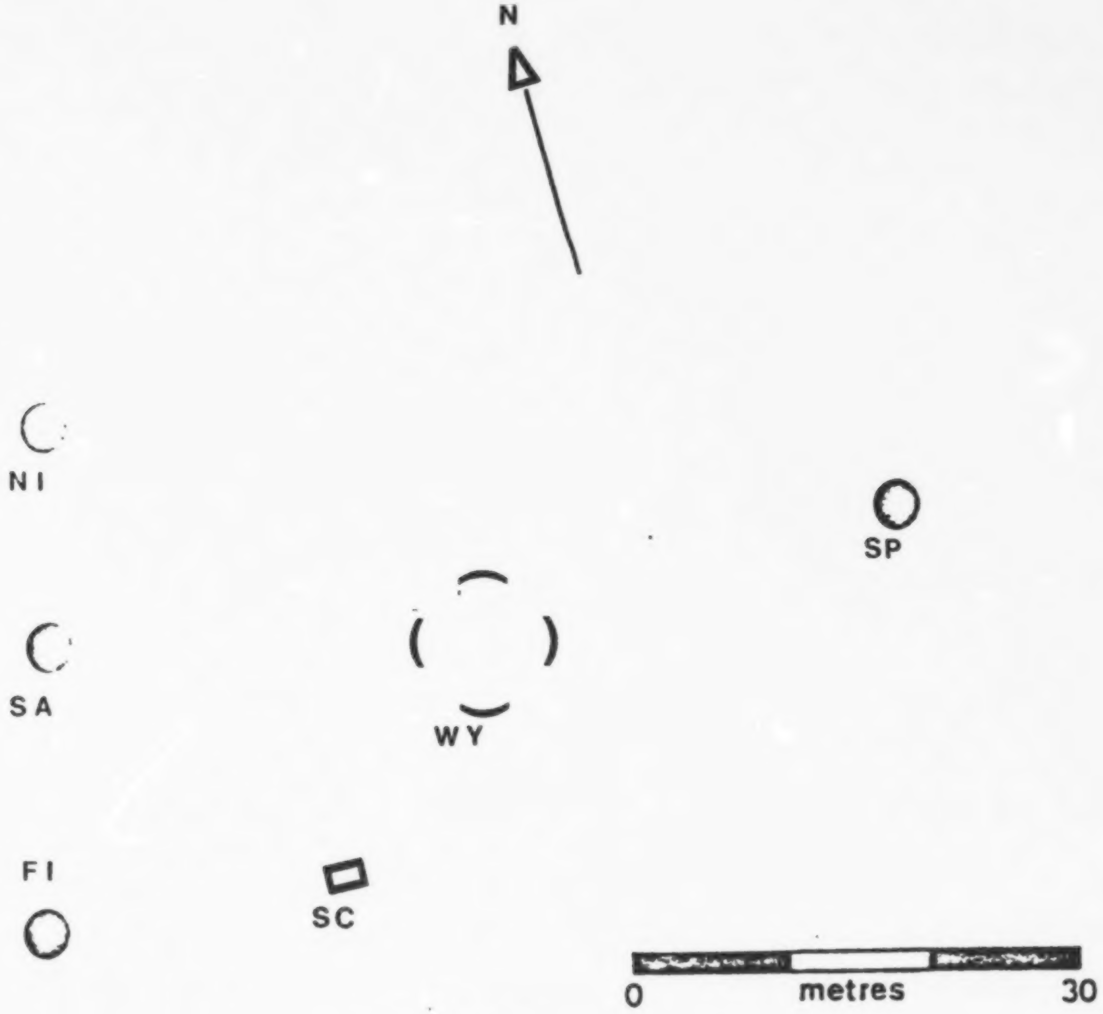

LEGEND

WY	Wyoming - shielded Belfort
SA	Alter - shielded Sacramento
FI	Nipher - shielded Fischer and Porter
NI	Standard Nipher - shielded gauge
SP	Alter - shielded standpipe
SC	Stevenson screen

FIGURE 2: Experimental Site for Winter of 1983-84

Nipher was constructed in the hope that it would enable the Fischer and Porter recording precipitation gauge to obtain snowfall water equivalent measurements comparable to the official A.E.S. Nipher-shielded gauge.

The Fischer and Porter recording gauge, the extension between the gauge and the shield, and the scaled up shield bring the orifice height to 1.7 m above ground. Further details on the installation of the various gauges at Regina over the five years are available from Jones (1982) and Cork (1978).

4. SNOWFALL CATCHES - DAILY MEASUREMENT GAUGES - WINTER 1983-84

Snowfall water eqivalents for each month of the winter of 1983-84 are given in Table 1 for the two recording gauges and for the standard AES Nipher which was read every weekday.

MONTH	AES STANDARD NIPHER	FISCHER & PORTER SCALED-UP NIPHER	BELFORT WYOMING
NOV	10.4	12.7	10.2
DEC	10.7	10.2	8.1
JAN	16.9	18.6	16.5
FEB	2.3	3.1	2.8
MAR	24.5	24.1	20.8
APR	1.0	1.5	1.5
TOTAL	65.8 (93.6%)	70.2 (100%)	59.9 (85%)

TABLE 1: Snow water equivalent (mm) from November 8, 1983 to April 10, 1984 with percent of highest catch.

Snowfall for the winter was well below normal with the month of February being especially dry, receiving only a couple of millimetres of snowfall. The results show the Nipher-shielded Fischer and Porter gauge had the highest snowfall catch followed closely by the A.E.S. standard Nipher-shielded snow gauge at 93.6% of the Fischer and Porter catch. The Belfort Wyoming ranked third among the three recording gauges catching 85.2% of the Fischer and Porter amount.

One gauge reading (January 30) had to be rejected for the standard Nipher-shielded gauge. A water equivalent of 10.2 mm was measured in this gauge. The two recording gauges and the Regina Weather Office Nipher-shielded gauge recorded under five millimetres of precipitation. The culprit was later identified as the fire hall. They had been practicing using their spray hoses that day and had gotten water into the Nipher-shielded gauge. The Regina Weather Office Nipher-shielded gauge reading of 4.8 mm water equivalent was substituted for this reading as measurments from these two gauges are usually within one-half millimetre of each other.

Table 2 gives the winter totals (83-84) for all five configurations (gauges and shields).

AES STANDARD NIPHER	FISCHER & PORTER SCALED-UP NIPHER	BELFORT WYOMING	STANDPIPE ALTER	SACRAMENTO ALTER
65.8 (93.6%)	70.2 (100%)	59.9 (85.2%)	43.7 (62.2%)	48.3 (68.8%)

TABLE 2: Snow water equivalent (mm) for the winter of 1983-84 with percent of highest catch for all gauges.

Both alter-shielded storage gauges caught considerably less snow than the Nipher-shielded gauges. This winter, however, the alter-shielded gauges and the Wyoming-shielded Belfort gauge caught an amount of snow closer to the Nipher totals. It is believed that the reason for this is that the winter of 1983-84 was noteworthy for its lack of wind. The winter of 1983-84 had an average monthly wind speed well below normal for every month or the winter (Table 3).

MONTH	AVERAGE SPEED (km/h)	NORMAL (km/h)
OCTOBER	14.6	20.5
NOVEMBER	14.3	20.9
DECEMBER	14.6	21.7
JANUARY	17.3	21.8
FEBRUARY	15.2	21.6
MARCH	15.1	22.0
APRIL	18.9	22.6

TABLE 3: Monthly average wind speed winter 1983-84 and comparative normals for Regina A.

The lack of wind this winter appears to have made the snowfall catch by any gauge less dependent on the type of shielding.

5. SNOWFALL CATCHES OVER THE FIVE WINTERS

Table 4 gives the snowfall catch over the last five winters. Results have proven to be surprisingly consistent. The last four years have seen the scaled-up Nipher shield on the Fischer & Porter catch the highest snowfall followed closely by the standard A.E.S. Nipher varying from 90 to 99% of the Fischer & Porter catch. The Wyoming shielded Belfort has consistently ranked third at 67 to 85% of the highest catch. The Alter shielded gauges caught considerably less snow in all years varying from 47 to 69% of the highest catch.

YEAR	AES STANDARD NIPHER	FISCHER & PORTER SCALED-UP NIPHER	BELFORT WYOMING	STANDPIPE ALTER	SACRAMENTO ALTER
79-80	35.1(100%)	33.0(94%)	23.6(67%)	-	-
80-81	43.6(90%)	48.3(100%)	37.8(78%)	24.9(52%)	23.9(49%)
81-82	113.8(98%)	116.3(100%)*	90.1(77%)	57.4(49%)	63.5(55%)
82-83	76.0(99%)	77.1(100%)	65.5(85%)	36.1(47%)	52.1(68%)
83-84	65.8(94%)	70.2(100%)	59.9(85%)	43.7(62%)	48.3(69%)
4 YR TOTAL	299.2(96%)	311.9(100%)	253.3(81%)	162.1(52%)	187.8(60%)

79-80 - January 18, 1980 to March 17, 1980
80-81 - October 24, 1980 to March 23, 1981
81-82 - November 17, 1981 to April 19, 1982
82-83 - November 15, 1982 to April 1, 1983
83-84 - November 8, 1983 to April 10, 1984

TABLE 4: Snow catch in mm water equivalent for five winters with percent of highest catch.

* (Period November 17 to November 26 estimated due to malfunction of gauge until November 26).

6. STATISTICAL CONFIDENCE

When a group comparison is made on the last four years of data, (Table 4), the variance between snowfall from year to year is so great that the estimate of variance becomes inflated by these yearly differences making it impossible to detect what could actually be a significant difference in gauge catch between any two gauges.

Since the variations from year to year are greater than the variations between gauges in any given year, a more appropriate statistical test is a paired comparison.

To estimate the mean difference between gauge catches and to test a hypothesis about these differences, one uses the difference between the members of each pair for a given year. Table 5 gives the results of a paired comparison between the standard A.E.S. Nipher-shielded gauge and the Wyoming-shielded Belfort gauge.

PAIR	AES STANDARD NIPHER	BELFORT WYOMING	DIFFERENCE $X_i = Y_{i1} - Y_{i2}$
79-80	35.1	23.6	11.5
80-81	43.6	37.8	5.8
81-82	113.8	90.1	23.7
82-83	76.0	65.5	10.5
83-84	65.8	59.9	5.9

TABLE 5: Paired comparisons of yearly snowfall in mm water equivalent.

From Table 5:

$$\Sigma X_i = 57.4 \qquad \bar{X} = 11.5$$

$$\Sigma (X_i - \bar{X})^2 = 213.7$$

The estimate of the variance of the population of differences is

$$S_x^2 = \frac{1}{n-1} \Sigma (X_i - \bar{X})^2$$

$$S_x^2 = \frac{213.7}{4} = 53.4$$

The variance of mean difference, $\bar{X}$ is estimated by

$$S_{\bar{x}}^2 = S_x^2/n$$

$$S_{\bar{x}}^2 = 53.4/5 - 10.7$$

$$S_{\bar{x}} = 3.27$$

Using the hypothesis that the gauges catch the same amount of snow,

$H_0: \mu_x = 0$, no difference against the alternate hypothesis

$H_a: \mu_x \neq 0$

The t-test at 95% confidence level with four degrees of freedom

$t_{.050,4} = 2.776$

The t-value from our five years of snowfall data

$$t = \frac{\overline{X} - \mu x}{S_{\overline{x}}} = \frac{11.5}{3.27} = 3.52$$

Therefore we can reject the null hypothesis and conclude that the A.E.S. standard Nipher-shielded gauge and the Wyoming-shielded Belfort do not catch an equal amount of snow (statistical confidence of 95.0%). Applying the same statistical test using the A.E.S. standard Nipher-shielded gauge and each of the two alter shielded storage gauges, we obtain a t-value of 3.93 for the Standpipe and a t-value of 3.67 for the Sacramento. The t-test at 95% confidence level with three degrees of freedom is $t_{.050,3} = 3.182$ Therefore in the case of the two Alter shielded gauges, we can again reject the null hypothesis and conclude that there is a significant difference in the seasonal catch of the A.E.S. standard Nipher-shielded gauge and that of either the Alter-shielded Sacramento or the Alter-shielded Standpipe gauges.

Table 6 is paired comparison of the Fischer and Porter gauge with the scaled-up Nipher and the standard A.E.S. Nipher-shielded gauge.

PAIR	SCALED-UP NIPHER FISCHER & PORTER	AES STANDARD NIPHER	DIFFERENCE $X_i = Yi1 = Y_2$
79-80	33.0	35.1	-2.1
80-81	48.3	43.6	4.7
81-82	116.3	113.8	2.5
82-83	77.1	76.0	1.1
83-84	70.2	65.8	4.4

TABLE 6: Paired comparison of snowfall catches in mm water equivalent

From Table 6 we have:

$\Sigma X_i = 10.6 \qquad \overline{X} = 2.1$

$\Sigma(X_i - \overline{X}) = 30.85$

Variance estimate of the population of differences is

$S_x^2 = \frac{30.85}{4} = 7.71$

Variance of the mean differences is then

$S_{\overline{x}}^2 = \frac{7.71}{5} = 1.54$ and $S_{\overline{x}} = 1.24$

The hypothesis is the same as before in that there is no difference in catch H_o: $\mu x = 0$. The alternate hypothesis H_a is

H_a: $\mu x \neq 0$.

The t-test at the 95% significance level with 4 degrees of freedom.

$t_{.050,4} = 2.776$

The t-value from five years of snowfall data

$t = \frac{\overline{X} - \mu x}{S_{\overline{x}}} = \frac{2.1}{1.24} - 1.69$

Therefore we cannot reject the null hypothesis at the 95% confidence limits and must conclude that the A.E.S. standard Nipher-shielded gauge and the Fischer and Porter gauge with the scaled-up Nipher shield have not shown any significant difference in seasonal catch amounts.

A one-tailed test on the five years of data shows that the Nipher shielded gauges catch more snow than the Wyoming or Alter shielded gauges. This can be stated with a statistical confidence of 95%. Testing of the snowfall catch of the scaled-up Nipher against the standard A.E.S. Nipher-shielded gauge has not revealed any significant difference. It can therefore be stated that the scaled-up Nipher shield can be placed on a recording gauge and yield results similar to those which would have been measured by a manually read standard Nipher-shielded at the same location.

7. SHIELD RELATIONSHIPS

The data over the five year test period has yielded consistent results. Because of this, it is of some benefit to study this relationship by means of regression analysis. Simple linear regression equations were fitted to the test data. Correlations and standard error for the regression estimates were also calculated. Table 7 contains the regression parameters based on the yearly snowfall data over five years.

In all cases, the predicted value Y is the amount of snowfall water equivalent in millimetres that the standard A.E.S. Nipher shielded gauge would have yielded.

$$Y = a + bX$$

	a	b	Correlation Coefficient	SE
SCALED-UP NIPHER FISCHER & PORTER	-.22	.97	.993	3.04
WYOMING SHIELDED BELFORT	1.26	1.18	.968	6.42
ALTER SHIELDED STANDPIPE	-5.86	1.99	.859	13.49
ALTER SHIELDED SACRAMENTO	-1.73	1.63	.859	13.46

TABLE 7: Regression parameters for predicting standard A.E.S. Nipher shielded gauge catch. Correlation coefficients and standard error of estimate for seasonal snowfall total water equivalent (mm).

8. SUMMARY

Determining the accuracy of gauge catch is difficult because it is not possible to define what the true catch should have been. On the wind-swept prairies, it is impossible to select a well-protected site and one must depend on artificial shields to provide protection from the wind.

Studies at the Regina site over the last few years have shown that gauges at the same location can show a considerable difference in catch totals depending on the type of shielding used on the gauge.

The two Nipher-shielded gauges consistently caught the most snow. The Wyoming-shielded gauge caught 80 percent of the amount that the Nipher-shielded gauges caught and the Alter-shielded gauges generally caught 50 to 60 percent of the Nipher-shielded gauges totals.

The snowfall catches of the standard A.E.S. Nipher-shielded gauge and the scaled-up Nipher shield mounted on the Fischer and Porter recording gauge are not significantly different. It appears that the scaled-up fiberglass shield designed to fit on recording gauges will give results compatible with the A.E.S. standard Nipher-shielded gauge used at principal meteorological stations across Canada.

9. CONCLUSION

It is concluded that the snow measurement comparison experiment at Regina Airport should be terminated. The consistent results from year to year have made vigorous statistical inferences possible and little more can be gained from another year of data.

11. REFERENCES

Cork, H.R., 1978: Wyoming-shielded storage gauge, Regina, 1977 and 1978. Hydrometeorological Report No. 29, 18 pp.

Dublin, J., 1981: A comparison of various snow gauges on the Canadian prairies. Regina, Central Region Scientific Services Report No. CSS-R81-03, 15 pp.

Goodison, B.E. and J.R. Metcalfe, 1980: MSC Nipher shields for recording precipitation gauges: an assessment. Downsview, Atmospheric Environment Service, Internal Document, 5 pp.

Jones, K.H., 1982: A comparison of various snow gauges on the Canadian prairies for the winter 1981-82. Regina, Central Region Scientific Services Report No. CSS-R83-01, 16 pp.

_____, 1983: A comparison of various snow gauges on the Canadian prairies for the winter 1982-83. Regina, Central Region Scientific Services Report No. CSS-R83-03, pp.

Larson, L.W., 1971: Shielding precipitation gauges from adverse wind effects with snow fences. Laramie, University of Wyoming, Water Resources Research Institute, Water Resources Series No. 25, 161 pp.

Rechard, P.A., 1975: Measurement of winter precipitation in windswept areas. Bismarck, North Dakota, Great Plains Agricultural Council, Pub. No. 73, 30 pp.

THE IMPACT OF AUTOMATION ON WINTER PRECIPITATION MEASUREMENT

by

B.E. Goodison

Canadian Climate Centre
Atmospheric Environment Service
Environment Canada
Downsview, Ontario
Canada

presented at

SNOW PROPERTY MEASUREMENTS WORKSHOP

Lake Louise, Alberta

1-3 April, 1985

TECHNICAL MEMORANDUM 140

Compiled By

P.R. Kry

NRCC 27594

THE IMPACT OF AUTOMATION ON WINTER PRECIPITATION MEASUREMENT

B.E. Goodison

Canadian Climate Centre

Atmospheric Environment Service

Environment Canada

Downsview, Ontario

INTRODUCTION

Precipitation is one of the most critical components of the hydrological cycle. Precipitation measurements - rainfall and snowfall - are currently made at about 2,500 Canadian observing stations operated by the Atmospheric Environment Service. Snowfall water equivalent is measured at 345 stations using the non-recording Nipher shielded snow gauge (the "official" Canadian snow gauge) and it is estimated at the remaining stations from ruler measurements of fresh snowfall, assuming a mean density of 100 kg m^{-3}. At best, therefore, 6-hourly snowfall totals are recorded at principal observing stations, while only twice daily or daily accumulations are available from all other network stations. The winter precipitation record is supplemented by measurements from approximately 190 storage gauges and 140 recording gauges operated by several agencies across Canada; these data are published annually by AES in **Supplementary Precipitation**. Unlike rainfall, where summer networks are operated at hundreds of grain elevators and provincial forest look-outs throughout the country, particularly in the West, there is no extensive supplemental snowfall or winter precipitation network other than data derived from the few snow pillows or the more extensive snow course network.

With reductions planned in the snow course network, more users are relying on precipitation measurements to estimate snow accumulation. However, as observing stations are automated and networks expanded through the use of data collection platforms (DCPs), new methods of snowfall measurement are required to replace the manual observations currently used. If new methods are not forthcoming for use at autostations, there will be a serious reduction in the number and quality of winter precipitation observations, and ultimately in our knowledge of Canada's snow resources. In an effort to address this problem, the Canadian Climate Centre of the Atmospheric Environment Service has been conducting research to evaluate the accuracy of current snowfall measurements and to develop suitable alternative techniques for the measurement of snowfall at automated stations.

Two developments which may resolve some of the uncertainty in winter precipitation measurement at automatic stations are improved shielding of recording precipitation gauges and the development of an automatic snow depth sensor. It has been found, in fact, that the use of both the precipitation gauge and snow depth sensor at unattended sites can be a very effective tool for determining precipitation totals, assessing the type of precipitation and providing an indication of the state of the snowpack (melting/non-melting).

Nipher-type Shield for Recording Precipitation Gauges

Considerable effort has been expended on assessing the accuracy and performance of snow gauges used by agencies. Earlier field tests (Goodison, 1978; 1981) and wind tunnel flow visualization experiments conducted at AES have shown that the non-recording Canadian MSC Nipher shielded snow gauge has a superior catch efficiency for measuring snowfall water equivalent than an unshielded or Alter-shielded Universal Belfort or Fischer & Porter recording precipitation gauge. However, recording gauges are the most feasible method, at least in the near future, for measuring winter precipitation at remote sites and at automatic observing stations. It was proposed, therefore, that a larger Nipher-type shield should be constructed, based on scaling-up the standard MSC Nipher shield to fit the 20.3 cm (8 inch) diameter recording gauges. The aim was to develop a shield which would not only provide more accurate recording gauge measurements of snowfall, but also would provide data which would be directly compatible with measurements from the official MSC Nipher shielded snow gauge.

Using a wooden mould constructed to the scaled-up specifications, fibreglass shields (general purpose polyester resin, chopped strand fibreglass reinforced, with glass loading of approximately 20-30%) were manufactured. An elongated tube of galvanized sheet metal (inside diameter, 20.3 cm) was used to extend the gauge orifice even with the top of the shield. The initial design had the 71 cm high fibreglass shield in a ring, which was supported by three 2.5 cm aluminum posts fixed to a base. The entire structure was guyed from the support ring to ground anchors. The shield was adapted to fit either the Fischer & Porter or Universal Belfort recording precipitation gauges.

The absolute physical size of the shield and its support structure caused some problems: difficulty in accurately positioning the shield around the orifice extension; levelling and centering the orifice inside the shield, and routine servicing of the precipitation gauge. Wind tunnel tests conducted subsequently, showed that the shield could be shortened by 30 cm without changing the flow pattern over the orifice (Goodison et al., 1983). This resulted in a lighter, easier to handle shield. By making the shield shorter, the original support structure could be eliminated, the orifice extension shortened and the shield could be fixed directly to the orifice extension, thus ensuring an even spacing between the extension and the shield. The gauge and the shield are now levelled as a single unit and the shield and orifice extension are supported by the precipitation gauge, thus allowing free access for gauge servicing. Some auxiliary guying is still recommended. As well, the orifice extension was teflon coated on the inside to minimize snow sticking to it, which could cause capping of the orifice.

Wind tunnel tests of the large Nipher-type shield were conducted at AES. Results are described in Goodison et al. (1983). On the basis of these tests, one would expect that a recording gauge shielded with this large Nipher-type shield should exhibit catch characteristics similar to the standard MSC Nipher shielded snow gauge.

Field results of the new shield have been very encouraging. Prototype shields were manufactured and fitted to Fischer & Porter and Universal Belfort recording gauges in the manner described above. Gauges were installed at eight sites in various climate regimes across Canada. A variety of local siting conditions were chosen to assess the shield's performance. For the purpose of this study, none of the gauge measurements was corrected for undercatch due to wind or for trace amounts. The MSC Nipher shielded snow gauge is used as the standard against which the other measurements are compared since it is the "official" Canadian snow gauge.

Table 1 summarizes the seasonal totals for gauges located at the Toronto Met Research Station. The unshielded and Alter-shielded gauges

TABLE 1
Snow Gauge Comparisons, Toronto Met Research Station*

			Snow Season		
	1977-78	1978-79	1980-81	1981-82	1982-83
MSC Nipher (mm)	82.0	102.6	120.8	76.4	204.6
Unshielded Belfort Gauge (%)		53	53	48	N/A
Alter-Shielded Belfort Gauge (%)		64	67	61	83
Nipher Shielded Belfort Gauge (%)		92	93	U/S	95
Alter-Shielded F&P Gauge (%)		59	61	U/S	N/A
Nipher Shielded F&P Gauge (%)		84	97	89	87
Wyoming Shielded Belfort Gauge (%)	68	71	79	82	N/A

*Note: None of the data has been corrected for undercatch due to wind, trace amounts or retention (where applicable); all totals include rainfall where applicable. Total accumulations are expressed as a percentage of the MSC Nipher total recorded the lowest totals (generally, 50-65% of the MSC Nipher), but this is in line with previous results (Goodison, 1978). The Befort and Fischer & Porter gauges shielded with the large Nipher-type shield recorded about 90% of the MSC Nipher total.

At Monticello, Ontario paired Nipher and Alter-shielded Fischer & Porter gauges were placed in both open and sheltered bush locations to assess the effect of siting on the performance of the large Nipher shield. At the open site the results were similar to those reported for the Toronto Met Research Station. However, the Nipher shielded Fischer & Porter gauge located in the small opening in the bush capped over early in the winter and it recorded no accumulation until it was cleared by hand. This would be a potential problem at remote sites. However, this type of shielding is not necessary at well sheltered sites as the catch of the Alter-shielded gauge at this site was comparable with that of the standard MSC Nipher snow gauge at the open site.

Data from test sites in Saskatchewan, at Bad Lake and Regina A, also confirm that the catch of a recording precipitation gauge fitted with a large Nipher-type shield is similar to that of the standard MSC Nipher shielded snow gauge. Tables 2 and 3 show that, at both stations, these two gauge configurations measured within 5 mm of each other over the winter season. Alter-shielded gauges, on the other hand, generally measured 40-60% of the MSC Nipher total, which is consistent with data from other sites. Jones (1984) analyzed data from various snow gauges located at Regina. He concluded that there was not a statistically significant difference between the snowfall catches of the MSC Nipher-shielded snow gauge and the F & P gauge fitted with a large Nipher shield. However, he found that there was a

TABLE 2
Winter Precipitation Measurements, Bad Lake Saskatchewan*

Date	MSC Nipher	Alter-Shielded F&P	Nipher-Shielded F&P
Feb-April, 1980	34.6 mm	12.7 mm	33.1 mm
% of MSC Nipher	100%	37%	96%
Jan-April, 1981	33.8 mm	20.1 mm	30.4 mm
% of MSC Nipher	100%	59%	90%
Dec 1982 - Apr 1983	44.6 mm	22.9 mm	48.3 mm
% of MSC Nipher	100%	51%	108%

* Data collected by Division of Hydrology, University of Saskatchewan

TABLE 3
Snow Gauge Comparison, Regina Saskatchewan*

Year	MSC Nipher (mm)	Nipher Shielded Fischer & Porter (mm)	$\frac{F\&P}{MSC}$ (%)
79-80	35.1	33.0	94
80-81	43.6	48.3	111
81-82	113.8	116.3	102
82-83	76.0	77.1	101
83-84	65.8	70.2	107

* Adapted from Jones (1984)

significant difference between the seasonal catch of the standard Nipher and an Alter-shielded Sacramento or an Alter-shielded standpipe gauge.

Data from other sites have provided similar results. Testing continues, with new sites being established in mountain areas so that shield performance can be assessed over a wider range of environments. Since the shield would be permanently affixed to the gauge, the performance of the shield during rain events must also be analyzed.

At this time, the field data indicate that the large Nipher-type shield can be used with recording gauges to provide measurements which are compatible with the official Canadian MSC Nipher snow gauge. The Nipher-type shield significantly improves gauge catch compared to unshielded and Alter-shielded gauges. There is little maintenance required and the new design will allow easy servicing of the gauge. However, snow can build up on the shield, even at open sites when the wind speed is low, and the gauge can cap over at sheltered sites. The design of the Nipher shield makes the gauge susceptible to catching blowing snow if it is mounted too close to the ground, but this is also a problem with the standard Nipher shielded snow gauge. At an automatic station however, there will be no on-site observer to make an adjustment or comment on whether the gauge measured falling or blowing snow or both. Use of the large Nipher-type shield on recording gauges would be one effective step in standardizing winter precipitation measurements.

Automatic Snow Depth Sensor

Snow depth on the ground is routinely measured at all synoptic and principal observing stations in Canada at 1200 Z, and since about 1980, all climatological stations have been asked to record daily snow depth as a standard observation. Before that time, only snow depth on the last day of the month was recorded at the climatological stations. Snow depth information is valuable in many hydrological, agricultural and forestry applications and it is often a substitute for snow water equivalent data when such data are unavailable. Snow depth measurements are made manually with a snow ruler. The observer uses his expertise and judgment in obtaining a representative areal measurement at the station. As stations are automated or new automatic stations are opened at remote locations, the snow depth measurement will be lost. There is a need, therefore, for an inexpensive automatic snow depth sensor, which can be used on future automatic hydrometeorological stations.

The Hydrometeorology Division and the Data Acquisition Services Branch of the Atmospheric Environment Service have been co-operating on the development of an inexpensive automatic snow-depth gauge which could be used at either manned or remote stations. Development began in 1982, with the first unit being tested during the winter of 1982-83. Two additional units have been built and deployed for testing during the past two winters.

A commercially available ultrasonic ranging kit from Polaroid Corporation provides an economical means of accurately measuring target distance in terms of time to target (Goodison et al., 1984). An on-board crystal oscillator provides a time base pulse train which is activated on a measurement request command from an integral microcontroller or from an external device such as a data logger or data collection platform (DCP). The time base pulse train is disabled when a target echo is received. In the present system, with appropriate processing, pulse counts stored in the microcontroller are directly equivalent to a distance to target. Since the speed of sound in air is highly temperature dependant, a correction must be applied in the calculation of target distance to allow for changes in the speed of sound related to changes in ambient air temperature. Significant modification to the system described in Goodison et al. (1984) now allows snow depth measurements to be made and corrected in real-time using the microcontroller and measurements from an ambient air-temperature sensor. The snow depth gauge as it is currently configured provides stand-alone operation with data being formatted for transmission to an appropriate peripheral for display and/or archiving. Details of the current system are given in Goodison et al., (1985).

Results from the first year of testing at the Dorset site (Goodison et al., 1984) indicated that the ultrasonic sensor undermeasured the ruler observations by about 6 cm, with individual observations differing by up to 13 cm. Part of the difference was attributable to overmeasurement of the snow depth by the observer and part due to the system configuration at that time. Results obtained during the first part of the 1984-85 season after sensor modifications were completed indicate a much improved sensor accuracy. Figure 1 shows that the persistent bias, which was evident in previous comparisons, has been nearly eliminated. The root-mean-square-error is less than 2.0 cm. Analysis of data from both the Dorset and Downsview test sites does suggest however, that there may be some degraded sensor performance related to signal scattering during periods of moderate to heavy snowfall. The Polaroid ultrasonic performed well outside during ambient air temperatures ranging from +10°C to -40°C. Rime ice or frost did not appear to build up on the sensor and had no effect on its operation.

This ultrasonic sensor provides a viable method for remotely measuring snow depth. Although it represents a point snow depth, as opposed to an areal snow depth, in most cases, with proper siting, a reasonable and accurate measurement of snow depth can be obtained. Hourly observations are feasible and would allow the user to monitor anomalies in the data. An ultrasonic snow depth gauge operating at a remote location in conjunction with a weighing type precipitation gauge and transmitting hourly observations can provide the hydrologist with an acceptable estimate of snow water equivalent.

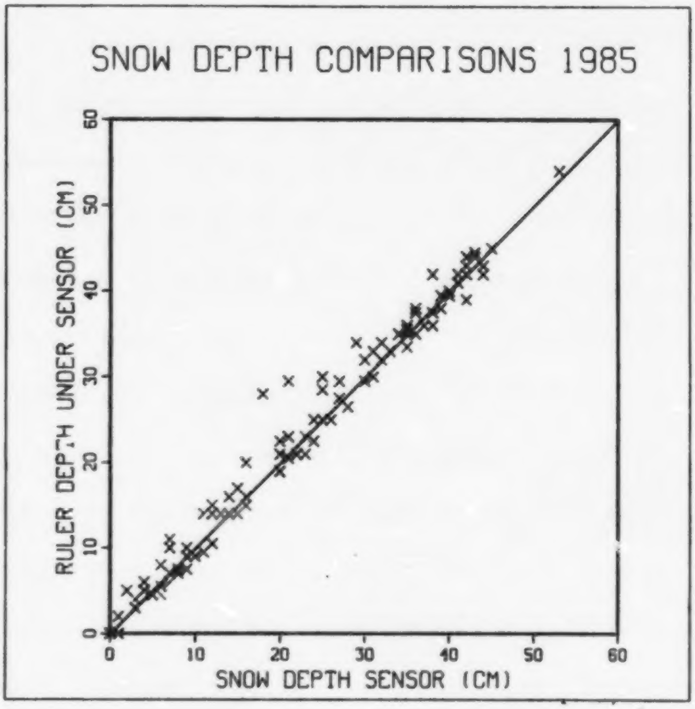

Figure 1

Comparison of snow depth measurements from the ultrasonic sensor and observed ruler measurements

The Challenge of Automation

The automation of hydrological, meteorological and climatological stations is a reality. Some stations have been automated; new auto-station networks have been initiated; and, discussions on climate station automation have begun. Current technology related to auto-station development presents us with a wide range of opportunities and options: on-site data logging for extended periods; receipt of real-time observations from unmanned remote sites using space technology; automatic quality control and archiving of data; reduction in the current number of manned observing stations; expansion of networks into regions from where observations were not previously available; more efficient scheduling of site visits; the capability to observe more elements than are currently measured, at say, climate stations; and, the elimination of observations because of the lack of suitable sensors for auto-stations. The challenge for scientists, engineers and managers is to work together to develop the best mix to meet the user community's needs. In Canada, what does this challenge mean for the measurement of winter precipitation, notably in the form of snow?

As noted above, current AES instruments for winter precipitation measurement at principal and climatological stations involve manned observations. Use of some type of recording weighing precipitation gauge is the most feasible method at present, but the accuracy of measurements from unshielded or Alter-shielded gauges is open to question especially at exposed locations. Use of the large Nipher type shield described above offers one viable method of minimizing gauge catch errors, and at the same time providing gauge measurements compatible with current standard MSC Nipher shielded snow gauge observations. But, even this alternative does not allow for an easy decision.

The decision process associated with automation must include a serious consideration of capital and operating costs of the proposed sensor/data logging system. Cost of the recording gauge, appropriate shielding, and interfacing to the data logging system are factors which cannot be ignored. AES uses the Fischer & Porter recording precipitation gauge almost exclusively in its supplementary precipitation network. Its general reliability, 500 mm capacity, ability to operate unattended for extended periods and the capability of having its punch paper tape record automatically processed have contributed to this preferred status. Interfacing to DCPs is accomplished using an absolute position shaft encoder permitting 1 mm increments to be recorded when used on an Inland Waters Directorate Bristol DCP. The resulting cost for gauge and shaft encoder is almost $6,000. This high cost certainly makes managers think twice before installing such sensors. A tipping bucket raingauge is much simpler to interface and at a cost of less than $1,000, it is an attractive alternative. The problem, of course, is that it can only measure rainfall; winter precipitation measurements would be lost using this configuration.

AES has deployed several types of auto-stations to meet operational needs, but in most cases, if precipitation is measured, only a tipping-bucket raingauge is used. The MAPS I prototype auto-station network, using Bristol DCPs, did use the Fischer-Porter gauge, but the more extensive MAPS II network (40 stations) currently being installed at former manned lighthouses will only have a tipping bucket raingauge. Cost of the Fischer-Porter and the marine location of most sites influenced the decision on instrument configuration.

AES also operates auto-stations which use land based communications rather than satellite telemetry, as does the MAPS stations. There are currently 50 MARS stations in this network, with 19 being co-located at manned observing stations; these 19 provide hourly data at night and on weekends when observers are not on duty. Only tipping bucket raingauges are used in the MARS network; weighing-type recording gauges have not been added to measure winter precipitation. Thus, a mix of types of observation, irregular timing of observation or no observation of winter precipitation results at these stations.

Other agencies are using other types of recording precipitation gauges, notably the Universal Belfort (300 mm) capacity and the large capacity Belfort (750 mm). Use of a potentiometer on these gauges instead of a shaft encoder makes interfacing to a data logger simpler and less expensive. The Hydrometeorology Division of AES has used both gauges for winter operations and has experienced some problems with the large capacity gauge, when it sometimes exhibits an apparently normal increase and then a sudden decrease in accumulation. The specific cause is unknown, although inquiries have been made to the company. Erroneous increases and decreases in accumulated precipitation are sometimes very difficult to detect; needless to say, they seriously limit use of the data not only in real-time, but also for climatological purposes. Problems such as this will present a challenge. One of the benefits of auto-stations is the potential availability of real-time data. Yet, very few people have had the chance to use and evaluate winter precipitation data in real-time. Is there precipitation occurring? Is it rain or snow? Is the measurement real? These are questions which we will have to be able to answer. There will no longer be an observer to provide comments which would assist in the interpretation of the record.

Table 4 is an example of the interpretation problems which could confront a user. Daily observations from a Type-B raingauge, MSC Nipher shielded snow gauge, snow board measurement of snowfall water equivalent, and four Fischer-Porter gauges with different shielding/siting configurations are compared for January, 1982. These data are given as they were recorded by each gauge, with no "quality control" applied. There are differences in timing between gauges because the standard F&P only records increments of 2.54 mm and because each has a different catch efficiency. There are days when totals are difficult to rationalize. For example, the measurement of 50.8 mm by the Wyoming shielded gauge on January 10-11 is significantly greater than other gauges. Was this a result of blowing snow? A similar problem occurred with the Nipher shielded and Alter-shielded F&P gauges on January 23. Did snow stick to the gauge orifice and extension and fall into the bucket later causing a sharp increase in accumulation? The reasons for such inconsistencies in the recorded gauge data must be understood before the gauges can be operated successfully at automatic stations in Canada. This intercomparison of data shows that quality control of real-time precipitation data will be a great challenge, one which we have yet to address fully.

Use of the automatic snow depth sensor described above may in fact be an extremely valuable complement to standard sensors on auto-stations. Measurements from this sensor will provide the user with independent data on snow accumulation rates, and the amount and timing of snowfall. When used in conjunction with precipitation gauge measurements the data will assist in determining precipitation type, state of the snowpack and providing an estimate of snowpack density.

TABLE 4

COMPARISON OF SNOW GAUGE MEASUREMENTS (mm), MONTICELLO, ONTARIO
JANUARY 1982

	RAIN GAUGE MAIN SITE	MSC NIPHER GAUGE MAIN SITE	SNOWBOARD MAIN SITE	ALTER SHIELDED F&P GAUGE MAIN SITE	NIPHER SHIELDED F&P GAUGE MAIN SITE	ALTER SHIELDED F&P GAUGE BUSH SITE	WYOMING SHIELDED F&P GAUGE
1	1.8	5.4 Blowing Snow	6.0	7.6	7.6		
2			0.4				
3	Trace						
4	13.8			22.9	25.4	12.7	15.2
5		7.0 Blowing Snow	7.0		5.1	2.5	2.5
6		1.4	1.4		7.6		
7		1.0	0.6				
8		1.8 Blowing Snow	1.4			2.5	5.1
9		2.4	1.8				
10		1.2	1.0	5.1	7.6	2.5	10.2
11		8.0 Blowing Snow	6.2	7.6	12.7	5.1	40.6
12		0.2	0.2		7.6		5.1
13		5.2	4.4		7.6	5.1	
14		1.0	0.6		2.5		2.5
15		Trace					2.5
16		2.6 Blowing Snow	2.6		5.1	5.1	5.1
17		0.8	1.0		2.5		5.1
18		0.2	0.2				
19					5.1		2.5
20		0.8	0.6				
21		1.8	1.8			2.5	
22		Trace					
23	0.5	7.0 Blowing Snow	6.3	30.5	27.9	17.8	17.8
24		0.8	0.8		7.6		2.5
25		2.0	2.8		2.5		
26		0.2	0.2				
27							
28		1.0	0.8			2.5	2.5
29							
30		7.2	7.6			5.1	
31		8.0	9.0	10.2	15.2	10.2	5.1
TOTALS	15.1 +	67.0 = 82.1 mm	64.7 mm	83.9 mm	149.6 mm	73.6 mm	124.3 mm

Technologically, there are still many questions which must be addressed. Is there a cheaper, easier to interface, but accurate and reliable shaft encoder for use on a Fischer-Porter gauge? Is gauge capacity a problem? If the large Nipher-type shield improves the catch efficiency as shown, gauges will have to be serviced more often. Regular monitoring of the data in near real-time, however, would allow more efficient scheduling of service trips. Should the precipitation gauge be redesigned for use in regions of heavy snowfall? Should a cheaper precipitation gauge be used in the national network? What are the power requirements of various gauges used at autostations? What is the appropriate gauge/shield combination for use at autostations? What sensors should be operated at automatic climate stations? What parameters do we need to measure?

The answers to these questions are critical if managers are to make sound judgments on the configuration of future autostation networks. Scientists and engineers have an obligation to provide managers with the best possible advice on equipment specifications, performance, reliability, and accuracy. We must demonstrate why winter precipitation measurements are important. Do we need them? If snow surveys are being discontinued, there will be an ever increasing dependence on precipitation measurements as an alternative. Many managers seem to feel precipitation gauge networks can be reduced because remote sensing will provide the answer. Appropriate remote sensing techniques may be developed in the future, but reliable algorithms must first be developed. Ground based data are in fact a critical component in algorithm development.

The challenge of automation of winter precipitation measurement is before us now. Although questions remain, we are making steady progress. The large Nipher-type shield and the ultrasonic snow gauge are but two developments which could be used at automatic stations. Other developments are feasible and necessary. But let us ensure that our snow data base is not eroded during the automation process.

ACKNOWLEDGEMENTS

The studies summarized in this paper are part of the snowfall measurement project of the Hydrometeorology Division. The assistance of personnel at the University of Saskatchewan (Division of Hydrology), Trent University (Dept. of Geography), and AES Region staff at Regina, Fredericton and Resolute have made possible the testing of the large Nipher-type shield across Canada. The ultrasonic snow depth gauge has been developed and tested in co-operation with AES Data Acquisition Services Branch personnel. Bob Wilson has been largely responsible for the development work on this sensor. Finally, many thanks are extended to John Metcalfe who has overall technical responsibility of the snowfall measurement project.

REFERENCES

Goodison, B.E., 1981: Compatability of Canadian Snowfall and Snowcover Measurements. Wat. Resour. Res., Vol. 17, No. 4, 893-900.

Goodison, B.E., 1978: Accuracy of Canadian Snow Gauge Measurements. Journal of Applied Meteorology, Vol. 17, No. 10, 1542-1548.

Goodison, B.E., B. Wilson and J. Metcalfe, 1985: An inexpensive remote snow depth gauge. Proc. TECIMO-III. WMO Technical Conference on Instruments and Methods of Observation, Ottawa, July 8-12, 1985 (in press)

Goodison, B.E., B. Wilson, K. Wu and J. Metcalfe, 1984: An inexpensive Remote Snow-Depth Gauge: An Assessment. Proc. Western Snow Conference, Sun Valley, Idaho, USA, April 17-19, 1984, 188-191.

Goodison, B.E., V.R. Turner and J.R. Metcalfe, 1983: A Nipher-type shield for recording precipitation gauges. Proc. 5th AMS Symposium on Meteorological Observations and Instrumentation, April 11-15, 1983. Toronto, pp. 21-26.

Jones, K.H., 1984: A comparison of various snow gauges on the Canadian Prairies over five winters. Atmospheric Environment Service Report No. CSS-R84-04, August, 1984, 15 pp.

SNOW RETENTION IN A LARGE CUTBLOCK

by

A.M.K. Nip and R.H. Swanson

Alberta Forest Service
Spruce Grove, Alberta
Canada

presented at

SNOW PROPERTY MEASUREMENTS WORKSHOP

Lake Louise, Alberta

1-3 April, 1985

TECHNICAL MEMORANDUM 140

Compiled By

P.R. Kry

NRCC 27594

SNOW RETENTION IN A LARGE CUTBLOCK

By

Allen M. K. Nip and Robert H. Swanson

Introduction

Snow is a form of delayed precipitation. The amount of snow that is on the ground at the time of snowmelt is very important in predicting water yield from clear-cut areas with the WRENSS procedure (U. S. Forest Service 1980). The WRENSS procedure is a methodology for estimating annual water yield from forested areas, and increases that might occur as a result of clear-cutting. Evapotranspiration is considered to be functionally related to seasonal precipitation. In partially clear-cut situations, the clearings and the residual treed patches are assumed to interact, so that snow is not distributed on the ground as it would have been had the clearings not been created, and the amount of winter and spring precipitation that is used to estimate evapotranspiration from clear-cuts is different from that used to estimate evapotranspiration from treed patches.

In WRENSS, the amount of snow to be considered as winter or spring precipitation in partially clear-cut situations is estimated with an empirically derived relationship between clear-cut size and the amount of snow retained in and around them compared to a fully forested situation. A snow retention coefficient for the clear-cuts (p_{cut}) for a 50% treed and clear-cut situations is derived from their graph reproduced here as Figure 1. The precipitation (presumably from precipitation gauge data) for the winter and spring seasons is adjusted upward or downward in the clear-cuts in accordance with their diameter as indicated by Figure 1.

A complimentary adjustment, $p_{for} = 1-p_{cut}$, is also made for the snow accumulation in the treed portions so that the combined total accumulation in treed and clear-cut portions is the same as that under a fully forested situation. However, if the clear-cuts are larger than 15 tree heights across, then the WRENSS procedure predicts a net loss due to evaporation from wind borne snow, that is, the areally-weighted total seasonal precipitation becomes less than that which would have occurred in the absence of any clear-cutting.

We have not documented less snow in clear-cuts than under forest as indicated by the right hand portion of Figure 1, in Alberta. However, most of the snow studies in Alberta have been done on clear-cuts considerably smaller than the 14-tree heights diameter, where the snow retention coefficient is greater than 1.0 (e.g. Stanton 1966, Golding and Swanson 1978). These Alberta studies have generally indicated accumulations in the clear-cuts ranging from 1.10 to 1.45 that under

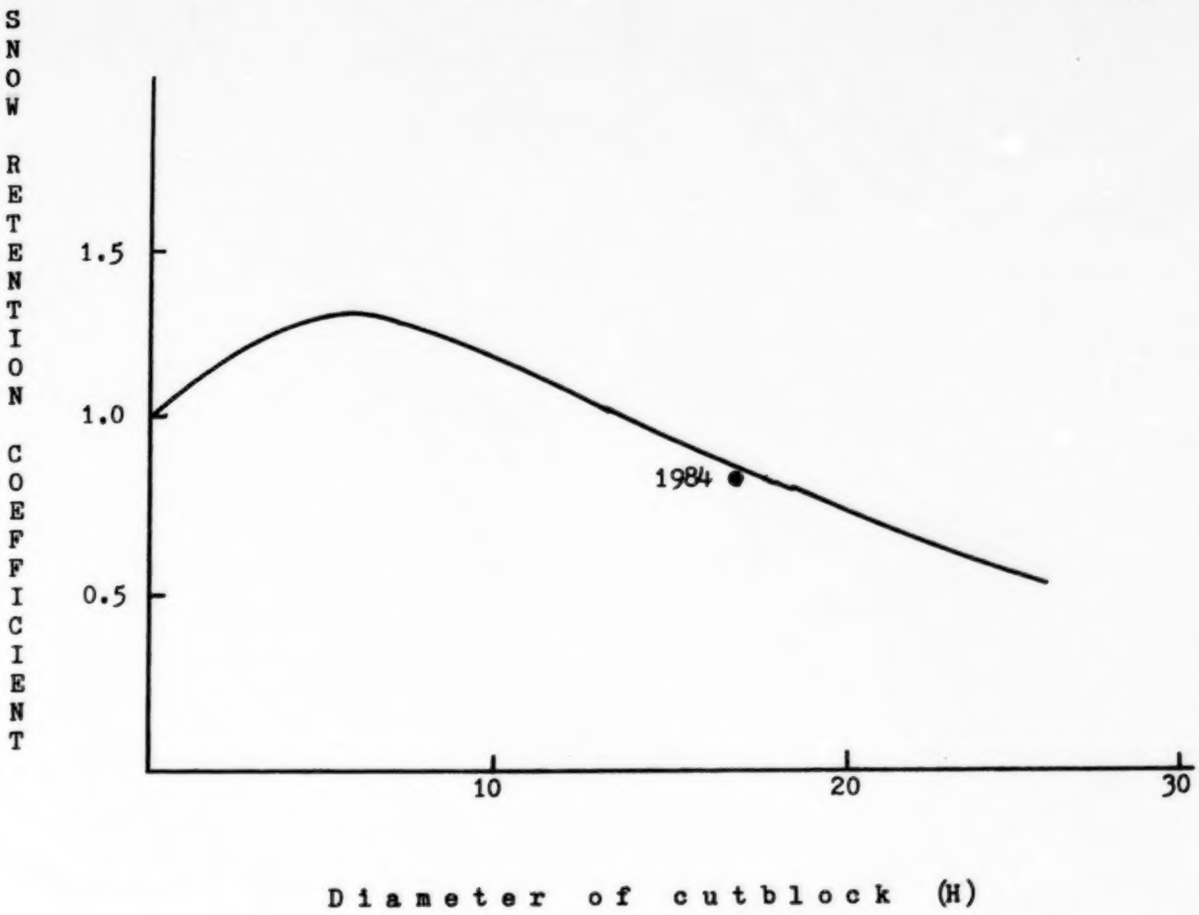

Figure 1: Snow Retention in Cutblock
Troendle and Leaf (1980)

full forest, and have been generally supportive of the left-hand portion of Figure 1.

The purpose of this study was to obtain some evidence that clear-cuts larger than 14 tree heights across, did accumulate less snow than an uncut forest situation. It is a sample of one and the results must be interpreted on that basis.

Study

One 31 ha clear-cut on the Tri Creeks Experimental Watershed was sampled. Three transects were established, Figure 2. Each transect traversed the clear-cut and extended 300 m into the forest on both ends. Sampling points were permanently marked at 20 m intervals (approximately one tree height). The snow depth, density and water

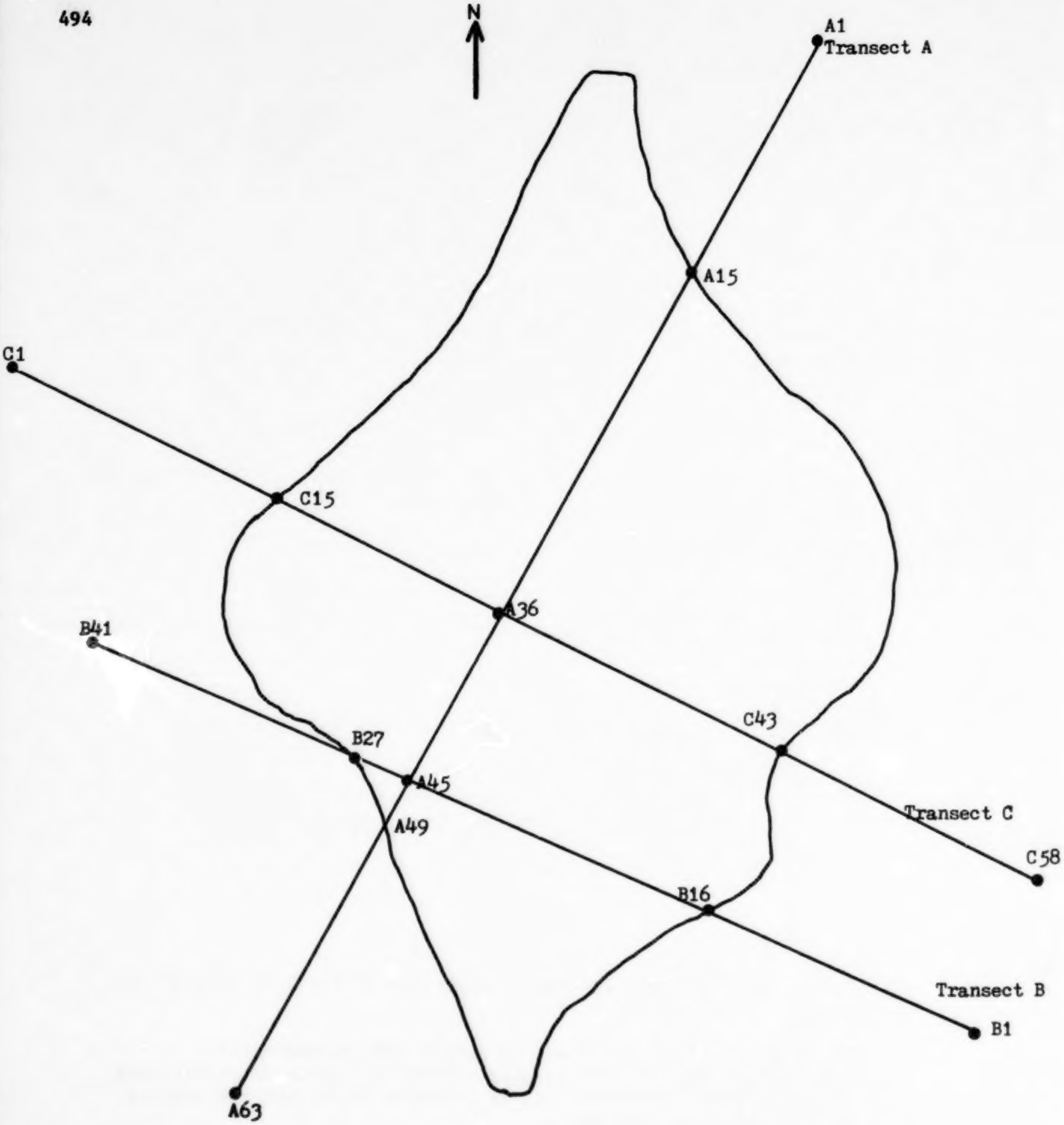
N
A1
Transect A
A15
C1
C15
A36
B41
C43
B27
A45
Transect C
A49
C58
B16
Transect B
B1
A63

Figure 2: Sampling Sites in Cutblock

equivalent were measured at each point with a Mount Rose sampler at approximately monthly intervals from December 1983 through April 1984.

The maximum width of the clear-cut is 813 m, which corresponds with a diameter of approximately 41 H (tree height, H, approximately 20 m). The diameter of a circle of equivalent area would be 31 H. As indicated on Figure 2, the shape is irregular, and the average diameter perpendicular to the wind is between 13 to 20 H, depending upon wind direction. The prevailing wind direction along the entire Eastern Slopes of Alberta is westerly; the average cross section width at each sampling point along transect A, which lies approximately perpendicular to the west, is 17 H.

The clear-cut and treed portions were divided into a number of 20 m wide tori, shaped similarily to the clear-cut, that intersected each transect twice and enclosed two sample points from each of the three transects. The mean snow water equivalent from the six points within each tori was multiplied by the area of that tori to obtain an area-weighted SWE. The SWE values from these individual tori were summed and divided by the summation of tori areas to obtain an area weighted values for the following three groups:

1) Control: An area within the surrounding forest between 10 and 15H from the clear-cut tree border. The snow accumulation within this area was considered to be relatively free of the influence of the clear-cut and has been used below as reasonably representative of the snow accumulation in an uncut forest condition.

2) Forest: An area from the clear-cut forest edge to 10H from it. This was considered to be within a zone where the clear-cut would influence the snow accumulation within it.

3) Clear-cut: The clear-cut itself.

A snow retention coefficient was obtained for the area within 10H surrounding the clear-cut (p_{for}), and for the clear-cut (p_{cut}), by dividing the value obtained for the SWE of them by that of the control. This was done with the data from each snow survey.

The data from the snow surveys are given in Table 1. They do not give a clear indication of whether the WRENSS snow retention coefficient is applicable or not. The snow accumulated in the clear-cut is less than or equal to that found in either the control or forest on four of the six snow survey dates. If one had access only the 02 February and/or 18 April data, then he would feel quite justified in using a coefficient that placed more snow in the trees than in clear-cuts. However, the data from the other survey dates do not support this.

Table 1. Snow accumulation data from Tri Creeks Experimental watershed, Alberta. Snow water equivalent in millimeters.

Date	Group			Retention Coefficient	
	Control	Forest	Clear-cut	Forest	Clear-cut
15 Dec 83	37	43	47	1.16	1.27
17 Jan 84	67	79	80	1.18	1.21
02 Feb 84	108	101	80	0.93	0.74
29 Feb 84	85	92	85	1.09	1.00
28 Mar 84	101	100	98	0.99	0.97
18 Apr 84	79	100	71	1.27	0.91

Discussion

These results are clear in one respect: there may be less snow on the ground in a clear-cut than under full forest. The cause of this lesser quantity is not so clear. The change in accumulated snow that occured between 02 and 29 February, thoroughly confounds the issue. During this interval, the amount of snow under the trees in both the control and forest decreased while that in the clear-cut increased. This is suggestive of greater ablation under the trees and is not particularily consistent with the theory used in WRENSS that predicts removal of snow from clear-cuts to the surrounding trees.

This study provides us with no definite direction as to whether or not snow redistribution from clearings to trees is applicable in the large clear-cuts of Alberta. Our instructions to WRENSS users prior to this study were to use caution in interpreting the results of predicted runoff from large clear-cuts. These instructions remain the same.

Literature Cited

Golding, D. L. and R. H. Swanson. 1978. Snow accumulation and melt in small forest openings in Alberta. Canadian Journal of Forest Research 8:390-388.

Stanton, C. R. 1968. Preliminary investigation of snow accumulation and melting in forested and cut-over areas of the Crowsnest forest. pp. 7-12 In: Proceedings Western Snow Conference, 34th annual meeting, 19-21 April, Seattle, Washington.

U. S. Forest Service. 1980. An approach to water resources evaluation of non-point silvicultural sources (a procedural handbook). United States Environmental Protection Agency, Environmental Research laboratory, Athens, Georgia. EPA-600/8-80-012. 861 pp.

SOIL HEAT FLUX, WETTING FRONT ADVANCE AND ICE LAYER GROWTH IN COLD, DRY SNOW COVERS

by

P. Marsh

National Hydrology Research Institute
Environment Canada
Ottawa, Ontario
Canada

M-k. Woo

Department of Geography
McMaster University
Hamilton, Ontario
Canada

presented at

SNOW PROPERTY MEASUREMENTS WORKSHOP

Lake Louise, Alberta

1-3 April, 1985

TECHNICAL MEMORANDUM 140

Compiled By

P.R. Kry

NRCC 27594

Abstract

A study of the changes in snow cover properties during melt was carried out at Resolute Bay and Eidsbotn Fiord in the Canadian High Arctic. Monitoring of the snow cover during this period is complicated by the fact that the snow is very close to its melting point and any disturbance can alter its properties substantially. The techniques used in this study were designed with this crucial point in mind. The resulting comprehensive field program consisted of snowpit sampling, dye tracing, lysimeters. snow and ground temperature, frozen soil infiltration measurements, and surface energy balance measurements.

Field observations showed that flow fingers developed at the leading edge of the wetting front and that ice layers grew in the zone between the deepest penetration of these fingers and the background wetting front. These ice layers were important in delaying the finger front advance and in releasing latent heat to warm the snow and underlying soil. When water reached the snow cover base a small amount of water infiltrated the soil. When infiltration ceased water froze to form a basal ice layer. The soil heat flux was always negative, therefore increasing the amount of water which froze as ice layers within and at the base of the snow cover. At times the soil heat flux was similar in magnitude to the surface melt rate. An important conclusion of this study is that it is necessary to 'ripen' both the snow and underlying soil when predicting runoff from cold snow underlain by frozen soil.

1. Introduction

In many cold regions, snowmelt runoff is influenced by snow cover melt metamorphism which significantly controls both the time at which water reaches the snow base and the volume of water available for runoff. Most previous studies considered mature snow covers underlain by unfrozen soils, but few have dealt with water movement into cold, initially dry snow underlain by frozen soils and the resulting metamorphism of the snow cover.

Snow cover melt metamorphism is a complex phenomenon which is dependent on a number of separate, but interrelated processes. Some of these are illustrated in Figure 1 and include: development of flow fingers at the leading edge of the wetting front, ice layer growth within and at the base of the snow cover, infiltration into frozen soil. heat flux from the snow to the frozen soil, and snow grain growth. in order to understand these processes it is necessary to monitor the changes which occur as meltwater enters the dry, below freezing snow. However, since the snow cover is close to 0 c, small disturbances result in significant changes to the snow cover, making observations difficult. Previous melt metamorphism work has concentrated on laboratory studies of individual processes such as grain growth (Wakahama 1968) and basal ice growth (Wakahama et al 1976), but have not been able to consider the entire melt metamorphism process. Field studies have relied on snowpit observations,

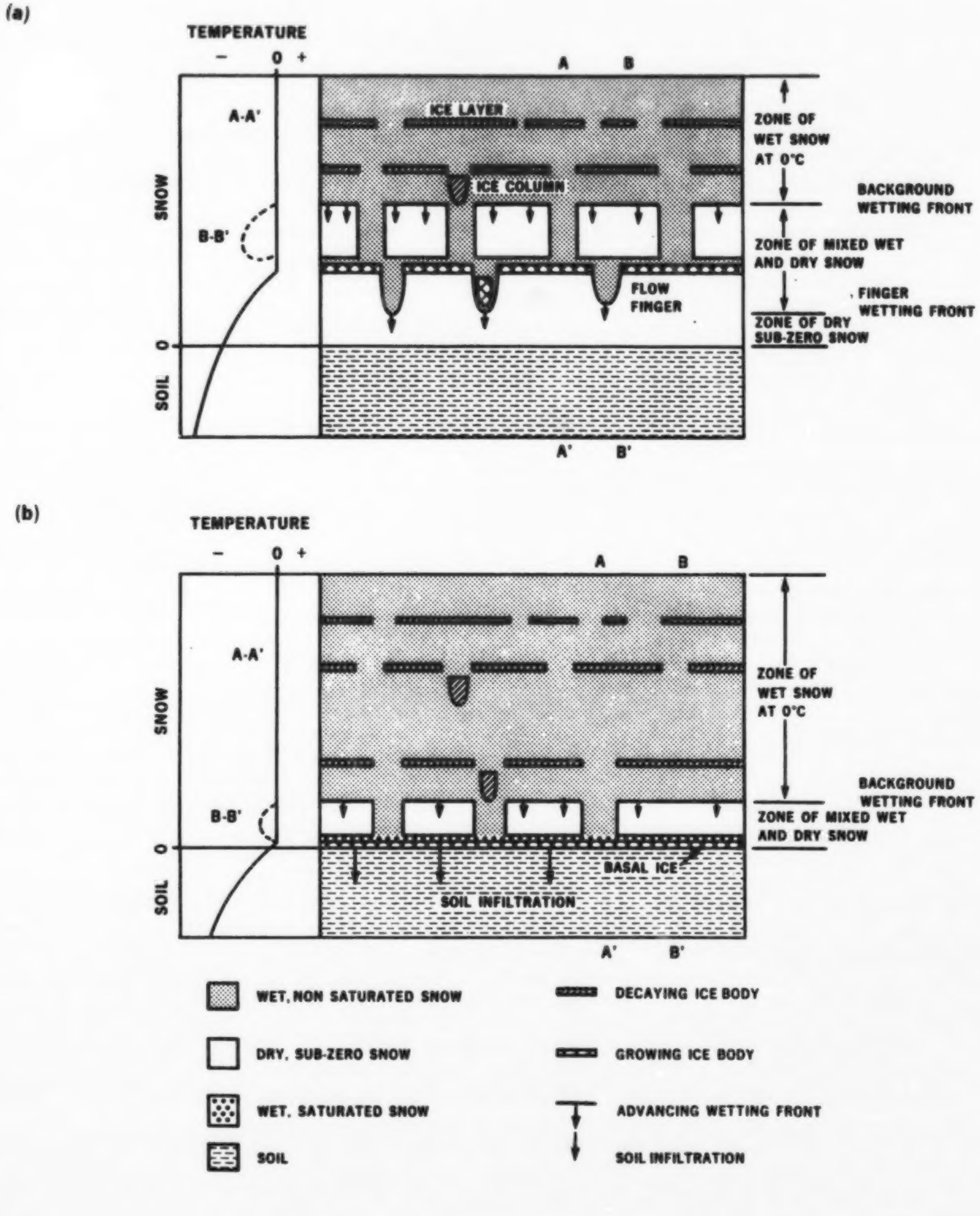
(a)
TEMPERATURE
–
0
+
A
B
ICE LAYER
A-A'
ZONE OF WET SNOW AT 0°C
SNOW
ICE COLUMN
BACKGROUND WETTING FRONT
B-B'
ZONE OF MIXED WET AND DRY SNOW
FLOW FINGER
FINGER WETTING FRONT
ZONE OF DRY SUB-ZERO SNOW
0
SOIL
A'
B'
(b)
TEMPERATURE
–
0
+
A
B
A-A'
SNOW
ZONE OF WET SNOW AT 0°C
BACKGROUND WETTING FRONT
B-B'
ZONE OF MIXED WET AND DRY SNOW
0
BASAL ICE
SOIL
SOIL INFILTRATION
A'
B'
WET, NON SATURATED SNOW
DRY, SUB-ZERO SNOW
WET, SATURATED SNOW
SOIL
DECAYING ICE BODY
GROWING ICE BODY
ADVANCING WETTING FRONT
SOIL INFILTRATION

Figure 1. Generalized diagram showing water movement into an initially cold, dry snow cover before and after meltwater reaches the snow cover base.

especially if a number of snow characteristics are required (IASH 1970), but the destructive nature of the sampling provides measurements at a single time, not day to day changes at a site. If sampling is to be repeated the snowpit is refilled with snow to protect it and is them resampled at a latter date (IASH 1970). This technique is not practical when frequent samples are required from a number of deep snow covers. This limitation has to some degree been overcome by the development of in-situ recording instruments such as profiling radioisotope snow gauges (Goodison et al 1981), but these are limited to measuring only one variable at a profile. What is required is a practical method to sample the day to day changes in a number of snow cover properties at a single site.

The primary objective of this paper is to describe simple field techniques to monitor snow cover melt metamorphism. The basic techniques used are documented in the literature, but they have been modified to minimize disturbance to the snow cover and to provide an integrated series of measurements. The resulting comprehensive field program consisted of:

(1) snow pit sampling to monitor the day to day changes in snow density, grain size, location of wetting front, liquid water content, ice layer location, size, density and ice type, basal ice thickness and density, and snow temperature

(2) dye injection and multi-compartment lysimeter to determine flow finger development at the leading edge of the

wetting front

(3) infiltration into frozen soils

(4) snow and soil temperature, and

(5) surface energy balance.

2. Study Area

Field observations were made in the Canadian High Arctic at Eidsbotn Fiord, Devon Island (76 10′ N, 91 30′ W) and at Resolute Bay, Cornwallis Island (74 45′ N, 94 50′ W). Measurements were carried out from early June to the end of snow melt in early July during both 1980 and 1981.

The High Arctic snow cover is influenced by the long duration of sub-zero air temperatures, frequent occurrence of blowing snow, low total precipitation, low net radiation, and low ground temperatures (Maxwell 1980). These processes produce a snow cover that is characterized by high density, small grain size, distinct depth hoar layer, well distinguished layering, variable snow depth, and cold temperature. The High Arctic snow cover has been described by Marsh (1982) and Marsh and Woo (1984a), and is similar to that of the Alaskan north slope (Benson et al 1974).

3. Methodology

The techniques used in this study were specially designed so that the changing properties of the snow cover can be obtained throughout the melt period. The resulting comprehensive field program consisted of snowpit sampling, dye tracing, lysimeters, snow and ground temperature, and surface energy balance measurement. All these techniques, though well documented, had to be modified to minimize disturbance to the snow cover.

Snowpit studies during melt

Throughout the 1980 and 1981 field seasons, changes in snow cover properties were monitored at five snowpits at Eidsbotn and Resolute. These sites were chosen because they provided a typical set of snow depths and snow properties as determined by a premelt snow cover study (Marsh and Woo 1984a).

An important aspect of the snowpit studies was ensuring that undisturbed natural snow was sampled and that day to day measurements were related to each other (ie. the same strata and ice layers were being sampled from day to day). The following two procedures ensured that these conditions were met. Firstly, between measurements the snowpits were protected with double layer mylar radiation shields to minimize melting of the pit wall (Figure 2). Secondly,

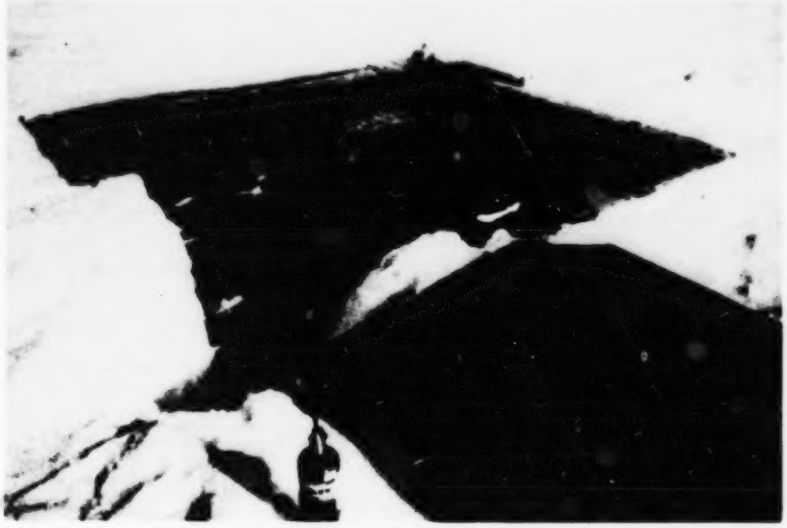

Figure 2. Typical snowpit showing mylar radiation shield.

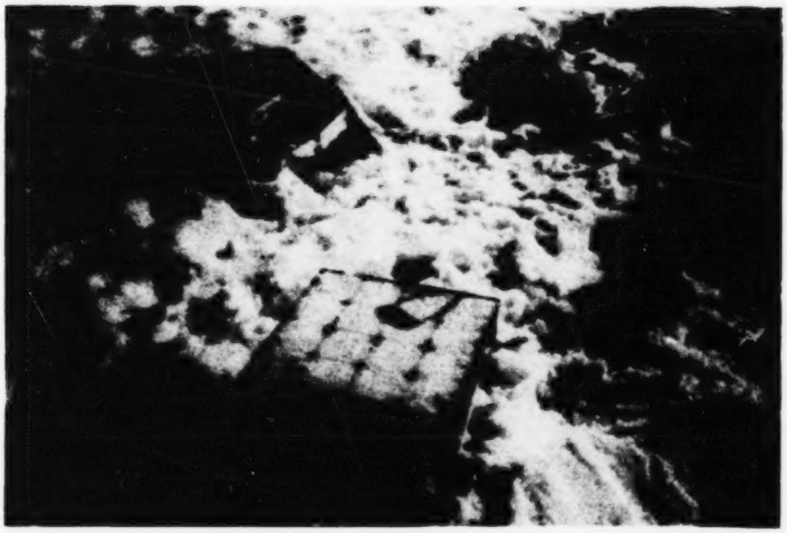

Figure 3. Multi-compartment lysimeter (0.25 m^2). Each separate compartment drains into a plastic bottle which is emptied daily.

immediately before snowpit sampling, half of the pit face was cleared back for approximately 0.2 m. Alternate sides of the pit were used on consecutive days to provide undisturbed snow for sampling and to allow the continuity of the layers to be determined. Observations of the condition of the pit wall and measurements of snow temperature from the snowpits compared to snow temperatures taken from a permanently installed thermistor rod, indicated that these procedures were successful.

One face of each pit was cleaned off with a wire brush or a scraper to highlight individual strata. Snow depth was measured as well as the thickness of individual stratigraphic layers. From each layer, samples were obtained by snow cutters (volume 50 to 250 cm^3). To determine density, these samples were weighed. The position of the wetting front was estimated as the depth at which the snow grains were wet and rounding of the grains had begun across the entire snowpit face. The location and thickness of all ice layers within and at the base of the snow cover were measured to the nearest 5 mm and observations were made on the horizontal extent, ice type, and uniformity of these layers. Occasional measurements of ice density were obtained by immersing preweighed samples in cold diesel oil to determine their volume. Whenever they were found, the size of vertical ice columns were measured and their location in relation to ice layers and stratigraphic boundaries noted. Since premelt observations demonstrated that horizontal variations in snow density were small, it was possible to estimate the liquid water content of the snow from measured changes in snow density (Marsh 1982). Snow temperatures were measured in the snowpit walls using Fenwall disc thermistors.

Snow and soil temperatures were obtained using Fenwall disc thermistors embedded in plexiglass tubes and attached to wooden rods at three sites near the snowpits. To minimize the conduction of heat down the rod and percolation of melt water along it, the snow thermistors were extended 0.1 m away from the wooden rod. The soil section of the thermistor rod was cut off at the soil surface, with the wires running along the ground for approximately 1 m and then up the snow thermistor rod. The soil thermistors were installed prior to snow accumulation, while the snow rod was installed at the end of winter. All thermistors were calibrated in an ice-water bath to an accuracy of +/- 0.1 c. This technique was successful in measuring soil temperatures and snow temperatures in the zone below the background wetting front (Figure 5).

Meltwater movement

Two techniques were used to study the wetting front advance into dry subzero snow. Before melt began, dye infiltration studies were conducted. A snowpit was excavated and the snow properties were measured as noted earlier. Then diluted dye at 0 c was slowly applied to the snow surface. After sufficient time elapsed, the snowpit face was cut back to reveal the dye path. The width and spacing of the flow fingers were measured and the position of the fingers in relation to the stratigraphic boundaries noted. The second technique involved the use of a multi-compartment lysimeter to measure the variability of flow over a small area. This allowed the the daily volume of flow to be partitioned into a finger and a background flow component. This lysimeter was 0.25 m^2 in area, had four 0.12 m high walls, and was divided into 16 separate compartments each of which was drained by a single hole leading to a collection bottle (Figure 3). All bottles were emptied every morning at the time of minimum flow. The installation procedure consisted of digging a snow pit in a 1.4 m deep snow cover, and inserting the lysimeter into a slot cut into the pit wall approximately 0.6 m above the ground. The collecting end of the lysimeter was at a minimum distance of 0.35 m from the pit wall. This notch was then refilled with snow. In addition, the snowpit face was protected with a double layer mylar radiation shield and the snowpit was covered with a mylar covered plywood sheet to minimize melting of the pit wall.

These procedures ensured that the lysimeter was in undisturbed snow and was not influenced by increased melt. Transfer errors were minimized by using a sufficiently large lysimeter in order to average the flow variations.

Daily flow from the multi-compartment lysimeter and from two recording lysimeters (1.0 and 0.25 m^2 in area) was always within +/- 10% of each other. Wankiewicz(1978) showed that problems due to hydraulic characteristics could be minimized if the raised limb of the lysimeter is equal to the pressure gradient zone which varies in height from 0.07 to 0.18 m depending on flow. For the flow conditions in this study, the 0.12 m lysimeter walls were sufficiently high to maximize catch efficiency.

Soil properties

Soil heat flux was estimated in two different ways. The first made use of the measured soil temperature profile and the soil thermal conductivity which was estimated using the method of Johansen (1975) and was recommended by Farouki(1981) after a comparison of four different approaches. The details of this procedure were reported in Marsh (1982). The second method made use of measured basal ice thickness to determine the soil heat flux. For periods when sufficient water is available at the soil-snow interface, the soil heat flux is equal to the latent heat released by the basal ice layer. In this case the soil heat flux (Qs) is

$$Qs = - (Lf * (pi - ps) * BI) / 86400 \qquad (1)$$

where Lf is the latent heat of fusion, pi and ps are the basal ice and snow density, BI is the daily increase in basal ice thickness, and the negative sign makes the soil heat flux negative when the heat flux is from the snow into the soil.

The total volume of water which may infiltrate the frozen soils was measured at two sites in each of the bog and polar desert soil types found in the Resolute study area. A constant head infiltrometer similar to that described by Hills (1970) was used. Steel cylinders, open at each end and 97 mm in diameter were placed into the soil in August 1980. In early June 1981, the snow overlying these cylinders was removed, and a known volume of water at 0 c was added until the infiltration ceased.

Snowmelt

Surface snowmelt during the 1981 study period was calculated using the energy balance approach described by Price and Dunne (1976) and applied to a High Arctic environment by Heron and Woo (1978). Instruments were installed at a level snow covered site (Marsh and Woo 1984a) before the beginning of melt. Air temperature and humidity were recorded with a Lambrecht thermohygrograph housed in a Stevenson screen, and recorder readings were checked at least twice daily with a mercury thermometer and an Assmann psychrometer. Net radiation was measured with a Swissteco net radiometer, and recorded on a Rustrak recorder. A Cassella sensitive cup anemometer and a Rustrak event recorder continuously monitored wind speed. The height of all instruments was frequently adjusted to maintain them at 1 m above the melting snow surface. Air pressure and rainfall measurements were obtained from the Atmospheric Environment Service weather station located 5 km south of the experimental site.

4. Melt metamorphism observations

Snow cover mass balance

During the melt period, the snow cover is composed of three separate components. These are defined as: (1) snow grains - loose granular ice grains, (2) liquid water - occupies the pores between the loose snow grains, and (3) ice - ice grains which are frozen together and form horizontal ice layers within the snow, vertical ice columns, and basal ice. Figure 4 shows the day to day changes in these constituents in 5 snowpits at Resolute.

As the melt proceeded the water equivalent of the snow portion of the pack gradually declined (Figure 4). The meltwater released by this melt was either stored in the snow as liquid water, froze to form ice, or was available for runoff. The total liquid water content slowly increased as the wetting front descended, but then increased as the

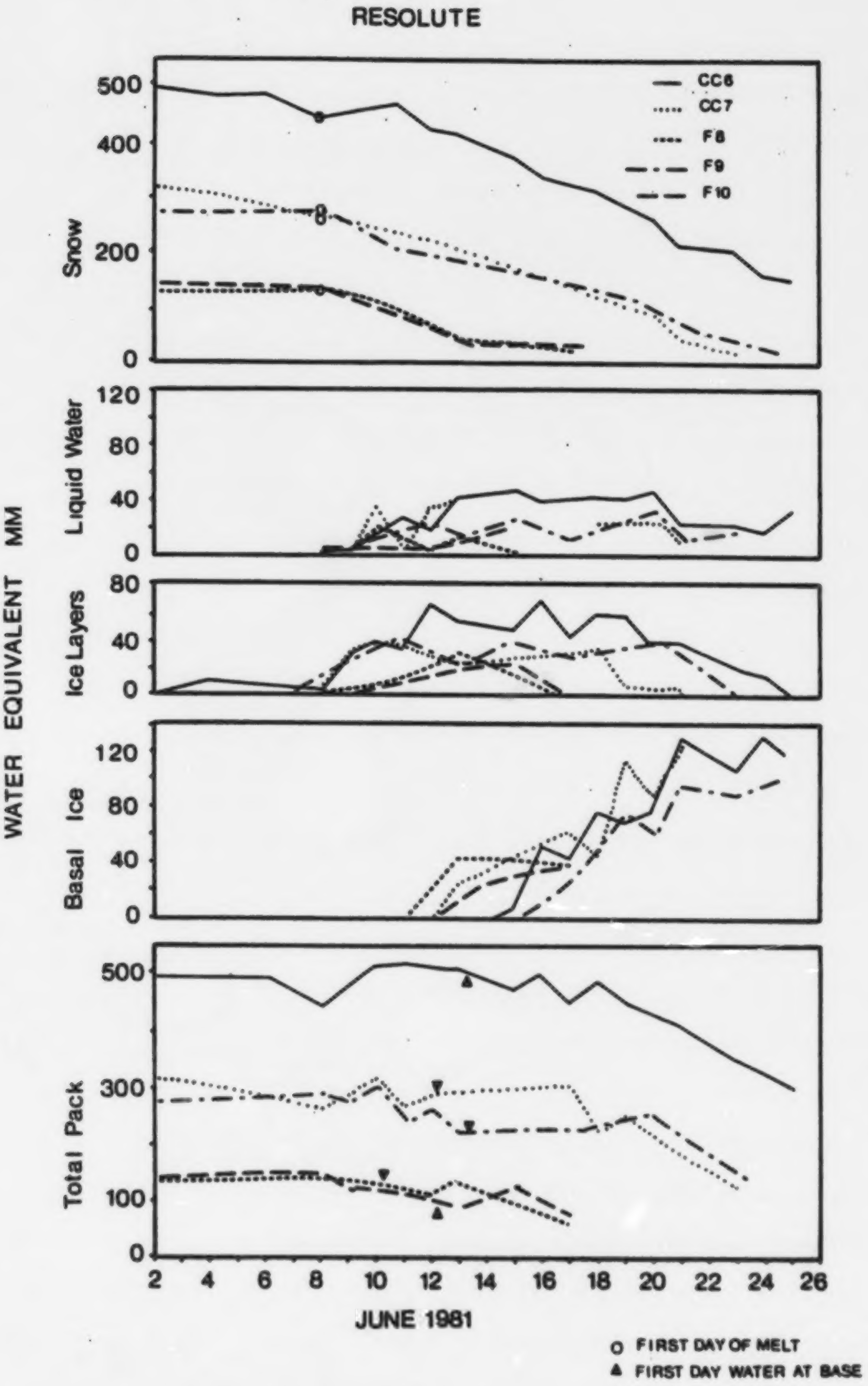

Figure 4. Daily changes in the individual components of the snow cover at snowpits monitored during the 1981 snowmelt period at Resolute.

snow depth diminishes (Figure 4). Storage ranged from 0 to 45 mm of water.

Field observations showed that the freezing of meltwater at the wetting front, or as ice columns, was small compared to ice layers. The ice layers were of two general types : (1) Discontinuous ice layers are thin (1 mm) and extend horizontally for only 0.1 to 0.2 m. They are not related to any observable premelt boundaries and do not contribute significantly to the snow cover mass.
(2) Continuous ice layers are much thicker (1 to 40 mm) and may be traced horizontally for at least 2 to 3 m. Their structure ranges from solid ice to frozen granular ice. Solid ice layers appear to have low permeability and measured mean density of 800 kg/m^3. Frozen granular layers are highly permeable and are composed of loosely bonded ice grains. These continuous ice layers were found to develop at all premelt stratigraphic boundaries.

Continuous ice layers began to grow at the beginning of melt and their total water equivalent (WE) increased as new layers formed below the advancing wetting front (Figure 4). The WE then decreased as layers near the surface decay. At maximum growth they accounted for 10 to 15% of the total pack water equivalent (Figure 4). Based on the premelt snowpit survey, the predicted number of ice layers in each vertical profile varied within and between the snow covers on different terrain units (Table 1), with the mean number of ice layers varying from 3 for the shallow snow covers lying on convex slpes to 7 on the deeper snow covers of concave slopes. Individual ice layers grew rapidly (up to a maximum of 21 mm/day WE) over a 24 to 36 hour period.

Once meltwater reached the snow base, up to 20 mm infiltrated the soil and froze. When this infiltration storage was filled, a basal ice layer began to form in the snow at all sites. It continued to grow throughout the melt period. It is denser than the other ice layers, with a mean density of 880 kg/m^3. Maximum thickness ranges from 50 to 150 mm, maximum WE of up to 120 mm (Figure 4) and accounts for 20 to 30% of the initial snow cover WE. This basal ice growth may consume a significant portion of the surface melt. As a result, the decrease in total snow cover WE is always less than the rate of surface melt (Figure 4).

Relationship between soil heat flux, wetting front and ice layers

As meltwater enters the dry snowcover, a distinct wetting front develops. A typical background wetting front is shown in Figure 5. This wetting front does not advance uniformly but it produces flow fingers at its leading edge. When a wetting front meets a stratigraphic boundary the water is first impounded above the interface and then spreads laterally to form a continuous wet layer (Figure 1 and 6). As water continues to accumulate above the horizontal boundary, new flow fingers penetrate the boundary, and the wetting front moves into the lower

Snow unit	Number of ice layers mean	 max	 min	mean snow depth (m)
flat	4	6	3	.45
convex slopes	3	4	2	.22
concave slopes	7	11	3	.88
gullies	6	7	3	1.44

Table 1. Predicted mean, maximum, and minimum number of continuous ice layers for each snow topographic unit, from premelt stratigraphy. Resolute 1981.

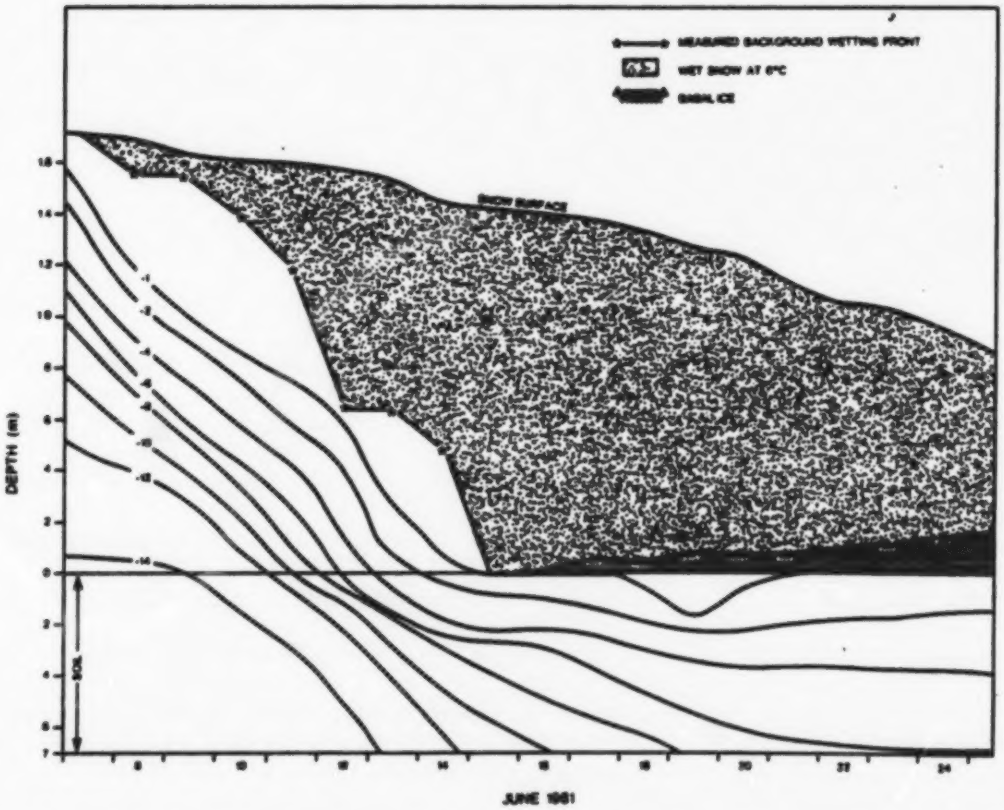

Figure 5. Snow-soil temperataure from the beginning of melt until June 25, 1981. Note that the background wetting front moves into snow which has already been warmed to near 0 c, and the basal ice continues to grow after the snow cover is isothermal at 0 c.

stratum. Flow finger movement is retarded at the lower boundary of the next stratigraphic unit and meltwater again spreads laterally until a new set of fingers is formed. Measurements of these flow fingers and of ice columns showed that their mean width was 36 mm and their mean separation averaged 131 mm.

These measurements, when projected on a horizontal plane, indicated that 22% of the area is covered by flow fingers (Marsh and Woo 1984a). Data from the multi-compartment lysimeter showed that shortly after the wetting front passed the lysimeter level, 22% of the area (ie. that covered by the fingers) conveyed 48% of the total flow (Figure 7). As a result, the mean flux in the finger compared to the surface flux is increased by

$$Ff = Fdf \ / \ Af \tag{2}$$

where Ff is mean flux in the finger, Fdf is the proportion of daily flow along the finger, and Af is the finger area. The above measurements demonstrate that the mean finger flux is 2.18 times higher than the average flux. This increased finger flux should enable the finger wetting front to move far ahead of the background front. However, field observations show that the finger front was seldom more than 0.2 m ahead of the background front. This may be explained by the growth of ice layers in the zone between the background and the finger wetting fronts (Figure 1). This

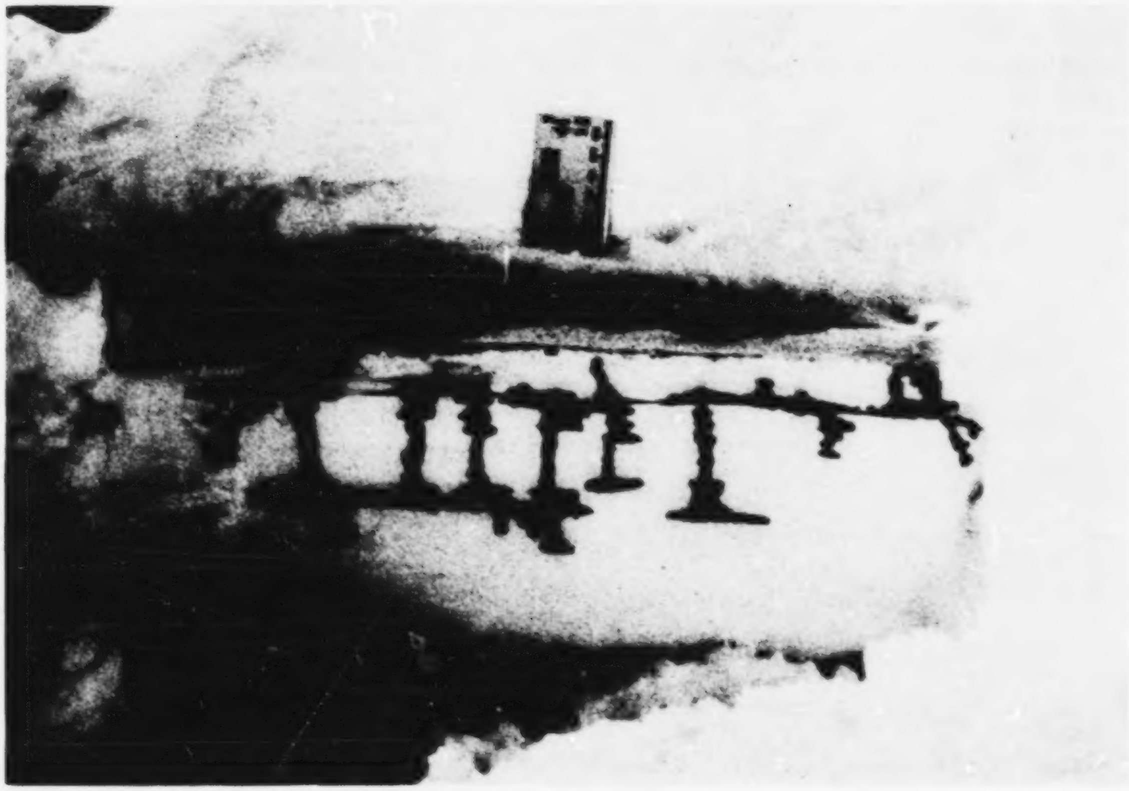

Figure 6. Development of flow fingers and wet layers at premelt horizons after dye injection into a dry, cold snow cover.

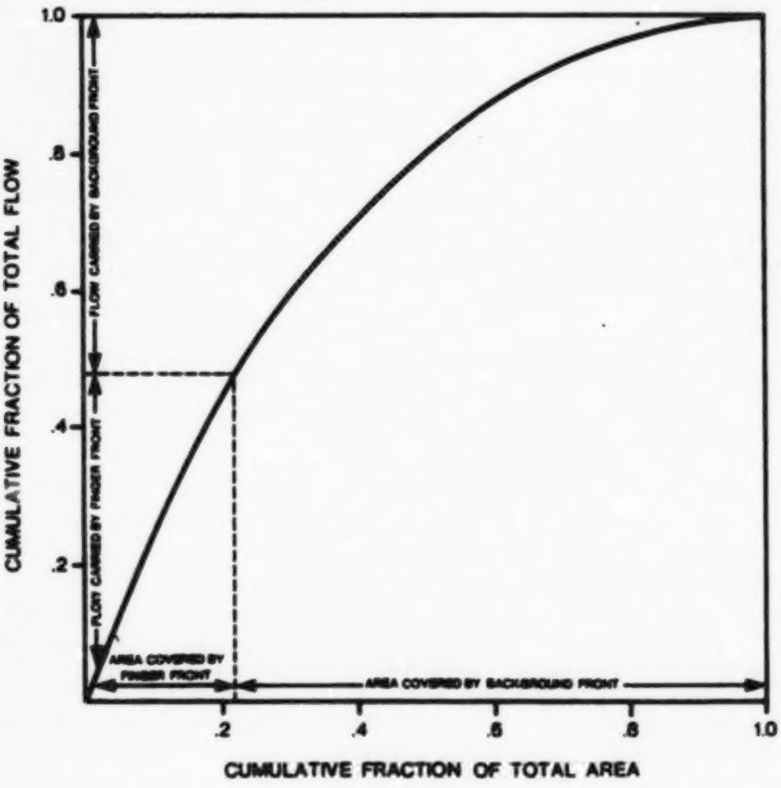

Figure 7. Measured flow variability soon after the wetting front passed the multi-compartment lysimeter level, June 16, 1981.

ice layer growth removed water from the flow fingers, thus limiting their downward movement. In warmer snow covers, ice layer growth is reduced and the flow fingers can move further ahead of the background wetting front. Marsh and Woo (1984b) provided a model to simulate the interaction of these processes.

The growth of these ice layers released large quantities of latent heat which was used to warm both the snow and underlying soil (Figure 8). During this period the soil heat flux was initially small (Figure 9), but increased rapidly as meltwater entered the snow. Soil heat flux consumed much of the energy needed to warm the snow cover and therefore increased the amount of water which froze as ice layers. This is especially important in shallow snow cover where the soil heat flux may represent up to 80% of the total ice layer growth.

Field observations showed a dramatic increase in soil heat flux as water reached the snow-soil interface (Figure 9), and it may reach a magnitude similar to the surface melt. As a result, all additional meltwater was frozen to form a basal ice layer yielding a considerable amount of latent heat to warm the soil (Figure 8). As the frozen soil gradually warmed the soil heat flux decreased and this retarded the basal ice growth. It is important to note that the soil heat flux stayed relatively large throughout the melt period and through the processes mentioned above, much of the meltwater was not immediately available for runoff.

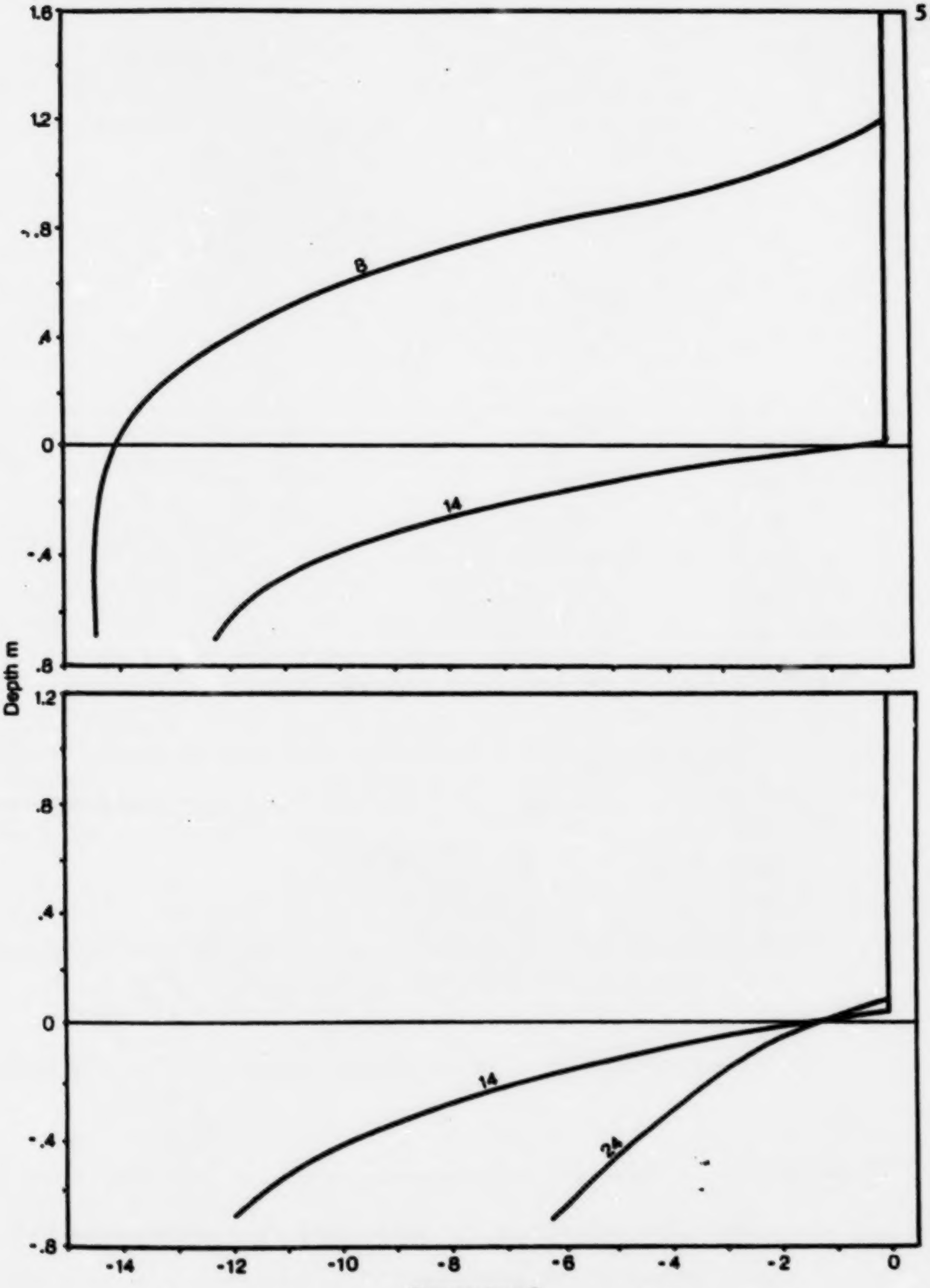

Figure 8. Warming of the snow and soil as a result of freezing within the snow, for the period before and after water reached the snow-soil interface. Zero depth marks the snow-soil interface.

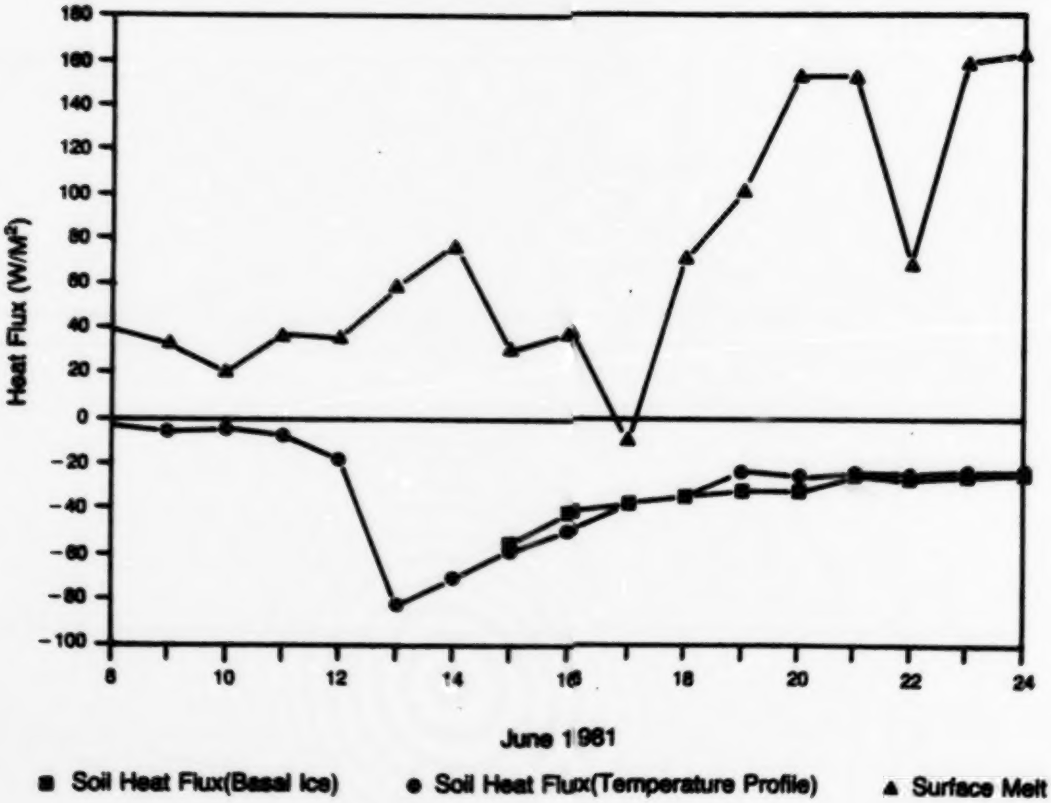

Figure 9. Soil heat flux throughout the melt period, Resolute, 1981. The estimates of soil heat flux were obtained from the soil temperature profile and from basal ice measurement. Surface snow melt heat flux is also given.

5. Conclusions

Field observations during the melt period demonstrated that the field techniques developed in this study were successful. The snowpit sampling technique allowed the day to day measurement of a number of snow properties at a single profile, and the method of dye injection and multi-compartment lysimeter allowed flow fingers to be studied. The comprhensive field program allowed the measurement of wetting front advance, development of flow fingers, volume of water carried by fingers, ice layer growth in the snow, basal ice growth, infiltration into frozen soils, snow-soil temperature, and soil heat flux.

These observations demonstrate that flow fingers developed at the leading edge of the wetting front. These fingers covered 22% of the area, but carried 48% of the total flow, enabling them to convey large amounts of water ahead of the background front. In the zone between the background and finger wetting fronts ice layers grew at all premelt stratigraphic boundaries. These ice layers are important in removing water from the flow fingers and therefore delaying wetting front advance. In addition, the growth of these ice layers releases large amounts of latent heat to warm the snow and the underlying soil. Soil heat flux is negative (from the snow to the soil) throughout the melt period, and at times it may be similar in magnitude to the surface melt rate and is responsible for increasing the amount of water that freezes as ice layers within and at the base fo the snow cover. An important conclusion of this study is that it is necessary to consider both the snow and soil when considering snow cover melt metamorphism. In fact it is necessary to "ripen" both the snow and the soil before meltwater runoff is generated.

Acknowldegements

The financial support for this work was provided by the Natural Sciences and Engineering Research Council of Canada, the Presidential Committee on Northern Studies of McMaster University, and the Arctic Institute of North America. The generous logistical support of Polar Continental Shelf Project, Department of Energy, Mines and Resources is gratefully acknowledged.

References

Benson,C., B. Holmgren, D. Trabant, and G. Weller. 1974. Physical characteristics of seasonal snow cover in northern Alaska. Proc. 42nd Western Snow Conf., 58-63.

Farouki,O.T. 1981. The thermal properties of soils in cold regions. Cold Regions Sci. and Technol., 5, 67-75.

Goodison,B.E., H.L Ferguson, and G.A. McKay. 1981. Measurement and Data Analysis in Handbook of Snow Principles, Processes, Management, and Use, edited by D.M. Gray and D.H. Male, 766 pp, Pergamon, New York.

Heron,R. and Woo,M.K. 1978. Snow melt computations for a High Arctic site. Proc. 35th Eastern Snow Conf., 162-172.

Hills,R.C. 1970. The determination of the infiltration capacity of field soils using the cylinder infiltrometer. British Geomor. Res. Group, Tech. Bull. 3, 25p.

IASH. 1970. Seasonal snow cover, A guide for measurement, compilation and assemblage of data, IASH-UNESCO-WMO, Technical papers in hydrology 2, 38 pp.

Johansen,O. 1975. Thermal Conductivity of Soils, Ph.D. Thesis, Trondheim, Norway.

Marsh,P. 1982. Ripening processes and meltwater movement in arctic snowpacks. Ph.D. thesis, 179p, McMaster University, Hamilton, Ontario.

Marsh,P. and M.K. Woo. 1984a. Wetting front advance and freezing of meltwater within a snow cover 1. Observations in the Canadian Arctic. Water Resour. Res. 20,1853-1864.

Marsh,P. and M.K. Woo. 1984b. Wetting front advance and freezing of meltwater within a snow cover 2. A simulation model. Water Resour. Res., 20, 1865-1874.

Maxwell,J.B.1980. The Climate of the Canadian Arctic Islands and adjacent waters, vol 1. Environment Canada, Atmospheric Environment Service, 532 p.

Price,A.J. and T.Dunne. 1976. Energy balance computation of snowmelt in a subarctic area. Water Resour. Res., 12, 686-694.

Wakahama,G. 1968. The metamorphism of wet snow, IASH AISH Publ., 79, 370-379.

Wakahama,G., D.Kuroiwa, T.Hasemi, and C.S. Benson. 1976. Field observations and experimental and theoretical studies on the superimosed ice of McCall Glacier. Alaska, J. Glaciol., 16, 135-149.

Wankiewics,A.C. 1978. Hydraulic characteristics of snow lysimeters. Proc. 35th Eastern Snow Conf., 105-116.

A list of Technical Memoranda of the Associate Commitee on Geotechnical Research may be obtained from the Secretary, Associate Committee on Geotechnical Research, c/o Institute for Research in Construction, National Research Council of Canada, Ottawa, Ontario K1A 0R6.

La liste des Technical Memoranda (mémoire techniques) du Comité associé de recherches géotechniques peut être obtenue auprès de secrétaire du Comité associé de recherches géotechniques, a/s Institut de recherche en construction, Conseil national de recherche du Canada, Ottawa, Ontario K1A 0R6.